Universidade de Aveiro Departamento de Química
2014

Hugo Daniel Carvalho de Azevedo Rocha

Disfunção mitocondrial nas doenças da β-oxidação dos ácidos gordos

Mitochondrial dysfunction in fatty acid β-oxidation disorders

Universidade de Aveiro Departamento de Química
2014

Hugo Daniel Carvalho de Azevedo Rocha

Disfunção mitocondrial nas doenças da β-oxidação dos ácidos gordos

Mitochondrial dysfunction in fatty acid β-oxidation disorders

Dissertação apresentada à Universidade de Aveiro para cumprimento dos requisitos necessários à obtenção do grau de Doutor em Bioquímica, realizada sob a orientação científica da Doutora Laura Ferreira Teixeira Vilarinho, Investigadora Auxiliar do Departamento de Genética do Instituto Nacional de Saúde Doutor Ricardo Jorge, do Doutor Francisco Manuel Lemos Amado, Professor Associado da Escola Superior de Saúde da Universidade de Aveiro e da Doutora Rita Maria Pinho Ferreira, Professora Auxiliar Convidada do Departamento de Química da Universidade de Aveiro

Dedico este trabalho à Raquel, ao André e à Leonor.

o júri

presidente

Doutor Carlos Manuel Martins da Costa
Professor Catedrático da Universidade de Aveiro

Doutora Catarina Isabel Neno Resende Oliveira
Professora Catedrática do Instituto de Bioquímica da Faculdade de Medicina da Universidade de Coimbra

Doutora Maria do Rosário Rodrigues de Almeida Martins
Professora Associada do Instituto de Ciências Biomédicas de Abel Salazar da Universidade do Porto

Doutor Fernando José dos Santos Rodrigues
Professor Associado da Escola de Ciências da Saúde da Universidade do Minho

Doutor Francisco Lemos Amado
Professor associado da Escola Superior de Saúde da Universidade de Aveiro

Doutor Cláudio Emanuel Moreira Gomes
Investigador auxiliar com agregação do Instituto de Tecnologia Química e Biológica da Universidade Nova de Lisboa

Doutora Laura Ferreira Teixeira Vilarinho
Investigadora auxiliar do Instituto Nacional de Saúde Doutor Ricardo Jorge

Doutora Maria do Rosário Gonçalves dos Reis Marques Domingues
Professora Auxiliar da Universidade de Aveiro

agradecimentos

Este trabalho só foi possível devido ao apoio e colaboração de várias pessoas a quem quero deixar os meus mais sinceros agradecimentos.

À Doutora Laura Vilarinho, que me criou o gosto pelo fascinante mundo das doenças metabólicas e com quem tanto aprendi e continuo a aprender, desde há dezoito anos, o meu obrigado pelo apoio, orientação e pela possibilidade de desenvolver este trabalho na Unidade de Rastreio Neonatal, Metabolismo e Genética do INSA, IP.

Ao Doutor Francisco Amado, agradeço a enorme generosidade com que me recebeu no seio do seu grupo de Proteómica no Departamento de Química da UA, assim como todo o apoio à realização deste trabalho.

À Doutora Rita Ferreira agradeço a amizade, a enorme disponibilidade, as sugestões e a inexcedível orientação científica. A forma abnegada e dedicada como assumiu, se envolveu e conduziu a orientação ficarão sempre para mim como um exemplo.

Ao Doutor Rui Vitorino, agradeço a amizade e toda a ajuda na análise e tratamento dos dados de espectrometria de massa das proteínas.

A todos os co-autores das publicações apresentadas no âmbito desta dissertação, agradeço a sua preciosa colaboração.

To Niels Gregersen and Rikke Olsen I have to thanks their belief in the collaboration we establish as well as the support during all the course of this project.

Às minhas colegas de trabalho Ana Marcão, Helena Fonseca, Carmen Sousa e Ivone Carvalho, obrigado pelo companheirismo. À Lurdes Lopes agradeço a colaboração com as culturas celulares e toda a amizade demonstrada.

Aos meus pais obrigado pela motivação, mas fundamentalmente por me terem ensinado a nunca desistir. À minha restante família agradeço o carinho e a ajuda fundamental a tratar dos meus filhos.

Aos meus filhos, André e Leonor, obrigado por todos os sorrisos e carinhos, que sempre me fazem querer ser melhor e acreditar que por Vós tudo vale a pena.

Por fim à Raquel, minha companheira, meu suporte, obrigado pelo incansável incentivo e apoio, fundamentais para a concretização deste projecto. A forma como assumiste as “despesas” familiares durante as minhas inúmeras ausências foi absolutamente extraordinária.

palavras-chave

Mitocôndria, proteoma mitocondrial, β-oxidação dos ácidos gordos, MADD, LCHADD

resumo

A mitocôndria desempenha um papel fundamental na regulação de vários processos celulares, com particular relevância na produção de energia, sendo a β-oxidação mitocondrial dos ácidos gordos uma das vias metabólicas que tem lugar neste organelo. Os défices da β-oxidação mitocondrial dos ácidos gordos estão entre os grupos de doenças metabólicas mais estudados, existindo contudo, algumas questões que continuam por esclarecer, como a sua prevalência ao nascimento em determinadas regiões da Europa e quais e de que forma os vários determinantes patofisiológicos interatuam para produzir um determinado fenótipo.

A análise dos dados de programas de rastreio neonatal da península Ibérica possibilitou estimar a prevalência ao nascimento dos défices da β-oxidação mitocondrial, tendo-se observado um dos valores mais elevados (particularmente em Portugal) no âmbito das regiões europeias, fundamentalmente devido à grande prevalência ao nascimento dos défices da desidrogenase dos ácidos gordos de cadeia média. Estes resultados realçam o impacto deste grupo de doenças genéticas nesta região europeia.

A caracterização do proteoma mitocondrial, a partir de fibroblastos em cultura, de doentes com défices da β-oxidação mitocondrial (especificamente défice múltiplo das desidogenases (MADD) e défice da desidrogenase dos ácidos 3-hidroxilados de cadeia longa (LCHADD)) permitiu obter uma perspetiva geral sobre a plasticidade do proteoma mitocondrial nestas doenças assim como avaliar quais as principais vias metabólicas envolvidas na sua patogénese. Em formas severas de MADD foi observada uma sobre-expressão de *chaperones*, enzimas antioxidantes e proteínas associadas à apoptose. Nestas células foi igualmente observada a sobre-expressão de enzimas glicolíticas, como adaptação ao bloqueio da β-oxidação. A análise de amostras de doentes com LCHADD também evidenciou uma sobre-expressão de enzimas glicolíticas, assim como de proteínas relacionadas com a apoptose, e a modulação do sistema de defesa antioxidante. O doente com uma forma severa de LCHADD apresentou níveis de *stress* oxidativo elevados, associados a uma sobre-expressão da MnSOD, enquanto o doente com uma forma moderada apresentou níveis mais baixos de stress oxidativo e uma sub-expressão da MnSOD. Estes resultados são provavelmente o reflexo do papel da MnSOD na regulação dos níveis de ROS, mantendo-os em níveis que não provoquem danos, mas que permitam iniciar processos de sinalização com vista à manutenção celular. A comparação de forma moderadas com severas de MADD não revelou diferenças significativas, muito provavelmente porque os níveis de *stress* oxidativo são suficientemente altos para despoletar uma resposta semelhante às formas severas. Os presentes resultados realçam as diferenças na modulação do sistema de defesa antioxidante no espectro dos défices da β-oxidação mitocondrial.

No seu conjunto os resultados obtidos revelam as principais vias moduladas nos défices da β-oxidação mitocondrial e a importância do *stress* oxidativo e sistema de defesa antioxidante para o fenótipo. Ao permitem compreender melhor a complexa interação entre os vários fatores que interagem com vista ao fenótipo e que podem ser de origem genética, epigenética ou ambiental, contribuem para o desenvolvimento de novas e mais eficazes abordagens terapêuticas.

keywords Mitochondria, mitochondrial proteome, fatty acid β-oxidation, MADD, LCHADD

abstract

Mitochondria are central organelles for cell survival with particular relevance in energy production and signalling, being mitochondrial fatty acid β–oxidation (FAO) one of the metabolic pathways harboured in this organelle.

FAO disorders (FAOD) are among the most well studied inborn errors of metabolism, mainly due to their impact in health. Nevertheless, some questions remain unsolved, as their prevalence in certain European regions and how pathophysiological determinants combine towards the phenotype.

Analysis of data from newborn screening programs from Portugal and Spain allowed the estimation of the birth prevalence of FAOD revealing that this group of disorders presents in Iberia (and particularly in Portugal) one of the highest European birth prevalence, mainly due to the high birth prevalence of medium chain acyl-CoA dehydrogenase deficiency. These results highlight the impact of this group of genetic disorders in this European region.

The characterization of mitochondrial proteome, from patients fibroblasts with FAOD, namely multiple acyl-CoA dehydrogenase deficiency (MADD) and long chain acyl-CoA dehydrogenase deficiency (LCHADD), provided a global perspective of the mitochondrial proteome plasticity in these disorders and highlights the main molecular pathways involved in their pathogenesis. Severe MADD forms show an overexpression of chaperones, antioxidant enzymes (MnSOD), and apoptotic proteins. An overexpression of glycolytic enzymes, which reflects cellular adaptation to energy deficiency due to FAO blockage, was also observed. When LCHADD fibroblasts were analysed a metabolic switching to glycolysis was also observed with overexpression of apoptotic proteins and modulation of the antioxidant defence system. Severe LCHADD present increased ROS alongside with up regulation of MnSOD while moderate forms have lower ROS and down-regulation of MnSOD. This probably reflects the role of MnSOD in buffering cellular ROS, maintain them at levels that allow cells to avoid damage and start a cellular response towards survival. When ROS levels are very high cells have to overexpress MnSOD for detoxifying proposes. When severe forms of MADD were compared to moderate forms no major differences were noticed, most probably because ROS levels in moderate MADD are high enough to trigger a response similar to that observed in severe forms. Our data highlights, for the first time, the differences in the modulation of antioxidant defence among FAOD spectrum.

Overall, the data reveals the main pathways modulated in FAOD and the importance of ROS levels and antioxidant defence system modulation for disease severity. These results highlight the complex interaction between phenotypic determinants in FAOD that include genetic, epigenetic and environmental factors. The development of future better treatment approaches is dependent on the knowledge on how all these determinants interact towards phenotype.

Table of Contents

List of Figures

Chapter I

Chapter III

Study 3

Chapter IV

Study 4

Chapter V

Study 5

Appendix – Supplementary data

List of Tables

Appendix – Supplementary data

List of Abbreviations

2DE-MS	Two dimensional electrophoresis-mass spectrometry
2D-LC-MS	Multidimentional liquid chromatography-mass spectrometry
ACAD	Acyl-CoA dehydrogenase
ADP	Adenosine diphosphate
AFLP	Acute fatty liver in the pregnancy
AMP	Adenosine monophosphate
ARDS	Acute repiratory distress syndrome
ATP	Adenosine triphosphate
CACT	Carnitine-acylcarnitine translocase
CoA	Coenzyme A
CPT I	Carnitine palmitoyl transferase I
CPT II	Carnitine palmitoyl transferase II
CUD	Carnitine uptake defect
DHA	Docosahexaenoic acid
DNA	Deoxyribonucleic acid
ETF	Electron transfer flavoprotein
ETF-QO	Electron transfer flavoprotein – ubiquinone oxidorreductase
FA	Fatty acids
FABPs	Fatty acid binding proteins
FAD	Flavin adenine dinucleotide
$FADH_2$	Flavin adenine dinucleotide – reduced form
FAO	Fatty acid β-oxidation
FAOD	Fatty acid β-oxidation disorders
FATPs	Fatty acid transport proteins
FFA	Free fatty acids
GAPDH	Glyceraldeyde-3-phosphate dehydrogenase
GDH	Glutamate dehydrogenase
H	Hydrogen
H_2O_2	Hydrogen peroxide
HELLP	Hemolysis, elevated liver enzymes and low platelets
HO^-	Hydroxyl radical
HSP	Heat shock protein
LCAD	Long chain acyl-CoA dehydrogenase
LC-CoA	Long chain fatty acid - CoenzymeA
LCEH	Long chain 2-enoyl-CoA hydratase
LCHAD	Long chain 3-hydroxyacyl-CoA dehydrogenase
LCHADD	Long chain 3-hydroxyacyl-CoA dehydrogenase deficiency
LCKAT	Long chain 3-ketoacyl-CoA thiolase
M/SCHAD	Medium/short chain 3-hydroxyacyl-CoA dehydrogenase
MADD	Multiple acyl-CoA dehydrogenation deficiency
MCAD	Medium chain acyl-CoA dehydrogenase
MCADD	Medium chain acyl-CoA dehydrogenase deficiency
MC-CoA	Medium chain fatty acid - CoenzymeA
MCKAT	Medium chain 3-ketoacyl-CoA thiolase
MIM	Mitochondrial inner membrane
MnSOD	Manganese Superoxide Dismutase
MOM	Mitochondrial outer membrane
mRNA	Messenger ribonucleic acid

MS/MS	Tandem mass spectrometry
MTP	Mitochondrial trifunctional protein
mtPQC	Mitochondrial protein quality control sytem
NAD^+	Nicotinamide adenine dinucleotide
NADH	Nicotinamide adenine dinucleotide – reduced form
NBS	Newborn screening
NO	Nitric oxide
O_2^-	Superoxide ion
OCTN2	Organic cation transporter 2
$ONOO^-$	Peroxynitrite
OXPHOS	Oxidative phosphorylation
PPAR	Peroxisome proliferator activator receptor
PPi	Inorganic pyrophosphate
PTM's	Post-transcriptional modifications
RNS	Reactive nitrogen species
ROS	Reactive oxygen species
RR-MADD	Riboflavin responsive multiple acyl-CoA dehydrogenation deficiency
SCAD	Short chain acyl-CoA dehydrogenase
SCADD	Short chain acyl-CoA dehydrogenase deficiency
SCEH	Short chain 2-enoyl-CoA hydratase
SCKAT	Short chain 3-ketoacyl-CoA thiolase
SDS-LC-MS	Sodium dodecyl-sulphate liquid chromatography-mass spectrometry
SIDS	Sudden infante death syndrome
TCA	Tricarboxilic acid
VLCAD	Very long chain acyl-CoA dehydrogenase
VLCADD	Very long chain acyl-CoA dehydrogenase deficiency

CHAPTER I

State of the art

1. General introduction

Mitochondria are crucial cellular organelles, which play a central role in energy production, being also deeply involved with intracellular signalling (Benard and Rossignol 2008). One of the main metabolic pathways that take place at mitochondria is fatty acid β-oxidation (FAO), which has a particular importance in energy production during periods of fasting or metabolic stress (Rinaldo, Matern et al. 2002). The oxidation of fatty acids molecules will result in the production of NADH and $FADH_2$, that will channel their electrons to oxidative phosphorylation (OXPHOS) for ATP production, and acetyl-CoA molecules that can be further oxidized via Krebs cycle or enter ketogenesis for ketone bodies production (Houten and Wanders 2010).

To accomplish its function FAO involves the coordinate action of about 25 distinct mitochondrial proteins, among enzymes and transporters. Deficiencies in several of these proteins have been associated to human diseases, the mitochondrial fatty acid β-oxidation disorders (FAOD), which include at least 15 distinct genetic disorders (Rinaldo, Matern et al. 2002, Vockley and Whiteman 2002, Kompare and Rizzo 2008, Moczulski, Majak et al. 2009). The clinical presentation associated to FAOD is very heterogeneous and may include hypoketotic hypoglycemia, Reye-like syndrome, cardiomyopahy, myopathy or rhabdomyolysis, with also heterogeneous degrees of severity, which can range from asymptomatic patients to neonatal sudden death, being acute episodes triggered by fasting or illness (Rinaldo, Matern et al. 2002). Treatment of FAOD relies mainly on avoiding fasting and diets supplemented with alternative fuel sources, like carbohydrates or medium chain fatty acids (Kompare and Rizzo 2008).

For a long time efforts have been made to understand the molecular basis underlying the observed clinical variability, which is noticed even between patients with the same genotype. It is believed that the pathophysiology of FAOD mainly relies on the resulting energy deficiency, on the accumulation of toxic metabolites, the shortness of vital components, altered enzyme products, loss of protein/protein interactions and in the accumulation of misfolded proteins (Gregersen and Olsen 2010, Olpin 2013). The contribution of each of these factors to the phenotype is different for each FAOD, depending on the defective protein, the nature of the mutation and the interaction of these determinants with other cellular and environmental factors. The ways all these disease determinants interact towards phenotype development are still poorly understood and it's

believed that study approaches like global proteomics will give a polygenic perspective, helping to understand it.

2. State of the art

2.1 Mitochondrial fatty acid β-oxidation

Fatty acids are a group of biological molecules characterised by a long hydrocarbon chain and a terminal carboxylate group. They play several important roles as they are key components of the cell membrane, enzymes and hormones, being also, alongside with carbohydrates and amino acids, one of the major energy sources in many organisms, including mammals (Moczulski, Majak et al. 2009). In the cells, fatty acids can undergo different oxidative degradation processes, namely alpha (α), beta (β) and omega (ω) oxidation, depending on the carbon involved in the oxidation process (Moczulski, Majak et al. 2009). The α-oxidation of fatty acids occurs in the peroxisomes and in humans is used to remove a single carbon from the carboxyl end of phytamic acid, that cannot undergo β-oxidation due to its β-methyl branch, transforming it into pristamic acid, which can; the ω-oxidation occurs in the endoplasmatic reticulum and is a minor pathway that only becomes relevant when β-oxidation is defective; the β-oxidation represents the major process by which fatty acids are oxidised, by a sequential removal of a two carbon units from the acyl chain, and takes place in the peroxisomes and in the mitochondria (Bartlett and Eaton 2004).

The β-oxidation of fatty acids is a key metabolic pathway for energy homeostasis in organs such as the liver, heart and skeletal muscle, being of particular importance in periods of fasting, high energy demanding as exercise, febrile illness or metabolic stress (Rinaldo, Matern et al. 2002). While in the heart and the skeletal muscle β-oxidation acts exclusively as a source of ATP, in the liver it also serves a different role by providing ketone bodies (acetoacetate and β-hydroxybutyrate) to peripheral tissues like the kidney (Thumelin, Forestier et al. 1993), the small intestine (Bekesi and Williamson 1990), white adipose tissue (Thumelin, Kohl et al. 1999) and the brain (Cullingford, Dolphin et al. 1998), that are ketogenic under certain circumstances, namely when glucose levels are low. The oxidation of long-chain fatty acids also provides the energy required for non-shivering thermogenesis by brown adipose tissue (Mitchell and Fukao 2006).

Georg Franz Knoop first discovered fatty acid β-oxidation, back in 1904 (Knoop 1904). By feeding dogs with different types of fatty acids, namely odd and even fatty acids, and then analysing the resulting metabolic products in dogs urine, he noticed that when the dogs were fed with odd chain fatty acids, hippuric acid was found in urine, and when the dogs were fed with even chain fatty acids phenaceturic acid was excreted. So he concluded that the metabolism of fatty acids proceeds by a successive removal of two carbon molecules and as the remaining fatty acids has to contain a carboxylic group. He also proposed that the oxidation took place in the β carbon atom (Knoop 1904).

The β-oxidation takes place in the peroxisomes and in the mitochondria where the oxidation of the fatty acids involves similar enzymatic steps (dehydrogenation, hydration, another dehydrogenation and finally a thiolytic cleavage) (Wanders, van Roermund et al. 2003, Houten and Wanders 2010). Besides these similarities major differences exist between the β-oxidation in both organelles, specifically in pathway regulation and substrates oxidised by each of the systems. While mitochondria β-oxidise palmitic acid, oleic acid and linoleic acids, the major fatty acids from diet, in the peroxisomes are oxidised a range of fatty acids and fatty acids derivatives that are not handled by mitochondria. These include very-long-chain fatty acids, pristamic acid and the bile acid intermediates, di- and trihydroxycholestanoic acid (Wanders and Waterham 2006). Quantitatively, most of the β-oxidation of fatty acids occurs in mitochondria, representing peroxisomal β-oxidation no more than 10% of the β-oxidation flux of long-chain-fatty-acids (Eaton 2002). The differences between the two β-oxidation systems are clear in the different clinical presentations of the patients affected by either a mitochondrial or peroxisomal β-oxidation defects (Rinaldo, Matern et al. 2002, Wanders and Waterham 2006). In this work we will focus on the mitochondrial β-oxidation of fatty acids.

So that the fatty acids (FA) can be fully β-oxidised in mitochondria, in order to originate ATP and/or ketone bodies, some sequential steps must be completed:

i. Transport of FA across the plasma membrane
ii. Transport of FA across the mitochondrial membrane – carnitine shuttle
iii. Mitochondrial β-oxidation cycles.

Each of these essential steps will now be presented.

2.1.1 Transport of FA across the plasma membrane

Long chain fatty acids represent the main source of energy for many organs and since most tissues contain only small amounts of storage lipids, they depend on a continuous supply of FA, mostly from adipose tissue (Rinaldo, Matern et al. 2002). FA are released by the action of lipases and then transported through the blood bounded to albumin to ensure solubility (Kerner and Hoppel 2000). Tissues then take them up by tissue-specific fatty acid transporters (Berk and Stump 1999), although passive uptake probably also occurs (Houten and Wanders 2010).

Fatty acid transport proteins (FATPs) are transmembrane proteins responsible for the uptake of very-long and long chain FA into the cell. In Humans, the family of FATPs encompass a group of six highly homologous proteins: $FATP_1$ to $FATP_6$, which are tissue specific. $FATP_1$ (SLC27A1) and $FATP_4$ (SLC27A4) are expressed in the skeletal muscle; in the heart are expressed $FATP_6$ (SLC27A6) and $FATP_1$ (SLC27A1); whereas in the liver it is $FATP_5$ (SLC27A5) that plays a crucial role in the uptake of FA (Gimeno, Ortegon et al. 2003, Doege and Stahl 2006). Besides FATPs other proteins, like fatty acid translocase and plasma membrane fatty acid binding protein are also involved in FA uptake (Glatz, Bonen et al. 2006, Kiens 2006).

FATPs have not only a transport function but they also have acyl-CoA synthetase activity, which suggests that FA are rapidly converted to their activated form – acyl-CoA's – once inside the cell, allowing them to participate in metabolic processes and drive the process (Houten and Wanders 2010). The activation of FA consists in the join of the FA to the SH group of CoenzymeA (CoA) through a thioester linkage (R-CO-SCoA), a high energy bound (Figure 1).

$$\text{R-COOH} + \text{CoA-SH} + \text{ATP} \Leftrightarrow \text{R-CO-SCoA} + \text{AMP} + \text{PPi}$$

Figure 1: Activation reaction of fatty acids.
Fatty acid activation is an energy dependent reaction that consists in linking a coenzyme A molecule to the fatty acid, through a thioester linkage.
R-COOH, fatty acid; CoA-SH, coenzyme A; ATP, adenosine triphospate; R-CO-SCoA, activated fatty acid; AMP, adenosine monophosphate; PPi, inorganic pyrophosphate.

The subsequent hydrolysis of PPi drives the reaction in the forward direction, maintaining a low cytosolic free fatty acid content (Moczulski, Majak et al. 2009). Nevertheless, the activation of FA is not exclusively performed by FATPs, being generally accepted that FA activation is also done by several acyl-CoA synthetases protein families which reside in the membrane of the mitochondria, peroxisomes and endoplasmic reticulum (Watkins 2008). While very long and long chain fatty acids are activated out of the mitochondria, medium and short chain fatty acids, are thought to directly enter to the mitochondrial matrix, being activated already inside mitochondria (Vockley and Whiteman 2002).

In order to stabilize and ensure FA solubility in the cytoplasm a group of binding proteins a is needed, the so called cytoplasmic fatty acid binding proteins (FABPs) (Schaap, Binas et al. 1999, Binas, Han et al. 2003, Erol, Kumar et al. 2004). These proteins are involved in reversibly binding intracellular hydrophobic ligands and trafficking them throughout cellular compartments, including the peroxisomes, mitochondria, endoplasmic reticulum and nucleus (Smathers and Petersen 2011). So far 9 different FABPs, with tissue-specific distribution, have been identified: L (liver), I (intestinal), H (muscle and heart), A (adipocyte), E (epidermal), Il (ileal), B (brain), M (myelin) and T (testis) (Chmurzynska 2006).

2.1.2 Transport of FA to the mitochondrial matrix

After FA activation, the resulting very long and long acyl-CoA esters cannot pass through the mitochondrial wall (Kerner and Hoppel 2000). Two membranes compose mitochondrial wall: the mitochondrial outer membrane (MOM) and the mitochondrial inner membrane (MIM), being the latter non-permeable to FA, more precisely to very long and long chain FA. In order to overpass this a shuttle is required – the carnitine shuttle (figure 2).

The carnitine shuttle is a mitochondrial membrane transport system that uses carnitine to assist FA transport, being its availability a crucial factor for FA transport. Carnitine (3-hydroxy-4-trimethylaminobutirate) (figure 3) can be obtained from the diet or through biosynthesis. In omnivorous Humans, the diet accounts for about 75 % of the body carnitine, being biosynthesis important in situations where diet cannot supply enough carnitine (Vaz and Wanders 2002). The substrate for the biosynthesis of carnitine is 6-N-trimethyl-lysine, that is a product of lysosomal and proteosomal degradation of proteins containing N-methylated lysines. Carnitine biosynthetic pathway involves a series of four enzymatic steps that take place mainly in the liver and in the kidneys (Vaz, Melegh et al.

2002, Strijbis, Vaz et al. 2010). Independently from its origin, and so it can reach tissues, carnitine must be actively transported through the plasma cell membrane. This transport is done by tissue specific plasma membrane carnitine transporters, which allow that carnitine concentration in the cytoplasm of cells to be as 50 times higher than the concentration in the plasma (Bremer 1983). Muscle, heart and renal tubes express OCTN2, the well-known plasma membrane carnitine transporter, while the liver expresses a different one (Nezu, Tamai et al. 1999).

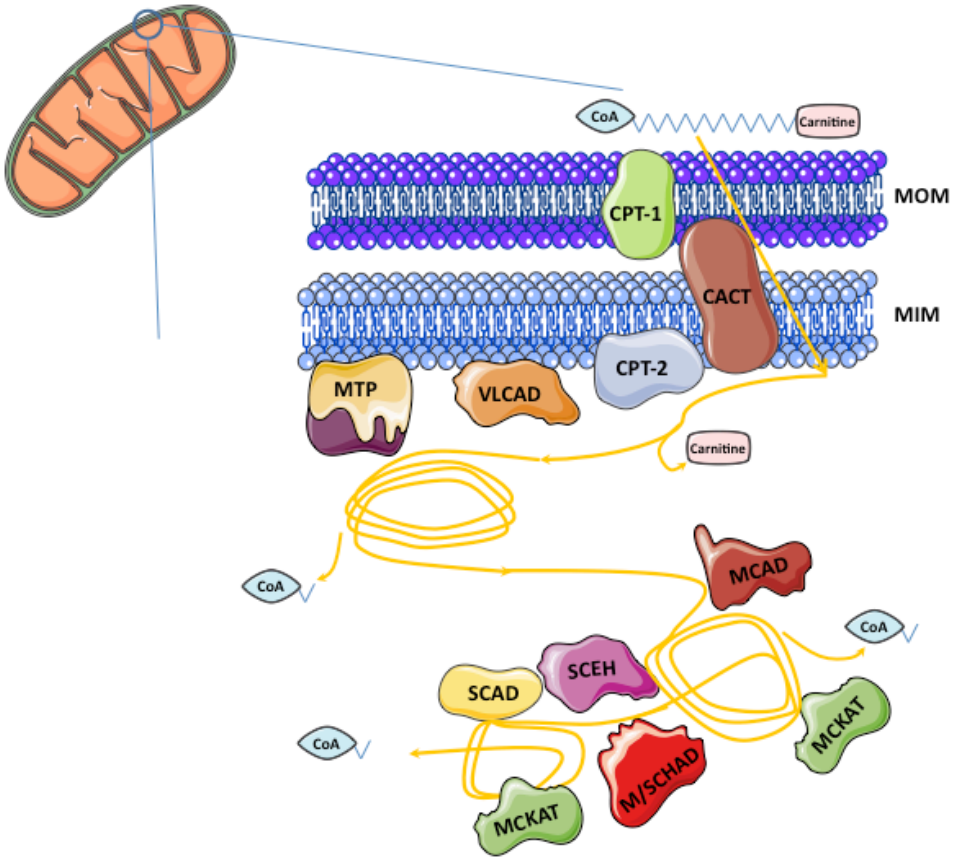

Figure 2: Representation of mitochondrial fatty acid β-oxidation machinery.
A schematic representation mitochondrial fatty acid β-oxidation pathway is shown. This mitochondrial pathway is responsible for the oxidation of fatty acids and encompasses the carnitine shuttle (CPT-1, CACT and CPT-2), that enables the transport of fatty acids to the mitochondrial matrix, and the β-oxidation cycles that oxidise the fatty acids to acetyl-CoA, with NADH and $FADH_2$ production.
CPT-1, carnitine palmitoyl transferase I; CPT-2, carnitine palmitoyl transferase II; CACT, carnitine-acylcarnitine translocase; MOM, mitochondrial outer membrane; MIM, mitochondrial inner membrane; VLCAD, very long chain acyl-CoA dehydrogenase; MTP, mitochondrial trifunctional protein; MCAD, medium chain acyl-CoA dehydrogenase; CoA, coenzyme A; MCKAT, medium chain 3-ketoacyl-CoA thiolase; SCEH, short chain 2-enoyl-CoA hydratase; M/SCHAD, medium/short chain 3-hydroxyacyl-CoA dehydrogenase; SCAD, short chain acyl-CoA dehydrogenase.

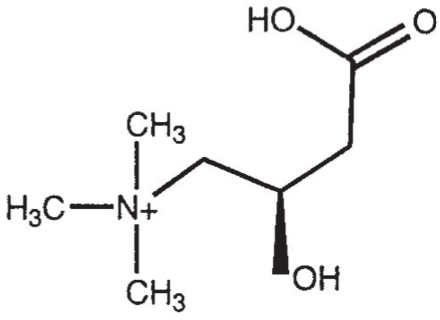

Figure 3: Structural formula of the carnitne molecule.

The carnitine shuttle involves the concerted action of a group of three proteins: carnitine palmitoyl transferase I (CPT I); Carnitine-acylcarnitine translocase (CACT); and carnitine palmitoyl transferase II (CPT II), all membrane bound (Kerner and Hoppel 2000) (Figure 2). CPT I is the first player in the shuttle catalyzing the formation of acylcarnitines from acyl-CoA's plus carnitine. It is a true transmembrane protein located in the MOM having its active and regulatory sites facing the cytosol (Kerner and Hoppel 2000). CPT I is the only enzyme of the mitochondrial β-oxidation that is known to exist in tissue specific isoforms: a liver type (CPT Ia), a muscle type (CPT Ib) and a brain type (CPT Ic) (Bonnefont, Djouadi et al. 2004). Although called liver type, CPT Ia is also expressed in the brain, kidney, lung, spleen, intestine, pancreas, ovary and fibroblasts, while CPT Ib is expressed in heart, skeletal muscle and testis (Houten and Wanders 2010). Type Ic is brain specific and its function still needs to be addressed (Bonnefont, Djouadi et al. 2004). After the formation of the acylcarnitines they are transported through the MIM by the action of CACT, a transmembrane protein, that exchanges acylcarnitine by a free carnitine molecule, from the mitochondrial matrix. The carnitine cycle is completed by the action of CPT II that is embedded in the MIM, with its active site facing the mitochondrial matrix, and that reverts the action of CPT I, hydrolyzing the acylcarnitines back to acyl-CoAs and free carnitine. The reaction catalysed by CPT II is reversible, as well as the CACT transport, allowing acylcarnitine export to the cytoplasm.

The resulting acyl-CoAs are now in the mitochondrial matrix and can undergo chain shortening through the β-oxidation cycles.

2.1.3 Mitochondrial β-oxidation cycles

Once inside the mitochondrial the activated form of the FA can now be fully oxidized to water and CO_2, by the action of β-oxidation, in tight collaboration with the Krebs cycle and mitochondrial respiratory chain. Mitochondrial β-oxidation is a cyclic pathway and FA will be subject to several oxidation cycles, that consist in the sequential occurrence of four enzymatic reactions, resulting in the removal of a two carbon molecule – acetyl-CoA, per cycle and leading to the correspondent chain shortening of the FA (Houten and Wanders 2010) (figure 4). The resulting acetyl-CoA molecule will be the substrate for the ketogenesis and/or be fully oxidised by the Krebs cycle, while the resulting FA will be subject to more β-oxidation cycles until the formation of two acetyl-CoA molecules in the last cycle (Houten and Wanders 2010).

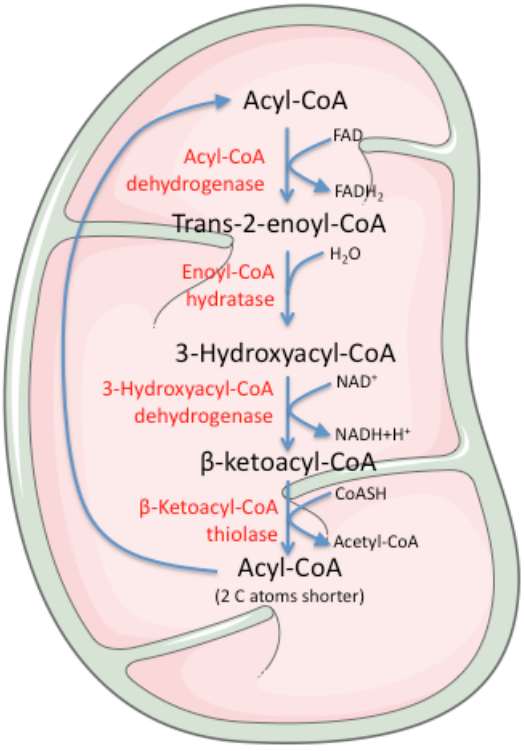

Figure 4: Reactions of the mitochondrial fatty acid β-oxidation cycles.
Mitochondrial β-oxidation cycles encompass a series of four sequential reactions: a dehydrogenation, a hydration, another dehydrogenation and finally a thiolytic cleavage. The result of each cycle is the formation of one $FADH_2$ and one NADH molecules as well as the release of an acetyl-CoA, alongside with the shortening of the oxidised fatty acid.
FAD, flavin adenine dinucleotide; $FADH_2$, flavin adenine dinucleotide – reduced form; NAD, nicotinamide adenine dinucleotide; NADH, nicotinamide adenine dinucleotide – reduced form; CoA, coenzyme A.

The β-oxidation cycle's reactions initiate by a dehydrogenation of the acyl-CoA ester to yield a trans-2-enoyl-CoA. This reaction involves several members of the acyl-CoA dehydrogenase family of FAD- requiring oxidoreductases (Rinaldo, Matern et al. 2002, Moczulski, Majak et al. 2009, Houten and Wanders 2010). These dehydrogenases are chain specific: very-long chain acyl-CoA dehydrogenase (VLCAD) (from C12 to C18), medium chain acyl-CoA dehydrogenase (MCAD) (from C6 to C10) and short chain acyl-CoA dehydrogenase (SCAD) (from C4 to C6) (Rinaldo, Matern et al. 2002). Another dehydrogenase, long chain acyl-CoA dehydrogenase (LCAD) has also been reported has having a chain length specificity between MCAD and VLCAD, although its role in fatty acid β-oxidation is unclear, due to its low expression levels (Kurtz, Rinaldo et al. 1998, Vockley and Whiteman 2002, Chegary, Brinke et al. 2009).

This second reaction involves the hydration of the double bound in the 2,3 position to produce a stereo specific L-3-hydroxyacyl-CoA species. This reaction is catalysed either by long-chain-enoyl-CoA-hydratase (LCEH) or by short chain-enoyl-CoA-hydratase (SCEH), also known as crotonase, which is responsible for the hydration of medium and short chain enoyl-CoA species (Kanazawa, Ohtake et al. 1993).

The third step consists in another dehydrogenation reaction to produce 3-keto-acyl-CoA molecules from the L-3-hydroxyacyl-CoA's. This reaction is catalysed either by long chain-3-hydroxy-acyl-CoA dehydrogenase (LCHAD), responsible for the reduction of long chain substrates, or by medium/short-chain-3-hydroxy-acyl-CoA dehydrogenase (M/SCHAD), with a broad chain length specificity and responsible by the reduction of medium and short chain L-3-hydroxyacyl-CoA's (Rinaldo, Matern et al. 2002, Vockley and Whiteman 2002, Moczulski, Majak et al. 2009, Houten and Wanders 2010).

The fourth and final step of the β-oxidation cycle is a thiolytic cleavage of the 3-keto-acyl-CoA to produce a two carbon chain shortened acyl-CoA plus an acetyl-CoA molecule. This final step is catalysed by long chain 3-ketoacyl-CoA thiolase (LCKAT) and medium chain 3-ketoacyl-CoA thiolase (MCKAT) (Rinaldo, Matern et al. 2002, Vockley and Whiteman 2002, Moczulski, Majak et al. 2009, Houten and Wanders 2010).

As a result of each complete cycle an acetyl-CoA molecule, a NADH, a $FADH_2$, and the shortened acyl-CoA molecule are formed. The reminiscent acyl-CoA enters another cycle, and so on until the formation of two acetyl-CoA molecules in the last cycle. Acetyl-CoA can have several metabolic fates, including entering Krebs cycle, for complete oxidation

and production of more reducing power (NADH) and ketogenisis. NADH and $FADH_2$ will deliver their electrons to the respiratory chain for ATP production (Houten and Wanders 2010) (figure 5).

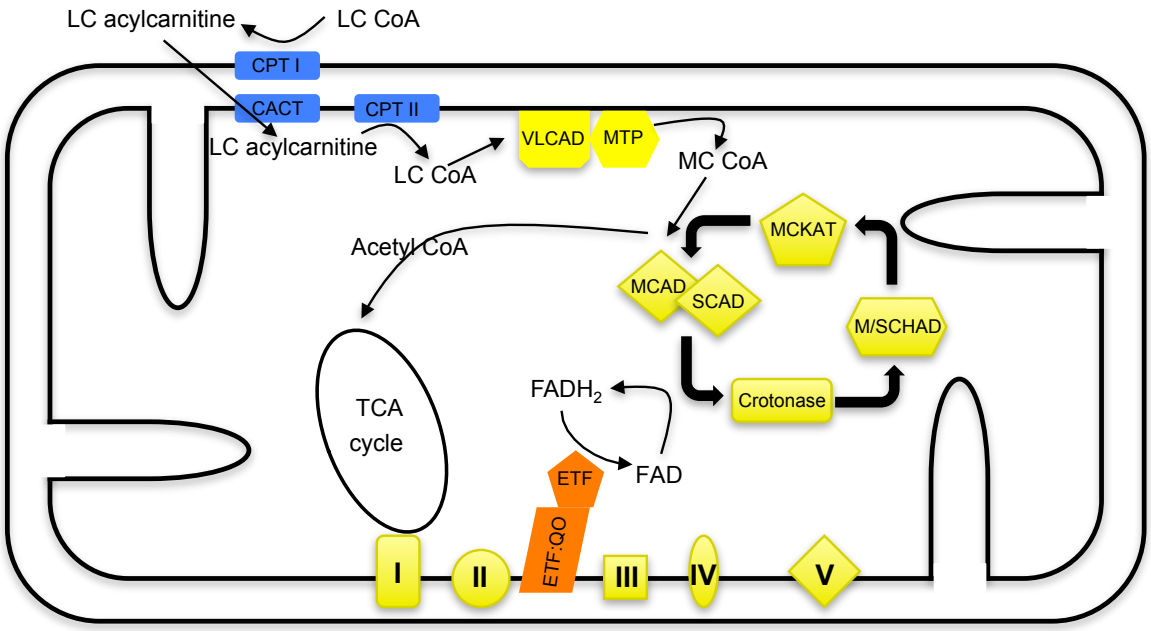

Figure 5: Representation of the relation between mitochondrial fatty acid β-oxidation, Krebs cycle (tricarboxylic acid cycle - TCA) and OXPHOS.
Mitochondrial fatty acid β-oxidation acts in close relation with other mitochondrial pathways in particular Krebs cycle and OXPHOS. NADH and $FADH_2$ produced during the β-oxidation cycles will deliver their electron at complex I and ubiquinone, respectively, for ATP production, while acetyl-CoA can be used as ketogenesis substrate or be fully oxidised at Krebs cycle with further production of NADH/$FADH_2$ molecules.
LC, long chain fatty acids; CoA – coenzyme A; CPT I; carnitine palmitoyl transferase I; CPT II, carnitine palmitoyl transferase II; CACT, carnitine-acylcarnitine translocase; VLCAD; very long chain acyl-CoA dehydrogenase; MTP, mitochondrial trifunctional protein; MC, medium chain fatty acids; MCKAT, medium chain 3-ketoacyl-CoA thiolase; MCAD, medium chain acyl-CoA dehydrogenase; SCAD, short chain acyl-CoA dehydrogenase; M/SCHAD, medium/short chain 3-hydroxyacyl-CoA dehydrogenase; TCA cycle, tricarboxylic acid cycle; ETF, electron transfer flavoprotein; ETF:QO, Electron transfer flavoprotein – ubiquinone oxidoreductase; FAD, flavin adenine dinucleotide; $FADH_2$, flavin adenine dinucleotide – reduced form; I, NADH dehydrogenase; II, succinate dehydrogenase; III, ubiquinone:cytochrome c oxidoreductase; IV, cytochome oxidase; V, ATP synthase.

After reaching the mitochondrial matrix long-chain acyl-CoA's are first metabolised by VLCAD and then mitochondrial trifunctional protein (MTP), both anchored to MIM. MTP

delivers three enzymatic activities: LCHAD, LCEK and LCKAT. MTP has a hetero-octamer structure, consisting in four α-subunits and four β-subunits, encoded by the *HADHA* (OMIM# 600890) and *HADHB* (OMIM# 143450) genes respectively, both located in the same region of chromosome 2p23 (Ushikubo, Aoyama et al. 1996). The α-subunit contains the long-chain enoyl-CoA hydratase (LCEH) and long-chain 3-hydroxyacyl-CoA dehydrogenase activities (LCHAD), while the β-subunit contains the long-chain 3-ketothiolase activity (LCKAT) (Vockley and Whiteman 2002).

After two or three cycles the resulting medium chain acyl-CoA's are metabolised by a group of enzymes, which are believed to be harboured in the matrix: MCAD, SCAD, M/SCHAD, MCKAT and crotonase (Rinaldo, Matern et al. 2002, Houten and Wanders 2010).

FA with an odd number of carbons are degraded in the same way, but the product of the last turn is propionyl-CoA, which is converted in succinyl-CoA that enters the Krebs cycle (Moczulski, Majak et al. 2009). The oxidation of monounsaturated FA requires the intervention of another mitochondrial enzyme, the decenoyl-CoA delta isomerase (3,2-trans-enoyl-CoA isomerase), while for the oxidation of polyunsaturated fatty acids another enzyme is also needed – 2,4-dienoyl-CoA reductase (Vockley and Whiteman 2002).

The resulting NADH molecules will deliver their electrons to the respiratory chain at the complex I (NADH dehydrogenase) level while $FADH_2$ will channel their electrons through the electron transfer flavoprotein complex to ubiquinone (Houten and Wanders 2010). The electron transfer flavoprotein complex is composed by two proteins: electron-transfer-flavoprotein: ubiquinone oxidoreductase (ETF:QO) and electron-transfer-flavoprotein (ETF). ETF is a mitochondrial matrix heterodimer with two subunits (α and β), containing one flavinadenine nucleotide (FAD) and one adenosine monophosphate, per molecule (Roberts, Frerman et al. 1996). ETF:QO is integrated in the MIM and contains one FAD molecule and a 4Fe4S cluster (Simkovic, Degala et al. 2002). These two proteins of the complex act coordinately to efficiently transfer the electrons from at least 11 dehydrogenases to ubiquinone, and recover the pool of FAD molecules inside the mitochondria (Schiff, Froissart et al. 2006).

To complete the mitochondrial β-oxidation of fatty acids, it is necessary the intervention and coordinated action of about 25 different proteins (table 1)

Table 1: Proteins involved in mitochondrial fatty acid oxidation

Metabolic process	Protein	Abbreviation
Fatty acid transport and activation	Fatty acid transporter(s)	FATP(s)
	Acyl-CoA synthetase(s)	---
Carnitine Uptake	Organic cation transporter 2 (plasma membrane carnitine transporter)	OCTN2
Carnitine cycle	Carnitine palmitoyl transferase I (liver)	lCPT I (CPT I)
	Carnitine palmitoyl transferase I (muscle)	mCPT I
	Carnitine palmitoyl transferase I (brain)	bCPT I
	Carnitine palmitoyl transferase II	CPT II
	Carnitine acyl-carnitine translocase	CACT
Mitochondrial β-oxidation spiral	Very long chain acyl-CoA dehydrogenase	VLCAD
	ACAD-9	ACAD-9
	Long chain acyl-CoA dehydrogenase	LCAD
	Medium chain acyl-CoA dehydrogenase	MCAD
	Shot chain acyl-CoA dehydrogenase	SCAD
	Trifunctional protein	MTP
	Long chain 3-hydroxyacyl-CoA dehydrogenase	LCHAD
	Long chain 2-enoyl-CoA hydratase	LCEH
	Long chain 3-ketoacyl-CoA thiolase	LCKAT
	Short chain 2-enoyl-CoA hydratase (crotonase)	SCEH
	Medium/short chain 3-hydroxyacyl-CoA dehydrogenase	M/SCHAD
	Medium chain 3-ketoacyl-CoA thiolase	MCKAT
Enzymes of β-oxidation of unsaturated fats	Long chain Δ^3, Δ^2- noyl-CoA isomerase	---
	Short chain Δ^3, Δ^2- noyl-CoA isomerase	---
	2,4 – dienoyl-CoA reductase	---
Electron transfer	Electron transfer flavoprotein	ETF
	ETF-ubiquinone oxidoreductase	ETF-QO

Although some FAO proteins are associated with/embedded in the MIM, like CPT II, VLCAD or MTP, and others believed to be in the mitochondrial matrix (like for example MCAD and SCAD), for the pathway to work efficiently all players in the sequentially processing of FAO substrates must be spatially organized in the so called FAO metabolome (Gregersen and Olsen 2010). Some hypotheses were raised on the organization of FAO metabolome, but common to all is the need of a close relation

between FAO proteins as well as a tight relation with other mitochondrial pathways, in particular the respiratory chain (Gregersen and Olsen 2010) (figure 6).

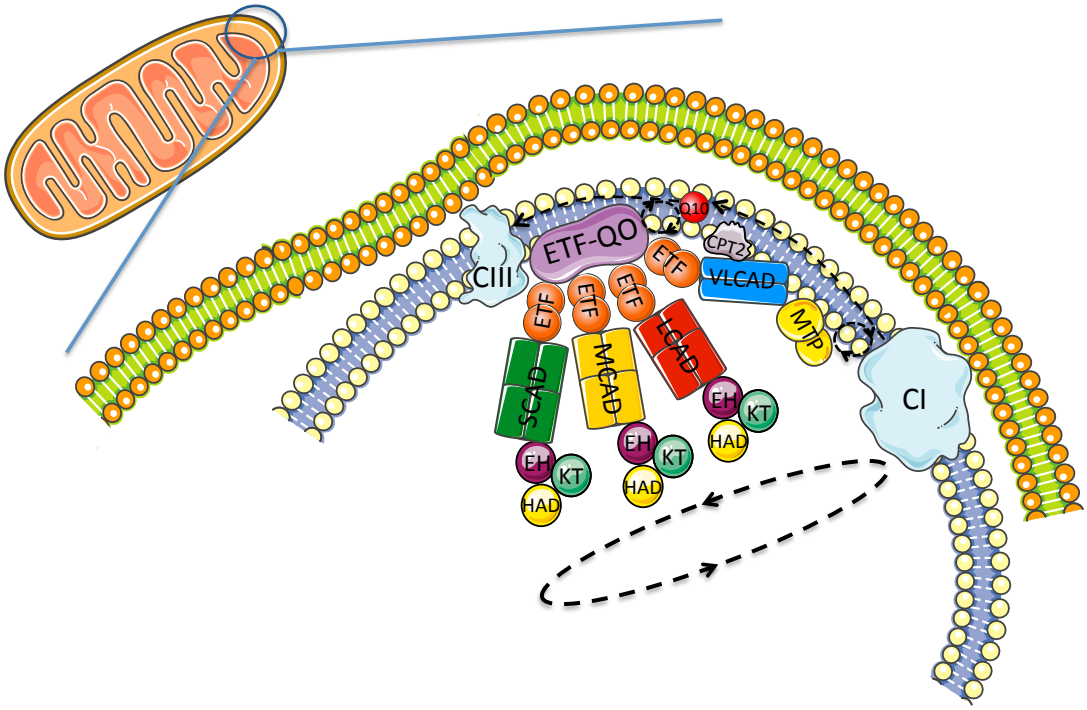

Figure 6: Hypothesis for the structural organisation of the FAO metabolome (adapted from (Gregersen and Olsen 2010))
For the efficient function of mitochondrial fatty acid β-oxidation a close spatial relation between all components is hypothesised. The proposed organization will maximise substrate channelling and pathway efficiency.
CI, NADH dehydrogenase; CIII, ubiquinone:cytochrome c oxidoreductase; CPT 2, carnitine palmitoyl transferase II; Q10, ubiquinone; VLCAD; very long chain acyl-CoA dehydrogenase; MTP, mitochondrial trifunctional protein; LCAD, long chain acyl-CoA dehydrogenase; MCAD, medium chain acyl-CoA dehydrogenase; SCAD, short chain acyl-CoA dehydrogenase; ETF, electron transfer flavoprotein; ETF:QO, Electron transfer flavoprotein – ubiquinone oxidoreductase; EH, enoyl hydratases; KT, 3-keto acyl-CoA thiolases; HAD, 3-hydroxy acyl-CoA dehydrogenases.

Due to the central role of mitochondrial fatty acid β-oxidation on cellular metabolism and to its relations with other metabolic pathways, it is subjected to tight metabolic control.

2.1.4. Regulation of mitochondrial fatty acid β-oxidation

The various tissues are to some extent flexible in the choice of the substrate they will use for energy production. In the majority of the tissues glucose is the first choice in the well-feed state, being the oxidation of fatty acids and ketone bodies more important during fasting. This relationship between the oxidation of glucose and fatty acids is known as the Randle cycle (Hue and Taegtmeyer 2009). Nevertheless, there are tissues that don't follow this logic in terms of fuel utilization. In the muscle the choice of substrate is complex and dependent on the type and duration of exercise. If the exercise is more intense and so more ATP needs to be available in a short period of time, then glucose is the choice, but on the other hand FAO is used at is maximum at moderate exercise intensity (Schulz 1994).

Nevertheless, the main determinant of which substrate oxidase to produce energy is its availability, with hormones playing a key role in the process (Hue and Taegtmeyer 2009). Insulin is secreted by pancreas in response to high plasma glucose concentrations, stimulating those pathways involved in glucose oxidation and storage (ex. glycolysis and glycogenesis), limiting fatty acid oxidation by inhibiting lipolysis. On the other hand, during periods of fasting, hormones like glucagon, adrenaline, noradrenaline and adrenocorticotropic hormone induce lipolysis and fatty acid utilization (Hue and Taegtmeyer 2009).

Free fatty acids (FFA) themselves also have a role in the regulation of the metabolic flux through FAO, but in a long-term perspective, since they affect the transcription of genes encoding for several of the FAO proteins. FFA stimulates the peroxisome proliferator activator receptor (PPAR), a transcription regulator, being the regulation of FAO by PPAR's a subject of intensive research in recent years (Djouadi and Bastin 2008). The relation was first established when Gulick and collaborators (Gulick, Cresci et al. 1994) showed that PPAR could increase the transcription of MCAD. The molecular mechanism was then elucidated; including the identification of the specific DNA sequence which allows binding of the activated PPAR on the promoter of the targeted gene (Gulick, Cresci et al. 1994). Three different isoforms were identified in Humans: PPAR α, PPAR δ and PPAR ϒ. PPAR ϒ is strongly expressed in the adipose tissue regulating the synthesis and storage of FA, but not affecting the enzymes involved in their oxidation (Djouadi and Bastin 2008). PPAR α and PPAR δ were shown to play important roles in FAO regulation in different tissues, regulating the expression of several FAO proteins, with PPAR α having particular importance in regulating energy metabolism in the liver where it is

abundantly expressed (Djouadi and Bastin 2008). But all regulation mechanisms that rely on manipulation of gene transcription are always considered long-term processes. Mechanisms of short-term control of pathways usually are based on the modulation of the activity of key enzymes of the pathways, normally the rate limiting steps.

CPT I is the key control point of FAO (Drynan, Quant et al. 1996). Modulating CPT I activity the amount of acylcarnitines produced will be controlled and, as a consequence, the FA transport to the mitochondria that will regulate the flux through the pathway. CPT I activity is regulated by its inhibitor malonyl-CoA, which binds the enzyme in a binding site that faces the cytoplasm (McGarry and Foster 1980, Saggerson 2008). Malonyl-CoA is not only an intermediate in the pathway of *de novo* fatty acid biosynthesis and fatty acid elongation, but also has important signalling functions through its allosteric inhibition of CPT I (McGarry and Foster 1980, Saggerson 2008). The amount of malonyl-CoA inside the cell reflects the availability of acetyl-CoA, the end product of FAO and the substrate for malonyl-CoA production, but also ATP, since the activity of acetyl-CoA carboxylase requires ATP to convert acetyl-CoA into malonyl-CoA. In this way, cellular availability of acetyl-CoA and ATP will shut down FAO (figure 7).

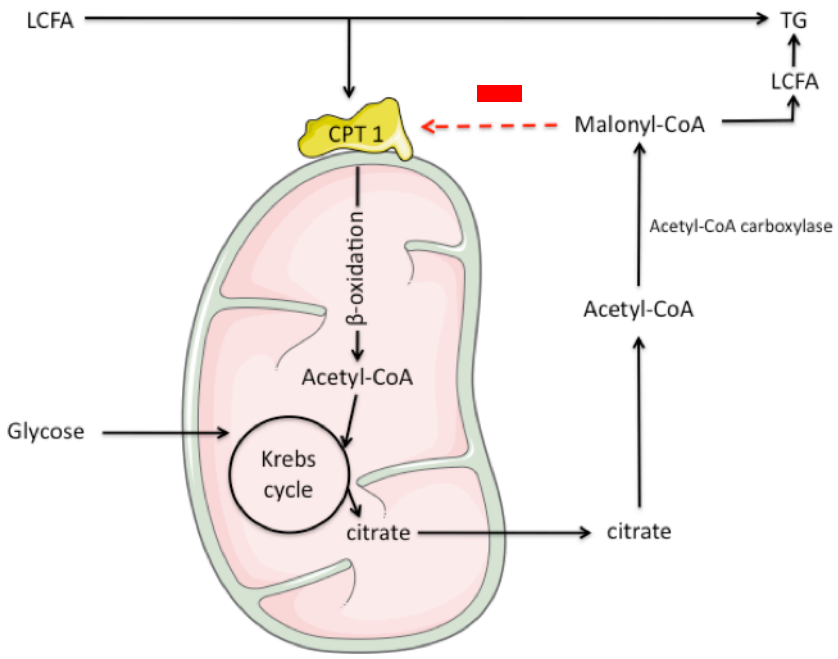

Figure 7: Control effect of malonyl-CoA over CPT1.
The amount of malonyl-CoA represents acetyl-CoA and ATP availability, being a key energy status sensor, and will regulate the metabolic flux through mitochondrial fatty acid β-oxidation by inhibiting CPT 1.
LCFA, long chain fatty acids; TG, triglycerides; CPT 1, carnitine palmitoyl transferase I

Although less important, there are other forms of FAO control, as for example redox control (based on the ratio NAD^+/NADH), feedback control (inhibition of the acyl-CoA dehydrogenases by their products and thiolases by acetyl-CoA) and availability of carnitine and CoA (Eaton 2002).

2.2. Mitochondrial fatty acid β-oxidation disorders

From the about 25 proteins, including enzymes and transport proteins, that must act co-ordinately to complete FAO, deficiencies in many of them are associated to Humans diseases. Mitochondrial fatty acid β-oxidation disorders (FAOD) are a group of inherited metabolic disorders, transmitted in an autosomal recessive pattern, which affect the oxidative metabolism of FA. FAOD are included in the group of diseases of the energetic metabolism, alongside with for example glycogen storage diseases and respiratory chain deficiencies.

FAO defects are known since 1973, when DiMauro described carnitine palmitoyl-CoA transferase II deficiency (DiMauro and DiMauro 1973) and since then several defects affecting the carnitine cycle as well as the acyl-CoA dehydrogenases activities were identified. Nowadays, about 15 mitochondrial FAO defects are known (Rinaldo, Matern et al. 2002, Vockley and Whiteman 2002, Kompare and Rizzo 2008, Moczulski, Majak et al. 2009) (table 2).

Deficient activity of another acyl-CoA dehydrogenase - ACAD 9, has been associated to disease, nevertheless its role in FAO is not fully elucidated (He, Rutledge et al. 2007). It is supposed that it acts as a chaperonin in the oxidative phosphorylation (OXPHOS) complex I, with yet unknown effect of FAO (Haack, Danhauser et al. 2010, Scheffler 2010, Gerards, van den Bosch et al. 2011, He, Pei et al. 2011).

In general, FAOD may present three different clinical presentations. The first one, the more severe and often lethal, has a predominant hepatic presentation that usually appears during infancy or in the neonatal period with severe hypoketotic hypoglycemia and Reye-like syndrome. This clinical presentation is usually triggered by a catabolic state associated for example to infections. The second type of clinical presentation includes the appearance, during infancy, of cardiac symptoms such as dilated or hypertrophic cardiomyopathy and/or arrhythmias. The third and last group includes the patients that present a milder and late on set disease, usually characterised by exercise induced

myopathy and rhabdomyolysis (Wanders, Vreken et al. 1999, Rinaldo, Matern et al. 2002). Some of the severe forms can present a combination of the symptoms presented above. FAOD have also been associated to sudden infant death syndrome (SIDS) (Lundemose, Kolvraa et al. 1997, Lovera, Porta et al. 2012) and maternal liver disease during pregnancy (acute fatty liver in the pregnancy (AFLP) and hemolysis, elevated liver enzymes and low platelets (HELLP) syndrome) (Browning, Levy et al. 2006, Ibdah 2006, Gutierrez Junquera, Balmaseda et al. 2009, Rector and Ibdah 2009).

Table 2: Defects of the mitochondrial fatty acid β-oxidation.

Deficient protein	Gene	Gene locus	First described	OMIM
FATP(s)	----	---	1998(Odaib, Shneider et al. 1998)	600691
OCTN2	*SLC22A5*	5q33	1975(Karpati, Carpenter et al. 1975)	212140
CPT I	*CPT1A*	11q13	1981(Bougneres, Saudubray et al. 1981)	255120
CPT II	*CPT2*	1p32	1973(DiMauro and DiMauro 1973)	25510/600649/ 668836
CACT	*SLC25A2*	3p21	1992(Stanley, Hale et al. 1992)	212138
VLCAD	*ACADVL*	17p11	1993(Bertrand, Largilliere et al. 1993)	201475
MTP	*HADHA*	2p23	1992(Jackson, Kler et al. 1992, Wanders, L et al. 1992)	609015
	HADHB	2p23	---	---
LCHAD (isolated)	*HADHA*	2p23	1989(Wanders, Duran et al. 1989)	609016
LCKAT (isolated)	*HADHB*	2p23	2006(Das, Illsinger et al. 2006)	143450
MCAD	*ACADM*	1p31	1976(Gregersen, Lauritzen et al. 1976)	201450
SCAD	*ACADS*	12q22	1984(Amendt, Greene et al. 1987)	201470
SCHAD	*HADHSC*	4q25	1991(Tein, De Vivo et al. 1991)	231530
MCKAT	---	---	1997(Kamijo, Indo et al. 1997)	602199
2,4 – dienoyl-CoA reductase	*DECR1*	8q21	1990(Roe, Millington et al. 1990)	222745
ETF (MADD)	*ETFA*	15q23	1976(Przyrembel, Wendel et al. 1976)	231680
	ETFB	19q13	---	---
ETF-QO (MADD)	*ETFDH*	4q32	---	---

A block in the FAO pathway usually results in a characteristic biochemical phenotype of hypoketotic hypoglycemia due to the shortage of acetyl-CoA, that is not only the substrate for ketogenisis but also a stimulating factor for pyruvate carboxylase, which will limit gluconeogenesis (Houten and Wanders 2010). Moreover, FAO malfunction will increase glucose oxidation, further contributing for hypoglycemia (Houten and Wanders 2010). However, in some cases, low blood sugar may not become evident until the metabolic crisis is well developed (Roe 2002, Olpin 2004). Another consequence of FAOD is the development of secondary hyperammonaemia, due to the decreasing availability of N-acetylglutamate, compromising the efficiency of the urea cycle (Moczulski, Majak et al. 2009).

In this group of inherited metabolic disorders, the severity of the symptoms covers a wide range that goes from neonatal sudden death to asymptomatic adults and there are overlapping phenotypes between the various enzyme defects. Moreover, the same defective enzyme may be associated with considerable clinical heterogeneity (Sim, Hammond et al. 2002). If not early treated, these disorders usually result in significant morbidity and mortality with some deceasing during acute episodes and those who don't may suffer from irreversible neurological trauma (Kompare and Rizzo 2008).

The main characteristics of the most common FAOD are now presented.

2.2.1 Carnitine Uptake Defect

Carnitine uptake defect (CUD) or primary carnitine deficiency (MIM# 212140), is caused by a defective OCTN2 transporter, and is characterised by carnitine loss due to defective renal reabsorption and depleted tissue levels of carnitine to a point that compromises the transport of long chain FA to the mitochondria (Vockley and Whiteman 2002). Plasma carnitine levels are extremely low or even undetectable in these patients. The clinical presentation can range from undiagnosed, almost asymptomatic, adults (mostly mothers detected through differential diagnosis of abnormal newborn screening results of their sons) (Lee, Tang et al. 2010) to presentations that include a progressive cardiac failure and skeletal muscle weakness. Hypoketotic hypoglycemia and coma may also be seen during periods of catabolic stress, mainly in the first months of life (Rinaldo, Matern et al. 2002, Vockley and Whiteman 2002). Treatment is based on L-carnitine supplementation

in order to restore intracellular carnitine levels, being treatment response very good as well as the clinical outcome (Rinaldo, Matern et al. 2002).

2.2.2 CPT I deficiency

Deficiency in any of the proteins of the mitochondrial carnitine shuttle compromises the transport of long chain FA to the mitochondria. Deficiency in CPT I (MIM# 255120) doesn't allow the formation of long chain acylcarnitines, and so their transport for the mitochondrial matrix. Although CPT I exists in three isoforms in Humans – liver, muscle and brain, only deficiencies in the liver type (CPT Ia) are known to cause disease (Moczulski, Majak et al. 2009). Clinical symptoms are mainly characterised by Reye-like attacks with hypoketotic hypoglycemia, beginning in infancy and multi organ failure. Muscle and cardiac symptoms although rare, have already been reported (Moczulski, Majak et al. 2009). Patients also present hyperammonaemia and very elevated free carnitine in plasma, alongside with very low acylcarnitines, being the most characteristic biochemical feature of this FAOD. Treatment is mainly based on avoiding fasting with frequent feedings, high carbohydrate/low fat diet and supplementation with medium chain triglycerides, since medium chain FA don't require CPT I to enter mitochondria (Kompare and Rizzo 2008).

2.2.3 CACT deficiency

CACT deficiency (MIM# 212138) generally presents with chronic progressive liver disease, servere hypoketotic hypoglycemia and cardiac arrhythmias and/or hypertrophy usually enhanced by intercurrent illness (Bonnet, Martin et al. 1999, Lopriore, Gemke et al. 2001). Hyperammonaemia is in this FAOD more frequent and skeletal myopathy is also a common feature. A few patients with milder phenotypes have been reported and biochemically, patients present low free carnitine and increase of long chain acylcarnitines (Vockley and Whiteman 2002). Treatment is based on avoiding fasting, frequent meals, high carbohydrate/low fat diet and supplemented with medium chain triglycerides (Kompare and Rizzo 2008).

2.2.2. CPT 2 deficiency

CPT II deficiency (MIM# 255110/600649/608836) is one of the most frequent disorders affecting FAO (Kompare and Rizzo 2008). In CPT II deficiency, long chain acylcarnitines are translocated to the mitochondrial matrix, but then they are not hydrolysed to acyl-CoA plus carnitine, compromising its oxidation. The hallmarks of this FAOD are the muscle symptoms that classically present in late childhood or early adulthood as recurrent

episodes of myoglobinuria following prolonged exercise, fasting, high fat intake, fever, viral infection or even emotional stress (Vockley and Whiteman 2002). Rhabdomyolisis can be severe enough to lead to acute renal failure. There is no tendency to hypoglycemia and patients are usually well between episodes. Three phenotypes of different severity can be identified: an adult onset, an infantile and a neonatal form, that are probably due to different levels of residual activity of the deficient enzyme (Moczulski, Majak et al. 2009). While the most common adult forms only have the typical muscular presentation, the infantile form may present with recurrent liver failure, hypoketotic hypoglycemia, leading sometimes to coma. It is a frequent cause of SIDS due to paroxysmal heartbeat and Reye-like syndrome (Fontaine, Briand et al. 1998). The most severe neonatal form present a multiple organ failure and all affected children die shortly after birth (Pollitt 1993). The phenotypic presentation can be highly variable even within the same family (Bonnefont, Demaugre et al. 1999). Biochemically, patients present with low free carnitine and increase of long chain acylcarnitines exactly as CACT patients and diagnosis must be clarified by direct enzyme or molecular analysis (Moczulski, Majak et al. 2009). Treatment depends on the severity of the clinical presentation with infantile forms requiring intravenous glucose during acute episodes. Diet should be based on a high carbohydrate/low fat diet, supplemented with medium chain triglycerides, avoid fasting and vigorous exercise (Kompare and Rizzo 2008).

2.2.5 VLCAD deficiency

VLCAD deficiency (VLCADD; MIM#201475) results in impaired ability to oxidise long-chain fatty acids (Voermans, van Engelen et al. 2006). It is commonly associated with an early onset of cardiac and skeletal myopathy, although hypoketotic hypoglycemia, hyperammonemia and liver failure also occur (Aoyama, Souri et al. 1995). The clinical presentation is then very heterogeneous, with a severe type that has an onset in the neonatal period with hypertrophic cardiomyopathy and hypoketotic hypoglycemia, being often fatal; a late onset infantile form presents with fasting hypoketotic hypoglycemia and lethargy, but without cardiomyopathy; at last a milder late onset form with a debut usually after adolescence, with predominant muscle involvement – exercise induced rhabdomyolysis and myoglobinuria (Doi, Abo et al. 2000, Hoffman, Steiner et al. 2006, Voermans, van Engelen et al. 2006). Treatment includes avoiding fasting, high carbohydrate diet and medium chain triglycerides supplementation when needed (situations of high energy demand) and carnitine supplementation (Kompare and Rizzo 2008).

Biochemically these patients are characterized by an accumulation of long chain acylcarnitines in blood, in particular tetradecenoylcarnitine (C14:1) (Kompare and Rizzo 2008).

2.2.6 MTP deficiencies

The mitochondrial trifunctional protein, an enzymatic complex bound to the mitochondrial inner membrane, catalyzes the last three of the four chain-shortening reactions in the mitochondrial β-oxidation of long chain fatty acids.

Distinct autosomal recessive disorders of fatty acid oxidation are associated to different degrees of MTP malfunction. Two groups first described general MTP deficiency independently in 1992 (Jackson, Kler et al. 1992, Wanders, L et al. 1992), which is defined by reduced activity of all three MTP enzymes and can be caused by a heterogeneous group of mutations in any of the *HADHA* or *HADHB* genes. Besides general MTP deficiency, isolated enzymatic defects were identified, namely LCKAT and LCHAD deficiencies, since no isolated LCEH deficient patient has been identified so far. Isolated LCKAT deficiency has only been reported in very few patients and associated to mutations in *HADHB* gene (Das, Illsinger et al. 2006), but isolated LCHAD deficiency (LCHADD), although rare, is the most common defect of the MTP complex (Rinaldo, Matern et al. 2002). Isolated LCHADD was first described in 1989 (Wanders, Duran et al. 1989) and is biochemically characterized by a reduced LCHAD activity with substantial preservation of the other two MTP enzymatic activities (>60% of the normal)(Olpin, Clark et al. 2005). This fatty acid oxidation pathway block results in the accumulation of long-chain 3-hydroxy fatty acids and their metabolites.

LCHADD is associated to mutations in the *HADHA* gene, in particular to c.1528G>C (p.Glu474Gln), in the exon 15, that is present in 56% (Ibdah, Bennett et al. 1999) to 87%(Ijlst, Ruiter et al. 1996) of the mutated alleles. This common mutation is located in the active site of LCHAD, compromising its activity but not affecting the normal levels of expression of the α-subunit neither the functional structure of the MTP complex, which results in nearly normal activities of LCEH and LCKAT (Barycki, O'Brien et al. 1999, Rector, Payne et al. 2008). Patients homozygous for c.1528G>C have undoubtedly isolated LCHADD deficiency, although patients heterozygous for the common mutation and for other on the α-subunit can have isolated LCHADD or general MTP deficiency, depending on the nature of the second mutation, being patients classification only accessed based on the enzymatic activities measurements (Diekman, Boelen et al. 2013).

Since it was first described in 1989 (Wanders, Duran et al. 1989), LCHADD is recognized as one of the most severe fatty acid oxidation disorders and besides the reduced genetic heterogeneity, due to the occurrence of a very common frequent mutation, LCHADD presents with heterogeneous phenotypes (den Boer, Wanders et al. 2002). Clinical manifestations can vary from early onset cardiomyopathy, hypoketotic hypoglycemia, hepatopathy (sometimes presenting as Reye like syndrome), coma and sudden death, to a later onset with myopathy, progressive neuropathy and pigmentary retinopathy (den Boer, Wanders et al. 2002). Current management relies mainly on fasting avoidance. Generally a low-fat, high carbohydrate diet is instituted alongside with the possibility of medium chain fatty acid supplementation (Spiekerkoetter, Lindner et al. 2009).

The presence of retinopathy is exclusive of MTP deficiencies, among the group of fatty acid oxidation disorders, and it is also documented that women who carry fetus with MTP defects (general or isolated) often develop AFLP and HELLP syndrome (Rector and Ibdah 2009). The severity and the particular features of the clinical presentations of isolated LCHADD are related with the pathomechanisms of this fatty acid oxidation disorder. It is believed that besides the energy deficiency, the toxic accumulation of 3-hydroxy fatty acids (3-hydroxydodecanoic, 3-hydroxytetradecanoic and 3-hydroxypalmitic acids) plays a key role on disease development (Ventura, Ruiter et al. 2005, Bennett 2010, Olpin 2013). These toxic 3-hydroxyacil metabolites are believed to be the cause of retinopathy development and progressive neuropathy (Tein, Vajsar et al. 1999). It was reported that accumulated fatty acids might play a role inducing oxidative stress (Tonin, Ferreira et al. 2010) and compromise OXPHOS activity (Tonin, Amaral et al. 2013). Nevertheless, we can't still explain why LCHADD patients, homozygous for the common mutation, can present so differently with some exhibiting significant morbidity, developing chorioretinopathy and neuropathy while others reach adulthood with minimal retinal changes as the only manifestations of the clinical disease (Spiekerkoetter and Wood 2010, Olpin 2013).

2.2.7. MCAD deficiency

The MCADD (MIM#201450) phenotype ranges from asymptomatic to Reye-like syndrome presentations and sudden death (Leydiker, Neidich et al. 2011, Lovera, Porta et al. 2012). Typical clinical presentation consists of a metabolic crisis, characterized by hypoketotic hypoglycemia, lethargy, coma, seizures or sudden death, and triggered by catabolic stress during fasting or illness (Hoflack, Caruba et al. 2010, Yusupov, Finegold et al. 2010). The disease usually manifests in the first few years, although presentations in

adulthood has also been described (Yang, Ding et al. 2000, Wilcken, Haas et al. 2007). Unusual manifestations, such as neonatal ventricular tachyarrhythmias (Maclean, Rasiah et al. 2005, Rice, Brazelton et al. 2007, Yusuf, Jirapradittha et al. 2010) and pulmonary haemorrhage(Maclean, Rasiah et al. 2005) have also been reported. The risk of neurological impairment after an acute metabolic decompensation is high (Grosse, Khoury et al. 2006). MCAD protein is encoded by the *ACADM* gene, located on chromosome 1p31. More than 80 mutations have been identified in this gene, most of which are missense mutations (Stenson, Ball et al. 2003). Approximately 80% of patients diagnosed clinically are homozygous for the common c.985A>G mutation (Waddell, Wiley et al. 2006, Hsu, Zytkovicz et al. 2008). Patients with the same genotype and belonging to the same family can present very distinct clinical presentations, with the occurrence of asymptomatic adults and SIDS cases within the same family. Biochemically, these patients present an elevation of medium chain acylcarnitines in blood. Treatment is mainly based on avoiding fasting (Kompare and Rizzo 2008).

2.2.8. SCAD deficiency

SCAD deficiency (SCADD; MIM#201470) impairs the last β-oxidation cycles, those where short-chain fatty acids are involved. There is a huge debate on whether this deficiency is really a disease or not (Jethva and Ficicioglu 2008). Clinical symptoms are very heterogeneous ranging from asymptomatic individual (mainly detected in newborn screening programs) to others that present clinically with episodic hypoglycemia with ketosis or with developmental delay. The presence of hypotonia, muscle weakness and seizures has also been reported (Gregersen, Andresen et al. 2001, Gregersen, Andresen et al. 2008, Jethva and Ficicioglu 2008). Biochemically they present an elevation of C4-carnitine in blood and increased ethylmalonic acid in urine. Treatment, when applied, is based on avoidance of fasting in periods of metabolic stress (Kompare and Rizzo 2008).

2.2.9. SCHAD deficiency

Medium and short-chain L-3-hydroxyacyl-CoA dehydrogenase (M/SCHAD, SCHAD) catalyzes the penultimate step in FAO, the NAD^+ dependent conversion of L-3-hydroxyacyl-CoA to 3-ketoacyl-CoA for medium- and short-chain acyl-CoA intermediates (C4-C12). The clinical phenotype of most patients that have been described with SCHAD deficiency (MIM#231530) is recurrent hypoglycemia associated with hyperinsulinism (Clayton 2001, Eaton, Chatziandreou et al. 2003, Molven, Matre et al. 2004). The mechanism of hyperinsulinism has been identified as loss of a non-enzymatic inhibitory effect of the SCHAD protein on glutamate dehydrogenase (GDH) – moonlighting effect. In

the absence of SCHAD protein, this inhibition is lost resulting in gain of activity of GDH and increased release of insulin, similar to that seen in patients with gain of function mutations in GDH (Li, Chen et al. 2010). Treatment includes diazoxide to control insulin secretion (Kompare and Rizzo 2008).

2.2.10. Multiple Acyl-CoA dehydrogenation deficiency

Multiple Acyl-CoA dehydrogenation deficiency, also known as glutaric aciduria type II (MADD; MIM#231680), is an autosomal recessive disorder that affect fatty acids, amino acids and choline metabolism, caused by defects in one of the two flavoproteins – ETF or ETF-QO, or in yet unidentified disturbances of riboflavin metabolism (Vockley and Whiteman 2002). In mitochondria, ETF receives electrons from several mitochondrial flavin-containing dehydrogenases, which are transferred to ETF-QO and subsequently passed to ubiquinone in the respiratory chain (Houten and Wanders 2010). ETF exists in the mitochondrial matrix as a heterodimer of alpha and beta subunits, while ETF-QO is a monomer embedded in the inner mitochondrial membrane (Gregersen and Olsen 2010). A deficiency in either ETF or ETF-QO will result in a secondary malfunction of all the 11 flavoprotein dehydrogenases that use ETF complex to channel the electrons resultants from dehydrogenation reactions to OXPHOS (Watmough and Frerman 2010)

Clinically, MADD patients can be classified into three phenotypic groups: neonatal onset forms, with (type I) or without (type II) congenital abnormalities and late onset forms (type III) (Schiff, Froissart et al. 2006). Neonatal onset forms are characterised by severe nonketotic hypoglicemias, hypotonia, failure to thrive, hyperamonaemia, metabolic acidosis and usually lead to an early death. Patients with late onset forms manifest proximal myopathy, hepatomegaly and encephalopathy usually associated with intermittent vomiting, abdominal pain, hypoglycemia and lethargy (Vockley and Whiteman 2002).

MADD is caused by mutations in the genes *ETFA*, *ETFB* and *ETFDH*, which encode ETF alpha subunit, ETF beta subunit and ETF-QO (Gregersen, Andresen et al. 2001, Olsen, Olpin et al. 2007). It was also observed some degree of genotype/phenotype correlation, with null mutations associated to neonatal onset form, and mutations that lead to the retention of some residual activity of the enzyme, associated to type III phenotypes (Olsen, Andresen et al. 2003, Gregersen, Bross et al. 2004). It was also realised that many of these patients, mainly type III, are responsive to riboflavin (riboflavin responsive

MADD; RR-MADD) treatment, with a significant positive effect on symptoms and metabolic control (Gregersen 1985).

For many years it was believed that the riboflavin responsive form of the disease was due to an inborn error affecting FAD cofactor formation from riboflavin (vitamin B2) (Gregersen, Wintzensen et al. 1982, Rhead, Roettger et al. 1993). Only when Olsen and collaborators, in 2007, reported that the majority of patients have molecular lesions on ETFDH gene, it became clear that this is the main cause of RR-MADD (Olsen, Olpin et al. 2007). All RR-MADD patients have at least one missense mutation on ETFDH gene, on or near the FAD – binding or ubiquinone-binding domains (Cornelius, Frerman et al. 2012). Nevertheless, very recently, genetic defects affecting riboflavin metabolism and transport were identified in a few RR-MADD patients (Green, Wiseman et al. 2010, Johnson, Gibbs et al. 2010, Bosch, Abeling et al. 2011, Ho, Yonezawa et al. 2011)

The mechanisms underlying riboflavin responsiveness in RR-MADD patients with ETFDH mutations, only very recently were described (Cornelius, Frerman et al. 2012). It was demonstrated that riboflavin response results from the ability of the FAD to promote the folding of the variant protein, stabilize their mature protein or folding intermediates (Cornelius, Frerman et al. 2012). MADD treatment is based on a fat restricted diet, sometimes with supplementation with coenzyme Q_{10} and riboflavin.

One important data to evaluate the health impact of a disorders or a group of disorders in a given population is its prevalence. Given the difficulties in calculating accurate epidemiological data based on symptomatic diagnosed patients, assessment of the true birth prevalence of FAOD is only possible through NBS data.

The knowledge on the birth prevalence of FAOD in a defined population is important so follow-up and public health policies can be properly defined and implemented. More robust data still require for some European populations, namely Iberia, where the only publication is from 2010, reporting the data from the screening of about 300000 Portuguese newborns and where FAO present a birth prevalence of 1:6325 (Vilarinho, Rocha et al. 2010).

2.3. Pathophysiology of mitochondrial fatty acid β-oxidation disorders

FAOD present a wide clinical phenotype spectrum that results from the interaction between genetic determinants and environmental factors, which act together towards the phenotype. Realising how all these players interact is the key to better understand this group of disorders and ultimately to the development of new and more effective treatment approaches. In this way, disclosing the pathophysiology of FAOD as well as molecular mechanisms underlying the observed clinical variability has gained importance in the last years, supported by innovative technological developments.

2.3.1 Phenotype determinants

Since the advances of molecular biology, in late 80's, and the discovery of a growing number of genes in the 90's, the study of the relationship between genotypes and phenotypes in genetic diseases become a main goal for the genetic community, in order to elucidate the pathophysiology and so predict the clinical outcome and improve treatment and diagnosis. Inborn errors of metabolism and more precisely FAOD were not an exception. Soon was realized that the initial naive idea that genetic information was the key answer to all questions, was an oversimplification of the system. The effect of genetic mutations and their interaction with other genes and other cellular/environmental factors was shown not to be straightforward in all situations. Nevertheless, it was possible to establish, for some genetic disorders some degree of correlation between the mutation and phenotype, with some examples between FAOD.

For some FAOD, namely CPT2, VLCADD and MADD, it is possible to establish a certain degree of relation between the nature of the molecular lesion, the residual enzymatic activity and the clinical phenotype. Complete enzymatic deficiencies, associated to severe mutations (nonsense, frameshift and splice site mutation resulting in mRNA degradation and protein absence) are associated with severe clinical disease while some missense mutations and small in frame deletions and insertions were associated to milder clinical presentations (Andresen, Olpin et al. 1999, Gregersen, Andresen et al. 2001, Olpin, Afifi et al. 2003, Olsen, Andresen et al. 2003). On the contrary, on FAOD affecting the oxidation of medium/short chain FA (MCADD and SCADD) it is not possible to establish any genotype/phenotype correlation (Gregersen, Andresen et al. 2001, Gregersen, Andresen et al. 2008, Arnold, Saavedra-Matiz et al. 2010). Even in the disorders in which it is possible to establish a correlation between the genotype and the phenotype it is not

possible to justify some of the differences observed between individual with milder forms (Olpin, Afifi et al. 2003).

Mutations in another genes coding to related proteins (from the same pathway or at least related to the deficient protein) have the power to modulate phenotypic expression of the disease. Supporting this idea is the concept of “synergistic heterozygocity”. Synergistic heterozygocity relies on the hypothesis that individuals that are heterozygous carriers for mutations in multiple genes coding for proteins in the same metabolic pathway or functionally related pathways, have a cumulative effect that cause a physiologically relevant reduction of the flux through the metabolic pathway (Vockley, Rinaldo et al. 2000, Vockley 2008, Zschocke 2008). There are reported cases of CPT2 carriers that present clinical symptoms, and in some of these it was demonstrated the presence of mutation(s) in another related genes (Vladutiu, Bennett et al. 2000, Vockley, Rinaldo et al. 2000, Vladutiu 2001, Vladutiu, Bennett et al. 2002).

So, phenotypic variability can, to some extent, be justified by the genotype, but many questions remain unsolved, namely those related to the interaction between genetic, epigenetic and environmental factors.

Energy depletion as a result of a FAO blockage is the most well known determinant of disease phenotype, but it is far from being the only one. Biochemical consequences of a FAOD can be grouped in six different categories (adapted from Olpin, 2013 (Olpin 2013)):

1-Inadequate supply of energy

In order to understand the pathophysiology of FAOD it is important not to forget the key importance of this metabolic pathway in energy production, where it participates in about 80% of ATP production during fasting (Olpin 2013). Deficient energy supply, namely during periods of high demand (as fasting, febrile illness, gastrointestinal illness, cold exposure or muscular exertion) is of major importance for triggering symptom development, reflecting the clinical signs tissue needs at the time of the metabolic stress. This way, in FAOD, when energy restriction is due to fasting, hepatic function will most probably be affected with less impact on skeletal and cardiac muscle function. On the other hand, if the stressor is exercise it is most likely to have an effect on muscles and myopatic signs are expected (Bennett 2010). It is believed that energy deficiency will have more impact in FAOD affecting the oxidation of long chain FA than in those affecting medium and short chain FA, because in the last ones there is a partial oxidation of long chain FA that will result in some energy production (Bennett 2010).

In the fasting liver, gluconeogenesis and ketogenesis are stimulated to provide energy for both hepatic and extra hepatic tissues. In the presence of a FAOD, there is a decreased availability of acetyl-CoA, $NADH+H^+$ and ATP that will sustain glucose and ketone bodies production, conducing to hypoketotic hypoglycemia. Another consequence of the decreased availability of acetyl-CoA and ATP is hyperammonaemia. In the myocardium, that even in the feed state relies mainly on the oxidation of FA to get energy, FAO blockage conducte to an alternative use of glucose that will lead to a profound, but poorly understood, remodelling that results in the hypertrophy of the myocardium (Ritchie and Delbridge 2006). In the skeletal muscle, decrease of FAO will result in hypotonia, muscle weakness and exercise intolerance (Olpin 2013).

2-Accumulation of toxic metabolites

Defects in the FAO pathway result in the accumulation of several intermediates from the pathway. These intermediates can be toxic by themselves or further metabolised to toxic derivates (Olpin 2013).

In MCADD, octanoyl-CoA has been reported to illicit oxidative damage, reduce glutathione reserves and inhibit cytochrome c activity (Schuck, Ferreira Gda et al. 2009); octanoic acid leads to inhibition of choroid plexus organic anion transport(Kim, Roe et al. 1992); decanoic acid accumulation results in uncouple OXPHOS (Schuck, Ferreira et al. 2009) and inhibition of complexes I-III, II-III and IV in rat liver (Scaini, Simon et al. 2012) while cis-4-decanoic acid uncouple OXPHOS in rat brain (Schuck, Ferreira Gda et al. 2010).

The accumulation of long-chain acylcarnitines observed in CPT2, CACT and VLCADD, has the potential to inhibit n-acetylglutamate synthase (Mak, Kramer et al. 1986), contribute to Reactive Oxidative Species (ROS) formation, cause lipid peroxidation (that can cause cardiac arrhythmias) (Sparagna, Hickson-Bick et al. 2000). Also, accumulated long chain acyl-CoA's present toxicity by causing the inhibition of OXPHOS (Ventura, Tavares de Almeida et al. 2007) and of the ATP/ADP carrier (Ventura, Ruiter et al. 2005).

The best known example of toxic effects of accumulated metabolites in FAOD, are those associated to long-chain 3-hydroxy acylcarnitines and long-chain 3-hydroxy acyl-CoA's that accumulate in MTP/LCHADD. They are the cause of the neuropathy and retinopathy that characterise these FAOD's. Moreover 3-hydroxydodecanoic acid might interfere with Docosahexaenoic acid (DHA) metabolism in retinal pigment epithelium/neural membrane (Tein, Vajsar et al. 1999), and 3-hydroxytetradecanoic acid can uncouple OXPHOS (Tyni, Pourfarzam et al. 2002).

In MADD the accumulation of short, medium and long chain fatty acids is thought to be one of the ROS sources observed in this FAOD (Scaini, Simon et al. 2012). It is important to highlight that the accumulation of toxic metabolites in FAOD has the power to induce mitochondrial dysfunction and ROS generation. This is of particular relevance, because oxidative stress is for long related to cell signalling, survival and apoptosis being extensively associated to disease development (Hamanaka and Chandel 2010).

3-Sequestration of vital components

FAO blockage will result in the shortage of CoA, due to excess formation of acyl-CoA intermediates. As the mitochondrial pool of CoA is finite, this compromises several metabolic processes where CoA is involved.

Another consequence of FAOD's (with exception of CPT1) is the decreased availability of carnitine, which results in a diminished free carnitine plasma concentration. In cases of very pronounced carnitine depletion the transport of FA into mitochondria is compromised, not allowing their oxidation. This is the basis of the phenotype developed in CUD. Carnitine is also important as a detoxification element, which facilitates the removal of unmetabolised acyl groups from the mitochondria, avoiding their accumulation and contributing to the rescue of CoA (Olpin 2013). For these reasons carnitine depletion may contribute to disease development.

4-Altered enzyme product

In MTP/LCHAD defects the occurrence of acute respiratory distress syndrome (ARDS) has been reported (Lundy, Shield et al. 2003, Olpin, Clark et al. 2005). It is believed that mitochondrial dysfunction and surfactant abnormalities are the mechanisms underlying ARDS occurrence in MTP/LCHAD deficiencies (Suhrie, Karunanidhi et al. 2011). It was proposed that accumulated fatty acid derivatives might alter the phospholipids of the surfactant, impairing its function. Another hypothesis is that as palmitoylmyristoylphosphatidylcholine is a component of surfactant, fatty acid shortening is probably needed for its formation (Olpin 2013).

5-Loss of protein/protein interaction

The best-documented example of protein/protein loss due to a FAOD is SCHADD. In this case the absence of SCHAD protein will conduce to the loss of its inhibitory effect over glutamate dehydrogenase, increasing its activity, which results in insulin overproduction (Li, Chen et al. 2010). Nevertheless, several protein interactions in the mitochondria have

been hypothesised (Gregersen and Olsen 2010), being expected the discovery and characterisation of more protein/protein interactions in FAOD in a near future.

6-Accumulation of misfolded proteins

The majority of mutations associated to FAOD are missense mutations (approximately two thirds) (Gregersen and Olsen 2010), that have the potential to not abolish mRNA expression/stability neither polypeptide biosynthesis, resulting in polypeptide with an abnormal conformation due to misfolding (Gregersen, Bross et al. 2006, Gregersen, Andresen et al. 2008, Gregersen and Olsen 2010). Besides missense mutations in exons, that alter aminoacids, some small in-frame deletions and insertions that result in additions or suppressions of one or more aminoacids can also be associated to protein misfolding (Gregersen and Olsen 2010).

When misfolded proteins accumulate inside mitochondria (and for this to occur is important that the mutation doesn't disrupt mitochondria leader sequence neither occur at exome splicing enhancer/silencers sites), they can undergo two distinct processes: degradation by the mitochondrial proteases that form the mitochondrial protein quality control system (mtPQC), or formation of protein aggregates (Pedersen, Bross et al. 2003, Pedersen, Kolvraa et al. 2008). In any of these processes mtPQC plays a key role since it is involved in the supervision of protein folding, counteracting aggregation and eliminating misfolded peptide chains before they can exert toxic effect, being this protecting ability dependent on internal and external factors (Gregersen, Bross et al. 2006).

As consequence of a mutation that results in a variant misfolded protein, a loss of function will occur and will be noticed by a decrease of enzymatic activity, which is dependent on the nature of the mutation and other cellular/environmental determinants (as temperature or capacity of the mtPQC system). The accumulation of this misfolded protein results in the gain of function, that alongside with loss of the original function, will contribute to cellular dysfunction and disease phenotype (Gregersen, Bross et al. 2006, Gregersen and Olsen 2010).

Several studies have related protein misfolding with the pathogenesis of FAOD. For example in MCADD many of the missense mutations found in the *ACADM* gene give origin to misfolded proteins (Maier, Gersting et al. 2009). In this disorder the highest levels of actanoilcarnitine are associated with the common missesse mutation p.Lys329Glu (c.985A>G), while in patients with other mutations levels are lower (Giak Sim, Carpenter et al. 2002, Maier, Liebl et al. 2005). It was also noticed that patients homozygous for the

common missense mutation present a high variability in the clinical phenotype, that ranges from a asymptomatic patients to others that present fatal attacks (Gregersen, Andresen et al. 2008). These two observations raised the hypothesis that the common missense mutation c.985A>G could result in a variable toxic gain of function (Gregersen, Andresen et al. 2008). It has been shown that the variant MCAD protein, due to the common mutation, is subject to misfolding (Bross, Andresen et al. 1993) and that its accumulation was temperature sensitive (Bross, Jespersen et al. 1995), being this a possible explanation for the clinical picture associated to febrile illness.

Another FAOD where misfolding seems to play an important role in disease development is SCADD. Pathophysiological relevance of the genetic variations in *ACADS* gene stills on debate, as the clinical significance of the disease itself (Jethva and Ficicioglu 2008, Pedersen, Kolvraa et al. 2008). Nevertheless, studies of *ACADS* variants (that strangely are mostly caused by missense mutations, for which so far there is no definitive justification (Gregersen, Andresen et al. 2008)) showed that some conduct to the accumulation of misfolded proteins, resulting on mitochondrial fission and oxidative stress in some conditions (Schmidt, Corydon et al. 2010, Schmidt, Corydon et al. 2010).

The fate of misfolded proteins depends on the nature of the gene variation, other genetic factors as well as cellular and environmental conditioners (Gregersen, Andresen et al. 2008), with this complex relationships influencing and inducing variability in the genotype/phenotype relationship. Considering the actual knowledge, some cases of FAOD can be included in the group of conformational protein misfolded diseases.

2.3.2 Oxidative stress and FAOD

Accumulation of toxic metabolites and misfolded proteins are known to cause oxidative stress, being its participation on cell signalling and survival extensively explored and subject for numerous publications (Bolisetty and Jaimes 2013). Considering the known effects of oxidative stress in the pathophysiology of several disorders it is supposed that it also plays an important role on FAO disease development (Schmidt, Corydon et al. 2010, Olsen, Cornelius et al. 2013).

It was back in 1984 when free radicals were described as “any species capable of independent existence that contains one or more impaired electrons” (Halliwell and Gutteridge 1984). The term ROS refers to a variety of reactive molecules derived from oxygen and can be free radical (superoxie – O_2^-), hydroxyl radical (OH) or non radicals as hydrogen peroxide (H_2O_2). On the other hand Reactive Nitrogen Species (RNS) are

derived from nitrogen and can be classified into ions (peroxynitrite – $ONOO^-$) or non-ions (nitric oxide – NO) (Bolisetty and Jaimes 2013).

Mitochondria is the main source of ROS in the cell, that are mainly produced as a consequence of electron leakage during the normal activity of the OXPHOS, being a side product of respiration (Turrens 2003, Murphy 2009). The main points of electron leak, in the electron transport chain are complex I (NADH ubiquinone oxidoreductase), complex II (succinate dehydrogenase) and complex III (ubiquinol cytochrome c reductase), and they will prematurely reduce oxygen and give origin to superoxide (Turrens 2003, Murphy 2009). Another point of ROS production in mitochondria, with particular interest for FAOD is ETF complex (Rodrigues and Gomes 2012, Olsen, Cornelius et al. 2013). Other enzymes like glycerol-3-phospate dehydrogenase, monoamine oxidase and diidrolipoamide dehydrogenase are also sites for ROS generation, but to a less extent (Drahota, Chowdhury et al. 2002, Maurel, Hernandez et al. 2003, Miwa, St-Pierre et al. 2003, Tretter and Adam-Vizi 2004, Seifert, Estey et al. 2010).

Considering that low levels of superoxide are constantly produced during normal mitochondrial activity there are several pathways involved in detoxification of this ion. Cellular antioxidants, particularly mitochondrial antioxidants, can be divided into two groups: the enzymatic and the non-enzymatic ones. From the enzymatic group the most important is manganese superoxide dismutase (MnSOD) a mitochondrial matrix enzyme that catalyses the conversion of superoxide into hydrogen peroxide. Hydrogen peroxide is then converted to water by the action of catalase, glutathione peroxidase and peroxiredoxins. In the group of the non-enzymatic antioxidants are for example glutathione, ascorbic acid and α-tocopherol (Bolisetty and Jaimes 2013).

Increased ROS generation as a consequence of mutations in proteins at the sites of ROS production (eg. MADD) (Rodrigues and Gomes 2012) or by secondary affection of the normal OXPHOS/mitochondrial function, will trigger a cascade of signalling pathways involved in inflammation, apoptosis, DNA repair, proliferation and cell cycle arrest (Bolisetty and Jaimes 2013). ROS also induces damage to mitochondria structures, like proteins and lipids, compromising its function (Bolisetty and Jaimes 2013). ROS are not only damaging to the mitochondria/cell, being also very important in signalling (mostly H_2O_2), namely in stress signalling and cell survival response (Hamanaka and Chandel 2010, Olsen, Cornelius et al. 2013).

ROS increase can be subdivided into two classes: a milder increase that induces autophagy (or mitophagy), acting as a survival mechanism eliminating damaged structures; and higher ROS levels that alter signalling pathways to induce autophagic or apoptotic cell death(Chen, McMillan-Ward et al. 2008, Nishida, Yamaguchi et al. 2008). (figure 8).

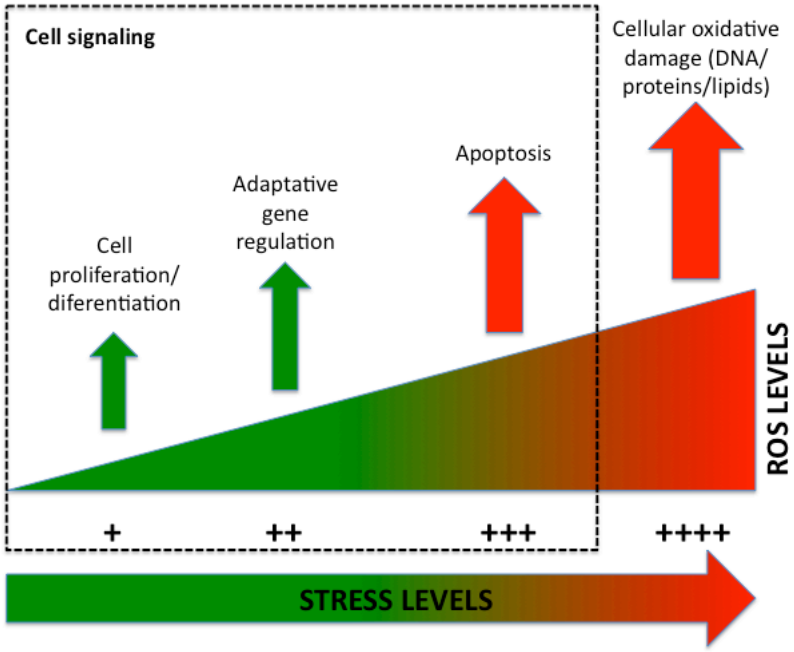

Figure 8: ROS levels are crucial for biological outcome (adapted from (Hamanaka and Chandel 2010)).
Low ROS levels are essential for cellular processes such as cell proliferation or differentiation. ROS production will result in adaptive programs for cell survival as the trigger of antioxidant defences. Higher ROS levels will initiate senescence and apoptosis while very high ROS will result in a non-signalling, irreversible damage to cellular components. ROS, Reactive Oxygen Species.

Besides the almost certain involvement of ROS in mitochondrial and cellular dysfunction in FAOD, the exact mechanisms by which ROS are produced and the consequences of its increase on phenotype still need to be addressed.

2.4. Laboratory approach to the diagnosis of fatty acid oxidation disorders.

During many years the state of the art in the diagnosis of FAOD was the analysis of the organic acids excretion in urine and the measurement of total and free carnitine in blood. Organic acids analysis allows the detection of dicarboxilic aciduria (high excretion of adipic, suberic and sebacic acids) produced as a result of a β-oxidation block (Hoffmann and Feyh 2003). Dicarboxilic aciduria is a normal finding in healthy children as a response to fasting, but here with ketosis (in FAOD the sum of dicarboxilis acids is higher than the sum of the ketone bodies). In the organic acids analysis is also possible to detect more specific glycine conjugates formed as consequence of FAOD (ex. hexanoylglycine in MCAD deficiency) (Hoffmann and Feyh 2003). The problem with this approach was the poor specificity and sensitivity to detect FAOD, with organic acids profiles looking normal between episodes. Nevertheless, combining the information from the organic acids analysis with the clinical history and enzymatic activity measurements it was possible to diagnose of at least the most severe forms of FAOD.

This scenario only changed in the 90's with the advances in mass spectrometry, more precisely in tandem mass spectrometry (MS/MS), with a significant cost reduction and technical developments that conducted to a more reliable and easy operation This new generation of MS/MS analysis allows the quantification of acylcarnitines in several body fluids, in a way they could be progressively introduced in metabolic laboratories. The sensitivity and specificity of acylcarnitine analysis in blood (where free carnitine and many acyl-conjugates are quantified) in the diagnosis of FAOD is much higher than those previously delivered by organic acid analysis in urine, namely in the inter crises periods.

The development of a new, more specific and sensitive method adapted to high throughput alongside with treatment efficacy in many of the FAOD, made this group of metabolic disorders a key target for Newborn Screening (NBS) programs. Since the publications of Millington in the 90's (Millington, Kodo et al. 1990, Van Hove, Zhang et al. 1993) that NBS programs all over the world have been introducing MS/MS in their daily practice, and nowadays the screening for FAOD is a reality in almost every developed country (Bodamer, Hoffmann et al. 2007).

Acylcarnitine analysis and more precisely acylcarnitine analysis in blood spots as a NBS practice, completely changed the diagnostic approach of FAOD and revealed a new set of questions and a new reality in the natural history of this group of disorders. First, the combination of a more sensitive approach with NBS busted the number of patients with FAOD diagnoses. When disease incidence before and after NBS are compared, for some FAOD they clearly double (Wilcken, Haas et al. 2007). Secondly, the follow-up of the

patients detected by NBS revealed that some of them remain asymptomatic through life, and that their genotypes were different from those detected clinically (eg. MCADD) (Andresen, Dobrowolski et al. 2001, Andresen, Lund et al. 2012). So, the increased number of patients detected through NBS is due not only to the detection of severe forms that most probably died in the neonatal period without diagnosis, but also due to an increased sensitivity that allowed the detection of milder forms, in patients that would probably remain asymptomatic through life. Thirdly, very differently clinical progressions were observed in patients with the same genotype. This, alongside with continuing clinical and pathophysiological research, raised some new questions on the factors contributing to disease development in FAOD, some of which were clearly addressed by Gregersen and collaborators (Gregersen, Andresen et al. 2008). In this paper, the highlighted questions were: why 80% of symptomatic patients with MCAD deficiency are homozygous for the prevalent c.985A>G whereas this is found only in about 50% of the newborns detected by NBS?; What is the connection between variations in *ETFDH* gene in RR-MADD, and the observed deficiency of a number of different mitochondrial dehydrogenases as well as deficiency of FAD and Coenzyme Q_{10}?; In SCAD deficiency, are *ACDS* gene variations disease-associated, especially combined with other genetic/cellular/environmental factors that may act synergistically? (Gregersen, Andresen et al. 2008)

These and many other questions can be raised on FAOD, but are almost all related to the understanding of the mechanisms by which factors like the nature of the mutation, interaction with other genetic factors and interaction with cellular, environmental conditions and stressors, influence the phenotype at the protein, cellular and clinical level. Until now, most proposed theories are mainly speculative with little supporting experimental evidence, with little sustained knowledge on its pathophysiology, above all at a cellular level (Gregersen, Andresen et al. 2008, Olpin 2013)

3. Aims of the study

The general goals of this work are to better understand the epidemiology of FAOD in Portugal and Iberia as well as to increase the knowledge on the way mitochondrial adapts and responds to a blockage on fatty acid oxidation. To accomplish the second one, a global proteomic approach was used, since it gives us with a broad perspective on mitochondrial adaptation.

Five specific aims were defined:

1. Characterise epidemiological parameters of FAOD in Portugal and in Iberia, to better understand their impact in health (study 1 and study 2);

2. Compare different experimental approaches for the characterization of the mitochondrial proteome from Human fibroblasts, envisioning the characterisation of mitochondrial adaptation to FAOD (study 3);

3. Characterization of mitochondrial proteome adaptation to a severe defect of ETF-QO (study 4);

4. Evaluate the mitochondrial proteome adaptation to a defect in LCHAD (study 5);

5. Compare the mitochondrial response to severe and mild defects of ETF-QO (study 6);

List of original research papers

Study 1 – Rocha H, Castiñeras D, Pecellin CD, Mellado J, Yahyaoui R, González Y, Sánches M, Gallego I, Rueda I, Varas L, Vilarinho L and Cocho J (2014). "Birth prevalence of fatty acid β-oxidation disorders in Iberia". *J Inherit Metab Dis Reports* (accepted for publication).

Study 2 – Couce ML, Sánchez-Pinto P, Diogo L, Leão-Teles E, Martins E, Santos H, Bueno M, Pecellín C, Castiñeras C, Cocho J, Villoria J, Ribes A, Fraga J and Rocha H (2013). "Newborn screening for medium-chain acyl-CoA dehydrogenase deficiency: regional experience and high incidence of carnitine deficiency". *Orphanet J Rare Dis* **8**:102

Study 3 – Ferreira R, Rocha H, Almeida V, Padrão A, Santa C, Vilarinho L, Amado F and Vitorino R (2013). “Mitochondrial proteome profiling: A comparative analysis between gel- and gel-free approaches”. *Talanta* **115**:277-83.

Study 4 – Rocha H, Ferreira R, Carvalho J, Vitorino R, Santa C, Lopes L, Gregersen N, Vilarinho L and Amado F (2011). “Characterization of mitochondrial proteome in a severe case of ETF-QO deficiency” *J Proteomics* **75**: 221-228.

Study 5 – Rocha H, Ferreira R, AlmeidaV, Vitorino R, Lopes L, Martins E, Nogueira C, Leão-Teles E, Amado F and Vilarinho L “Unravelling the impact of long-chain 3-hydroxyacyl-CoA dehydrogenase deficiency on mitochondrial proteome” (submitted for publication).

CHAPTER II

Study 1 - Birth prevalence of fatty acid β-oxidation disorders in Iberia.

(Accepted for publication on Journal of Inherited Metabolic Disease -Reports)

Birth prevalence of fatty acid β-oxidation disorders in Iberia

Hugo Rocha[1], Daisy Castiñeiras[2], Carmen Delgado[3], José Egea[4], Raquel Yahyaoui[5], Yolanda González[6], Manuel Conde[3], Inmaculada González[4], Inmaculada Rueda[5],Luis Rello[6], Laura Vilarinho[1] and José Cocho[2].

1 – Newborn Screening, Metabolism and Genetics Unit - Genetics Department, National Institute of Health Ricardo Jorge, Porto, Portugal.
2 – Hospital Clínico Universitario, Santiago de Compostela, Spain;
3 – Unidad de Metabolopatías del Hospital Universitario Virgen del Rocio, Seville, Spain;
4 – Laboratorio de Metabolopatías, Centro de Bioquímica y Genetica Clínica, H.U. Virgen de la Arrixaca, Murcia, Spain
5 – Laboratorio de Metabolopatías, Carlos Haya University Hospital, Málaga, Spain
6 – Unidad de Metabolopatías, Servicio de Bioquimica Clínica, Hospital Universitario Miguel Servet, Zaragoza, Spain

Correspondence to:

Hugo Rocha
Newborn Screening, Metabolism and Genetics Unit - Genetics Department
National Institute of Health Ricardo Jorge
Rua Alexandre Herculano, 321; 4000-055 Porto, Portugal.
Phone: +351 223401100
Phone (direct): +351 223401150
Fax: +351 223401109
email: hugo.rocha@insa.min-saude.pt

Abstract

Mitochondrial fatty acid β-oxidation disorders (FAOD) are main targets for newborn screening (NBS) programs, which are excellent data sources for accurate estimations of disease birth's prevalence. Epidemiological data is of key importance for the understanding of the natural history of the disorders as well as to define more effective public health strategies. In order to estimate FAOD birth prevalence in Iberia, the authors collected data from six NBS programs from Portugal and Spain, encompassing the screening of more than 1.6 million newborns by tandem mass spectrometry (MS/MS), and compare it with available data from other populations. The participating NBS programs are responsible for the screening of about 46% of all Iberian newborns. Data reveals that Iberia has one of the highest FAOD prevalence in Europe (1:7,914) and that Portugal has the highest birth prevalence of FAOD reported so far (1:6,351), strongly influenced by the high prevalence of medium-chain acyl-CoA dehydrogenase deficiency (MCADD; 1:8,380), one of the highest ever reported. This is justified by the fact that more than 90% of Portuguese MCADD patients are of Gypsy origin, a community characterized by high inbreeding. From the comparative analysis of various populations with comparable data other differences emerge, what points to the existence of significant variations in FAOD prevalence's among different populations, but without any clear European variation pattern. Considering that FAOD are one of the justifications for MS/MS NBS, the birth prevalence's now estimated stress the need to screen all Iberian newborns for this group of inherited metabolic disorders.

Introduction

Mitochondrial fatty acid β-oxidation is a key metabolic pathway to the provision of energy for the organism, particularly during periods of fasting and metabolic stress (Bartlett and Eaton 2004; Houten and Wanders 2010). To carry out the process, at least 25 enzymes and specific transport proteins are involved and defects in many of them are associated with human diseases (Kompare and Rizzo 2008; Houten and Wanders 2010).

Fatty acid oxidation defects (FAOD) are a group of inherited metabolic disorders that present with heterogeneous clinical phenotypes mainly affecting heart, liver and skeletal muscles (Kompare and Rizzo 2008). Some patients present with the full spectrum and multisystemic disease, while others may stay asymptomatic and only exhibit hypoketotic hypoglycemia during illness or periods of rhabdomyolysis due to vigorous exercise (Wilcken 2010). Presumed pathophysiology of FAOD is supposed to rely mainly on inadequate energy supply, on the toxicity of accumulated metabolites or mutated proteins, and in some cases carnitine depletion. Pathophysiological threshold of some of these factors can be triggered by external factors like insufficient caloric intake, diet changes or infections (Olpin 2013).

Treatment options includes avoiding fasting, that in some cases complemented with carnitine, riboflavin or CoQ10 supplementation (Spiekerkoetter, Bastin et al. 2010) and leads in most cases to favourable prognosis following diagnosis, being FAOD associated with high mortality/morbidity rates for those diagnosed later in a symptomatic phase (Baruteau, Sachs et al. 2012). The effectiveness of available treatments for most of FAOD patients, the availability of high throughput adapted tests

(acylcarnitine analysis on dried blood spots) and the advantages of an early intervention made this group of disorders main targets for Newborn Screening (NBS) programs worldwide (Lindner, Hoffmann et al. 2010; Baruteau, Sachs et al. 2012).

NBS programs, besides public health programs that allow on an early and positive intervention on affected newborns, are valuable data sources on the screened disorders. Since the introduction of FAOD in the screening panels of NBS programs, generated data pointed to significant increase in disease incidence (Wilcken, Haas et al. 2007) that is now believed to be about 1:9,000, although some significant differences can be observed between different populations (Zytkovicz, Fitzgerald et al. 2001; Wilcken, Wiley et al. 2003; Frazier, Millington et al. 2006; Kasper, Ratschmann et al. 2010; Lindner, Gramer et al. 2011; Lund, Hougaard et al. 2012). In the pre-NBS era, diagnosis was achieved mainly through organic acid analysis in urine of symptomatic patients what resulted in a low detection rate, which together with the detection of potentially asymptomatic patients through NBS, justifies the observed difference (Sturm, Herebian et al. 2012).

NBS programs have facilitated the expansion of epidemiological knowledge of screened disorders, with clear advantages over prevalence estimations calculated based on diagnosis of symptomatic cases. The present work incorporates population data derived from the use of tandem mass spectrometry by Iberian NBS programs and has the aim to obtain up to date estimates of birth prevalence of FAOD in Iberia and compare it with those of other reported population-based studies.

The increased knowledge on epidemiology is useful for the better understanding of the natural history of the disorders, and so we can define better treatments and public health strategies.

Material and methods

Study design

The present study includes data from the metabolic screening by tandem mass spectrometry of 1,672,286 Iberian newborns (812,902 Portuguese and 859,384 Spanish) (table 1). Data was collected from six NBS programs, the Portuguese one and five from Spain (Galicia, Murcia, Western Andalucia, Eastern Andalucia and Aragón/La Rioja) during several years. All participating programs are well-implemented public health programs that virtually screen all newborns from their regions. All together, participating NBS programs screen about 46.2% of all annual birth's in Iberia.

Patient detection

FAO detection criteria applied in the participating NBS programs are identical (all according to the best-accepted practices) and present similar levels of ascertainment. The panel of FAOD screened in the different programs is similar with exception of the Portuguese that doesn't screen for short-chain acyl-CoA dehydrogenase deficiency. After the initial suspicion of FAOD, based on the acylcarnitine profile, all diagnosis were confirmed by molecular and/or enzymatic approaches.

Statistical analysis

FAOD birth prevalence in Iberia was determined by dividing the number of diagnosed patients by the total number of newborns screened. The calculation of the confidence interval of the prevalence was as calculated using Wilson's score method.

Results and discussion

Accurate assessment of the birth prevalence of screened disorders requires analysis of test results from a birth cohort representative of a geographic population. In this work, data from well-defined Iberian populations was used to assess the birth prevalence of FAOD in this European region.

Analysing the variation of FAOD prevalence within Iberian populations, what clearly emerges is that the prevalence of FAOD in Portugal (1/6,351) is the double of that observed in Spain (1/12,104). If we compare it excluding SCADD (not screened in Portugal) the difference is even bigger (1/6,351 *versus* 1/14,817). Undoubtedly, MCADD is the major contributor for this difference; nevertheless, all other FAOD present in Portugal higher birth prevalence than in Spain. In Portugal, the prevalence of MCADD, (1:8,380 : 95% CI; 1:10,221 to 1:6,869) is higher than in any Spanish region and than in any other country with available data reported so far (table 1). This high prevalence of MCADD can be justified by the fact that the great majority of the patients are of Gypsy origin (over 90%, and all homozygous for the most common mutation c.985 A>G), a community characterised by high inbreeding and where the high occurrence of genetic diseases, namely MCADD is known (Martinez, Garcia-Lozano et al. 1998; Kalaydjieva, Gresham et al. 2001). The same is observed in Spain but to a less extent. This bias in the ethnical distribution of MCADD patients represents a significant difference in MCADD epidemiology in Iberia, namely Portugal, in comparison to other European countries where patients are almost exclusively of non-Gypsy origin (Khalid, Oerton et al. 2008). This particular characteristic of Portuguese Gypsy community is the main justification for the observed birth prevalence of FAOD in Portugal, the highest among countries with available comparable data. These results are in disagreement with a pre-NBS assumption that there was in Europe a north to south gradient in the incident of MCADD (Tanaka, Gregersen et al. 1997).

SCADD prevalence in Iberia reflects its birth prevalence only in Spain, since this FAOD is not screened in Portugal. It has a prevalence of 1:66,106 in line with other available data for Europe, with exception of Italy where this FAOD seems to be significantly more prevalent.

VLCADD presented a birth prevalence of 1:209,036 in our cohort. Its prevalence in Iberia doesn't present significant differences to what is reported to other European populations, with exception of Italy where it presents a prevalence of 1:45,765. Indeed in this country, and in comparison with the other southern countries Portugal and Spain, and besides an overall similar birth prevalence of FAOD, there are some

differences in individual FAOD. Besides the differences in SCADD and VLCADD is also clear a lower birth prevalence of MCADD in Italy in respect to Portugal and Spain.

For LCHADD Iberia has a prevalence of 1:139,357, similar to that of Germany and Denmark, but less than in Austria. Concerning CUD, Iberia presents a birth prevalence of 1/139,357 in line with available data from other European populations. Comparing available data from Europe, the USA and Australia, it looks that CUD is less prevalent in the USA.

The analysis of the birth prevalence of MADD, CPT1 and CPT2 encompasses some difficulties due to their low frequency, requiring higher numbers of screened newborns in order to get more accurate prevalence estimations.

In Iberia, and influenced by Portuguese population data, MCADD has a birth prevalence of 1: 11,945 one of the highest reported in European countries, alongside with UK, Denmark and the Netherlands. This is higher than those observed, for example, in Austria (1/24,900) or Germany (1/14,080) as well as in the USA or Australia (table1).

Iberia presents birth prevalence for FAOD of 1:7,914 one of the highest in Europe, only comparable with Denmark and Michigan-USA. MCADD is the most prevalent FAOD in our cohort (66.3%), being followed by SCADD (12.0%), CUD and LCHADD (5.7%), VLCADD (3.8%), CPT 2 (2.8%), MADD (2.4%) and finally CPT 1 (1.4 %) (values corrected for the number of screened newborns). Comparing our data with those from the world collaborative NBS project – Region4genetics (McHugh, Cameron et al. 2011), what emerges is a higher proportion of MCADD (66.3% versus 56.3%) and lower contribution of SCADD (12.0% versus 15.7%) and VLCADD (3.8% versus 12.2%), for the total number of FAOD patients.

In conclusion, Portugal has the highest birth prevalence of FAOD reported, estimated based on NBS data. Iberian as a whole presents a birth prevalence of FAOD in agreement with available data from other Caucasian populations, but exhibiting one of the highest values reported. As FAOD are one of the main justifications for MS/MS screening in Caucasian populations, the birth prevalence now estimated stresses the need to screen all Iberian newborns for this group of disorders.

Region	Screened newborns	Fatty acid β-oxidation disorders																					
Iberia		SCADD		MCADD		VLCADD		LCHADD		MADD		CPT1		CPT2		CUD		Overall	
Portugal	812,902	not screened		97	1/8,380	8	1/101,613	7	1/116,129	3	1/270,967	2	1/406,451	3	1/270,967	8	1/101,613	1/6,351	
Galiza	278,371	5	1/55,674	14	1/19,884	0	0	3	1/92,790	0	0	0	0	0	0	0	0	1/12,653	
Múrcia	124,942	1	1/124,942	3	1/41,647	0	0	2	1/62,471	1	1/124,942	0	0	0	0	1	1/124,942	1/15,618	
Western Andalucia	272,462	3	1/90,981	15	1/18,196	0	0	0	0	1	1/272,462	1	1/272,462	0	0	1	1/272,462	1/12,997	
Aragón/La Rioja	54,901	1	1/54,901	3	1/18,300	0	0	0	0	0	0	0	0	0	0	0	0	1/13,725	
Eastern Andalucia	128,228	3	1/42,743	8	1/16,029	0	0	0	0	0	0	0	0	3	1/42,743	2	1/60,114	1/8,014	
Overall	1,672,286	13	1/66,106 (95% CI: 1/113,111 - 1/38,834)	140	1/11,945 (95% CI: 1/14,093 - 1/10,122)	8	1/209,036 (95% CI: 1/415,522 - 1/105,923)	12	1/139,357 (95% CI: 1/243,603 - 1/79,720)	5	1/334,457 (95% CI: 1/783,014 - 1/142,860)	3	1/557,429 (95% CI: 1/1,639,060- 1/189,576)	6	1/278,714 (95% CI: 1/608,135 - 1/127,737)	11	1/139,357 (95% CI: 1/272,250 - 1/84,891)	1/7.914 (95% CI: 1/9,054 - 1/6,916)	
Austria(Kasper, Ratschmann et al.	622,489	1/155,622		1/24,900		1/88,927		1/69,165		1/311,245		0		0		1/311,245		1/12,704	
Germany(Lindner, Gramer et al. 2011)	583,555[a]/1,084,195[b]	1/64,839[a]		1/14,080[b]		1/180,699[b]		1/216,839[b]		1/194,517[a]		1/1,084,195[b]		1/1,084,195[b]		1/194,518[a]		1/9,198	
Denmark(Lund, Hougaard et al. 2012)	190,287[a]/504,049[b]/363,538[c]	1/190,287[a]		1/9,164[b]		1/168,016[b]		1/168,016[b]		0[c]		1/363,538[c]		0[c]		1/100,810[b]		1/7,691	
Italy [a]	640,707	1/27,857		1/22,882		1/45,765		1/640,707		0		1/640,707		1/640,707		1/128,141		1/8,777	
Greece(Loukas, Soumelas et al. 2010)	45,000	0		1/45,000		0		0		0		0		0		0		1/45,000	
Switzerland(Rhead 2006)	57,000			1/11,500															
UK(Oerton, Khalid et al. 2011)	1,500,000			1/10,204															
Belgium(Bodamer and Pollitt 2005)	120,000			1/15,000															
Netherlands(Derks, Boer et al. 2008)	182,850			1/9,624															
USA																			
New England(Zytkovicz,	164,000	1/32,800		1/16,400		1/164,000		0		0		0		1/164,000		0		1/9,647	
North Carolina(Frazier, Millington et al. 2006)	944,078	1/118,010		1/12,933		1/78,673		1/314,693		0		0		1/472,039		0		1/9,633	
California(Feuchtbaum, Lorey et al. 2006)	353,894	1/19,661		1/27,223		1/353,894		1/353,894		1/176,947		0		0		0		1/10,111	
Michigan [b]	708,257	1/16,097		1/13,620		1/88,532		1/708,257		1/354,129		0		1/708,257		1/354,129		1/6,439	
Japan(Bodamer and Pollitt 2005)	102,000			1/51,000															
Saudi Arabia(Al-Hassnan, Imtiaz et al.	237,812			1/18,293															
Australia(Wilcken, Wiley et al. 2003)	362,000	1/72,400		1/21,294		1/120,667		0		0		0		0		1/120,667		1/12,929	

Table 1: Number of FAOD detected in the participating Iberian NBS programs and estimated birth prevalence's, as well as in other NBS programs with available data reported. [a] - data from Italy was extracted from national NBS reports from 2006 to 2012 (available on http://www.simmesn.it/it/documents/rt_screening/index.html; accessed on December 2013); [b] - data from the Michigan NBS program was extracted from program reports from 2006 to 2011 (available on www-michigan.gov/mdch/0,1607,7-132-2942_2950-233593--,00.html , accessed on September 2013). CI – Confidence interval, calculated using Wilson's score method.

References

Al-Hassnan ZN, Imtiaz F, Al-Amoudi M, et al. (2010) Medium-chain acyl-CoA dehydrogenase deficiency in Saudi Arabia: incidence, genotype, and preventive implications. *J Inherit Metab Dis*.

Andresen BS, Lund AM, Hougaard DM, et al. (2012) MCAD Deficiency in Denmark. *Molecular Genetics and Metabolism*.

Bartlett K, Eaton S (2004) Mitochondrial beta-oxidation. *Eur J Biochem* 271(3): 462-469.

Baruteau J, Sachs P, Broue P, et al. (2012) Clinical and biological features at diagnosis in mitochondrial fatty acid beta-oxidation defects: a French pediatric study of 187 patients. *J Inherit Metab Dis*.

Bodamer O, Pollitt RJ (2005) Newborn screening and MCAD. *Workshop results 37th European Metabolic Group Meeting, Prague, Milupa, Friedrichsdorf*.

Derks TG, Boer TS, van Assen A, et al. (2008) Neonatal screening for medium-chain acyl-CoA dehydrogenase (MCAD) deficiency in The Netherlands: the importance of enzyme analysis to ascertain true MCAD deficiency. *J Inherit Metab Dis* 31(1): 88-96.

Feuchtbaum L, Lorey F, Faulkner L, et al. (2006) California's experience implementing a pilot newborn supplemental screening program using tandem mass spectrometry. *Pediatrics* 117(5 Pt 2): S261-269.

Frazier DM, Millington DS, McCandless SE, et al. (2006) The tandem mass spectrometry newborn screening experience in North Carolina: 1997–2005. *Journal of Inherited Metabolic Disease* 29(1): 76-85.

Houten SM, Wanders RJA (2010) A general introduction to the biochemistry of mitochondrial fatty acid β-oxidation. *Journal of Inherited Metabolic Disease* 33(5): 469-477.

Kalaydjieva L, Gresham D, Calafell F (2001) Genetic studies of the Roma (Gypsies): a review. *BMC medical genetics* 2: 5.

Kasper DC, Ratschmann R, Metz TF, et al. (2010) The national Austrian newborn screening program - eight years experience with mass spectrometry. past, present, and future goals. *Wiener klinische Wochenschrift* 122(21-22): 607-613.

Khalid JM, Oerton J, Cortina-Borja M, et al. (2008) Ethnicity of children with homozygous c.985A>G medium-chain acyl-CoA dehydrogenase deficiency: findings from screening approximately 1.1 million newborn infants. *Journal of Medical Screening* 15(3): 112-117.

Kompare M, Rizzo WB (2008) Mitochondrial fatty-acid oxidation disorders. *Semin Pediatr Neurol* 15(3): 140-149.

Lindner M, Gramer G, Haege G, et al. (2011) Efficacy and outcome of expanded newborn screening for metabolic diseases - Report of 10 years from South-West Germany *. *Orphanet Journal of Rare Diseases* 6(1): 44.

Lindner M, Hoffmann GF, Matern D (2010) Newborn screening for disorders of fatty-acid oxidation: experience and recommendations from an expert meeting. *Journal of Inherited Metabolic Disease* 33(5): 521-526.

Loukas YL, Soumelas GS, Dotsikas Y, et al. (2010) Expanded newborn screening in Greece: 30 months of experience. *J Inherit Metab Dis* 33 Suppl 3: 341-348.

Lund AM, Hougaard DM, Simonsen H, et al. (2012) Biochemical screening of 504,049 newborns in Denmark, the Faroe Islands and Greenland - Experience and development of a routine program for expanded newborn screening. *Mol Genet Metab* 107(3): 281-293.

Lund AM, Joensen F, Hougaard DM, et al. (2007) Carnitine transporter and holocarboxylase synthetase deficiencies in The Faroe Islands. *J Inherit Metab Dis* 30(3): 341-349.

Martinez G, Garcia-Lozano JR, Ribes A, et al. (1998) High risk of medium chain acyl-coenzyme A dehydrogenase deficiency among gypsies. *Pediatr Res* 44(1): 83-84.

McHugh DM, Cameron CA, Abdenur JE, et al. (2011) Clinical validation of cutoff target ranges in newborn screening of metabolic disorders by tandem mass spectrometry: a worldwide collaborative project. *Genet Med* 13(3): 230-254.

Oerton J, Khalid J, Besley G, et al. (2011) Newborn screening for medium chain acyl-CoA dehydrogenase deficiency in England: prevalence predictive value and test validity based on 1.5 million screened babies. *J Med Screen* 18: 173-181.

Olpin SE (2013) Pathophysiology of fatty acid oxidation disorders and resultant phenotypic variability. *J Inherit Metab Dis*.

Rhead WJ (2006) Newborn screening for medium-chain acyl-CoA dehydrogenase deficiency: A global perspective. *Journal of Inherited Metabolic Disease* 29(2-3): 370-377.

Spiekerkoetter U, Bastin J, Gillingham M, Morris A, Wijburg F, Wilcken B (2010) Current issues regarding treatment of mitochondrial fatty acid oxidation disorders. *J Inherit Metab Dis* 33(5): 555-561.

Sturm M, Herebian D, Mueller M, Laryea MD, Spiekerkoetter U (2012) Functional effects of different medium-chain acyl-CoA dehydrogenase genotypes and identification of asymptomatic variants. *PLoS One* 7(9): e45110.

Tanaka J, Gregersen N, Ribes A, et al. (1997) A survey of the newborn populations in Belgium, Germany, Poland, Czech Republic, Hungary, Bulgaria, Spain, Turkey, and Japan for the G985 variant allele with haplotype analysis at the medium chain acyl-CoA dehydrogenase gene locul: clinical and evolutionary consideration. *Pediatr Res* 41: 201-209.

Wilcken B (2010) Fatty acid oxidation disorders: outcome and long-term prognosis. *J Inherit Metab Dis*.

Wilcken B, Haas M, Joy P, et al. (2007) Outcome of neonatal screening for medium-chain acyl-CoA dehydrogenase deficiency in Australia: a cohort study. *The Lancet* 369(9555): 37-42.

Wilcken B, Wiley V, Hammond J, Carpenter K (2003) Screening newborns for inborn errors of metabolism by tandem mass spectrometry. *N Engl J Med* 348(23): 2304-2312.

Zytkovicz TH, Fitzgerald EF, Marsden D, et al. (2001) Tandem mass spectrometric analysis for amino, organic, and fatty acid disorders in newborn dried blood spots: a two-year summary from the New England Newborn Screening Program. *Clin Chem* 47(11): 1945-1955.

Study 2 - Newborn screening for medium-chain acyl-CoA dehydrogenase deficiency: regional experience and high incidence of carnitine deficiency.

Couce et al. Orphanet Journal of Rare Diseases 2013, 8:102
http://www.ojrd.com/content/8/1/102

ORPHANET JOURNAL OF RARE DISEASES

RESEARCH Open Access

Newborn screening for medium-chain acyl-CoA dehydrogenase deficiency: regional experience and high incidence of carnitine deficiency

Maria Luz Couce[1*], Paula Sánchez-Pintos[1], Luisa Diogo[2], Elisa Leão-Teles[3], Esmeralda Martins[4], Helena Santos[5], Maria Amor Bueno[6], Carmen Delgado-Pecellín[7], Daisy E Castiñeiras[8], José A Cocho[8], Judit García-Villoria[9], Antonia Ribes[9], José M Fraga[1] and Hugo Rocha[10]

Abstract

Background: Medium-chain acyl-CoA dehydrogenase deficiency (MCADD) is the most common inherited defect in the mitochondrial fatty acid oxidation pathway, resulting in significant morbidity and mortality in undiagnosed patients.
Newborn screening (NBS) has considerably improved MCADD outcome, but the risk of complication remains in some patients. The aim of this study was to evaluate the relationship between genotype, biochemical parameters and clinical data at diagnosis and during follow-up, in order to optimize monitoring of these patients.

Methods: We carried out a multicenter study in southwest Europe, of MCADD patients detected by NBS. Evaluated NBS data included free carnitine (C0) and the acylcarnitines C8, C10, C10:1 together with C8/C2 and C8/C10 ratios, clinical presentation parameters and genotype, in 45 patients. Follow-up data included C0 levels, duration of carnitine supplementation and occurrence of metabolic crises.

Results: C8/C2 ratio and C8 were the most accurate biomarkers of MCADD in NBS. We found a high number of patients homozygous for the prevalent c.985A > G mutation (75%). Moreover, in these patients C8, C8/C10 and C8/C2 were higher than in patients with other genotypes, while median value of C0 was significantly lower (23 μmol/L vs 36 μmol/L).
The average follow-up period was 43 months. To keep carnitine levels within the normal range, carnitine supplementation was required in 82% of patients, and for a longer period in patients homozygotes for the c.985A>G mutation than in patients with other genotypes (average 31 vs 18 months). Even with treatment, median C0 levels remained lower in homozygous patients than in those with other genotypes (14 μmol/L vs 22 μmol/L). Two patients died and another three suffered a metabolic crisis, all of whom were homozygous for the c.985 A>G mutation.

Conclusions: Our data show a direct association between homozygosity for c.985A>G and lower carnitine values at diagnosis, and a higher dose of carnitine supplementation for maintenance within the normal range. This study contributes to a better understanding of the relationship between genotype and phenotype in newborn patients with MCADD detected through screening which could be useful in improving follow-up strategies and clinical outcome.

Keywords: L-carnitine, Metabolic decompensation, Mitochondrial fatty acid oxidation, Mutations, Newborn screening, Rare disease

* Correspondence: maria.luz.couce.pico@sergas.es
[1]Unidad de Diagnóstico y Tratamiento de Enfermedades Congénitas del Metabolismo, Departamento de Pediatría, Hospital Clínico Universitario, Universidad de Santiago, Santiago de Compostela, Spain
Full list of author information is available at the end of the article

Background

Medium-chain acyl-CoA dehydrogenase deficiency (MCADD) is the most common inherited fatty acid β-oxidation (FAO) defect and is a potentially fatal disorder. FAO is a metabolic pathway of particular importance as an energy source during fasting, when glucose supply becomes limited [1]. The overall incidence of MCADD, evaluated by tandem mass spectrometry (MS/MS) newborn screening, is approximately 1:14600, which is 2- to 3-fold higher than the incidence estimated by clinical diagnosis [2]. Incidence varies widely by region, with a higher incidence in the population of northern Europe [3,4].

The MCADD phenotype ranges from asymptomatic [5] to Reye-like syndrome. Typical clinical presentation consists of a metabolic crisis, characterized by hypoketotic hypoglycemia, lethargy, coma [6], seizures or sudden death [7], and triggered by catabolic stress during fasting or illness. The disease usually manifests in the first few years [8], although first presentation in adulthood has also been described [9]. Unusual manifestations, such as neonatal ventricular tachyarrhythmias [10-12], pulmonary haemorrhage [10], and abnormal motor behavior during sleep [13] have also been described. There is a risk of neurological impairment after an acute metabolic decompensation [8,14]. The long term follow up of a Dutch cohort of clinically diagnosed cases of MCADD identified disabilities in 21% of patients [15]. The mortality rate in the first 72 hours of birth is 4%, with and additional mortality rate of 5-7% by 6 years of age in affected unscreened children [8,16].

Newborn screening (NBS) by MS/MS started in the 1990s. It has since been demonstrated to be accurate and effective [2] with a clear benefit in countries with a high percentage of Caucasians [17], contributing to a reduction in MCADD morbidity and mortality [18]. However, severe metabolic crises still occur, particularly in the early post-natal period prior to NBS [8,19,20] and before screening results are available [12,21]. Patients with fatal neonatal presentation show low residual MCAD enzyme activities (<1%) [22].

Elevations of octanoylcarnitine (C8), C8/C10 and C8/C2 ratios are the most commonly reported markers in screening for MCADD [23-26]. It is important to bear in mind that C8 values are likely to be lower when screening samples are collected 72 h after birth [27]. C8/C10 and C8/C2 ratios does not seem to be affected by time of sampling [4].

MCAD protein is encoded by the *ACADM* gene (OMIM 607008), located on chromosome 1p31. More than 80 mutations have been identified in this gene (HGMD®), most of which are missense mutations. While screening programs have greatly improved clinical outcome and contributed to current understanding of MCADD, several questions remain. Two of the most important of these are how genotype and phenotype are related [3,25,28] and the clinical relevance of novel variants of *ACADM*, as identified by newborn screening. Approximately 80% of patients diagnosed clinically are homozygous for the common c.985A>G mutation [25,29]. Patients diagnosed as a result of screening show a different mutational spectrum, with a lower proportion (30-71%) of homozygotes for the common mutation [3,20,21,23,25,27,30-35]. This diagnosis-dependent difference in frequency of the homozygous c.985A>G mutation could be due to the increased detection of milder biochemical phenotypes by newborn screening, with a relatively low risk of developing clinical disease, and associated to mutations found only in screened populations [4,31,36]. Notably, residual MCAD activity is significantly lower in patients with the common mutation (range 0-8%), compared to those with other variants (range 0-63%) [22].

Although most reports indicate that patients homozygous for the most common mutation have a poorer outcome [2,37,38], some homozygous patients who were asymptomatic until adulthood were also reported [4,8,38,39].

The main goal of the present study was to evaluate any relationships between biochemical findings at diagnosis, genotype, free carnitine (C0) levels during follow-up, and clinical outcome, in patients with MCADD detected by NBS.

Methods

Study population

The present study population comprised MCADD patients diagnosed by two of the Spanish regional (Galicia and western Andalusia) and one Portuguese (north/central) NBS programs. From the initiation of newborn screening by MS/MS in each region (in Galicia in 2000, in Andalusia in 2009, and in Portugal in 2004) until December 2011, the total number of MCADD cases detected were, 13 in Galicia (incidence 1:18736), 8 in Andalusia (incidence 1:23656) and 28 in north/central Portugal (incidence 1:11799). Global frequency is 1:15575. Four cases lacking sufficient genetic or follow-up data were excluded. The final ethnic breakdown was 31 Gypsy and 14 Caucasian patients.

At diagnosis, the following parameters were evaluated: age at which analytical samples were taken for NBS, presence or absence of clinical symptoms, C0, medium chain acylcarnitines (C8, C6, C10, C10:1) and ratios of C8/C2 and C8/C10 on the NBS blotter. Diagnosis was confirmed by mutation analysis of the *ACADM* gene. Clinical course was subsequently monitored.

During follow-up patients received a normal diet, according to age and avoiding prolonged fasting and lipolysis. A daily intake of 1-2 g/kg of slow absorption

carbohydrates was recommended from eight months of age. During any acute intercurrent illness the treatment protocol was: careful management with frequent administration of drinks containing an appropriate amount of glucose until the patient improved. In case of vomiting or clinical deterioration, an urgent hospital admission for intravenous glucose infusion was recommended. Biochemical follow-up included measurement of C0 in blood spot/plasma at each visit (average frequency of 3 months) and an annual determination of general biochemical parameters including transaminase levels. Few data exist on the consequences of low carnitine in MCADD; supplementation was prescribed if C0 fell below 12 μmol/L in blood spots or below 20 μmol/L in plasma. Supplementation was only stopped after 2 independent determinations showed free carnitine higher than μmol/L in blood spots or 20 μmol/L in plasma. Carnitine was reintroduced if it fell again below the control values.

Informed consent was obtained from the parents of all patients. The study was approved by the Ethics Committee of each Hospital. Institutional Review Board: Fundación Ramón Dominguez G 15796683. Address: Travesía da Choupana s/n. 15706 Santiago de Compostela, A Coruña. Spain.

Analytical methods

NBS

Acylcarnitines in blood spots were studied by the standard method of butylation and analysis by MS/MS. MCADD was suspected in a newborn if the medium chain acylcarnitines and/or C8/C2 or C8/C10 ratios were higher than the 99.9th percentile of the specific medium acylcarnitine (C8) and/or the ratios C8/C2 or C8/C10 (C8 p99.9 = 0.52 μM; C8/C2 p99.9 = 0.02; C8/C10 p99.9 = 1.8).

Molecular testing

DNA was isolated and sequenced by standard procedures for blood samples of all patients and their parents, except for two patients conceived by in vitro fertilization with oocyte donation (Patients 1 and 16, Additional file 1), and whose biological mothers were not available for analysis. Molecular analysis of *ACADM* was performed using standard procedures. Primers were designed to overlap the coding sequences and their flanking regions (sequences available on request). PCR products were purified by ExoSap (usb®) enzyme and sequenced using a Big Dye Terminator Cycler Sequencing Ready reaction kit and the manufacturer's protocol (Applied Biosystems). The sequencing reactions were performed in an ABI 3130XL Genetic Analyser.

Biochemical follow-up

C0 was evaluated in blood spots or plasma samples. When using blood spots it was measured by MS/MS, according to the method of Zytkovicz et al [27]. In plasma, C0 was measured by the classical enzymatic/spectrophotometric assay [40].

When appropriate, data were statistically analyzed using the Student's t-test (with $p < 0.05$ taken to indicate significance).

Results

During the study period we evaluated 45 patients with MCADD detected by NBS, with the following geographical distribution: 26 cases from Portugal, 13 from Galicia, and 6 from Andalusia. The average age of analytical sample collection during screening was 7 days (range: 0-35), with a median of 5 days and a mode of 4 days. In 82.2% cases samples were obtained during the first week of life (37/45). In the remaining 8 cases (17.8%) repeat samples were analyzed subsequently, due to invalidity of the first sample. At diagnosis, all patients were asymptomatic with increased levels of medium chain acylcarnitines.

As shown in Additional file 1, all but patient 39 exhibited a marked elevation of C8 (average 4.8 ± 4.1 μmol/L; CV < 0.52). On the fourth day of postnatal age, patient 39 had a C8 value between percentiles 99.5 (0.37 μM) and 99.9 (0.52 μM), but a higher than normal C8/C2 ratio (0.04). A repeat sample, taken at 23 days of age showed a slight increase in C8 (0.54 μM) and C8/C2 (0.05), justifying a genetic study. The C8/C2 ratio was highly increased in all patients, with an average value of 0.28 ± 0.21 (CV < 0.02). A similar tendency was observed with the C8/C10 ratio, with an average value of 9.8 ± 5.7 μmol/L (CV < 1.85), but in patients 35 and 39 this ratio was normal (C8/C10 = 1.6 and 1). On resampling this ratio increased slightly (C8/C10 = 1.81). Increased levels of C10 or C10:1 was seen in nineteen and thirty nine patients respectively.

A diagnosis of MCADD was confirmed by molecular testing in all patients; 34 patients were homozygous for the prevalent c.985A>G (p.Lys329Glu) mutation and 10 patients were compound heterozygous for the prevalent and another mutation. Only patient 45 did not carry the c.985A>G mutation in any of the alleles (Additional file 1). Three of the mutations detected, c.600G>T (p.Trp200Cys), c.245G>C (p.Trp82Ser) and c.542A>G (p.Asp181Gly), are novel. Among our screened cases the prevalence of the common mutation was 86% (78 out of 90 alleles).

Levels of C8 and ratios of C8/C10 and C8/C2 were significantly higher ($p = 0.016$), while C0 was significantly lower ($p < 0.001$) in patients who were homozygous for the prevalent c.985A>G mutation, compared to with those with other genotypes (Additional file 1).

After diagnosis, all patients received dietary recommendations, but supplementation with L-carnitine (20-60 mg/kg/day) was prescribed only to thirty-two patients, having a low C0.

The average follow-up period was 3 years and 7 months (range 2 months-10 years 7 months). Follow-up data were available in 39 out of 45 cases (28 homozygous for the c.985A>G mutation and 11 with other genotypes). Eighty-two percent of patients (32/39) were given carnitine supplementation. Carnitine was not administered to 6 patients as their levels were consistently within the control range. One patient did not receive supplementation because his parents declined treatment, despite fulfilling the biochemical indication as per our protocol. Following carnitine treatment, the average C0 levels were significantly lower in patients homozygous for the common mutation than in patients with other mutations (14 μmol/L vs 22 μmol/L, $p < 0.001$) (Additional file 1). Among the 28 cases homozygous for the c.985A>G mutation, 26 (92.8%) required L-carnitine supplementation to reach normal levels, while fewer patients with other genotypes needed supplementation (6/11; 54.5%). The average follow-up period for homozygous patients was 31 months while the average for other patients was 18 months. According to our protocol, carnitine supplementation could never be stopped in eleven homozygous patients (34.3%). Supplementation was stopped in 15 homozygous patients but, reintroduction was necessary in 11 patients. Among 11 patients with a genotype other than homozygosity for the common mutation, carnitine supplementation was only required in one of them continuously (9.1%).

Two patients of Gypsy ethnicity (patients 4 and 33; Additional file 1) died at 15 and 32 months of age, respectively. Despite frequent carnitine supplementation, patient 4 consistently showed low C0 levels (average 10 μM). This patient died in a hospital not participating in the study, due to a lower respiratory tract infection. Patient 33 frequently showed low C0 levels (average 11.5 μM), but supplementation of carnitine was not always complied with. This patient died after presenting with gastroenteritis, decreased consciousness, hypotonia and in cardiorespiratory arrest.

Another three (patients 13, 17 and 21, Additional file 1), also of Gypsy ethnicity, suffered metabolic crises with episodes of hypoglycaemia and vomiting, triggered by infection. The remaining patients never had a metabolic crisis, although one (patient 31, Additional file 1) was also diagnosed with maple syrup urine disease.

Discussion

C8 levels and several other ratios are utilized in screening for MCADD. We analysed the C8, C8/C2 and C8/C10 in our study and found C8/C2 ratio to be more accurate than either C8 and C8/C10, as it was elevated in all patients. By comparison, C8 was elevated in 44/45 and C8/C10 in 43/45 patients. We therefore consider the calculation of C8/C2 ration very important in screening for MCADD. This was exemplified in patients 35 and 39 whose diagnosis could easily have been missed without referral to the C8/C2 ratio. Both these patients were compound heterozygous for the common c.985A>G mutation as well as for other reported pathogenic mutations (c.683C>A [41] and c.199T>C [3]), respectively. It is thought that these latter two mutations might confer a more attenuated biochemical phenotype [3,41]. Patient 39 presented a biochemical profile similar to MCAD carrier, as also described Hsu et al. [42], and never showed clinical signs. The percentage of cases homozygous for the common mutation (76%) detected in our cohort was higher than previously reported, ranging from 30% to 71% (47.4% [3]; 43% [4]; 53% [19]; 61% [21]; 37% [27]; 71% [30]; 40% [31]; 63% [32]; 36.4% [33]; 52% [34]; 30% [35]). Our results could have a bias due to the high proportion of patients of Gypsy ethnicity (31/45, 69%), in whom the common allele shows a high population frequency [43]; 22/26 (84.6%) of our patients from Portugal were homozygous for the common mutation, while the remaining 12 homozygous patients were from Spain. We have previously observed that the prevalence for the common mutation in patients from Galicia (north-west Spain) was also high, at 63% [24].

The higher plasma C8 levels and C8/C10 and C8/C2 ratios that we have found in patients homozygous for the c.985A>G mutation agree with previous reports [3,4,20,23,24,34,38,44]. We noted a statistically significant association between low C0 level at NBS and homozygosity. As shown in Additional file 1, patients homozygous for the common mutation tended to maintain lower levels of C0 and carnitine supplementation is more frequent necessary in order that the plasma carnitine levels remain within the normal range. Treatment for MCADD is based mainly on diet: avoidance of fasting and ensuring high carbohydrate intake during illness. L-carnitine treatment has been proposed in MCADD therapy [45], although there is as yet no good evidence to support this recommendation. A survey of thirty-one centers in Europe, North America, Asia and Australia showed L-carnitine supplementation in MCADD to be controversial: 36% of the centers routinely used oral carnitine whereas 32% used it only in cases of proven carnitine deficiency or intercurrent infection [46]. Bzduch et al [47] reported a homozygous patient who had suffered two Reye-like episodes and whose C0 decreased continuously from an acute crisis for a further 8-13 days but then returned to normal by the 25th day after the episode.

Apart from the c.985A>G mutation, it is well documented that most of the *ACADM* mutations seen in MCADD patients who have been diagnosed as a result of NBS are associated with asymptomatic or moderate clinical forms [48] of the disease. While it is also known that patients with these less commonly seen *ACADM* genotypes are also at risk of metabolic decompensation during periods of illness or metabolic stress [7,43,49,50],

in our cohort clinical symptoms were only manifest in 11% of patients (5/45), all of whom were homozygous for the c.985A>G mutation.

In conclusion, our study points to that the *ACADM* genotype most commonly seen in MCADD might be of particular relevance in refining a follow-up protocol, since plasma carnitine levels in patients homozygous for c.985A>G tend to be lower and supplementation is required to maintain carnitine within the normal range. Nevertheless, this associations needs to be further supported by future studies with larger patients cohorts. Our results suggest that dietary management should be complemented with close monitoring of C0 levels and carnitine should be supplemented when necessary, and point to that this might be of particularly importance in patients homozygous for the common mutation. By demonstrating an association between carnitine levels and homozygosity for the c.985A>G mutation, the current study also contributes to our understanding of the relationship between genotype/biochemical markers and phenotype in MCADD. To a large extent, however, MCAD deficiency remains unpredictable, indicating the need for further prospective studies.

Additional file

Additional file 1: Table S1. Summary of levels of acylcarnitines at diagnosis, mutations, carnitine free levels, treatment and evolution of MCADD patients.

Abbreviations

C10: Decanoylcarnitine (); FAO: Fatty acid β-oxidation; C0: Free carnitine; MCADD: Medium-chain acyl-CoA dehydrogenase deficiency; NBS: Newborn screening; C8: Octanoylcarnitine; MS/MS: Tandem mass spectrometry.

Competing interests

None of the authors have any conflict of interest to declare.

Authors' contributions

MLC, PSP and HR reviewed the literature and conceived the study. LD was involved in patient selection, monitoring and data collection at Coimbra Hospital. ELT was involved in patient selection, monitoring and data collection at S Joao-Porto Hospital. EM was involved in patient selection, monitoring and data collection at María Pía-Porto Hospital. HS was involved in patient selection, monitoring and data collection at Gaia Hospital. MAB and CDP were involved in patient selection, monitoring and data collection at Virgen del Rocío Hospital. DEC and JAC were involved in patient selection, monitoring and data collection at Santiago de Compostela Hospital. JGV and AR interpreted the results of mutation analyses and were involved in the statistical analysis. MLC, AR and JMF reviewed and edited the manuscript. All authors critically revised the manuscript and approved the final version.

Acknowledgements

We thank all patients and their families for kindly participating in the study.

Author details

[1]Unidad de Diagnóstico y Tratamiento de Enfermedades Congénitas del Metabolismo, Departamento de Pediatría, Hospital Clínico Universitario, Universidad de Santiago, Santiago de Compostela, Spain. [2]Centro de Desenvolvimento da Criança Luís Borges, Hospital Pediátrico de Coimbra, Coimbra, Portugal. [3]Unidade Doenças Metabólicas, Hospital Pediátrico Integrado, Centro Hospitalar de S. João, EPE, Porto, Portugal. [4]Unidade de Doenças Metabólicas, Hospital de Crianças Maria Pia, Centro Hospitalar do Porto, Porto, Portugal. [5]Departamento de Pediatria, Centro Hospitalar Gaia/Espinho, Gaia, Portugal. [6]Unidad de Metabolopatías y Nutrición Infantil, Departamento de Pediatría, Hospital Universitario Virgen del Rocio, Sevilla, Spain. [7]Departamento de Bioquímica Clínica, Hospital Universitario Virgen del Rocío, Sevilla, Spain. [8]Unidad de Diagnóstico y Tratamiento de Enfermedades Congénitas del Metabolismo, Laboratorio de Metabolopatías, Hospital Clínico Universitario, Universidad de Santiago, Santiago de Compostela, Spain. [9]Sección de Errores Congénitos del Metabolismo-IBC, Servicio de Bioquímica y Genética Molecular, Hospital Clínic y Centro de Investigación Biomédica en Red de Enfermedades Raras (CIBERER), Barcelona, Spain. [10]Unidade de Rastreio Neonatal, Departamento de Genética do Instituto Nacional de Saúde Doutor Ricardo Jorge, Porto, Portugal.

Received: 7 March 2013 **Accepted:** 5 July 2013
Published: 10 July 2013

References

1. Houten SM, Wanders RJA: **A general introduction to the biochemistry of mitochondrial fatty acid oxidation.** *J Inherit Metab Dis* 2010, **33:**469–477.
2. Rhead WJ: **Newborn screening for medium-chain acyl-CoA dehydrogenase deficiency: a global perspective.** *J Inherit Metab Dis* 2006, **29:**370–377.
3. Maier EM, Liebl B, Röschinger W, Nennstiel-Ratzel U, Fingerhut R, Olgemöller B, Busch U, Krone N, Kries R, Roscher AA: **Population spectrum of ACADM genotypes correlated to biochemical phenotypes in newborn screening for medium-chain acyl-CoA dehydrogenase deficiency.** *Hum Mutat* 2005, **25:**443–452.
4. Andresen BJ, Lund AM, Hougaard DM, Christensen E, Gahrn B, Christensen M, Bross P, Vested A, Simonsen H, Skogstrand K, Olpin S, Brandt NJ, Skovby F, Nørgaard-Pedersen B, Gregersen N: **MCAD deficiency in Denmark.** *Mol Genet Metab* 2012, **106:**175–188.
5. Leydiker KB, Neidich JA, Lorey F, Barr EM, Puckett RL, Lobo RM, Abdenur JE: **Maternal medium-chain acyl-CoA dehydrogenase deficiency identified by newborn screening.** *Mol Genet Metab* 2011, **103:**92–95.
6. Hoflack M, Caruba C, Pitelet G, Hass H, Mas JC, Paquis V, Berard E: **Infant coma in the emergency department: 2 cases of MCAD deficiency.** *Arch Pediatr* 2010, **17:**1074–1077.
7. Yusupov R, Finegold DN, Naylor EW, Sahai I, Wainsbren S, Levy HL: **Sudden death in medium chain acyl-coenzyme a dehydrogenase deficiency (MCADD) despite newborn screening.** *Mol Genet Metab* 2010, **101:**33–39.
8. Wilcken B, Haas M, Joy P, Wiley V, Chaplin M, Black C, Fletcher J, McGill J, Boneh A: **Outcome of neonatal screening for medium-chain acyl-CoA dehydrogenase deficiency in Australia: a cohort study.** *Lancet* 2007, **369:**37–42.
9. Schatz UA, Ensenauer R: **The clinical manifestation of MCAD deficiency: challenges towards adulthood in the screened population.** *J Inherit Metab Dis* 2010, **33:**513–520.
10. Maclean K, Rasiah VS, Kirk EPE, Carpenter K, Cooper S, Lui K, Oei J: **Pulmonary haemorrhage and cardiac dysfunction in a neonate with medium-chain acyl-CoA dehydrogenase (MCAD) deficiency.** *Acta Paediatr* 2005, **94:**114–6.
11. Rice G, Brazelton T, Maginot K, Srinivasan S, Hollman G, Wolff JA: **Medium chain acyl-coenzyme A dehydrogenase deficiency in a neonate.** *N Engl J Med* 2007, **357:**1781.
12. Yusuf K, Jirapradittha J, Amin HJ, Yu W, Hasan SU: **Neonatal ventricular tachyarrhythmias in medium chain acyl-CoA dehydrogenase deficiency.** *Neonatology* 2010, **98:**260–264.
13. Meng X, Mao W, Sun W, Li L, Zhan S, Wu X, Huang Z, Zhang X, Ma Y, Wang Y: **Sleep induces abnormal motor behaviors caused by medium-chain acyl-CoA dehydrogenase deficiency: a case report.** *Sleep Med* 2012, **13:**115–117.
14. Grosse SD, Khoury MJ, Greene CL, Crider KS, Pollit RJ: **The epidemiology of medium chain acyl-CoA dehydrogenase deficiency: an update.** *Genet Med* 2006, **8:**205–212.
15. Derks TG, Rejngoud DJ, Waterham HR, Gerver WJ, van den Berg M, Sauer PJ, Smit GP: **The natural history of medium-chain acyl CoA dehydrogenase deficiency in The Netherlands: clinical presentation and outcome.** *J Pediatr* 2006, **148:**665–70.
16. Wilcken B: **Fatty acid oxidation disorders: outcome and long-term prognosis.** *J Inherit Metab Dis* 2010, **33:**501–506.
17. Lindner M, Hoffman GF, Matern D: **Newborn screening for disorders of fatty-acid oxidation: experience and recommendations from an expert meeting.** *J Inherit Metab Dis* 2010, **33:**521–526.

18. Nennstiel-Ratzel U, Arenz S, Maier EM, Knerr I, Baumkötter J, Röschinger W, Liebl B, Hadorn HB, Roscher AA, von Kries R: **Reduced incidence of severe metabolic crisis or death in children with medium chain acyl-CoA dehydrogenase deficiency homozygous for c.985A > G identified by neonatal screening.** *Mol Genet Metab* 2005, **85:**157–59.
19. Cyriac J, Venkatesh V, Gupta C: **A fatal neonatal presentation of medium-chain acyl coenzyme A dehydrogenase deficiency.** *J Int Med Res* 2008, **36:**609–610.
20. Oerton J, Khalid JM, Besley G, Dalton RN, Downing M, Green A, Henderson M, Krywawych S, Leonard J, Andresen BS, Dezateux C: **Newborn screening for medium chain acyl-CoA dehydrogenase deficiency in England: prevalence, predictive value and test validity based on 1.5million screened babies.** *J Med Screen* 2011, **18:**173–181.
21. Frazier D, Millington D, McCandless S, Koebert D, Weavil S, Chaing S, Boney A, Moore E, Frazier DM: **The tandem mass spectrometry newborn screening experience in North Carolina: 1997-2005.** *J Inherit Metab Dis* 2006, **29:**76–85.
22. Touw CM, Smit GP, de Vries M, de Klerk JB, Bosch AM, Visser G, Mulder MF, Rubio-Gozalbo ME, Elvers B, Niezen-Koning KE, Wanders RJ, Waterham HR, Reijngoud DJ, Derks TG: **Risk stratification by residual enzyme activity after newborn screening for medium-chain acyl-CoA dehydrogenase deficiency: data from a cohort study.** *Orphanet J Rare Dis* 2012, **7:**30.
23. Blois B, Riddell C, Dooley K, Dyack S: **Newborns with C8 acylcarnitine level over the 90th centile have an increased frequency of the common MCAD 985A > G mutation.** *J Inherit Metab Dis* 2005, **28:**551–556.
24. Couce ML, Castiñeiras DE, Moure JD, Cocho JA, Sánchez-Pintos P, García-Villoria J, Quelhas D, Gregersen N, Andresen BS, Ribes A, Fraga JM: **Relevance of expanded neonatal screening of medium-chain acyl Co-A dehydrogenase deficiency: outcome of a decade in Galicia (Spain).** *JIMD Reports* 2011, **28:**131–136.
25. Arnold GL, Saavedra- Matiz CA, Galvin-Parton PA, Erbe R, DeVicentis E, Kronn D, Mofidi S, Wasserstein M, Pellegrino JE, Levy PA, Adams DJ, Nichols M, Caggana M: **Lack of genotype-phenotype correlations and outcome in MCAD deficiency diagnosed by newborn screening in New York State.** *Mol Genet Metab* 2010, **99:**263–268.
26. McHugh DM, Cameron CA, Abdenur JE, Abdulrahman M, Adair O, Al Nuaimi SA, Ahlman H, Allen JJ, Antonozzi I, Archer S, et al: **Clinical validation of cutoff target ranges in newborn screening of metabolic disorders by tandem mass spectrometry: a worldwide collaborative project.** *Genet Med* 2011, **13:**230-254.
27. Zytkovicz TH, Fitzgerald EF, Marsden D, Larson CA, Shih VE, Johnson DM, Strauss AW, Comeau AM, Eaton RB, Grady GF: **Tandem mass spectrometric analysis for amino, organic, and fatty acid disorders in newborn dried bloodspots: a two-year summary from the New England Newborn Screening Program.** *Clin Chem* 2001, **47:**1945–1955.
28. Gregersen N, Andresen BS, Pedersen CB, Olsen RKJ, Corydon TJ, Bross P: **Mitochondrial fatty acid oxidation defects-remaining challenges.** *J Inherit Metab Dis* 2008, **31:**643–657.
29. Gregersen N, Winter V, Curtis D, Deufel T, Mack M, Hendrickx J, Willems PJ, Ponzone A, Parrella T, Ponzone R, *et al*: **Medium-chain acyl-CoA dehydrogenase deficiency: the prevalent mutation G985 is subject to a strong founder effect from northwestern Europe.** *Hum Heredity* 1993, **43:**342–50.
30. Yokota I, Coates P, Hale DE, Rinaldo P, Tanaka K: **Molecular survey of a prevalent mutation, 985 A-to-G transition, and identification of five infrequent mutations in the medium-chain acyl-CoA dehydrogenase (MCAD) gene in 55 patients with MCAD deficiency.** *Am J Hum Genet* 1991, **49:**1280–1291.
31. Derks TG, Boer TS, van Assen A, Bos T, Ruiter J, Waterham HR, Niezen-Koning KE, Wanders RJ, Rondeel JM, Loeber JG, Ten Kate LP, Smit GP, Reijngoud DJ: **Neonatal screening for medium-chain acyl-CoA dehydrogenase (MCAD) deficiency in The Netherlands: the importance of enzyme analysis to ascertain true MCAD deficiency.** *J Inherit Metab Dis* 2008, **31:**88–96.
32. Andresen BS, Dobrowolski SF, O'Reilly L, Muenzer J, McCandless SE, Frazier DM, Udvari S, Bross P, Knudsen I, Banas R, Chace DH, Engel P, Naylor EW, Gregersen N: **Medium-chain acyl-CoA dehydrogenase (MCAD) mutations identified by MS/MS-based prospective screening of newborns differ from those observed in patients with clinical symptoms: identification and characterization of a new, prevalent mutation that results in mild MCAD deficiency.** *Am J Hum Genet* 2001, **68:**108–118.
33. Carpenter K, Wiley V, Sim K, Heath D, Wilcken B: **Evaluation of newborn screening for medium chain acyl-CoA dehydrogenase deficiency in 275000 babies.** *Arch Dis Child Fetal Neonatal Ed* 2001, **85:**F105–F109.
34. Kennedy S, Potter BK, Wilson K, Fisher L, Geraghty M, Milburn J, Chakraborty P: **The first three years of screening for medium chain acyl-CoA dehydrogenase deficiency (MCADD) by newborn screening Ontario.** *BMC Pediatr* 2010, **10:**82.
35. Nichols MJ, Saavedra-Matiz CA, Kenneth AP, Caggana M: **Novel mutations causing medium chain acyl-CoA dehydrogenase deficiency: under representation of the common c.985 A > G mutation in the New York State population.** *Am J Med Genet A* 2008, **146A:**610–619.
36. Zschocke J, Schulze A, Lindner M, Fiesel S, Olgemöller K, Hoffman GF, Penzien J, Ruiter JP, Wanders RJ, Mayatepek E: **Molecular and functional characterization of mild MCAD deficiency.** *Hum Genet* 2001, **108:**404–8.
37. Hsu H-W, Zytkovicz TH, Comeau AM, Strauss AW, Marsden D, Shih VE, Grady GF, Eaton RB: **Spectrum of medium-chain acyl-CoA dehydrogenase deficiency detected by newborn screening.** *Pediatrics* 2008, **121:**108–114.
38. Waddell L, Wiley V, Carpenter K, Bennetts B, Angel L, Andresen BS, Wilcken B: **Medium-chain acyl-CoA dehydrogenase deficiency: genotype-biochemical phenotype correlations.** *Mol Genet Metab* 2006, **87:**32–39.
39. Duran M, Hofkamp M, Rhead WJ, Saudubray JM, Wadman SK: **Sudden child death and "healthy · affected family members with medium-chain acyl-CoA dehydrogenase deficiency.** *Pediatrics* 1986, **78:**1052–1057.
40. Wieland OH: **Methods of Enzymatic analysis**. In *Volume 8*. 3rd edition. Edited by Bergmeyer HU. Florida: VCH Verlagsgesellschaft, Weinhiem Deerfield Beach; 1965:481–488.
41. McKinney JT, Longo N, Hahn SH, Matern D, Rinaldo P, Strauss AW, Dobrowolski SF: **Rapid, comprehensive screening of the human medium chain acyl-CoA dehydrogenase gene.** *Mol Genet Metab* 2004, **82:**112–120.
42. Hsu HW, Zytkovicz TH, Comeau AM, Strauss AW, Marsden D, Shih VE, Grady GF, Eaton RB: **Spectrum of medium-chain acyl-CoA dehydrogenase deficiency detected by newborn screening.** *Pediatrics* 2008, **121:**e1108–14.
43. Martinez G, Garcia-Lozano JR, Ribes A, Maldonado MD, Baldellou A, de Pablo R, Nuñez-Roldan A: **High risk of medium chain acyl-coenzyme A dehydrogenase deficiency among gypsies.** *Pediatr Res* 1998, **44:**83–84.
44. Smith EH, Tomas C, McHugh D, Gavrilov D, Raymond K, Rinaldo P, Tortorelli S, Matern D, Highsmith WE, Oglesbee D: **Allelic diversity in MCAD deficiency: the biochemical classification of 54 variants identified during 5 years of ACADM sequencing.** *Mol Genet Metab* 2010, **100:**241–250.
45. Feillet F, Ogier H, Cheillan D, Aquaviva C, Labarthe F, Baruteau J, Chabrol B, de Lonlay P, Valayanopoulos V, Garnotel R, Dobbelaere D, Briand G, Jeannesson E, Vassault A, Vianey-Saban C: **SFEIM: Medium-chain acyl-CoA -dehydrogenase (MCAD) deficiency: French consensus for neonatal screening, diagnosis, and management.** *Arch Pediatr* 2012, **19:**184–193.
46. Walter JH: **L-carnitine in inborn errors of metabolism: what is the evidence?** *J Inherit Metab Dis* 2003, **26:**181–188.
47. Bzduch V, Behulova D, Salingova A, Ponec J, Fabriciova K, Kozak L: **Serum free carnitine in medium chain acyl-CoA dehydrogenase deficiency.** *Bratisl Lek Listy* 2003, **104:**405–407.
48. Maier EM, Pongratz J, Muntau AC, Liebl B, Nennstiel-Ratzel U, Busch U, Fingerhut R, Olgemöller B, Roscher AA, Röschinger W: **Dissection of biochemical borderline phenotypes in carriers and genetic variants of medium-chain acyl-CoA dehyrogenase deficiency: implications for newborn screening [corrected].** *Clin Genet* 2010, **77:**304.
49. Purevsuren J, Kobayashi H, Hasegawa Y, Mushimoto Y, Li H, Fukuda S, Shigematsu Y, Fukao T, Yamaguchi S: **A novel molecular aspect of Japanese patients with medium-chain acyl-CoA dehydrogenase deficiency (MCADD): c.449-452delCTGA is a common mutation in Japanese patients with MCADD.** *Mol Genet Metab* 2009, **96:**77–79.
50. Thodi G, Georgiou V, Molou E, Loukas YL, Dotsikas Y, Biti S, Papadopoulos K, Doulgerakis E: **Characterization of the molecular spectrum of Medium-Chain Acyl-CoA Dehydrogenase Deficiency in a Greek newborns cohort: Identification of a novel variant.** *Clin Biochem* 2012, **45:**116–1172.

doi:10.1186/1750-1172-8-102
Cite this article as: Couce *et al.*: Newborn screening for medium-chain acyl-CoA dehydrogenase deficiency: regional experience and high incidence of carnitine deficiency. *Orphanet Journal of Rare Diseases* 2013 **8:**102.

CHAPTER III

Study 3 - Mitochondria proteome profiling: A comparative analysis between gel- and gel-free approaches.

Talanta ▮ (▮▮▮▮) ▮▮▮–▮▮▮

Contents lists available at SciVerse ScienceDirect

Talanta

journal homepage: www.elsevier.com/locate/talanta

Mitochondria proteome profiling: A comparative analysis between gel- and gel-free approaches

Rita Ferreira [a], Hugo Rocha [b], Vanessa Almeida [a], Ana I. Padrão [a], Cátia Santa [a], Laura Vilarinho [b], Francisco Amado [a,c], Rui Vitorino [a,*]

[a] QOPNA, Department of Chemistry, University of Aveiro, Aveiro, Portugal
[b] I&D Unit, Genetics Department, National Institute of Health Ricardo Jorge, Porto, Portugal
[c] School of Health Sciences, University of Aveiro, Portugal

ARTICLE INFO

Article history:
Received 16 November 2012
Received in revised form
29 March 2013
Accepted 8 April 2013
Available online 22 April 2013

Keywords:
Gel-based
Gel-free
Electrophoresis
LC-MS/MS
PTMs
Proteomics

ABSTRACT

Mitochondrial proteomics emerged aiming to disclose the dynamics of mitochondria under various pathophysiological conditions. In the present study we investigated the relative merits of gel-based (2DE and SDS-LC) and gel-free (2D-LC) protein separation approaches and protein identification algorithms (Mascot and Paragon) in the proteome profiling of mitochondria isolated from cultured fibroblasts, a sample traditionally used for diagnosis purposes.

Combining data retrieved from 2DE, 2D-LC and SDS-LC and search methods, a total of 696 non-redundant proteins were identified. An overlap of only 19% between the proteins identified by the three different methods was observed when Mascot and Paragon were used. Regarding protein ID, a consistency in the number of identified proteins *per* sample was noticed for 2DE approach. Independent of the methodological approach chosen, it was noticed that the predominance in mitochondria of hydrophilic proteins with 20–50 kDa and p*I* 5–6 and 8–9; however, 2D-LC and SDS-LC allowed the enrichment of proteins with a mass below 30 kDa and of basic proteins with p*I* values above 8. In conclusion, data from the present study highlight the power of integrating different separation technologies and protein identification algorithms.

1. Introduction

Mitochondrial dysfunctions are associated with many pathophysiological conditions, such as metabolic disorders, diabetes mellitus, cancer, neurodegenerative diseases and aging [1,2]. Among these, metabolic disorders involving defects in proteins/enzymes from pathways harbored in mitochondria are rare but related with high morbidity and mortality [3]. Many effects of these disease processes have been studied using classic biochemical methods focused on a particular protein [4]. Recent developments in proteomics have allowed a global perception into protein expression, localization, and interaction, and how they are modulated by pathophysiological conditions. Indeed, proteome profiling has been intensely used for the investigation of pathogenic mechanisms and functional correlations on protein levels in a non-biased manner [2,4,5]. Among the protein separation procedures used for mitochondria proteome profiling, two-dimensional gel electrophoresis (2DE) as well as multidimensional liquid chromatography (2D-LC) have been adopted [1,6–8]. While 2DE, a classical proteomic technology, separates proteins based on their isoelectric point (p*I*) and molecular weight (MW) with a limited dynamic range, 2D-LC partially overcomes the shortcomings of 2DE such as limitations in detecting proteins with extreme alkalinity, hydrophobicity, and molecular mass, allowing large-scale, discovery-driven proteomics [1,4,9–11].

Cultured skin fibroblasts are an attractive sample for diagnostic testing and research of metabolic diseases involving defects in mitochondrial proteins, considering the minimally invasive character of sampling and the large amount of cell material that can be obtained by culturing [12]. For the diagnosis of certain diseases, enzymatic measurements or molecular genetic analysis of tissue and/or cell samples is required [3] and for that, tissue biopsy is often needed. Although tissues like heart, skeletal muscle and liver are among the main targets of metabolic disorders, such as fatty acid oxidation defects [13], skin biopsy is usually preferred. Besides being ethically straightforward, the isolated fibroblasts can be used to measure ATP synthesis, oxygen consumption, electric membrane potential, and substrate oxidation rates [3,12,13]. Moreover, fibroblasts can be stored and retested when desired and might be used as a model system to study diseases' pathogenesis [3]. Despite all these advantages, few studies have

* Correspondence to: Department of Chemistry, University of Aveiro, 3810-193, Aveiro, Portugal. Fax: +35 1234370084.
E-mail address: rvitorino@ua.pt (R. Vitorino).

0039-9140/$ - see front matter © 2013 Elsevier B.V. All rights reserved.
http://dx.doi.org/10.1016/j.talanta.2013.04.026

been performed focused on mitochondrial protein profiling in cultured fibroblasts [1,6,7] and their use might be advantageous in the investigation of complex defects where several factors may contribute to disease [1].

In order to clarify the strengths and limitations of proteomics to study the mitochondrial proteome in fibroblasts and the potential implications for the comprehension of metabolic diseases' pathogenesis, we performed a comparative analysis of gel-based and gel-free protein separation approaches, and protein identification algorithms (Mascot and Paragon). We report the advantages of combining multidimensional approaches to get a deep protein profile screening of mitochondria isolated from cultured fibroblasts aiming a more comprehensive and effective manner to investigate the mitochondrial proteome. Nevertheless, from the separation approaches tested, a higher number of identified mitochondrial proteins were achieved with SDS-LC approach, apart from the protein identification algorithm chosen.

2. Material and methods

2.1. Reagents

Unless otherwise stated, all reagents such as triethylammonium bicarbonate (TEAB), trifluoroacetic acid (TFA), protease inhibitor cocktail, formic acid, α-cyano-4-hydroxycinnamic acid (α-CHCA), urea, CHAPS were purchased from Sigma-Aldrich. Immobiline drystrip and ampholytes were from GE Healthcare. Sequencing grade modified trypsin (bovine) was from ABSciex (ABSciex, USA).

2.2. Cell culture

Skin fibroblasts from healthy individuals ($n=3$) were grown in Ham F10 nutrient mixture supplemented with 10% fetal calf serum, 2 mmol/L glutamine, 1% penicillin, streptomycin and fungizone, in 75 cm^2 culture flasks. Ten culture flasks from each sample were grown to subconfluence before mitochondria isolation.

2.3. Mitochondria isolation and protein extraction

Isolation of mitochondria from the cell pellet was performed at 4 °C according to Schwab et al. [14] with minor modifications. Briefly, the cell pellet was suspended in isolation buffer (250 mM sucrose, 1 mM EGTA, 10 mM HEPES and 5 g/L BSA, pH 7.5) and was then centrifuged at 500 × g for 2 min. The supernatant was discarded and the remaining pellet was suspended in 500 μL of isolation buffer. The cell suspension was homogenized in a tight-fitting Potter homogenizer (Teflon pestle). After centrifugation at 1500 × g for 10 min, the supernatant was kept on ice. The pellet was homogenized and centrifuged as described above. The two supernatants were pooled and centrifuged at 10,000 × g for 10 min. The resulting mitochondrial pellet was washed with 100 μL of BSA-free isolation buffer. Mitochondrial proteins were extracted according to the different separation procedures tested and protein content was determined with RC DC Protein Assay kit (Bio-Rad, Hercules, CA, USA).

Following fibroblast mitochondria isolation, three different procedures were used for protein characterization (Fig. 1).

2.4. Two-dimensional electrophoresis (2DE)

Two-dimensional electrophoresis (2DE) was performed as previously reported with minor modifications [6]. In brief, 250 μg of mitochondrial protein extract were diluted to 250 μL with a rehydration solution containing 8 M urea, 2 M thiourea, 2% CHAPS, 0.5% IPG buffer (pH 3–10 NL), 0.2% DTT and loaded on 13 cm IPG strips (pH 3–10 NL; GE Healthcare). Isoelectric separation was performed using the following focusing program: 12 h at 50 mV (rehydration), 2 h at 150 V (gradient), 1 h at 500 V (gradient), 1 h at 1000 V (gradient) and 3 h at 8000 V ("step-n-hold"). After IEF separation, the gel strips were applied on top of a sodium dodecyl sulfate-polyacrylamide gel electrophoresis (SDS-PAGE) gel (12.5%) and proteins were separated at 200 V constant current until the bromophenol blue front reached the bottom of the gel. At least three gels were generated for further gel image analysis and mass spectrometry characterization. The gels were stained with Coomassie Colloidal-G250, and scanned with Gel Doc XR (Bio-Rad). The "Spot Detection Wizard" function in PdQuest software (v8.0.1, Bio-Rad) was used to automate the process of finding protein spots and based on the automated spot detection results, misdetected spots were added or removed using visual inspection. All detected spots were manually excised for in-gel digestion.

2.5. One-dimensional gel electrophoresis (SDS-PAGE)

Seventy micrograms of protein were incubated with SDS sample buffer (10% (w/v) sodium dodecyl sulfate (SDS), 50 mM Tris–HCl (pH 6.8), 4% glycerol, bromophenol blue (w/v)) for 5 min at 100 °C. Samples were loaded onto Laemli gel (12.5%) and electrophoresis was carried out at a constant voltage of 200 V current until the bromophenol blue front reached the bottom of the gel. Gels were stained with Coomassie Colloidal-G250. Following image acquisition, the entire gel lanes were manually cut out lengthwise and divided into 16 gel slices for in-gel digestion.

2.6. In-gel/band protein digestion

Annotated spots or bands were in-gel digested with trypsin. Briefly, gel pieces were washed three times with 25 mM ammonium bicarbonate/50% acetonitrile and further dried in a Speed-Vac. Then, 10 μL of 25 μg/mL modified bovine trypsin (ABSciex, USA) in 25 mM ammonium bicarbon ate was added to the dried gel pieces and the samples were incubated overnight at 37 °C. Extraction of tryptic peptides was performed by the addition of 10% formic acid/50% acetonitrile, which was repeated three times, followed by dryness in a Speed-Vac. 2DE spot's tryptic peptides were resuspended in acetonitrile/formic acid solution and mixed (1:1) with a matrix consisting of α-cyano-4-hydroxycinnamic acid (5 mg in 1 ml of 50% acetonitrile/0.1% trifluoracetic acid). Aliquots of samples were spotted onto MALDI sample target plates. SDS-PAGE bands tryptic peptides were resuspended in acetonitrile/trifluoroacetic acid (5% and 0.01%, respectively) for reverse-phase LC separation.

2.7. In-solution protein digestion

Seventy micrograms of protein was used for digestion which was performed as described previously [15]. Protein was precipitated by incubation with cold acetone (6 volumes) overnight (−20 °C) and centrifuged at 20,000 × g for 30 min. Pellet samples were then ressuspended with triethyl ammonium bicarbonate buffer (TEAB) (1 M, pH 8.5) and RapiGest (Waters) to a final concentration of 0.5 M and 0.1%, respectively. Samples were reduced with 5 mM tris(2-carboxyethyl) phosphine (TCEP) for 1 h at 37 °C and alkylated with 10 mM S-methyl methanethiosulfonate (MMTS) for 10 min at room temperature. Two micrograms of trypsin were added to each sample and the digestion was performed for 18 h at 37 °C. Samples were dried in a Speed-Vac and then ressupended for peptide separation in high pH reverse phase separation.

Please cite this article as: R. Ferreira, et al., Talanta (2013), http://dx.doi.org/10.1016/j.talanta.2013.04.026

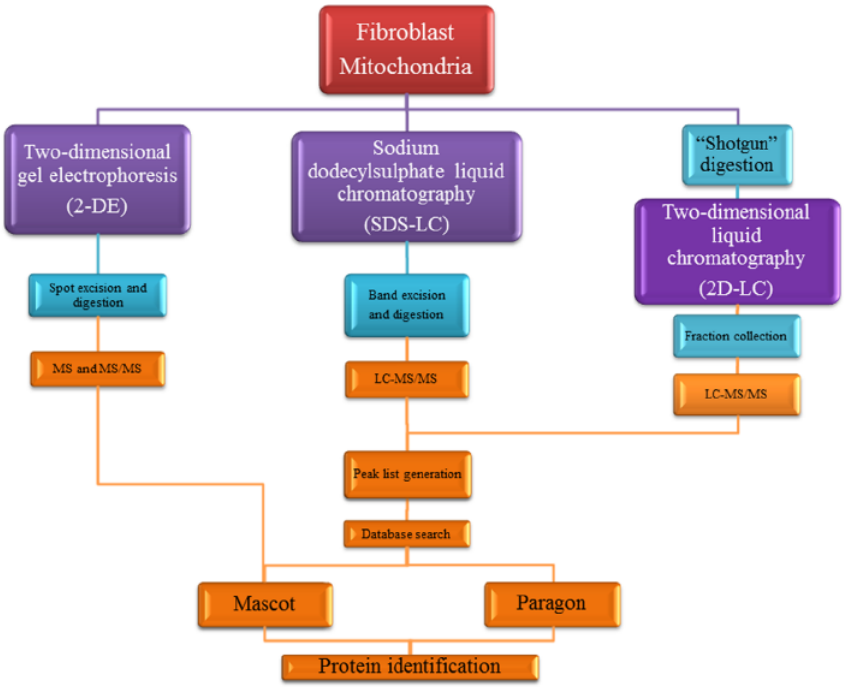

Fig. 1. Schematic flowchart of the methodological strategy used in this study.

2.8. LC analysis

2.8.1. High pH reverse-phase separation

Tryptic peptides from in-solution digestions were ressuspended in buffer A (72 mM triethylamine (TEA), 52 mM acetic acid in H_2O, pH 10). Sample loading was performed at 200 μL/min with buffers A and B (72 mM TEA, 52 mM acetic acid in ACN, pH 10) (98% A: 2% B). After 5 min of sample loading and washing, peptide fractionation was performed in a C18 Acclaim PP2 column (3 μm, 2.1 × 150 mm; Dionex) with linear gradient to 50% B over 35 min followed by a 100% B step. Sixteen fractions were collected, evaporated, and ressuspended in 2% ACN, 0.1% TFA for acidic reverse phase separation.

2.8.2. Reverse-phase separation

Collected tryptic peptide fractions and SDS-PAGE band tryptic peptides were separated as previously described [13]. Briefly, peptides loaded onto a C18 pre-column (5 μm particle size, 5 mm, from Dionex) connected to a PepMap100 C18 (150 mm × 75 μm I.D., 3 μm particle size) column. The flow rate was set at 300 nL/min. The mobile phases A and B were 2% ACN, 0.1% TFA in water and 95% ACN, 0.045% TFA, respectively. The gradient was started at 10 min and ramped to 60% B till 50 min and 100% B at 55 min and retained at 100% B till 65 min. The column was equilibrated with solvent A for 20 min before the next sample was injected. The separation was monitored at 214 nm using a UV detector (Dionex/LC Packings, Sunnyvale, CA) equipped with a 3 nL flow cell. Using the micro-collector Probot (Dionex/LC Packings) and, after a lag time of 5 min, peptides eluting from the capillary column were mixed with a continuous flow of α-CHCA matrix solution (270 nL/min, 2 mg/mL in 70% ACN/0.3% TFA and internal standard Glu-Fib at 15 fmol) were directly deposited onto the LC-MALDI plates at 12 s intervals for each spot (150 nL/fraction). For every separation run, 208 fractions in total were collected.

2.9. Gel-based ID

Peptide mass spectra were obtained on a MALDI-TOF/TOF mass spectrometer (4800 Proteomics Analyzer, Applied Biosystems, Foster City, CA, USA) in the positive ion reflector mode. Spectra were obtained in the mass range between 700 and 4500 Da with ca. 1500 laser shots. For each sample spot, a data dependent acquisition method was created to select the six most intense peaks, excluding those from the matrix, trypsin autolysis, or acrylamide peaks, for subsequent MS/MS data acquisition. Trypsin autolysis peaks were used for internal calibration of the mass spectra, allowing a routine mass accuracy of better than 20 ppm. Spectra were processed and analyzed by the Global Protein Server Workstation (Applied Biosystems, Foster City, CA, USA), which uses internal Mascot (v2.1.1. Matrix Science Ltd., UK) software for searching the peptide mass fingerprints and MS/MS data. Searches were performed against the Swissprot (release 010111) under all taxonomic categories and the following parameters: (i) two missed cleavages by trypsin; (ii) mass tolerance of precursor ions 25 ppm and product ions 0.3 Da; and (iii) oxidation of methionine and cysteine, phosphorylation (tyrosine, serine and tryptophan) and acetylation (N-terminal and lysine) as variable modifications.

2.10. LC-based ID

Acquisition parameters were similar to Gel-based ID using Glu-Fib for internal calibration. MS/MS data was searched against the Swissprot non-redundant protein database (peptide fragment fingerprinting) (UniProt release 2012-04) with paragon algorithm from ProteinPilot™ software (version 4.0, Applied Biosystems, USA) and Mascot (v2.1.1. Matrix Science Ltd., UK). In order to confidently compare results from Paragon and Mascot, peak lists from 2D-LC and SDS-LC experiments were generated using the Peaks2Mascot (4000 series explorer, Absciex) using the following parameter settings were used: mass range from 65 Da to the precursor mass −35 Da, minimal S/N ratio of 10, minimal area

Please cite this article as: R. Ferreira, et al., Talanta (2013), http://dx.doi.org/10.1016/j.talanta.2013.04.026

of 100, maximum of 20 peaks per 100 Da and maximum of 60 peaks per precursor. For Paragon, the search parameters were the following: enzyme (trypsin), special factor (gel-based ID in case of SDS-LC), species (*Homo sapiens*), ID focus (biological modification), detected protein threshold: more than 1 (99%) and running the false discovery rate (FDR). Cut-off score value for accepting protein identification for Paragon® was a ProteoScore of 1.3 (95% confidence). For Mascot (v2.1.1. Matrix Science Ltd., UK), the search parameters were: species (*Homo sapiens*); two missed cleavages by trypsin; mass tolerance of precursor ions 25 ppm and product ions 0.3 Da; and oxidation of methionine, cysteine oxidation (methylthio, in case of SDS-LC), phosphorylation (tyrosine, serine and tryptophan) and acetylation (N-terminal and lysine) as variable modifications. A reverse decoy database was created for all Swissprot to calculate the FDR. Protein identifications were considered reliable when: (i) at least two peptides *per* protein were detected with individual ion score for each peptide greater than or equal to 30; (ii) a single peptide hit with a minimum individual score of 30 (confidence level of at least 95%) and a minimum sequence tag of four amino acids (five consecutive peaks in the MS/MS spectrum).

2.11. Gene network pathway analysis

Gene Ontology (GO) annotations were analyzed with the PANTHER Protein Classification System (database version 6.1, http://www.pantherdb.org/) to identify functional annotations. Protein lists identified by gel- and gel-free methodologies were mapped onto biological pathways that were significantly represented. To evaluate the protein cellular location, the protein lists were analyzed using the ClueGo plugin from cytoscape (v2.8.3) and applying the Gene Ontology database (release date, September 19, 2012). Ontology selection as enrichment analysis was done by right-side hyper-geometric statistic test and its probability value was corrected by the bonferroni method [16].

2.12. Western blotting

Twenty micrograms were subjected to electrophoresis by 15% SDS-PAGE gel, followed by blotting onto a nitrocellulose membrane (Hybond-ECL; Amersham Pharmacia Biotech, Buckinghamshire, UK). After blotting, non-specific binding was blocked with 5% (w/v) non-fat dry milk in TTBS (Tris-buffered saline (TBS) with Tween 20) and the membrane was incubated with primary antibodies diluted 1:1000 in 5% (w/v) non-fat dry milk in TTBS (anti-mitofilin ab48139 and anti-ATPB ab14730 from Abcam; anti-vimentin V6630 from Sigma) for 2 h at room temperature, washed and incubated with secondary horseradish peroxidase-conjugated antibody (GE Healthcare). The blots were developed by using enhanced chemiluminescence detection system (Amersham Pharmacia Biotech, Buckinghamshire, UK) according to manufacturer's instructions, followed by exposure to X-ray films (Kodak Biomax Light Film, Sigma, St. Louis, USA). The protein bands on films were visualized using a GelDoc XR (Bio-Rad) and quantified by Quantity One® Imaging software (v4.6.3, Bio-Rad).

3. Results and discussion

In the present study, a systematic evaluation of mitochondrial proteome was performed using different methodological approaches, gel- and gel free-based. Proteomic analyses were conducted on freshly isolated fibroblast mitochondria from human skin biopsies. The purity of mitochondria was assessed by immunoblotting, which demonstrated the enrichment of mitochondrial proteins (mitofilin, ATP synthase subunit beta) in the mitochondrial fraction isolated from fibroblasts and depletion of the abundant cytosolic protein vimentin (Scheme 1). The yield of isolated mitochondria from this kind of cells is low (approximately 300 μg of mitochondrial proteins per 10^7 cells), which is in accordance with the previously reported by Palmfeldt et al. [1].

Proteomic characterization of isolated mitochondria was performed using three different approaches: 2DE, SDS-LC and 2D-LC, coupled with mass spectrometry for protein identification (Fig. 1). Technical replicates were considered in all the analysis performed (replicates of $n=3$), with an overlapping average of $76 \pm 11\%$ for SDS-LC and 2D-LC. Mascot and Paragon were used for MS/MS processing data. Protein false discovery rates were estimated by the use of reverse decoy sequences during database searching, which were relatively low (≤0.01%). As can be seen in Table 1, a higher number of identified proteins was achieved with SDS-LC approach. Combining data retrieved from all these approaches and search methods, a total of 696 non-redundant proteins were identified, using Swiss-Prot as protein ID search database (Table S1). Based upon the human genome, approximately 2000–2500 mitochondrial proteins are predicted; however, just over 600 have been identified at the protein level (reviewed by [4]). Nonetheless, according to Hermann and Hermann [17], this number can be very variable, ranging from 600 to 4000 proteins. In mitochondria isolated from cultured fibroblasts, more than 1000 distinct proteins were identified using IPI database for protein ID search [1]. The lower number of mitochondrial proteins identified in our study might be justified, at least partially, by the database used for protein ID. Whereas Swiss-Prot database follows a gene-centric approach, with one gene represented by one master protein sequence, IPI database represent a cluster of entries from the source databases and consider splice isoforms as separate entities [18]. Regarding MS/MS processing data with Mascot, an overlap of 14% was observed between the proteins identified by the three different methods (Fig. 2A). When Mascot and Paragon were combined for LC-MS/MS protein identification, this overlap increases to 19% (Fig. 2B). For 2D-LC, 73 unique proteins were identified using Mascot and 136 using Paragon, whereas an overlapping of 42% was noticed (Fig. 2C). In the case of SDS-LC, the same tendency was observed with higher unique proteins identified with Paragon analysis (104 vs. 47). Nevertheless, an overlap of 74% was observed for this methodological approach (Fig. 2D). Using a multidimensional approach combining IEF and LC and comparing with SDS-LC, McDonald et al. [8] only verified an overlap of 9% for inner mitochondria membrane proteins. In the present study, an overlap of 71% was observed when a multidimensional approach combining high pH RP with a standard low pH RP (2D-LC approach) and SDS-LC were used (Fig. 2B), which could be explained by the higher separation efficiency and a more homogenous distribution of eluted peptides [9,19,20]. Interestingly, the intersection between data from the methodological approaches and MS/MS search algorithms for protein ID studied highlights the consistency of 2DE using Mascot in the number of identified proteins. Despite the higher sample amount needed for 2DE, approximately 6-fold greater than the required for

Table 1
Summary of the number of proteins identified by each method and algorithm.

Approach	Proteins identified				Total proteins	
	Replicate A		Replicate B			
	Mascot	ProteinPilot	Mascot	ProteinPilot	Mascot	ProteinPilot
2DE	298	N/A	293	N/A	298	N/A
2D-LC	168	265	172	266	186	284
SDS-LC	417	522	467	513	486	535

Please cite this article as: R. Ferreira, et al., Talanta (2013), http://dx.doi.org/10.1016/j.talanta.2013.04.026

SDS-LC and 2D-LC, more distinct proteins were identified using these last two approaches. Indeed, multidimensional chromatographic procedures allow the identification of lower abundant proteins due, at least in part, to the higher resolution underlying the chromatographic separation [19]. However, 2DE allows to distinguish multiple forms of proteins with differences in molecular mass, isoelectric point or PTMs (e.g. phosphorylation) that induces changes in the molecular mass and p*I*, potentially detected

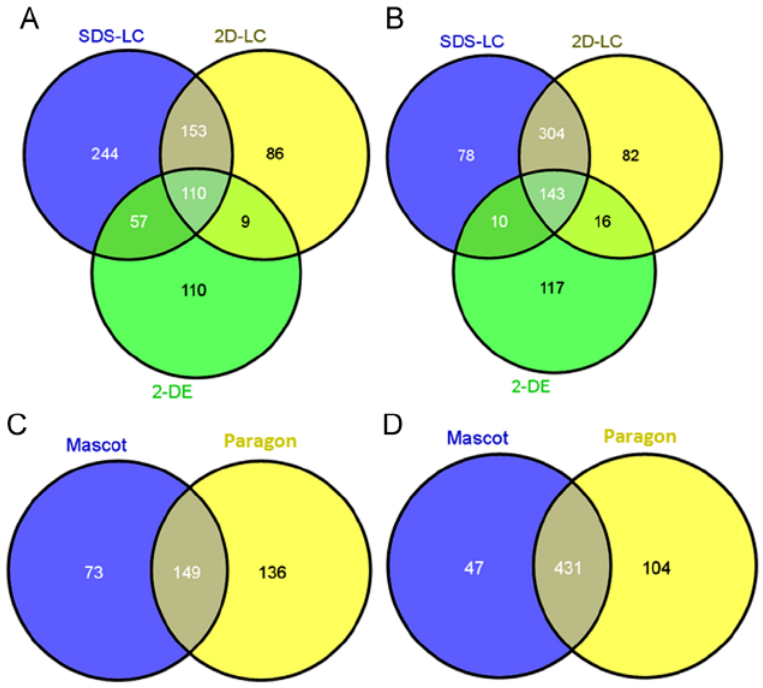

Fig. 2. Venn diagrams indicating the distribution of unique proteins identified using 2D-LC, SDS-LC and 2DE approaches. (A) refers to the distribution of proteins between separation approaches using Mascot. (B) refers to the distribution of proteins between separation approaches combining Mascot and Paragon for SDS-LC and 2D-LC. (C) and (D) refer to the distribution of unique proteins identified with Mascot and Protein Pilot using 2D-LC and SDS-LC, respectively.

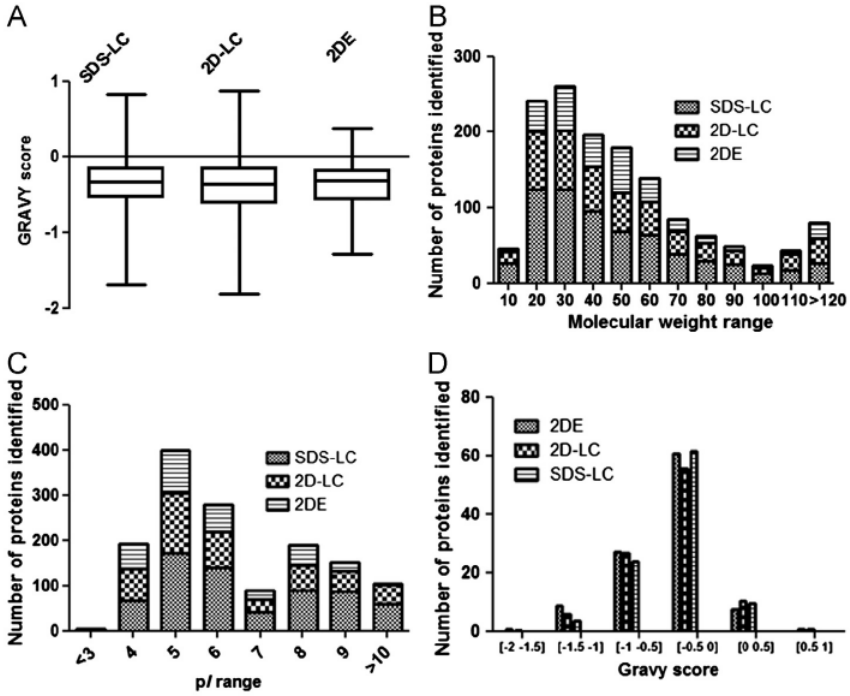

Fig. 3. Gravy score (A), molecular weight (B) and p*I* (C) distribution of identified proteins as a function of protein separation approaches. (D) refers to the Gravy score distribution of unique proteins as a function of separation approaches.

Please cite this article as: R. Ferreira, et al., Talanta (2013), http://dx.doi.org/10.1016/j.talanta.2013.04.026

by deviations in gel's protein migration [21]. In 2DE and SDS-LC some mitochondrial proteins were identified in more than one spot/band (e.g. ATP synthase subunits alpha and beta and aconitate hydratase), evidencing their high turnover [22,23], not distinguished with 2D-LC approach.

In order to search for a potential methodological impact in the intrinsic properties of identified proteins, GRAVY score, molecular weight and isoelectric point were analyzed (Fig. 3). In overall, p*I*, mass and GRAVY score calculations presented a similar tendency among the three methodological approaches used. However, when unique proteins were analyzed in terms of GRAVY score, SDS-LC approach retrieved more hydrophobic proteins (positive GRAVY score) though in relatively lower amount (Fig. 3D). With gel-based approaches involving SDS-PAGE, a significantly higher number of hydrophobic peptides can be recovered [20], which is particularly relevant for mitochondria analysis considering the approximately 33% of membrane proteins (Scheme 2). Even with the optimization of solubilization and running conditions, 2DE does not permit the analysis of proteins with extreme masses (>200 kDa and <10 kDa), hydrophobicity and p*I* [4,21]. 2D-LC and SDS-LC allow the enrichment of proteins with molecular weight below 30 kDa and of basic proteins with p*I* values above 8 (Fig. 3). Independent of the methodological approach chosen, the predominance in mitochondria of hydrophilic proteins (Fig. 3A) with 20–50 kDa (Fig. 3B) and p*I* 5–6 and 8–9 (Fig. 3C) was noticed.

In order to perform cellular localization analysis of all identified proteins, ClueGo [16] was used to determine the association strength between the Gene Ontology (GO) terms. As can be depicted in Scheme 2, most of the identified proteins belong to different organelle compartments related to mitochondria (around 54%). The contribution of ribosomal proteins is also worth of note, justified by the close association between mitochondrial outer membrane and cytosolic ribosomes [24]. Moreover, it has been estimated that approximately 15% of mitochondrial proteins have dual-localization [25]. Regarding biological function, the top three clusters to which these proteins belong are, according to PANTHER bioinformatic tool [26], metabolic processes, cellular processes and transport (Fig. 4) further supported by BiNGO analysis [27] (Scheme 3). Considering the molecular function, the top three clusters retrieved by PANTHER analysis are catalytic activity, structural molecule activity and binding. Despite the similar cluster distribution trend among the three methodological approaches, with 2DE we observed an enrichment of proteins belonging to developmental and cell cycle clusters, and presenting catalytic and antioxidant activity.

In order to get a deep characterization of mitochondria proteome, phosphorylated and acetylated peptides were searched (Fig. 5). These PTMs are known to regulate mitochondrial processes leading to energy production and the synthesis of mitochondrially-encoded subunits of OXPHOS complexes. Though their role in the regulation of cellular events has been known for decades, the extent of this mode of regulation is just beginning to be disclosed for which has contributed the availability of high-resolution mass spectrometers and the development of powerful tools for high scale analysis of PTMs [28,29]. In overall, 101 distinct peptides corresponding to 49 different proteins were found

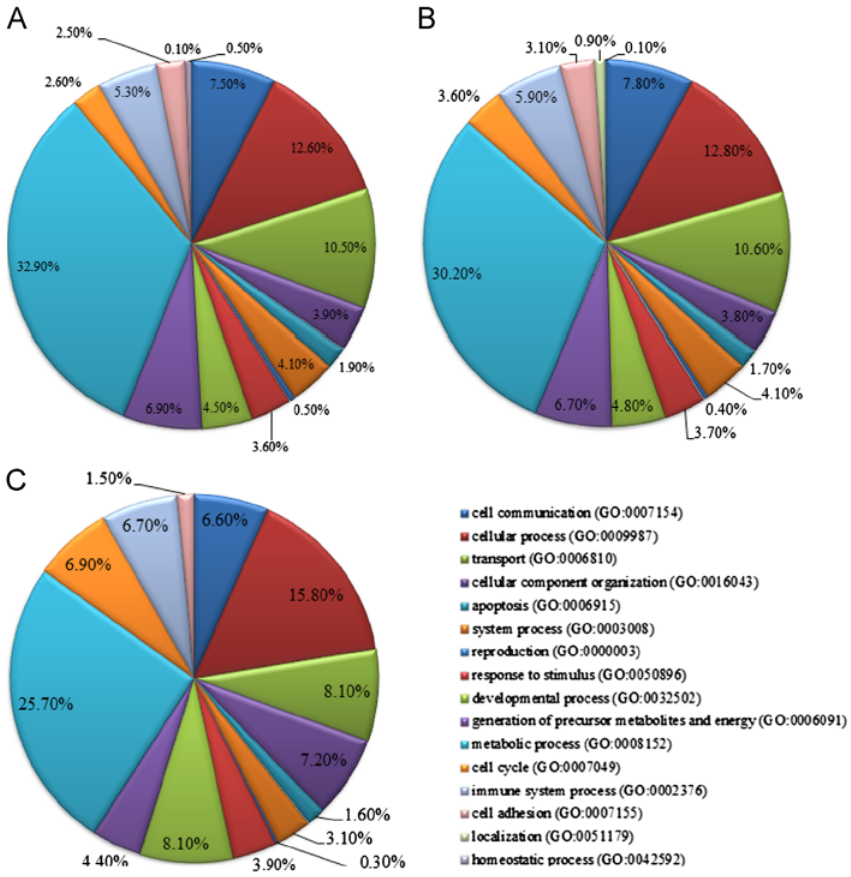

Fig. 4. Pie chart showing the biological function category for the identified proteins using SDS-LC (A), 2D-LC (B) and 2DE (C).

Please cite this article as: R. Ferreira, et al., Talanta (2013), http://dx.doi.org/10.1016/j.talanta.2013.04.026

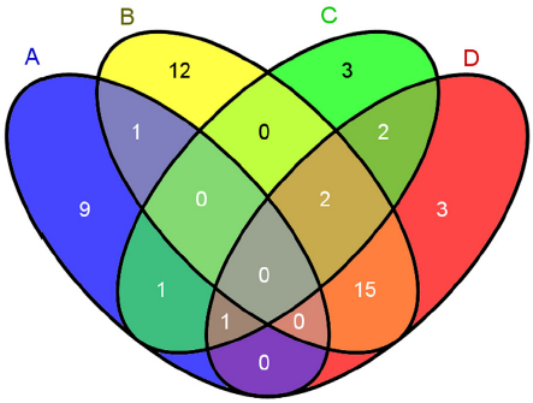

Fig. 5. Venn diagram indicating the distribution of phosphorylated and acetylated proteins using 2D-LC combined with Mascot (A), SDS-LC with Mascot (B), 2D-LC with Paragon (C) and SDS-LC with Paragon (D).

acetylated and phosphorylated. From these, 13 and 30 unique modified proteins were identified by 2D-LC and SDS-LC, respectively. PTMs search with both algorithms produced a similar number of phosphorylated/acetylate peptides identified. Despite the high number of modifications already annotated in Swiss-Prot for the identified mitochondrial proteins, only one peptide from the membrane-associated progesterone receptor component 1 (PGRC1_HUMAN) was found phosphorylated by 2D-LC. Using PTMs Peptide Scanner (v1.0, 〈http://pps.biocuckoo.org/〉), we detected new acetylated sites in the 78 kDa glucose-regulated protein (GRP78_HUMAN; in Lys^{585}), in cytoskeleton-associated protein 4 (CKAP4_HUMAN; in Lys^{551}) and in electron transfer flavoprotein subunit beta (ETFB_HUMAN; in Lys^{201}), using either 2D-LC or SDS-LC and Mascot or Paragon. No enrichment procedures were used for the analysis of acetylation and phosphorylation in mitochondrial proteins, which justify the relatively low number of identified peptides with these PTMs.

4. Conclusion

Data highlight the impact of protein separation methods for protein characterization in mitochondria isolated from cultured fibroblasts. Despite the higher number of identified proteins retrieved by SDS-LC, 2DE allows the identification of a significant content of unique proteins and so might be seen as a complementary approach in a deeper protein profiling of mitochondria. These gel-based approaches are promising when quantitative strategies using metabolic labeling (SILAC) is meant. Nevertheless, 2DE requires a considerable amount of starting protein quantity, which is a limitation for the analysis of mitochondria isolated from samples as cultured fibroblasts. Overall, the results show the power of integrating different separation technologies and protein identification algorithms and suggest caution in making the assumption that similar findings are expected using different separation methods and algorithms.

Acknowledgments

This work was supported by the Portuguese Foundation for Science and Technology (FCT) [Grant number PEst-C/QUI/UI0062/2011]. We thank John Cottrell (Matrix Science Ltd.) for helping with searching data in Mascot.

Appendix A. Supporting information

Supplementary data associated with this article can be found in the online version at http://dx.doi.org/10.1016/j.talanta.2013.04.026.

References

[1] J. Palmfeldt, S. Vang, V. Stenbroen, C.B. Pedersen, J.H. Christensen, P. Bross, N. Gregersen, Proteome Sci. 7 (2009) 20.
[2] N. Gregersen, J. Hansen, J. Palmfeldt, J. Inherit. Metab. Dis. 35 (2012) 715–726.
[3] R.J.T. Rodenburg, J. Inherit. Metab. Dis. 34 (2011) 283–292.
[4] Y. Jiang, X. Wang, J. Hematol. Oncol. 5 (2012) 11.
[5] M.F. Lopez, S. Melov, Circ. Res. 90 (2002) 380–389.
[6] H. Rocha, R. Ferreira, J. Carvalho, R. Vitorino, C. Santa, L. Lopes, N. Gregersen, L. Vilarinho, F. Amado, J. Proteomics 75 (2011) 221–228.
[7] C.B. Pedersen, Z. Zolkipli, S. Vang, J. Palmfeldt, M. Kjeldsen, V. Stenbroen, S.P. Schmidt, R.J.A. Wanders, J.P.N. Ruiter, F. Wibrand, I. Tein, N. Gregersen, J. Inherit. Metab. Dis. 33 (2010) 211–222.
[8] T. McDonald, S. Sheng, B. Stanley, D. Chen, Y. Ko, R.N. Cole, P. Pedersen, J.E. Van Eyk, Mol. Cell. Proteomics 5 (2006) 2392–2411.
[9] B. Manadas, V.M. Mendes, J. English, M.J. Dunn, Expert Rev. Proteomics 7 (2010) 655–663.
[10] B. Manadas, J.A. English, K.J. Wynne, D.R. Cotter, M.J. Dunn, Proteomics 9 (2009) 5194–5198.
[11] P.C. Wright, J. Noirel, S.Y. Ow, A. Fazeli, Theriogenology 77 (2012) 738–765, e752.
[12] B. De Paepe, J. Smet, A. Vanlander, S. Seneca, W. Lissens, L. De Meirleir, M. Vandewoestyne, D. Deforce, R.J. Rodenburg, R. Van Coster, Pediatr. Res. 72 (2012) 232–240.
[13] U. Spiekerkoetter, J. Inherit. Metab. Dis. 33 (2010) 527–532.
[14] M.A. Schwab, S. Kolker, L.P. van den Heuvel, S. Sauer, N.I. Wolf, D. Rating, G.F. Hoffmann, J.A. Smeitink, J.G. Okun, Clin. Chem. 51 (2005) 151–160.
[15] R. Vitorino, S. Guedes, B. Manadas, R. Ferreira, F. Amado, J. Proteomics 75 (2012) 5140–5165.
[16] G. Bindea, B. Mlecnik, H. Hackl, P. Charoentong, M. Tosolini, A. Kirilovsky, W.H. Fridman, F. Pages, Z. Trajanoski, J. Galon, Bioinformatics 25 (2009) 1091–1093.
[17] P.C. Herrmann, E.C. Herrmann, Methods Mol. Biol. 823 (2012) 265–277.
[18] P.J. Kersey, J. Duarte, A. Williams, Y. Karavidopoulou, E. Birney, R. Apweiler, Proteomics 4 (2004) 1985–1988.
[19] L. Antberg, P. Cifani, M. Sandin, F. Levander, P. James, J. Proteome Res. 11 (2012) 2644–2652.
[20] D. Botelho, M.J. Wall, D.B. Vieira, S. Fitzsimmons, F. Liu, A. Doucette, J. Proteome Res. 9 (2010) 2863–2870.
[21] T. Rabilloud, M. Chevallet, S. Luche, C. Lelong, J. Proteomics 73 (2010) 2064–2077.
[22] A.I. Padrao, R.M.P. Ferreira, R. Vitorino, R.M.P. Alves, M.J. Neuparth, J.A. Duarte, F. Amado, BBA-Bioenergetics 2011 (1807) 1106–1113.
[23] R.M. Alves, R. Vitorino, P. Figueiredo, J.A. Duarte, R. Ferreira, F. Amado, J. Gerontol. Ser. A Biol. Sci. Med. Sci. 65 (2010) 832–842.
[24] N.P. Chappell, P.N. Teng, B.L. Hood, G. Wang, K.M. Darcy, C.A. Hamilton, G.L. Maxwell, T.P. Conrads, J. Proteome Res. 11 (2012) 4605–4614.
[25] S.E. Calvo, V.K. Mootha, Annu. Rev. Genomics Hum. Genet. 11 (2010) 25–44.
[26] P.D. Thomas, A. Kejariwal, M.J. Campbell, H. Mi, K. Diemer, N. Guo, I. Ladunga, B. Ulitsky-Lazareva, A. Muruganujan, S. Rabkin, J.A. Vandergriff, O. Doremieux, Nucleic Acids Res. 31 (2003) 334–341.
[27] S. Maere, Bioinformatics 21 (2005) 3448–3449.
[28] E.C. Koc, H. Koc, Biochim. Biophys. Acta 2012 (1819) 1055–1066.
[29] X. Zhao, I.R. Leon, S. Bak, M. Mogensen, K. Wrzesinski, K. Hojlund, O.N. Jensen, Mol. Cell. Proteomics 10 (2011) 1–14.
[30] S. Maere, K. Heymans, M. Kuiper, Bioinformatics 21 (2005) 3448–3449.

CHAPTER IV

Study 4 - Characterization of mitochondrial proteome in a severe case of ETF-QO deficiency.

JOURNAL OF PROTEOMICS 75 (2011) 221–228

available at www.sciencedirect.com

www.elsevier.com/locate/jprot

Characterization of mitochondrial proteome in a severe case of ETF-QO deficiency

H. Rocha[a,b,*], R. Ferreira[b], J. Carvalho[b], R. Vitorino[b], C. Santa[b], L. Lopes[a], N. Gregersen[c], L. Vilarinho[a], F. Amado[b]

[a] I&D unit, Genetics Department, Medical Genetics Center Jacinto Magalhães of National Institute of Health Ricardo Jorge, Porto, Portugal
[b] Chemical Department, Aveiro University, Aveiro, Portugal
[c] The Research Unit for Molecular Medicine, Aarhus University Hospital and Faculty of Health Sciences, Skejby Sygehus, Aarhus, Denmark

ARTICLE INFO

Available online 7 May 2011

Keywords:
Fatty acid oxidation
Mitochondrial proteome
Mitochondrial dysfunction
MADD

ABSTRACT

Multiple acyl-CoA dehydrogenase deficiency (MADD) is a mitochondrial fatty acid oxidation disorder caused by mutations that affect electron transfer flavoprotein (ETF) or ETF:ubiquinone oxidoreductase (ETF-QO) or even due to unidentified disturbances of riboflavin metabolism. Besides all the available data on the molecular basis of FAO disorders, including MADD, the pathophysiological mechanisms underlying clinical phenotype development, namely at the mitochondrial level, are poorly understood. In order to contribute to the elucidation of these mechanisms, we isolated mitochondria from cultured fibroblasts, from a patient with a severe MADD presentation due to ETF-QO deficiency, characterize its mitochondrial proteome and compare it with normal controls. The used approach (2-DE-MS/MS) allowed the positive identification of 287 proteins in both patient and controls, presenting 35 of the significant differences in their relative abundance. Among the differentially expressed are proteins associated to binding/folding functions, mitochondrial antioxidant enzymes as well as proteins associated to apoptotic events. The overexpression of chaperones like Hsp60 or mitochondrial Grp75, antioxidant enzymes and apoptotic proteins reflects the mitochondrial response to a complete absence of ETF-QO.

Our study provides a global perspective of the mitochondrial proteome plasticity in a severe case of MADD and highlights the main molecular pathways involved in its pathogenesis.

1. Introduction

β-oxidation represents an important source of energy for the body during times of fasting and metabolic stress, providing carbon substrates for gluconeogenesis and contributing with electrons to the respiratory chain for energy production. Mitochondrial fatty acid oxidation (FAO) is predominantly responsive for the oxidation of fatty acids of carbon length 20 or less, while peroxisomes are more relevant for oxidation of longer chain fatty acids. To carry out the process, about 25

Abbreviations: FAO, fatty acid oxidation; MADD, multiple acyl-CoA dehydrogenase deficiency; ETF, electron transfer flavoprotein; ETF-QO, ETF:ubiquinone oxidoreductase; GAPDH, glyceraldehyde-3-phosphate dehydrogenase; ETFB, electron transfer flavoprotein subunit beta; ATPB, ATP synthase subunit beta.

* *Corresponding author at:* I&D Unit, Genetics Department, Medical Genetics Center Jacinto Magalhães, National Institute of Health Ricardo Jorge, Praça Pedro Nunes, 88, 4099-028 Porto, Portugal. Tel.: +351 226070341; fax: +351 226070399.
E-mail address: hugo.rocha@insa.min-saude.pt (H. Rocha).

1874-3919/$ – see front matter © 2011 Elsevier B.V. All rights reserved.
doi:10.1016/j.jprot.2011.04.025

enzymes and specific transport proteins are involved, and defects in several of them have been shown to cause disease in humans [1].

FAO disorders are a group of inherited metabolic disorders that encompass at least twelve distinct enzyme or transporter deficiencies, including multiple acyl-CoA-dehydrogenase deficiency (MADD). MADD, also known as glutaric aciduria type II, is an autosomal recessive disorder that affects fatty acids, amino acid and choline metabolism, caused by defects in one of the two flavoproteins — electron transfer flavoprotein (ETF) and ETF:ubiquinone oxidoreductase (ETF-QO), or in yet unidentified disturbances of riboflavin metabolism [2]. In mitochondria, ETF receives electrons from several mitochondrial flavin-containing dehydrogenases, which are transferred to ETF-QO and subsequently passed to ubiquinone in the respiratory chain [1]. ETF exists in the mitochondrial matrix as a heterodimer of alpha and beta subunits, while ETF-QO is a monomer embedded in the inner mitochondrial membrane [3].

Clinically, MADD patients can be classified into three phenotypic groups: neonatal onset forms, with (type I) or without (type II) congenital abnormalities and late onset forms (type III). Neonatal onset forms are characterized by severe nonketotic hypoglycemias, hypotonia, failure to thrive, hyperammonemia, metabolic acidosis and usually lead to an early death. Patients with late onset forms manifest proximal myopathy, hepatomegaly and encephalopathy usually associated with intermittent vomiting, abdominal pain, hypoglycemia and lethargy [2]. Many of these patients, mainly type III, are responsive to riboflavin treatment, with a positive effect on symptoms and metabolic control [4]. If not treated, these disorders result in significant morbidity and mortality.

MADD is caused by mutations in the genes *ETFA*, *ETFB* and *ETFDH*, which encode ETF alpha subunit, ETF beta subunit and ETF-QO, being *ETFDH* mutations reported to be associated to riboflavin responsive patients [4,5]. It was also observed some degree of genotype/phenotype correlation, with null mutations associated to neonatal onset forms, while mutations leading to the retention of some residual activity of the enzyme are usually associated to type III phenotype [6,7].

Pathophysiological mechanisms leading to clinical phenotype are believed to rely mainly on the resulting energy deficiency. However, the true extent on the effect of these deficiencies on mitochondrial/cellular functions is still unknown [1,8,9]. In order to better characterize the degree of mitochondrial dysfunction in MADD, and so contribute to the elucidation of the molecular mechanisms underlying the disease development, we studied the mitochondrial proteome in cultured fibroblasts from a patient with severe MADD due to ETF-QO defect. The genetic and phenotypic specificity as well as the rarity of this metabolic disorder, justify the analysis of each case individually with the aim of definitive therapeutic strategies.

2. Materials and methods

2.1. Samples

Fibroblasts from a MADD patient and control individuals (n = 3) were analyzed. The patient had a severe form of MADD as result of ETF-QO deficiency. The patient was the 4th son of a consanguineous couple, who had two previous brothers that died in the neonatal period and presented in the first 14 h of life hyporeactivity, generalized hypotonia along side with hypoglycemia and metabolic acidosis. This patient died at day 5. Laboratory investigations reveal high blood ammonia, generalized aminoaciduria and an organic acid profile compatible with MADD. β-oxidation studies in fibroblasts reveal a decreased palmitate and octanoic oxidation in comparison to controls (5% and 3% respectively). The molecular studies revealed the presence of the mutation p.X618QextX14 in homozygous form in the *ETFDH* gene.

Control fibroblasts were obtained from individuals with no apparent related disease. Control fibroblasts were used, anonymously, after each subject/legal guardian gave written informed consent.

2.2. Cell culture

Skin fibroblasts were grown in Ham F10 nutrient mixture supplemented with 10% fetal calf serum, 2 mmol/L glutamine, 1% penicillin, streptomycin and fungizone, in 75 cm^2 culture flasks. Ten culture flasks from each sample were grown to confluence before mitochondria isolation.

2.3. Mitochondria isolation

Isolation of mitochondria from the cell pellet was performed at 4 °C according to Schwab et al. [10] with minor modifications. Briefly, the cell pellet was suspended in isolation buffer (250 mM sucrose, 1 mM EGTA, 10 mM HEPES and 5 g/L BSA pH 7.5) and was then centrifugated at 500 *g* for 2 min. The supernatant was discarded and the remaining pellet was suspended in isolation buffer. The cell suspension was homogenized in a tight-fitting Potter homogenizer (Teflon pestle). After centrifugation at 1500 *g* for 10 min, the supernatant was kept on ice. The pellet was homogenized and centrifuged as described above. The two supernatants were pooled and centrifuged at 10,000 *g* for 10 min. The resulting mitochondrial pellet was washed with BSA-free isolation buffer. Protein content was determined with RC DC Protein Assay kit (Bio-Rad, Hercules, CA, USA).

2.4. Two-dimensional electrophoresis

Two-dimensional electrophoresis (2-DE) was performed as previously reported with minor modifications [11]. In brief, 200 μg proteins of mitochondrial fractions from patient and control cells were diluted to 250 μL with a rehydration solution containing 8 mol/L urea, 2 M thiourea, 2% CHAPS, 0.5% IPG buffer (pH 3–10), 0.2% DTT and loaded on 13 cm IPG strips (pH 3–10 NL; GE Healthcare) with a pH 3–10. Isoelectric separation was performed using the following focusing program: 12 h at 50 mV in rehydration, 2 h at 150 V (gradient), 1 h at 500 V (gradient), 1 h at 1000 V (gradient) and 3 h at 8000 V ("step-n-hold"). After IEF separation, the gel strips were applied on top of a sodium dodecyl sulfate–polyacrylamide gel electrophoresis (SDS–PAGE) gel (12×14 cm; 12.5%) and proteins were separated at 200 V constant current until the bromophenol blue front reached the bottom of the gel. The gels were stained with Coomassie Colloidal, and scanned with GelDoc XR (Bio-Rad). The PdQuest

version 8.0.1 (Bio-Rad) was used to assemble the matchset from biological replicates that had correlation coefficient values of at least 0.8. Saturated spots were excluded from analysis. Following automatic spot detection, matching was performed.

The spot boundary tool was applied to detect large spots. The patterns in sections of the gels in appropriate magnification were checked and spots were added manually to the master gel to allow matching unique spots present in the individual gels. The spot quantity table containing all matched spots was generated. The quantity of missing spots was estimated by the software. The means of logarithmic ratio method was used for normalization. The means of log ratio method of normalization calculates the normalization factor of a gel by calculating the means of all log ratios (log spot quantity of gel/log spot quantity of master gel) of all matched spots (master gel–gel). The quantity table was exported to a spreadsheet of SPSS (v15.0) and submitted to statistical analyses.

2.5. *Tryptic digestion and MS analysis*

For tryptic digestion of proteins from 2-DE gels, spots were excised manually from the gel, destained with 25 mM ammonium bicarbonate/50% acetonitrile, and dried in vacuum concentrator (SpeedVac, Thermo Savant). The dried gel pieces were rehydrated with 25 μL of 10 μg/mL trypsin in 50 mM ammonium bicarbonate and digested overnight at 37 °C. Tryptic peptides were dried in a vacuum concentrator and resuspended in 10 μL of a 50% acetonitrile/0.1% formic acid solution. MS was performed on a matrix-assisted laser desorption/ionization-time-of-flight MALDI-TOF/TOF mass spectrometer (4800 Proteomics Analyzer, Applied Biosystems, Foster City, CA, USA) in the positive ion reflector mode. A data-dependent acquisition method was created to select the six most intense peaks in each sample spot spectrum for subsequent tandem mass spectrometry (MS/MS) data acquisition, excluding those from the matrix, due to trypsin autolysis or acrylamide peaks. Mass spectra were externally calibrated with auto-digest peaks of trypsin (MH^+: 842.5, 2211.42 Da).

Spectra were processed and analyzed by the Global Protein Server Workstation (Applied Biosystems, Foster City, CA, USA), which uses internal MASCOT software (v2.0 Matrix Science, London, UK) on searching the peptide mass fingerprints and MS/MS data. Swiss-Prot nonredundant protein sequence database (21, January 2008) was used for all searches under *Human*. Database search parameters are as follows: carbamidomethylation and propionamide of cysteine as a variable modification as well as oxidation of methionine, and the allowance for up to two missed tryptic cleavages. The peptide mass tolerance was 30 ppm and fragment ion mass tolerance was 0.3 Da. Positive identifications were accepted up to 95% of confidence level. All proteins were identified by more than four unique peptides to minimize false-positive identification.

2.6. *Western blotting*

Equal amounts of proteins from each individual analyzed were subjected to electrophoresis by 15% SDS–PAGE gel, followed by blotting onto a nitrocellulose membrane (Hybond-ECL; Amersham Pharmacia Biotech, Buckinghamshire, UK). After blotting, non-specific binding was blocked with 5% (w/v) nonfat dry milk in TTBS (Tris-buffered saline (TBS) with Tween 20) and the membrane was incubated with primary antibodies diluted 1:1000 in 5% (w/v) nonfat dry milk in TTBS (anti-ETFB, abcam ab73986; anti ETFDH, abcam ab91508; anti-GAPDH, ab9485 or anti-ATPB, abcam ab14730) for 2 h at room temperature, washed and incubated with secondary horseradish peroxidase-conjugated antibody (GE Healthcare). The blots were developed by using enhanced chemiluminescence detection system (Amersham Pharmacia Biotech, Buckinghamshire, UK) according to manufacturer's instructions, followed by exposure to X-ray films (Kodak Biomax Light Film, Sigma, St. Louis, USA). The protein bands on films were visualized using a GelDoc XR (Bio-Rad) and quantified by Quantity One® Imaging software (v4.6.3, Bio-Rad).

2.7. *Spectrophotometric assay of ATP synthase activity*

The activity of respiratory chain complex V was measured according to Simon et al. [12]. The phosphate produced by hydrolysis of ATP reacts with ammonium molybdate in the presence of reducing agents to form a blue-color complex, the intensity of which is proportional to the concentration of phosphate in solution. Oligomycin was used as an inhibitor of mitochondrial ATPase activity.

2.8. *Statistics*

Optical densities of differentially expressed protein spots in 2-DE maps were exported from PdQuest to SPSS (v15.0). Significant differences between MADD patient and control individuals were evaluated with the Wilcoxon test for all data (i.e., immunoblotting, ATP synthase activity and 2-DE OD values). A p value < 0.05 was considered significant.

3. Results

3.1. *Analysis of ETF-QO expression*

The expression of ETF-QO was analyzed by Western blotting in isolated mitochondria from replicates of three independent cultivated fibroblasts from all individuals analyzed. As it can be seen in Fig. 1, this dehydrogenase was not detected in MADD patient's blot, which indicates its absence in mitochondria.

3.2. *Global mitochondrial proteome profiling from cultivated fibroblasts*

In order to detect the proteome alterations induced by a severe deficiency of ETF-QO, we have performed a 2-DE analysis of mitochondria isolated from cultivated human skin fibroblasts from control individuals and from a patient with ETF-QO deficiency, presenting a severe phenotype of MADD. Replicates of two independent cultivation studies were analyzed for all individuals included in this study.

The analysis of 2-DE gels allowed the identification of 516 ± 54 spots in the patient vs 400 ± 70 in the control individuals (Fig. 2),

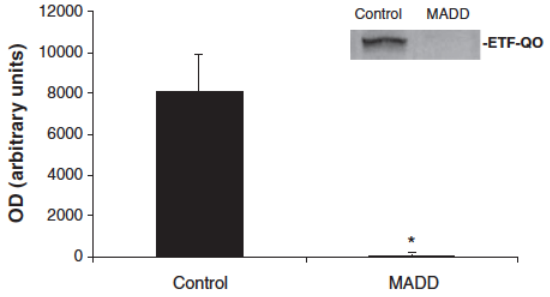

Fig. 1 – Western blotting analysis of ETF-QO (69 kDa) expression in control individuals and MADD patient. A representative panel of immunoblots is presented above the histogram. Results represent the mean ± STDESV of the patient and control (n = 3) replicates of three independent analyses. (*p < 0.05).

having extracted a total of 381 and 333 spots, respectively, to be analyzed by MALDI-TOF/TOF. A total of 287 different proteins were positively identified in all samples analyzed with a confidence degree over 95% (supporting information Table S1). Cluster analysis assigned these proteins, according to Gene Ontology Annotation Database (GOA) and literature data [13], to 11 different functional classes including metabolism (62 proteins), structure (56), signal transduction (43), protein binding/folding (29), DNA/RNA/protein synthesis (25), redox (21), OXPHOS (17), transport (14), proteolysis (12), apoptosis (11), adhesion (7) and five proteins of unknown function (Figure S1). Given the central role of mitochondria in fibroblasts metabolism, it was not surprising that the most significant cluster of identified proteins (21%) was involved in amino acids, lipids and carbohydrate metabolism.

3.3. *Profiling of differentially expressed mitochondrial proteins between MADD patient and control individuals*

Comparative analysis of controls and MADD patient's mitochondria 2-DE spot profile with PdQuest software revealed 35 proteins differentially expressed (Fig. 2 and Table 1). Ten of these proteins belong to the functional cluster "metabolism". Indeed, MADD-related lower OD values were noticed for proteins from fatty acid oxidation and nitrogen and glutamate metabolism, whereas glycolytic proteins were up-regulated. A decrease of more than 3-fold was noticed for the medium-chain specific acyl-CoA dehydrogenase (spot 11) in the patient. The subunit alpha of electron transfer flavoprotein (spot 20), which together with ETF-QO serves as a short electron transfer pathway [14], was also down-regulated in MADD patient. Besides the higher levels in fibroblasts from MADD patient of cathepsino D (spot 27) and of the signaling proteins 14-3-3 protein epsilon (spot 31), Rho GDP-dissociation inhibitor (spot 32) and cofilin-1 (spot 33), the following MADD-induced proteins were up-regulated: the chaperones HSP90 (spot 21), HSP beta-1 (spot 26), the mitochondrial HSP60 (spot 24), Stress-70 protein (spot 23), and redox proteins like MnSOD (spot 30) and glutathione S-transferase (spot 28). For instance, the levels of the mitochondrial Stress-70 protein, also known as 75 kDa glucose-regulated protein, were more than 4-fold higher in the patient compared to the controls. Also noteworthy is the 6-fold increase of the signaling protein Girdin (spot 35) in MADD patient.

All the proteins differentially expressed among controls and MADD patient were further analyzed with the PANTHER (Protein Analysis Though Evolutionary Relationships) classification system (http://www.pantherdb.org) to identify biological processes and molecular functions distinctly regulated due to the presence or absence of ETF-QO in mitochondria. According to this bioinformatic tool, 42% of the differentially

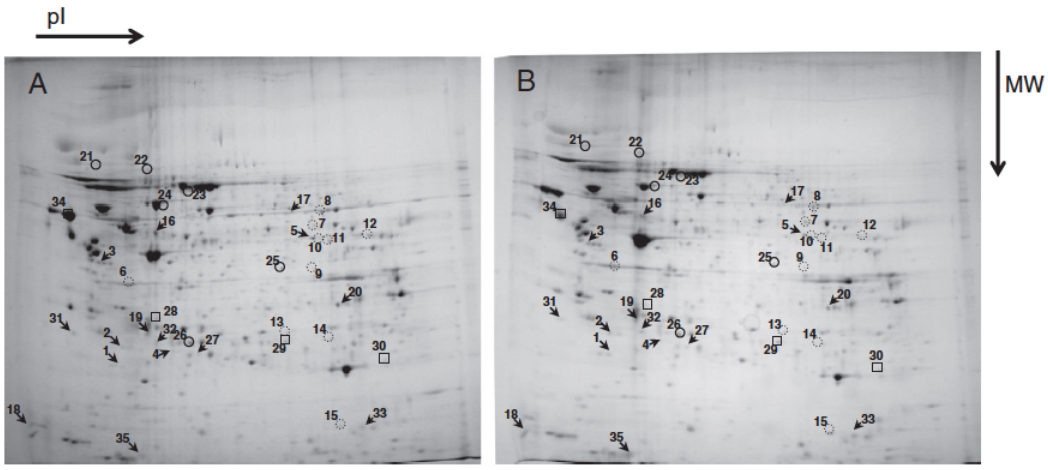

Fig. 2 – Two-dimensional electrophoresis of control (A) and MADD patient (B) mitochondria. Differential expressed proteins are marked with a number with correspondence in Table 1. To better compare A and B maps, proteins belonging to the functional clusters metabolism (namely GAPDH (spot 6), short-chain specific acyl-CoA dehydrogenase (spot 9), medium-chain specific acyl-CoA dehydrogenase (spot 11) and 3-ketoacyl-CoA thiolase (spot 12)) are highlighted with dotted circles, whereas the ones from protein binding/folding (like Stress 70 protein (spot 23) and Hsp60 (spot 24)) and redox (gluthatione S-transferase (spot 28), peroxiredoxin-6 (spot 29), MnSOD (spot 30) and protein disulfide isomerase A3 (spot 34)) are identified with linear circles and squares, respectively. Proteins from other functional clusters are identified with arrows.

expressed proteins belong to "metabolic process" and 12% to "generation of precursor metabolites and energy". The other significant biological process represented was "immune system process" (Figure S2-A). Regarding molecular function, most of these proteins have "catalytic activity" (45%) and "binding function" (21%) (Figure S2-B). The most significant alterations related to ETF-QO deficit analyzed in this study seem to be related with enzymes involved in metabolic pathways and with proteins with binding functions like the chaperone ones.

To validate the expression pattern observed in this study, ETFB, ATPB and GAPDH were selected for further characterization by Western blotting. Replicates of three independent samples from each individual were analyzed. As can be seen in Fig. 3A, the Western blot results were in agreement with 2-DE data (Table 1), with lower OD values observed in MADD patients for ETFB and ATPB. An opposite behavior was noticed for GAPDH. The MADD-related down-regulation of ATP synthase subunits alpha and beta (spots 16 and 17) was also related with the decreased activity of this respiratory chain complex (Fig. 3B), highlighting the bioenergetics' impairment induced by *ETFDH* mutations.

4. Discussion

In the present study we have used a mass spectrometry based proteomic approach to characterize the mitochondrial dysfunction in fibroblasts from a patient with a severe phenotype of MADD, which most probably represents the edge of mitochondrial abnormalities found in FAO disorders. Besides the overall characterization of mitochondrial dysfunction, new data in the field of FAO disorders is provided.

The studied patient is homozygous for a mutation (p.X618QextX14) in the *ETFDH* gene, that results in a protein extension of 13 amino acids at C′ terminal. It is known that this mutation leads to a severe clinical and biochemical phenotype, although its effect on protein stability and translocation was unknown. We looked for the protein in the mitochondrial and extramitochondrial fractions by Western blotting and we did not detect the mutated protein inside the mitochondria (Fig. 1). Although not affecting the typical *mitochondrial targeting sequence*, located at the N′ terminal [15,16], the mutation most probably impairs protein folding, compromising its translocation into mitochondria The mitochondrial adaptation to this ETF-QO absence was analyzed in skin fibroblasts, whose utility to study mitochondrial imbalance and cellular stress was previously shown [17]. By 2-DE-MS/MS, we successfully identified 287 distinct mitochondrial proteins (Table S1) from different functional clusters (Figures S1 and S2), more than previously achieved in studies where mitochondria from fibroblasts were analyzed [17]. When the mitochondrial proteome profile from this MADD patient was compared with controls, 35 proteins presenting significant expression differences were identified. These proteins were allocated to several functional clusters, with particular relevance to protein binding/folding, metabolism and apoptosis (Table 1).

Several mitochondrial proteins belonging to the functional cluster *protein binding/folding*, particularly mitochondrial chaperones like Stress-70 protein, a 75 kDa glucose-regulated protein from the HSP70 family, or HSP60 was overexpressed in the patient. This probably reflects a cellular response to counteract the instability/disorganization inside the mitochondria, with the consequent activation of the mitochondrial protein quality control (PQC) system [18,19]. Since mutated ETF-QO is not imported into the mitochondria, there is no direct activation of the mtURP (mitochondrial Unfolded Protein Response) as generally observed when abnormal mitochondrial proteins (due to missense mutations) accumulate inside the organelle, triggering an all set of mitochondrial pathological features [20–23].

Concomitantly with chaperones' up-regulation, our data suggest a metabolic adaptation to EFT-QO absence, with an overall down-regulation of several enzymes involved in β-oxidation (spots 9, 11 and 12; Table 1). These results are in agreement with the patient biochemical phenotype, which evidenced an accumulation of several β-oxidation intermediate metabolites, due to a secondary inhibition of the FAD-dependent enzymes [3]. Subunits alpha and beta of ATP synthase were down-regulated in the patient, which were paralleled by the impaired activity of this respiratory chain complex (Fig. 3B). These results are in agreement with previous findings from Song and collaborators [24]. These authors demonstrated the MADD-related limitation in proton translocation through mitochondrial ATP synthase, limiting oxygen consumption and therefore ATP synthesis, which most probably contributes to the clinical phenotype development.

Impairment of mitochondrial metabolism, namely fatty acid oxidation, may result in oxidative stress [25], increasing reactive oxygen species (ROS) generation. ROS production may arise due to an inability to channel reducing equivalents into the respiratory chain, as well as by other sites, including ETF/ETF-QO complex and by mitochondrial FAO deficient enzymes [22]. In this sense, MADD-induced ROS production might explain the overexpression of the mitochondrial antioxidant enzymes like MnSOD, glutathione-S-transferase and peroxiredoxin-6 observed in the present study (Fig. 2 and Table 1). However, in severe presentations of MADD, ROS production most probably overwhelms ROS neutralization capacity, leading to severe mitochondrial dysfunction and ultimately to apoptosis. Several apoptotic proteins were overexpressed in the patient, reflecting not only the high degree of mitochondrial dysfunction that impairs cell viability, but also the central role of this organelle in apoptotic pathways. The huge expression of Diablo homolog protein (spot 1; Fig. 2 and Table 1), a key player in caspase activity process, generally precludes apoptosis activation [26]. Other proteins recently found involved in the activation of apoptosis were also identified in higher levels in MADD patient, including Girdin, an AKT phosphorylation enhancer [27,28].

Several glycolytic enzymes (GAPDH, alpha enolase, phosphoglycerate mutase and triosephosphate isomerase) were found to be overexpressed in the patient, probably reflecting the metabolic shift to glycolysis in order to compensate ATP deficiency due to mitochondrial dysfunction. However, GAPDH elevation in mitochondrial fraction can also be associated to apoptotic events. According to Huand and collaborators [29], the translocation of GAPDH to mitochondria plays a pivotal role in apoptosis. These authors demonstrated that mitochondrial respiratory chain inhibitors induce GAPDH overexpression, promoting its accumulation, increasing protein insolubility

Table 1 – Proteins differentially expressed in mitochondria isolated from controls and MADD patient's fibroblasts identified in 2-DE gels ($p < 0.05$). Spot numbers have correspondence in 2-DE maps. Biological function assigned to each protein is in accordance with Gene Ontology Annotation Database (GOA). Patient/control ratio represents the mean ± STDESV of OD values obtained from PdQuest analysis of replicates of two independent 2-DE maps from patient and controls (n = 3).

Spot number	Protein name	Accession number	Protein MW	Protein PI	Patient/control ratio	Functional cluster
1	Diablo homolog, mitochondrial OS=*Homo sapiens* GN=DIABLO PE=1 SV=1	DBLOH_HUMAN	27113.7	5.68	+4.7±2.0	Apoptosis
2	Translationally-controlled tumor protein OS=*Homo sapiens* GN=TPT1 PE=1 SV=1	TCTP_HUMAN	19582.6	4.84	+2.2±0.6	Apoptosis/transport
3	40S ribosomal protein SA OS=*Homo sapiens* GN=RPSA PE=1 SV=4	RSSA_HUMAN	32833.4	4.79	+1.9±0.4	DNA/RNA/protein biosynthesis
4	Zinc finger protein 462 OS=*Homo sapiens* GN=ZNF462 PE=1 SV=3	ZN462_HUMAN	284505.9	7.53	+2.1±0.4	DNA/RNA/protein biosynthesis
5	Elongation factor Tu, mitochondrial OS=*Homo sapiens* GN=TUFM PE=1 SV=2	EFTU_HUMAN	49510.2	7.26	−2.0±0.4	DNA/RNA/protein biosynthesis
6	Glyceraldehyde-3-phosphate dehydrogenase OS=*Homo sapiens* GN=GAPDH PE=1 SV=3	G3P_HUMAN	36030.4	8.57	+3.5±2.3	Metabolism
7	Alpha-enolase OS=*Homo sapiens* GN=ENO1 PE=1 SV=2	ENOA_HUMAN	47139.3	7.01	+3.3±1.0	Metabolism
8	Glutamate dehydrogenase 1, mitochondrial OS=*Homo sapiens* GN=GLUD1 PE=1 SV=2	DHE3_HUMAN	61359.2	7.66	−2.0±0.5	Metabolism
9	Short-chain specific acyl-CoA dehydrogenase, mitochondrial OS=*Homo sapiens* GN=ACADS PE=1 SV=1	ACADS_HUMAN	44268.8	8.13	−2.7±0.3	Metabolism
10	Isocitrate dehydrogenase [NADP] cytoplasmic OS=*Homo sapiens* GN=IDH1 PE=1 SV=2	IDHC_HUMAN	46629.5	6.53	+2.3±0.6	Metabolism
11	Medium-chain specific acyl-CoA dehydrogenase, mitochondrial OS=*Homo sapiens* GN=ACADM PE=1 SV=1	ACADM_HUMAN	46558.6	8.61	−3.6±0.4	Metabolism
12	3-ketoacyl-CoA thiolase, mitochondrial OS=*Homo sapiens* GN=ACAA2 PE=1 SV=2	THIM_HUMAN	41897.6	8.32	−2.2±0.6	Metabolism
13	Phosphoglycerate mutase 1 OS=*Homo sapiens* GN=PGAM1 PE=1 SV=2	PGAM1_HUMAN	28785.8	6.67	+4.5±2.8	Metabolism
14	Triosephosphate isomerase OS=*Homo sapiens* GN=TPI1 PE=1 SV=2	TPIS_HUMAN	26652.7	6.45	+2.2±0.5	Metabolism
15	Peptidyl-prolyl cis-trans isomerase A OS=*Homo sapiens* GN=PPIA PE=1 SV=2	PPIA_HUMAN	18000.9	7.68	+5.0±0.7	Metabolism
16	ATP synthase subunit beta, mitochondrial OS=*Homo sapiens* GN=ATP5B PE=1 SV=3	ATPB_HUMAN	56524.6	5.26	−4.1±0.4	OXPHOS
17	ATP synthase subunit alpha, mitochondrial OS=*Homo sapiens* GN=ATP5A1 PE=1 SV=1	ATPA_HUMAN	59713.6	9.16	−1.5±0.3	OXPHOS
18	Cytochrome b5 OS=*Homo sapiens* GN=CYB5A PE=1 SV=2	CYB5_HUMAN	15320.5	4.88	+2.7±0.8	OXPHOS
19	NADH dehydrogenase [ubiquinone] flavoprotein 2, mitochondrial OS=*Homo sapiens* GN=NDUFV2 PE=1 SV=2	NDUV2_HUMAN	27374.0	8.22	+2.1±0.5	OXPHOS
20	Electron transfer flavoprotein subunit alpha, mitochondrial OS=*Homo sapiens* GN=ETFA PE=1 SV=1	ETFA_HUMAN	35057.6	8.62	−2.2±0.2	OXPHOS
21	Heat shock protein HSP 90-beta OS=*Homo sapiens* GN=HSP90AB1 PE=1 SV=4	HS90B_HUMAN	83212.1	4.97	+1.6±0.2	Protein binding/folding
22	78 kDa glucose-regulated protein OS=*Homo sapiens* GN=HSPA5 PE=1 SV=2	GRP78_HUMAN	72288.4	5.07	+2.1±0.7	Protein binding/folding
23	Stress-70 protein, mitochondrial OS=*Homo sapiens* GN=HSPA9 PE=1 SV=2	GRP75_HUMAN	73634.8	5.87	+4.5±2.7	Protein binding/folding
24	60 kDa heat shock protein, mitochondrial OS=*Homo sapiens* GN=HSPD1 PE=1 SV=2	CH60_HUMAN	61016.4	5.7	+2.1±0.3	Protein binding/folding
25	28S ribosomal protein S22, mitochondrial OS=*Homo sapiens* GN=MRPS22 PE=1 SV=1	RT22_HUMAN	41254.4	7.7	+3.4±0.3	Protein binding/folding
26	Heat shock protein beta-1 OS=*Homo sapiens* GN=HSPB1 PE=1 SV=2	HSPB1_HUMAN	22768.5	5.98	+1.6±0.1	Protein binding/folding
27	Cathepsin D OS=*Homo sapiens* GN=CTSD PE=1 SV=1	CATD_HUMAN	44523.6	6.1	+2.1±0.5	Proteolysis
28	Glutathione S-transferase P OS=*Homo sapiens* GN=GSTP1 PE=1 SV=2	GSTP1_HUMAN	23341.0	5.43	+2.3±0.8	Redox
29	Peroxiredoxin-6 OS=*Homo sapiens* GN=PRDX6 PE=1 SV=3	PRDX6_HUMAN	25019.2	6	+1.7±0.2	Redox

Table 1 (continued)

Spot number	Protein name	Accession number	Protein MW	Protein PI	Patient/ control ratio	Functional cluster
30	Superoxide dismutase [Mn], mitochondrial OS=*Homo sapiens* GN=SOD2 PE=1 SV=2	SODM_HUMAN	24706.6	8.35	+1.5±0.2	Redox
31	14-3-3 protein epsilon OS=*Homo sapiens* GN=YWHAE PE=1 SV=1	1433E_HUMAN	29155.4	4.63	+3.7±0.9	Signal transduction
32	Rho GDP-dissociation inhibitor 1 OS=*Homo sapiens* GN=ARHGDIA PE=1 SV=3	GDIR1_HUMAN	23192.7	5.02	+2.0±0.3	Signal transduction
33	Cofilin-1 OS=*Homo sapiens* GN=CFL1 PE=1 SV=3	COF1_HUMAN	18490.7	8.22	+2.3±0.4	Signal transduction
34	Protein disulfide-isomerase A3 OS=*Homo sapiens* GN=PDIA3 PE=1 SV=4	PDIA3_HUMAN	56746.8	5.98	−1.9±0.2	Signal transduction/redox
35	Girdin OS=*Homo sapiens* GN=CCDC88A PE=1 SV=2	GRDN_HUMAN	215909.1	5.9	+6.0±4.1	Signal transduction/transport

and ultimately leading to apoptotic cell death [29]. The presence and accumulation of GAPDH inside the mitochondria and the related induction of pro-apoptotic mitochondrial membrane permeabilization, a decisive event of the intrinsic pathway to apoptosis, was also reported [30].

In overall, our study provides a global perspective of the mitochondrial proteome plasticity in a severe case of MADD and highlights the main molecular pathways involved in its pathogenesis. The overexpression of chaperones, antioxidant enzymes and apoptotic proteins reflects the mitochondrial response to a complete absence of ETF-QO.

Supplementary materials related to this article can be found online at doi:10.1016/j.jprot.2011.04.025.

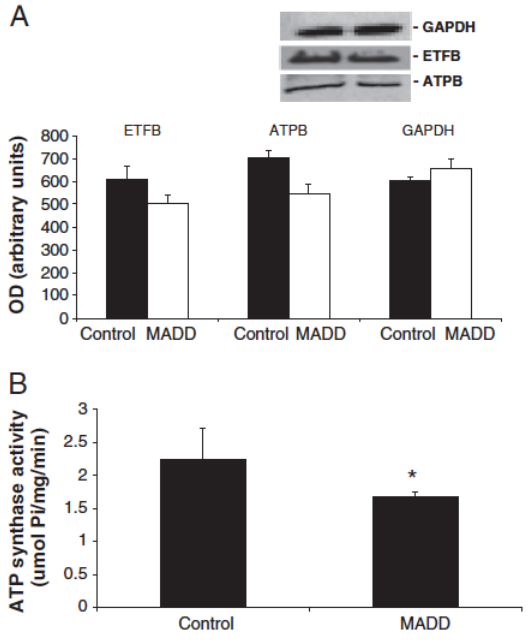

Fig. 3 – Comparison of relative quantities of ETFB (28 kDa), ATPB (52 kDa) and GAPDH (37 kDa) in mitochondrial fractions from controls and MADD patient determined by Western blotting analysis. Representative panels of immunoblots are presented above the histogram (A). Activity of ATP synthase, spectrophotometrically assessed, in controls and MADD patient (B). Results represent the mean ± STDESV of the patient and control (n=3) replicates of three independent analyses. (*$p<0.05$).

REFERENCES

[1] Houten SM, Wanders RJ. A general introduction to the biochemistry of mitochondrial fatty acid beta-oxidation. J Inherit Metab Dis 2010;33:469–77.
[2] Vockley J, Whiteman DA. Defects of mitochondrial beta-oxidation: a growing group of disorders. Neuromuscul Disord 2002;12:235–46.
[3] Gregersen N, Olsen RK. Disease mechanisms and protein structures in fatty acid oxidation defects. J Inherit Metab Dis 2010;33(5):547–53.
[4] Olsen RK, Olpin SE, Andresen BS, Miedzybrodzka ZH, Pourfarzam M, Merinero B, et al. ETFDH mutations as a major cause of riboflavin-responsive multiple acyl-CoA dehydrogenation deficiency. Brain 2007;130:2045–54.
[5] Gregersen N, Andresen BS, Corydon MJ, Corydon TJ, Olsen RK, Bolund L, et al. Mutation analysis in mitochondrial fatty acid oxidation defects: exemplified by acyl-CoA dehydrogenase deficiencies, with special focus on genotype-phenotype relationship. Hum Mutat 2001;18:169–89.
[6] Olsen RK, Andresen BS, Christensen E, Bross P, Skovby F, Gregersen N. Clear relationship between ETF/ETFDH genotype and phenotype in patients with multiple acyl-CoA dehydrogenation deficiency. Hum Mutat 2003;22:12–23.
[7] Liang WC, Ohkuma A, Hayashi YK, Lopez LC, Hirano M, Nonaka I, et al. ETFDH mutations, CoQ10 levels, and respiratory chain activities in patients with riboflavin-responsive multiple acyl-CoA dehydrogenase deficiency. Neuromuscul Disord 2009;19:212–6.
[8] Gregersen N, Andresen BS, Pedersen CB, Olsen RK, Corydon TJ, Bross P. Mitochondrial fatty acid oxidation defects—remaining challenges. J Inherit Metab Dis 2008;31:643–57.
[9] Bennett MJ. Pathophysiology of fatty acid oxidation disorders. J Inherit Metab Dis 2009;33(5):533–7.
[10] Schwab MA, Kolker S, van den Heuvel LP, Sauer S, Wolf NI, Rating D, et al. Optimized spectrophotometric assay for the completely activated pyruvate dehydrogenase complex in fibroblasts. Clin Chem 2005;51:151–60.
[11] Vitorino R, Ferreira R, Neuparth M, Guedes S, Williams J, Tomer KB, et al. Subcellular proteomics of mice gastrocnemius and soleus muscles. Anal Biochem 2007;366:156–69.

[12] Simon N, Morin C, Urien S, Tillement JP, Bruguerolle B. Tacrolimus and sirolimus decrease oxidative phosphorylation of isolated rat kidney mitochondria. Br J Pharmacol 2003;138:369–76.
[13] Ferreira R, Vitorino R, Alves RM, Appell HJ, Powers SK, Duarte JA, et al. Subsarcolemmal and intermyofibrillar mitochondria proteome differences disclose functional specializations in skeletal muscle. Proteomics 2010;10:3142–54.
[14] Watmough NJ, Frerman FE. The electron transfer flavoprotein:ubiquinone oxidoreductases. Biochim Biophys Acta 2010;1797:1910–6.
[15] Baker MJ, Frazier AE, Gulbis JM, Ryan MT. Mitochondrial protein-import machinery: correlating structure with function. Trends Cell Biol 2007;17:456–64.
[16] Stojanovski D, Johnston AJ, Streimann I, Hoogenraad NJ, Ryan MT. Import of nuclear-encoded proteins into mitochondria. Exp Physiol 2003;88:57–64.
[17] Palmfeldt J, Vang S, Stenbroen V, Pedersen CB, Christensen JH, Bross P, et al. Mitochondrial proteomics on human fibroblasts for identification of metabolic imbalance and cellular stress. Proteome Sci 2009;7:20.
[18] Tatsuta T, Langer T. Quality control of mitochondria: protection against neurodegeneration and ageing. EMBO J 2008;27:306–14.
[19] Voos W. Mitochondrial protein homeostasis: the cooperative roles of chaperones and proteases. Res Microbiol 2009;160:718–25.
[20] Schmidt SP, Corydon TJ, Pedersen CB, Vang S, Palmfeldt J, Stenbroen V, et al. Toxic response caused by a misfolding variant of the mitochondrial protein short-chain acyl-CoA dehydrogenase. J Inherit Metab Dis 2011;34(2):465–75.
[21] Gregersen N, Bross P, Vang S, Christensen JH. Protein misfolding and human disease. Annu Rev Genomics Hum Genet 2006;7:103–24.
[22] Gregersen N, Bross P. Protein misfolding and cellular stress: an overview. Methods Mol Biol 2010;648:3–23.
[23] Schmidt SP, Corydon TJ, Pedersen CB, Bross P, Gregersen N. Misfolding of short-chain acyl-CoA dehydrogenase leads to mitochondrial fission and oxidative stress. Mol Genet Metab 2010;100:155–62.
[24] Song Y, Selak MA, Watson CT, Coutts C, Scherer PC, Panzer JA, et al. Mechanisms underlying metabolic and neural defects in zebrafish and human multiple acyl-CoA dehydrogenase deficiency (MADD). PLoS One 2009;4:e8329.
[25] Wallace DC. A mitochondrial paradigm of metabolic and degenerative diseases, aging, and cancer: a dawn for evolutionary medicine. Annu Rev Genet 2005;39:359–407.
[26] Verhagen AM, Ekert PG, Pakusch M, Silke J, Connolly LM, Reid GE, et al. Identification of DIABLO, a mammalian protein that promotes apoptosis by binding to and antagonizing IAP proteins. Cell 2000;102:43–53.
[27] Dan HC, Sun M, Kaneko S, Feldman RI, Nicosia SV, Wang HG, et al. Akt phosphorylation and stabilization of X-linked inhibitor of apoptosis protein (XIAP). J Biol Chem 2004;279:5405–12.
[28] Kizhakkayil J, Thayyullathil F, Chathoth S, Hago A, Patel M, Galadari S. Modulation of curcumin-induced Akt phosphorylation and apoptosis by PI3K inhibitor in MCF-7 cells. Biochem Biophys Res Commun 2010;394:476–81.
[29] Huang J, Hao L, Xiong N, Cao X, Liang Z, Sun S, et al. Involvement of glyceraldehyde-3-phosphate dehydrogenase in rotenone-induced cell apoptosis: relevance to protein misfolding and aggregation. Brain Res 2009;1279:1–8.
[30] Tarze A, Deniaud A, Le Bras M, Maillier E, Molle D, Larochette N, et al. GAPDH, a novel regulator of the pro-apoptotic mitochondrial membrane permeabilization. Oncogene 2007;26:2606–20.

CHAPTER V

Study 5 – Unravelling the impact of long-chain 3-hydroxyacyl-CoA dehydrogenase deficiency on mitochondrial proteome.
(submitted)

Unravelling the impact of long-chain 3-hydroxyacyl-CoA dehydrogenase deficiency on mitochondrial proteome

Rocha H[1,2], Ferreira R[2], Almeida V[2], Vitorino R[2], Lopes L[1], Martins E[3], Nogueira C[1,] Leão-Teles E[4], Amado F[5] and Vilarinho L[1].

[1] Newborn Screening, Metabolism and Genetics Unit, Genetics Department, National Institute of Health Ricardo Jorge, Porto, Portugal;
[2] QOPNA, Department of Chemistry, University of Aveiro, Aveiro, Portugal
[3] Unidade de doenças metabólicas, Centro Hospitalar do Porto, Porto, Portugal
[4] Unidade doenças metabólicas, Hospital Pediátrico Integrado, Centro Hospitalar de S. João, EPE, Porto, Portugal
[5] QOPNA, School of Health Sciences, University of Aveiro, Portugal

Abstract

Isolated long-chain 3-hydroxyacyl-CoA dehydrogenase deficiency (LCHADD) is a mitochondrial fatty acid β-oxidation disorder, which affects the oxidation of long chain fatty acids. LCHADD is clinically characterized by cardiomyopathy, hypoketotic hypoglycemia, hepathopathy and sometimes myopathy, neuropathy and pigmentary retinopathy. The resulting energy deficiency and the accumulation of toxic long chain 3-hydroxy fatty acids are believed to be the main pathological determinants. Nevertheless, we can still not explain why patients homozygous for the most common mutation may exhibit so major differences in disease severity. In order to disclose the main molecular pathways modulated in LCHADD we applied a nanoLC-MS/MS approach to the protein profiling of mitochondria isolated from fibroblasts of two patients homozygous for the most common mutation (c.1528 G>C), but with different clinical outcomes. Data reveal a metabolic reprogramming that results in a shift to glycolysis for energy production, modulation of apoptotic pathways and of the mitochondrial antioxidant defence system. The patient with the most severe phenotype revealed increased ROS levels with overexpression of MnSOD, while the other presented borderline ROS increase and down-regulation of MnSOD. Our data highlights the main molecular pathways modulated in LCHADD as well as the role of ROS and ROS buffering for disease progression.

Introduction

Mitochondrial β-oxidation of fatty acids is an important source of energy, particularly in metabolically active tissues such as skeletal muscles and myocardium, playing also an essential role during periods of fasting and metabolic stress [1]. The mitochondrial trifunctional protein, an enzymatic complex bound to the mitochondrial inner membrane, catalyzes the last three of the four chain-shortening reactions in the mitochondrial β-oxidation of long chain fatty acids. The mitochondrial trifunctional protein – MTP, has a hetero-octamer structure, consisting in four α-subunits and four β-subunits, encoded by the *HADHA* (OMIM# 600890) and *HADHB* (OMIM# 143450) genes respectively, both located in the same region of chromosome 2p23 [2]. The α-subunit contains the long-chain enoyl-CoA hydratase (LCEH) and long-chain 3-hydroxyacyl-CoA dehydrogenase activities (LCHAD), while the β-subunit contains the long-chain 3-ketothiolase activity (LKAT) [3].

Distinct autosomal recessive disorders of fatty acid oxidation are associated to different degrees of MTP malfunction. General MTP deficiency, described in 1992 [4, 5], is defined by reduced activity of all three MTP enzymes and can be caused by a heterogeneous group of mutations in any of the *HADHA* or *HADHB* genes. Besides general MTP deficiency, isolated enzymatic defects were identified, namely LKAT and LCHAD deficiencies, with no isolated LCEH deficient patient identified so far. Isolated LKAT deficiency, associated to mutations in *HADHB* gene, has been reported in very few patients [6], whereas isolated LCHAD deficiency (LCHADD), although rare, is by far the most common defect of the MTP complex, with an estimated birth prevalence ranging from 1/69,165 to 1/216,839 in European populations [7, 8]. Isolated LCHADD was first described in 1989 [9] and is biochemically characterized by a reduced LCHAD activity with substantial preservation of the other two MTP enzymatic activities (>60% of the normal) [10]. This fatty acid oxidation pathway blockage results in the accumulation of long-chain 3-hydroxy fatty acids and their metabolites [10].

LCHADD is associated to mutations in the *HADHA* gene, in particular to c.1528G>C (p.Glu474Gln), in the exon 15, that is present in 60% [11] to 86% [12] of the mutated alleles. This common mutation is located in the active site of LCHAD, compromising its activity but not affecting the expression levels of

the α-subunit neither the functional structure of the MTP complex [13, 14]. Patients homozygous for c.1528G>C have undoubtedly isolated LCHADD deficiency, although patients heterozygous for the common mutation and for other on the α-subunit can have isolated LCHADD or general MTP deficiency, depending on the nature of the second mutation. Patients classification is only accessed based on the enzymatic activities measurements [15]. Clinically manifestations of LCHADD can vary from early onset cardiomyopathy, hypoketotic hypoglycemia, hapatopathy (sometimes presenting as Reye like syndrome), coma and sudden death, to a later onset with myopathy, progressive neuropathy and pigmentary retinopathy [10, 12]. It is believed that besides the energy deficiency, the accumulation of 3-hydroxy fatty acids (3-hydroxydodecanoic, 3-hydroxytetradecanoic and 3-hydroxypalmitic acids) plays a key role on disease development [16-18]. 3-Hydroxyacyl metabolites are supposed to be the cause of MTP-related retinopathy and progressive neuropathy, being also reported that they might induce oxidative stress [19] and compromise OXPHOS activity [20]. Nevertheless, we cannot still explain why LCHADD patients, homozygous for the common mutation, can present so differently with some exhibiting significant morbidity, develop chorioretinopathy and neuropathy while other reach adulthood with minimal retinal changes as the only manifestations of the clinical disease [18, 21].

In order to bring new insights on the cellular pathophysiology of LCHADD, we applied a global mitochondrial proteomic approach to the study of isolated LCHADD patients, homozygous for the common mutation and with different clinical presentations.

Material and Methods

Samples

Skin fibroblasts from two LCHADD patients and control individuals, with no apparent related disease (n=5) were analysed. Patients are both homozygous for the common mutation c.1528G>C in the *HADHA* gene. Patient 1 (Pt1) is classified as a mild LCHADD, and according to available information presented in infancy cardiomyopathy and hepatopathy. In adulthood, the clinical presentation includes retinopathy without myopatic signs. Patient 2

(Pt2) presented a severe clinical phenotype in the first months of age with severe cardiomyopathy, which result in patient death at the age of 7 months. Fibroblasts were used de-identified according to local ethic regulations. All samples were obtained in accordance with the current revision of the Helsinki Declaration.

Cell culture

Skin fibroblasts were grown in Ham F10 nutrient mixture supplemented with 10% fetal calf serum, 2mmol/L glutamine, 1% penicillin, streptomycin and fungizone. Ten 75cm^2 culture flasks from each sample were grown to pre-confluence before mitochondria isolation.

Mitochondrial isolation

Isolation of mitochondria from the cell pellet was performed at 4 °C according to Rocha et al. [22]. Briefly, the cell pellet was suspended in isolation buffer (250mM sucrose, 1mM EGTA, 10mM HEPES and 5g/L BSA pH 7.5) and was then centrifuged at 500g for 2min. The supernatant was discarded and the remaining pellet was suspended in isolation buffer. The cell suspension was homogenized in a tight-fitting Potter homogenizer (Teflon pestle). After centrifugation at 1500 *g* for 10min, the supernatant was kept on ice. The pellet was homogenized and centrifuged as described above. The two supernatants were pooled and centrifuged at 10000 *g* for 10 min. The resulting mitochondrial pellet was washed with BSA-free isolation buffer. Protein content was determined with RC DC Protein Assay kit (Bio-Rad, Hercules, CA, USA).

iTRAQs comparative analysis of isolated mitochondria

For iTRAQ analysis, mitochondrial extracts from LCHADD patients and controls (pool of mitochondria isolated from fibroblasts of 5 healthy subjects) were used. Aliquots of 100µg of protein were analyzed in duplicate. An in-solution digestion was performed for iTRAQ labelling according to the protocol provided by the manufacturer (Applied Biosystems, Foster City, CA). Two independent runs were carried out. Briefly, proteins were reduced, alkylated and digested. Samples were mixed with triethyl ammonium bicarbonate buffer

(TEAB) (1M, pH 8.5) and RapiGest (Waters) to a final concentration of 0.5M and 0.1%, respectively, and then reduced with 50mM tris(2-carboxyethyl) phosphine (TCEP) for 1h at 37◦C and alkylated with 10mM S-methyl methanethiosulfonate (MMTS) for 10 min at room temperature. The aliquots were digested with trypsin (Promega, Madison, WI) at a protein-to-enzyme ratio of 10:1 at 37°C overnight and then dried in a Speed-Vac (Thermo Savant, NY).

After protein digestion, the extracted peptides were labelled with iTRAQ reagents (8-plex) according to the manufacturer's instructions (Applied Biosystems, Foster City, CA). Briefly, one vial of iTRAQ reagent, previously dissolved in 70µL of ethanol, was added to each aliquot and incubated for 2h at room temperature. The reaction was stopped by adding water and the labelled digests corresponding to each of the four of 8-plex experiments were combined and dried in the Speed-Vac (Thermo Savant, NY).

The tryptic labelled digests were separated by a multidimensional approach based on a first dimension with high pH reverse-phase and a second dimension with the acidic reverse-phase system as previously described[23]. Briefly, sample loading was performed at 200 µL/min with buffers (A) 2% ammonium hydroxide and 0.014% formic acid in water, pH 10 and (B) 2% ammonium hydroxide and 90% acetonitrile (ACN) in water, pH 10. After 5 minutes of sample loading and washing, peptide fractionation was performed with linear gradient to 70 % B over 85 min. Sixty fractions were collected, dried in a SpeedVac and resuspended in 5% ACN and 0.1% trifluoroacetic acid (TFA). Collected fractions were then separated by LC. Collected fractions were separated using an Ultimate 3000 (Dionex, LCPackings, Sunnyvale, CA) onto a 150mm × 75µm Pepmap100 capillary analytical C18 column with 3µm particle size (Dionex, LC Packings) at a flow rate of 300nL/min. The mobile phases A and B were 2% ACN 0.1% TFA in water and 95% ACN, 0.045% TFA, respectively. The gradient started at 10 min and ramped to 60 % B till 50min and 100% B at 55min and retained 100% B till 65min. The chromatographic separation was monitored at 214nm using a UV detector (Dionex/LC Packings) equipped with a 3nL flow cell. The peptides eluted from the column were mixed with a continuous flow of matrix solution (270nL/min, 2mg/mL α-CHCA in 70% ACN/0.1% TFA and internal standard Glu-Fib at

15ftmol) in a fractions microcollector (Probot, Dionex/LC Packings) and directly deposited onto the LC-MALDI plates at 12s intervals for each spot (150- nL/fraction). For every chromatographic run, a total of 208 fractions were collected.

MALDI-TOF/TOF MS analysis was performed using a 4800 MALDI-TOF/TOF Analyzer (Applied Biosystems, Foster City, CA), as described by Vitorino et al.[23]. A S/N threshold of 50 was used to select peaks for MS/MS analyses. The spectra were processed and analyzed by the ProteinPilot software (v4.0 AB Sciex, USA), which uses paragon algorithm for protein/peptide identification based on MS/MS data. Searches were performed against the SwissProt protein database (release date 01032013) for *Homo sapiens*. Default search parameters were: specifying trypsin as the digestion enzyme, fixed modification of methylathion on cysteine residue and iTRAQ 8-Plex, biological modification with emphasis on phosphorylation and urea denaturation as the variable modification setting. The mass tolerances for precursor and fragments were default values for ProteinPilot®. The cut-off score value for protein identification with ProteinPilot® was a ProteoScore of 1.3 (95% confidence). A decoy database search strategy was also used to estimate the false discovery rate (FDR), defined as the percentage of decoy proteins identified against the total protein identification. The local FDR was calculated by searching the spectra against SwissProt (*Homo sapiens*) decoy database. The estimated low FDR of 0.9% indicated a high reliability in the proteins identified (four proteins identified in decoy database). Data was normalized for loading error by bias correction, which is an algorithm in ProteinPilot that corrects for unequal mixing when combining the labelled samples of one experiment. It does so by calculating the median protein ratio for all proteins reported in each sample, adjusted to unity and assigning an autobias factor to it. Nevertheless, the quantification results were reviewed manually for all proteins found to be differentially expressed (iTRAQ ratio>1.3 or<0.7 according to Vitorino et al. [24]).

Quantitative acylcarnitine profiling in intact fibroblasts

In vitro acylcarnitine assay in intact fibroblasts was performed as previously described [25], with minor modifications. At confluence fibroblasts were

harvested and seeded in 6 well plates (approximately 5x 10^5 cells) and settled for 24 hours to form a cell monolayer. Two wells were prepared for each sample in each batch. After 24 hours the culture medium was replaced by 2.5mL of reaction mixture. The reaction mixture contained ^{13}C-palmitic acid (C.I.L.) 0.11mmol/L complexed with bovine serum albumin (essential fatty acid free) 0.5mg/mL, L-carnitine 0.4mmol/L and fetal calf serum 10%, in Ham F10 culture medium. Incubation was performed at 37°C for 96 hours. The reaction medium was transferred for a tube for acylcarnitine analysis and cell monolayer retained for proteins quantification.

For acylcarnitine analysis, 15µL of the reaction mixture was mixed with 100µL of internal deuterated standards mixture (C.I.L.) in methanol and keep on ice for 15min. Then it was centrifuge at 15000g for 5 min to remove the precipitate. The supernatant was dried under a nitrogen stream and derivatized with 100µL of butanolic-hydrochloric acid 1N for 15 min at 70°C, and dried again. The dried butylated sample was reconstituted with 100µL of acetonitrile/water (50/50, 0.01% formic acid). Acylcarnitines were analysed using an API 2000 LC electrospray ionization tandem mass spectrometer (ABSciex), detecting the precursors of m/z 85.1. Quantification was performed by intensity comparison with deuterated internal standards.

For protein quantification, cells were harvested and washed twice with PBS and then hydrolysed by sonication and centrifuge. Total protein content was measure in the supernatant by Lowry protein assay method.

Measurement of mitochondrial ROS levels

Mitochondrial superoxide levels were measured using the MitoSOX™ RED Mitochondrial Superoxide Indicator (Invitrogen, USA) following the procedure described by Suski et al [26] with minor modifications. MitoSOX is a live cell permanent indicator that is rapidly and selectively targeted to mitochondria. In this organelle it is oxidised by superoxide anion and not by other ROS or reactive nitrogen species. Cells were harvested and seeded in a dark, clear bottom 96 well microplate, with 25000 cells *per* well, and allowed to adhere overnight. Next day cells were washed twice with Hanks' Balanced Salt Solution (HBSS) and allowed to incubate with HBSS for 30 min. The pre-

incubation HBSS was replaced by 100µL of the MitoSOX solution (5µM of MitoSOx in HBSS) and incubated for 10' at 37°C. Then, cells were gently washed twice with warm HBSS, 100µL of HBSS was added and fluorescence was measured at 510nm excitation and 590nm emission wavelengths.

Western blottting

For the expression analysis of target proteins, equal amounts of proteins from each sample were loaded on a 12.5% SDS-PAGE gel prepared according to Laemmli [27]. After separation at 180V, proteins were transferred from the gel to a nitrocellulose membrane (Millipore®, 0.45µm porosity) by electroblotting for 2 hours at 200mA in transfer buffer (25mM Tris, 192mM glycine, 20% methanol). After blotting, non-specific binding was blocked with 5% (w/v) nonfat dry milk in TTBS (100mM Tris pH 8.0, 150mM NaCl, and 0.05% Tween 20) and the membrane was incubated with primary antibodies diluted 1:1000 in 5% (w/v) nonfat dry milk in TTBS (rabbit polyclonal anti-paraplegin, sc-135026, Santa Cruz Biotechnology; rabbit polyclonal anti-Tfam, ab47548, abcam; mouse monoclonal anti-ATP synthase subunit β, ab14730, abcam; mouse monoclonal anti-MnSOD, ALX-804-265, Alexis;) for 2 hours at room temperature or overnight at 4°C. After 3 washes for 10 min with TTBS, membranes were incubated with secondary horseradish peroxidase-conjugated antibody (GE Healthcare®) for 1 hour, and after that 3 washes were made for 10 min with TTBS.

The blots were developed using the chemiluminescence ECL reagent (Amersham Pharmacia Biotech®, Buckinghamshire, UK), followed by exposure to X-ray films (Kodak Biomax Light Film, Sigma®, St. Louis, USA). Film images were acquired using GelDoc XR system (Bio-Rad, Hercules, CA.) and quantitative analysis of optical density (OD) was performed with QuantityOne® 1-D Analysis Software (Bio-Rad, Hercules, CA).

mtDNA relative quantification in fibroblasts

Mitochondrial DNA (mtDNA) copy number was calculated from the standard curve and threshold cycle number using the ratios *ND1/rRNA18S* and *ND4/rRNA18S*. Calibration curves were prepared in triplicate for two mitochondrial genes (*ND1* and *ND4*) and one nuclear gene (*rRNA18S*), using

serial dilutions of the PCR product of the target gene. For qPCR reaction was used 1.25mL of 1x GoTaq (Promega), 1.5mL of each primer (Supplemental table S1) – forward and reverse (5mM), 3mL of $MgCl_2$ 25mM (Promega), 2mL of dNTPs 2.5mM (Promega), 1.25mL of Eva Green (Biotium), 5ng of DNA (sample or calibrator) and water in a final volume of 25mL. The qPCR amplification conditions were 2 min at 50°C and 10 min at 95°C, followed by 40 cycles of 15s of denaturation at 95°C and 60s of annealing/extension at 60°C. At the end of the amplification process, melting curves were analyzed between 60-95ºC (temperature transition of 0.1ºC/s), with continuous fluorescence monitoring to control for the absence of nonspecific products. The fluorescent signal intensity of PCR products was recorded and analyzed in a Rotor-Gene 6000 (Corbett, Life Sciences).

Statistical analysis

Data is presented as mean ± standard deviation of replicates (in the case of LCHADD patients) and replicates of n=5 in the case of controls. Analysis of the statistical significance of differences between each LCHADD patient and controls in relation to OD measures were performed with the GraphPad Prism version 5.0 for Windows (GraphPad Software, San Diego California, USA). . Significant differences were evaluated with the unpaired Student's *t* test followed by a Bonferroni post hoc test. The level of significance was set at $p < 0.05$.

Results

In order to investigate and disclose the cellular processes harboured in mitochondria that are impacted by LCHAD deficiency, a global proteomic profiling based on nanoLC-MS/MS was applied to mitochondria isolated from cultured skin fibroblasts of two patients. Patients with isolated LCHAD deficiency were selected, both homozygous for the most common mutation c.1528 G>C, avoiding the variability associated to the nature of disease-related gene mutation. Once α-subunit of MTP (ECHA_HUMAN) strongly interacts with other fatty acid β-oxidation enzymes (according to String 9.0 – http://string-db.org), one might expect that the decreased activity of LCHAD

will directly impact the metabolic processes related to lipid oxidation/metabolism (Supplemental figure S1).

The levels of acylcarnitines accumulated by fibroblasts were determined to evaluate their potential contribution to LCHADD pathogenesis. Data evidenced a significant elevation of tetradecanoylcarnitine, 3-hydroxytetradecenoylcarnitie, palmitoylcarnitine and 3-hydroxypalmitoylcarnitine (figure 1). No major differences were observed between both patients analysed, in respect to the accumulation of long chain 3-hydroxy fatty acids and tetradecanoylcarnitine, being the only significant difference noticed in palmitoylcarnitine accumulation, more pronounced in patient 2 ($p<0.05$).

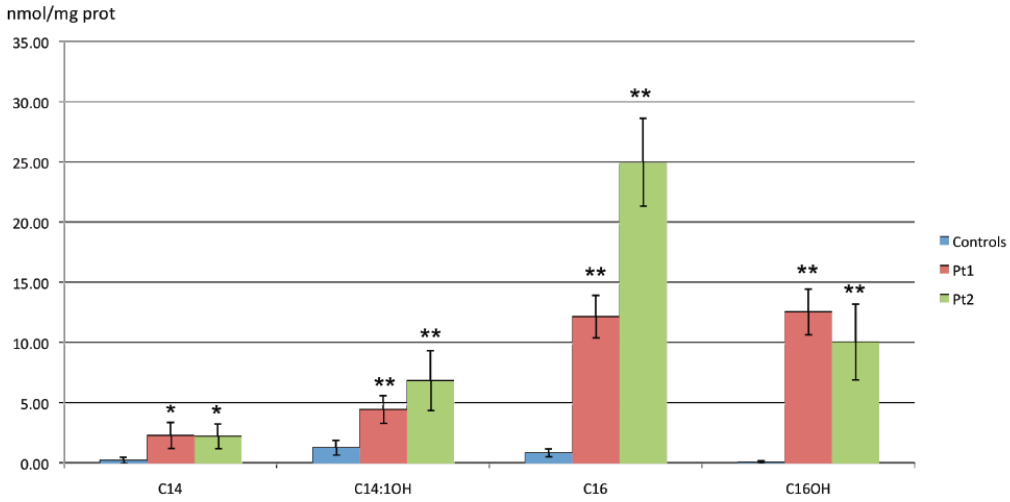

Figure 1: Accumulated acylcarnitines in the culture medium after the incubation of patient's fibroblasts with ^{13}C-palmitic acid for 96 hours. Values are expressed as mean ± standard deviation (*$p<0.05$ *vs* CONT; **$p<0.01$ *vs* CONT). C14 – tetradecanoylcarnitine; C14:1OH – 3-hydroxytetradecenoylcarnitine; C16 – palmitoylcarnitine; C16OH – 3-hydroxypalmitoylcarnitine.

To give new insights into the molecular pathways modulated by the presence of the c.1528 G>C in homozygous condition, we applied a LC-MS/MS analysis of isolated mitochondria that resulted in the identification of 942 distinct proteins (Supplemental table S2A), with a confidence degree over 95%, from which 42% were assigned to mitochondria, according to MitoMiner [28]. A significant proportion of the identified proteins had more than one

subcellular location, for which its biological significance remains to be disclosed. One possibility is that multi-residential proteins support mitochondrial protein trafficking and connection with other organelles [29]. The five most significantly enriched biological process clusters to which these proteins belong were metabolic process, cellular process, localization, developmental process and cellular organization or biogenesis. Similarly, the top five molecular function clusters were catalytic activity, binding, structure molecule activity, transporter activity and receptor activity (figure 2).

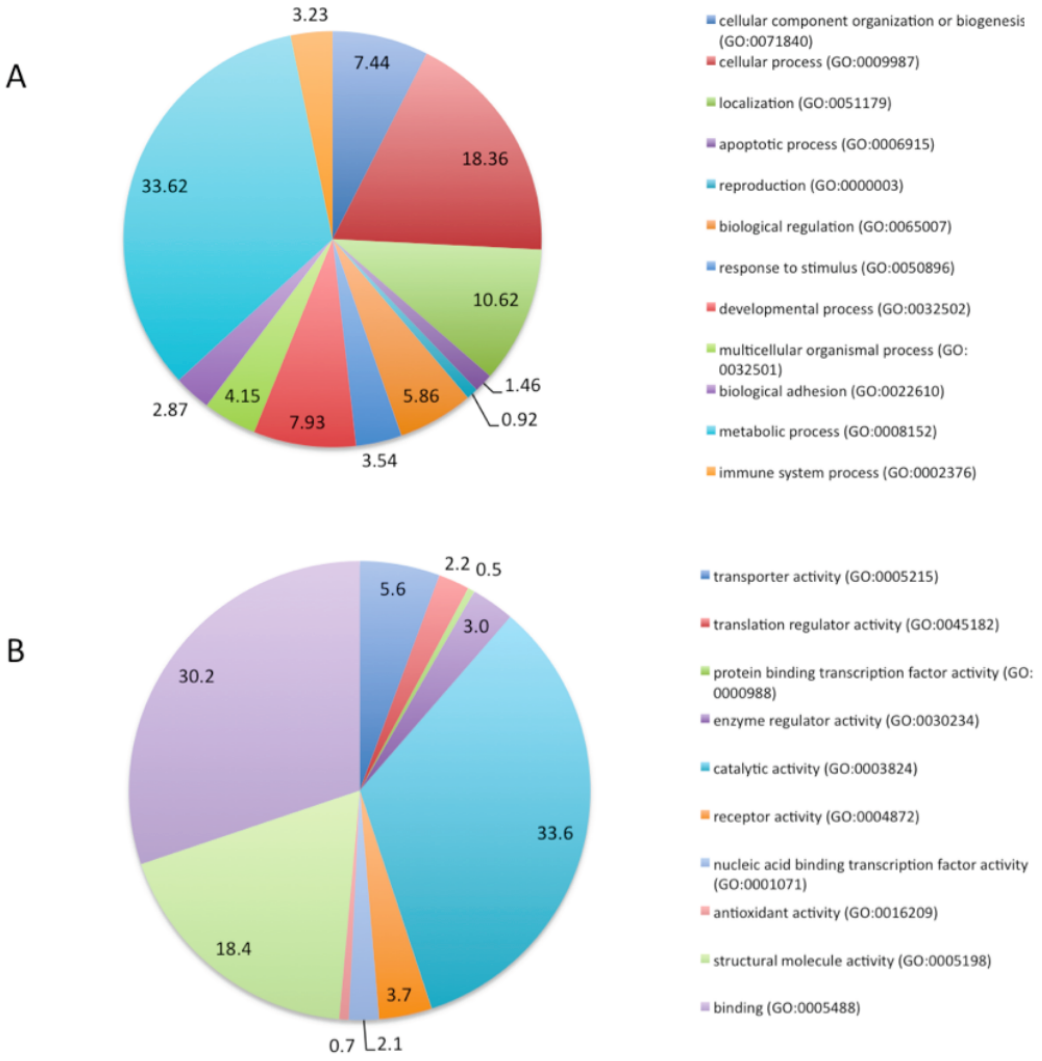

Figure 2: Pie charts showing the biological processes (A) and molecular functions (B) categories for the identified proteins, assigned by Panther. Values indicate the percentage of each cluster.

In order to detect variations in protein abundance between LCAHDD patients and healthy subjects, iTRAQ-based quantification was performed. From the 942 distinct proteins identified, 395 were successfully quantified with a $p<0.05$ and from these 153 were found to be modulated by isolated LCHADD deficiency (Supplemental table S2B). In Pt1 111 proteins were found up or down regulated and in Pt2 97 (figure 3).

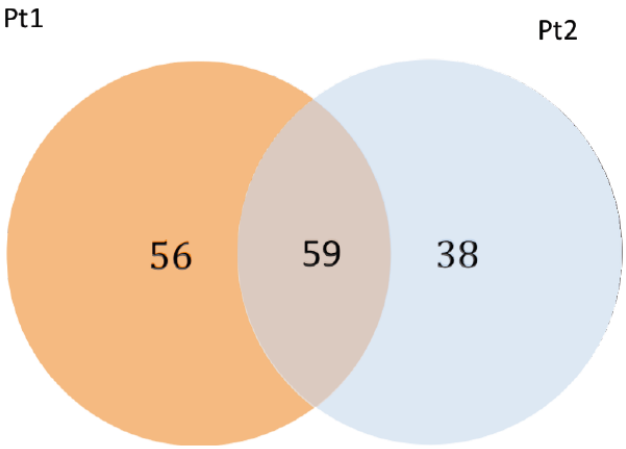

Figure 3: Venn diagram representing the modulated proteins identified by comparative analysis of the mitochondrial fraction of each of the patients studied with control subjects.

An integrated analysis of the proteins modulated by the disease in each patient was performed using Cytoscape v3.0. The most significant clusters positively modulated in both patients were apoptotic process, mitochondrial organisation and mitochondrial membrane adaptations while negatively modulated clusters were peptidyl-proline modifications and glycerol ether metabolic process. Individual patients presented specific regulated processes. Pt1 evidenced a positive regulation of cellular component size, vesicle fusion and cytoskeleton adaptations with a negative modulation of fibroblast proliferation. Pt2 presented a positive modulation of intrinsic signalling in response to oxidative stress and oxidative stress metabolic process with a negative regulation of fatty acid metabolic process (figures 4A and 4B).

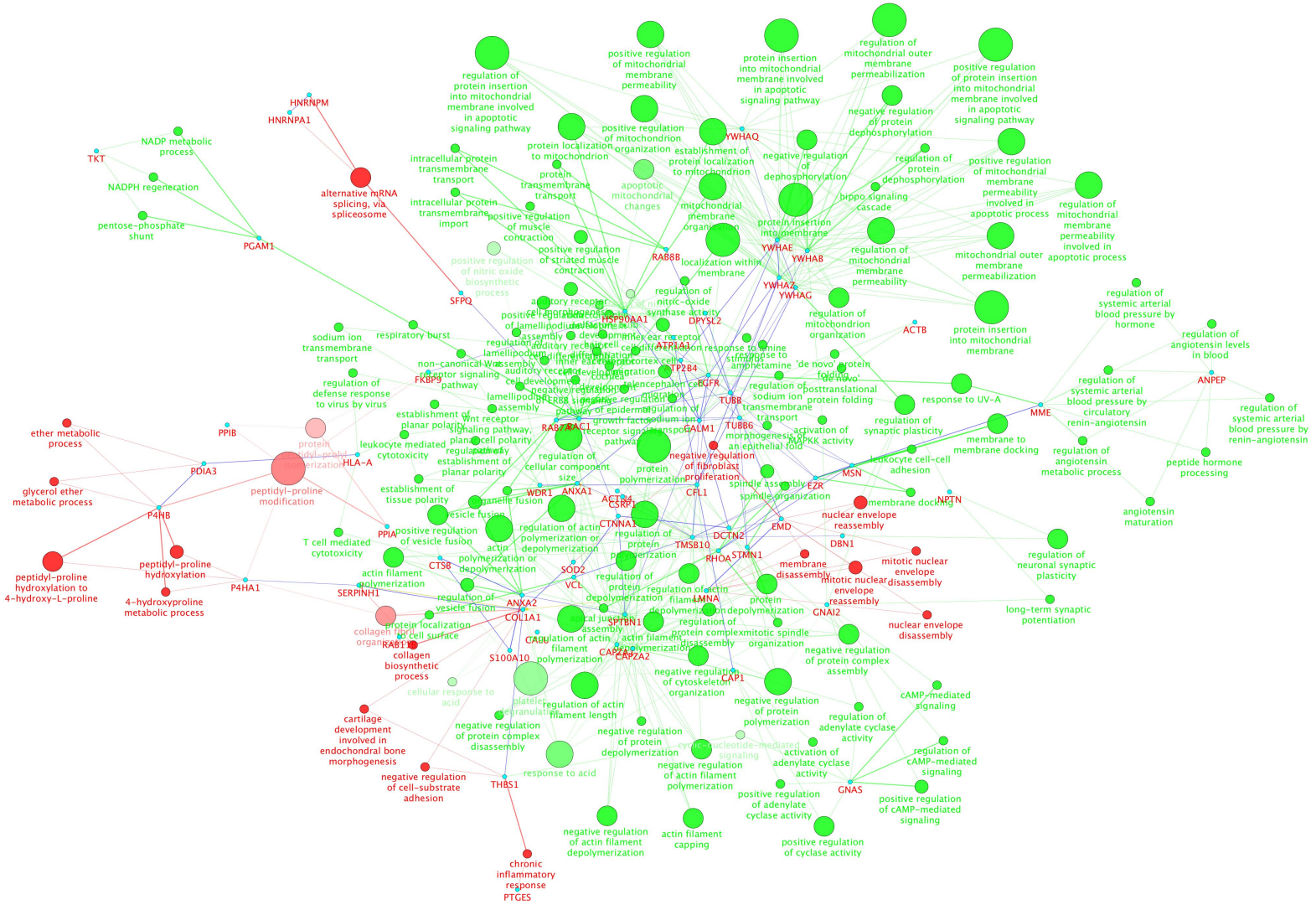

Figure 4A: Integrated analysis of modulated proteins in Pt1, using Cytoscape. Green dots represent up regulated processes and red down regulated processes.

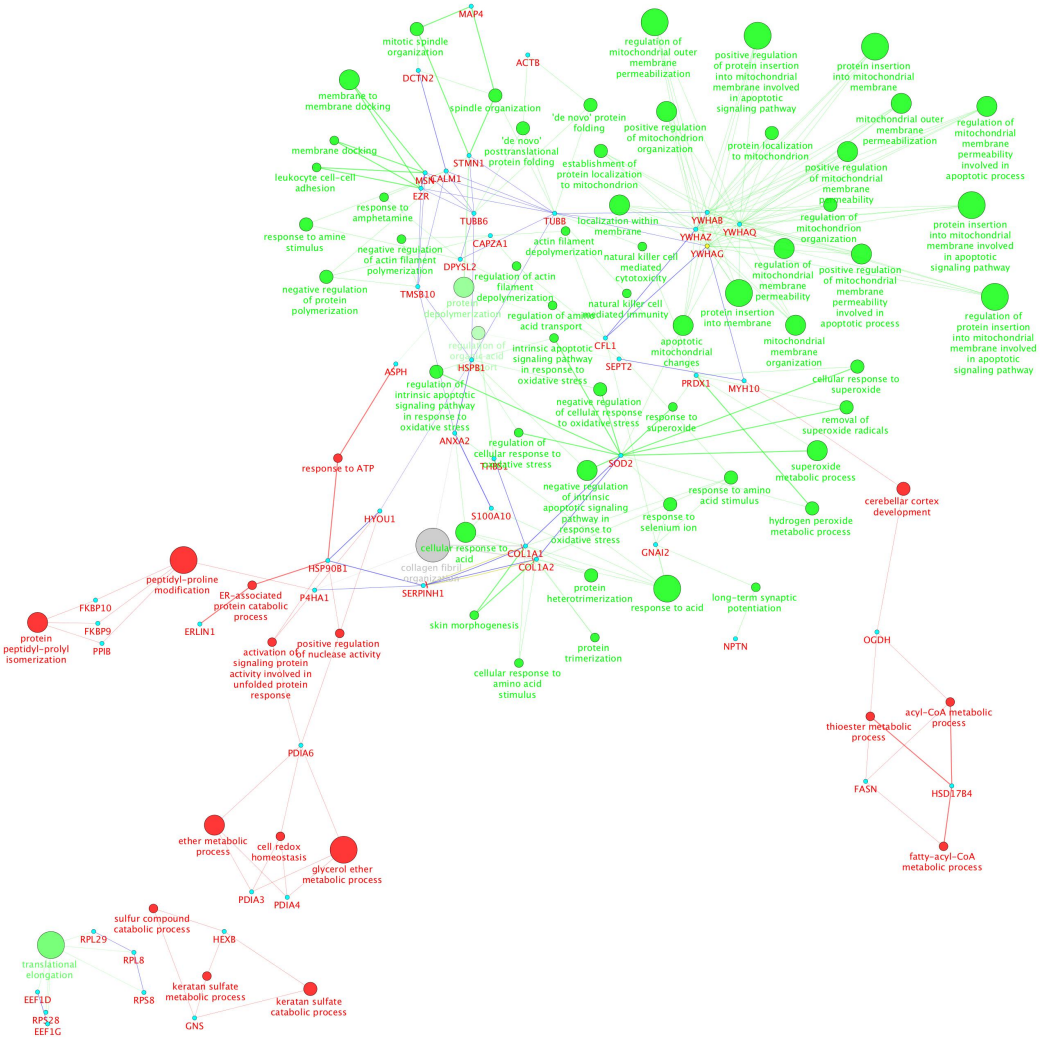

Figure 4B: Integrated analysis of modulated proteins in Pt2, using Cytoscape. Green dots represent up regulated processes and red down regulated processes.

Looking to the differentially abundant proteins in patients, it becomes evident an overrepresentation of cytoskeleton-related proteins, probably reflecting the interaction of these proteins to patients' mitochondria, which is supposed to be enhanced in dysfunctional mitochondria [30, 31]. Patients' fibroblasts presented higher levels of signalling molecules (e.g. 14-3-3 proteins, A-kinase anchor protein and protein S100 family members), chaperones (e.g. HSP90 and HSP beta-1), glycolytic enzymes (e.g. alpha enolase and pyruvate kinase) and apoptotic proteins (e.g. cofilin and galectin-1) (figure 5 and Supplemental table S2B). The presence of glycolytic enzymes in the mitochondrial fractions is probably a reflexion of their tight interaction with mitochondria. This proximity enhances metabolite channelling from glycolysis to mitochondria for complete oxidation [32, 33].

Figure 5 illustrates the comparison of the log ratio of the relative intensity (Pt1/CONT and Pt2/CONT) to better visualize the mitochondrial proteins differentially modulated by LCHADD. As can be depicted from this figure, there is a significant proportion of LCHADD-modulated proteins with the same variation tendency with others presenting differences between patients, like HSP90, tranketolase and peroxiredoxin-1. Point differences in proteins abundance were expected based on the individuality of the response to LCHADD associated to each of the patients. However, divergent expression differences between patients were noticed for MnSOD, which was overexpressed in Pt2 and underexpressed in Pt1. Western blotting analysis confirmed this tendency in MnSOD expression (figure 6C). To better understand this apparent divergent response to oxidative stress we measured the mitochondrial superoxide production in fibroblasts using MitoSox assay. Results showed similar ROS levels between Pt1 and controls while Pt2 presented significantly higher superoxide levels (figure 7), supporting the higher abundance of MnSOD noticed in mitochondria from Pt2.

In order to validate the data retrieved from our analysis, besides MnSOD we evaluate the expression of ATP synthase subunit beta by western blotting. The results obtained for ATP synthase β subunit revealed no statistical significant expression differences between patients and controls (figure 6A), corroborating LC-MS/MS analysis data.

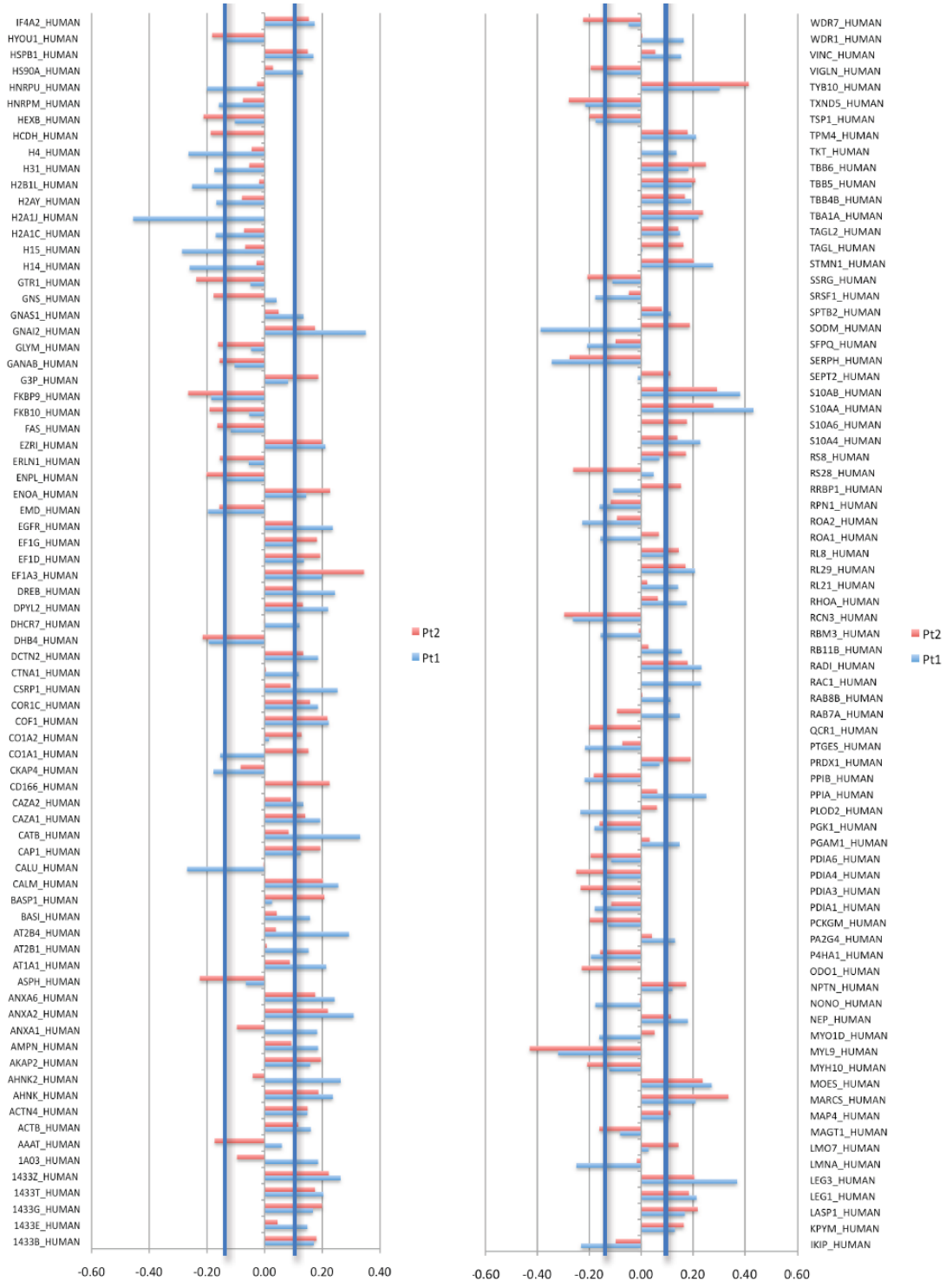

Figure 5: Representation of up and down regulated proteins in both patients (Log (Pt/controls)). Vertical blue lines represent used cut-off's (-0.15 and 0.11).

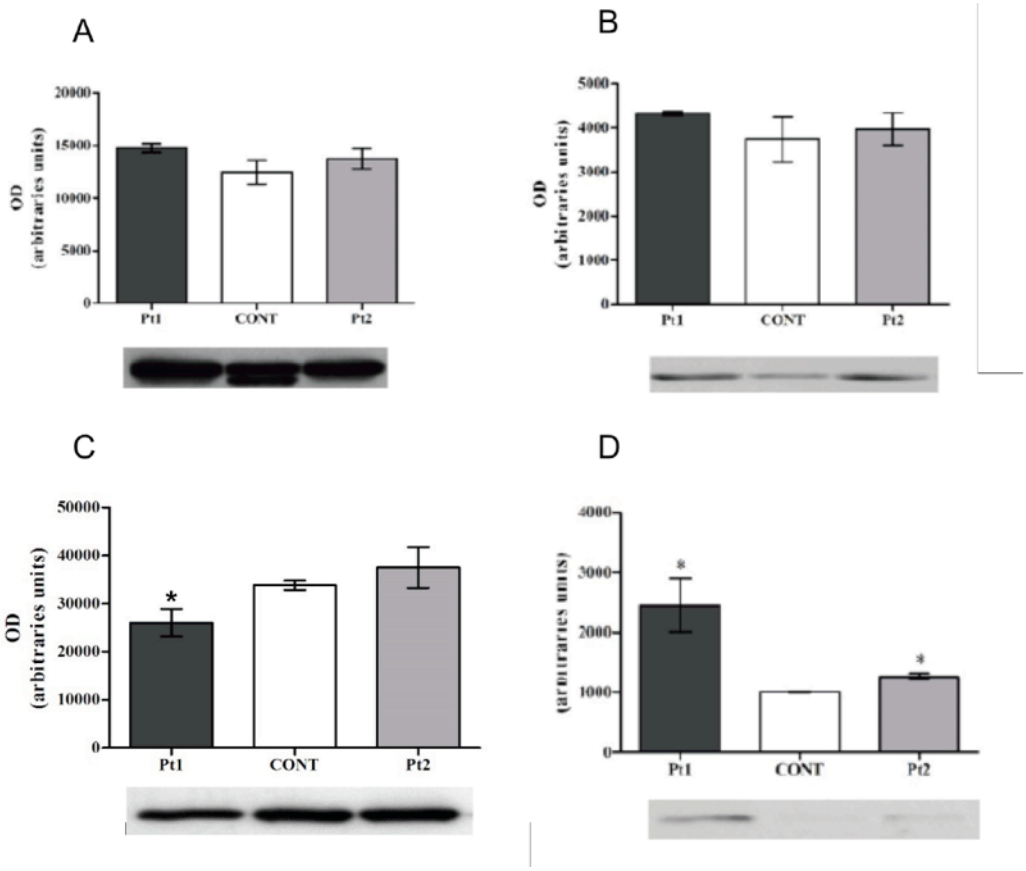

Figure 6: Western blotting analysis of ATP synthase beta (A), paraplegin (B), MnSOD (C) and mtTFA (D) expression in isolated mitochondria. Representative immunoblots are presented below the graphs. Values are expressed as mean ± standard deviation of optical density values presented as arbitrary units (*p<0.05 *vs* CONT; **p<0.01 *vs* CONT).

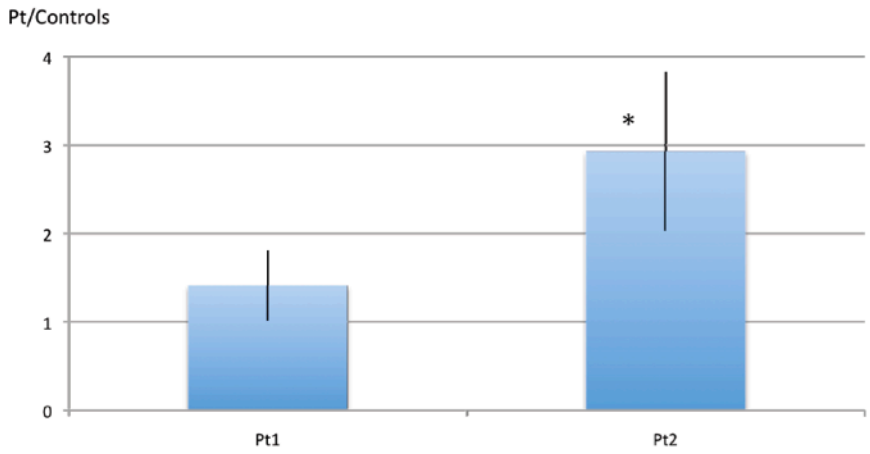

Figure 7: ROS generation in LCHADD patient fibroblasts. Oxidative stress levels were determined with the mitochondrial targeted probe, MitoSOX. Results are expressed as fold change over controls mean. Error bars represent standard deviation (*p<0.05 *vs* CONT)

Our study was further complemented with the expression assessment of other proteins from key pathways, namely mitochondrial protein quality control (mtPQC) system and mtDNA maintenance (paraplegin and mtTFA, respectively) (figure 6).

In order to evaluate the contribution of mitochondrial PQC to the pathogenesis of LCHADD, the expression of paraplegin was evaluated by western blotting. This m-AAA (membrane-bound ATP-dependent) protease has a crucial function in the degradation of misfolded/damage proteins [34]; however, no significant expression differences related to LCHADD were observed. The expression of mitochondrial transcriptional factor mtTFA was also evaluated, since mtDNA maintenance is of key importance for mitochondrial function. In both patients it was observed a statistically significant increase of mtTFA expression. These results were correlated with data retrieved from qPCR analysis of *ND1/rRNA18S* and *ND4/rRNA18S.* No differences were noticed between LCHADD patients and healthy subjects suggesting similar mtDNA relative abundance (data not shown). Figure 8 integrates the molecular pathways that are affected by LCHADD.

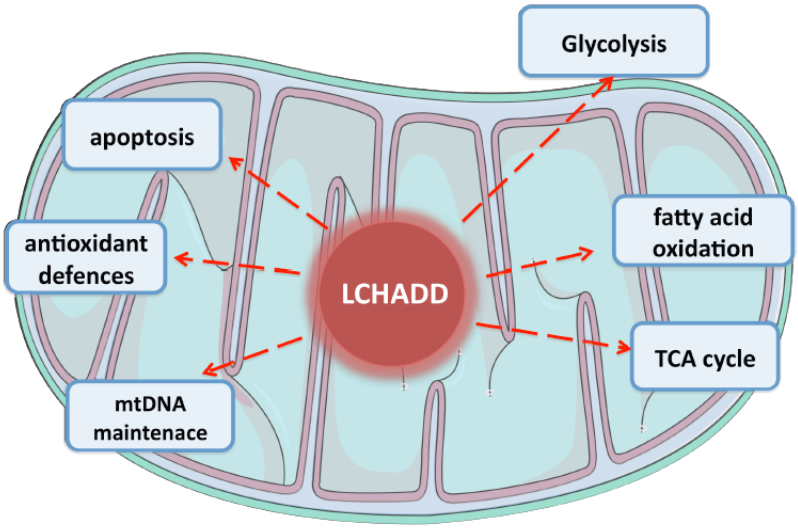

Figure 8: Representation of the main processes modulated in LCHADD.

Discussion

In the present study we applied a nanoLC-MS/MS approach to characterize the mitochondrial dysfunction in two patients with LCHADD caused by the mutation p.Glu474Gln (c.1528 G>C) in homozygous condition, in the *HADHA* gene. Despite the same genotype, the patients studied presented distinct clinical outcomes with Pt2 evidencing a worse disease phenotype. Metabolite analysis of fibroblasts cultures evidenced a similar accumulation of long chain 3-hydroxy acylcarnitines in both patients with an elevation of palmitoylcarnitine in Pt2 in comparison to Pt1. Despite this difference, the similar accumulation of 3-hydroxy-palmitoylcarnitine puts both patients in the same group in respect to metabolite accumulation [35], don't allowing any correlation with clinical phenotype. These alterations in the metabolite profile were related to the remodelling of mitochondrial proteome in LCHADD characterized by similar adaptations to the disease, as increased susceptibility to apoptosis and mitochondrial membrane adaptations, and by individual ones, with negative modulation of fibroblast proliferation overrepresented in Pt1 and an enhanced response to oxidative stress noticed in Pt2.

The comparison of the mitochondrial proteome profile of LCHADD patients with healthy controls highlighted the up-regulation of apoptotic processes in both patients, reflecting the inability of the cells to counteract LCHADD. One of the markers of this process is cofilin, found significantly abundant in patients' samples. The translocation of this actin-binding protein to the mitochondria is an early step in apoptosis induction and occurs before caspase activation [36]. An up-regulation of glycolytic enzymes was also noticed, namely α-enolase, piruvate kinase, being also observed in Pt2 an elevation of glyceraldehyde-3-phosphate dehydrogenase. This profile of glycolytic enzymes is characteristic of the Warburg effect [37], usually associated to cancer cells, though it was previously reported in multiple-acyl-CoA dehydrogenation deficiency [22]. This metabolic reprogramming process represents a cellular adaptation to ensure enough ATP to fulfil cellular needs. The Warburg effect might result from HIF 1α activation through the regulation

of its hydroxylation in proline residues by prolyl-4-hydroxylase domain proteins (PHD), which is known to regulate HIF 1α stability [38, 39]. In both patients analysed PHD1 (prolyl 4-hydroxylase subunit alpha-1) was found down regulated what could point to a lower hydroxylation and consequently to a higher activity of HIF 1α, contributing to the observed metabolic reprogramming. HIF 1α stimulation in these patients might also be mediated by ROS [40], which levels were increased in Pt1 and slight increased in Pt2.

LCHADD-related metabolic adaptation was paralleled with increased levels of the mitochondrial transcription factor mtTFA, the nuclear encoded transcription factor that control mtDNA replication and transcription [41], despite no alterations of mtDNA-to-nDNA content. Though remaining to be disclosed, the stabilization of mtDNA nucleoid formation and mtDNA copy number in conditions of oxidative stress [42] presents as an attractive hypothesis to justify mtTFA over-expression.

Besides the LCHADD-related remodelling of the mitochondrial proteome, an individual specific signature was noticed between patients. One of the more notorious differences was related to the expression of mitochondrial antioxidant enzymes: MnSOD and peroxiredoxin-1. In Pt1 MnSOD was found down-regulated while in Pt2 it was up-regulated, alongside with peroxiredoxin-1, being Pt2 the only that presented significantly high ROS levels given by MitoSox assay. Curiously, no differences in the content of mitochondrial chaperones like HSP 60 and HSP 70 and of the mAAA protease paraglegin were noticed, given by iTRAQ and western blotting data, respectively. Such discrepancy in the regulation of MnSOD was previously reported in fatty acid β-oxidation disorders, namely between severe and riboflavin responsive forms of multiple acyl-CoA dehydrogenase deficiency [40]. The proposed justification relies on the critical role of MnSOD in buffering cellular ROS, maintaining them at levels that avoid damage but start a cellular response towards survival[40]. When ROS levels are very high cells have to overexpress MnSOD for detoxifying purposes. The distinct mitochondrial proteome profiles presented by LCHADD patients seem to correlate with the distinct clinical outcomes. Pt2 has a much severe clinical presentation that Pt1 and present higher ROS levels and up-regulation of MnSOD while Pt1 present borderline elevated ROS and down-regulation of MnSOD. These results

alongside with the others reported for MADD, make us hypothesise that in FAOD ROS levels and the individual ability to buffer them are of key importance for disease progression and outcome. Severe FAOD forms seem to be associated with significant ROS increase that forces an up-regulation of MnSOD, while less severe forms that present a slight ROS increase have a MnSOD down-regulation, what is expected to be associated to a better prognosis. Most probably other genetic factors than the disease causing mutation, might justify the distinct response of LCHADD patients to stress.

In conclusion, fibroblasts from LCHADD patients reveal signs of metabolic reprogramming shifting from oxidative phosphorylation towards glycolysis as a pro-survival adaptive process, modulation of the mitochondrial antioxidant defence system and apoptosis. Despite the same disease causing mutation, different responses to stress were observed between patients, considering mitochondrial ROS levels and MnSOD expression content, which are in agreement with the clinical phenotype. These observations highlight the importance of other regulatory factors in mitochondrial response to fatty acid β-disorders that can be on the basis of the reported clinical heterogeneity.

References

1. Rinaldo, P., D. Matern, and M.J. Bennett, *Fatty acid oxidation disorders.* Annu Rev Physiol, 2002. **64**: p. 477-502.
2. Ushikubo, S., et al., *Molecular characterization of mitochondrial trifunctional protein deficiency: formation of the enzyme complex is important for stabilization of both alpha- and beta-subunits.* Am J Hum Genet, 1996. **58**(5): p. 979-88.
3. Vockley, J. and D.A. Whiteman, *Defects of mitochondrial beta-oxidation: a growing group of disorders.* Neuromuscul Disord, 2002. **12**(3): p. 235-46.
4. Jackson, S., et al., *Combined enzyme defect of mitochondrial fatty acid oxidation.* J Clin Invest, 1992. **90**(4): p. 1219-25.
5. Wanders, R.J., et al., *Human trifunctional protein deficiency: a new disorder of mitochondrial fatty acid beta-oxidation.* Biochem Biophys Res Commun, 1992. **188**(3): p. 1139-45.
6. Das, A.M., et al., *Isolated mitochondrial long-chain ketoacyl-CoA thiolase deficiency resulting from mutations in the HADHB gene.* Clin Chem, 2006. **52**(3): p. 530-4.

7. Kasper, D.C., et al., *The national Austrian newborn screening program - eight years experience with mass spectrometry. past, present, and future goals.* Wien Klin Wochenschr, 2010. **122**(21-22): p. 607-13.
8. Lindner, M., et al., *Efficacy and outcome of expanded newborn screening for metabolic diseases--report of 10 years from South-West Germany.* Orphanet J Rare Dis, 2011. **6**: p. 44.
9. Wanders, R.J., et al., *Sudden infant death and long-chain 3-hydroxyacyl-CoA dehydrogenase.* Lancet, 1989. **2**(8653): p. 52-3.
10. Olpin, S.E., et al., *Biochemical, clinical and molecular findings in LCHAD and general mitochondrial trifunctional protein deficiency.* J Inherit Metab Dis, 2005. **28**(4): p. 533-44.
11. Ibdah, J.A., M.J. Dasouki, and A.W. Strauss, *Long-chain 3-hydroxyacyl-CoA dehydrogenase deficiency: variable expressivity of maternal illness during pregnancy and unusual presentation with infantile cholestasis and hypocalcaemia.* J Inherit Metab Dis, 1999. **22**(7): p. 811-4.
12. den Boer, M.E., et al., *Long-chain 3-hydroxyacyl-CoA dehydrogenase deficiency: clinical presentation and follow-up of 50 patients.* Pediatrics, 2002. **109**(1): p. 99-104.
13. Barycki, J.J., et al., *Biochemical characterization and crystal structure determination of human heart short chain L-3-hydroxyacyl-CoA dehydrogenase provide insights into catalytic mechanism.* Biochemistry, 1999. **38**(18): p. 5786-98.
14. Rector, R.S., R.M. Payne, and J.A. Ibdah, *Mitochondrial trifunctional protein defects: clinical implications and therapeutic approaches.* Adv Drug Deliv Rev, 2008. **60**(13-14): p. 1488-96.
15. Diekman, E.F., et al., *Necrotizing enterocolitis and respiratory distress syndrome as first clinical presentation of mitochondrial trifunctional protein deficiency.* JIMD Rep, 2013. **7**: p. 1-6.
16. Ventura, F.V., et al., *Differential inhibitory effect of long-chain acyl-CoA esters on succinate and glutamate transport into rat liver mitochondria and its possible implications for long-chain fatty acid oxidation defects.* Mol Genet Metab, 2005. **86**(3): p. 344-52.
17. Bennett, M.J., *Pathophysiology of fatty acid oxidation disorders.* J Inherit Metab Dis, 2010. **33**: p. 533-537.
18. Olpin, S.E., *Pathophysiology of fatty acid oxidation disorders and resultant phenotypic variability.* J Inherit Metab Dis, 2013.
19. Tonin, A.M., et al., *Long-chain 3-hydroxy fatty acids accumulating in LCHAD and MTP deficiencies induce oxidative stress in rat brain.* Neurochem Int, 2010. **56**(8): p. 930-6.
20. Tonin, A.M., et al., *Long-chain 3-hydroxy fatty acids accumulating in long-chain 3-hydroxyacyl-CoA dehydrogenase and mitochondrial trifunctional protein deficiencies uncouple oxidative phosphorylation in heart mitochondria.* J Bioenerg Biomembr, 2013. **45**(1-2): p. 47-57.
21. Spiekerkoetter, U. and P.A. Wood, *Mitochondrial fatty acid oxidation disorders: pathophysiological studies in mouse models.* J Inherit Metab Dis, 2010. **33**(5): p. 539-46.
22. Rocha, H., et al., *Characterization of mitochondrial proteome in a severe case of ETF-QO deficiency.* J Proteomics, 2011. **75**(1): p. 221-8.

23. Vitorino, R., et al., *Toward a standardized saliva proteome analysis methodology.* J Proteomics, 2012. **75**(17): p. 5140-65.
24. Vitorino, R., et al., *Evaluation of different extraction procedures for salivary peptide analysis.* Talanta, 2012. **94**: p. 209-15.
25. Sim, K.G., et al., *Acylcarnitine profiles in fibroblasts from patients with respiratory chain defects can resemble those from patients with mitochondrial fatty acid beta-oxidation disorders.* Metabolism, 2002. **51**(3): p. 366-71.
26. Suski, J.M., et al., *Relation between mitochondrial membrane potential and ROS formation.* Methods Mol Biol, 2012. **810**: p. 183-205.
27. Laemmli, U.K., *Cleavage of structural proteins during the assembly of the head of bacteriophage T4.* Nature, 1970. **227**(5259): p. 680-5.
28. Smith, A.C., J.A. Blackshaw, and A.J. Robinson, *MitoMiner: a data warehouse for mitochondrial proteomics data.* Nucleic Acids Res, 2012. **40**(Database issue): p. D1160-7.
29. Deng, N., et al., *Phosphoproteome analysis reveals regulatory sites in major pathways of cardiac mitochondria.* Mol Cell Proteomics, 2011. **10**(2): p. M110 000117.
30. Anesti, V. and L. Scorrano, *The relationship between mitochondrial shape and function and the cytoskeleton.* Biochim Biophys Acta, 2006. **1757**(5-6): p. 692-9.
31. Tang, H.L., A.H. Le, and H.L. Lung, *The increase in mitochondrial association with actin precedes Bax translocation in apoptosis.* Biochem J, 2006. **396**(1): p. 1-5.
32. Graham, J.W., et al., *Glycolytic enzymes associate dynamically with mitochondria in response to respiratory demand and support substrate channeling.* Plant Cell, 2007. **19**(11): p. 3723-38.
33. Williams, T.C., L.J. Sweetlove, and R.G. Ratcliffe, *Capturing metabolite channeling in metabolic flux phenotypes.* Plant Physiol, 2011. **157**(3): p. 981-4.
34. Rugarli, E.I. and T. Langer, *Translating m-AAA protease function in mitochondria to hereditary spastic paraplegia.* Trends Mol Med, 2006. **12**(6): p. 262-9.
35. Giak Sim, K., et al., *Quantitative fibroblast acylcarnitine profiles in mitochondrial fatty acid beta-oxidation defects: phenotype/metabolite correlations.* Mol Genet Metab, 2002. **76**(4): p. 327-34.
36. Chua, B.T., et al., *Mitochondrial translocation of cofilin is an early step in apoptosis induction.* Nat Cell Biol, 2003. **5**(12): p. 1083-9.
37. Zhou, W., et al., *Proteomic analysis reveals Warburg effect and anomalous metabolism of glutamine in pancreatic cancer cells.* J Proteome Res, 2012. **11**(2): p. 554-63.
38. Page, E.L., et al., *Hypoxia-inducible factor-1alpha stabilization in nonhypoxic conditions: role of oxidation and intracellular ascorbate depletion.* Mol Biol Cell, 2008. **19**(1): p. 86-94.
39. Boulahbel, H., R.V. Duran, and E. Gottlieb, *Prolyl hydroxylases as regulators of cell metabolism.* Biochem Soc Trans, 2009. **37**(Pt 1): p. 291-4.
40. Olsen, R.K.J., N. Cornelius, and N. Gregersen, *Genetic and cellular modifiers of oxidative stress: What can we learn from fatty acid oxidation defects?* Molecular Genetics and Metabolism, 2013.

41. Campbell, C.T., J.E. Kolesar, and B.A. Kaufman, *Mitochondrial transcription factor A regulates mitochondrial transcription initiation, DNA packaging, and genome copy number.* Biochim Biophys Acta, 2012. **1819**(9-10): p. 921-9.
42. Xu, S., et al., *Overexpression of Tfam protects mitochondria against beta-amyloid-induced oxidative damage in SH-SY5Y cells.* FEBS J, 2009. **276**(14): p. 3800-9.

CHAPTER VI

Study 6 – Disclosing the differences in mitochondrial pathway modulation between severe and mild multiple acyl-CoA dehydrogenation deficiencies.
(in preparation)

Disclosing the differences in mitochondrial pathway modulation between severe and mild multiple acyl-CoA dehydrogenation deficiencies

Rocha H[1,2], Vitorino R[2], Amado F[3], Vilarinho L[1] and Ferreira R[2]

1- Newborn Screening, Metabolism and Genetics Unit, Genetics Department, National Institute of Health Ricardo Jorge, Porto, Portugal;
2- QOPNA, Department of Chemistry, University of Aveiro, Aveiro, Portugal
3- QOPNA, School of Health Sciences, University of Aveiro, Portugal

Abstract

Multiple acyl-CoA dehydrogenation deficiency is a mitochondrial fatty acid oxidation disorder caused, in most cases, by genetic mutations on electron transfer flavoprotein subunits (ETF subunits α of β) or in electron transfer flavoprotein ubiquinone oxidoreductase (ETF:QO). Defects in ETF/ETF:QO impair electron transfer from the dehydrogenation reactions of 12 flavoproteins to oxidative phosphorylation, compromising energy production. Clinically, patients can present with heterogeneous phenotypes and are usually grouped in severe or milder forms. Nevertheless the knowledge on the molecular basis of the disease, the way the pathological determinants interact towards the phenotype is still poor understood. We previously showed that in the severe forms, fatty acid oxidation, glycolysis, antioxidant defence systems and apoptosis are among the modulated pathways. In order to discriminate the pathways modulated among different severity phenotypes, we compared the mitochondrial proteome of severe and milder forms using an iTRAQ nanoLC-MS/MS proteomic approach. Our results revealed that in both phenotypic groups there is a metabolic reprogramming towards glycolysis and an up-regulation of MnSOD. The main difference was related to apoptosis, more pronounced in the severe forms. These results highlight the importance of integrated mitochondrial metabolism, intermediary metabolism and redox balance for FAOD cell survival.

Introduction

Mitochondrial fatty acid β-oxidation (FAO) is a key metabolic pathway for energy production, manly during periods of fasting, metabolic stress or illness [1]. To accomplish its function of providing substrates for gluconeogenesis/krebs cycle and electrons for the respiratory chain for energy production, about 25 proteins have to act coordinately enabling not only the transport of fatty acids (FA) to the mitochondria but also their complete oxidation to acetyl-CoA[1]. Deficiencies in several of these proteins are associated to human diseases forming the group of mitochondrial fatty acid β-oxidation disorders (FAOD), which are inherited metabolic disorders, that encompass at least 15 distinct enzyme and transport deficiencies[2, 3]. Among them is multiple acyl-CoA dehydrogenation deficiency (MADD; OMIM#231680; glutaric aciduria type II), an autosomal recessive inborn error of metabolism that affects the metabolism of fatty acids, amino acids and choline and is caused by defects in one of two flavoproteins: electron transfer flavoprotein (ETF) and ETF:ubiquinone oxidoreductase (ETF:QO)[4]. ETF exists in the mitochondrial matrix as an heterodimer of an alpha and beta subunits while ETF:QO is a monomer embedded in the inner mitochondrial membrane[5]. The role of ETF complex (ETF plus ETF:QO) in FAO is the acceptance of electrons from several mitochondrial flavin-containing dehydrogenases and their transfer to ubiquinone (coenzyme Q10) in the respiratory chain[5].

Clinically, MADD patients can be classified in three groups: neonatal onset forms, with (type I) or without (type II) congenital abnormalities and a late onset form (type III). Type I and type II can also be referred as severe MADD (S:MADD) while type III as mild MADD (M:MADD). Severe forms are characterized by hypoketotic hypoglycemias, hypotonia, failure to thrive, hyperammonemia, metabolic acidosis and usually result in early death. Milder forms may present proximal myopathy, hepatomegaly and encephalopathy usually associated to intermittent vomiting, hypoglycemia and lethargy[4]. Some of MADD patients, namely milder forms, respond positively to riboflavin supplementation what allows the definition of another sub group, the riboflavin

responsive MADD (RR:MADD)[6]. MADD is caused by mutations in the genes encoding for the alpha and beta ETF subunits (*ETFA* and *ETFB*) or in the one coding for ETF:QO (*ETFDH*). In MADD as well as in other FAOD affecting the oxidation of long chain fatty acids, is possible to establish some degree of genotype/phenotype correlation. Patients harbouring genetic variations that result in null or very little corresponding protein show more severe clinical, biochemical and cellular phenotype, while patients with genetic variations that allow the retention of some residual protein amounts and enzyme activity are usually associated to milder phenotypes[5, 7, 8]. Moreover, some patients with mutations in the *ETFDH* gene, more precisely in the FAD or ubiquinone binding domains, are associated with RR:MADD forms[6]. In this cases riboflavin acts as a chaperone, stabilizing the structure and activity level of the misfolded ETF:QO variant[9]. Nevertheless, pathophysiological mechanisms of the disease are not fully understood, namely the extent of the effect of enzyme deficiencies on mitochondrial and cellular functions. We previously shown that the mitochondrial response to a complete absence of ETF:QO was mainly characterized by an overexpression of chaperones, antioxidant enzymes and apoptotic proteins[10], what represented an extreme response to a severe deficiency. In order to better characterize pathway modulation in MADD, proteome profiling of isolated mitochondria from two MADD patient groups: severe and mild, non-riboflavin responsive, was performed by applying an iTRAQ nanoLC-MS/MS quantitative approach. Data highlight the similarities and differences of mitochondria proteome between patients with distinct disease phenotypes, contributing for the elucidation of the molecular mechanisms underlying disease development, with the ultimately aim of better define treatment strategies.

Material and Methods

Samples

Skin fibroblasts from three MADD patients and control individuals (n=4) were analysed. One patient presented a severe MADD form (S:MADD) and the other two mild forms (M:MADD1 and M:MADD2), all with mutations in *ETFDH*.

The S:MADD patient is homozygous for the mutation p.X618QextX14, that results in a protein extension of 13 amino acid residues at the C-terminal, and the M:MADD1 and M:MADD2 are both homozygous for the mutation p.R175H (c.524 G>A) in *ETFDH* exon 5.

Control fibroblasts were obtained from individuals with no apparent related disease and aged matched. Controls and patients fibroblasts were used, anonymously, after each subject/legal guardian gave written informed consent.

Cell culture

Skin fibroblasts were grown in Ham F10 nutrient mixture supplemented with 10% fetal calf serum, 2mmol/L glutamine, 1% penicillin, streptomycin and fungizone. Ten 75cm^2 culture flasks from each sample were grown to pre-confluence before mitochondria isolation.

Mitochondrial isolation

Isolation of mitochondria from the cell pellet was performed at 4 °C according to Rocha et al.[10]. Briefly, the cell pellet was suspended in isolation buffer (250mM sucrose, 1mM EGTA, 10mM HEPES and 5g/L BSA pH 7.5) and was then centrifuged at 500g for 2min. The supernatant was discarded and the remaining pellet was suspended in isolation buffer. The cell suspension was homogenized in a tight-fitting Potter homogenizer (Teflon pestle). After centrifugation at 1500g for 10min, the supernatant was kept on ice. The pellet was homogenized and centrifuged as described above. The two supernatants were pooled and centrifuged at 10,000g for 10min. The resulting mitochondrial pellet was washed with BSA-free isolation buffer. Protein content was determined with RC DC Protein Assay kit (Bio-Rad, Hercules, CA, USA).

iTRAQs comparative analysis of isolated mitochondria

For iTRAQ analysis, mitochondrial extracts from MADD patients and controls (pool of mitochondria isolated from fibroblasts of 4 healthy subjects) were used. Aliquots of 100µg of protein were analyzed in duplicate. An in-solution digestion was performed for iTRAQ labelling according to the protocol

provided by the manufacturer (Applied Biosystems, Foster City, CA). Two independent runs were carried out. Briefly, proteins were reduced, alkylated and digested. Samples were mixed with triethyl ammonium bicarbonate buffer (TEAB) (1M, pH 8.5) and RapiGest (Waters) to a final concentration of 0.5M and 0.1%, respectively, and then reduced with 50mM tris(2-carboxyethyl) phosphine (TCEP) for 1h at 37◦C and alkylated with 10mM S-methyl methanethiosulfonate (MMTS) for 10min at room temperature. The aliquots were digested with trypsin (Promega, Madison, WI) at a protein-to-enzyme ratio of 10:1 at 37°C overnight and then dried in a Speed-Vac (Thermo Savant, NY).

After protein digestion, the extracted peptides were labelled with iTRAQ reagents (8-plex) according to the manufacturer's instructions (Applied Biosystems, Foster City, CA). Briefly, one vial of iTRAQ reagent, previously dissolved in 70µL of ethanol, was added to each aliquot and incubated for 2h at room temperature. The reaction was stopped by adding water and the labelled digests corresponding to each of the four of 8-plex experiments were combined and dried in the Speed-Vac (Thermo Savant, NY).

The tryptic labelled digests were separated by a multidimensional approach based on a first dimension with high pH reverse-phase and a second dimension with the acidic reverse-phase system as previously described[11]. Briefly, sample loading was performed at 200 µL/min with buffers (A) 2% ammonium hydroxide and 0.014% formic acid in water, pH 10 and (B) 2% ammonium hydroxide and 90% acetonitrile (ACN) in water, pH 10. After 5 minutes of sample loading and washing, peptide fractionation was performed with linear gradient to 70 % B over 85 min. Sixty fractions were collected, dried in a SpeedVac and resuspended in 5% ACN and 0.1% trifluoroacetic acid (TFA). Collected fractions were then separated by LC. Collected fractions were separated using an Ultimate 3000 (Dionex, LCPackings, Sunnyvale, CA) onto a 150mm × 75µm Pepmap100 capillary analytical C18 column with 3µm particle size (Dionex, LC Packings) at a flow rate of 300nL/min. The mobile phases A and B were 2% ACN 0.1% TFA in water and 95% ACN, 0.045% TFA, respectively. The gradient started at 10 min and ramped to 60 % B till 50min and 100% B at 55min and retained 100% B till 65min. The chromatographic separation was monitored at 214nm using a UV detector

(Dionex/LC Packings) equipped with a 3nL flow cell. The peptides eluted from the column were mixed with a continuous flow of matrix solution (270nL/min, 2mg/mL α-CHCA in 70% ACN/0.1% TFA and internal standard Glu-Fib at 15ftmol) in a fractions microcollector (Probot, Dionex/LC Packings) and directly deposited onto the LC-MALDI plates at 12s intervals for each spot (150- nL/fraction). For every chromatographic run, a total of 208 fractions were collected.

MALDI-TOF/TOF MS analysis was performed using a 4800 MALDI-TOF/TOF Analyzer (Applied Biosystems, Foster City, CA), as described by Vitorino et al.[11]. A S/N threshold of 50 was used to select peaks for MS/MS analyses. A fragmentation voltage of 2kV was used throughout the automated runs. The spectra were processed and analyzed by the ProteinPilot software (v4.0 AB Sciex, USA), which uses paragon algorithm for protein/peptide identification based on MS/MS data. Searches were performed against the SwissProt protein database (release date 01032013) for *Homo sapiens*. Default search parameters were: specifying trypsin as the digestion enzyme, fixed modification of methylathion on cysteine residue and iTRAQ 8-Plex, biological modification with emphasis on phosphorylation and urea denaturation as the variable modification setting. The mass tolerances for precursor and fragments were default values for ProteinPilot®. The cut-off score value for protein identification with ProteinPilot® was a ProteoScore of 1.3 (95% confidence). A decoy database search strategy was also used to estimate the false discovery rate (FDR), defined as the percentage of decoy proteins identified against the total protein identification. The local FDR was calculated by searching the spectra against SwissProt (*Homo sapiens*) decoy database. The estimated low FDR of 0.9% indicated a high reliability in the proteins identified. Data was normalized for loading error by bias correction, which is an algorithm in ProteinPilot that corrects for unequal mixing when combining the labelled samples of one experiment. It does so by calculating the median protein ratio for all proteins reported in each sample, adjusted to unity and assigning an autobias factor to it. Nevertheless, the quantification results were reviewed manually for all proteins found to be differentially expressed (iTRAQ ratio>1.3 or<0.7 according to Vitorino et al. [12]).

Statistical analysis

Data is presented as mean of replicates. Significant differences among groups were evaluated with the unpaired student's *t* test, using GraphPad Prism® software (version 5.00). The level of significance was set at $p < 0.05$.

Results

In order to investigate the differences and similarities in the modulation of mitochondrial proteome between severe and mild forms of MADD, a global proteomic profiling approach based on nanoLC-MS/MS was applied to mitochondria isolated from cultured fibroblasts. The option for isolated mitochondria was based on the need to detect the modulation of mitochondrial pathways with greater sensitivity. One patient with severe and two with mild MADD, all harbouring mutations in *ETFDH* gene, as well as four aged matched controls were included in the present study.

We were able to successfully identify 454 proteins with a degree of confidence of over 95% (supplemental table 1), from which 48% were assigned to mitochondria, according to MitoMiner [13]. A significant proportion of the identified proteins had more than one sub-cellular location, for which its biological significance remains to be disclosed. One possibility is that multi-residential proteins support mitochondrial protein trafficking and connection with other organelles [14]. The clustering of the identified proteins according to Gene Ontology, revealed that the five most enriched biological processes were metabolic process, cellular process, localization, cellular component organization or biogenesis and immune system process (figure 1a). Similarly, the top five molecular function clusters were catalytic activity, binding, structural molecule activity, transport activity and receptor activity (figure 1b).

From the 454 distinct proteins identified, 95 were successfully quantified by iTRAQ-based nanoLC-MS/MS with a $p<0.05$, from which 52 were found modulated by MADD. In S:MADD we found 36 modulated proteins, in M:MADD1 31 and in M:MADD2 29 (table 1). Comparing the common modulated proteins between the patients, 15 were common to all of them,

being clear the higher similarities between M:MADD patients than between these and the S:MADD (figure 2).

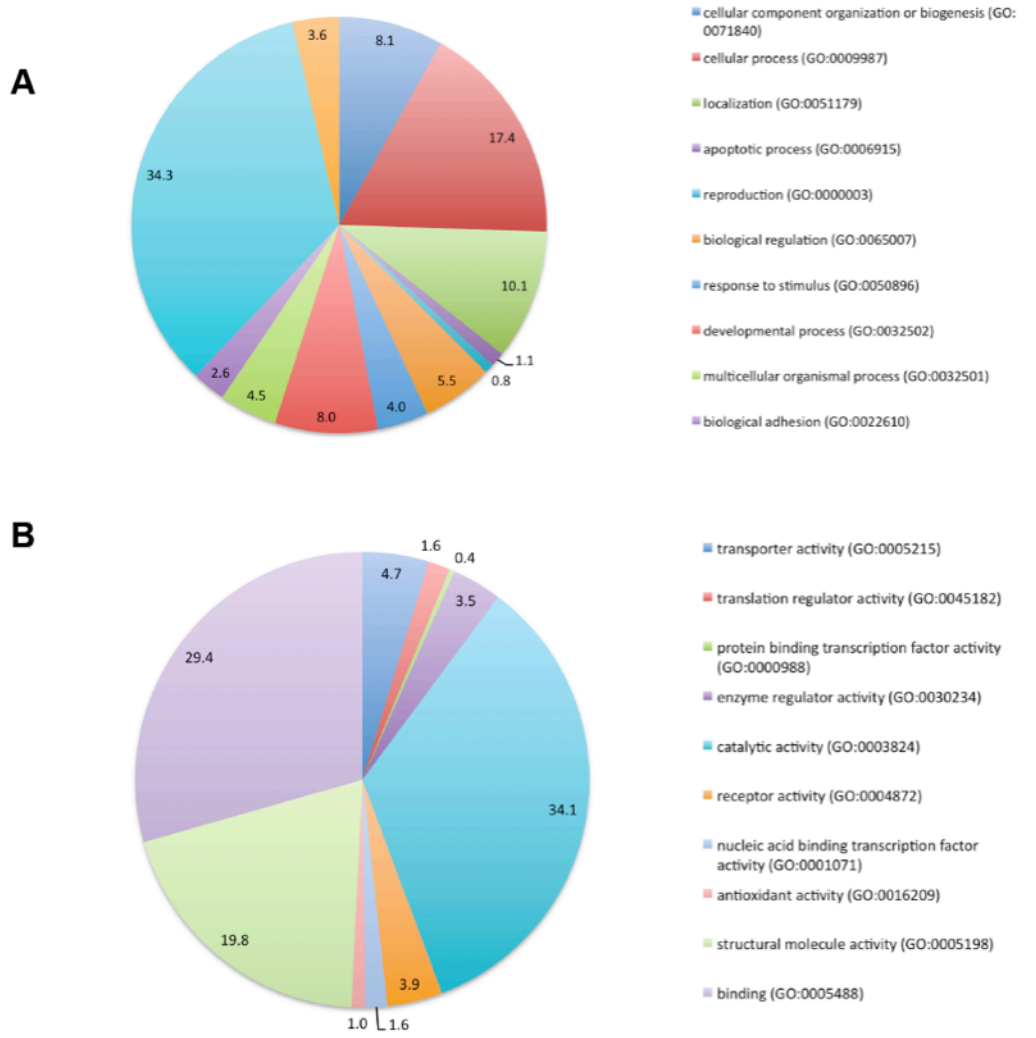

Figure 1: Pie charts showing the biological processes (A) and molecular functions (B) categories for the identified proteins, assigned by Panther. Values indicate the percentage of each cluster.

Table 1: Up and down-regulated proteins differentially expressed in the studied patients.

	Up-regulated	Down-regulated	Total
S:MADD	24	12	36
M:MADD1	26	5	31
M:MADD2	25	4	29

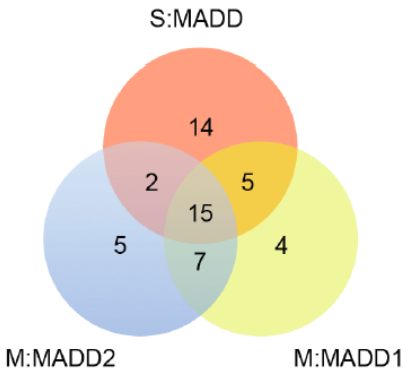

Figure 2: Venn diagram representing the modulated proteins identified in each of the patients studied

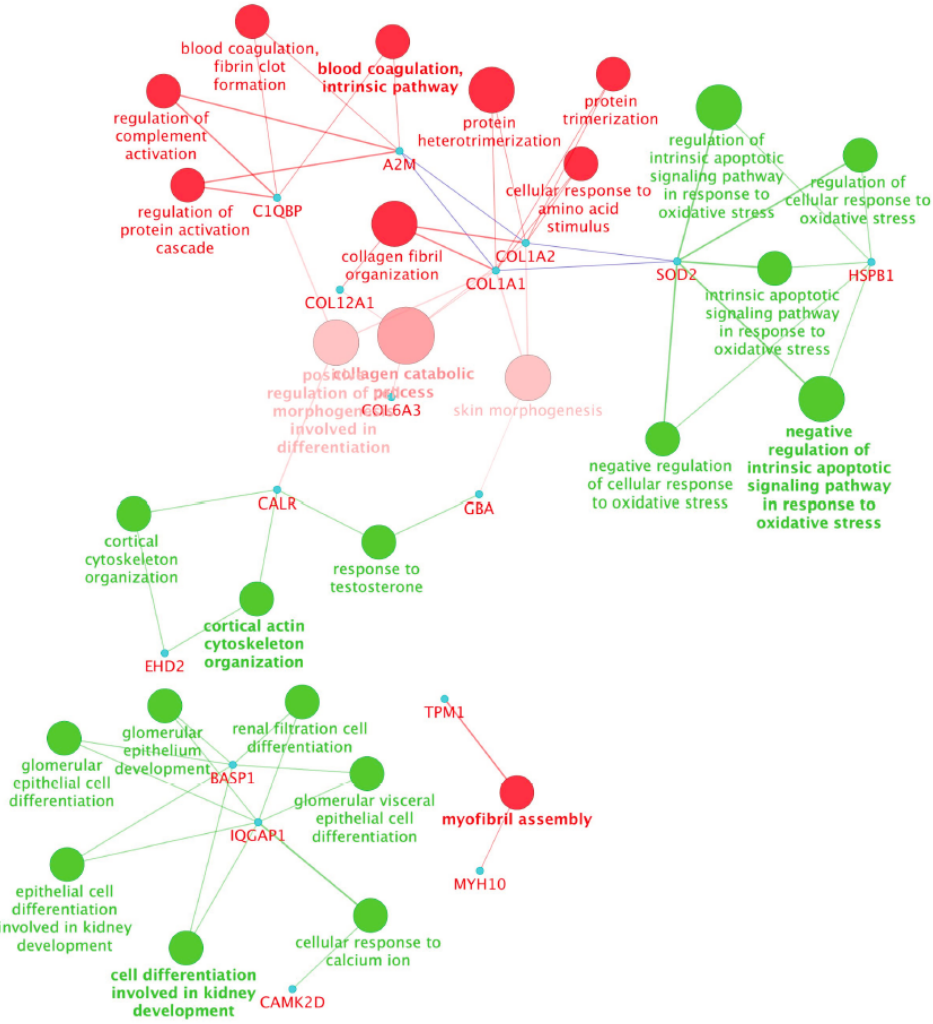

Figure 3: Integrated analysis of modulated proteins in S:MADD, using Cytoscape. Green dots represent up-regulated processes and red down-regulated processes.

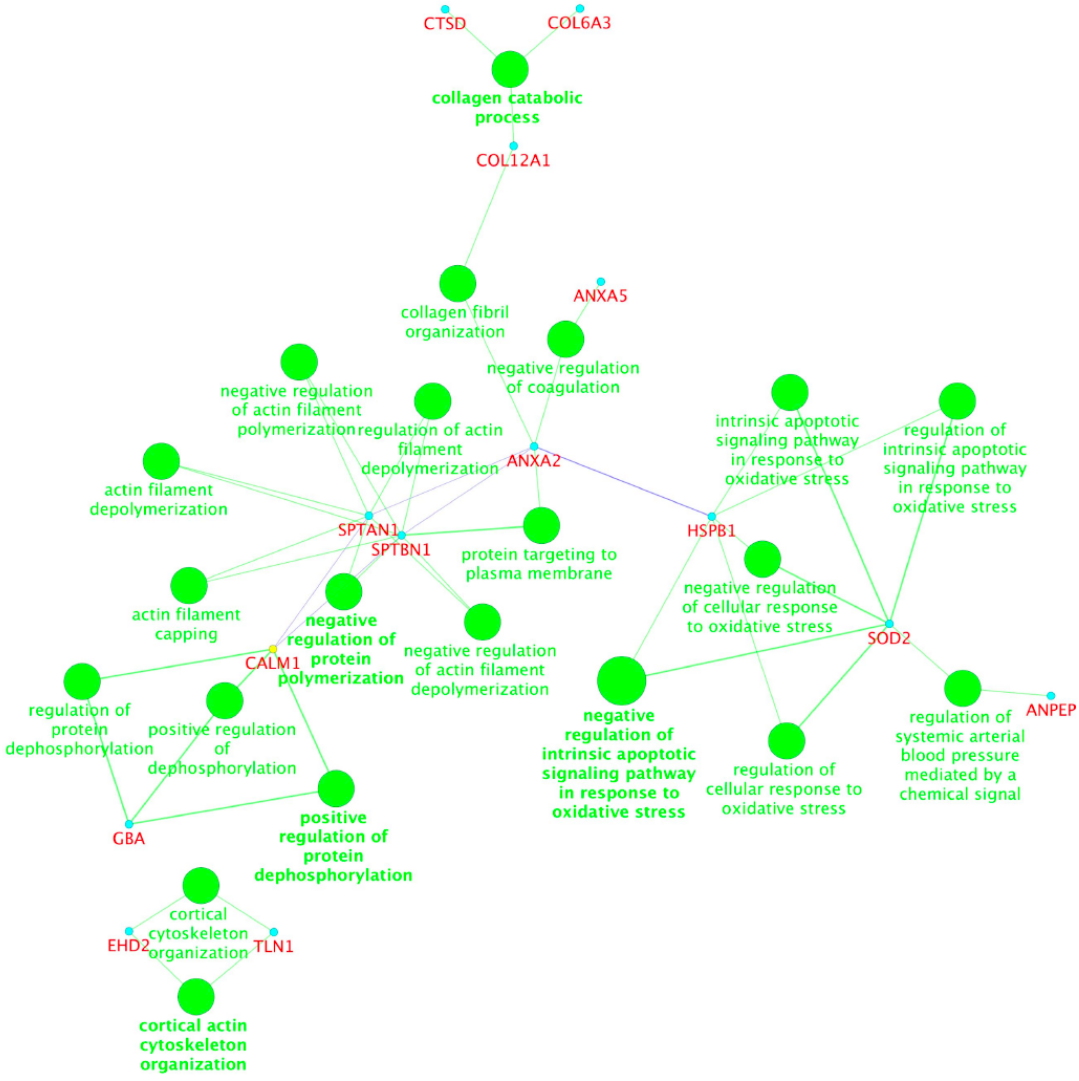

Figure 4: Integrated analysis of modulated proteins in M:MADD, using Cytoscape. Green dots represent up-regulated processes and red down-regulated processes.

An integrated analysis of modulated proteins in each group was performed using Cytoscape V3.0 (figures 3 and 4). Common to both MADD forms was the positive regulation of cellular response to oxidative stress and the negative regulation of the intrinsic apoptotic pathway in response to oxidative stress. In S:MADD (figure 3) was highlighted a positive modulation of cytoskeleton organization and negative modulation of collagen catabolic process, while in M:MADD (figure 4) was observed the positive modulation of actin metabolism and collagen catabolic process.

The analysis of biological processes and molecular functions influenced by the two MADD forms was done using WebGestalt [15]. In S:MADD the main biological processes modulated by the disease were cellular component organization or biogenesis, organism processes and response to wounding (figure 5) while in M:MADD it was observed a significant modulation of cellular component organization or biogenesis and other organization processes (figure 6).

Looking at the differentially expressed proteins in MADD patients, it gets clear that all three patients share common characteristics (table 2). One is the overrepresentation of cytoskeleton related proteins (e.g. tubulin alpha-1C, collagen alpha 3(VI) or septin-2), that most probably reflect a tight interaction with dysfunctional mitochondria [16]. It was also observed the overexpression of glycolytic enzymes, like alpha enolase, whose detection is not surprising given the close relation between glycolysis and mitochondria in order to maximise the metabolic flux towards energy production[17, 18]. Besides these, the modulation of proteins involved in signalling (e.g. Ras GTPase-activating-like protein), proteases (e.g. cathepsin D or tripeptidyl peptidase 1), redox (MnSOD) and apoptosis related proteins (e.g. annexin A5) were also observed.

Comparing S:MADD with M:MADD some differences emerge, like with glyceraldehyde-3-phosphate dehydrogenase, presented in higher levels only in S:MADD or vimentin, only elevated in the mild forms. It is worth notice the down regulation of ATP synthase subunit alpha in the S:MADD, in accordance to our previous observation[10].

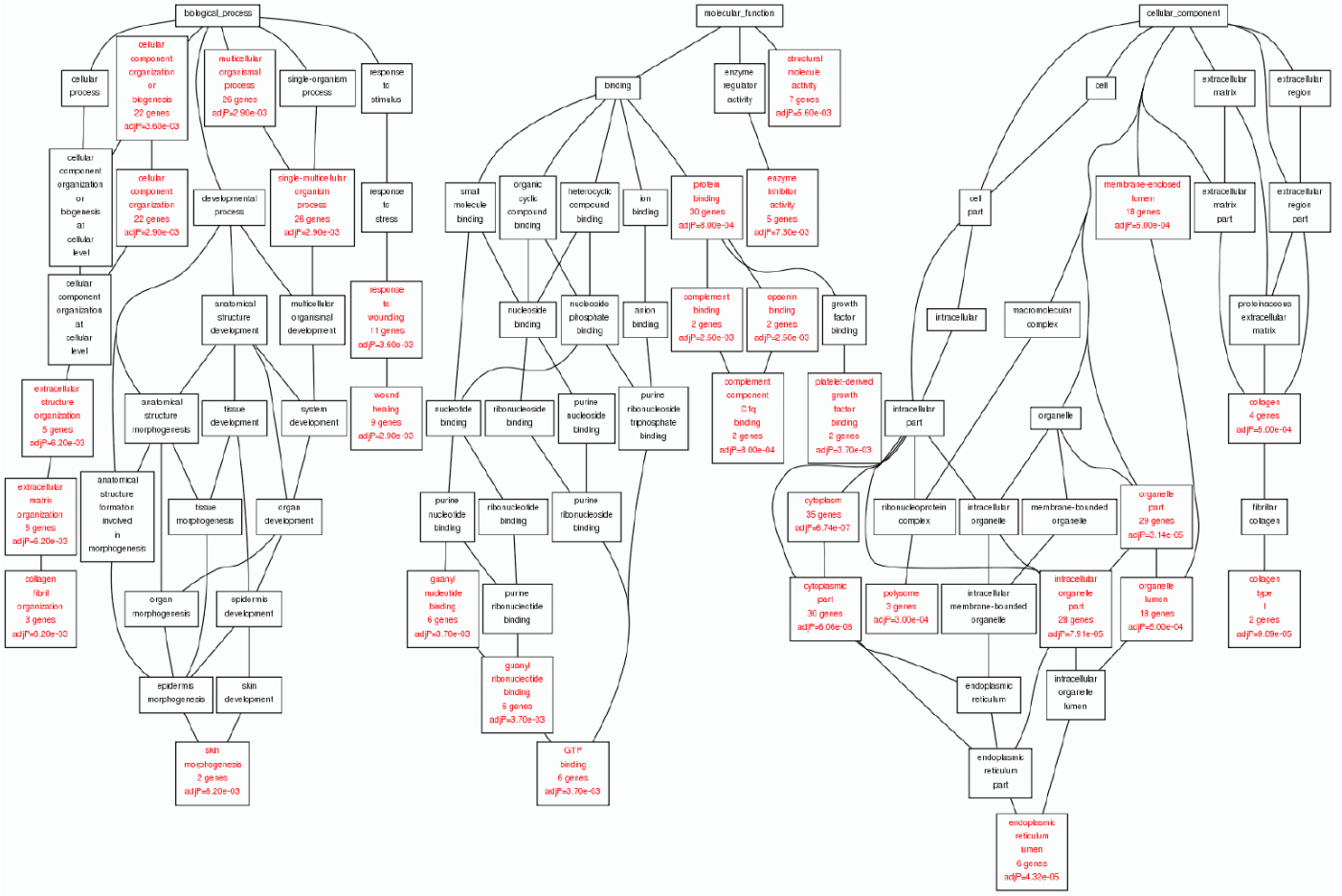

Figure 5: Proteins modulated in S:MADD clustered by biological process, molecular function and cellular component, according to Webgestalt.

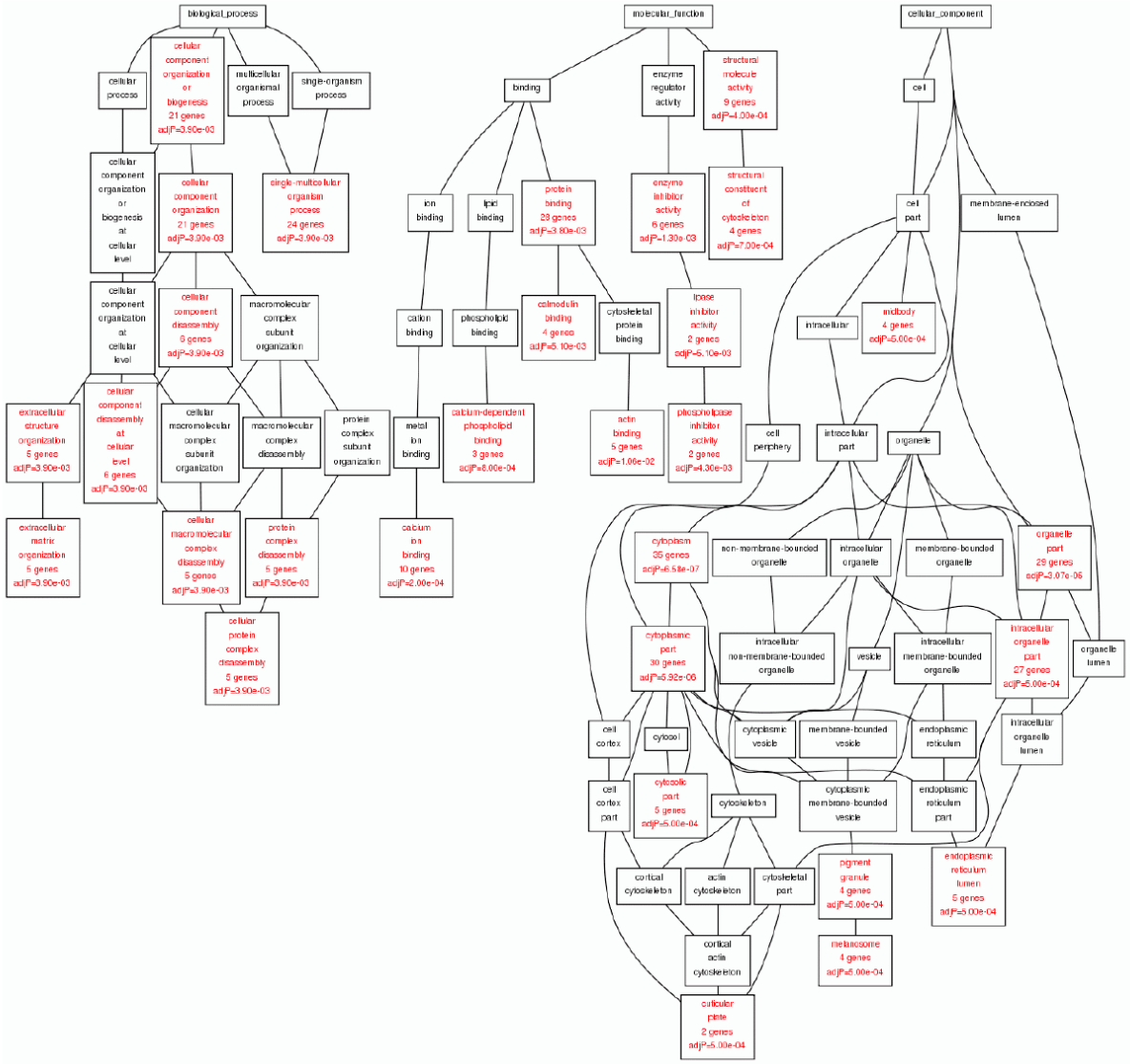

Figure 6: Proteins modulated in M:MADD clustered by biological process, molecular function and cellular component, according to Webgestalt.

Table 2: Differentially expressed proteins identified by comparative analysis of mitochondrial fraction of each of the patients studied with control subjects by nanoLC-MS/MS with iTRAQ labeling. In yellow are the down-regulated and in red the up-regulated ones.

Name	M:MADD1	M:MADD2	S:MADD
40S ribosomal protein S10 OS=Homo sapiens GN=RPS10 PE=1 SV=1	0.73	0.61	0.90
40S ribosomal protein S18 OS=Homo sapiens GN=RPS18 PE=1 SV=3	0.66	0.70	0.88
40S ribosomal protein S4, X isoform OS=Homo sapiens GN=RPS4X PE=1 SV=2	1.17	1.05	1.47
60S ribosomal protein L7a OS=Homo sapiens GN=RPL7A PE=1 SV=2	0.79	0.67	0.81
Adenylate kinase isoenzyme 4, mitochondrial OS=Homo sapiens GN=AK4 PE=1 SV=1	1.62	1.64	1.38
Alpha-2-macroglobulin OS=Homo sapiens GN=A2M PE=1 SV=3	0.64	0.96	0.47
Alpha-enolase OS=Homo sapiens GN=ENO1 PE=1 SV=2	2.33	2.06	1.79
Aminopeptidase N OS=Homo sapiens GN=ANPEP PE=1 SV=4	1.36	1.78	0.94
Annexin A2 OS=Homo sapiens GN=ANXA2 PE=1 SV=2	1.32	1.55	1.15
Annexin A5 OS=Homo sapiens GN=ANXA5 PE=1 SV=2	3.31	2.37	3.85
Annexin A6 OS=Homo sapiens GN=ANXA6 PE=1 SV=3	1.44	1.73	2.74
ATP synthase subunit alpha, mitochondrial OS=Homo sapiens GN=ATP5A1 PE=1 SV=1	0.79	0.81	0.59
Brain acid soluble protein 1 OS=Homo sapiens GN=BASP1 PE=1 SV=2	0.66	1.69	1.52
Calcium/calmodulin-dependent protein kinase type II subunit delta OS=Homo sapiens GN=CAMK2D PE=1 SV=3	1.19	0.96	1.91
Calmodulin OS=Homo sapiens GN=CALM1 PE=1 SV=2	1.24	1.47	0.91
Calreticulin OS=Homo sapiens GN=CALR PE=1 SV=1	1.20	1.05	1.66
Cathepsin D OS=Homo sapiens GN=CTSD PE=1 SV=1	1.30	1.01	1.26
CD44 antigen OS=Homo sapiens GN=CD44 PE=1 SV=3	0.73	0.97	1.42
Collagen alpha-1(I) chain OS=Homo sapiens GN=COL1A1 PE=1 SV=5	1.14	1.18	0.46
Collagen alpha-1(XII) chain OS=Homo sapiens GN=COL12A1 PE=1 SV=2	1.17	1.30	0.66
Collagen alpha-2(I) chain OS=Homo sapiens GN=COL1A2 PE=1 SV=7	0.97	1.01	0.58
Collagen alpha-3(VI) chain OS=Homo sapiens GN=COL6A3 PE=1 SV=5	1.77	1.81	1.43
Complement component 1 Q subcomponent-binding protein, mitochondrial OS=Homo sapiens GN=C1QBP PE=1 SV=1	0.81	0.89	0.65
Cytochrome b5 OS=Homo sapiens GN=CYB5A PE=1 SV=2	1.00	0.94	0.60
Developmentally-regulated GTP-binding protein 1 OS=Homo sapiens GN=DRG1 PE=1 SV=1	4.08	1.95	2.34
Dipeptidyl peptidase 1 OS=Homo sapiens GN=CTSC PE=1 SV=2	0.98	0.49	0.52
EH domain-containing protein 2 OS=Homo sapiens GN=EHD2 PE=1 SV=2	2.40	1.86	2.54
Galectin-3 OS=Homo sapiens GN=LGALS3 PE=1 SV=5	1.39	1.86	1.29
Glucosylceramidase OS=Homo sapiens GN=GBA PE=1 SV=3	1.78	1.41	2.13
Glyceraldehyde-3-phosphate dehydrogenase OS=Homo sapiens GN=GAPDH PE=1 SV=3	1.11	1.12	1.38
Heat shock protein beta-1 OS=Homo sapiens GN=HSPB1 PE=1 SV=2	1.43	1.71	1.62
Histone H2A type 1-J OS=Homo sapiens GN=HIST1H2AJ PE=1 SV=3	1.32	0.77	0.79
Mitochondrial inner membrane protein OS=Homo sapiens GN=IMMT PE=1 SV=1	0.69	0.76	0.53
Myosin-10 OS=Homo sapiens GN=MYH10 PE=1 SV=3	0.60	1.01	0.69
NADH-cytochrome b5 reductase 3 OS=Homo sapiens GN=CYB5R3 PE=1 SV=3	1.33	1.23	1.33
Peptidyl-prolyl cis-trans isomerase B OS=Homo sapiens GN=PPIB PE=1 SV=2	1.40	1.25	1.41
Plastin-3 OS=Homo sapiens GN=PLS3 PE=1 SV=4	2.02	1.74	1.83
Protein S100-A10 OS=Homo sapiens GN=S100A10 PE=1 SV=2	1.66	1.99	1.23
Ras GTPase-activating-like protein IQGAP1 OS=Homo sapiens GN=IQGAP1 PE=1 SV=1	1.82	1.54	1.42
Ras-related protein Rab-7a OS=Homo sapiens GN=RAB7A PE=1 SV=1	0.89	0.77	1.62
Reticulocalbin-1 OS=Homo sapiens GN=RCN1 PE=1 SV=1	1.42	1.10	0.99
Reticulocalbin-3 OS=Homo sapiens GN=RCN3 PE=1 SV=1	1.22	1.36	1.17
Septin-2 OS=Homo sapiens GN=SEPT2 PE=1 SV=1	1.46	1.33	1.35
Spectrin alpha chain, non-erythrocytic 1 OS=Homo sapiens GN=SPTAN1 PE=1 SV=3	1.40	1.57	1.24
Spectrin beta chain, non-erythrocytic 1 OS=Homo sapiens GN=SPTBN1 PE=1 SV=2	1.26	1.36	0.95
Stress-70 protein, mitochondrial OS=Homo sapiens GN=HSPA9 PE=1 SV=2	0.75	0.81	0.67
Superoxide dismutase [Mn], mitochondrial OS=Homo sapiens GN=SOD2 PE=1 SV=2	2.44	2.72	1.82
Talin-1 OS=Homo sapiens GN=TLN1 PE=1 SV=3	1.30	1.20	1.02
Tripeptidyl-peptidase 1 OS=Homo sapiens GN=TPP1 PE=1 SV=2	1.06	1.10	1.49
Tropomyosin alpha-1 chain OS=Homo sapiens GN=TPM1 PE=1 SV=2	1.21	1.20	0.63
Tubulin alpha-1C chain OS=Homo sapiens GN=TUBA1C PE=1 SV=1	1.78	1.76	2.29
Vimentin OS=Homo sapiens GN=VIM PE=1 SV=4	1.55	1.75	0.88

Discussion

In the present study we applied a nanoLC-MS/MS global proteomic approach to characterize mitochondria isolated from cultured fibroblasts of MADD patients, tracing a proteome signature of MADD pathogenesis. Disease pathogenesis in MADD is believed to rely mainly on the resultant energy

deficiency, the accumulation of toxic metabolites and misfolded proteins (depending on the nature of the disease causing mutation) and on the resulting oxidative stress[5, 19, 20]. We previously shown that the main modulated pathways in the severe MADD forms were protein quality control system, antioxidant defences, glycolysis and apoptosis[10]. However, how different MADD forms impact the molecular pathways harboured in mitochondria remained to be disclosed. The comparison of the mitochondrial proteome from MADD patients and normal controls highlighted the overrepresentation of cytoskeleton related proteins that assist in the maintenance of mitochondrial structure and function[21, 22], probably reflecting an installed mitochondrial dysfunction. It was also observed an overexpression of glycolytic enzymes like alpha enolase and glyceraldehyde-3-phosphate dehydrogenase (the last in S:MADD). This is in agreement with our previous observation [10] and with the occurrence of the Warburg effect, that represents a shifting from oxygen dependent oxidative phosphorylation to glycolysis for energy production. The Warburg effect has initially been reported in cancer cells[23], where it allows a more rapidly ATP production and generates molecular precursors and NADPH via the pentose phosphate shunt for anabolic metabolism, essential for cell proliferation[24]. In FAOD it represents an alternative to an inefficient ATP production at the mitochondria, allowing also a decrease of ROS production, contributing to bring them to a level where cells can evade damage [20]. This metabolic reprogramming has been reported by us in S:MADD[10] and in long chain-3-hydroxy-acyl-CoA dehydrogenase deficiency (unpublished data) and by Edhager's group in short chain-acyl-CoA dehydrogenase deficiency[25]. Such metabolic adaptation seems to represent a hallmark of FAOD, independently of the type of enzyme deficiency and the severity of the clinical picture. It is noteworthy the overrepresentation of tubulin in the MADD patients, that is reported to block VDAC, turning mitochondrial metabolism off and so, playing an important role on the Warburg effect installation[24].

ETF complex is one of the mitochondrial sites for ROS production, with pathological variants associated to increased ROS [26, 27], being reported that oxidative defence systems are positively modulated in severe MADD [10] and negatively modulated in riboflavin responsive forms [20]. Present data

reveals that in the mild forms (non-riboflavin responsive), as in the severe ones, is present an over-expression of MnSOD. In M:MADD ROS seem high enough to push for an up-regulation of MnSOD. Nevertheless, ROS levels are supposed to be lower than in the severe forms, based on the higher expression levels of glyceraldehyde-3-phosphate dehydrogenase noticed in S:MADD. This enzyme, besides its glycolytic role is also known to be a signalling component in oxidative stress induced cell death [28, 29], being its translocation to mitochondria an event that facilitates apoptosis [30]. Depending on ROS levels the cell adopts different molecular strategies that will ultimately lead to different fates.

Data analysis suggests that ROS levels most probably overwhelm cellular detoxifying capacity, with the activation of apoptotic mechanisms, evidenced by the overexpression of annexin A5. The translocation of annexin A5 to mitochondria have recently been associated to apoptosis, via the modulation of mitochondrial membrane potential and apoptogenic factors [31]. This is in agreement with the previously reported overexpression of Diablo homolog protein in S:MADD[10]. Nevertheless, data seems to point that in S:MADD the mitochondrial dysfunction is more pronounced than in M:MADD. In S:MADD we observed a significant down regulation of mitochondrial inner membrane protein (mitofilin) and complement component 1Q subcomponent-binding protein, that are more pronounced than in M:MADD. Mitochondrial inner membrane protein is a key protein in mitochondrial membrane organization and its down-regulation has been associated to altered mitochondrial morphology leading to mitochondrial dysfunction[32] and to an increased release of cytochrome c, which in cytoplasm activates apoptosis[33]. Complement component 1Q subcomponent-binding protein (p32 protein) down regulation is associated to an enhanced mitochondrial fragmentation [34]. On the other hand in M:MADD there was an overrepresentation of proteins associated to mitochondrial stabilization and pro-survival processes, like annexin A2[35], galectin-3[36], vimentin[37] and aminopeptidase N[38].

In conclusion, in both MADD phenotypic groups it was observed a metabolic reprogramming towards glycolysis as a response to a dysfunctional mitochondria and an up-regulation of MnSOD .

The main differences between S:MADD and M:MADD are associated to the positive modulation of apoptosis that is more pronounced in the severe form. Our work also underscores the importance of integrated mitochondrial metabolism, intermediary metabolism and redox balance for cell survival in FAOD.

References

1. Houten, S.M. and R.J.A. Wanders, *A general introduction to the biochemistry of mitochondrial fatty acid β-oxidation.* Journal of Inherited Metabolic Disease, 2010. **33**(5): p. 469-477.
2. Kompare, M. and W. Rizzo, *Mitochondrial Fatty-Acid Oxidation Disorders.* Seminars in Pediatric Neurology, 2008. **15**(3): p. 140-149.
3. Moczulski, D., I. Majak, and D. Mamczur, *An overview of beta-oxidation disorders.* Postepy Hig Med Dosw (Online), 2009. **63**: p. 266-77.
4. Vockley, J. and D.A. Whiteman, *Defects of mitochondrial beta-oxidation: a growing group of disorders.* Neuromuscul Disord, 2002. **12**(3): p. 235-46.
5. Gregersen, N. and R.K. Olsen, *Disease mechanisms and protein structures in fatty acid oxidation defects.* J Inherit Metab Dis, 2010.
6. Olsen, R.K., et al., *ETFDH mutations as a major cause of riboflavin-responsive multiple acyl-CoA dehydrogenation deficiency.* Brain, 2007. **130**(Pt 8): p. 2045-54.
7. Olsen, R.K., et al., *Clear relationship between ETF/ETFDH genotype and phenotype in patients with multiple acyl-CoA dehydrogenation deficiency.* Hum Mutat, 2003. **22**(1): p. 12-23.
8. Gregersen, N., et al., *Mutation analysis in mitochondrial fatty acid oxidation defects: Exemplified by acyl-CoA dehydrogenase deficiencies, with special focus on genotype-phenotype relationship.* Hum Mutat, 2001. **18**(3): p. 169-89.
9. Cornelius, N., et al., *Molecular mechanisms of riboflavin responsiveness in patients with ETF-QO variations and multiple acyl-CoA dehydrogenation deficiency.* Hum Mol Genet, 2012. **21**(15): p. 3435-48.
10. Rocha, H., et al., *Characterization of mitochondrial proteome in a severe case of ETF-QO deficiency.* J Proteomics, 2011. **75**(1): p. 221-8.
11. Vitorino, R., et al., *Toward a standardized saliva proteome analysis methodology.* J Proteomics, 2012. **75**(17): p. 5140-65.
12. Vitorino, R., et al., *Evaluation of different extraction procedures for salivary peptide analysis.* Talanta, 2012. **94**: p. 209-15.
13. Smith, A.C., J.A. Blackshaw, and A.J. Robinson, *MitoMiner: a data warehouse for mitochondrial proteomics data.* Nucleic Acids Res, 2012. **40**(Database issue): p. D1160-7.
14. Deng, N., et al., *Phosphoproteome analysis reveals regulatory sites in major pathways of cardiac mitochondria.* Mol Cell Proteomics, 2011. **10**(2): p. M110 000117.

15. Wang, J., et al., *WEB-based GEne SeT AnaLysis Toolkit (WebGestalt): update 2013.* Nucleic Acids Res, 2013. **41**(Web Server issue): p. W77-83.
16. Kuznetsov, A.V., et al., *Cytoskeleton and regulation of mitochondrial function: the role of beta-tubulin II.* Front Physiol, 2013. **4**: p. 82.
17. Williams, T.C., L.J. Sweetlove, and R.G. Ratcliffe, *Capturing metabolite channeling in metabolic flux phenotypes.* Plant Physiol, 2011. **157**(3): p. 981-4.
18. Graham, J.W., et al., *Glycolytic enzymes associate dynamically with mitochondria in response to respiratory demand and support substrate channeling.* Plant Cell, 2007. **19**(11): p. 3723-38.
19. Olpin, S.E., *Pathophysiology of fatty acid oxidation disorders and resultant phenotypic variability.* J Inherit Metab Dis, 2013.
20. Olsen, R.K.J., N. Cornelius, and N. Gregersen, *Genetic and cellular modifiers of oxidative stress: What can we learn from fatty acid oxidation defects?* Molecular Genetics and Metabolism, 2013.
21. Anesti, V. and L. Scorrano, *The relationship between mitochondrial shape and function and the cytoskeleton.* Biochim Biophys Acta, 2006. **1757**(5-6): p. 692-9.
22. Knowles, M.K., et al., *Cytoskeletal-assisted dynamics of the mitochondrial reticulum in living cells.* Proc Natl Acad Sci U S A, 2002. **99**(23): p. 14772-7.
23. Dakubo, G.D., *The Warburg Phenomenon and Other Metabolic Alterations of Cancer Cells.* 2010: p. 39-66.
24. Maldonado, E.N. and J.J. Lemasters, *Warburg revisited: regulation of mitochondrial metabolism by voltage-dependent anion channels in cancer cells.* J Pharmacol Exp Ther, 2012. **342**(3): p. 637-41.
25. Edhager, A.V., et al., *Proteomic investigation of cultivated fibroblasts from patients with mitochondrial short-chain acyl-CoA dehydrogenase deficiency.* Mol Genet Metab, 2014.
26. Rodrigues, J.V. and C.M. Gomes, *Mechanism of superoxide and hydrogen peroxide generation by human electron-transfer flavoprotein and pathological variants.* Free Radic Biol Med, 2012. **53**(1): p. 12-9.
27. Cornelius, N., et al., *Secondary coenzyme Q10 deficiency and oxidative stress in cultured fibroblasts from patients with riboflavin responsive multiple Acyl-CoA dehydrogenation deficiency.* Hum Mol Genet, 2013. **22**(19): p. 3819-27.
28. Chen, J.K., et al., *Oxidative stress-induced attenuation of thrombospondin-1 expression in primary rat astrocytes.* J Cell Biochem, 2011. **112**(1): p. 59-70.
29. Ito, Y., et al., *Oxidative stress increases glyceraldehyde-3-phosphate dehydrogenase mRNA levels in isolated rabbit aorta.* Am J Physiol, 1996. **270**(1 Pt 2): p. H81-7.
30. Tarze, A., et al., *GAPDH, a novel regulator of the pro-apoptotic mitochondrial membrane permeabilization.* Oncogene, 2007. **26**(18): p. 2606-20.
31. Jeong, J.J., et al., *Role of Annexin A5 in Cisplatin-induced Toxicity in Renal Cells: MOLECULAR MECHANISM OF APOPTOSIS.* J Biol Chem, 2014. **289**(4): p. 2469-81.

32. von der Malsburg, K., et al., *Dual role of mitofilin in mitochondrial membrane organization and protein biogenesis.* Dev Cell, 2011. **21**(4): p. 694-707.
33. Yang, R.F., et al., *Mitofilin regulates cytochrome c release during apoptosis by controlling mitochondrial cristae remodeling.* Biochem Biophys Res Commun, 2012. **428**(1): p. 93-8.
34. Hu, M., et al., *p32 protein levels are integral to mitochondrial and endoplasmic reticulum morphology, cell metabolism and survival.* Biochem J, 2013. **453**(3): p. 381-91.
35. Bao, H., et al., *Overexpression of Annexin II affects the proliferation, apoptosis, invasion and production of proangiogenic factors in multiple myeloma.* Int J Hematol, 2009. **90**(2): p. 177-85.
36. Yu, F., et al., *Galectin-3 translocates to the perinuclear membranes and inhibits cytochrome c release from the mitochondria. A role for synexin in galectin-3 translocation.* J Biol Chem, 2002. **277**(18): p. 15819-27.
37. Tang, H.L., et al., *Vimentin supports mitochondrial morphology and organization.* Biochem J, 2008. **410**(1): p. 141-6.
38. Piedfer, M., et al., *Aminopeptidase-N/CD13 is a potential proapoptotic target in human myeloid tumor cells.* FASEB J, 2011. **25**(8): p. 2831-42.

CHAPTER VII

General discussion

General discussion

Mitochondria fatty acid β-oxidation disorders are one of the main groups of inherited metabolic diseases alongside glycogen storage disease, organic acidurias, urea cycle defects and OXPHOS defects, only to cite some. Without an early intervention the majority of FAOD leads to high morbidity and mortality, which makes them key targets for NBS programs.

Data from NBS programs allow a better comprehension of the natural history of these disorders being also, due to their high coverage and detection rate, one of the best ways to estimate the birth prevalence of a disorder or group of disorders. This epidemiological index is one of the important parameters to decide if a disease should or should not be included in screening programs, due to its impact in screening value (Andermann, Blancquaert et al. 2008).

Since the beginning of the XXI century that NBS programs in Europe started to introduce MS/MS screening for metabolic disorders in their practice (Loeber, Burgard et al. 2012) and since then several reports on the birth prevalence of FAOD in European countries became available (Kasper, Ratschmann et al. 2010, Lindner, Gramer et al. 2011, Lund, Hougaard et al. 2012), all revealing MCADD as the most frequent FAOD. It also became clear that this group of metabolic disorders was much more frequent than previously expected based on clinical evaluation (Wilcken, Haas et al. 2007, Spiekerkoetter 2010). This is mostly due to the identification of patients that could remain asymptomatic or with minor symptoms throughout life and, on the other hand, to the detection of patients with severe forms that could die without diagnosis. Nevertheless, data from Iberia is scarce with the only report representing data from the NBS of about 300,000 Portuguese newborns (Vilarinho, Rocha et al. 2010). There was also no report integrating available data on birth prevalence of FAOD in Europe. In order to fulfil this gap, data from six Iberian NBS programs were collected (Portugal, Galicia, Aragon/LaRioja, Murcia, Western Andalucia and Eastern Andalucia) resulting in the compilation of the results from the screening of more than 1.6 million newborns, which was compared to available data from other European populations (study 1). Our data reveal that the global birth prevalence of FAOD in Iberia is one of the highest reported (1:7,914; 95% CI: 1:9,054 to 1:6,916) in line with Denmark (1:7,691) (Lund, Hougaard et al. 2012) and Italy (1:8,777) (data extracted from Italian national NBS reports from 2006 to 2012, available on

http://www.simmesn.it/it/documents/rt_screening/index.html; accessed on December 2013) and much higher than the observed in Austria and Greece (1:12,704 and 1:45,000 respectively) (Kasper, Ratschmann et al. 2010, Loukas, Soumelas et al. 2010). However, significant differences were also noticed between Iberian regions, with Portugal presenting higher birth prevalence of FAOD than Spain. Portugal with a birth prevalence of FAOD of 1:6,351 newborns, almost the double of Spain (1:12,104), has one of the highest birth prevalence of FAOD ever reported. The major contributor for this result is the high frequency of MCADD in Portugal that presents a birth prevalence of 1:8,380, one of the highest reported. The most probable explanation for this is the fact that the great majority of Portuguese MCADD patients are Gypsies, a community classically associated to high inbreeding. Overall, data highlight the importance of screening all Iberian newborns for this group of disorders.

In order to understand better the relationship between genotype, biochemical parameters and clinical data at diagnosis and during follow up in MCADD patients, a multicenter research project was established between Portuguese and Spanish groups (study 2). Data from this project revealed that the percentage of MCADD patients homozygous for the common mutation c.985 A>G is 76% among the studied cohort and higher than previously reported for other populations, that range from 30% to 71% (Yokota, Coates et al. 1991, Nichols, Saavedra-Matiz et al. 2008). This is mostly due to the high occurrence of this disorder among Iberian Gypsy communities, particularly in Portugal, and represents an important epidemiological difference when in comparison with other European populations. It was also observed a statistically significant association between low free carnitine levels at the time of NBS and homozygosity for the common mutation. Although carnitine supplementation in MCADD patients is controversial (Walter 2003) this result points to the need of a different follow-up protocol depending on the genotype, with a tight monitoring of carnitine levels in homozygous for the common mutation. This study also contributed to a better understanding of the relationship between genotype and biochemical phenotype. Nevertheless, MCADD remains an unpredictable FAOD, indicating the need of further studies to disclose its pathophysiology.

To go deeper into the pathophysiology of inherited metabolic disorders in general and of FAOD in particular, we have to look at them not as purely monogenic disorders and study them in a polygenic perspective. In order to achieve it, a global mitochondrial proteomic approach was applied to mitochondria extracts obtained from FAOD patients' fibroblasts. Mitochondrial proteomics allows disclosing mitochondrial dynamics under various

pathophysiological conditions and provides an integrated perception into mitochondrial protein relative abundance, highlighting pathways activation/inhibition.

Although liver, heart and skeletal muscle are the most affected tissues in FAOD, skin fibroblasts are usually the sample of choice for the enzymatic confirmation of diagnosis, being also a model system for the study of disease pathogenesis (Palmfeldt, Vang et al. 2009, Gregersen, Hansen et al. 2012). Fibroblasts are an attractive sample considering the minimal invasive character of sampling and the large amount of cell material that can be obtained by culturing. Besides these advantages very few studies focused on mitochondrial protein profiling in cultured fibroblasts were reported. In order to define the strengths and limitations of a proteomic approach to the study of mitochondrial proteome in fibroblasts and the potential implications for the comprehension of metabolic disease pathogenesis, a comparative analysis of gel-based and gel-free protein approaches and protein identification algorithms (Mascot and Paragon) was performed (study 3). Three separation approaches were compared: two dimensional electrophoresis (2DE-MS), sodium dodecyl-sulphate liquid chromatography (SDS-LC-MS) and multidimentional liquid chromatography (2D-LC-MS), followed by mass spectrometry analysis for protein identification. The combined data from all these approaches and search methods allowed the identification of 696 non-redundant proteins. Despite the high sample amount needed for 2DE, approximately six times more than for SDS-LC or 2D-LC, fewer proteins were identified in comparison with the other two separation methods. However, 2DE allows distinguishing multiple forms of proteins with differences in molecular mass, isoelectric point and with post-transcriptional modifications (PTM's) (e.g. phosphorylation). Data highlighted the impact of protein separation methods on the characterization of mitochondrial proteome from cultured fibroblasts. Although the higher number of proteins identified by SDS-LC, 2DE allows the identification of a significant content of unique proteins and so must be seen as a complementary approach for a deeper protein profiling of mitochondria. The results show the power of integrating different separation technologies and protein identification algorithms.

To describe the mitochondrial proteome response to FAOD, fibroblasts from patients with MADD (severe and moderate forms, all with mutations in *ETFDH* gene and non responsive to riboflavin) and LCHADD (homozygous for the common mutation) were chosen. The choice of these disorders was based on the possibility of analysing two groups – mild and severe – that could potentiate the discriminatory power on the mitochondrial response to different deficiency degrees, enabling also comparisons

between them, looking for similarities and differences. The generated data could then be compared to that reported for less severe FAOD.

The characterization of mitochondrial proteome of a severe MADD by 2DE-MS/MS allowed the identification of 286 distinct proteins from several functional clusters, with particular relevance to protein binding/folding, metabolism and apoptosis (study 4). The main observed differences in protein abundance included the overexpression of chaperones (e.g. Hsp 60 and Hsp 70), antioxidant enzymes (e.g. MnSOD and peroxiredoxin-6), apoptotic proteins (e.g. Girdin) and glycolytic enzymes (e.g. glyceraldeyde-3-phospate dehydrogenase (GAPDH and α-enolase), alongside a down-representation of some β-oxidation enzymes (e.g. MCAD and SCAD).

The obtained data reveals a cellular adaptation to the lack of energy production through β-oxidation of fatty acids with a shift to glycolysis, represented by an overrepresentation of glycolytic enzymes and down-representation of β-oxidation ones. Another relevant finding was the down-representation of some OXPHOS related proteins (e.g. ATP synthase α and β, and NADH dehydrogenase flavoprotein 2), which highlights the close link between OXPHOS and FAO, at least in ETF complex defects. ATP synthase activity was decreased, being most probably OXPHOS secondary dysfunction a contributor for the pathophysiology in ETF complex deficiencies. The overexpression of chaperones probably reflects a cellular response to counteract the instability/disorganization inside the mitochondria due to the absence of ETF-QO, with the consequent activation of the mtPQC system. The observed over-expression of mitochondrial antioxidant enzymes, like MnSOD, glutathione-S-transferase or peroxiredoxin-6, was most probably triggered by the increased ROS observed in these cells. Nevertheless, the presence of an increased quantity of apoptotic proteins, points out that cellular aggressors overwhelm cellular capacity to neutralize and control them, resulting in mitochondrial/cellular damage and ultimately in cellular death.

In order to trace a pattern of mitochondrial response to LCHADD we proceed to the mitochondrial proteome analysis of one severe and one mild LCHADD patients (study 5). The obtained results revealed that as in severe MADD, there is a metabolic shift to glycolysis in response to the FAO blockage, with an overrepresentation of glycolytic enzymes. Signs of apoptosis were also noticed, like the overrepresentation of cofilin, whose translocation to the mitochondria is an early step in apoptosis induction, occurring before caspase activation (Chua, Volbracht et al. 2003). The comparison of mitochondrial

proteome between both patients highlighted a different regulation of the antioxidant defence system. The patient with the severe clinical phenotype presented an over-expression of MnSOD associated with a significant increase in ROS levels, while the mild LCHADD patient presented slightly ROS elevation and MnSOD down-regulation. This was particularly interesting since both patients were homozygous for the same disease causing mutation. Probably in individuals with lower ROS levels there is the need for a MnSOD down-regulation so they can increase and act as signalling molecules driving the metabolic reprogramming, while in the forms with high ROS, MnSOD must be up-regulated for detoxifying purposes. These results suggest that mitochondrial ROS levels and the individual ability to buffer them are of key importance for disease progression and outcome. It also becomes clear that other determinants than the disease causing mutation modulate the distinct clinical outcomes of LCHADD patients.

When a comparison between severe (S:MADD) and mild (M:MADD; non-riboflavin responsive) MADD forms was made (study 6) a metabolic reprogramming towards glycolysis and apoptotic pathway modulation was observed in all patients. Nevertheless, such adaptation was more notorious in S:MADD than in M:MADD with a more pronounced positive modulation of the apoptotic process. In respect to antioxidant system regulation, in all three patients an MnSOD up-regulation was observed. ROS levels in M:MADD seem to be high enough to trigger a MnSOD overexpression. Howerver, ROS levels in M:MADD are expected to be lower than in S:MADD based on the less apoptotic signs and on the lower levels of glyceraldehyde-3-phosphate dehydrogenase, a signalling component of oxidative stress cell death (Ito, Pagano et al. 1996, Chen, Zhan et al. 2011). These alterations in ROS levels probably underlie the differences in apoptotic pathway modulation, contributing to the clinical phenotype.

Merging the data from MADD and LCHADD it is possible to trace similarities in the response mechanisms of mitochondria to a FAO blockage. It was observed in all patients a metabolic reprogramming towards glycolysis – the Warburg effect. This was also reported recently in SCADD patients (Edhager, Stenbroen et al. 2014) which points out that it is a hallmark of FAOD, independently of the enzyme deficiency and of disease severity. While in cancer cells the Warburg effect aims at rapidly generating ATP, molecular precursors and NADPH to support cell proliferation, in FAO it seems to be a cellular adaptation to dysfunctional mitochondria, in order to increase survival. The Warburg effect may result from the activation of the transcription factor hypoxia-inducible factor 1-alpha (HIF 1α). A down regulation of prolyl 4 hydroxylase, which prompts to a

decrease HIF 1α degradation, was observed in LCHADD. Moreover, it has been proposed that ROS are also responsible for HIF 1α stimulation (Nazarewicz, Dikalova et al. 2013, Olsen, Cornelius et al. 2013). This links the observed oxidative stress, mitochondrial antioxidant system modulation and pro-survival metabolic reprogramming.

The data here obtained and that reported by others (Pedersen, Zolkipli et al. 2010, Schmidt, Corydon et al. 2010, Olsen, Cornelius et al. 2013) allows to hypothesise a mechanism for MnSOD modulation in FAOD (figure 1).

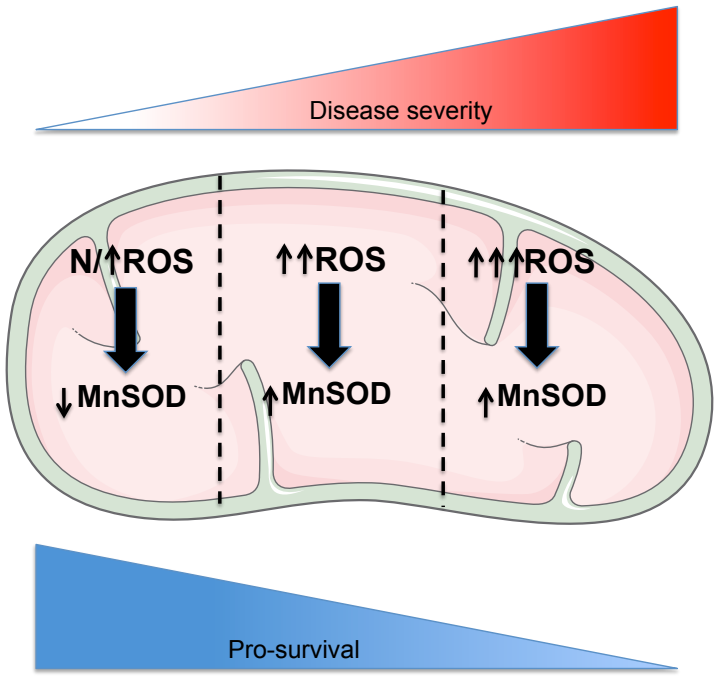

Figure 1: Hypothetical model for the modulation of MnSOD in FAOD.
According to this hypothetical model, in FAOD cells with lower ROS levels there is a down-regulation of MnSOD so they can increase and act as signalling molecules, and when ROS levels are higher MnSOD is over-expressed for detoxifying purposes.
N, normal; MnSOD, manganese superoxide dismutase; ROS, reactive oxygen species.

It is probable that due to a FAO blockage, and to the resulting mitochondrial dysfunction, cells shift to glycolysis for ATP production being ROS a key signalling in this process (Nazarewicz, Dikalova et al. 2013). In FAOD cells that due to the nature of the enzyme deficiency, the nature of the disease causing mutation or individual response to stress, have lower oxidative stress levels, MnSOD is down-regulated in order to increase ROS, namely superoxide which was suggested to be a signalling molecule towards Warburg effect (Sarsour, Kalen et al. 2012, Nazarewicz, Dikalova et al. 2013). On the other hand, when FAO deficient mitochondria already generate significant amounts of ROS, cell overexpress MnSOD for detoxifying purposes, which can lead to cellular death when ROS

levels are very high (Bolisetty and Jaimes 2013). According to this hypothesis low ROS-inducing MnSOD down-regulation are more favourable than high ROS and MnSOD overexpression. This hypothetical model on the possible contribution of ROS for pathophysiology of FAOD might help to explain why individuals with the same disease causing mutation may present divergent clinical pictures, based on ROS levels generated by their mitochondria. Nevertheless, more data is needed to corroborate the proposed hypothesis.

It is important to keep in mind that, although important, ROS are only part of the players that contribute to disease development in FAOD. Due to the combination and relation between genetic, epigenetic and environmental factors, the initial genetic mutation that leads to a defect on the function of a FAO enzyme may be seen as a risk factor for developing disease. Risk level depends on the deficient enzyme, the nature of the mutation itself, individual cellular response capacity and environmental factors (as fever or fasting), being the risk higher in disorders affecting the oxidation of long chain FA and lower in those affecting the oxidation of medium and short chain fatty acids.

CHAPTER VIII

Conclusions

Conclusions

Mitochondrial fatty acid β-oxidation disorders are a group of inherited metabolic diseases in which some epidemiological parameters (including birth prevalence) are not estimated for Iberia, and in which mitochondrial dysfunction is believed to play a critical role in its pathophysiology; however the mechanisms involved are not disclosed. To give new insights on these issues, NBS data was collected within an Iberian collaboration and mitochondrial proteome profiling of fibroblasts obtained from FAOD patients, namely MADD and LCHADD, was performed. Data obtained allowed to conclude that:

i. FAOD presents in Iberia one of the highest birth prevalence comparing with other European countries. Particularly in Portugal, FAOD has one of the highest values ever reported, mainly due to the high birth prevalence of MCADD. This data highlights the importance and impact of this group of disorders in this European region.
ii. Mitochondrial proteome response in severe MADD forms reflects a metabolic shift from FAO to glycolysis (Warburg effect) and shows an over-expression of mtPQC system components and antioxidant enzymes, probably trying to counteract the instability/disorganization on the mitochondria and increased ROS. The over-representation of apoptotic proteins seems to reflect an overwhelmed cellular defence capacity, resulting in cell death.
iii. In LCHADD fibroblast cell lines the observed mitochondrial response is much like the one observed in severe MADD, with over-expression of glycolytic enzymes and apoptosis related proteins alongside with antioxidant defence system modulation. Severe LCHADD present high ROS levels with MnSOD over-expression while moderate forms present lower ROS and MnSOD down-regulation, highlighting the contribution of oxidative stress and MnSOD modulation for the phenotype.
iv. The comparison between severe and moderate MADD forms does not reveal major differences in the pathways involved in mitochondrial response neither in MnSOD modulation. Most probably ROS are high enough to trigger a mitochondrial response similar to severe MADD.

In overall, experimental findings presented in this thesis highlight the significant birth prevalence of FAOD in Iberia and particularly in Portugal. It also allows tracing, for the first time, a pattern of mitochondrial response to FAOD blockages with a key metabolic

reprogramming towards glycolysis and antioxidant defence system modulation. Data also support the growing idea of ROS as a keystone in cellular pathophysiology of FAOD.

Future studies focused on how metabolic shifting and antioxidant defence systems are regulated and contribute to disease in distinct FAOD will not only contribute for a better prediction of disease progression and severity but will also open possibilities to establish and develop new therapeutic strategies.

REFERENCES

Amendt, B. A., C. Greene, L. Sweetman, J. Cloherty, V. Shih, A. Moon, L. Teel and W. J. Rhead (1987). "Short-chain acyl-coenzyme A dehydrogenase deficiency. Clinical and biochemical studies in two patients." J Clin Invest **79**(5): 1303-1309.

Andermann, A., I. Blancquaert, S. Beauchamp and V. Dery (2008). "Revisiting Wilson and Jungner in the genomic age: a review of screening criteria over the past 40 years." Bull World Health Organ **86**(4): 317-319.

Andresen, B. S., S. F. Dobrowolski, L. O'Reilly, J. Muenzer, S. E. McCandless, D. M. Frazier, S. Udvari, P. Bross, I. Knudsen, R. Banas, D. H. Chace, P. Engel, E. W. Naylor and N. Gregersen (2001). "Medium-chain acyl-CoA dehydrogenase (MCAD) mutations identified by MS/MS-based prospective screening of newborns differ from those observed in patients with clinical symptoms: identification and characterization of a new, prevalent mutation that results in mild MCAD deficiency." Am J Hum Genet **68**(6): 1408-1418.

Andresen, B. S., A. M. Lund, D. M. Hougaard, E. Christensen, B. Gahrn, M. Christensen, P. Bross, A. Vested, H. Simonsen, K. Skogstrand, S. Olpin, N. J. Brandt, F. Skovby, B. Nørgaard-Pedersen and N. Gregersen (2012). "MCAD Deficiency in Denmark." Molecular Genetics and Metabolism.

Andresen, B. S., S. Olpin, B. J. Poorthuis, H. R. Scholte, C. Vianey-Saban, R. Wanders, L. Ijlst, A. Morris, M. Pourfarzam, K. Bartlett, E. R. Baumgartner, J. B. deKlerk, L. D. Schroeder, T. J. Corydon, H. Lund, V. Winter, P. Bross, L. Bolund and N. Gregersen (1999). "Clear correlation of genotype with disease phenotype in very-long-chain acyl-CoA dehydrogenase deficiency." Am J Hum Genet **64**(2): 479-494.

Aoyama, T., M. Souri, I. Ueno, T. Kamijo, S. Yamaguchi, W. J. Rhead, K. Tanaka and T. Hashimoto (1995). "Cloning of human very-long-chain acyl-coenzyme A dehydrogenase and molecular characterization of its deficiency in two patients." Am J Hum Genet **57**(2): 273-283.

Arnold, G. L., C. A. Saavedra-Matiz, P. A. Galvin-Parton, R. Erbe, E. DeVincentis, D. Kronn, S. Mofidi, M. Wasserstein, J. E. Pellegrino and P. A. Levy (2010). "Lack of genotype–phenotype correlations and outcome in MCAD deficiency diagnosed by newborn screening in New York State." Molecular Genetics and Metabolism **99**(3): 263-268.

Bartlett, K. and S. Eaton (2004). "Mitochondrial beta-oxidation." Eur J Biochem **271**(3): 462-469.

Barycki, J. J., L. K. O'Brien, J. M. Bratt, R. Zhang, R. Sanishvili, A. W. Strauss and L. J. Banaszak (1999). "Biochemical characterization and crystal structure determination of human heart short chain L-3-hydroxyacyl-CoA dehydrogenase provide insights into catalytic mechanism." Biochemistry **38**(18): 5786-5798.

Bekesi, A. and D. H. Williamson (1990). "An explanation for ketogenesis by the intestine of the suckling rat: the presence of an active hydroxymethylglutaryl-coenzyme A pathway." Biol Neonate **58**(3): 160-165.

Benard, G. and R. Rossignol (2008). "Ultrastructure of the mitochondrion and its bearing on function and bioenergetics." Antioxid Redox Signal **10**(8): 1313-1342.

Bennett, M. J. (2010). "Pathophysiology of fatty acid oxidation disorders." J Inherit Metab Dis **33**: 533-537.

Berk, P. D. and D. D. Stump (1999). "Mechanisms of cellular uptake of long chain free fatty acids." Mol Cell Biochem **192**(1-2): 17-31.

Bertrand, C., C. Largilliere, M. T. Zabot, M. Mathieu and C. Vianey-Saban (1993). "Very long chain acyl-CoA dehydrogenase deficiency: identification of a new inborn error of mitochondrial fatty acid oxidation in fibroblasts." Biochim Biophys Acta **1180**(3): 327-329.

Binas, B., X. X. Han, E. Erol, J. J. Luiken, J. F. Glatz, D. J. Dyck, R. Motazavi, P. J. Adihetty, D. A. Hood and A. Bonen (2003). "A null mutation in H-FABP only partially

inhibits skeletal muscle fatty acid metabolism." Am J Physiol Endocrinol Metab **285**(3): E481-489.
Bodamer, O. A., G. F. Hoffmann and M. Lindner (2007). "Expanded newborn screening in Europe 2007." Journal of Inherited Metabolic Disease **30**(4): 439-444.
Bolisetty, S. and E. A. Jaimes (2013). "Mitochondria and reactive oxygen species: physiology and pathophysiology." Int J Mol Sci **14**(3): 6306-6344.
Bonnefont, J. P., F. Demaugre, C. Prip-Buus, J. M. Saudubray, M. Brivet, N. Abadi and L. Thuillier (1999). "Carnitine palmitoyltransferase deficiencies." Mol Genet Metab **68**(4): 424-440.
Bonnefont, J. P., F. Djouadi, C. Prip-Buus, S. Gobin, A. Munnich and J. Bastin (2004). "Carnitine palmitoyltransferases 1 and 2: biochemical, molecular and medical aspects." Mol Aspects Med **25**(5-6): 495-520.
Bonnet, D., D. Martin, L. Pascale De, E. Villain, P. Jouvet, D. Rabier, M. Brivet and J. M. Saudubray (1999). "Arrhythmias and conduction defects as presenting symptoms of fatty acid oxidation disorders in children." Circulation **100**(22): 2248-2253.
Bosch, A. M., N. G. Abeling, L. Ijlst, H. Knoester, W. L. van der Pol, A. E. Stroomer, R. J. Wanders, G. Visser, F. A. Wijburg, M. Duran and H. R. Waterham (2011). "Brown-Vialetto-Van Laere and Fazio Londe syndrome is associated with a riboflavin transporter defect mimicking mild MADD: a new inborn error of metabolism with potential treatment." J Inherit Metab Dis **34**(1): 159-164.
Bougneres, P. F., J. M. Saudubray, C. Marsac, O. Bernard, M. Odievre and J. Girard (1981). "Fasting hypoglycemia resulting from hepatic carnitine palmitoyl transferase deficiency." J Pediatr **98**(5): 742-746.
Bremer, J. (1983). "Carnitine--metabolism and functions." Physiol Rev **63**(4): 1420-1480.
Bross, P., B. S. Andresen, V. Winter, F. Krautle, T. G. Jensen, A. Nandy, S. Kolvraa, S. Ghisla, L. Bolund and N. Gregersen (1993). "Co-overexpression of bacterial GroESL chaperonins partly overcomes non-productive folding and tetramer assembly of E. coli-expressed human medium-chain acyl-CoA dehydrogenase (MCAD) carrying the prevalent disease-causing K304E mutation." Biochim Biophys Acta **1182**(3): 264-274.
Bross, P., C. Jespersen, T. G. Jensen, B. S. Andresen, M. J. Kristensen, V. Winter, A. Nandy, F. Krautle, S. Ghisla, L. Bolundi and et al. (1995). "Effects of two mutations detected in medium chain acyl-CoA dehydrogenase (MCAD)-deficient patients on folding, oligomer assembly, and stability of MCAD enzyme." J Biol Chem **270**(17): 10284-10290.
Browning, M. F., H. L. Levy, L. E. Wilkins-Haug, C. Larson and V. E. Shih (2006). "Fetal fatty acid oxidation defects and maternal liver disease in pregnancy." Obstet Gynecol **107**(1): 115-120.
Chegary, M., H. Brinke, J. P. Ruiter, F. A. Wijburg, M. S. Stoll, P. E. Minkler, M. van Weeghel, H. Schulz, C. L. Hoppel, R. J. Wanders and S. M. Houten (2009). "Mitochondrial long chain fatty acid beta-oxidation in man and mouse." Biochim Biophys Acta **1791**(8): 806-815.
Chen, J. K., Y. J. Zhan, C. S. Yang and S. F. Tzeng (2011). "Oxidative stress-induced attenuation of thrombospondin-1 expression in primary rat astrocytes." J Cell Biochem **112**(1): 59-70.
Chen, Y., E. McMillan-Ward, J. Kong, S. J. Israels and S. B. Gibson (2008). "Oxidative stress induces autophagic cell death independent of apoptosis in transformed and cancer cells." Cell Death Differ **15**(1): 171-182.
Chmurzynska, A. (2006). "The multigene family of fatty acid-binding proteins (FABPs): function, structure and polymorphism." J Appl Genet **47**(1): 39-48.
Chua, B. T., C. Volbracht, K. O. Tan, R. Li, V. C. Yu and P. Li (2003). "Mitochondrial translocation of cofilin is an early step in apoptosis induction." Nat Cell Biol **5**(12): 1083-1089.

Clayton, P. T. (2001). "Hyperinsulinism in short-chain l-3-hydroxyacyl-CoA dehydrogenase deficiency reveals the importance of beta-oxidation in insulin secretion." Journal of Clinical Investigation **108**(3): 457-465.

Cornelius, N., F. E. Frerman, T. J. Corydon, J. Palmfeldt, P. Bross, N. Gregersen and R. K. Olsen (2012). "Molecular mechanisms of riboflavin responsiveness in patients with ETF-QO variations and multiple acyl-CoA dehydrogenation deficiency." Hum Mol Genet **21**(15): 3435-3448.

Cullingford, T. E., C. T. Dolphin, K. K. Bhakoo, S. Peuchen, L. Canevari and J. B. Clark (1998). "Molecular cloning of rat mitochondrial 3-hydroxy-3-methylglutaryl-CoA lyase and detection of the corresponding mRNA and of those encoding the remaining enzymes comprising the ketogenic 3-hydroxy-3-methylglutaryl-CoA cycle in central nervous system of suckling rat." Biochem J **329 (Pt 2)**: 373-381.

Das, A. M., S. Illsinger, T. Lucke, H. Hartmann, J. P. Ruiter, U. Steuerwald, H. R. Waterham, M. Duran and R. J. Wanders (2006). "Isolated mitochondrial long-chain ketoacyl-CoA thiolase deficiency resulting from mutations in the HADHB gene." Clin Chem **52**(3): 530-534.

den Boer, M. E., R. J. Wanders, A. A. Morris, I. J. L, H. S. Heymans and F. A. Wijburg (2002). "Long-chain 3-hydroxyacyl-CoA dehydrogenase deficiency: clinical presentation and follow-up of 50 patients." Pediatrics **109**(1): 99-104.

Diekman, E. F., C. C. Boelen, B. H. Prinsen, L. Ijlst, M. Duran, T. J. de Koning, H. R. Waterham, R. J. Wanders, F. A. Wijburg and G. Visser (2013). "Necrotizing enterocolitis and respiratory distress syndrome as first clinical presentation of mitochondrial trifunctional protein deficiency." JIMD Rep **7**: 1-6.

DiMauro, S. and P. M. DiMauro (1973). "Muscle carnitine palmityltransferase deficiency and myoglobinuria." Science **182**(4115): 929-931.

Djouadi, F. and J. Bastin (2008). "PPARs as therapeutic targets for correction of inborn mitochondrial fatty acid oxidation disorders." J Inherit Metab Dis.

Doege, H. and A. Stahl (2006). "Protein-mediated fatty acid uptake: novel insights from in vivo models." Physiology (Bethesda) **21**: 259-268.

Doi, T., W. Abo, M. Tateno, K. Hayashi, T. Hori, T. Nakada, T. Fukao, Y. Takahashi and N. Terada (2000). "Milder childhood form of very long-chain acyl-CoA dehydrogenase deficiency in a 6-year-old Japanese boy." Eur J Pediatr **159**(12): 908-911.

Drahota, Z., S. K. Chowdhury, D. Floryk, T. Mracek, J. Wilhelm, H. Rauchova, G. Lenaz and J. Houstek (2002). "Glycerophosphate-dependent hydrogen peroxide production by brown adipose tissue mitochondria and its activation by ferricyanide." J Bioenerg Biomembr **34**(2): 105-113.

Drynan, L., P. A. Quant and V. A. Zammit (1996). "Flux control exerted by mitochondrial outer membrane carnitine palmitoyltransferase over beta-oxidation, ketogenesis and tricarboxylic acid cycle activity in hepatocytes isolated from rats in different metabolic states." Biochem J **317 (Pt 3)**: 791-795.

Eaton, S. (2002). "Control of mitochondrial beta-oxidation flux." Prog Lipid Res **41**(3): 197-239.

Eaton, S., I. Chatziandreou, S. Krywawych, S. Pen, P. T. Clayton and K. Hussain (2003). "Short-chain 3-hydroxyacyl-CoA dehydrogenase deficiency associated with hyperinsulinism: a novel glucose-fatty acid cycle?" Biochem Soc Trans **31**(Pt 6): 1137-1139.

Edhager, A. V., V. Stenbroen, N. S. Nielsen, P. Bross, R. K. Olsen, N. Gregersen and J. Palmfeldt (2014). "Proteomic investigation of cultivated fibroblasts from patients with mitochondrial short-chain acyl-CoA dehydrogenase deficiency." Mol Genet Metab.

Erol, E., L. S. Kumar, G. W. Cline, G. I. Shulman, D. P. Kelly and B. Binas (2004). "Liver fatty acid binding protein is required for high rates of hepatic fatty acid oxidation but not for the action of PPARalpha in fasting mice." FASEB J **18**(2): 347-349.

Fontaine, M., G. Briand, C. Largilliere, P. Degand, P. Divry, C. Vianey-Saban, B. Mousson and J. Vamecq (1998). "Metabolic studies in a patient with severe carnitine palmitoyltransferase type II deficiency." Clin Chim Acta **273**(2): 161-170.

Gerards, M., B. J. van den Bosch, K. Danhauser, V. Serre, M. van Weeghel, R. J. Wanders, G. A. Nicolaes, W. Sluiter, K. Schoonderwoerd, H. R. Scholte, H. Prokisch, A. Rotig, I. F. de Coo and H. J. Smeets (2011). "Riboflavin-responsive oxidative phosphorylation complex I deficiency caused by defective ACAD9: new function for an old gene." Brain **134**(Pt 1): 210-219.

Giak Sim, K., K. Carpenter, J. Hammond, J. Christodoulou and B. Wilcken (2002). "Quantitative fibroblast acylcarnitine profiles in mitochondrial fatty acid beta-oxidation defects: phenotype/metabolite correlations." Mol Genet Metab **76**(4): 327-334.

Gimeno, R. E., A. M. Ortegon, S. Patel, S. Punreddy, P. Ge, Y. Sun, H. F. Lodish and A. Stahl (2003). "Characterization of a heart-specific fatty acid transport protein." J Biol Chem **278**(18): 16039-16044.

Glatz, J. F., A. Bonen, D. M. Ouwens and J. J. Luiken (2006). "Regulation of sarcolemmal transport of substrates in the healthy and diseased heart." Cardiovasc Drugs Ther **20**(6): 471-476.

Green, P., M. Wiseman, Y. J. Crow, H. Houlden, S. Riphagen, J. P. Lin, F. L. Raymond, A. M. Childs, E. Sheridan, S. Edwards and D. J. Josifova (2010). "Brown-Vialetto-Van Laere syndrome, a ponto-bulbar palsy with deafness, is caused by mutations in c20orf54." Am J Hum Genet **86**(3): 485-489.

Gregersen, N. (1985). "Riboflavin-responsive defects of beta-oxidation." J Inherit Metab Dis **8 Suppl 1**: 65-69.

Gregersen, N., B. S. Andresen, M. J. Corydon, T. J. Corydon, R. K. Olsen, L. Bolund and P. Bross (2001). "Mutation analysis in mitochondrial fatty acid oxidation defects: Exemplified by acyl-CoA dehydrogenase deficiencies, with special focus on genotype-phenotype relationship." Hum Mutat **18**(3): 169-189.

Gregersen, N., B. S. Andresen, C. B. Pedersen, R. K. Olsen, T. J. Corydon and P. Bross (2008). "Mitochondrial fatty acid oxidation defects--remaining challenges." J Inherit Metab Dis **31**(5): 643-657.

Gregersen, N., P. Bross and B. S. Andresen (2004). "Genetic defects in fatty acid beta-oxidation and acyl-CoA dehydrogenases. Molecular pathogenesis and genotype-phenotype relationships." Eur J Biochem **271**(3): 470-482.

Gregersen, N., P. Bross, S. Vang and J. H. Christensen (2006). "Protein misfolding and human disease." Annu Rev Genomics Hum Genet **7**: 103-124.

Gregersen, N., J. Hansen and J. Palmfeldt (2012). "Mitochondrial proteomics--a tool for the study of metabolic disorders." J Inherit Metab Dis **35**(4): 715-726.

Gregersen, N., R. Lauritzen and K. Rasmussen (1976). "Suberylglycine excretion in the urine from a patient with dicarboxylic aciduria." Clin Chim Acta **70**(3): 417-425.

Gregersen, N. and R. K. Olsen (2010). "Disease mechanisms and protein structures in fatty acid oxidation defects." J Inherit Metab Dis.

Gregersen, N., H. Wintzensen, S. K. Christensen, M. F. Christensen, N. J. Brandt and K. Rasmussen (1982). "C6-C10-dicarboxylic aciduria: investigations of a patient with riboflavin responsive multiple acyl-CoA dehydrogenation defects." Pediatr Res **16**(10): 861-868.

Grosse, S. D., M. J. Khoury, C. L. Greene, K. S. Crider and R. J. Pollitt (2006). "The epidemiology of medium chain acyl-CoA dehydrogenase deficiency: an update." Genet Med **8**(4): 205-212.

Gulick, T., S. Cresci, T. Caira, D. D. Moore and D. P. Kelly (1994). "The peroxisome proliferator-activated receptor regulates mitochondrial fatty acid oxidative enzyme gene expression." Proc Natl Acad Sci U S A **91**(23): 11012-11016.

Gutierrez Junquera, C., E. Balmaseda, E. Gil, A. Martinez, M. Sorli, I. Cuartero, B. Merinero and M. Ugarte (2009). "Acute fatty liver of pregnancy and neonatal long-chain 3-hydroxyacyl-coenzyme A dehydrogenase (LCHAD) deficiency." Eur J Pediatr **168**(1): 103-106.

Haack, T. B., K. Danhauser, B. Haberberger, J. Hoser, V. Strecker, D. Boehm, G. Uziel, E. Lamantea, F. Invernizzi, J. Poulton, B. Rolinski, A. Iuso, S. Biskup, T. Schmidt, H. W. Mewes, I. Wittig, T. Meitinger, M. Zeviani and H. Prokisch (2010). "Exome sequencing identifies ACAD9 mutations as a cause of complex I deficiency." Nat Genet **42**(12): 1131-1134.

Halliwell, B. and J. M. Gutteridge (1984). "Oxygen toxicity, oxygen radicals, transition metals and disease." Biochem J **219**(1): 1-14.

Hamanaka, R. B. and N. S. Chandel (2010). "Mitochondrial reactive oxygen species regulate cellular signaling and dictate biological outcomes." Trends Biochem Sci **35**(9): 505-513.

He, M., Z. Pei, A. W. Mohsen, P. Watkins, G. Murdoch, P. P. Van Veldhoven, R. Ensenauer and J. Vockley (2011). "Identification and characterization of new long chain acyl-CoA dehydrogenases." Mol Genet Metab **102**(4): 418-429.

He, M., S. L. Rutledge, D. R. Kelly, C. A. Palmer, G. Murdoch, N. Majumder, R. D. Nicholls, Z. Pei, P. A. Watkins and J. Vockley (2007). "A new genetic disorder in mitochondrial fatty acid beta-oxidation: ACAD9 deficiency." Am J Hum Genet **81**(1): 87-103.

Ho, G., A. Yonezawa, S. Masuda, K.-i. Inui, K. G. Sim, K. Carpenter, R. K. J. Olsen, J. J. Mitchell, W. J. Rhead, G. Peters and J. Christodoulou (2011). "Maternal riboflavin deficiency, resulting in transient neonatal-onset glutaric aciduria Type 2, is caused by a microdeletion in the riboflavin transporter gene GPR172B." Human Mutation **32**(1): E1976-E1984.

Hoffman, J. D., R. D. Steiner, L. Paradise, C. O. Harding, L. Ding, A. W. Strauss and P. Kaplan (2006). "Rhabdomyolysis in the military: recognizing late-onset very long-chain acyl Co-A dehydrogenase deficiency." Mil Med **171**(7): 657-658.

Hoffmann, G. and P. Feyh (2003). Organic acid analysis. Physician's guide to the laboratory diagnosis of metabolic diseases. N. Blau, M. Duran, M. E. Blaskovics and K. M. Gibson. Germany, Springer.

Hoflack, M., C. Caruba, G. Pitelet, H. Haas, J. C. Mas, V. Paquis and E. Berard (2010). "[Infant coma in the emergency department: 2 cases of MCAD deficiency]." Arch Pediatr **17**(7): 1074-1077.

Houten, S. M. and R. J. A. Wanders (2010). "A general introduction to the biochemistry of mitochondrial fatty acid β-oxidation." Journal of Inherited Metabolic Disease **33**(5): 469-477.

Hsu, H. W., T. H. Zytkovicz, A. M. Comeau, A. W. Strauss, D. Marsden, V. E. Shih, G. F. Grady and R. B. Eaton (2008). "Spectrum of Medium-Chain Acyl-CoA Dehydrogenase Deficiency Detected by Newborn Screening." Pediatrics **121**(5): e1108-e1114.

Hue, L. and H. Taegtmeyer (2009). "The Randle cycle revisited: a new head for an old hat." Am J Physiol Endocrinol Metab **297**(3): E578-591.

Ibdah, J. A. (2006). "Acute fatty liver of pregnancy: an update on pathogenesis and clinical implications." World J Gastroenterol **12**(46): 7397-7404.

Ibdah, J. A., M. J. Bennett, P. Rinaldo, Y. Zhao, B. Gibson, H. F. Sims and A. W. Strauss (1999). "A fetal fatty-acid oxidation disorder as a cause of liver disease in pregnant women." N Engl J Med **340**(22): 1723-1731.

Ijlst, L., J. P. Ruiter, J. M. Hoovers, M. E. Jakobs and R. J. Wanders (1996). "Common missense mutation G1528C in long-chain 3-hydroxyacyl-CoA dehydrogenase deficiency. Characterization and expression of the mutant protein, mutation analysis

on genomic DNA and chromosomal localization of the mitochondrial trifunctional protein alpha subunit gene." J Clin Invest **98**(4): 1028-1033.
Ito, Y., P. J. Pagano, K. Tornheim, P. Brecher and R. A. Cohen (1996). "Oxidative stress increases glyceraldehyde-3-phosphate dehydrogenase mRNA levels in isolated rabbit aorta." Am J Physiol **270**(1 Pt 2): H81-87.
Jackson, S., R. S. Kler, K. Bartlett, H. Briggs, L. A. Bindoff, M. Pourfarzam, D. Gardner-Medwin and D. M. Turnbull (1992). "Combined enzyme defect of mitochondrial fatty acid oxidation." J Clin Invest **90**(4): 1219-1225.
Jethva, R. and C. Ficicioglu (2008). "Clinical outcomes of infants with short-chain acyl-coenzyme A dehydrogenase deficiency (SCADD) detected by newborn screening." Mol Genet Metab **95**(4): 241-242.
Johnson, J. O., J. R. Gibbs, L. Van Maldergem, H. Houlden and A. B. Singleton (2010). "Exome sequencing in Brown-Vialetto-van Laere syndrome." Am J Hum Genet **87**(4): 567-569; author reply 569-570.
Kamijo, T., Y. Indo, M. Souri, T. Aoyama, T. Hara, S. Yamamoto, S. Ushikubo, P. Rinaldo, I. Matsuda, A. Komiyama and T. Hashimoto (1997). "Medium chain 3-ketoacyl-coenzyme A thiolase deficiency: a new disorder of mitochondrial fatty acid beta-oxidation." Pediatr Res **42**(5): 569-576.
Kanazawa, M., A. Ohtake, H. Abe, S. Yamamoto, Y. Satoh, M. Takayanagi, H. Niimi, M. Mori and T. Hashimoto (1993). "Molecular cloning and sequence analysis of the cDNA for human mitochondrial short-chain enoyl-CoA hydratase." Enzyme Protein **47**(1): 9-13.
Karpati, G., S. Carpenter, A. G. Engel, G. Watters, J. Allen, S. Rothman, G. Klassen and O. A. Mamer (1975). "The syndrome of systemic carnitine deficiency. Clinical, morphologic, biochemical, and pathophysiologic features." Neurology **25**(1): 16-24.
Kasper, D. C., R. Ratschmann, T. F. Metz, T. P. Mechtler, D. Moslinger, V. Konstantopoulou, C. B. Item, A. Pollak and K. R. Herkner (2010). "The national Austrian newborn screening program - eight years experience with mass spectrometry. past, present, and future goals." Wien Klin Wochenschr **122**(21-22): 607-613.
Kerner, J. and C. Hoppel (2000). "Fatty acid import into mitochondria." Biochim Biophys Acta **1486**(1): 1-17.
Kiens, B. (2006). "Skeletal muscle lipid metabolism in exercise and insulin resistance." Physiol Rev **86**(1): 205-243.
Kim, C. S., C. R. Roe, J. D. Mann and G. R. Breese (1992). "Octanoic acid produces accumulation of monoamine acidic metabolites in the brain: interaction with organic anion transport at the choroid plexus." J Neurochem **58**(4): 1499-1503.
Knoop, F. (1904). "Der Abbau aromastischer Fettsauren im Tierkorper." Beitr Chem Physiol Pathol **6**: 12.
Kompare, M. and W. Rizzo (2008). "Mitochondrial Fatty-Acid Oxidation Disorders." Seminars in Pediatric Neurology **15**(3): 140-149.
Kompare, M. and W. B. Rizzo (2008). "Mitochondrial fatty-acid oxidation disorders." Semin Pediatr Neurol **15**(3): 140-149.
Kurtz, D. M., P. Rinaldo, W. J. Rhead, L. Tian, D. S. Millington, J. Vockley, D. A. Hamm, A. E. Brix, J. R. Lindsey, C. A. Pinkert, W. E. O'Brien and P. A. Wood (1998). "Targeted disruption of mouse long-chain acyl-CoA dehydrogenase gene reveals crucial roles for fatty acid oxidation." Proc Natl Acad Sci U S A **95**(26): 15592-15597.
Lee, N. C., N. L. Tang, Y. H. Chien, C. A. Chen, S. J. Lin, P. C. Chiu, A. C. Huang and W. L. Hwu (2010). "Diagnoses of newborns and mothers with carnitine uptake defects through newborn screening." Mol Genet Metab **100**(1): 46-50.

Leydiker, K. B., J. A. Neidich, F. Lorey, E. M. Barr, R. L. Puckett, R. M. Lobo and J. E. Abdenur (2011). "Maternal medium-chain acyl-CoA dehydrogenase deficiency identified by newborn screening." Molecular Genetics and Metabolism.

Li, C., P. Chen, A. Palladino, S. Narayan, L. K. Russell, S. Sayed, G. Xiong, J. Chen, D. Stokes, Y. M. Butt, P. M. Jones, H. W. Collins, N. A. Cohen, A. S. Cohen, I. Nissim, T. J. Smith, A. W. Strauss, F. M. Matschinsky, M. J. Bennett and C. A. Stanley (2010). "Mechanism of hyperinsulinism in short-chain 3-hydroxyacyl-CoA dehydrogenase deficiency involves activation of glutamate dehydrogenase." J Biol Chem **285**(41): 31806-31818.

Lindner, M., G. Gramer, G. Haege, J. Fang-Hoffmann, K. O. Schwab, U. Tacke, F. K. Trefz, E. Mengel, U. Wendel, M. Leichsenring, P. Burgard and G. F. Hoffmann (2011). "Efficacy and outcome of expanded newborn screening for metabolic diseases--report of 10 years from South-West Germany." Orphanet J Rare Dis **6**: 44.

Loeber, J. G., P. Burgard, M. C. Cornel, T. Rigter, S. S. Weinreich, K. Rupp, G. F. Hoffmann and L. Vittozzi (2012). "Newborn screening programmes in Europe; arguments and efforts regarding harmonization. Part 1. From blood spot to screening result." J Inherit Metab Dis **35**(4): 603-611.

Lopriore, E., R. J. Gemke, N. M. Verhoeven, C. Jakobs, R. J. Wanders, A. B. Roeleveld-Versteeg and B. T. Poll-The (2001). "Carnitine-acylcarnitine translocase deficiency: phenotype, residual enzyme activity and outcome." Eur J Pediatr **160**(2): 101-104.

Loukas, Y. L., G. S. Soumelas, Y. Dotsikas, V. Georgiou, E. Molou, G. Thodi, M. Boutsini, S. Biti and K. Papadopoulos (2010). "Expanded newborn screening in Greece: 30 months of experience." J Inherit Metab Dis **33 Suppl 3**: 341-348.

Lovera, C., F. Porta, A. Caciotti, S. Catarzi, M. Cassanello, U. Caruso, M. R. Gallina, A. Morrone and M. Spada (2012). "Sudden unexpected infant death (SUDI) in a newborn due to medium chain acyl CoA dehydrogenase (MCAD) deficiency with an unusual severe genotype." Ital J Pediatr **38**: 59.

Lund, A. M., D. M. Hougaard, H. Simonsen, B. S. Andresen, M. Christensen, M. Duno, K. Skogstrand, R. K. Olsen, U. G. Jensen, A. Cohen, N. Larsen, P. Saugmann-Jensen, N. Gregersen, N. J. Brandt, E. Christensen, F. Skovby and B. Norgaard-Pedersen (2012). "Biochemical screening of 504,049 newborns in Denmark, the Faroe Islands and Greenland--experience and development of a routine program for expanded newborn screening." Mol Genet Metab **107**(3): 281-293.

Lundemose, J. B., S. Kolvraa, N. Gregersen, E. Christensen and M. Gregersen (1997). "Fatty acid oxidation disorders as primary cause of sudden and unexpected death in infants and young children: an investigation performed on cultured fibroblasts from 79 children who died aged between 0-4 years." Mol Pathol **50**(4): 212-217.

Lundy, C. T., J. P. Shield, E. A. Kvittingen, O. J. Vinorum, E. R. Trimble and A. A. Morris (2003). "Acute respiratory distress syndrome in long-chain 3-hydroxyacyl-CoA dehydrogenase and mitochondrial trifunctional protein deficiencies." J Inherit Metab Dis **26**(6): 537-541.

Maclean, K., V. S. Rasiah, E. P. Kirk, K. Carpenter, S. Cooper, K. Lui and J. Oei (2005). "Pulmonary haemorrhage and cardiac dysfunction in a neonate with medium-chain acyl-CoA dehydrogenase (MCAD) deficiency." Acta Paediatr **94**(1): 114-116.

Maier, E. M., S. W. Gersting, K. F. Kemter, J. M. Jank, M. Reindl, D. D. Messing, M. S. Truger, C. P. Sommerhoff and A. C. Muntau (2009). "Protein misfolding is the molecular mechanism underlying MCADD identified in newborn screening." Hum Mol Genet **18**(9): 1612-1623.

Maier, E. M., B. Liebl, W. Roschinger, U. Nennstiel-Ratzel, R. Fingerhut, B. Olgemoller, U. Busch, N. Krone, R. v. Kries and A. A. Roscher (2005). "Population spectrum ofACADM genotypes correlated to biochemical phenotypes in newborn screening

for medium-chain acyl-CoA dehydrogenase deficiency." Human Mutation **25**(5): 443-452.
Mak, I. T., J. H. Kramer and W. B. Weglicki (1986). "Potentiation of free radical-induced lipid peroxidative injury to sarcolemmal membranes by lipid amphiphiles." J Biol Chem **261**(3): 1153-1157.
Maurel, A., C. Hernandez, O. Kunduzova, G. Bompart, C. Cambon, A. Parini and B. Frances (2003). "Age-dependent increase in hydrogen peroxide production by cardiac monoamine oxidase A in rats." Am J Physiol Heart Circ Physiol **284**(4): H1460-1467.
McGarry, J. D. and D. W. Foster (1980). "Regulation of hepatic fatty acid oxidation and ketone body production." Annu Rev Biochem **49**: 395-420.
Millington, D. S., N. Kodo, D. L. Norwood and C. R. Roe (1990). "Tandem mass spectrometry: a new method for acylcarnitine profiling with potential for neonatal screening for inborn errors of metabolism." J Inherit Metab Dis **13**(3): 321-324.
Mitchell, G. A. and T. Fukao (2006). Inborn errors of ketone body metabolism. Scriver's online metabolic and molecular basis of inherited disease. . D. Valle, A. L. Beaudet, B. Vogelstein et al., McGraw Hill.
Miwa, S., J. St-Pierre, L. Partridge and M. D. Brand (2003). "Superoxide and hydrogen peroxide production by Drosophila mitochondria." Free Radic Biol Med **35**(8): 938-948.
Moczulski, D., I. Majak and D. Mamczur (2009). "An overview of beta-oxidation disorders." Postepy Hig Med Dosw (Online) **63**: 266-277.
Molven, A., G. E. Matre, M. Duran, R. J. Wanders, U. Rishaug, P. R. Njolstad, E. Jellum and O. Sovik (2004). "Familial hyperinsulinemic hypoglycemia caused by a defect in the SCHAD enzyme of mitochondrial fatty acid oxidation." Diabetes **53**(1): 221-227.
Murphy, Michael P. (2009). "How mitochondria produce reactive oxygen species." Biochemical Journal **417**(1): 1.
Nazarewicz, R. R., A. Dikalova, A. Bikineyeva, S. Ivanov, I. A. Kirilyuk, I. A. Grigor'ev and S. I. Dikalov (2013). "Does scavenging of mitochondrial superoxide attenuate cancer prosurvival signaling pathways?" Antioxid Redox Signal **19**(4): 344-349.
Nezu, J., I. Tamai, A. Oku, R. Ohashi, H. Yabuuchi, N. Hashimoto, H. Nikaido, Y. Sai, A. Koizumi, Y. Shoji, G. Takada, T. Matsuishi, M. Yoshino, H. Kato, T. Ohura, G. Tsujimoto, J. Hayakawa, M. Shimane and A. Tsuji (1999). "Primary systemic carnitine deficiency is caused by mutations in a gene encoding sodium ion-dependent carnitine transporter." Nat Genet **21**(1): 91-94.
Nichols, M. J., C. A. Saavedra-Matiz, K. A. Pass and M. Caggana (2008). "Novel mutations causing medium chain acyl-CoA dehydrogenase deficiency: under-representation of the common c.985 A > G mutation in the New York state population." Am J Med Genet A **146A**(5): 610-619.
Nishida, K., O. Yamaguchi and K. Otsu (2008). "Crosstalk between autophagy and apoptosis in heart disease." Circ Res **103**(4): 343-351.
Odaib, A. A., B. L. Shneider, M. J. Bennett, B. R. Pober, M. Reyes-Mugica, A. L. Friedman, F. J. Suchy and P. Rinaldo (1998). "A defect in the transport of long-chain fatty acids associated with acute liver failure." N Engl J Med **339**(24): 1752-1757.
Olpin, S. E. (2004). "Implications of impaired ketogenesis in fatty acid oxidation disorders." Prostaglandins Leukot Essent Fatty Acids **70**(3): 293-308.
Olpin, S. E. (2013). "Pathophysiology of fatty acid oxidation disorders and resultant phenotypic variability." J Inherit Metab Dis.
Olpin, S. E., A. Afifi, S. Clark, N. J. Manning, J. R. Bonham, A. Dalton, J. V. Leonard, J. M. Land, B. S. Andresen, A. A. Morris, F. Muntoni, D. Turnbull, M. Pourfarzam, S. Rahman and R. J. Pollitt (2003). "Mutation and biochemical analysis in carnitine palmitoyltransferase type II (CPT II) deficiency." J Inherit Metab Dis **26**(6): 543-557.

Olpin, S. E., S. Clark, B. S. Andresen, C. Bischoff, R. K. Olsen, N. Gregersen, A. Chakrapani, M. Downing, N. J. Manning, M. Sharrard, J. R. Bonham, F. Muntoni, D. N. Turnbull and M. Pourfarzam (2005). "Biochemical, clinical and molecular findings in LCHAD and general mitochondrial trifunctional protein deficiency." J Inherit Metab Dis **28**(4): 533-544.

Olsen, R. K., B. S. Andresen, E. Christensen, P. Bross, F. Skovby and N. Gregersen (2003). "Clear relationship between ETF/ETFDH genotype and phenotype in patients with multiple acyl-CoA dehydrogenation deficiency." Hum Mutat **22**(1): 12-23.

Olsen, R. K., S. E. Olpin, B. S. Andresen, Z. H. Miedzybrodzka, M. Pourfarzam, B. Merinero, F. E. Frerman, M. W. Beresford, J. C. Dean, N. Cornelius, O. Andersen, A. Oldfors, E. Holme, N. Gregersen, D. M. Turnbull and A. A. Morris (2007). "ETFDH mutations as a major cause of riboflavin-responsive multiple acyl-CoA dehydrogenation deficiency." Brain **130**(Pt 8): 2045-2054.

Olsen, R. K. J., N. Cornelius and N. Gregersen (2013). "Genetic and cellular modifiers of oxidative stress: What can we learn from fatty acid oxidation defects?" Molecular Genetics and Metabolism.

Palmfeldt, J., S. Vang, V. Stenbroen, C. B. Pedersen, J. H. Christensen, P. Bross and N. Gregersen (2009). "Mitochondrial proteomics on human fibroblasts for identification of metabolic imbalance and cellular stress." Proteome Sci **7**: 20.

Pedersen, C. B., P. Bross, V. S. Winter, T. J. Corydon, L. Bolund, K. Bartlett, J. Vockley and N. Gregersen (2003). "Misfolding, degradation, and aggregation of variant proteins. The molecular pathogenesis of short chain acyl-CoA dehydrogenase (SCAD) deficiency." J Biol Chem **278**(48): 47449-47458.

Pedersen, C. B., S. Kolvraa, A. Kolvraa, V. Stenbroen, M. Kjeldsen, R. Ensenauer, I. Tein, D. Matern, P. Rinaldo, C. Vianey-Saban, A. Ribes, W. Lehnert, E. Christensen, T. J. Corydon, B. S. Andresen, S. Vang, L. Bolund, J. Vockley, P. Bross and N. Gregersen (2008). "The ACADS gene variation spectrum in 114 patients with short-chain acyl-CoA dehydrogenase (SCAD) deficiency is dominated by missense variations leading to protein misfolding at the cellular level." Hum Genet **124**(1): 43-56.

Pedersen, C. B., Z. Zolkipli, S. Vang, J. Palmfeldt, M. Kjeldsen, V. Stenbroen, S. P. Schmidt, R. J. A. Wanders, J. P. N. Ruiter, F. Wibrand, I. Tein and N. Gregersen (2010). "Antioxidant dysfunction: potential risk for neurotoxicity in ethylmalonic aciduria." Journal of Inherited Metabolic Disease **33**(3): 211-222.

Pollitt, R. J. (1993). "Defects in mitochondrial fatty acid oxidation: clinical presentations and their role in sudden infant death." Padiatr Padol **28**(1): 13-17.

Przyrembel, H., U. Wendel, K. Becker, H. J. Bremer, L. Bruinvis, D. Ketting and S. K. Wadman (1976). "Glutaric aciduria type II: report on a previously undescribed metabolic disorder." Clin Chim Acta **66**(2): 227-239.

Rector, R. S. and J. A. Ibdah (2009). "Fatty acid oxidation disorders: maternal health and neonatal outcomes." Semin Fetal Neonatal Med **15**(3): 122-128.

Rector, R. S., R. M. Payne and J. A. Ibdah (2008). "Mitochondrial trifunctional protein defects: clinical implications and therapeutic approaches." Adv Drug Deliv Rev **60**(13-14): 1488-1496.

Rhead, W., V. Roettger, T. Marshall and B. Amendt (1993). "Multiple acyl-coenzyme A dehydrogenation disorder responsive to riboflavin: substrate oxidation, flavin metabolism, and flavoenzyme activities in fibroblasts." Pediatr Res **33**(2): 129-135.

Rice, G., T. Brazelton, 3rd, K. Maginot, S. Srinivasan, G. Hollman and J. A. Wolff (2007). "Medium chain acyl-coenzyme A dehydrogenase deficiency in a neonate." N Engl J Med **357**(17): 1781.

Rinaldo, P., D. Matern and M. J. Bennett (2002). "Fatty acid oxidation disorders." Annu Rev Physiol **64**: 477-502.

Ritchie, R. H. and L. M. Delbridge (2006). "Cardiac hypertrophy, substrate utilization and metabolic remodelling: cause or effect?" Clin Exp Pharmacol Physiol **33**(1-2): 159-166.

Roberts, D. L., F. E. Frerman and J. J. Kim (1996). "Three-dimensional structure of human electron transfer flavoprotein to 2.1-A resolution." Proc Natl Acad Sci U S A **93**(25): 14355-14360.

Rodrigues, J. V. and C. M. Gomes (2012). "Mechanism of superoxide and hydrogen peroxide generation by human electron-transfer flavoprotein and pathological variants." Free Radic Biol Med **53**(1): 12-19.

Roe, C. R. (2002). "Inherited disorders of mitochondrial fatty acid oxidation: a new responsibility for the neonatologist." Semin Neonatol **7**(1): 37-47.

Roe, C. R., D. S. Millington, D. L. Norwood, N. Kodo, H. Sprecher, B. S. Mohammed, M. Nada, H. Schulz and R. McVie (1990). "2,4-Dienoyl-coenzyme A reductase deficiency: a possible new disorder of fatty acid oxidation." J Clin Invest **85**(5): 1703-1707.

Saggerson, D. (2008). "Malonyl-CoA, a Key Signaling Molecule in Mammalian Cells." Annual Review of Nutrition **28**(1): 253-272.

Sarsour, E. H., A. L. Kalen, Z. Xiao, T. D. Veenstra, L. Chaudhuri, S. Venkataraman, P. Reigan, G. R. Buettner and P. C. Goswami (2012). "Manganese superoxide dismutase regulates a metabolic switch during the mammalian cell cycle." Cancer Res **72**(15): 3807-3816.

Scaini, G., K. R. Simon, A. M. Tonin, E. N. Busanello, A. P. Moura, G. C. Ferreira, M. Wajner, E. L. Streck and P. F. Schuck (2012). "Toxicity of octanoate and decanoate in rat peripheral tissues: evidence of bioenergetic dysfunction and oxidative damage induction in liver and skeletal muscle." Mol Cell Biochem **361**(1-2): 329-335.

Schaap, F. G., B. Binas, H. Danneberg, G. J. van der Vusse and J. F. Glatz (1999). "Impaired long-chain fatty acid utilization by cardiac myocytes isolated from mice lacking the heart-type fatty acid binding protein gene." Circ Res **85**(4): 329-337.

Scheffler, I. E. (2010). "Assembling complex I with ACAD9." Cell Metab **12**(3): 211-212.

Schiff, M., R. Froissart, R. K. Olsen, C. Acquaviva and C. Vianey-Saban (2006). "Electron transfer flavoprotein deficiency: functional and molecular aspects." Mol Genet Metab **88**(2): 153-158.

Schmidt, S. P., T. J. Corydon, C. B. Pedersen, P. Bross and N. Gregersen (2010). "Misfolding of short-chain acyl-CoA dehydrogenase leads to mitochondrial fission and oxidative stress." Mol Genet Metab **100**(2): 155-162.

Schmidt, S. P., T. J. Corydon, C. B. Pedersen, S. Vang, J. Palmfeldt, V. Stenbroen, R. J. A. Wanders, J. P. N. Ruiter and N. Gregersen (2010). "Toxic response caused by a misfolding variant of the mitochondrial protein short-chain acyl-CoA dehydrogenase." Journal of Inherited Metabolic Disease **34**(2): 465-475.

Schuck, P. F., G. C. Ferreira, A. P. Moura, E. N. Busanello, A. M. Tonin, C. S. Dutra-Filho and M. Wajner (2009). "Medium-chain fatty acids accumulating in MCAD deficiency elicit lipid and protein oxidative damage and decrease non-enzymatic antioxidant defenses in rat brain." Neurochem Int **54**(8): 519-525.

Schuck, P. F., C. Ferreira Gda, E. B. Tahara, F. Klamt, A. J. Kowaltowski and M. Wajner (2010). "cis-4-decenoic acid provokes mitochondrial bioenergetic dysfunction in rat brain." Life Sci **87**(5-6): 139-146.

Schuck, P. F., C. Ferreira Gda, A. M. Tonin, C. M. Viegas, E. N. Busanello, A. P. Moura, A. Zanatta, F. Klamt and M. Wajner (2009). "Evidence that the major metabolites accumulating in medium-chain acyl-CoA dehydrogenase deficiency disturb mitochondrial energy homeostasis in rat brain." Brain Res **1296**: 117-126.

Schulz, H. (1994). "Regulation of fatty acid oxidation in heart." J Nutr **124**(2): 165-171.

Seifert, E. L., C. Estey, J. Y. Xuan and M. E. Harper (2010). "Electron transport chain-dependent and -independent mechanisms of mitochondrial H2O2 emission during long-chain fatty acid oxidation." J Biol Chem **285**(8): 5748-5758.

Sim, K. G., J. Hammond and B. Wilcken (2002). "Strategies for the diagnosis of mitochondrial fatty acid beta-oxidation disorders." Clin Chim Acta **323**(1-2): 37-58.

Simkovic, M., G. D. Degala, S. S. Eaton and F. E. Frerman (2002). "Expression of human electron transfer flavoprotein-ubiquinone oxidoreductase from a baculovirus vector: kinetic and spectral characterization of the human protein." Biochem J **364**(Pt 3): 659-667.

Smathers, R. L. and D. R. Petersen (2011). "The human fatty acid-binding protein family: evolutionary divergences and functions." Hum Genomics **5**(3): 170-191.

Sparagna, G. C., D. L. Hickson-Bick, L. M. Buja and J. B. McMillin (2000). "A metabolic role for mitochondria in palmitate-induced cardiac myocyte apoptosis." Am J Physiol Heart Circ Physiol **279**(5): H2124-2132.

Spiekerkoetter, U. (2010). "Mitochondrial fatty acid oxidation disorders: clinical presentation of long-chain fatty acid oxidation defects before and after newborn screening." J Inherit Metab Dis.

Spiekerkoetter, U., M. Lindner, R. Santer, M. Grotzke, M. R. Baumgartner, H. Boehles, A. Das, C. Haase, J. B. Hennermann, D. Karall, H. de Klerk, I. Knerr, H. G. Koch, B. Plecko, W. Roschinger, K. O. Schwab, D. Scheible, F. A. Wijburg, J. Zschocke, E. Mayatepek and U. Wendel (2009). "Management and outcome in 75 individuals with long-chain fatty acid oxidation defects: results from a workshop." J Inherit Metab Dis **32**(4): 488-497.

Spiekerkoetter, U. and P. A. Wood (2010). "Mitochondrial fatty acid oxidation disorders: pathophysiological studies in mouse models." J Inherit Metab Dis **33**(5): 539-546.

Stanley, C. A., D. E. Hale, G. T. Berry, S. Deleeuw, J. Boxer and J. P. Bonnefont (1992). "Brief report: a deficiency of carnitine-acylcarnitine translocase in the inner mitochondrial membrane." N Engl J Med **327**(1): 19-23.

Stenson, P. D., E. V. Ball, M. Mort, A. D. Phillips, J. A. Shiel, N. S. Thomas, S. Abeysinghe, M. Krawczak and D. N. Cooper (2003). "Human Gene Mutation Database (HGMD): 2003 update." Hum Mutat **21**(6): 577-581.

Strijbis, K., F. M. Vaz and B. Distel (2010). "Enzymology of the carnitine biosynthesis pathway." IUBMB Life **62**(5): 357-362.

Suhrie, K. R. S., A. K. Karunanidhi, W. M. Mohen, M. R. M. Reys-Mugia and J. Vockley (2011). "Long chain acyl-CoA dehydrogenase deficiency: a new inborn error of metabolism manifestating as congenital surfactant deficiency." J Inherit Metab Dis **34**(Suppl 3).

Tein, I., D. C. De Vivo, D. E. Hale, J. T. Clarke, H. Zinman, R. Laxer, A. Shore and S. DiMauro (1991). "Short-chain L-3-hydroxyacyl-CoA dehydrogenase deficiency in muscle: a new cause for recurrent myoglobinuria and encephalopathy." Ann Neurol **30**(3): 415-419.

Tein, I., J. Vajsar, L. MacMillan and W. G. Sherwood (1999). "Long-chain L-3-hydroxyacyl-coenzyme A dehydrogenase deficiency neuropathy: response to cod liver oil." Neurology **52**(3): 640-643.

Thumelin, S., M. Forestier, J. Girard and J. P. Pegorier (1993). "Developmental changes in mitochondrial 3-hydroxy-3-methylglutaryl-CoA synthase gene expression in rat liver, intestine and kidney." Biochem J **292 (Pt 2)**: 493-496.

Thumelin, S., C. Kohl, J. Girard and J. P. Pegorier (1999). "Atypical expression of mitochondrial 3-hydroxy-3-methylglutaryl-CoA synthase in subcutaneous adipose tissue of male rats." J Lipid Res **40**(6): 1071-1077.

Tonin, A. M., A. U. Amaral, E. N. Busanello, M. Grings, R. F. Castilho and M. Wajner (2013). "Long-chain 3-hydroxy fatty acids accumulating in long-chain 3-hydroxyacyl-CoA dehydrogenase and mitochondrial trifunctional protein deficiencies uncouple

oxidative phosphorylation in heart mitochondria." J Bioenerg Biomembr **45**(1-2): 47-57.
Tonin, A. M., G. C. Ferreira, M. Grings, C. M. Viegas, E. N. Busanello, A. U. Amaral, A. Zanatta, P. F. Schuck and M. Wajner (2010). "Disturbance of mitochondrial energy homeostasis caused by the metabolites accumulating in LCHAD and MTP deficiencies in rat brain." Life Sci **86**(21-22): 825-831.
Tretter, L. and V. Adam-Vizi (2004). "Generation of reactive oxygen species in the reaction catalyzed by alpha-ketoglutarate dehydrogenase." J Neurosci **24**(36): 7771-7778.
Turrens, J. F. (2003). "Mitochondrial formation of reactive oxygen species." J Physiol **552**(Pt 2): 335-344.
Tyni, T., M. Pourfarzam and D. M. Turnbull (2002). "Analysis of mitochondrial fatty acid oxidation intermediates by tandem mass spectrometry from intact mitochondria prepared from homogenates of cultured fibroblasts, skeletal muscle cells, and fresh muscle." Pediatr Res **52**(1): 64-70.
Ushikubo, S., T. Aoyama, T. Kamijo, R. J. Wanders, P. Rinaldo, J. Vockley and T. Hashimoto (1996). "Molecular characterization of mitochondrial trifunctional protein deficiency: formation of the enzyme complex is important for stabilization of both alpha- and beta-subunits." Am J Hum Genet **58**(5): 979-988.
Van Hove, J. L., W. Zhang, S. G. Kahler, C. R. Roe, Y. T. Chen, N. Terada, D. H. Chace, A. K. Iafolla, J. H. Ding and D. S. Millington (1993). "Medium-chain acyl-CoA dehydrogenase (MCAD) deficiency: diagnosis by acylcarnitine analysis in blood." Am J Hum Genet **52**(5): 958-966.
Vaz, F. M., B. Melegh, J. Bene, D. Cuebas, D. A. Gage, A. Bootsma, P. Vreken, A. H. van Gennip, L. L. Bieber and R. J. Wanders (2002). "Analysis of carnitine biosynthesis metabolites in urine by HPLC-electrospray tandem mass spectrometry." Clin Chem **48**(6 Pt 1): 826-834.
Vaz, F. M. and R. J. Wanders (2002). "Carnitine biosynthesis in mammals." Biochem J **361**(Pt 3): 417-429.
Ventura, F. V., J. Ruiter, L. Ijlst, I. T. de Almeida and R. J. Wanders (2005). "Differential inhibitory effect of long-chain acyl-CoA esters on succinate and glutamate transport into rat liver mitochondria and its possible implications for long-chain fatty acid oxidation defects." Mol Genet Metab **86**(3): 344-352.
Ventura, F. V., I. Tavares de Almeida and R. J. Wanders (2007). "Inhibition of adenine nucleotide transport in rat liver mitochondria by long-chain acyl-coenzyme A beta-oxidation intermediates." Biochem Biophys Res Commun **352**(4): 873-878.
Vilarinho, L., H. Rocha, C. Sousa, A. Marcao, H. Fonseca, M. Bogas and R. V. Osorio (2010). "Four years of expanded newborn screening in Portugal with tandem mass spectrometry." J Inherit Metab Dis.
Vladutiu, G. D. (2001). "Heterozygosity: an expanding role in proteomics." Mol Genet Metab **74**(1-2): 51-63.
Vladutiu, G. D., M. J. Bennett, N. M. Fisher, D. Smail, R. Boriack, J. Leddy and D. R. Pendergast (2002). "Phenotypic variability among first-degree relatives with carnitine palmitoyltransferase II deficiency." Muscle Nerve **26**(4): 492-498.
Vladutiu, G. D., M. J. Bennett, D. Smail, L. J. Wong, R. T. Taggart and H. B. Lindsley (2000). "A variable myopathy associated with heterozygosity for the R503C mutation in the carnitine palmitoyltransferase II gene." Mol Genet Metab **70**(2): 134-141.
Vockley, J. (2008). "Metabolism as a complex genetic trait, a systems biology approach: implications for inborn errors of metabolism and clinical diseases." J Inherit Metab Dis **31**(5): 619-629.
Vockley, J., P. Rinaldo, M. J. Bennett, D. Matern and G. D. Vladutiu (2000). "Synergistic heterozygosity: disease resulting from multiple partial defects in one or more metabolic pathways." Mol Genet Metab **71**(1-2): 10-18.

Vockley, J. and D. A. Whiteman (2002). "Defects of mitochondrial beta-oxidation: a growing group of disorders." Neuromuscul Disord **12**(3): 235-246.
Voermans, N. C., B. G. van Engelen, L. A. Kluijtmans, N. M. Stikkelbroeck and A. R. Hermus (2006). "Rhabdomyolysis caused by an inherited metabolic disease: very long-chain acyl-CoA dehydrogenase deficiency." Am J Med **119**(2): 176-179.
Waddell, L., V. Wiley, K. Carpenter, B. Bennetts, L. Angel, B. Andresen and B. Wilcken (2006). "Medium-chain acyl-CoA dehydrogenase deficiency: Genotype–biochemical phenotype correlations." Molecular Genetics and Metabolism **87**(1): 32-39.
Walter, J. H. (2003). "L-carnitine in inborn errors of metabolism: what is the evidence?" J Inherit Metab Dis **26**(2-3): 181-188.
Wanders, R. J., M. Duran, L. Ijlst, J. P. de Jager, A. H. van Gennip, C. Jakobs, L. Dorland and F. J. van Sprang (1989). "Sudden infant death and long-chain 3-hydroxyacyl-CoA dehydrogenase." Lancet **2**(8653): 52-53.
Wanders, R. J., I. J. L, F. Poggi, J. P. Bonnefont, A. Munnich, M. Brivet, D. Rabier and J. M. Saudubray (1992). "Human trifunctional protein deficiency: a new disorder of mitochondrial fatty acid beta-oxidation." Biochem Biophys Res Commun **188**(3): 1139-1145.
Wanders, R. J., C. W. van Roermund, W. F. Visser, S. Ferdinandusse, G. A. Jansen, D. M. van den Brink, J. Gloerich and H. R. Waterham (2003). "Peroxisomal fatty acid alpha- and beta-oxidation in health and disease: new insights." Adv Exp Med Biol **544**: 293-302.
Wanders, R. J., P. Vreken, M. E. den Boer, F. A. Wijburg, A. H. van Gennip and I. J. L (1999). "Disorders of mitochondrial fatty acyl-CoA beta-oxidation." J Inherit Metab Dis **22**(4): 442-487.
Wanders, R. J. and H. R. Waterham (2006). "Peroxisomal disorders: the single peroxisomal enzyme deficiencies." Biochim Biophys Acta **1763**(12): 1707-1720.
Watkins, P. A. (2008). "Very-long-chain acyl-CoA synthetases." J Biol Chem **283**(4): 1773-1777.
Watmough, N. J. and F. E. Frerman (2010). "The electron transfer flavoprotein: ubiquinone oxidoreductases." Biochim Biophys Acta **1797**(12): 1910-1916.
Wilcken, B., M. Haas, P. Joy, V. Wiley, M. Chaplin, C. Black, J. Fletcher, J. McGill and A. Boneh (2007). "Outcome of neonatal screening for medium-chain acyl-CoA dehydrogenase deficiency in Australia: a cohort study." Lancet **369**(9555): 37-42.
Wilcken, B., M. Haas, P. Joy, V. Wiley, M. Chaplin, C. Black, J. Fletcher, J. McGill and A. Boneh (2007). "Outcome of neonatal screening for medium-chain acyl-CoA dehydrogenase deficiency in Australia: a cohort study." The Lancet **369**(9555): 37-42.
Yang, B. Z., J. H. Ding, C. Zhou, M. M. Dimachkie, L. Sweetman, M. J. Dasouki, J. Wilkinson and C. R. Roe (2000). "Identification of a novel mutation in patients with medium-chain acyl-CoA dehydrogenase deficiency." Mol Genet Metab **69**(3): 259-262.
Yokota, I., P. M. Coates, D. E. Hale, P. Rinaldo and K. Tanaka (1991). "Molecular survey of a prevalent mutation, 985A-to-G transition, and identification of five infrequent mutations in the medium-chain Acyl-CoA dehydrogenase (MCAD) gene in 55 patients with MCAD deficiency." Am J Hum Genet **49**(6): 1280-1291.
Yusuf, K., J. Jirapradittha, H. J. Amin, W. Yu and S. U. Hasan (2010). "Neonatal ventricular tachyarrhythmias in medium chain acyl-CoA dehydrogenase deficiency." Neonatology **98**(3): 260-264.
Yusupov, R., D. N. Finegold, E. W. Naylor, I. Sahai, S. Waisbren and H. L. Levy (2010). "Sudden death in medium chain acyl-coenzyme a dehydrogenase deficiency (MCADD) despite newborn screening." Mol Genet Metab **101**(1): 33-39.
Zschocke, J. (2008). "Dominant versus recessive: molecular mechanisms in metabolic disease." J Inherit Metab Dis **31**(5): 599-618.

APPENDIX – Supplementary data

Study 2- Newborn screening for medium-chain acyl-CoA dehydrogenase deficiency: regional experience and high incidence of carnitine deficiency.

Table S1. Summary of levels of acylcarnitines at diagnosis, mutations, carnitine free levels, treatment and evolution of MCADD patients.

CV: control values; FS: Free of Symptoms; MD: Metabolic decompensation; n.d.= not done; n.f: not found in this moment m: month; y: year; bs (blood spot samples); *ps (plasma samples)* *All mutations were named according to the nucleotide change.

	Diagnosis								*Follow-up*				
Patients	Days at collection	C0 (CV<12 µM)	C8 (CV<0.52 µM)	C10 (CV<0.50 µM)	C10:1 (CV<0.33 µM)	C8/C10 (CV<1.8)	C8/C2 (CV<0.02)	Genotype*	C0 median (range) (µM) bs *(cursive.ps)*	Carnitine supplementaion (duration)	Inicial dose (mg/kg/day)	Follow up	Present status
1	4	14	**1.3**	0.20	0.27	**6.6**	**0.12**	c.985A>G/ c.985A>G	9.9 (5.4-15)	Yes (6y)	20	10y 3m	FS
2	7	16	**1.2**	0.17	0.20	**7.3**	**0.11**	c.985A>G/ c.985A>G	n.d.	No	-	10y 1m	FS
3	10	**9**	**3.0**	0.38	**0.66**	**7.9**	**0.34**	c.985A>G/ c.985A>G	8.8 (3.7-15)	Yes (7y)	20	9 y	FS
4	23	21	**5.8**	**0.56**	**0.47**	**10**	**0.67**	c.985A>G/ c.985A>G	10 (6.3-15)	Yes (6m)	20	1y 3m	Exitus
5	6	18	**1.9**	0.17	0.22	**11**	**0.09**	c.985A>G/ c.985A>G	n.d.	No	-	7y 5m	FS
6	4	41	**9.4**	**0.71**	**0.97**	**13**	**0.74**	c.985A>G/ c.985A>G	11 (4.2-17)	Yes (1y 6m)	20	3y 2m	FS
7	4	35	**4.6**	0.40	**0.55**	**11**	**0.55**	c.985A>G/ c.985A>G	n.d.	No	-	3y 2m	FS
8	6	22	**0.8**	**0.50**	**0.33**	1.6	**0.07**	c.985A>G/ c.199T>C	19 (11-29)	Yes (3m)	20	9y 10m	FS
9	6	34	**1.7**	0.22	**0.61**	**7.5**	**0.22**	c.245G>C c.985A>G	16 (11-21)	Yes (6m)	20	10y 7m	FS
10	3	45	**1.3**	**0.51**	**0.39**	**2.4**	**0.12**	c.985A>G / c.1247T>C	28 (26-30)	No	-	1y 7m	FS
11	4	43	**5.2**	**0.81**	**0.56**	**6.4**	**0.60**	c.542A>G/ c.799G>A	20 (14-23)	No	-	1y 10m	FS
12	2	34	**16**	**1.3**	**1.8**	**12**	**0.72**	c.600G>T/ c.985A>G	16 (9.5-25)	Yes (3m)	20	1y 1m	FS
13	4	35	0.42	0.39	0.22	1.0	**0.04**	c.683C>A/ c.985A>G	23 (21-30)	No	-	2y	FS
14	5	33	**7.6**	**0.64**	**0.62**	**12**	**0.33**	c.985A>G/ c.985A>G	*42 (19-71) ps*	Yes (continuo)	30	7y 1m	FS
15	5	12	**3.0**	0.42	**1.4**	**7.3**	**0.18**	c.985A>G/ c.985A>G	*32 (13-49)ps*	Yes (continuo)	60	6y 9m	FS
16	6	25	**5.7**	0.46	**1.3**	**12**	**0.40**	c.985A>G/ c.985A>G	n.d.	No	-	6y 1m	FS
17	6	25	**6.5**	**0.74**	**0.89**	**8.8**	**0.76**	c.985A>G/ c.985A>G	*50 (20-87)ps*	Yes (continuo)	50	5y 6m	FS
18	5	17	**1.9**	0.24	**0.47**	**8.0**	**0.19**	c.985A>G/ c.985A>G	*50 (22-83)ps*	Yes (continuo)	50	5y 6m	FS
19	6	12	**4.3**	0.42	0.30	**10**	**0.20**	c.985A>G/ c.985A>G	16 (4.0-23)	Yes (3y 6m)	30	5y 6m	MD
20	7	29	**13**	**1.1**	**0.42**	**11**	**0.31**	c.985A>G/ c.985A>G	*62 (26-83)ps*	Yes (continuo)	50	4y 8m	FS
21	5	39	**4.9**	**0.53**	**0.94**	**9.4**	**0.29**	c.985A>G/ c.1189dupT	*51 (25-85)ps*	Yes (continuo)	50	4y 4m	
22	4	44	**2.0**	**0.79**	**0.57**	**2.5**	**0.05**	c.653C>G/ c.985A>G	25 (12- 43)	Yes (3y)	30	4y 5m	FS
23	5	20	**1.8**	0.27	**0.66**	**6.7**	**0.14**	c.985A>G/ c.985A>G	22 (10-36)	Yes (2y)	30	4y 1m	FS
24	5	20	**4.6**	0.39	**0.64**	**12**	**0.23**	c.985A>G/ n.f.	25 (3.0-55)	Yes (8m)	35	3y 10m	FS
25	13	22	**2.0**	0.16	**0.36**	**13**	**0.27**	c.985A>G/ c.985A>G	17 (13-20.3)	No	-	2y 11m	FS
26	6	27	**6.9**	**0.59**	**1.1**	**12**	**0.46**	c.985A>G/ c.985A>G	15 (11-21)	Yes (4m)		1y 10m	MD
27	3	29	**21**	**1.3**	**1.0**	**16**	**0.85**	c.985A>G/ c.985A>G	*27 (18-34)ps*	Yes (7m)	25	1y 7m	FS
28	2	31	**4.2**	0.37	**0.36**	**12**	**0.17**	c.985A>G/ c.985A>G	12 (9.5-15)	Yes (continuo)		1y 6m	FS
29	4	24	**5.7**	**0.55**	**0.55**	**11**	**0.15**	c.985A>G/ c.985A>G	n.d.	No	-	1y 5m	FS
30	4	31	**2.5**	0.24	**0.34**	**11**	**0.10**	c.985A>G/ c.985A>G	15 (5.6-21)	Yes (1y)	30	2y 1m	MD
31	8	20	**2.8**	0.25	**0.36**	**11**	**0.26**	c.985A>G/ c.985A>G	15 (11-19)	Yes (4m)	30	1y 1m	FS

	Diagnosis								*Follow-up*				
Patients	Days at collection	C0 (CV<12 µM)	C8 (CV<0.52 µM)	C10 (CV<0.50 µM)	C10:1 (CV<0.33 µM)	C8/C10 (CV<1.8)	C8/C2 (CV<0.02)	Genotype*	C0 median (range) (µM) bs (*cursive.ps*)	Carnitine supplementaion (duration)	Inicial dose (mg/kg/day)	Follow up	Present status
32	0	27	**8.1**	**0.73**	**1.06**	**11**	**0.56**	c.985A>G/ c.985A>G	16 (10-22)	Yes (1y)	60	1y 1m	FS
33	4	37	**9.7**	**0.61**	**0.81**	**16**	**0.39**	c.985A>G/ c.985A>G	20 (11-33)	Yes (1y)	30	1y 4m	FS
34	20	22	**4.4**	0.44	**0.95**	**9.9**	**0.26**	c.985A>G/ c.985A>G	n.d.	No	-	6m	FS
35	4	26	**6.9**	**0.54**	**0.73**	**13**	**0.29**	c.985A>G/ c.985A>G	17 (14-20)	Yes (3m)	30	1y	FS
36	5	28	**2.4**	0.41	**0.35**	**5.8**	**0.21**	c.985A>G/ c.985A>G	18 (11-26)	Yes (continuo)	30	4m	FS
37	6	56	**3.1**	0.29	**0.41**	**11**	**0.12**	c.250C>T/ c.985A>G	28 (18-46)	No	-	2m	FS
38	3	20	**3.0**	0.38	**0.76**	**8.1**	**0.13**	c.985A>G/ c.985A>G	12 (3.9- 20)	Yes (3m)	20	1y 1m	FS
39	35	14	**2.3**	0.45	**0.56**	**5.2**	**0.28**	c.985A>G/ c.985A>G	13 (3.1-29)	Yes (continuo)	20	11m	FS
40	13	**11**	**1.4**	0.18	**0.53**	**7.8**	**0.07**	c.985A>G/ c.985A>G	10 (5.0-15)	No	-	2y	FS
41	18	25	**6.5**	**0.74**	**0.89**	**8.7**	**0.15**	c.985A>G/ c.985A>G	15 (11-31)	Yes (continuo)	30	1y 9m	FS
42	5	18	**2.8**	0.44	**0.85**	**6.9**	**0.17**	c.985A>G/ c.985A>G	14 (9.9-30)	Yes (continuo)	50	2y 8m	FS
43	7	29	**13**	**1.1**	**0.42**	**11**	**0.37**	c.985A>G/ c.985A>G	13 (9.4-28)	Yes (continuo)	20	2y 8m	Exitus
44	4	21	**1.4**	0.15	0.04	**9.9**	**0.06**	c.985A>G/ c.985A>G	7.8 (4.9-12)	Yes (2y 2m)	40	3y	FS
45	4	25	**1.2**	0.23	**0.33**	**5.2**	**0.07**	c.250C>T / c.985A>G	20 (15-23)	No	-	2y10m	FS

Study 3 - Mitochondria proteome profiling: A comparative analysis between gel- and gel-free approaches.

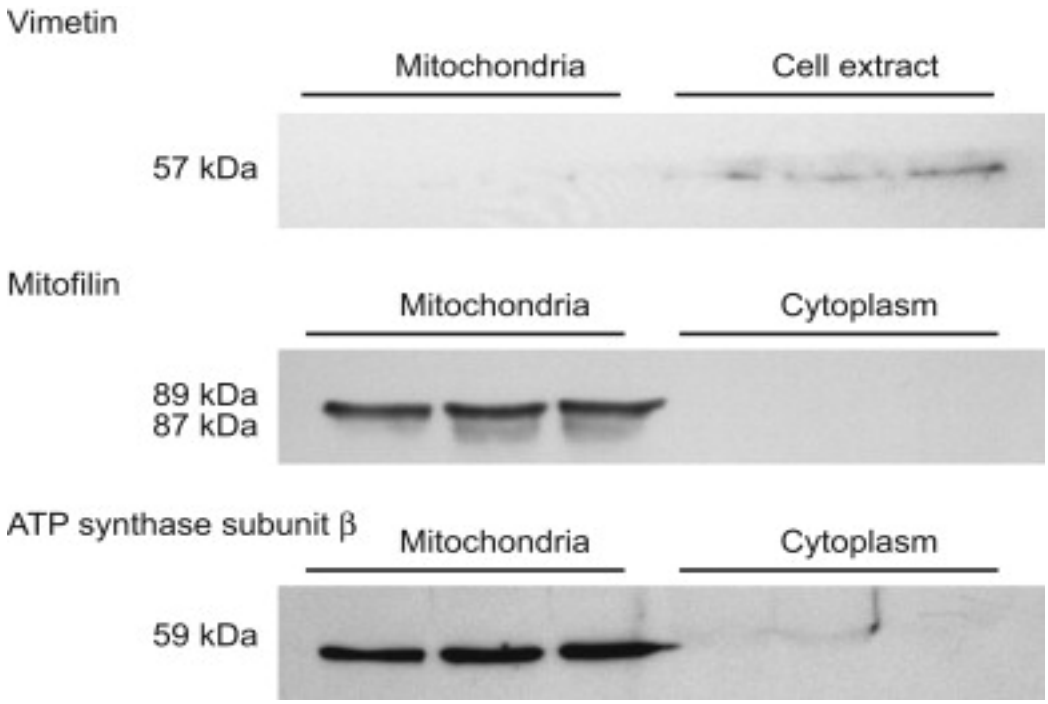

Supplemental figure S1: Immunobloting analysis of mitochondrial fraction and cell extract, evidencing the successful enrichment of mitochondria from cultured fibroblasts.

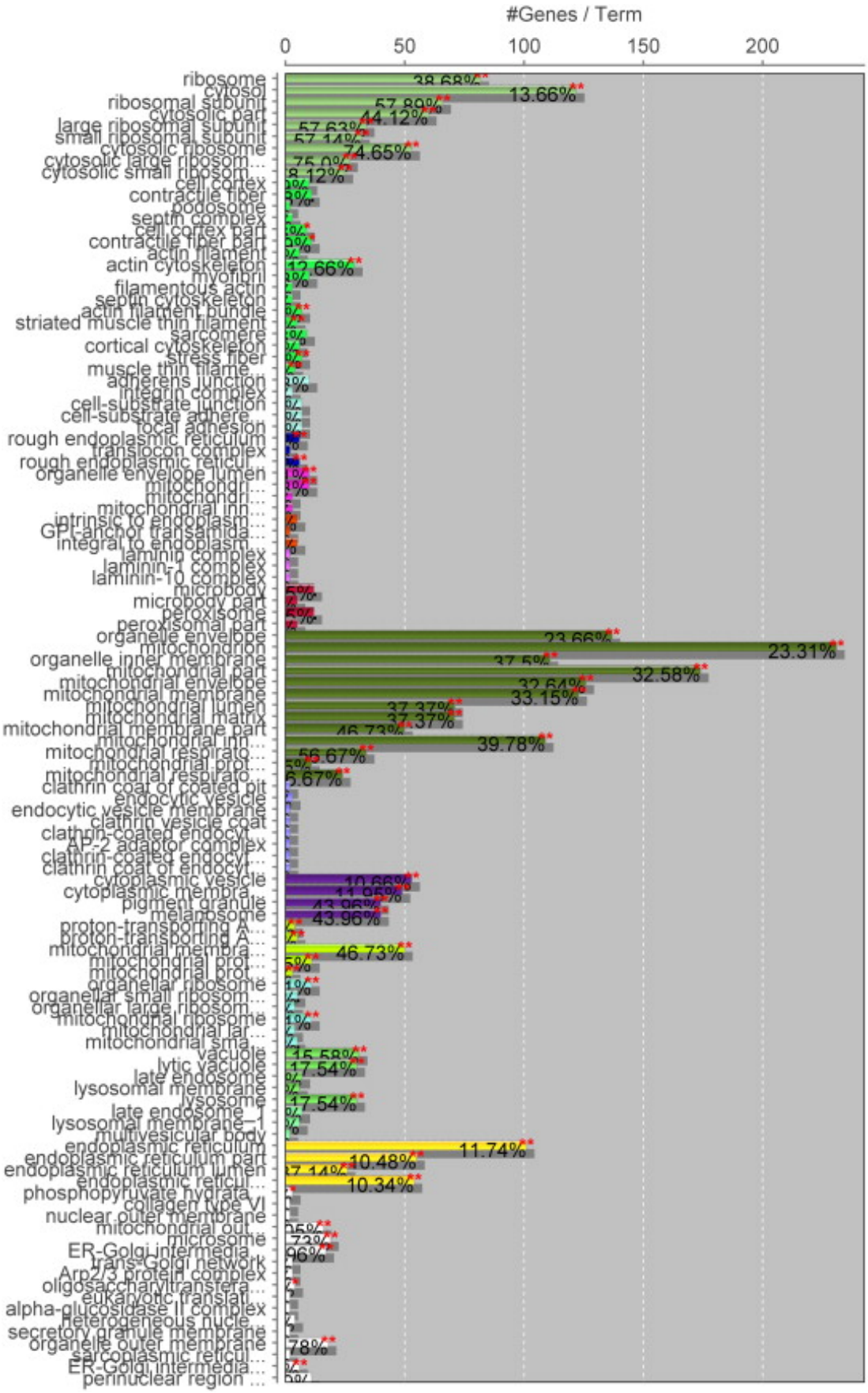

Supplemental figure S2: Gene Ontology Analysis for subcellular location of identified proteins using the ClueGo bioinformatic tool.

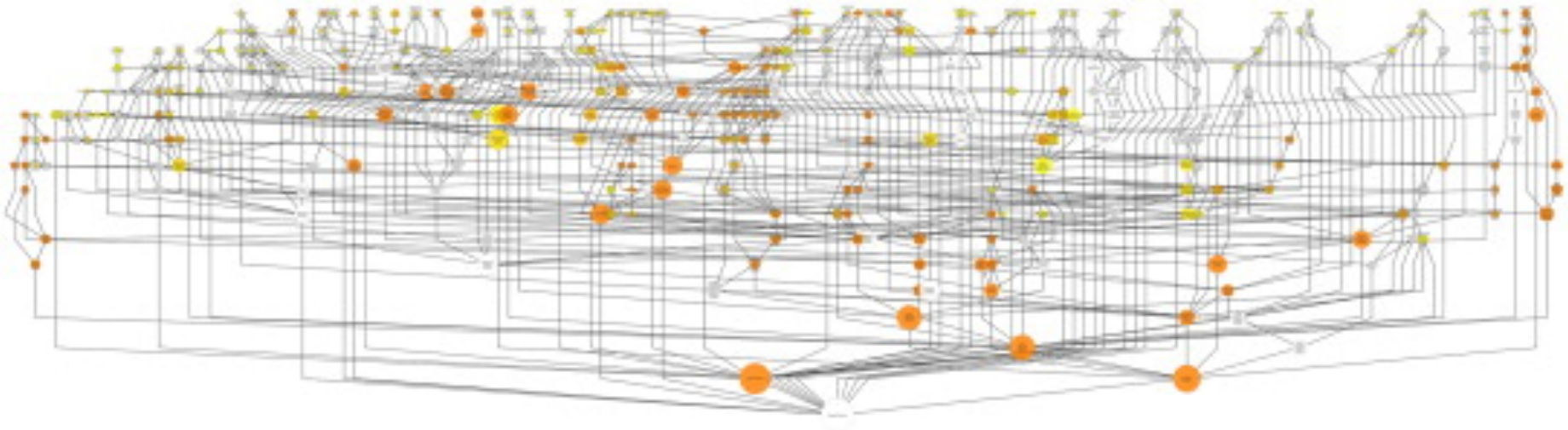

Supplemental figure S3: Hierarchical representation of BiNGO analysis, in terms of biological processes based on all identified proteins in isolated mitochondria

Supplemental table S1: Proteins identified using Mascot 2D-LC

prot_hit_nı	prot_acc	prot_desc	prot_score	prot_mass	prot_matches	prot_cover	prot_pi
1	PDIA1_HUMAN	Protein disulfide-isomerase OS=Homo sapiens GN=P4HB PE=1 SV=3	626	57081	19	25.6	4.76
2	MYH9_HUMAN	Myosin-9 OS=Homo sapiens GN=MYH9 PE=1 SV=4	557	226392	22	13.3	5.5
3	CO6A3_HUMAN	Collagen alpha-3(VI) chain OS=Homo sapiens GN=COL6A3 PE=1 SV=5	552	343457	34	7.9	6.26
4	CALR_HUMAN	Calreticulin OS=Homo sapiens GN=CALR PE=1 SV=1	509	48112	14	20.9	4.29
5	GRP78_HUMAN	78 kDa glucose-regulated protein OS=Homo sapiens GN=HSPA5 PE=1 SV=2	478	72288	25	26	5.07
6	ATPB_HUMAN	ATP synthase subunit beta, mitochondrial OS=Homo sapiens GN=ATP5B PE=1 SV=3	446	56525	14	28.4	5.26
7	AMPN_HUMAN	Aminopeptidase N OS=Homo sapiens GN=ANPEP PE=1 SV=4	430	109471	12	12.5	5.31
8	BASP1_HUMAN	Brain acid soluble protein 1 OS=Homo sapiens GN=BASP1 PE=1 SV=2	398	22680	7	41.9	4.64
9	TOM22_HUMAN	Mitochondrial import receptor subunit TOM22 homolog OS=Homo sapiens GN=TOMM22 PE=1 SV=3	347	15512	4	26.1	4.27
10	MYH10_HUMAN	Myosin-10 OS=Homo sapiens GN=MYH10 PE=1 SV=3	317	228858	23	9.5	5.44
11	K2C1_HUMAN	Keratin, type II cytoskeletal 1 OS=Homo sapiens GN=KRT1 PE=1 SV=6	299	65999	2	6.2	8.15
12	ANXA2_HUMAN	Annexin A2 OS=Homo sapiens GN=ANXA2 PE=1 SV=2	274	38580	14	35.7	7.57
13	THIL_HUMAN	Acetyl-CoA acetyltransferase, mitochondrial OS=Homo sapiens GN=ACAT1 PE=1 SV=1	260	45171	6	11.7	8.98
14	SODM_HUMAN	Superoxide dismutase [Mn], mitochondrial OS=Homo sapiens GN=SOD2 PE=1 SV=2	254	24707	4	22.1	8.35
15	CH60_HUMAN	60 kDa heat shock protein, mitochondrial OS=Homo sapiens GN=HSPD1 PE=1 SV=2	249	61016	10	19.4	5.7
16	GANAB_HUMAN	Neutral alpha-glucosidase AB OS=Homo sapiens GN=GANAB PE=1 SV=3	239	106807	8	9.2	5.74
17	VIME_HUMAN	Vimentin OS=Homo sapiens GN=VIM PE=1 SV=4	226	53619	7	15.5	5.06
18	RRBP1_HUMAN	Ribosome-binding protein 1 OS=Homo sapiens GN=RRBP1 PE=1 SV=4	223	152381	15	12.4	8.69
19	RL15_HUMAN	60S ribosomal protein L15 OS=Homo sapiens GN=RPL15 PE=1 SV=2	221	24131	9	30.4	11.62
20	MYOF_HUMAN	Myoferlin OS=Homo sapiens GN=MYOF PE=1 SV=1	220	234561	10	4.5	5.84
21	RLA2_HUMAN	60S acidic ribosomal protein P2 OS=Homo sapiens GN=RPLP2 PE=1 SV=1	219	11658	2	16.5	4.42
22	POTEF_HUMAN	POTE ankyrin domain family member F OS=Homo sapiens GN=POTEF PE=1 SV=2	214	121367	25	11.1	5.83
23	ACTB_HUMAN	Actin, cytoplasmic 1 OS=Homo sapiens GN=ACTB PE=1 SV=1	214	41710	16	18.7	5.29
24	POTEE_HUMAN	POTE ankyrin domain family member E OS=Homo sapiens GN=POTEE PE=1 SV=3	214	121286	24	11	5.83
25	MOES_HUMAN	Moesin OS=Homo sapiens GN=MSN PE=1 SV=3	208	67778	8	18.2	6.08
26	CALD1_HUMAN	Caldesmon OS=Homo sapiens GN=CALD1 PE=1 SV=3	201	93175	2	3.8	5.62
27	PLEC_HUMAN	Plectin OS=Homo sapiens GN=PLEC PE=1 SV=3	184	531466	21	4.7	5.74
28	CALX_HUMAN	Calnexin OS=Homo sapiens GN=CANX PE=1 SV=2	182	67526	9	12.3	4.47
29	K1C9_HUMAN	Keratin, type I cytoskeletal 9 OS=Homo sapiens GN=KRT9 PE=1 SV=3	180	62027	3	10.1	5.14
30	YBOX1_HUMAN	Nuclease-sensitive element-binding protein 1 OS=Homo sapiens GN=YBX1 PE=1 SV=3	179	35903	5	30.9	9.87
31	RS29_HUMAN	40S ribosomal protein S29 OS=Homo sapiens GN=RPS29 PE=1 SV=2	179	6672	5	19.6	10.17
32	ENPL_HUMAN	Endoplasmin OS=Homo sapiens GN=HSP90B1 PE=1 SV=1	171	92411	15	17.7	4.76
33	EFTU_HUMAN	Elongation factor Tu, mitochondrial OS=Homo sapiens GN=TUFM PE=1 SV=2	167	49510	9	14.6	7.26
34	ATP5J_HUMAN	ATP synthase-coupling factor 6, mitochondrial OS=Homo sapiens GN=ATP5J PE=1 SV=1	164	12580	2	18.5	9.52
35	GRP75_HUMAN	Stress-70 protein, mitochondrial OS=Homo sapiens GN=HSPA9 PE=1 SV=2	158	73635	10	12.7	5.87
36	FKB10_HUMAN	Peptidyl-prolyl cis-trans isomerase FKBP10 OS=Homo sapiens GN=FKBP10 PE=1 SV=1	158	64204	6	7.4	5.36
37	G3P_HUMAN	Glyceraldehyde-3-phosphate dehydrogenase OS=Homo sapiens GN=GAPDH PE=1 SV=3	150	36030	6	33.1	8.57
39	PDIA6_HUMAN	Protein disulfide-isomerase A6 OS=Homo sapiens GN=PDIA6 PE=1 SV=1	148	48091	4	17.7	4.95
40	RCN3_HUMAN	Reticulocalbin-3 OS=Homo sapiens GN=RCN3 PE=1 SV=1	147	37470	3	6.7	4.74
41	1C07_HUMAN	HLA class I histocompatibility antigen, Cw-7 alpha chain OS=Homo sapiens GN=HLA-C PE=1 SV=3	145	40623	3	18.9	5.7
42	CYB5_HUMAN	Cytochrome b5 OS=Homo sapiens GN=CYB5A PE=1 SV=2	143	15321	4	29.1	4.88
43	IMMT_HUMAN	Mitochondrial inner membrane protein OS=Homo sapiens GN=IMMT PE=1 SV=1	142	83626	6	11.9	6.08
44	FUMH_HUMAN	Fumarate hydratase, mitochondrial OS=Homo sapiens GN=FH PE=1 SV=3	142	54602	4	7.1	8.85
45	ATPA_HUMAN	ATP synthase subunit alpha, mitochondrial OS=Homo sapiens GN=ATP5A1 PE=1 SV=1	142	59714	11	18.1	9.16
46	RL18_HUMAN	60S ribosomal protein L18 OS=Homo sapiens GN=RPL18 PE=1 SV=2	140	21621	5	18.6	11.73
47	DLDH_HUMAN	Dihydrolipoyl dehydrogenase, mitochondrial OS=Homo sapiens GN=DLD PE=1 SV=2	140	54143	10	14.9	7.95
48	ACTBL_HUMAN	Beta-actin-like protein 2 OS=Homo sapiens GN=ACTBL2 PE=1 SV=2	138	41976	10	9.6	5.39
49	PDIA3_HUMAN	Protein disulfide-isomerase A3 OS=Homo sapiens GN=PDIA3 PE=1 SV=4	136	56747	5	10.7	5.98
50	GLYM_HUMAN	Serine hydroxymethyltransferase, mitochondrial OS=Homo sapiens GN=SHMT2 PE=1 SV=3	136	55958	4	9.5	8.76
51	PGRC1_HUMAN	Membrane-associated progesterone receptor component 1 OS=Homo sapiens GN=PGRMC1 PE=1 SV=3	136	21658	5	22.6	4.56
52	DESM_HUMAN	Desmin OS=Homo sapiens GN=DES PE=1 SV=3	134	53503	3	5.7	5.21
53	QCR7_HUMAN	Cytochrome b-c1 complex subunit 7 OS=Homo sapiens GN=UQCRB PE=1 SV=2	133	13522	5	28.8	8.73
54	1C08_HUMAN	HLA class I histocompatibility antigen, Cw-8 alpha chain OS=Homo sapiens GN=HLA-C PE=2 SV=1	133	40747	6	21.6	6.52
55	1B56_HUMAN	HLA class I histocompatibility antigen, B-56 alpha chain OS=Homo sapiens GN=HLA-B PE=2 SV=1	132	40453	6	20.7	5.77
57	ACTH_HUMAN	Actin, gamma-enteric smooth muscle OS=Homo sapiens GN=ACTG2 PE=1 SV=1	129	41850	13	19.9	5.31
60	RL7_HUMAN	60S ribosomal protein L7 OS=Homo sapiens GN=RPL7 PE=1 SV=1	124	29207	4	8.1	10.66
61	COQ9_HUMAN	Ubiquinone biosynthesis protein COQ9, mitochondrial OS=Homo sapiens GN=COQ9 PE=1 SV=1	124	35487	1	6.6	5.61
62	PREP_HUMAN	Presequence protease, mitochondrial OS=Homo sapiens GN=PITRM1 PE=1 SV=2	122	117380	6	7.2	6.5
63	RCN2_HUMAN	Reticulocalbin-2 OS=Homo sapiens GN=RCN2 PE=1 SV=1	120	36854	3	13.9	4.26
64	ACSL1_HUMAN	Long-chain-fatty-acid--CoA ligase 1 OS=Homo sapiens GN=ACSL1 PE=1 SV=1	120	77893	3	5.3	6.81
65	P5CS_HUMAN	Delta-1-pyrroline-5-carboxylate synthase OS=Homo sapiens GN=ALDH18A1 PE=1 SV=2	119	87248	4	6.2	6.66
66	DBPA_HUMAN	DNA-binding protein A OS=Homo sapiens GN=CSDA PE=1 SV=4	118	40066	5	22	9.77
67	PPIA_HUMAN	Peptidyl-prolyl cis-trans isomerase A OS=Homo sapiens GN=PPIA PE=1 SV=2	118	18001	4	20	7.68
68	2AAA_HUMAN	Serine/threonine-protein phosphatase 2A 65 kDa regulatory subunit A alpha isoform OS=Homo sapiens G	117	65267	4	7.8	5
69	TPP1_HUMAN	Tripeptidyl-peptidase 1 OS=Homo sapiens GN=TPP1 PE=1 SV=2	115	61210	4	12.3	6.01
70	NDUS6_HUMAN	NADH dehydrogenase [ubiquinone] iron-sulfur protein 6, mitochondrial OS=Homo sapiens GN=NDUFS6 PE=1	113	13703	3	17.7	8.59
71	ETFA_HUMAN	Electron transfer flavoprotein subunit alpha, mitochondrial OS=Homo sapiens GN=ETFA PE=1 SV=1	110	35058	5	19.2	8.62
72	MGST3_HUMAN	Microsomal glutathione S-transferase 3 OS=Homo sapiens GN=MGST3 PE=1 SV=1	110	16506	2	9.9	9.46
73	KPYM_HUMAN	Pyruvate kinase isozymes M1/M2 OS=Homo sapiens GN=PKM PE=1 SV=4	109	57900	4	7.7	7.96
74	CISY_HUMAN	Citrate synthase, mitochondrial OS=Homo sapiens GN=CS PE=1 SV=2	108	51680	3	6.7	8.45
75	FKBP9_HUMAN	Peptidyl-prolyl cis-trans isomerase FKBP9 OS=Homo sapiens GN=FKBP9 PE=1 SV=2	108	63044	3	7.4	4.91
76	KAD4_HUMAN	Adenylate kinase isoenzyme 4, mitochondrial OS=Homo sapiens GN=AK4 PE=1 SV=1	107	25252	6	33.6	8.47
77	CATB_HUMAN	Cathepsin B OS=Homo sapiens GN=CTSB PE=1 SV=3	107	37797	4	11.8	5.88
78	ANXA1_HUMAN	Annexin A1 OS=Homo sapiens GN=ANXA1 PE=1 SV=2	107	38690	3	11	6.57
79	RL6_HUMAN	60S ribosomal protein L6 OS=Homo sapiens GN=RPL6 PE=1 SV=3	106	32708	7	20.5	10.59
80	SND1_HUMAN	Staphylococcal nuclease domain-containing protein 1 OS=Homo sapiens GN=SND1 PE=1 SV=1	106	101934	11	13.7	6.74
81	RCN1_HUMAN	Reticulocalbin-1 OS=Homo sapiens GN=RCN1 PE=1 SV=1	105	38866	3	4.8	4.86
82	VATA_HUMAN	V-type proton ATPase catalytic subunit A OS=Homo sapiens GN=ATP6V1A PE=1 SV=2	105	68260	4	5.3	5.35
83	CH10_HUMAN	10 kDa heat shock protein, mitochondrial OS=Homo sapiens GN=HSPE1 PE=1 SV=2	105	10925	11	53.9	8.89
84	CD44_HUMAN	CD44 antigen OS=Homo sapiens GN=CD44 PE=1 SV=3	105	81487	2	3.2	5.13
85	RSSA_HUMAN	40S ribosomal protein SA OS=Homo sapiens GN=RPSA PE=1 SV=4	104	32833	3	12.2	4.79
86	SAP_HUMAN	Proactivator polypeptide OS=Homo sapiens GN=PSAP PE=1 SV=2	104	58074	4	6.1	5.06
87	AT1A1_HUMAN	Sodium/potassium-transporting ATPase subunit alpha-1 OS=Homo sapiens GN=ATP1A1 PE=1 SV=1	104	112824	7	9.1	5.33
88	TBA1B_HUMAN	Tubulin alpha-1B chain OS=Homo sapiens GN=TUBA1B PE=1 SV=1	104	50120	3	6.7	4.94
89	CKAP4_HUMAN	Cytoskeleton-associated protein 4 OS=Homo sapiens GN=CKAP4 PE=1 SV=2	103	65983	9	18.9	5.63
90	ODPB_HUMAN	Pyruvate dehydrogenase E1 component subunit beta, mitochondrial OS=Homo sapiens GN=PDHB PE=1 SV=3	102	39208	3	4.5	6.2
91	1433Z_HUMAN	14-3-3 protein zeta/delta OS=Homo sapiens GN=YWHAZ PE=1 SV=1	102	27728	5	27.3	4.73
92	EXOC5_HUMAN	Exocyst complex component 5 OS=Homo sapiens GN=EXOC5 PE=1 SV=1	102	81801	4	4.9	6.27
93	HMGA1_HUMAN	High mobility group protein HMG-I/HMG-Y OS=Homo sapiens GN=HMGA1 PE=1 SV=3	102	11669	7	61.7	10.32
94	GLSK_HUMAN	Glutaminase kidney isoform, mitochondrial OS=Homo sapiens GN=GLS PE=1 SV=1	101	73414	5	11.1	7.85
95	SPTN1_HUMAN	Spectrin alpha chain, non-erythrocytic 1 OS=Homo sapiens GN=SPTAN1 PE=1 SV=3	100	284364	12	5.7	5.22
96	IDH3B_HUMAN	Isocitrate dehydrogenase [NAD] subunit beta, mitochondrial OS=Homo sapiens GN=IDH3B PE=1 SV=2	100	42157	3	9.6	8.64
97	PABP3_HUMAN	Polyadenylate-binding protein 3 OS=Homo sapiens GN=PABPC3 PE=1 SV=2	100	69987	4	4.3	9.68

prot_hit_nı	prot_acc	prot_desc	prot_score	prot_mass	prot_matches	prot_cover	prot_pi
98	CY1_HUMAN	Cytochrome c1, heme protein, mitochondrial OS=Homo sapiens GN=CYC1 PE=1 SV=3	99	35399	2	9.5	9.15
99	TOM70_HUMAN	Mitochondrial import receptor subunit TOM70 OS=Homo sapiens GN=TOMM70A PE=1 SV=1	97	67412	1	3	6.75
100	PHB2_HUMAN	Prohibitin-2 OS=Homo sapiens GN=PHB2 PE=1 SV=2	97	33276	3	9.4	9.83
101	NB5R3_HUMAN	NADH-cytochrome b5 reductase 3 OS=Homo sapiens GN=CYB5R3 PE=1 SV=3	96	34213	5	22.9	7.18
102	STML2_HUMAN	Stomatin-like protein 2 OS=Homo sapiens GN=STOML2 PE=1 SV=1	96	38510	7	20.8	6.88
103	TXTP_HUMAN	Tricarboxylate transport protein, mitochondrial OS=Homo sapiens GN=SLC25A1 PE=1 SV=2	96	33991	5	8.7	9.91
104	COX20_HUMAN	Cytochrome c oxidase protein 20 homolog OS=Homo sapiens GN=COX20 PE=1 SV=2	96	13283	2	10.2	9
105	SERPH_HUMAN	Serpin H1 OS=Homo sapiens GN=SERPINH1 PE=1 SV=2	94	46411	3	10.3	8.75
106	RL4_HUMAN	60S ribosomal protein L4 OS=Homo sapiens GN=RPL4 PE=1 SV=5	94	47667	6	14.1	11.07
107	ECHA_HUMAN	Trifunctional enzyme subunit alpha, mitochondrial OS=Homo sapiens GN=HADHA PE=1 SV=2	94	82947	7	12.6	9.16
108	TBA3C_HUMAN	Tubulin alpha-3C/D chain OS=Homo sapiens GN=TUBA3C PE=1 SV=3	93	49928	3	10.7	4.97
109	QCR2_HUMAN	Cytochrome b-c1 complex subunit 2, mitochondrial OS=Homo sapiens GN=UQCRC2 PE=1 SV=3	92	48413	3	11.9	8.74
110	PLOD1_HUMAN	Procollagen-lysine,2-oxoglutarate 5-dioxygenase 1 OS=Homo sapiens GN=PLOD1 PE=1 SV=2	92	83497	6	12.5	6.47
111	SSRA_HUMAN	Translocon-associated protein subunit alpha OS=Homo sapiens GN=SSR1 PE=1 SV=3	92	32215	2	8	4.39
112	LAMB1_HUMAN	Laminin subunit beta-1 OS=Homo sapiens GN=LAMB1 PE=1 SV=2	90	197909	8	6.8	4.83
113	1A29_HUMAN	HLA class I histocompatibility antigen, A-29 alpha chain OS=Homo sapiens GN=HLA-A PE=2 SV=2	88	40837	5	15.3	6.52
114	E41L3_HUMAN	Band 4.1-like protein 3 OS=Homo sapiens GN=EPB41L3 PE=1 SV=2	87	120603	8	6.3	5.09
115	HCD2_HUMAN	3-hydroxyacyl-CoA dehydrogenase type-2 OS=Homo sapiens GN=HSD17B10 PE=1 SV=3	87	26906	1	6.5	7.66
116	AKA12_HUMAN	A-kinase anchor protein 12 OS=Homo sapiens GN=AKAP12 PE=1 SV=4	87	191367	6	4.8	4.37
117	ATP5H_HUMAN	ATP synthase subunit d, mitochondrial OS=Homo sapiens GN=ATP5H PE=1 SV=3	85	18479	2	13	5.21
118	ITAV_HUMAN	Integrin alpha-V OS=Homo sapiens GN=ITGAV PE=1 SV=2	85	115964	11	8.9	5.45
119	MDHM_HUMAN	Malate dehydrogenase, mitochondrial OS=Homo sapiens GN=MDH2 PE=1 SV=3	85	35481	3	15.1	8.92
120	SPNS1_HUMAN	Protein spinster homolog 1 OS=Homo sapiens GN=SPNS1 PE=1 SV=1	84	56594	1	2.7	6.19
121	ANXA6_HUMAN	Annexin A6 OS=Homo sapiens GN=ANXA6 PE=1 SV=3	83	75826	6	9.5	5.42
122	RS18_HUMAN	40S ribosomal protein S18 OS=Homo sapiens GN=RPS18 PE=1 SV=3	82	17708	8	34.9	10.99
123	NEP_HUMAN	Neprilysin OS=Homo sapiens GN=MME PE=1 SV=2	82	85460	4	4.1	5.54
124	LAMP1_HUMAN	Lysosome-associated membrane glycoprotein 1 OS=Homo sapiens GN=LAMP1 PE=1 SV=3	82	44854	4	14.9	9
125	SQRD_HUMAN	Sulfide:quinone oxidoreductase, mitochondrial OS=Homo sapiens GN=SQRDL PE=1 SV=1	81	49929	2	5.6	9.18
126	ODO1_HUMAN	2-oxoglutarate dehydrogenase, mitochondrial OS=Homo sapiens GN=OGDH PE=1 SV=3	80	115861	6	8.6	6.4
127	RL26_HUMAN	60S ribosomal protein L26 OS=Homo sapiens GN=RPL26 PE=1 SV=1	80	17248	7	15.9	10.55
128	TIM8B_HUMAN	Mitochondrial import inner membrane translocase subunit Tim8 B OS=Homo sapiens GN=TIMM8B PE=1 SV=1	80	9338	2	25.3	5.02
129	CNPY2_HUMAN	Protein canopy homolog 2 OS=Homo sapiens GN=CNPY2 PE=1 SV=1	80	20639	1	8.8	4.81
130	SKP1_HUMAN	S-phase kinase-associated protein 1 OS=Homo sapiens GN=SKP1 PE=1 SV=2	80	18646	1	7.4	4.4
131	HNRPK_HUMAN	Heterogeneous nuclear ribonucleoprotein K OS=Homo sapiens GN=HNRNPK PE=1 SV=1	80	50944	6	12.7	5.39
132	1433E_HUMAN	14-3-3 protein epsilon OS=Homo sapiens GN=YWHAE PE=1 SV=1	79	29155	1	7.5	4.63
133	EIF3M_HUMAN	Eukaryotic translation initiation factor 3 subunit M OS=Homo sapiens GN=EIF3M PE=1 SV=1	79	42476	1	4.8	5.41
134	TMM43_HUMAN	Transmembrane protein 43 OS=Homo sapiens GN=TMEM43 PE=1 SV=1	79	44847	3	2.3	7.86
135	PPIB_HUMAN	Peptidyl-prolyl cis-trans isomerase B OS=Homo sapiens GN=PPIB PE=1 SV=2	79	23728	5	18.1	9.42
136	SEPT7_HUMAN	Septin-7 OS=Homo sapiens GN=SEPT7 PE=1 SV=2	79	50648	1	2.7	8.76
137	C1QBP_HUMAN	Complement component 1 Q subcomponent-binding protein, mitochondrial OS=Homo sapiens GN=C1QBP PE=1	78	31343	4	20.6	4.74
138	ANXA4_HUMAN	Annexin A4 OS=Homo sapiens GN=ANXA4 PE=1 SV=4	77	35860	2	3.4	5.84
139	AHNK_HUMAN	Neuroblast differentiation-associated protein AHNAK OS=Homo sapiens GN=AHNAK PE=1 SV=2	77	628699	18	4.6	5.8
140	3HIDH_HUMAN	3-hydroxyisobutyrate dehydrogenase, mitochondrial OS=Homo sapiens GN=HIBADH PE=1 SV=2	76	35306	2	8.6	8.38
141	IF2B2_HUMAN	Insulin-like growth factor 2 mRNA-binding protein 2 OS=Homo sapiens GN=IGF2BP2 PE=1 SV=2	76	66081	4	7.5	8.48
142	IF2B_HUMAN	Eukaryotic translation initiation factor 2 subunit 2 OS=Homo sapiens GN=EIF2S2 PE=1 SV=2	76	38364	3	15.3	5.6
143	HDGF_HUMAN	Hepatoma-derived growth factor OS=Homo sapiens GN=HDGF PE=1 SV=1	76	26772	1	11.3	4.7
144	RS5_HUMAN	40S ribosomal protein S5 OS=Homo sapiens GN=RPS5 PE=1 SV=4	76	22862	4	15.2	9.73
145	ALDH2_HUMAN	Aldehyde dehydrogenase, mitochondrial OS=Homo sapiens GN=ALDH2 PE=1 SV=2	75	56346	2	5.2	6.63
146	CALU_HUMAN	Calumenin OS=Homo sapiens GN=CALU PE=1 SV=2	75	37084	4	8.3	4.47
147	DHE3_HUMAN	Glutamate dehydrogenase 1, mitochondrial OS=Homo sapiens GN=GLUD1 PE=1 SV=2	74	61359	8	9.5	7.66
148	1A34_HUMAN	HLA class I histocompatibility antigen, A-34 alpha chain OS=Homo sapiens GN=HLA-A PE=1 SV=1	74	41029	2	8.2	5.89
149	NDUS5_HUMAN	NADH dehydrogenase [ubiquinone] iron-sulfur protein 5 OS=Homo sapiens GN=NDUFS5 PE=1 SV=3	74	12509	3	14.2	9.27
150	NDUA9_HUMAN	NADH dehydrogenase [ubiquinone] 1 alpha subcomplex subunit 9, mitochondrial OS=Homo sapiens GN=NDUF	74	42483	4	9.8	9.81
151	SPTB2_HUMAN	Spectrin beta chain, non-erythrocytic 1 OS=Homo sapiens GN=SPTBN1 PE=1 SV=2	74	274439	13	5.2	5.39
152	RS3_HUMAN	40S ribosomal protein S3 OS=Homo sapiens GN=RPS3 PE=1 SV=2	73	26671	2	8.6	9.68
153	RAB10_HUMAN	Ras-related protein Rab-10 OS=Homo sapiens GN=RAB10 PE=1 SV=1	73	22527	2	11	8.59
154	HXK1_HUMAN	Hexokinase-1 OS=Homo sapiens GN=HK1 PE=1 SV=3	71	102420	7	10	6.36
155	NDUS8_HUMAN	NADH dehydrogenase [ubiquinone] iron-sulfur protein 8, mitochondrial OS=Homo sapiens GN=NDUFS8 PE=1	71	23690	2	9.5	6
156	DPP2_HUMAN	Dipeptidyl peptidase 2 OS=Homo sapiens GN=DPP7 PE=1 SV=3	71	54307	2	5.1	5.91
157	RS4X_HUMAN	40S ribosomal protein S4, X isoform OS=Homo sapiens GN=RPS4X PE=1 SV=2	71	29579	3	13.7	10.16
158	ATD3C_HUMAN	ATPase family AAA domain-containing protein 3C OS=Homo sapiens GN=ATAD3C PE=1 SV=2	71	46350	3	9.2	9.37
159	ATD3A_HUMAN	ATPase family AAA domain-containing protein 3A OS=Homo sapiens GN=ATAD3A PE=1 SV=2	71	71325	3	4.9	9.08
160	LRP1_HUMAN	Prolow-density lipoprotein receptor-related protein 1 OS=Homo sapiens GN=LRP1 PE=1 SV=2	70	504276	52	13.8	5.16
161	VATG1_HUMAN	V-type proton ATPase subunit G 1 OS=Homo sapiens GN=ATP6V1G1 PE=1 SV=3	69	13749	1	9.3	8.93
162	FLNA_HUMAN	Filamin-A OS=Homo sapiens GN=FLNA PE=1 SV=4	69	280564	20	9.2	5.7
163	NDUS1_HUMAN	NADH-ubiquinone oxidoreductase 75 kDa subunit, mitochondrial OS=Homo sapiens GN=NDUFS1 PE=1 SV=3	68	79417	5	9.8	5.89
164	ATPD_HUMAN	ATP synthase subunit delta, mitochondrial OS=Homo sapiens GN=ATP5D PE=1 SV=2	68	17479	1	8.3	5.38
165	RS15_HUMAN	40S ribosomal protein S15 OS=Homo sapiens GN=RPS15 PE=1 SV=2	68	17029	5	24.1	10.39
166	NLTP_HUMAN	Non-specific lipid-transfer protein OS=Homo sapiens GN=SCP2 PE=1 SV=2	68	58956	2	8.6	6.44
167	RL13_HUMAN	60S ribosomal protein L13 OS=Homo sapiens GN=RPL13 PE=1 SV=4	68	24247	6	20.4	11.65
168	LPPRC_HUMAN	Leucine-rich PPR motif-containing protein, mitochondrial OS=Homo sapiens GN=LRPPRC PE=1 SV=3	67	157805	6	6.1	5.81
169	GOGA5_HUMAN	Golgin subfamily A member 5 OS=Homo sapiens GN=GOLGA5 PE=1 SV=3	67	82974	1	2.5	5.6
170	CACP_HUMAN	Carnitine O-acetyltransferase OS=Homo sapiens GN=CRAT PE=1 SV=5	67	70812	4	5.4	8.63
171	MPCP_HUMAN	Phosphate carrier protein, mitochondrial OS=Homo sapiens GN=SLC25A3 PE=1 SV=2	66	40069	2	3.3	9.45
172	IPO5_HUMAN	Importin-5 OS=Homo sapiens GN=IPO5 PE=1 SV=4	66	123550	3	4.2	4.83
173	HMOX2_HUMAN	Heme oxygenase 2 OS=Homo sapiens GN=HMOX2 PE=1 SV=2	65	36010	2	12	5.31
174	RL35_HUMAN	60S ribosomal protein L35 OS=Homo sapiens GN=RPL35 PE=1 SV=2	65	14543	2	16.3	11.04
175	IF5A1_HUMAN	Eukaryotic translation initiation factor 5A-1 OS=Homo sapiens GN=EIF5A PE=1 SV=2	65	16821	1	7.8	5.08
176	SSBP_HUMAN	Single-stranded DNA-binding protein, mitochondrial OS=Homo sapiens GN=SSBP1 PE=1 SV=1	65	17249	3	16.2	9.59
177	TMX1_HUMAN	Thioredoxin-related transmembrane protein 1 OS=Homo sapiens GN=TMX1 PE=1 SV=1	65	31771	1	7.5	4.92
178	THY1_HUMAN	Thy-1 membrane glycoprotein OS=Homo sapiens GN=THY1 PE=1 SV=2	65	17923	3	9.9	8.96
179	RT36_HUMAN	28S ribosomal protein S36, mitochondrial OS=Homo sapiens GN=MRPS36 PE=1 SV=2	65	11459	3	33	9.99
180	FRIH_HUMAN	Ferritin heavy chain OS=Homo sapiens GN=FTH1 PE=1 SV=2	64	21212	4	19.7	5.3
181	LDHA_HUMAN	L-lactate dehydrogenase A chain OS=Homo sapiens GN=LDHA PE=1 SV=2	64	36665	3	11.1	8.44
182	NDUV1_HUMAN	NADH dehydrogenase [ubiquinone] flavoprotein 1, mitochondrial OS=Homo sapiens GN=NDUFV1 PE=1 SV=4	63	50785	4	8.8	8.51
183	OAT_HUMAN	Ornithine aminotransferase, mitochondrial OS=Homo sapiens GN=OAT PE=1 SV=1	62	48504	1	2.5	6.57
184	AL1L2_HUMAN	Mitochondrial 10-formyltetrahydrofolate dehydrogenase OS=Homo sapiens GN=ALDH1L2 PE=1 SV=2	60	101681	6	8.1	6.13
185	FINC_HUMAN	Fibronectin OS=Homo sapiens GN=FN1 PE=1 SV=4	60	262460	9	4.9	5.46
186	THIM_HUMAN	3-ketoacyl-CoA thiolase, mitochondrial OS=Homo sapiens GN=ACAA2 PE=1 SV=2	60	41898	5	10.3	8.32
187	NNTM_HUMAN	NAD(P) transhydrogenase, mitochondrial OS=Homo sapiens GN=NNT PE=1 SV=3	60	113823	9	7.1	8.31
188	G6PE_HUMAN	GDH/6PGL endoplasmic bifunctional protein OS=Homo sapiens GN=H6PD PE=1 SV=2	60	88836	4	8	6.84

Supplemental table S2: Proteins identified using Mascot SDS-LC

prot_hit_n	prot_acc	prot_desc	prot_score	prot_mass	prot_matches	prot_cover	prot_pi
1	K2C1_HUMAN	Keratin, type II cytoskeletal 1 OS=Homo sapiens GN=KRT1 PE=1 SV=6	4011	65999	94	62.7	8.15
2	ACTB_HUMAN	Actin, cytoplasmic 1 OS=Homo sapiens GN=ACTB PE=1 SV=1	2421	41710	72	59.2	5.29
3	CKAP4_HUMAN	Cytoskeleton-associated protein 4 OS=Homo sapiens GN=CKAP4 PE=1 SV=2	2273	65983	56	48.3	5.63
4	ANXA2_HUMAN	Annexin A2 OS=Homo sapiens GN=ANXA2 PE=1 SV=2	2223	38580	93	74	7.57
5	K1C9_HUMAN	Keratin, type I cytoskeletal 9 OS=Homo sapiens GN=KRT9 PE=1 SV=3	2221	62027	54	48.2	5.14
6	PDIA3_HUMAN	Protein disulfide-isomerase A3 OS=Homo sapiens GN=PDIA3 PE=1 SV=4	2043	56747	71	52.9	5.98
7	CALR_HUMAN	Calreticulin OS=Homo sapiens GN=CALR PE=1 SV=1	1971	48112	50	50.8	4.29
8	GRP78_HUMAN	78 kDa glucose-regulated protein OS=Homo sapiens GN=HSPA5 PE=1 SV=2	1706	72288	65	64.2	5.07
9	CO6A3_HUMAN	Collagen alpha-3(VI) chain OS=Homo sapiens GN=COL6A3 PE=1 SV=5	1675	343457	84	24.5	6.26
10	ECHA_HUMAN	Trifunctional enzyme subunit alpha, mitochondrial OS=Homo sapiens GN=HADHA PE=1 SV=2	1667	82947	51	45.6	9.16
11	GRP75_HUMAN	Stress-70 protein, mitochondrial OS=Homo sapiens GN=HSPA9 PE=1 SV=2	1587	73635	50	48.3	5.87
12	ENPL_HUMAN	Endoplasmin OS=Homo sapiens GN=HSP90B1 PE=1 SV=1	1490	92411	68	45.5	4.76
13	ATPB_HUMAN	ATP synthase subunit beta, mitochondrial OS=Homo sapiens GN=ATP5B PE=1 SV=3	1333	56525	39	61.2	5.26
14	ATPA_HUMAN	ATP synthase subunit alpha, mitochondrial OS=Homo sapiens GN=ATP5A1 PE=1 SV=1	1217	59714	53	66.4	9.16
15	POTEE_HUMAN	POTE ankyrin domain family member E OS=Homo sapiens GN=POTEE PE=1 SV=3	1211	121286	38	14.5	5.83
16	MYH9_HUMAN	Myosin-9 OS=Homo sapiens GN=MYH9 PE=1 SV=4	1206	226392	79	36.5	5.5
17	PDIA1_HUMAN	Protein disulfide-isomerase OS=Homo sapiens GN=P4HB PE=1 SV=3	1164	57081	39	50.6	4.76
18	VIME_HUMAN	Vimentin OS=Homo sapiens GN=VIM PE=1 SV=4	1112	53619	54	55.8	5.06
19	AMPN_HUMAN	Aminopeptidase N OS=Homo sapiens GN=ANPEP PE=1 SV=4	1087	109471	66	42.6	5.31
20	SERPH_HUMAN	Serpin H1 OS=Homo sapiens GN=SERPINH1 PE=1 SV=2	1033	46411	24	51.2	8.75
21	PDIA6_HUMAN	Protein disulfide-isomerase A6 OS=Homo sapiens GN=PDIA6 PE=1 SV=1	1022	48091	27	39.8	4.95
22	MYOF_HUMAN	Myoferlin OS=Homo sapiens GN=MYOF PE=1 SV=1	1010	234561	59	29.9	5.84
23	GANAB_HUMAN	Neutral alpha-glucosidase AB OS=Homo sapiens GN=GANAB PE=1 SV=3	1005	106807	45	44.3	5.74
24	RRBP1_HUMAN	Ribosome-binding protein 1 OS=Homo sapiens GN=RRBP1 PE=1 SV=4	1001	152381	38	24.5	8.69
25	CATB_HUMAN	Cathepsin B OS=Homo sapiens GN=CTSB PE=1 SV=3	963	37797	25	27.1	5.88
26	MOES_HUMAN	Moesin OS=Homo sapiens GN=MSN PE=1 SV=3	958	67778	50	40.6	6.08
27	CH60_HUMAN	60 kDa heat shock protein, mitochondrial OS=Homo sapiens GN=HSPD1 PE=1 SV=2	897	61016	28	47.8	5.7
28	K22E_HUMAN	Keratin, type II cytoskeletal 2 epidermal OS=Homo sapiens GN=KRT2 PE=1 SV=2	831	65393	44	39.1	8.07
29	VDAC1_HUMAN	Voltage-dependent anion-selective channel protein 1 OS=Homo sapiens GN=VDAC1 PE=1 SV=2	763	30754	20	74.2	8.62
30	SODM_HUMAN	Superoxide dismutase [Mn], mitochondrial OS=Homo sapiens GN=SOD2 PE=1 SV=2	759	24707	22	60.8	8.35
31	PPIB_HUMAN	Peptidyl-prolyl cis-trans isomerase B OS=Homo sapiens GN=PPIB PE=1 SV=2	747	23728	32	75.9	9.42
32	PLEC_HUMAN	Plectin OS=Homo sapiens GN=PLEC PE=1 SV=3	725	531466	90	19	5.74
33	ANXA6_HUMAN	Annexin A6 OS=Homo sapiens GN=ANXA6 PE=1 SV=3	722	75826	42	51.9	5.42
34	NEP_HUMAN	Neprilysin OS=Homo sapiens GN=MME PE=1 SV=2	720	85460	31	39.3	5.54
35	CALX_HUMAN	Calnexin OS=Homo sapiens GN=CANX PE=1 SV=2	715	67526	33	28.9	4.47
36	PHB2_HUMAN	Prohibitin-2 OS=Homo sapiens GN=PHB2 PE=1 SV=2	658	33276	25	67.6	9.83
37	CALU_HUMAN	Calumenin OS=Homo sapiens GN=CALU PE=1 SV=2	646	37084	36	42.9	4.47
39	SPTN1_HUMAN	Spectrin alpha chain, non-erythrocytic 1 OS=Homo sapiens GN=SPTAN1 PE=1 SV=3	621	284364	37	18.6	5.22
40	ACTN1_HUMAN	Alpha-actinin-1 OS=Homo sapiens GN=ACTN1 PE=1 SV=2	619	102993	35	41.6	5.25
41	AL1L2_HUMAN	Mitochondrial 10-formyltetrahydrofolate dehydrogenase OS=Homo sapiens GN=ALDH1L2 PE=1 SV=2	613	101681	32	33.6	6.13
42	K1C10_HUMAN	Keratin, type I cytoskeletal 10 OS=Homo sapiens GN=KRT10 PE=1 SV=6	611	58792	35	37.8	5.13
43	RL6_HUMAN	60S ribosomal protein L6 OS=Homo sapiens GN=RPL6 PE=1 SV=3	604	32708	27	39.9	10.59
44	SQRD_HUMAN	Sulfide:quinone oxidoreductase, mitochondrial OS=Homo sapiens GN=SQRDL PE=1 SV=1	572	49929	27	43.6	9.18
45	DHE3_HUMAN	Glutamate dehydrogenase 1, mitochondrial OS=Homo sapiens GN=GLUD1 PE=1 SV=2	567	61359	29	40	7.66
46	ACTN4_HUMAN	Alpha-actinin-4 OS=Homo sapiens GN=ACTN4 PE=1 SV=2	564	104788	28	34.4	5.27
47	SEPT7_HUMAN	Septin-7 OS=Homo sapiens GN=SEPT7 PE=1 SV=2	559	50648	21	33.6	8.76
48	ANXA5_HUMAN	Annexin A5 OS=Homo sapiens GN=ANXA5 PE=1 SV=2	557	35914	22	72.8	4.94
49	EFTU_HUMAN	Elongation factor Tu, mitochondrial OS=Homo sapiens GN=TUFM PE=1 SV=2	532	49510	21	28.5	7.26
50	OST48_HUMAN	Dolichyl-diphosphooligosaccharide--protein glycosyltransferase 48 kDa subunit OS=Homo sapiens GN=DD	531	50769	15	19.7	6.09
51	SFXN3_HUMAN	Sideroflexin-3 OS=Homo sapiens GN=SFXN3 PE=2 SV=2	516	35956	15	50.8	9.25
52	PDIA4_HUMAN	Protein disulfide-isomerase A4 OS=Homo sapiens GN=PDIA4 PE=1 SV=2	514	72887	33	39.8	4.96
53	AOFA_HUMAN	Amine oxidase [flavin-containing] A OS=Homo sapiens GN=MAOA PE=1 SV=1	481	59644	20	39.3	7.94
54	HSP7C_HUMAN	Heat shock cognate 71 kDa protein OS=Homo sapiens GN=HSPA8 PE=1 SV=1	469	70854	23	29.3	5.37
55	HYEP_HUMAN	Epoxide hydrolase 1 OS=Homo sapiens GN=EPHX1 PE=1 SV=1	463	52915	21	34.9	6.77
56	G3P_HUMAN	Glyceraldehyde-3-phosphate dehydrogenase OS=Homo sapiens GN=GAPDH PE=1 SV=3	461	36030	28	50.4	8.57
57	ALDH2_HUMAN	Aldehyde dehydrogenase, mitochondrial OS=Homo sapiens GN=ALDH2 PE=1 SV=2	436	56346	16	28.4	6.63
58	FUMH_HUMAN	Fumarate hydratase, mitochondrial OS=Homo sapiens GN=FH PE=1 SV=3	434	54602	19	30.8	8.85
59	FLNA_HUMAN	Filamin-A OS=Homo sapiens GN=FLNA PE=1 SV=4	430	280564	41	15.5	5.7
60	RPN1_HUMAN	Dolichyl-diphosphooligosaccharide--protein glycosyltransferase subunit 1 OS=Homo sapiens GN=RPN1 PE	429	68527	20	32.3	5.96
61	NDUS1_HUMAN	NADH-ubiquinone oxidoreductase 75 kDa subunit, mitochondrial OS=Homo sapiens GN=NDUFS1 PE=1 SV=3	427	79417	19	32.6	5.89
62	MDHM_HUMAN	Malate dehydrogenase, mitochondrial OS=Homo sapiens GN=MDH2 PE=1 SV=3	422	35481	14	41.1	8.92
63	SEPT2_HUMAN	Septin-2 OS=Homo sapiens GN=SEPT2 PE=1 SV=1	418	41461	15	26.9	6.15
64	TBB2A_HUMAN	Tubulin beta-2A chain OS=Homo sapiens GN=TUBB2A PE=1 SV=1	408	49875	11	29.4	4.78
65	TBB4B_HUMAN	Tubulin beta-4B chain OS=Homo sapiens GN=TUBB4B PE=1 SV=1	407	49799	14	34.6	4.79
66	TBB5_HUMAN	Tubulin beta chain OS=Homo sapiens GN=TUBB PE=1 SV=2	405	49639	15	40.1	4.78
67	SND1_HUMAN	Staphylococcal nuclease domain-containing protein 1 OS=Homo sapiens GN=SND1 PE=1 SV=1	404	101934	33	31	6.74
68	HCD2_HUMAN	3-hydroxyacyl-CoA dehydrogenase type-2 OS=Homo sapiens GN=HSD17B10 PE=1 SV=3	399	26906	12	44.8	7.66
69	IMMT_HUMAN	Mitochondrial inner membrane protein OS=Homo sapiens GN=IMMT PE=1 SV=1	389	83626	24	19.9	6.08
70	DHSA_HUMAN	Succinate dehydrogenase [ubiquinone] flavoprotein subunit, mitochondrial OS=Homo sapiens GN=SDHA PE	381	72645	22	29.2	7.06
71	PHB_HUMAN	Prohibitin OS=Homo sapiens GN=PHB PE=1 SV=1	381	29786	17	51.1	5.57
72	SFXN1_HUMAN	Sideroflexin-1 OS=Homo sapiens GN=SFXN1 PE=1 SV=4	376	35596	16	37.9	9.22
73	RAB7A_HUMAN	Ras-related protein Rab-7a OS=Homo sapiens GN=RAB7A PE=1 SV=1	374	23475	16	44	6.4
74	K2C6B_HUMAN	Keratin, type II cytoskeletal 6B OS=Homo sapiens GN=KRT6B PE=1 SV=5	368	60030	30	17.2	8.09
75	LEG3_HUMAN	Galectin-3 OS=Homo sapiens GN=LGALS3 PE=1 SV=5	365	26136	15	26.4	8.57
76	THIL_HUMAN	Acetyl-CoA acetyltransferase, mitochondrial OS=Homo sapiens GN=ACAT1 PE=1 SV=1	365	45171	17	43.3	8.98
77	RCN1_HUMAN	Reticulocalbin-1 OS=Homo sapiens GN=RCN1 PE=1 SV=1	352	38866	24	26	4.86
78	P3H1_HUMAN	Prolyl 3-hydroxylase 1 OS=Homo sapiens GN=LEPRE1 PE=1 SV=2	352	83341	14	20	5.05
79	CISY_HUMAN	Citrate synthase, mitochondrial OS=Homo sapiens GN=CS PE=1 SV=2	351	51680	17	34.8	8.45
80	RADI_HUMAN	Radixin OS=Homo sapiens GN=RDX PE=1 SV=1	345	68521	27	18.5	6.03
81	GLYM_HUMAN	Serine hydroxymethyltransferase, mitochondrial OS=Homo sapiens GN=SHMT2 PE=1 SV=3	343	55958	17	37.3	8.76
82	EZRI_HUMAN	Ezrin OS=Homo sapiens GN=EZR PE=1 SV=4	336	69370	32	18.8	5.94
83	RSSA_HUMAN	40S ribosomal protein SA OS=Homo sapiens GN=RPSA PE=1 SV=4	327	32833	11	19	4.79
84	RCN3_HUMAN	Reticulocalbin-3 OS=Homo sapiens GN=RCN3 PE=1 SV=1	325	37470	15	28.4	4.74
85	PCKGM_HUMAN	Phosphoenolpyruvate carboxykinase [GTP], mitochondrial OS=Homo sapiens GN=PCK2 PE=1 SV=3	320	70685	14	21.7	7.57
86	GLSK_HUMAN	Glutaminase kidney isoform, mitochondrial OS=Homo sapiens GN=GLS PE=1 SV=1	317	73414	11	11.7	7.85
87	LPPRC_HUMAN	Leucine-rich PPR motif-containing protein, mitochondrial OS=Homo sapiens GN=LRPPRC PE=1 SV=3	313	157805	21	18.5	5.81
88	ANXA1_HUMAN	Annexin A1 OS=Homo sapiens GN=ANXA1 PE=1 SV=2	309	38690	15	47.7	6.57
89	RS16_HUMAN	40S ribosomal protein S16 OS=Homo sapiens GN=RPS16 PE=1 SV=2	303	16435	14	61.6	10.21
90	RL7A_HUMAN	60S ribosomal protein L7a OS=Homo sapiens GN=RPL7A PE=1 SV=2	302	29977	28	40.6	10.61
91	PGRC1_HUMAN	Membrane-associated progesterone receptor component 1 OS=Homo sapiens GN=PGRMC1 PE=1 SV=3	300	21658	11	34.9	4.56
92	AATM_HUMAN	Aspartate aminotransferase, mitochondrial OS=Homo sapiens GN=GOT2 PE=1 SV=3	300	47487	14	34	9.14
93	ATLA3_HUMAN	Atlastin-3 OS=Homo sapiens GN=ATL3 PE=1 SV=1	296	60503	9	8.1	5.43
94	ECHB_HUMAN	Trifunctional enzyme subunit beta, mitochondrial OS=Homo sapiens GN=HADHB PE=1 SV=3	293	51262	16	33.1	9.45

prot_hit_nı	prot_acc	prot_desc	prot_score	prot_mass	prot_matches	prot_cover	prot_pi
95	AT5F1_HUMAN	ATP synthase subunit b, mitochondrial OS=Homo sapiens GN=ATP5F1 PE=1 SV=2	293	28890	16	41	9.37
96	RL15_HUMAN	60S ribosomal protein L15 OS=Homo sapiens GN=RPL15 PE=1 SV=2	292	24131	13	37.7	11.62
97	RS19_HUMAN	40S ribosomal protein S19 OS=Homo sapiens GN=RPS19 PE=1 SV=2	292	16051	10	51.7	10.31
98	QCR2_HUMAN	Cytochrome b-c1 complex subunit 2, mitochondrial OS=Homo sapiens GN=UQCRC2 PE=1 SV=3	291	48413	16	41.5	8.74
99	ODO1_HUMAN	2-oxoglutarate dehydrogenase, mitochondrial OS=Homo sapiens GN=OGDH PE=1 SV=3	286	115861	28	23.2	6.4
100	ETFA_HUMAN	Electron transfer flavoprotein subunit alpha, mitochondrial OS=Homo sapiens GN=ETFA PE=1 SV=1	285	35058	18	54.1	8.62
101	RS18_HUMAN	40S ribosomal protein S18 OS=Homo sapiens GN=RPS18 PE=1 SV=3	281	17708	19	58.6	10.99
102	FKB10_HUMAN	Peptidyl-prolyl cis-trans isomerase FKBP10 OS=Homo sapiens GN=FKBP10 PE=1 SV=1	276	64204	23	26.8	5.36
103	OAT_HUMAN	Ornithine aminotransferase, mitochondrial OS=Homo sapiens GN=OAT PE=1 SV=1	276	48504	15	33.7	6.57
104	ACON_HUMAN	Aconitate hydratase, mitochondrial OS=Homo sapiens GN=ACO2 PE=1 SV=2	275	85372	17	27.1	7.36
105	NDUS3_HUMAN	NADH dehydrogenase [ubiquinone] iron-sulfur protein 3, mitochondrial OS=Homo sapiens GN=NDUFS3 PE=1	274	30223	9	39.4	6.99
106	ATPG_HUMAN	ATP synthase subunit gamma, mitochondrial OS=Homo sapiens GN=ATP5C1 PE=1 SV=1	271	32975	8	28.9	9.23
107	K2C5_HUMAN	Keratin, type II cytoskeletal 5 OS=Homo sapiens GN=KRT5 PE=1 SV=3	270	62340	24	16.4	7.59
108	ECH1_HUMAN	Delta(3,5)-Delta(2,4)-dienoyl-CoA isomerase, mitochondrial OS=Homo sapiens GN=ECH1 PE=1 SV=2	269	35793	7	18.3	8.16
109	TXND5_HUMAN	Thioredoxin domain-containing protein 5 OS=Homo sapiens GN=TXNDC5 PE=1 SV=2	266	47599	15	20.4	5.63
110	IDHP_HUMAN	Isocitrate dehydrogenase [NADP], mitochondrial OS=Homo sapiens GN=IDH2 PE=1 SV=2	266	50877	15	32.7	8.88
111	ENOA_HUMAN	Alpha-enolase OS=Homo sapiens GN=ENO1 PE=1 SV=2	265	47139	12	28.8	7.01
112	RS3A_HUMAN	40S ribosomal protein S3a OS=Homo sapiens GN=RPS3A PE=1 SV=2	265	29926	13	25.8	9.75
113	ADRO_HUMAN	NADPH:adrenodoxin oxidoreductase, mitochondrial OS=Homo sapiens GN=FDXR PE=1 SV=3	261	53803	15	22.6	8.72
114	RL4_HUMAN	60S ribosomal protein L4 OS=Homo sapiens GN=RPL4 PE=1 SV=5	260	47667	17	41.2	11.07
115	LMNA_HUMAN	Prelamin-A/C OS=Homo sapiens GN=LMNA PE=1 SV=1	257	74095	17	24.2	6.57
116	ENPLL_HUMAN	Putative endoplasmin-like protein OS=Homo sapiens GN=HSP90B2P PE=5 SV=1	257	45830	15	19.8	5.14
117	PGRC2_HUMAN	Membrane-associated progesterone receptor component 2 OS=Homo sapiens GN=PGRMC2 PE=1 SV=1	256	23804	14	32.3	4.76
118	MYL6_HUMAN	Myosin light polypeptide 6 OS=Homo sapiens GN=MYL6 PE=1 SV=2	253	16919	7	43.7	4.56
119	SEP11_HUMAN	Septin-11 OS=Homo sapiens GN=SEPT11 PE=1 SV=3	253	49367	19	20	6.36
120	ATP5H_HUMAN	ATP synthase subunit d, mitochondrial OS=Homo sapiens GN=ATP5H PE=1 SV=3	249	18479	15	73.9	5.21
121	MTCH2_HUMAN	Mitochondrial carrier homolog 2 OS=Homo sapiens GN=MTCH2 PE=1 SV=1	249	33309	8	22.4	8.25
122	AL4A1_HUMAN	Delta-1-pyrroline-5-carboxylate dehydrogenase, mitochondrial OS=Homo sapiens GN=ALDH4A1 PE=1 SV=3	249	61681	14	19.2	8.25
123	BASP1_HUMAN	Brain acid soluble protein 1 OS=Homo sapiens GN=BASP1 PE=1 SV=2	247	22680	12	71.4	4.64
124	VDAC2_HUMAN	Voltage-dependent anion-selective channel protein 2 OS=Homo sapiens GN=VDAC2 PE=1 SV=2	242	31547	12	37.4	7.49
125	SCRB2_HUMAN	Lysosome membrane protein 2 OS=Homo sapiens GN=SCARB2 PE=1 SV=2	238	54255	12	18.6	5
126	IDH3A_HUMAN	Isocitrate dehydrogenase [NAD] subunit alpha, mitochondrial OS=Homo sapiens GN=IDH3A PE=1 SV=1	236	39566	9	29.8	6.47
127	CATD_HUMAN	Cathepsin D OS=Homo sapiens GN=CTSD PE=1 SV=1	234	44524	10	18.7	6.1
128	LAMP1_HUMAN	Lysosome-associated membrane glycoprotein 1 OS=Homo sapiens GN=LAMP1 PE=1 SV=3	231	44854	9	13.2	9
129	MYH10_HUMAN	Myosin-10 OS=Homo sapiens GN=MYH10 PE=1 SV=3	229	228858	39	16.1	5.44
130	RL14_HUMAN	60S ribosomal protein L14 OS=Homo sapiens GN=RPL14 PE=1 SV=4	229	23417	18	35.8	10.94
131	RL7_HUMAN	60S ribosomal protein L7 OS=Homo sapiens GN=RPL7 PE=1 SV=1	228	29207	18	35.5	10.66
132	NDUA9_HUMAN	NADH dehydrogenase [ubiquinone] 1 alpha subcomplex subunit 9, mitochondrial OS=Homo sapiens GN=NDUF	228	42483	7	17.2	9.81
133	NB5R3_HUMAN	NADH-cytochrome b5 reductase 3 OS=Homo sapiens GN=CYB5R3 PE=1 SV=3	223	34213	24	42.2	7.18
134	PCYOX_HUMAN	Prenylcysteine oxidase 1 OS=Homo sapiens GN=PCYOX1 PE=1 SV=3	221	56604	8	15.8	5.8
135	USMG5_HUMAN	Up-regulated during skeletal muscle growth protein 5 OS=Homo sapiens GN=USMG5 PE=1 SV=1	220	6453	3	44.8	9.78
136	THIM_HUMAN	3-ketoacyl-CoA thiolase, mitochondrial OS=Homo sapiens GN=ACAA2 PE=1 SV=2	220	41898	13	38	8.32
137	SUCB2_HUMAN	Succinyl-CoA ligase [GDP-forming] subunit beta, mitochondrial OS=Homo sapiens GN=SUCLG2 PE=1 SV=2	219	46481	10	24.5	6.15
138	AL1L1_HUMAN	Cytosolic 10-formyltetrahydrofolate dehydrogenase OS=Homo sapiens GN=ALDH1L1 PE=1 SV=2	219	98767	12	8.1	5.63
139	ARSA_HUMAN	Arylsulfatase A OS=Homo sapiens GN=ARSA PE=1 SV=3	215	53554	8	13.2	5.65
140	TBA1A_HUMAN	Tubulin alpha-1A chain OS=Homo sapiens GN=TUBA1A PE=1 SV=1	214	50104	15	31.9	4.94
141	ODPB_HUMAN	Pyruvate dehydrogenase E1 component subunit beta, mitochondrial OS=Homo sapiens GN=PDHB PE=1 SV=3	213	39208	6	20.9	6.2
142	MGST3_HUMAN	Microsomal glutathione S-transferase 3 OS=Homo sapiens GN=MGST3 PE=1 SV=1	213	16506	4	18.4	9.46
143	ECHM_HUMAN	Enoyl-CoA hydratase, mitochondrial OS=Homo sapiens GN=ECHS1 PE=1 SV=4	212	31367	11	37.2	8.34
144	HEXB_HUMAN	Beta-hexosaminidase subunit beta OS=Homo sapiens GN=HEXB PE=1 SV=3	212	63071	16	24.3	6.29
145	HORN_HUMAN	Hornerin OS=Homo sapiens GN=HRNR PE=1 SV=2	212	282228	8	3.2	10.05
146	RS8_HUMAN	40S ribosomal protein S8 OS=Homo sapiens GN=RPS8 PE=1 SV=2	208	24190	13	48.1	10.32
147	QCR1_HUMAN	Cytochrome b-c1 complex subunit 1, mitochondrial OS=Homo sapiens GN=UQCRC1 PE=1 SV=3	207	52612	17	39.8	5.94
148	STML2_HUMAN	Stomatin-like protein 2 OS=Homo sapiens GN=STOML2 PE=1 SV=1	206	38510	8	33.1	6.88
149	DHSB_HUMAN	Succinate dehydrogenase [ubiquinone] iron-sulfur subunit, mitochondrial OS=Homo sapiens GN=SDHB PE=	206	31609	14	38.6	9.03
150	NCLN_HUMAN	Nicalin OS=Homo sapiens GN=NCLN PE=1 SV=2	204	62935	7	13.5	6.4
151	RLA0_HUMAN	60S acidic ribosomal protein P0 OS=Homo sapiens GN=RPLP0 PE=1 SV=1	203	34252	11	25.2	5.71
152	RL12_HUMAN	60S ribosomal protein L12 OS=Homo sapiens GN=RPL12 PE=1 SV=1	203	17808	8	40.6	9.48
153	LRP1_HUMAN	Prolow-density lipoprotein receptor-related protein 1 OS=Homo sapiens GN=LRP1 PE=1 SV=2	202	504276	52	11.9	5.16
154	SSRD_HUMAN	Translocon-associated protein subunit delta OS=Homo sapiens GN=SSR4 PE=1 SV=1	201	18987	7	29.5	5.76
155	COX41_HUMAN	Cytochrome c oxidase subunit 4 isoform 1, mitochondrial OS=Homo sapiens GN=COX4I1 PE=1 SV=1	200	19564	10	42	9.52
156	CYB5_HUMAN	Cytochrome b5 OS=Homo sapiens GN=CYB5A PE=1 SV=2	199	15321	7	49.3	4.88
157	CYC_HUMAN	Cytochrome c OS=Homo sapiens GN=CYCS PE=1 SV=2	197	11741	8	29.5	9.59
158	RL35_HUMAN	60S ribosomal protein L35 OS=Homo sapiens GN=RPL35 PE=1 SV=2	197	14543	10	55.3	11.04
159	LONM_HUMAN	Lon protease homolog, mitochondrial OS=Homo sapiens GN=LONP1 PE=1 SV=2	197	106422	17	19.8	6.01
160	TIM50_HUMAN	Mitochondrial import inner membrane translocase subunit TIM50 OS=Homo sapiens GN=TIMM50 PE=1 SV=2	196	39622	10	25.8	8.55
161	LEG1_HUMAN	Galectin-1 OS=Homo sapiens GN=LGALS1 PE=1 SV=2	194	14706	4	40.7	5.34
162	RL8_HUMAN	60S ribosomal protein L8 OS=Homo sapiens GN=RPL8 PE=1 SV=2	194	28007	19	38.5	11.03
163	GLU2B_HUMAN	Glucosidase 2 subunit beta OS=Homo sapiens GN=PRKCSH PE=1 SV=2	194	59388	13	14.2	4.33
164	ADT2_HUMAN	ADP/ATP translocase 2 OS=Homo sapiens GN=SLC25A5 PE=1 SV=7	193	32831	16	40.6	9.71
165	HSP72_HUMAN	Heat shock-related 70 kDa protein 2 OS=Homo sapiens GN=HSPA2 PE=1 SV=1	192	69978	15	20.5	5.56
166	DHB4_HUMAN	Peroxisomal multifunctional enzyme type 2 OS=Homo sapiens GN=HSD17B4 PE=1 SV=3	189	79636	16	19.6	8.96
167	HS71L_HUMAN	Heat shock 70 kDa protein 1-like OS=Homo sapiens GN=HSPA1L PE=1 SV=2	188	70331	15	15.8	5.76
168	1433Z_HUMAN	14-3-3 protein zeta/delta OS=Homo sapiens GN=YWHAZ PE=1 SV=1	187	27728	10	41.6	4.73
169	PRDX4_HUMAN	Peroxiredoxin-4 OS=Homo sapiens GN=PRDX4 PE=1 SV=1	183	30521	6	20.7	5.86
170	DECR_HUMAN	2,4-dienoyl-CoA reductase, mitochondrial OS=Homo sapiens GN=DECR1 PE=1 SV=1	183	36045	9	23	9.35
171	S10AA_HUMAN	Protein S100-A10 OS=Homo sapiens GN=S100A10 PE=1 SV=2	182	11196	6	49.5	6.82
172	MPCP_HUMAN	Phosphate carrier protein, mitochondrial OS=Homo sapiens GN=SLC25A3 PE=1 SV=2	182	40069	12	17.7	9.45
173	ACADV_HUMAN	Very long-chain specific acyl-CoA dehydrogenase, mitochondrial OS=Homo sapiens GN=ACADVL PE=1 SV=1	182	70345	7	11.8	8.92
174	PABP1_HUMAN	Polyadenylate-binding protein 1 OS=Homo sapiens GN=PABPC1 PE=1 SV=2	180	70626	15	24.2	9.52
175	SCOT1_HUMAN	Succinyl-CoA:3-ketoacid coenzyme A transferase 1, mitochondrial OS=Homo sapiens GN=OXCT1 PE=1 SV=1	179	56122	8	18.1	7.14
176	ATD3A_HUMAN	ATPase family AAA domain-containing protein 3A OS=Homo sapiens GN=ATAD3A PE=1 SV=2	178	71325	15	23.5	9.08
177	LAMB1_HUMAN	Laminin subunit beta-1 OS=Homo sapiens GN=LAMB1 PE=1 SV=2	176	197909	20	13.8	4.83
178	SPTB2_HUMAN	Spectrin beta chain, non-erythrocytic 1 OS=Homo sapiens GN=SPTBN1 PE=1 SV=2	176	274439	27	11.8	5.39
179	ANXA4_HUMAN	Annexin A4 OS=Homo sapiens GN=ANXA4 PE=1 SV=4	176	35860	8	22.9	5.84
180	THY1_HUMAN	Thy-1 membrane glycoprotein OS=Homo sapiens GN=THY1 PE=1 SV=2	173	17923	6	9.9	8.96
181	TMED9_HUMAN	Transmembrane emp24 domain-containing protein 9 OS=Homo sapiens GN=TMED9 PE=1 SV=2	173	27260	5	15.7	7.82
182	HSP71_HUMAN	Heat shock 70 kDa protein 1A/1B OS=Homo sapiens GN=HSPA1A PE=1 SV=5	170	70009	10	13.1	5.48
183	RL13_HUMAN	60S ribosomal protein L13 OS=Homo sapiens GN=RPL13 PE=1 SV=4	170	24247	14	37	11.65
184	RL10_HUMAN	60S ribosomal protein L10 OS=Homo sapiens GN=RPL10 PE=1 SV=4	170	24588	18	49.5	10.11
185	HEXA_HUMAN	Beta-hexosaminidase subunit alpha OS=Homo sapiens GN=HEXA PE=1 SV=2	170	60664	7	10.4	5.04
186	RL40_HUMAN	Ubiquitin-60S ribosomal protein L40 OS=Homo sapiens GN=UBA52 PE=1 SV=2	170	14719	20	36.7	9.87
187	RS27A_HUMAN	Ubiquitin-40S ribosomal protein S27a OS=Homo sapiens GN=RPS27A PE=1 SV=2	169	17953	19	28.2	9.68

prot_hit_nı	prot_acc	prot_desc	prot_score	prot_mass	prot_matches	prot_cover	prot_pi
188	SYG_HUMAN	Glycine--tRNA ligase OS=Homo sapiens GN=GARS PE=1 SV=3	168	83113	13	20.8	6.61
189	PGK1_HUMAN	Phosphoglycerate kinase 1 OS=Homo sapiens GN=PGK1 PE=1 SV=3	167	44586	9	26.9	8.3
190	ADT3_HUMAN	ADP/ATP translocase 3 OS=Homo sapiens GN=SLC25A6 PE=1 SV=4	167	32845	16	30.9	9.76
191	RCN2_HUMAN	Reticulocalbin-2 OS=Homo sapiens GN=RCN2 PE=1 SV=1	167	36854	3	16.7	4.26
192	TPM4_HUMAN	Tropomyosin alpha-4 chain OS=Homo sapiens GN=TPM4 PE=1 SV=3	167	28504	12	40.7	4.67
193	GBLP_HUMAN	Guanine nucleotide-binding protein subunit beta-2-like 1 OS=Homo sapiens GN=GNB2L1 PE=1 SV=3	167	35055	11	30.9	7.6
194	MYO1D_HUMAN	Unconventional myosin-Id OS=Homo sapiens GN=MYO1D PE=1 SV=2	165	116129	26	21.2	9.44
195	ERG7_HUMAN	Lanosterol synthase OS=Homo sapiens GN=LSS PE=1 SV=1	163	83255	15	19	6.16
196	ERP29_HUMAN	Endoplasmic reticulum resident protein 29 OS=Homo sapiens GN=ERP29 PE=1 SV=4	161	28975	7	29.9	6.77
197	QOR_HUMAN	Quinone oxidoreductase OS=Homo sapiens GN=CRYZ PE=1 SV=1	160	35185	4	17	8.56
198	TPP1_HUMAN	Tripeptidyl-peptidase 1 OS=Homo sapiens GN=TPP1 PE=1 SV=2	160	61210	6	13.1	6.01
199	P5CR1_HUMAN	Pyrroline-5-carboxylate reductase 1, mitochondrial OS=Homo sapiens GN=PYCR1 PE=1 SV=2	159	33340	7	32.6	7.18
200	RS20_HUMAN	40S ribosomal protein S20 OS=Homo sapiens GN=RPS20 PE=1 SV=1	159	13364	6	38.7	9.95
201	NDUA2_HUMAN	NADH dehydrogenase [ubiquinone] 1 alpha subcomplex subunit 2 OS=Homo sapiens GN=NDUFA2 PE=1 SV=3	159	10915	1	21.2	9.62
202	RL19_HUMAN	60S ribosomal protein L19 OS=Homo sapiens GN=RPL19 PE=1 SV=1	156	23451	8	22.4	11.48
203	CH10_HUMAN	10 kDa heat shock protein, mitochondrial OS=Homo sapiens GN=HSPE1 PE=1 SV=2	156	10925	10	68.6	8.89
204	ACOT1_HUMAN	Acyl-coenzyme A thioesterase 1 OS=Homo sapiens GN=ACOT1 PE=1 SV=1	154	46248	9	23.8	6.9
205	FKBP9_HUMAN	Peptidyl-prolyl cis-trans isomerase FKBP9 OS=Homo sapiens GN=FKBP9 PE=1 SV=2	154	63044	17	19.5	4.91
206	RS26_HUMAN	40S ribosomal protein S26 OS=Homo sapiens GN=RPS26 PE=1 SV=3	154	13007	9	74.8	11.01
207	HS90B_HUMAN	Heat shock protein HSP 90-beta OS=Homo sapiens GN=HSP90AB1 PE=1 SV=4	153	83212	12	17.8	4.97
208	RS14_HUMAN	40S ribosomal protein S14 OS=Homo sapiens GN=RPS14 PE=1 SV=3	149	16263	8	41.7	10.07
209	NDUV1_HUMAN	NADH dehydrogenase [ubiquinone] flavoprotein 1, mitochondrial OS=Homo sapiens GN=NDUFV1 PE=1 SV=4	148	50785	9	25.6	8.51
210	SEPT9_HUMAN	Septin-9 OS=Homo sapiens GN=SEPT9 PE=1 SV=2	148	65361	11	18.6	9.06
211	THTR_HUMAN	Thiosulfate sulfurtransferase OS=Homo sapiens GN=TST PE=1 SV=4	148	33408	7	25.6	6.77
212	PRDX3_HUMAN	Thioredoxin-dependent peroxide reductase, mitochondrial OS=Homo sapiens GN=PRDX3 PE=1 SV=3	148	27675	8	27.3	7.67
213	GNS_HUMAN	N-acetylglucosamine-6-sulfatase OS=Homo sapiens GN=GNS PE=1 SV=3	147	62042	5	6.9	8.6
214	TLN1_HUMAN	Talin-1 OS=Homo sapiens GN=TLN1 PE=1 SV=3	147	269599	22	8.9	5.77
215	RS17L_HUMAN	40S ribosomal protein S17-like OS=Homo sapiens GN=RPS17L PE=3 SV=1	147	15540	7	39.3	9.85
216	ERGI1_HUMAN	Endoplasmic reticulum-Golgi intermediate compartment protein 1 OS=Homo sapiens GN=ERGIC1 PE=1 SV=1	147	32571	11	30.3	6.59
217	COX5B_HUMAN	Cytochrome c oxidase subunit 5B, mitochondrial OS=Homo sapiens GN=COX5B PE=1 SV=2	146	13687	5	30.2	9.07
218	1A29_HUMAN	HLA class I histocompatibility antigen, A-29 alpha chain OS=Homo sapiens GN=HLA-A PE=2 SV=2	145	40837	7	28.5	6.52
219	RS13_HUMAN	40S ribosomal protein S13 OS=Homo sapiens GN=RPS13 PE=1 SV=2	144	17212	12	51.7	10.53
220	NDUB4_HUMAN	NADH dehydrogenase [ubiquinone] 1 beta subcomplex subunit 4 OS=Homo sapiens GN=NDUFB4 PE=1 SV=3	144	15199	8	53.5	9.85
221	HCDH_HUMAN	Hydroxyacyl-coenzyme A dehydrogenase, mitochondrial OS=Homo sapiens GN=HADH PE=1 SV=3	144	34272	9	25.8	8.88
222	RS15A_HUMAN	40S ribosomal protein S15a OS=Homo sapiens GN=RPS15A PE=1 SV=2	143	14830	10	35.4	10.14
223	CY1_HUMAN	Cytochrome c1, heme protein, mitochondrial OS=Homo sapiens GN=CYC1 PE=1 SV=3	143	35399	7	15.4	9.15
224	FRIL_HUMAN	Ferritin light chain OS=Homo sapiens GN=FTL PE=1 SV=2	142	20007	7	33.7	5.51
225	ADAS_HUMAN	Alkyldihydroxyacetonephosphate synthase, peroxisomal OS=Homo sapiens GN=AGPS PE=1 SV=1	142	72866	9	13.8	6.99
226	ETFB_HUMAN	Electron transfer flavoprotein subunit beta OS=Homo sapiens GN=ETFB PE=1 SV=3	141	27826	7	25.1	8.24
227	SCMC1_HUMAN	Calcium-binding mitochondrial carrier protein SCaMC-1 OS=Homo sapiens GN=SLC25A24 PE=1 SV=2	140	53320	10	18.7	6
228	NDUB9_HUMAN	NADH dehydrogenase [ubiquinone] 1 beta subcomplex subunit 9 OS=Homo sapiens GN=NDUFB9 PE=1 SV=3	140	21817	7	36.9	8.58
229	NDUBA_HUMAN	NADH dehydrogenase [ubiquinone] 1 beta subcomplex subunit 10 OS=Homo sapiens GN=NDUFB10 PE=1 SV=3	139	20763	13	51.7	8.72
230	RS9_HUMAN	40S ribosomal protein S9 OS=Homo sapiens GN=RPS9 PE=1 SV=3	139	22578	15	38.1	10.66
231	ACOT2_HUMAN	Acyl-coenzyme A thioesterase 2, mitochondrial OS=Homo sapiens GN=ACOT2 PE=1 SV=6	138	53185	9	19.7	8.7
232	1A01_HUMAN	HLA class I histocompatibility antigen, A-1 alpha chain OS=Homo sapiens GN=HLA-A PE=1 SV=1	138	40820	9	27.1	6.08
233	CNPY2_HUMAN	Protein canopy homolog 2 OS=Homo sapiens GN=CNPY2 PE=1 SV=1	136	20639	4	23.6	4.81
234	ATIF1_HUMAN	ATPase inhibitor, mitochondrial OS=Homo sapiens GN=ATPIF1 PE=1 SV=1	136	12241	5	33	9.34
235	AL1B1_HUMAN	Aldehyde dehydrogenase X, mitochondrial OS=Homo sapiens GN=ALDH1B1 PE=1 SV=3	136	57170	9	21.5	6.36
236	TMM43_HUMAN	Transmembrane protein 43 OS=Homo sapiens GN=TMEM43 PE=1 SV=1	135	44847	11	39.3	7.86
237	ATP5L_HUMAN	ATP synthase subunit g, mitochondrial OS=Homo sapiens GN=ATP5L PE=1 SV=3	135	11421	4	46.6	9.65
238	GSTP1_HUMAN	Glutathione S-transferase P OS=Homo sapiens GN=GSTP1 PE=1 SV=2	134	23341	3	22.4	5.43
239	CHCH3_HUMAN	Coiled-coil-helix-coiled-coil-helix domain-containing protein 3, mitochondrial OS=Homo sapiens GN=C	134	26136	7	26	8.48
240	AP2A2_HUMAN	AP-2 complex subunit alpha-2 OS=Homo sapiens GN=AP2A2 PE=1 SV=2	134	103895	5	5.9	6.53
241	NDKB_HUMAN	Nucleoside diphosphate kinase B OS=Homo sapiens GN=NME2 PE=1 SV=1	133	17287	6	38.8	8.52
242	EF2_HUMAN	Elongation factor 2 OS=Homo sapiens GN=EEF2 PE=1 SV=4	133	95277	28	21.9	6.41
243	MMSA_HUMAN	Methylmalonate-semialdehyde dehydrogenase [acylating], mitochondrial OS=Homo sapiens GN=ALDH6A1 PE=	133	57803	9	15	8.72
244	AP2A1_HUMAN	AP-2 complex subunit alpha-1 OS=Homo sapiens GN=AP2A1 PE=1 SV=3	132	107478	17	21.4	6.63
245	1A34_HUMAN	HLA class I histocompatibility antigen, A-34 alpha chain OS=Homo sapiens GN=HLA-A PE=1 SV=1	132	41029	8	28.2	5.89
246	COQ9_HUMAN	Ubiquinone biosynthesis protein COQ9, mitochondrial OS=Homo sapiens GN=COQ9 PE=1 SV=1	131	35487	3	14.2	5.61
247	PPIA_HUMAN	Peptidyl-prolyl cis-trans isomerase A OS=Homo sapiens GN=PPIA PE=1 SV=2	131	18001	10	28.5	7.68
248	THIK_HUMAN	3-ketoacyl-CoA thiolase, peroxisomal OS=Homo sapiens GN=ACAA1 PE=1 SV=2	130	44264	6	13.2	8.76
249	RS11_HUMAN	40S ribosomal protein S11 OS=Homo sapiens GN=RPS11 PE=1 SV=3	128	18419	14	38.6	10.31
250	PLBL2_HUMAN	Putative phospholipase B-like 2 OS=Homo sapiens GN=PLBD2 PE=1 SV=2	127	65430	6	8.5	6.34
251	TPIS_HUMAN	Triosephosphate isomerase OS=Homo sapiens GN=TPI1 PE=1 SV=3	127	30772	5	9.8	5.65
252	NDUV2_HUMAN	NADH dehydrogenase [ubiquinone] flavoprotein 2, mitochondrial OS=Homo sapiens GN=NDUFV2 PE=1 SV=2	127	27374	5	20.5	8.22
253	K1C14_HUMAN	Keratin, type I cytoskeletal 14 OS=Homo sapiens GN=KRT14 PE=1 SV=4	127	51529	19	28	5.09
254	ML12B_HUMAN	Myosin regulatory light chain 12B OS=Homo sapiens GN=MYL12B PE=1 SV=2	127	19767	5	19.2	4.71
255	RL26_HUMAN	60S ribosomal protein L26 OS=Homo sapiens GN=RPL26 PE=1 SV=1	127	17248	12	50.3	10.55
256	FINC_HUMAN	Fibronectin OS=Homo sapiens GN=FN1 PE=1 SV=4	126	262460	21	9.7	5.46
257	COX6C_HUMAN	Cytochrome c oxidase subunit 6C OS=Homo sapiens GN=COX6C PE=1 SV=2	126	8776	8	46.7	10.38
258	NDUAD_HUMAN	NADH dehydrogenase [ubiquinone] 1 alpha subcomplex subunit 13 OS=Homo sapiens GN=NDUFA13 PE=1 SV=3	126	16688	6	40.3	8.04
259	VATA_HUMAN	V-type proton ATPase catalytic subunit A OS=Homo sapiens GN=ATP6V1A PE=1 SV=2	126	68260	9	11.8	5.35
260	SSRA_HUMAN	Translocon-associated protein subunit alpha OS=Homo sapiens GN=SSR1 PE=1 SV=3	125	32215	5	9.1	4.39
261	TOM22_HUMAN	Mitochondrial import receptor subunit TOM22 homolog OS=Homo sapiens GN=TOMM22 PE=1 SV=3	124	15512	4	33.8	4.27
262	M2OM_HUMAN	Mitochondrial 2-oxoglutarate/malate carrier protein OS=Homo sapiens GN=SLC25A11 PE=1 SV=3	124	34040	5	12.1	9.92
263	1B46_HUMAN	HLA class I histocompatibility antigen, B-46 alpha chain OS=Homo sapiens GN=HLA-B PE=2 SV=1	124	40415	11	36.7	6.17
264	NDUAC_HUMAN	NADH dehydrogenase [ubiquinone] 1 alpha subcomplex subunit 12 OS=Homo sapiens GN=NDUFA12 PE=1 SV=1	124	17104	5	28.3	9.63
265	MTX1_HUMAN	Metaxin-1 OS=Homo sapiens GN=MTX1 PE=1 SV=2	123	51445	7	11.8	9.8
266	RL11_HUMAN	60S ribosomal protein L11 OS=Homo sapiens GN=RPL11 PE=1 SV=2	122	20240	7	26.4	9.64
267	RS7_HUMAN	40S ribosomal protein S7 OS=Homo sapiens GN=RPS7 PE=1 SV=1	122	22113	7	26.3	10.09
268	RB11A_HUMAN	Ras-related protein Rab-11A OS=Homo sapiens GN=RAB11A PE=1 SV=3	122	24378	10	41.2	6.12
269	H4_HUMAN	Histone H4 OS=Homo sapiens GN=HIST1H4A PE=1 SV=2	122	11360	5	40.8	11.36
270	CD63_HUMAN	CD63 antigen OS=Homo sapiens GN=CD63 PE=1 SV=2	121	25619	6	5	8.14
271	1433B_HUMAN	14-3-3 protein beta/alpha OS=Homo sapiens GN=YWHAB PE=1 SV=3	120	28065	7	25.6	4.76
272	AMPL_HUMAN	Cytosol aminopeptidase OS=Homo sapiens GN=LAP3 PE=1 SV=3	120	56131	8	16.8	8.03
273	DJB11_HUMAN	DnaJ homolog subfamily B member 11 OS=Homo sapiens GN=DNAJB11 PE=1 SV=1	119	40489	9	27.4	5.81
274	RL10A_HUMAN	60S ribosomal protein L10a OS=Homo sapiens GN=RPL10A PE=1 SV=2	119	24816	6	25.3	9.94
275	ESYT1_HUMAN	Extended synaptotagmin-1 OS=Homo sapiens GN=ESYT1 PE=1 SV=1	119	122780	12	13.2	5.57
276	P4HA1_HUMAN	Prolyl 4-hydroxylase subunit alpha-1 OS=Homo sapiens GN=P4HA1 PE=1 SV=2	118	61011	15	19.9	5.7
277	AIFM1_HUMAN	Apoptosis-inducing factor 1, mitochondrial OS=Homo sapiens GN=AIFM1 PE=1 SV=1	118	66859	14	13.9	9.04
278	ALDOA_HUMAN	Fructose-bisphosphate aldolase A OS=Homo sapiens GN=ALDOA PE=1 SV=2	117	39395	10	19.2	8.3
279	NDUA7_HUMAN	NADH dehydrogenase [ubiquinone] 1 alpha subcomplex subunit 7 OS=Homo sapiens GN=NDUFA7 PE=1 SV=3	117	12544	6	49.6	10.19
280	RS12_HUMAN	40S ribosomal protein S12 OS=Homo sapiens GN=RPS12 PE=1 SV=3	116	14505	2	7.6	6.81

prot_hit_nı	prot_acc	prot_desc	prot_score	prot_mass	prot_matches	prot_cover	prot_pi
281	MMAB_HUMAN	Cob(I)yrinic acid a,c-diamide adenosyltransferase, mitochondrial OS=Homo sapiens GN=MMAB PE=1 SV=1	116	27371	6	18.8	8.86
282	SUCA_HUMAN	Succinyl-CoA ligase [ADP/GDP-forming] subunit alpha, mitochondrial OS=Homo sapiens GN=SUCLG1 PE=1 S	116	36227	5	12.1	9.01
283	SUMF2_HUMAN	Sulfatase-modifying factor 2 OS=Homo sapiens GN=SUMF2 PE=1 SV=2	116	33822	6	21.9	7.78
284	AT1A1_HUMAN	Sodium/potassium-transporting ATPase subunit alpha-1 OS=Homo sapiens GN=ATP1A1 PE=1 SV=1	115	112824	18	23	5.33
285	RRAS_HUMAN	Ras-related protein R-Ras OS=Homo sapiens GN=RRAS PE=1 SV=1	115	23466	6	24.8	6.43
286	GPDM_HUMAN	Glycerol-3-phosphate dehydrogenase, mitochondrial OS=Homo sapiens GN=GPD2 PE=1 SV=3	114	80802	13	15.4	7.57
287	TXD12_HUMAN	Thioredoxin domain-containing protein 12 OS=Homo sapiens GN=TXNDC12 PE=1 SV=1	114	19194	6	34.9	5.24
288	IF5A1_HUMAN	Eukaryotic translation initiation factor 5A-1 OS=Homo sapiens GN=EIF5A PE=1 SV=2	114	16821	1	7.8	5.08
289	RM23_HUMAN	39S ribosomal protein L23, mitochondrial OS=Homo sapiens GN=MRPL23 PE=1 SV=1	113	17770	4	21.6	9.69
290	RS24_HUMAN	40S ribosomal protein S24 OS=Homo sapiens GN=RPS24 PE=1 SV=1	112	15413	2	17.3	10.79
291	GDIR1_HUMAN	Rho GDP-dissociation inhibitor 1 OS=Homo sapiens GN=ARHGDIA PE=1 SV=3	112	23193	6	24	5.02
292	1B57_HUMAN	HLA class I histocompatibility antigen, B-57 alpha chain OS=Homo sapiens GN=HLA-B PE=1 SV=1	112	40199	8	26	5.89
293	H2AX_HUMAN	Histone H2A.x OS=Homo sapiens GN=H2AFX PE=1 SV=2	111	15135	4	25.9	10.74
294	SYJ2B_HUMAN	Synaptojanin-2-binding protein OS=Homo sapiens GN=SYNJ2BP PE=1 SV=2	111	15918	3	22.1	5.87
295	6PGD_HUMAN	6-phosphogluconate dehydrogenase, decarboxylating OS=Homo sapiens GN=PGD PE=1 SV=3	111	53106	5	14.1	6.8
296	PLOD2_HUMAN	Procollagen-lysine,2-oxoglutarate 5-dioxygenase 2 OS=Homo sapiens GN=PLOD2 PE=1 SV=2	111	84632	9	8.5	6.24
297	CHP1_HUMAN	Calcineurin B homologous protein 1 OS=Homo sapiens GN=CHP1 PE=1 SV=3	110	22442	3	19.5	4.98
298	UCRI_HUMAN	Cytochrome b-c1 complex subunit Rieske, mitochondrial OS=Homo sapiens GN=UQCRFS1 PE=1 SV=2	110	29649	6	20.4	8.55
299	DPP2_HUMAN	Dipeptidyl peptidase 2 OS=Homo sapiens GN=DPP7 PE=1 SV=3	109	54307	8	16.5	5.91
300	ATPK_HUMAN	ATP synthase subunit f, mitochondrial OS=Homo sapiens GN=ATP5J2 PE=1 SV=3	109	10911	5	47.9	9.7
301	CAH2_HUMAN	Carbonic anhydrase 2 OS=Homo sapiens GN=CA2 PE=1 SV=2	109	29228	6	11.5	6.87
302	AL9A1_HUMAN	4-trimethylaminobutyraldehyde dehydrogenase OS=Homo sapiens GN=ALDH9A1 PE=1 SV=3	108	53767	4	10.9	5.69
303	PRDX1_HUMAN	Peroxiredoxin-1 OS=Homo sapiens GN=PRDX1 PE=1 SV=1	108	22096	7	21.1	8.27
304	1C16_HUMAN	HLA class I histocompatibility antigen, Cw-16 alpha chain OS=Homo sapiens GN=HLA-C PE=2 SV=1	108	40727	7	26.8	6.09
305	KAD3_HUMAN	GTP:AMP phosphotransferase, mitochondrial OS=Homo sapiens GN=AK3 PE=1 SV=4	107	25550	8	33.9	9.15
306	SSBP_HUMAN	Single-stranded DNA-binding protein, mitochondrial OS=Homo sapiens GN=SSBP1 PE=1 SV=1	107	17249	9	62.2	9.59
307	RL31_HUMAN	60S ribosomal protein L31 OS=Homo sapiens GN=RPL31 PE=1 SV=1	106	14454	6	31.2	10.54
308	RS15_HUMAN	40S ribosomal protein S15 OS=Homo sapiens GN=RPS15 PE=1 SV=2	104	17029	7	24.1	10.39
309	RS5_HUMAN	40S ribosomal protein S5 OS=Homo sapiens GN=RPS5 PE=1 SV=4	104	22862	8	32.8	9.73
310	GBB1_HUMAN	Guanine nucleotide-binding protein G(I)/G(S)/G(T) subunit beta-1 OS=Homo sapiens GN=GNB1 PE=1 SV=3	103	37353	7	17.9	5.6
311	ODPA_HUMAN	Pyruvate dehydrogenase E1 component subunit alpha, somatic form, mitochondrial OS=Homo sapiens GN=P	103	43268	10	21.8	8.35
312	K2C4_HUMAN	Keratin, type II cytoskeletal 4 OS=Homo sapiens GN=KRT4 PE=1 SV=4	102	57250	11	14.6	6.25
313	C1QBP_HUMAN	Complement component 1 Q subcomponent-binding protein, mitochondrial OS=Homo sapiens GN=C1QBP PE=1	102	31343	6	37.6	4.74
314	BCAT2_HUMAN	Branched-chain-amino-acid aminotransferase, mitochondrial OS=Homo sapiens GN=BCAT2 PE=1 SV=2	102	44259	5	10.5	8.88
315	PTCD3_HUMAN	Pentatricopeptide repeat-containing protein 3, mitochondrial OS=Homo sapiens GN=PTCD3 PE=1 SV=3	102	78500	10	18.4	6
316	GT251_HUMAN	Procollagen galactosyltransferase 1 OS=Homo sapiens GN=GLT25D1 PE=1 SV=1	101	71590	11	15.6	6.85
317	RT07_HUMAN	28S ribosomal protein S7, mitochondrial OS=Homo sapiens GN=MRPS7 PE=1 SV=2	101	28116	7	24	10
318	LAMP2_HUMAN	Lysosome-associated membrane glycoprotein 2 OS=Homo sapiens GN=LAMP2 PE=1 SV=2	101	44932	5	7.1	5.35
319	PRDX5_HUMAN	Peroxiredoxin-5, mitochondrial OS=Homo sapiens GN=PRDX5 PE=1 SV=4	101	22073	6	28.5	8.93
320	RS2_HUMAN	40S ribosomal protein S2 OS=Homo sapiens GN=RPS2 PE=1 SV=2	101	31305	8	21.5	10.25
321	SPB6_HUMAN	Serpin B6 OS=Homo sapiens GN=SERPINB6 PE=1 SV=3	100	42594	3	9.6	5.18
322	HS90A_HUMAN	Heat shock protein HSP 90-alpha OS=Homo sapiens GN=HSP90AA1 PE=1 SV=5	100	84607	14	17.3	4.94
323	ETFD_HUMAN	Electron transfer flavoprotein-ubiquinone oxidoreductase, mitochondrial OS=Homo sapiens GN=ETFDH PE	100	68452	6	11.2	7.31
324	P5CS_HUMAN	Delta-1-pyrroline-5-carboxylate synthase OS=Homo sapiens GN=ALDH18A1 PE=1 SV=2	100	87248	10	12.5	6.66
325	RL13A_HUMAN	60S ribosomal protein L13a OS=Homo sapiens GN=RPL13A PE=1 SV=2	100	23562	8	31.5	10.94
326	TXTP_HUMAN	Tricarboxylate transport protein, mitochondrial OS=Homo sapiens GN=SLC25A1 PE=1 SV=2	99	33991	10	23.5	9.91
327	RS23_HUMAN	40S ribosomal protein S23 OS=Homo sapiens GN=RPS23 PE=1 SV=3	99	15798	6	30.1	10.5
328	CO1A2_HUMAN	Collagen alpha-2(I) chain OS=Homo sapiens GN=COL1A2 PE=1 SV=7	98	129235	9	7.8	9.08
329	RL28_HUMAN	60S ribosomal protein L28 OS=Homo sapiens GN=RPL28 PE=1 SV=3	98	15738	10	35	12.02
330	PPT1_HUMAN	Palmitoyl-protein thioesterase 1 OS=Homo sapiens GN=PPT1 PE=1 SV=1	97	34171	7	22.9	6.07
331	GBB2_HUMAN	Guanine nucleotide-binding protein G(I)/G(S)/G(T) subunit beta-2 OS=Homo sapiens GN=GNB2 PE=1 SV=3	97	37307	4	13.2	5.6
332	NDUB6_HUMAN	NADH dehydrogenase [ubiquinone] 1 beta subcomplex subunit 6 OS=Homo sapiens GN=NDUFB6 PE=1 SV=3	97	15479	4	25.8	9.63
333	GPNMB_HUMAN	Transmembrane glycoprotein NMB OS=Homo sapiens GN=GPNMB PE=1 SV=2	96	63882	6	6.5	6.17
334	LMAN2_HUMAN	Vesicular integral-membrane protein VIP36 OS=Homo sapiens GN=LMAN2 PE=1 SV=1	95	40203	7	25.6	6.46
335	IDH3B_HUMAN	Isocitrate dehydrogenase [NAD] subunit beta, mitochondrial OS=Homo sapiens GN=IDH3B PE=1 SV=2	95	42157	4	14.8	8.64
336	4F2_HUMAN	4F2 cell-surface antigen heavy chain OS=Homo sapiens GN=SLC3A2 PE=1 SV=3	95	67952	4	8.1	4.89
337	AT2A2_HUMAN	Sarcoplasmic/endoplasmic reticulum calcium ATPase 2 OS=Homo sapiens GN=ATP2A2 PE=1 SV=1	94	114683	7	7.3	5.23
338	RL27_HUMAN	60S ribosomal protein L27 OS=Homo sapiens GN=RPL27 PE=1 SV=2	94	15788	9	55.1	10.56
339	RL27A_HUMAN	60S ribosomal protein L27a OS=Homo sapiens GN=RPL27A PE=1 SV=2	94	16551	8	30.4	11
340	SYIM_HUMAN	Isoleucine--tRNA ligase, mitochondrial OS=Homo sapiens GN=IARS2 PE=1 SV=2	92	113719	7	7.3	6.78
341	CAZA1_HUMAN	F-actin-capping protein subunit alpha-1 OS=Homo sapiens GN=CAPZA1 PE=1 SV=3	92	32902	3	15	5.45
342	PCP_HUMAN	Lysosomal Pro-X carboxypeptidase OS=Homo sapiens GN=PRCP PE=1 SV=1	92	55764	6	10.9	6.75
343	RS3_HUMAN	40S ribosomal protein S3 OS=Homo sapiens GN=RPS3 PE=1 SV=2	91	26671	12	36.2	9.68
344	TMEDA_HUMAN	Transmembrane emp24 domain-containing protein 10 OS=Homo sapiens GN=TMED10 PE=1 SV=2	91	24960	6	35.6	6.97
345	RDH11_HUMAN	Retinol dehydrogenase 11 OS=Homo sapiens GN=RDH11 PE=1 SV=2	90	35363	4	14.8	9.05
346	RL24_HUMAN	60S ribosomal protein L24 OS=Homo sapiens GN=RPL24 PE=1 SV=1	90	17768	9	30.6	11.26
347	SYCM_HUMAN	Probable cysteine--tRNA ligase, mitochondrial OS=Homo sapiens GN=CARS2 PE=1 SV=1	90	62185	5	12.6	8.58
348	APMAP_HUMAN	Adipocyte plasma membrane-associated protein OS=Homo sapiens GN=APMAP PE=1 SV=2	89	46451	6	15.9	5.82
349	RL18_HUMAN	60S ribosomal protein L18 OS=Homo sapiens GN=RPL18 PE=1 SV=2	89	21621	6	31.4	11.73
350	ECI1_HUMAN	Enoyl-CoA delta isomerase 1, mitochondrial OS=Homo sapiens GN=ECI1 PE=1 SV=1	89	32795	5	15.2	8.8
351	GNAI2_HUMAN	Guanine nucleotide-binding protein G(i) subunit alpha-2 OS=Homo sapiens GN=GNAI2 PE=1 SV=3	88	40425	3	10.4	5.34
352	RLA1_HUMAN	60S acidic ribosomal protein P1 OS=Homo sapiens GN=RPLP1 PE=1 SV=1	88	11507	3	14	4.26
353	GNA11_HUMAN	Guanine nucleotide-binding protein subunit alpha-11 OS=Homo sapiens GN=GNA11 PE=1 SV=2	88	42097	3	10	5.51
354	MOGS_HUMAN	Mannosyl-oligosaccharide glucosidase OS=Homo sapiens GN=MOGS PE=1 SV=5	88	91861	7	11.2	8.97
355	ACSL1_HUMAN	Long-chain-fatty-acid--CoA ligase 1 OS=Homo sapiens GN=ACSL1 PE=1 SV=1	88	77893	7	10.7	6.81
356	GALT2_HUMAN	Polypeptide N-acetylgalactosaminyltransferase 2 OS=Homo sapiens GN=GALNT2 PE=1 SV=1	87	64691	6	9.1	8.63
357	CUTA_HUMAN	Protein CutA OS=Homo sapiens GN=CUTA PE=1 SV=2	87	19104	1	7.8	5.42
358	1433E_HUMAN	14-3-3 protein epsilon OS=Homo sapiens GN=YWHAE PE=1 SV=1	86	29155	3	15.3	4.63
359	HNRPK_HUMAN	Heterogeneous nuclear ribonucleoprotein K OS=Homo sapiens GN=HNRNPK PE=1 SV=1	86	50944	6	12.3	5.39
360	PGK2_HUMAN	Phosphoglycerate kinase 2 OS=Homo sapiens GN=PGK2 PE=1 SV=3	86	44767	5	11.3	8.74
361	TERA_HUMAN	Transitional endoplasmic reticulum ATPase OS=Homo sapiens GN=VCP PE=1 SV=4	86	89266	10	17.1	5.14
362	5NTD_HUMAN	5'-nucleotidase OS=Homo sapiens GN=NT5E PE=1 SV=1	86	63327	8	11.8	6.58
363	NIPS1_HUMAN	Protein NipSnap homolog 1 OS=Homo sapiens GN=NIPSNAP1 PE=1 SV=1	85	33289	8	20.4	9.35
364	RL23_HUMAN	60S ribosomal protein L23 OS=Homo sapiens GN=RPL23 PE=1 SV=1	85	14856	3	7.1	10.51
365	ATPO_HUMAN	ATP synthase subunit O, mitochondrial OS=Homo sapiens GN=ATP5O PE=1 SV=1	85	23263	6	38.5	9.97
366	DAD1_HUMAN	Dolichyl-diphosphooligosaccharide--protein glycosyltransferase subunit DAD1 OS=Homo sapiens GN=DAD1	84	12489	2	19.5	6.52
367	LAMC1_HUMAN	Laminin subunit gamma-1 OS=Homo sapiens GN=LAMC1 PE=1 SV=3	84	177489	13	7.8	5.01
368	NDUS2_HUMAN	NADH dehydrogenase [ubiquinone] iron-sulfur protein 2, mitochondrial OS=Homo sapiens GN=NDUFS2 PE=1	84	52512	8	20.7	7.21
369	SYFA_HUMAN	Phenylalanine--tRNA ligase alpha subunit OS=Homo sapiens GN=FARSA PE=1 SV=3	83	57528	1	2.2	7.31
370	GSTK1_HUMAN	Glutathione S-transferase kappa 1 OS=Homo sapiens GN=GSTK1 PE=1 SV=3	83	25480	5	27.4	8.5
371	COX20_HUMAN	Cytochrome c oxidase protein 20 homolog OS=Homo sapiens GN=COX20 PE=1 SV=2	83	13283	4	22.9	9
372	RALA_HUMAN	Ras-related protein Ral-A OS=Homo sapiens GN=RALA PE=1 SV=1	83	23552	4	19.9	6.66
373	RS4X_HUMAN	40S ribosomal protein S4, X isoform OS=Homo sapiens GN=RPS4X PE=1 SV=2	83	29579	5	16.7	10.16

prot_hit_nı	prot_acc	prot_desc	prot_score	prot_mass	prot_matches	prot_cover	prot_pi
374	AL7A1_HUMAN	Alpha-aminoadipic semialdehyde dehydrogenase OS=Homo sapiens GN=ALDH7A1 PE=1 SV=5	83	58450	8	11.9	8.21
375	STX4_HUMAN	Syntaxin-4 OS=Homo sapiens GN=STX4 PE=1 SV=2	82	34159	1	6.4	5.92
376	HNRH1_HUMAN	Heterogeneous nuclear ribonucleoprotein H OS=Homo sapiens GN=HNRNPH1 PE=1 SV=4	82	49198	4	7.6	5.89
377	1433F_HUMAN	14-3-3 protein eta OS=Homo sapiens GN=YWHAH PE=1 SV=4	82	28201	6	22.4	4.76
378	CATA_HUMAN	Catalase OS=Homo sapiens GN=CAT PE=1 SV=3	81	59719	10	24.1	6.9
379	PLOD1_HUMAN	Procollagen-lysine,2-oxoglutarate 5-dioxygenase 1 OS=Homo sapiens GN=PLOD1 PE=1 SV=2	81	83497	7	10.9	6.47
380	RAB5C_HUMAN	Ras-related protein Rab-5C OS=Homo sapiens GN=RAB5C PE=1 SV=2	81	23468	6	24.1	8.64
381	GNAS2_HUMAN	Guanine nucleotide-binding protein G(s) subunit alpha isoforms short OS=Homo sapiens GN=GNAS PE=1 S	81	45636	9	13.7	5.59
382	VPS35_HUMAN	Vacuolar protein sorting-associated protein 35 OS=Homo sapiens GN=VPS35 PE=1 SV=2	81	91649	4	6.8	5.32
383	RL26L_HUMAN	60S ribosomal protein L26-like 1 OS=Homo sapiens GN=RPL26L1 PE=1 SV=1	80	17246	10	49	10.55
384	SE1L1_HUMAN	Protein sel-1 homolog 1 OS=Homo sapiens GN=SEL1L PE=1 SV=3	80	88698	6	6.5	5.23
385	PLOD3_HUMAN	Procollagen-lysine,2-oxoglutarate 5-dioxygenase 3 OS=Homo sapiens GN=PLOD3 PE=1 SV=1	80	84731	8	9.1	5.69
386	NCPR_HUMAN	NADPH--cytochrome P450 reductase OS=Homo sapiens GN=POR PE=1 SV=2	80	76641	13	17.6	5.38
387	TPBG_HUMAN	Trophoblast glycoprotein OS=Homo sapiens GN=TPBG PE=1 SV=1	80	46003	6	12.6	6.35
388	ERLN1_HUMAN	Erlin-1 OS=Homo sapiens GN=ERLIN1 PE=1 SV=1	80	38901	3	10.7	7.67
389	PIGS_HUMAN	GPI transamidase component PIG-S OS=Homo sapiens GN=PIGS PE=1 SV=3	79	61617	5	9.2	6.05
390	VAPB_HUMAN	Vesicle-associated membrane protein-associated protein B/C OS=Homo sapiens GN=VAPB PE=1 SV=3	79	27211	12	32.9	6.85
391	LDHA_HUMAN	L-lactate dehydrogenase A chain OS=Homo sapiens GN=LDHA PE=1 SV=2	79	36665	4	14.5	8.44
392	HIBCH_HUMAN	3-hydroxyisobutyryl-CoA hydrolase, mitochondrial OS=Homo sapiens GN=HIBCH PE=1 SV=2	78	43454	10	17.1	8.38
393	PGH1_HUMAN	Prostaglandin G/H synthase 1 OS=Homo sapiens GN=PTGS1 PE=1 SV=2	78	68642	6	12.2	6.81
394	AFG32_HUMAN	AFG3-like protein 2 OS=Homo sapiens GN=AFG3L2 PE=1 SV=2	78	88528	11	15.9	8.81
395	HSPB1_HUMAN	Heat shock protein beta-1 OS=Homo sapiens GN=HSPB1 PE=1 SV=2	77	22768	4	27.3	5.98
396	TBCA_HUMAN	Tubulin-specific chaperone A OS=Homo sapiens GN=TBCA PE=1 SV=3	77	12847	3	42.6	5.25
397	VDAC3_HUMAN	Voltage-dependent anion-selective channel protein 3 OS=Homo sapiens GN=VDAC3 PE=1 SV=1	77	30639	3	18.7	8.85
398	CPT2_HUMAN	Carnitine O-palmitoyltransferase 2, mitochondrial OS=Homo sapiens GN=CPT2 PE=1 SV=2	77	73730	8	12.8	8.38
399	HYOU1_HUMAN	Hypoxia up-regulated protein 1 OS=Homo sapiens GN=HYOU1 PE=1 SV=1	77	111266	10	7.7	5.16
400	TRAP1_HUMAN	Heat shock protein 75 kDa, mitochondrial OS=Homo sapiens GN=TRAP1 PE=1 SV=3	76	80060	14	18.9	8.3
401	CATZ_HUMAN	Cathepsin Z OS=Homo sapiens GN=CTSZ PE=1 SV=1	76	33846	6	15.2	6.7
402	HSDL2_HUMAN	Hydroxysteroid dehydrogenase-like protein 2 OS=Homo sapiens GN=HSDL2 PE=1 SV=1	76	45366	9	17.7	8.07
403	ODP2_HUMAN	Dihydrolipoyllysine-residue acetyltransferase component of pyruvate dehydrogenase complex, mitochon	76	68953	9	13	7.96
404	GLCM_HUMAN	Glucosylceramidase OS=Homo sapiens GN=GBA PE=1 SV=3	76	59678	6	6.9	7.29
405	DHB12_HUMAN	Estradiol 17-beta-dehydrogenase 12 OS=Homo sapiens GN=HSD17B12 PE=1 SV=2	76	34302	6	13.1	9.34
406	ACADM_HUMAN	Medium-chain specific acyl-CoA dehydrogenase, mitochondrial OS=Homo sapiens GN=ACADM PE=1 SV=1	75	46559	6	19.5	8.61
407	QCR8_HUMAN	Cytochrome b-c1 complex subunit 8 OS=Homo sapiens GN=UQCRQ PE=1 SV=4	75	9900	6	59.8	10.07
408	DLDH_HUMAN	Dihydrolipoyl dehydrogenase, mitochondrial OS=Homo sapiens GN=DLD PE=1 SV=2	74	54143	5	6.9	7.95
409	RS29_HUMAN	40S ribosomal protein S29 OS=Homo sapiens GN=RPS29 PE=1 SV=2	74	6672	2	32.1	10.17
410	AT1A2_HUMAN	Sodium/potassium-transporting ATPase subunit alpha-2 OS=Homo sapiens GN=ATP1A2 PE=1 SV=1	74	112193	8	12.5	5.47
411	H2AV_HUMAN	Histone H2A.V OS=Homo sapiens GN=H2AFV PE=1 SV=3	74	13501	3	15.6	10.58
412	RAB10_HUMAN	Ras-related protein Rab-10 OS=Homo sapiens GN=RAB10 PE=1 SV=1	74	22527	5	24.5	8.59
413	RAB6A_HUMAN	Ras-related protein Rab-6A OS=Homo sapiens GN=RAB6A PE=1 SV=3	74	23578	6	21.6	5.42
414	RB39B_HUMAN	Ras-related protein Rab-39B OS=Homo sapiens GN=RAB39B PE=1 SV=1	74	24607	5	11.7	7.7
415	RB43L_HUMAN	Putative Rab-43-like protein ENSP00000330714 OS=Homo sapiens PE=5 SV=3	74	20197	3	9.4	6.1
416	RAB8A_HUMAN	Ras-related protein Rab-8A OS=Homo sapiens GN=RAB8A PE=1 SV=1	74	23653	4	13.5	9.15
417	RB39A_HUMAN	Ras-related protein Rab-39A OS=Homo sapiens GN=RAB39A PE=2 SV=2	74	24991	3	11.5	7.57
418	ITAV_HUMAN	Integrin alpha-V OS=Homo sapiens GN=ITGAV PE=1 SV=2	73	115964	21	15.6	5.45
419	MYO1C_HUMAN	Unconventional myosin-Ic OS=Homo sapiens GN=MYO1C PE=1 SV=4	73	121606	18	13.1	9.46
420	CO6A1_HUMAN	Collagen alpha-1(VI) chain OS=Homo sapiens GN=COL6A1 PE=1 SV=3	73	108462	18	11.1	5.26
421	NDUS5_HUMAN	NADH dehydrogenase [ubiquinone] iron-sulfur protein 5 OS=Homo sapiens GN=NDUFS5 PE=1 SV=3	72	12509	4	34.9	9.27
422	NPTN_HUMAN	Neuroplastin OS=Homo sapiens GN=NPTN PE=1 SV=2	72	44360	2	6.8	8.11
423	CS010_HUMAN	UPF0556 protein C19orf10 OS=Homo sapiens GN=C19orf10 PE=1 SV=1	72	18783	3	23.1	6.2
424	SDF2_HUMAN	Stromal cell-derived factor 2 OS=Homo sapiens GN=SDF2 PE=1 SV=2	72	23011	4	28	6.83
425	RS21_HUMAN	40S ribosomal protein S21 OS=Homo sapiens GN=RPS21 PE=1 SV=1	72	9106	4	51.8	8.68
426	BAP31_HUMAN	B-cell receptor-associated protein 31 OS=Homo sapiens GN=BCAP31 PE=1 SV=3	71	27974	3	13.8	8.44
427	SYSM_HUMAN	Serine--tRNA ligase, mitochondrial OS=Homo sapiens GN=SARS2 PE=1 SV=1	71	58246	8	12.4	8.35
428	NPS3A_HUMAN	Protein NipSnap homolog 3A OS=Homo sapiens GN=NIPSNAP3A PE=1 SV=2	71	28449	9	20.2	9.21
429	MGST1_HUMAN	Microsomal glutathione S-transferase 1 OS=Homo sapiens GN=MGST1 PE=1 SV=1	71	17587	3	18.1	9.41
430	DDAH1_HUMAN	N(G),N(G)-dimethylarginine dimethylaminohydrolase 1 OS=Homo sapiens GN=DDAH1 PE=1 SV=3	71	31102	4	16.1	5.53
431	MIMIT_HUMAN	Mimitin, mitochondrial OS=Homo sapiens GN=NDUFAF2 PE=1 SV=1	71	19844	3	23.1	8.94
432	RM15_HUMAN	39S ribosomal protein L15, mitochondrial OS=Homo sapiens GN=MRPL15 PE=1 SV=1	71	33399	6	18.2	10.02
433	ITB1_HUMAN	Integrin beta-1 OS=Homo sapiens GN=ITGB1 PE=1 SV=2	71	88357	9	13.9	5.27
434	RALB_HUMAN	Ras-related protein Ral-B OS=Homo sapiens GN=RALB PE=1 SV=1	70	23394	6	27.7	6.24
435	1433T_HUMAN	14-3-3 protein theta OS=Homo sapiens GN=YWHAQ PE=1 SV=1	70	27747	9	35.9	4.68
436	SC61G_HUMAN	Protein transport protein Sec61 subunit gamma OS=Homo sapiens GN=SEC61G PE=2 SV=1	70	7736	3	44.1	10.01
437	BGAL_HUMAN	Beta-galactosidase OS=Homo sapiens GN=GLB1 PE=1 SV=2	69	76027	5	5.6	6.1
438	ERLN2_HUMAN	Erlin-2 OS=Homo sapiens GN=ERLIN2 PE=1 SV=1	69	37815	4	10.3	5.47
439	UBA1_HUMAN	Ubiquitin-like modifier-activating enzyme 1 OS=Homo sapiens GN=UBA1 PE=1 SV=3	69	117774	7	7.8	5.49
440	TOR1A_HUMAN	Torsin-1A OS=Homo sapiens GN=TOR1A PE=1 SV=1	69	37784	2	5.4	6.51
441	ODO2_HUMAN	Dihydrolipoyllysine-residue succinyltransferase component of 2-oxoglutarate dehydrogenase complex,	68	48724	10	19.4	9.11
442	CX6B1_HUMAN	Cytochrome c oxidase subunit 6B1 OS=Homo sapiens GN=COX6B1 PE=1 SV=2	68	10186	6	45.3	6.54
443	RM30_HUMAN	39S ribosomal protein L30, mitochondrial OS=Homo sapiens GN=MRPL30 PE=1 SV=1	68	18534	2	16.8	10.01
444	LYRIC_HUMAN	Protein LYRIC OS=Homo sapiens GN=MTDH PE=1 SV=2	68	63799	4	6	9.33
445	PREP_HUMAN	Presequence protease, mitochondrial OS=Homo sapiens GN=PITRM1 PE=1 SV=2	68	117380	19	16.7	6.5
446	ISOC2_HUMAN	Isochorismatase domain-containing protein 2, mitochondrial OS=Homo sapiens GN=ISOC2 PE=1 SV=1	67	22323	3	18.5	7.67
447	NDUS8_HUMAN	NADH dehydrogenase [ubiquinone] iron-sulfur protein 8, mitochondrial OS=Homo sapiens GN=NDUFS8 PE=1	67	23690	4	16.2	6
448	MAP1B_HUMAN	Microtubule-associated protein 1B OS=Homo sapiens GN=MAP1B PE=1 SV=2	66	270468	21	10.2	4.73
449	QCR9_HUMAN	Cytochrome b-c1 complex subunit 9 OS=Homo sapiens GN=UQCR10 PE=1 SV=3	66	7304	1	27	9.45
450	RS26L_HUMAN	Putative 40S ribosomal protein S26-like 1 OS=Homo sapiens GN=RPS26P11 PE=5 SV=1	66	12994	8	64.3	10.55
451	ACOT9_HUMAN	Acyl-coenzyme A thioesterase 9, mitochondrial OS=Homo sapiens GN=ACOT9 PE=1 SV=2	66	49870	6	16.6	8.81
452	HXK1_HUMAN	Hexokinase-1 OS=Homo sapiens GN=HK1 PE=1 SV=3	66	102420	14	18.9	6.36
453	NAGAB_HUMAN	Alpha-N-acetylgalactosaminidase OS=Homo sapiens GN=NAGA PE=1 SV=2	66	46534	1	2.7	4.98
454	MPPB_HUMAN	Mitochondrial-processing peptidase subunit beta OS=Homo sapiens GN=PMPCB PE=1 SV=2	66	54331	7	18	6.38
455	DBLOH_HUMAN	Diablo homolog, mitochondrial OS=Homo sapiens GN=DIABLO PE=1 SV=1	66	27114	4	11.3	5.68
456	VINC_HUMAN	Vinculin OS=Homo sapiens GN=VCL PE=1 SV=4	65	123722	13	11.4	5.5
457	RL36L_HUMAN	60S ribosomal protein L36a-like OS=Homo sapiens GN=RPL36AL PE=1 SV=3	65	12461	10	48.1	10.67
458	ATP5J_HUMAN	ATP synthase-coupling factor 6, mitochondrial OS=Homo sapiens GN=ATP5J PE=1 SV=1	64	12580	2	23.1	9.52
459	PPIF_HUMAN	Peptidyl-prolyl cis-trans isomerase F, mitochondrial OS=Homo sapiens GN=PPIF PE=1 SV=1	64	22026	4	11.1	9.48
460	TM173_HUMAN	Transmembrane protein 173 OS=Homo sapiens GN=TMEM173 PE=1 SV=1	64	42166	6	10.3	6.6
461	CRTAP_HUMAN	Cartilage-associated protein OS=Homo sapiens GN=CRTAP PE=1 SV=1	64	46532	8	11.5	5.5
462	RL17_HUMAN	60S ribosomal protein L17 OS=Homo sapiens GN=RPL17 PE=1 SV=3	63	21383	5	32.6	10.18
463	RT11_HUMAN	28S ribosomal protein S11, mitochondrial OS=Homo sapiens GN=MRPS11 PE=1 SV=2	63	20603	4	23.7	10.82
464	LMAN1_HUMAN	Protein ERGIC-53 OS=Homo sapiens GN=LMAN1 PE=1 SV=2	63	57513	8	16.5	6.3
465	SAM50_HUMAN	Sorting and assembly machinery component 50 homolog OS=Homo sapiens GN=SAMM50 PE=1 SV=3	62	51943	4	9.6	6.44
466	AMRP_HUMAN	Alpha-2-macroglobulin receptor-associated protein OS=Homo sapiens GN=LRPAP1 PE=1 SV=1	62	41441	5	13.4	8.73

prot_hit_nı	prot_acc	prot_desc	prot_score	prot_mass	prot_matches	prot_cover	prot_pi
467	COX5A_HUMAN	Cytochrome c oxidase subunit 5A, mitochondrial OS=Homo sapiens GN=COX5A PE=1 SV=2	62	16752	5	33.3	6.3
468	FKBP2_HUMAN	Peptidyl-prolyl cis-trans isomerase FKBP2 OS=Homo sapiens GN=FKBP2 PE=1 SV=2	62	15639	4	14.1	9.24
469	RAC3_HUMAN	Ras-related C3 botulinum toxin substrate 3 OS=Homo sapiens GN=RAC3 PE=1 SV=1	62	21365	8	15.1	8.43
470	RL36_HUMAN	60S ribosomal protein L36 OS=Homo sapiens GN=RPL36 PE=1 SV=3	62	12246	5	41.9	11.59
471	SPHM_HUMAN	N-sulphoglucosamine sulphohydrolase OS=Homo sapiens GN=SGSH PE=1 SV=1	62	56659	4	9	6.46
472	NDUS6_HUMAN	NADH dehydrogenase [ubiquinone] iron-sulfur protein 6, mitochondrial OS=Homo sapiens GN=NDUFS6 PE=1	62	13703	3	24.2	8.59
473	CACP_HUMAN	Carnitine O-acetyltransferase OS=Homo sapiens GN=CRAT PE=1 SV=5	61	70812	3	6.1	8.63
474	K1C12_HUMAN	Keratin, type I cytoskeletal 12 OS=Homo sapiens GN=KRT12 PE=1 SV=1	61	53478	8	9.3	4.7
475	K1C15_HUMAN	Keratin, type I cytoskeletal 15 OS=Homo sapiens GN=KRT15 PE=1 SV=3	61	49181	6	10.1	4.71
476	MCCB_HUMAN	Methylcrotonoyl-CoA carboxylase beta chain, mitochondrial OS=Homo sapiens GN=MCCC2 PE=1 SV=1	61	61294	10	19.2	7.57
477	NDUA4_HUMAN	NADH dehydrogenase [ubiquinone] 1 alpha subcomplex subunit 4 OS=Homo sapiens GN=NDUFA4 PE=1 SV=1	61	9364	4	46.9	9.42
478	MMP14_HUMAN	Matrix metalloproteinase-14 OS=Homo sapiens GN=MMP14 PE=1 SV=3	61	65852	8	12.5	7.63
479	ES1_HUMAN	ES1 protein homolog, mitochondrial OS=Homo sapiens GN=C21orf33 PE=1 SV=3	60	28153	3	22.8	8.5
480	K2C72_HUMAN	Keratin, type II cytoskeletal 72 OS=Homo sapiens GN=KRT72 PE=1 SV=2	60	55842	11	19.2	6.54
481	S39A7_HUMAN	Zinc transporter SLC39A7 OS=Homo sapiens GN=SLC39A7 PE=1 SV=2	60	50087	3	3	6.36
482	TM109_HUMAN	Transmembrane protein 109 OS=Homo sapiens GN=TMEM109 PE=1 SV=1	60	26194	5	14	10.48
483	DUT_HUMAN	Deoxyuridine 5'-triphosphate nucleotidohydrolase, mitochondrial OS=Homo sapiens GN=DUT PE=1 SV=4	60	26547	3	19	9.46
484	FBLN1_HUMAN	Fibulin-1 OS=Homo sapiens GN=FBLN1 PE=1 SV=4	60	77162	9	10.8	5.07
485	NDUS4_HUMAN	NADH dehydrogenase [ubiquinone] iron-sulfur protein 4, mitochondrial OS=Homo sapiens GN=NDUFS4 PE=1	60	20095	1	6.3	10.3
486	RM04_HUMAN	39S ribosomal protein L4, mitochondrial OS=Homo sapiens GN=MRPL4 PE=1 SV=1	60	34897	6	18.6	9.73

Supplemental table S3: Proteins identified using Protein Pilot 2D-LC

N	Unused	Total	% Cov	Accession #	Name	Species	Peptides(95%)
1	47.51	47.51	30	sp|P35579|MYH9_HU	Myosin-9 OS=Homo sapiens GN=MYH9 PE=1 SV=4	HUMAN	34
2	37.3	37.3	48.2	sp|P11021|GRP78_HU	78 kDa glucose-regulated protein OS=Homo sapiens GN=HSPA5 PE=1 SV=2	HUMAN	27
3	34.49	34.49	22.4	sp|P12111|CO6A3_HU	Collagen alpha-3(VI) chain OS=Homo sapiens GN=COL6A3 PE=1 SV=5	HUMAN	20
4	33.64	33.64	17.4	sp|Q15149|PLEC_HUM	Plectin OS=Homo sapiens GN=PLEC PE=1 SV=3	HUMAN	18
5	32.24	32.24	34.3	sp|P15144|AMPN_HU	Aminopeptidase N OS=Homo sapiens GN=ANPEP PE=1 SV=4	HUMAN	25
6	30.43	30.43	64.1	sp|P06576|ATPB_HUM	ATP synthase subunit beta, mitochondrial OS=Homo sapiens GN=ATP5B PE=1 SV=3	HUMAN	22
7	29.49	29.49	56.9	sp|P08670|VIME_HUM	Vimentin OS=Homo sapiens GN=VIM PE=1 SV=4	HUMAN	25
8	28.35	28.35	52.5	sp|P07355|ANXA2_HU	Annexin A2 OS=Homo sapiens GN=ANXA2 PE=1 SV=2	HUMAN	23
9	28.2	28.2	42	sp|P14625|ENPL_HUM	Endoplasmin OS=Homo sapiens GN=HSP90B1 PE=1 SV=1	HUMAN	16
10	27.04	27.04	53.2	sp|P27797|CALR_HUM	Calreticulin OS=Homo sapiens GN=CALR PE=1 SV=1	HUMAN	21
11	26.86	26.86	38.6	sp|P30101|PDIA3_HU	Protein disulfide-isomerase A3 OS=Homo sapiens GN=PDIA3 PE=1 SV=4	HUMAN	18
12	24.7	24.7	47.2	sp|P07237|PDIA1_HU	Protein disulfide-isomerase OS=Homo sapiens GN=P4HB PE=1 SV=3	HUMAN	23
13	22.86	22.86	48.3	sp|P63261|ACTG_HUM	Actin, cytoplasmic 2 OS=Homo sapiens GN=ACTG1 PE=1 SV=1	HUMAN	25
14	22.41	22.41	22.1	sp|Q14697|GANAB_H	Neutral alpha-glucosidase AB OS=Homo sapiens GN=GANAB PE=1 SV=3	HUMAN	9
15	21.44	21.44	20.3	sp|Q09666|AHNK_HU	Neuroblast differentiation-associated protein AHNAK OS=Homo sapiens GN=AHNAK PE=1 SV=2	HUMAN	10
16	20.63	24.49	18.4	sp|P35580|MYH10_H	Myosin-10 OS=Homo sapiens GN=MYH10 PE=1 SV=3	HUMAN	13
17	20.31	20.31	32.4	sp|P38646|GRP75_HU	Stress-70 protein, mitochondrial OS=Homo sapiens GN=HSPA9 PE=1 SV=2	HUMAN	15
18	17.59	17.59	15.7	sp|Q9NZM1|MYOF_H	Myoferlin OS=Homo sapiens GN=MYOF PE=1 SV=1	HUMAN	8
19	17.11	17.11	13.5	sp|P21333|FLNA_HUM	Filamin-A OS=Homo sapiens GN=FLNA PE=1 SV=4	HUMAN	9
20	16.92	16.92	42.1	sp|P25705|ATPA_HUM	ATP synthase subunit alpha, mitochondrial OS=Homo sapiens GN=ATP5A1 PE=1 SV=1	HUMAN	18
21	16.35	16.35	29.6	sp|P00367|DHE3_HUM	Glutamate dehydrogenase 1, mitochondrial OS=Homo sapiens GN=GLUD1 PE=1 SV=2	HUMAN	10
22	16.03	16.03	45.4	sp|P10809|CH60_HUM	60 kDa heat shock protein, mitochondrial OS=Homo sapiens GN=HSPD1 PE=1 SV=2	HUMAN	13
23	15.92	15.92	30.9	sp|P40939|ECHA_HUM	Trifunctional enzyme subunit alpha, mitochondrial OS=Homo sapiens GN=HADHA PE=1 SV=2	HUMAN	11
24	15.51	15.51	30.2	sp|P27824|CALX_HUM	Calnexin OS=Homo sapiens GN=CANX PE=1 SV=2	HUMAN	7
25	14.04	14.04	31.2	sp|Q07065|CKAP4_HU	Cytoskeleton-associated protein 4 OS=Homo sapiens GN=CKAP4 PE=1 SV=2	HUMAN	8
26	13.65	13.65	36.4	sp|Q15084|PDIA6_HU	Protein disulfide-isomerase A6 OS=Homo sapiens GN=PDIA6 PE=1 SV=1	HUMAN	8
27	13.31	13.31	37.6	sp|P50454|SERPH_HU	Serpin H1 OS=Homo sapiens GN=SERPINH1 PE=1 SV=2	HUMAN	8
28	13.05	13.05	47	sp|Q96D15|RCN3_HU	Reticulocalbin-3 OS=Homo sapiens GN=RCN3 PE=1 SV=1	HUMAN	10
29	12.99	12.99	48.7	sp|P04406|G3P_HUM	Glyceraldehyde-3-phosphate dehydrogenase OS=Homo sapiens GN=GAPDH PE=1 SV=3	HUMAN	13
30	12.92	12.92	18.4	sp|P26038|MOES_HU	Moesin OS=Homo sapiens GN=MSN PE=1 SV=3	HUMAN	7
31	11.92	11.92	20.6	sp|Q7KZF4|SND1_HU	Staphylococcal nuclease domain-containing protein 1 OS=Homo sapiens GN=SND1 PE=1 SV=1	HUMAN	7
32	11.69	11.69	35.1	sp|Q02878|RL6_HUM	60S ribosomal protein L6 OS=Homo sapiens GN=RPL6 PE=1 SV=3	HUMAN	9
33	11.48	11.48	28.9	sp|O43852|CALU_HU	Calumenin OS=Homo sapiens GN=CALU PE=1 SV=2	HUMAN	8
34	10.22	10.22	21.1	sp|Q9P2E9|RRBP1_HU	Ribosome-binding protein 1 OS=Homo sapiens GN=RRBP1 PE=1 SV=4	HUMAN	7
35	9.82	9.82	15.3	sp|Q16822|PCKGM_H	Phosphoenolpyruvate carboxykinase [GTP], mitochondrial OS=Homo sapiens GN=PCK2 PE=1 SV=3	HUMAN	7
36	9.26	9.26	50.5	sp|P23284|PPIB_HUM	Peptidyl-prolyl cis-trans isomerase B OS=Homo sapiens GN=PPIB PE=1 SV=2	HUMAN	7
37	9.22	9.22	22.9	sp|Q96AY3|FKB10_HU	Peptidyl-prolyl cis-trans isomerase FKBP10 OS=Homo sapiens GN=FKBP10 PE=1 SV=1	HUMAN	6
38	9.18	9.18	25.7	sp|P42765|THIM_HUM	3-ketoacyl-CoA thiolase, mitochondrial OS=Homo sapiens GN=ACAA2 PE=1 SV=2	HUMAN	6
39	8.63	8.63	22.3	sp|P26373|RL13_HUM	60S ribosomal protein L13 OS=Homo sapiens GN=RPL13 PE=1 SV=4	HUMAN	5
40	8.63	8.63	49.6	sp|P14927|QCR7_HUM	Cytochrome b-c1 complex subunit 7 OS=Homo sapiens GN=UQCRB PE=1 SV=2	HUMAN	4
41	8.3	8.3	20.4	sp|O75390|CISY_HUM	Citrate synthase, mitochondrial OS=Homo sapiens GN=CS PE=1 SV=2	HUMAN	5
42	8.29	8.29	41.2	sp|P61313|RL15_HUM	60S ribosomal protein L15 OS=Homo sapiens GN=RPL15 PE=1 SV=2	HUMAN	4
43	8.27	8.27	20	sp|P08473|NEP_HUM	Neprilysin OS=Homo sapiens GN=MME PE=1 SV=2	HUMAN	6
44	8.19	8.19	14	sp|Q3SY69|AL1L2_HU	Mitochondrial 10-formyltetrahydrofolate dehydrogenase OS=Homo sapiens GN=ALDH1L2 PE=1 SV=2	HUMAN	4
45	8.16	8.16	23	sp|P07858|CATB_HUM	Cathepsin B OS=Homo sapiens GN=CTSB PE=1 SV=3	HUMAN	5
46	8	8	15.7	sp|P24752|THIL_HUM	Acetyl-CoA acetyltransferase, mitochondrial OS=Homo sapiens GN=ACAT1 PE=1 SV=1	HUMAN	5
47	7.88	7.88	25.5	sp|P12236|ADT3_HUM	ADP/ATP translocase 3 OS=Homo sapiens GN=SLC25A6 PE=1 SV=4	HUMAN	5
48	7.87	7.88	11.9	sp|O43707|ACTN4_HU	Alpha-actinin-4 OS=Homo sapiens GN=ACTN4 PE=1 SV=2	HUMAN	4
49	7.79	7.79	37.1	sp|O75380|NDUS6_H	NADH dehydrogenase [ubiquinone] iron-sulfur protein 6, mitochondrial OS=Homo sapiens GN=NDUFS6 PE=1 SV=1	HUMAN	5
50	7.74	7.75	32.5	sp|P08758|ANXA5_HU	Annexin A5 OS=Homo sapiens GN=ANXA5 PE=1 SV=2	HUMAN	5
51	7.62	7.62	14.9	sp|P31040|DHSA_HUM	Succinate dehydrogenase [ubiquinone] flavoprotein subunit, mitochondrial OS=Homo sapiens GN=SDHA PE=1 SV=2	HUMAN	4
52	7.62	7.62	22.2	sp|P62081|RS7_HUM	40S ribosomal protein S7 OS=Homo sapiens GN=RPS7 PE=1 SV=1	HUMAN	4
53	7.6	7.6	22.6	sp|P09622|DLDH_HUM	Dihydrolipoyl dehydrogenase, mitochondrial OS=Homo sapiens GN=DLD PE=1 SV=2	HUMAN	5
54	7.57	7.57	19.2	sp|P08133|ANXA6_HU	Annexin A6 OS=Homo sapiens GN=ANXA6 PE=1 SV=3	HUMAN	4
55	7.53	7.53	26.3	sp|P07954|FUMH_HU	Fumarate hydratase, mitochondrial OS=Homo sapiens GN=FH PE=1 SV=3	HUMAN	3
56	7.46	7.46	34.4	sp|Q07000|1C15_HUM	HLA class I histocompatibility antigen, Cw-15 alpha chain OS=Homo sapiens GN=HLA-C PE=1 SV=1	HUMAN	4
57	7.41	7.41	51.4	sp|P62241|RS8_HUM	40S ribosomal protein S8 OS=Homo sapiens GN=RPS8 PE=1 SV=2	HUMAN	4
58	7.41	7.41	30.9	sp|P62269|RS18_HUM	40S ribosomal protein S18 OS=Homo sapiens GN=RPS18 PE=1 SV=3	HUMAN	4
59	7.24	7.24	6.5	sp|Q01082|SPTB2_HU	Spectrin beta chain, non-erythrocytic 1 OS=Homo sapiens GN=SPTBN1 PE=1 SV=2	HUMAN	4
60	7.19	7.19	11.4	sp|P04181|OAT_HUM	Ornithine aminotransferase, mitochondrial OS=Homo sapiens GN=OAT PE=1 SV=1	HUMAN	4
61	7.11	7.11	17.2	sp|Q9BQE3|TBA1C_H	Tubulin alpha-1C chain OS=Homo sapiens GN=TUBA1C PE=1 SV=1	HUMAN	4
62	7.09	7.09	60.7	sp|P20674|COX5A_HU	Cytochrome c oxidase subunit 5A, mitochondrial OS=Homo sapiens GN=COX5A PE=1 SV=2	HUMAN	6
63	7.06	7.06	13.9	sp|P49411|EFTU_HUM	Elongation factor Tu, mitochondrial OS=Homo sapiens GN=TUFM PE=1 SV=2	HUMAN	4
64	7.06	7.06	17.4	sp|O14773|TPP1_HUM	Tripeptidyl-peptidase 1 OS=Homo sapiens GN=TPP1 PE=1 SV=2	HUMAN	4
65	6.87	6.87	13.2	sp|P13639|EF2_HUMA	Elongation factor 2 OS=Homo sapiens GN=EEF2 PE=1 SV=4	HUMAN	5
66	6.86	6.86	44.1	sp|P61604|CH10_HUM	10 kDa heat shock protein, mitochondrial OS=Homo sapiens GN=HSPE1 PE=1 SV=2	HUMAN	5
67	6.82	6.82	31.9	sp|P00387|NB5R3_HU	NADH-cytochrome b5 reductase 3 OS=Homo sapiens GN=CYB5R3 PE=1 SV=3	HUMAN	4
68	6.79	6.79	13.3	sp|P04083|ANXA1_HU	Annexin A1 OS=Homo sapiens GN=ANXA1 PE=1 SV=2	HUMAN	3
69	6.78	6.78	15.1	sp|Q16181|SEPT7_HU	Septin-7 OS=Homo sapiens GN=SEPT7 PE=1 SV=2	HUMAN	5
70	6.71	6.71	22.6	sp|O00264|PGRC1_HU	Membrane-associated progesterone receptor component 1 OS=Homo sapiens GN=PGRMC1 PE=1 SV=3	HUMAN	5
71	6.59	6.59	43.7	sp|P60660|MYL6_HUM	Myosin light polypeptide 6 OS=Homo sapiens GN=MYL6 PE=1 SV=2	HUMAN	6
72	6.55	6.55	11.6	sp|Q13813|SPTN1_HU	Spectrin alpha chain, non-erythrocytic 1 OS=Homo sapiens GN=SPTAN1 PE=1 SV=3	HUMAN	3
73	6.5	6.5	35.7	sp|P34897|GLYM_HUM	Serine hydroxymethyltransferase, mitochondrial OS=Homo sapiens GN=SHMT2 PE=1 SV=3	HUMAN	4
74	6.26	6.26	31.5	sp|Q9UJZ1|STML2_HU	Stomatin-like protein 2 OS=Homo sapiens GN=STOML2 PE=1 SV=1	HUMAN	4
75	6.25	6.25	12	sp|P54886|P5CS_HUM	Delta-1-pyrroline-5-carboxylate synthase OS=Homo sapiens GN=ALDH18A1 PE=1 SV=2	HUMAN	4
76	6.24	6.26	33.3	sp|P04179|SODM_HU	Superoxide dismutase [Mn], mitochondrial OS=Homo sapiens GN=SOD2 PE=1 SV=2	HUMAN	6
77	6.24	6.24	41.9	sp|P80723|BASP1_HU	Brain acid soluble protein 1 OS=Homo sapiens GN=BASP1 PE=1 SV=2	HUMAN	6
78	6.22	6.22	17.4	sp|Q14257|RCN2_HUM	Reticulocalbin-2 OS=Homo sapiens GN=RCN2 PE=1 SV=1	HUMAN	3
79	6.15	6.15	34	sp|P40926|MDHM_HU	Malate dehydrogenase, mitochondrial OS=Homo sapiens GN=MDH2 PE=1 SV=3	HUMAN	7
80	6.07	6.07	13.3	sp|P05023|AT1A1_HU	Sodium/potassium-transporting ATPase subunit alpha-1 OS=Homo sapiens GN=ATP1A1 PE=1 SV=1	HUMAN	5
81	6.04	6.04	20.1	sp|O75489|NDUS3_H	NADH dehydrogenase [ubiquinone] iron-sulfur protein 3, mitochondrial OS=Homo sapiens GN=NDUFS3 PE=1 SV=1	HUMAN	3
82	6.01	6.01	9.9	sp|P07942|LAMB1_HU	Laminin subunit beta-1 OS=Homo sapiens GN=LAMB1 PE=1 SV=2	HUMAN	4
83	6	6	39.4	sp|P62937|PPIA_HUM	Peptidyl-prolyl cis-trans isomerase A OS=Homo sapiens GN=PPIA PE=1 SV=2	HUMAN	4
84	6	6	12.4	sp|P05091|ALDH2_HU	Aldehyde dehydrogenase, mitochondrial OS=Homo sapiens GN=ALDH2 PE=1 SV=2	HUMAN	3
85	6	6	20.6	sp|Q16698|DECR_HUM	2,4-dienoyl-CoA reductase, mitochondrial OS=Homo sapiens GN=DECR1 PE=1 SV=1	HUMAN	4
86	5.89	5.89	9.5	sp|P16435|NCPR_HUM	NADPH--cytochrome P450 reductase OS=Homo sapiens GN=POR PE=1 SV=2	HUMAN	3
87	5.84	5.84	17.1	sp|P22090|RS4Y1_HU	40S ribosomal protein S4, Y isoform 1 OS=Homo sapiens GN=RPS4Y1 PE=2 SV=2	HUMAN	3
88	5.59	5.59	15.3	sp|O94925|GLSK_HUM	Glutaminase kidney isoform, mitochondrial OS=Homo sapiens GN=GLS PE=1 SV=1	HUMAN	3
89	5.57	5.57	18.3	sp|P12109|CO6A1_HU	Collagen alpha-1(VI) chain OS=Homo sapiens GN=COL6A1 PE=1 SV=3	HUMAN	5
90	5.51	5.51	39.8	sp|O75947|ATP5H_HU	ATP synthase subunit d, mitochondrial OS=Homo sapiens GN=ATP5H PE=1 SV=3	HUMAN	4
91	5.48	5.48	9.6	sp|O95302|FKBP9_HU	Peptidyl-prolyl cis-trans isomerase FKBP9 OS=Homo sapiens GN=FKBP9 PE=1 SV=2	HUMAN	3
92	5.42	5.42	20.1	sp|P04843|RPN1_HUM	Dolichyl-diphosphooligosaccharide--protein glycosyltransferase subunit 1 OS=Homo sapiens GN=RPN1 PE=1 SV=1	HUMAN	3
93	5.34	5.34	22.8	sp|P35232|PHB_HUM	Prohibitin OS=Homo sapiens GN=PHB PE=1 SV=1	HUMAN	3
94	5.25	5.25	25.9	sp|Q8NB59|TXND5_H	Thioredoxin domain-containing protein 5 OS=Homo sapiens GN=TXNDC5 PE=1 SV=2	HUMAN	6
95	5.1	5.1	8.5	sp|P07339|CATD_HUM	Cathepsin D OS=Homo sapiens GN=CTSD PE=1 SV=1	HUMAN	4
96	5.08	5.08	16.9	sp|P36578|RL4_HUM	60S ribosomal protein L4 OS=Homo sapiens GN=RPL4 PE=1 SV=5	HUMAN	3
97	5.07	5.08	40.9	sp|P19105|ML12A_HU	Myosin regulatory light chain 12A OS=Homo sapiens GN=MYL12A PE=1 SV=2	HUMAN	3
98	5.06	5.06	33.8	sp|Q9NS69|TOM22_H	Mitochondrial import receptor subunit TOM22 homolog OS=Homo sapiens GN=TOMM22 PE=1 SV=3	HUMAN	3
99	5.01	5.01	23.7	sp|Q9BWM7|SFXN3_H	Sideroflexin-3 OS=Homo sapiens GN=SFXN3 PE=2 SV=2	HUMAN	4
100	5	5	24.5	sp|Q15293|RCN1_HU	Reticulocalbin-1 OS=Homo sapiens GN=RCN1 PE=1 SV=1	HUMAN	5
101	4.98	6.48	25.9	sp|P11142|HSP7C_HU	Heat shock cognate 71 kDa protein OS=Homo sapiens GN=HSPA8 PE=1 SV=1	HUMAN	6
102	4.98	4.98	17.5	sp|P28331|NDUS1_HU	NADH-ubiquinone oxidoreductase 75 kDa subunit, mitochondrial OS=Homo sapiens GN=NDUFS1 PE=1 SV=3	HUMAN	3
103	4.94	4.94	18.3	sp|P08865|RSSA_HUM	40S ribosomal protein SA OS=Homo sapiens GN=RPSA PE=1 SV=4	HUMAN	3
104	4.92	4.92	19.8	sp|Q16891|IMMT_HU	Mitochondrial inner membrane protein OS=Homo sapiens GN=IMMT PE=1 SV=1	HUMAN	2

N	Unused	Total	% Cov	Accession #	Name	Species	Peptides(95%)
105	4.88	4.88	42.5	sp|P00167|CYB5_HUM	Cytochrome b5 OS=Homo sapiens GN=CYB5A PE=1 SV=2	HUMAN	5
106	4.84	4.84	15.5	sp|P30084|ECHM_HU	Enoyl-CoA hydratase, mitochondrial OS=Homo sapiens GN=ECHS1 PE=1 SV=4	HUMAN	3
107	4.69	4.69	19.9	sp|Q05682|CALD1_HI	Caldesmon OS=Homo sapiens GN=CALD1 PE=1 SV=3	HUMAN	2
108	4.67	4.67	25.9	sp|P08574|CY1_HUM	Cytochrome c1, heme protein, mitochondrial OS=Homo sapiens GN=CYC1 PE=1 SV=3	HUMAN	4
109	4.67	4.67	8.9	sp|P15586|GNS_HUM	N-acetylglucosamine-6-sulfatase OS=Homo sapiens GN=GNS PE=1 SV=3	HUMAN	3
110	4.65	4.65	26.7	sp|P00505|AATM_HU	Aspartate aminotransferase, mitochondrial OS=Homo sapiens GN=GOT2 PE=1 SV=3	HUMAN	3
111	4.61	4.61	50.4	sp|P10606|COX5B_HU	Cytochrome c oxidase subunit 5B, mitochondrial OS=Homo sapiens GN=COX5B PE=1 SV=2	HUMAN	4
112	4.55	4.55	29.6	sp|P67809|YBOX1_HU	Nuclease-sensitive element-binding protein 1 OS=Homo sapiens GN=YBX1 PE=1 SV=3	HUMAN	3
113	4.51	4.51	14.4	sp|P36957|ODO2_HU	Dihydrolipoyllysine-residue succinyltransferase component of 2-oxoglutarate dehydrogenase complex, mitochondrial OS=Homo sapiens GN=DLST PE=1 SV=4	HUMAN	3
114	4.48	4.48	13.4	sp|P11177|ODPB_HU	Pyruvate dehydrogenase E1 component subunit beta, mitochondrial OS=Homo sapiens GN=PDHB PE=1 SV=3	HUMAN	2
115	4.35	4.35	7.8	sp|P07602|SAP_HUM	Proactivator polypeptide OS=Homo sapiens GN=PSAP PE=1 SV=2	HUMAN	4
116	4.25	4.25	10.2	sp|Q5JRX3|PREP_HU	Presequence protease, mitochondrial OS=Homo sapiens GN=PITRM1 PE=1 SV=2	HUMAN	3
117	4.25	4.25	17.2	sp|P61254|RL26_HUM	60S ribosomal protein L26 OS=Homo sapiens GN=RPL26 PE=1 SV=1	HUMAN	2
118	4.19	4.19	14.8	sp|P53007|TXTP_HUM	Tricarboxylate transport protein, mitochondrial OS=Homo sapiens GN=SLC25A1 PE=1 SV=2	HUMAN	2
119	4.17	4.17	21.2	sp|P22695|QCR2_HUM	Cytochrome b-c1 complex subunit 2, mitochondrial OS=Homo sapiens GN=UQCRC2 PE=1 SV=3	HUMAN	2
120	4.07	4.07	28.8	sp|Q99623|PHB2_HU	Prohibitin-2 OS=Homo sapiens GN=PHB2 PE=1 SV=2	HUMAN	4
121	4.02	4.02	10.6	sp|Q14165|MLEC_HU	Malectin OS=Homo sapiens GN=MLEC PE=1 SV=1	HUMAN	3
122	4	4	22.5	sp|P04264|K2C1_HUM	Keratin, type II cytoskeletal 1 OS=Homo sapiens GN=KRT1 PE=1 SV=6	HUMAN	3
123	4	4	37.8	sp|P16104|H2AX_HUM	Histone H2A.x OS=Homo sapiens GN=H2AFX PE=1 SV=2	HUMAN	2
124	4	4	16.1	sp|P06733|ENOA_HU	Alpha-enolase OS=Homo sapiens GN=ENO1 PE=1 SV=2	HUMAN	2
125	4	4	19.7	sp|O75915|PRAF3_HU	PRA1 family protein 3 OS=Homo sapiens GN=ARL6IP5 PE=1 SV=1	HUMAN	2
126	4	4	16.5	sp|P05387|RLA2_HUM	60S acidic ribosomal protein P2 OS=Homo sapiens GN=RPLP2 PE=1 SV=1	HUMAN	5
127	4	4	18.4	sp|O14880|MGST3_H	Microsomal glutathione S-transferase 3 OS=Homo sapiens GN=MGST3 PE=1 SV=1	HUMAN	2
128	3.96	3.96	25.5	sp|P56134|ATPK_HUM	ATP synthase subunit f, mitochondrial OS=Homo sapiens GN=ATP5J2 PE=1 SV=3	HUMAN	2
129	3.94	3.94	21.6	sp|P46776|RL27A_HU	60S ribosomal protein L27a OS=Homo sapiens GN=RPL27A PE=1 SV=2	HUMAN	3
130	3.91	3.91	15.8	sp|Q02218|ODO1_HU	2-oxoglutarate dehydrogenase, mitochondrial OS=Homo sapiens GN=OGDH PE=1 SV=3	HUMAN	2
131	3.89	3.89	15.3	sp|Q9BTV4|TMM43_H	Transmembrane protein 43 OS=Homo sapiens GN=TMEM43 PE=1 SV=1	HUMAN	2
132	3.87	3.87	25.2	sp|P07437|TBB5_HUM	Tubulin beta chain OS=Homo sapiens GN=TUBB PE=1 SV=2	HUMAN	3
133	3.85	3.85	3.8	sp|Q07954|LRP1_HUM	Prolow-density lipoprotein receptor-related protein 1 OS=Homo sapiens GN=LRP1 PE=1 SV=2	HUMAN	2
134	3.84	3.85	13.3	sp|Q07020|RL18_HUM	60S ribosomal protein L18 OS=Homo sapiens GN=RPL18 PE=1 SV=2	HUMAN	4
135	3.77	3.82	7.4	sp|Q9NVI7|ATD3A_HU	ATPase family AAA domain-containing protein 3A OS=Homo sapiens GN=ATAD3A PE=1 SV=2	HUMAN	2
136	3.75	3.75	7.5	sp|P42704|LPPRC_HU	Leucine-rich PPR motif-containing protein, mitochondrial OS=Homo sapiens GN=LRPPRC PE=1 SV=3	HUMAN	2
137	3.74	3.74	11.6	sp|Q02809|PLOD1_HU	Procollagen-lysine,2-oxoglutarate 5-dioxygenase 1 OS=Homo sapiens GN=PLOD1 PE=1 SV=2	HUMAN	2
138	3.59	3.59	23.8	sp|Q07021|C1QBP_HU	Complement component 1 Q subcomponent-binding protein, mitochondrial OS=Homo sapiens GN=C1QBP PE=1 SV=1	HUMAN	2
139	3.58	3.59	14.9	sp|P30040|ERP29_HU	Endoplasmic reticulum resident protein 29 OS=Homo sapiens GN=ERP29 PE=1 SV=4	HUMAN	2
140	3.52	3.52	31.2	sp|Q9GZT3|SLIRP_HU	SRA stem-loop-interacting RNA-binding protein, mitochondrial OS=Homo sapiens GN=SLIRP PE=1 SV=1	HUMAN	4
141	3.52	3.52	24.2	sp|P83731|RL24_HUM	60S ribosomal protein L24 OS=Homo sapiens GN=RPL24 PE=1 SV=1	HUMAN	2
142	3.46	3.46	17	sp|Q9Y2B0|CNPY2_HU	Protein canopy homolog 2 OS=Homo sapiens GN=CNPY2 PE=1 SV=1	HUMAN	2
143	3.45	3.45	28.4	sp|Q13162|PRDX4_HU	Peroxiredoxin-4 OS=Homo sapiens GN=PRDX4 PE=1 SV=1	HUMAN	2
144	3.41	3.41	22.9	sp|Q96L21|RL10L_HU	60S ribosomal protein L10-like OS=Homo sapiens GN=RPL10L PE=1 SV=3	HUMAN	2
145	3.37	3.37	15.7	sp|P18124|RL7_HUM	60S ribosomal protein L7 OS=Homo sapiens GN=RPL7 PE=1 SV=1	HUMAN	2
146	3.3	3.3	8.5	sp|P16070|CD44_HUM	CD44 antigen OS=Homo sapiens GN=CD44 PE=1 SV=3	HUMAN	2
147	3.29	3.29	16.8	sp|P30048|PRDX3_HU	Thioredoxin-dependent peroxide reductase, mitochondrial OS=Homo sapiens GN=PRDX3 PE=1 SV=3	HUMAN	3
148	3.29	3.29	10.2	sp|Q9Y6N5|SQRD_HU	Sulfide:quinone oxidoreductase, mitochondrial OS=Homo sapiens GN=SQRDL PE=1 SV=1	HUMAN	3
149	3.26	3.26	22.7	sp|P63241|IF5A1_HU	Eukaryotic translation initiation factor 5A-1 OS=Homo sapiens GN=EIF5A PE=1 SV=2	HUMAN	2
150	3.23	3.23	36	sp|P61026|RAB10_HU	Ras-related protein Rab-10 OS=Homo sapiens GN=RAB10 PE=1 SV=1	HUMAN	2
151	3.23	3.23	15.3	sp|P67936|TPM4_HU	Tropomyosin alpha-4 chain OS=Homo sapiens GN=TPM4 PE=1 SV=3	HUMAN	3
152	3.22	3.22	32.9	sp|P62158|CALM_HU	Calmodulin OS=Homo sapiens GN=CALM1 PE=1 SV=2	HUMAN	2
153	3.15	3.15	17.7	sp|P35613|BASI_HUM	Basigin OS=Homo sapiens GN=BSG PE=1 SV=2	HUMAN	2
154	3.14	3.14	24.1	sp|P62841|RS15_HUM	40S ribosomal protein S15 OS=Homo sapiens GN=RPS15 PE=1 SV=2	HUMAN	2
155	3.1	3.1	38.9	sp|P18859|ATPSJ_HU	ATP synthase-coupling factor 6, mitochondrial OS=Homo sapiens GN=ATP5J PE=1 SV=1	HUMAN	3
156	3.06	3.06	14.1	sp|P55084|ECHB_HUM	Trifunctional enzyme subunit beta, mitochondrial OS=Homo sapiens GN=HADHB PE=1 SV=3	HUMAN	3
157	3.06	3.06	9.5	sp|P04844|RPN2_HUM	Dolichyl-diphosphooligosaccharide--protein glycosyltransferase subunit 2 OS=Homo sapiens GN=RPN2 PE=1 SV=3	HUMAN	2
158	3.06	3.06	9.5	sp|Q06830|PRDX1_HU	Peroxiredoxin-1 OS=Homo sapiens GN=PRDX1 PE=1 SV=1	HUMAN	2
159	2.98	2.98	7.6	sp|P55072|TERA_HUM	Transitional endoplasmic reticulum ATPase OS=Homo sapiens GN=VCP PE=1 SV=4	HUMAN	2
160	2.88	2.88	13	sp|O43837|IDH3B_HU	Isocitrate dehydrogenase [NAD] subunit beta, mitochondrial OS=Homo sapiens GN=IDH3B PE=1 SV=2	HUMAN	2
161	2.85	2.85	27.6	sp|Q86TX2|ACOT1_HU	Acyl-coenzyme A thioesterase 1 OS=Homo sapiens GN=ACOT1 PE=1 SV=1	HUMAN	2
162	2.82	2.82	12.8	sp|P10515|ODP2_HUM	Dihydrolipoyllysine-residue acetyltransferase component of pyruvate dehydrogenase complex, mitochondrial OS=Homo sapiens GN=DLAT PE=1 SV=3	HUMAN	2
163	2.78	2.78	12	sp|P18621|RL17_HUM	60S ribosomal protein L17 OS=Homo sapiens GN=RPL17 PE=1 SV=3	HUMAN	2
164	2.76	2.76	25.2	sp|P47985|UCRI_HUM	Cytochrome b-c1 complex subunit Rieske, mitochondrial OS=Homo sapiens GN=UQCRFS1 PE=1 SV=2	HUMAN	3
165	2.74	2.74	16.5	sp|Q02818|NUCB1_H	Nucleobindin-1 OS=Homo sapiens GN=NUCB1 PE=1 SV=4	HUMAN	1
166	2.74	2.74	4.9	sp|P13473|LAMP2_HU	Lysosome-associated membrane glycoprotein 2 OS=Homo sapiens GN=LAMP2 PE=1 SV=2	HUMAN	1
167	2.73	2.73	10.9	sp|P33121|ACSL1_HU	Long-chain-fatty-acid--CoA ligase 1 OS=Homo sapiens GN=ACSL1 PE=1 SV=1	HUMAN	1
168	2.65	2.65	26	sp|Q8N183|MIMIT_H	Mimitin, mitochondrial OS=Homo sapiens GN=NDUFAF2 PE=1 SV=1	HUMAN	2
169	2.61	2.61	37.3	sp|P09669|COX6C_HU	Cytochrome c oxidase subunit 6C OS=Homo sapiens GN=COX6C PE=1 SV=2	HUMAN	1
170	2.6	2.6	39	sp|P42766|RL35_HUM	60S ribosomal protein L35 OS=Homo sapiens GN=RPL35 PE=1 SV=2	HUMAN	2
171	2.58	2.58	12.6	sp|P50213|IDH3A_HU	Isocitrate dehydrogenase [NAD] subunit alpha, mitochondrial OS=Homo sapiens GN=IDH3A PE=1 SV=1	HUMAN	2
172	2.53	2.53	12.6	sp|P82675|RT05_HUM	28S ribosomal protein S5, mitochondrial OS=Homo sapiens GN=MRPS5 PE=1 SV=2	HUMAN	2
173	2.51	2.51	8	sp|Q9Y4L1|HYOU1_H	Hypoxia up-regulated protein 1 OS=Homo sapiens GN=HYOU1 PE=1 SV=1	HUMAN	3
174	2.51	2.51	8.2	sp|P38117|ETFB_HUM	Electron transfer flavoprotein subunit beta OS=Homo sapiens GN=ETFB PE=1 SV=3	HUMAN	1
175	2.49	4.95	28.2	sp|P30512|1A29_HUM	HLA class I histocompatibility antigen, A-29 alpha chain OS=Homo sapiens GN=HLA-A PE=2 SV=2	HUMAN	2
176	2.46	2.46	12.6	sp|Q9Y512|SAM50_H	Sorting and assembly machinery component 50 homolog OS=Homo sapiens GN=SAMM50 PE=1 SV=3	HUMAN	2
177	2.45	2.45	9.3	sp|P13667|PDIA4_HU	Protein disulfide-isomerase A4 OS=Homo sapiens GN=PDIA4 PE=1 SV=2	HUMAN	2
178	2.43	2.43	27.8	sp|P62263|RS14_HUM	40S ribosomal protein S14 OS=Homo sapiens GN=RPS14 PE=1 SV=3	HUMAN	1
179	2.4	2.4	12.5	sp|Q13011|ECH1_HUM	Delta(3,5)-Delta(2,4)-dienoyl-CoA isomerase, mitochondrial OS=Homo sapiens GN=ECH1 PE=1 SV=2	HUMAN	1
180	2.39	2.39	8.1	sp|O95479|G6PE_HUM	GDH/6PGL endoplasmic bifunctional protein OS=Homo sapiens GN=H6PD PE=1 SV=2	HUMAN	1
181	2.37	2.37	17.4	sp|P62913|RL11_HUM	60S ribosomal protein L11 OS=Homo sapiens GN=RPL11 PE=1 SV=2	HUMAN	1
182	2.34	2.34	15.3	sp|O75306|NDUS2_H	NADH dehydrogenase [ubiquinone] iron-sulfur protein 2, mitochondrial OS=Homo sapiens GN=NDUFS2 PE=1 SV=2	HUMAN	1
183	2.31	2.31	12.6	sp|P60866|RS20_HUM	40S ribosomal protein S20 OS=Homo sapiens GN=RPS20 PE=1 SV=1	HUMAN	1
184	2.26	2.26	30.4	sp|P10109|ADX_HUM	Adrenodoxin, mitochondrial OS=Homo sapiens GN=FDX1 PE=1 SV=1	HUMAN	1
185	2.26	2.26	8	sp|Q9ULV4|COR1C_H	Coronin-1C OS=Homo sapiens GN=CORO1C PE=1 SV=1	HUMAN	1
186	2.23	2.23	10.5	sp|P43307|SSRA_HUM	Translocon-associated protein subunit alpha OS=Homo sapiens GN=SSR1 PE=1 SV=3	HUMAN	1
187	2.22	2.22	14.1	sp|Q15019|SEPT2_HU	Septin-2 OS=Homo sapiens GN=SEPT2 PE=1 SV=1	HUMAN	1
188	2.21	2.21	15.4	sp|Q99798|ACON_HU	Aconitate hydratase, mitochondrial OS=Homo sapiens GN=ACO2 PE=1 SV=2	HUMAN	3
189	2.21	2.21	16	sp|P17931|LEG3_HUM	Galectin-3 OS=Homo sapiens GN=LGALS3 PE=1 SV=5	HUMAN	4
190	2.2	2.2	18.8	sp|P27144|KAD4_HUM	Adenylate kinase isoenzyme 4, mitochondrial OS=Homo sapiens GN=AK4 PE=1 SV=1	HUMAN	1
191	2.18	2.18	14.2	sp|O43920|NDUS5_H	NADH dehydrogenase [ubiquinone] iron-sulfur protein 5 OS=Homo sapiens GN=NDUFS5 PE=1 SV=3	HUMAN	1
192	2.16	2.16	18.1	sp|P11940|PABP1_HU	Polyadenylate-binding protein 1 OS=Homo sapiens GN=PABPC1 PE=1 SV=2	HUMAN	1
193	2.14	2.14	6.4	sp|Q32P28|P3H1_HUM	Prolyl 3-hydroxylase 1 OS=Homo sapiens GN=LEPRE1 PE=1 SV=2	HUMAN	2
194	2.12	2.12	17.4	sp|P07099|HYEP_HUM	Epoxide hydrolase 1 OS=Homo sapiens GN=EPHX1 PE=1 SV=1	HUMAN	2
195	2.08	2.08	13.5	sp|P35527|K1C9_HUM	Keratin, type I cytoskeletal 9 OS=Homo sapiens GN=KRT9 PE=1 SV=3	HUMAN	1
196	2.07	2.07	8.2	sp|P53634|CATC_HUM	Dipeptidyl peptidase 1 OS=Homo sapiens GN=CTSC PE=1 SV=2	HUMAN	2
197	2.02	2.02	30.3	sp|P39019|RS19_HUM	40S ribosomal protein S19 OS=Homo sapiens GN=RPS19 PE=1 SV=2	HUMAN	1
198	2.01	2.01	31.5	sp|P48047|ATPO_HUM	ATP synthase subunit O, mitochondrial OS=Homo sapiens GN=ATP5O PE=1 SV=1	HUMAN	1
199	2.01	2.01	11.8	sp|O94826|TOM70_H	Mitochondrial import receptor subunit TOM70 OS=Homo sapiens GN=TOMM70A PE=1 SV=1	HUMAN	1
200	2.01	2.01	14.2	sp|Q99714|HCD2_HU	3-hydroxyacyl-CoA dehydrogenase type-2 OS=Homo sapiens GN=HSD17B10 PE=1 SV=3	HUMAN	1
201	2.01	2.01	17.6	sp|P54819|KAD2_HUM	Adenylate kinase 2, mitochondrial OS=Homo sapiens GN=AK2 PE=1 SV=2	HUMAN	1
202	2.01	2.01	14.9	sp|P50914|RL14_HUM	60S ribosomal protein L14 OS=Homo sapiens GN=RPL14 PE=1 SV=4	HUMAN	1
203	2	2	66.4	sp|P17096|HMGA1_H	High mobility group protein HMG-I/HMG-Y OS=Homo sapiens GN=HMGA1 PE=1 SV=3	HUMAN	1
204	2	2	35.7	sp|Q99879|H2B1M_H	Histone H2B type 1-M OS=Homo sapiens GN=HIST1H2BM PE=1 SV=3	HUMAN	1
205	2	2	19.2	sp|P61978|HNRPK_HU	Heterogeneous nuclear ribonucleoprotein K OS=Homo sapiens GN=HNRNPK PE=1 SV=1	HUMAN	1
206	2	2	8.9	sp|Q9HA77|SYCM_HU	Probable cysteine--tRNA ligase, mitochondrial OS=Homo sapiens GN=CARS2 PE=1 SV=1	HUMAN	1
207	2	2	23.3	sp|P63104|1433Z_HU	14-3-3 protein zeta/delta OS=Homo sapiens GN=YWHAZ PE=1 SV=1	HUMAN	1
208	2	2	22	sp|P62258|1433E_HU	14-3-3 protein epsilon OS=Homo sapiens GN=YWHAE PE=1 SV=1	HUMAN	1

N	Unused	Total	% Cov	Accession #	Name	Species	Peptides(95%)	
209	2	2	31.2	sp|P56556|NDUA6_H	NADH dehydrogenase [ubiquinone] 1 alpha subcomplex subunit 6 OS=Homo sapiens GN=NDUFA6 PE=1 SV=3	HUMAN		1
210	2	2	8.9	sp|P43155|CACP_HUI	Carnitine O-acetyltransferase OS=Homo sapiens GN=CRAT PE=1 SV=5	HUMAN		1
211	2	2	4.9	sp|P11498|PYC_HUM	Pyruvate carboxylase, mitochondrial OS=Homo sapiens GN=PC PE=1 SV=2	HUMAN		1
212	2	2	8.9	sp|P05556|ITB1_HUN	Integrin beta-1 OS=Homo sapiens GN=ITGB1 PE=1 SV=2	HUMAN		1
213	2	2	22.3	sp|O75208|COQ9_HU	Ubiquinone biosynthesis protein COQ9, mitochondrial OS=Homo sapiens GN=COQ9 PE=1 SV=1	HUMAN		1
214	2	2	7	sp|Q9H2V7|SPNS1_HI	Protein spinster homolog 1 OS=Homo sapiens GN=SPNS1 PE=1 SV=1	HUMAN		1
215	2	2	29.3	sp|P62847|RS24_HUI	40S ribosomal protein S24 OS=Homo sapiens GN=RPS24 PE=1 SV=1	HUMAN		1
216	2	2	17.9	sp|P51858|HDGF_HUI	Hepatoma-derived growth factor OS=Homo sapiens GN=HDGF PE=1 SV=1	HUMAN		1
217	2	2	41.9	sp|P14854|CX6B1_HU	Cytochrome c oxidase subunit 6B1 OS=Homo sapiens GN=COX6B1 PE=1 SV=2	HUMAN		1
218	2	2	7	sp|P14618|KPYM_HU	Pyruvate kinase isozymes M1/M2 OS=Homo sapiens GN=PKM PE=1 SV=4	HUMAN		1
219	2	2	11	sp|P09525|ANXA4_HI	Annexin A4 OS=Homo sapiens GN=ANXA4 PE=1 SV=4	HUMAN		1
220	2	2	4.8	sp|Q15758|AAAT_HUI	Neutral amino acid transporter B(0) OS=Homo sapiens GN=SLC1A5 PE=1 SV=2	HUMAN		1
221	2	2	11.2	sp|P62899|RL31_HUM	60S ribosomal protein L31 OS=Homo sapiens GN=RPL31 PE=1 SV=1	HUMAN		1
222	2	2	24.9	sp|P30050|RL12_HUM	60S ribosomal protein L12 OS=Homo sapiens GN=RPL12 PE=1 SV=1	HUMAN		1
223	2	2	13.7	sp|P02794|FRIH_HUM	Ferritin heavy chain OS=Homo sapiens GN=FTH1 PE=1 SV=2	HUMAN		1
224	2	2	5.3	sp|Q9Y224|CN166_HI	UPF0568 protein C14orf166 OS=Homo sapiens GN=C14orf166 PE=1 SV=1	HUMAN		1
225	2	2	7.6	sp|Q9UNL2|SSRG_HU	Translocon-associated protein subunit gamma OS=Homo sapiens GN=SSR3 PE=1 SV=1	HUMAN		2
226	2	2	7.5	sp|Q9H3N1|TMX1_HI	Thioredoxin-related transmembrane protein 1 OS=Homo sapiens GN=TMX1 PE=1 SV=1	HUMAN		1
227	2	2	4.2	sp|Q16563|SYPL1_HU	Synaptophysin-like protein 1 OS=Homo sapiens GN=SYPL1 PE=1 SV=1	HUMAN		1
228	2	2	10.5	sp|P99999|CYC_HUM	Cytochrome c OS=Homo sapiens GN=CYCS PE=1 SV=2	HUMAN		1
229	2	2	6.5	sp|P62834|RAP1A_HU	Ras-related protein Rap-1A OS=Homo sapiens GN=RAP1A PE=1 SV=1	HUMAN		1
230	2	2	17.7	sp|P60059|SC61G_HU	Protein transport protein Sec61 subunit gamma OS=Homo sapiens GN=SEC61G PE=2 SV=1	HUMAN		1
231	2	2	8.5	sp|P60033|CD81_HUM	CD81 antigen OS=Homo sapiens GN=CD81 PE=1 SV=1	HUMAN		1
232	2	2	4.2	sp|P31937|3HIDH_HU	3-hydroxyisobutyrate dehydrogenase, mitochondrial OS=Homo sapiens GN=HIBADH PE=1 SV=2	HUMAN		1
233	2	2	5.3	sp|P27695|APEX1_HU	DNA-(apurinic or apyrimidinic site) lyase OS=Homo sapiens GN=APEX1 PE=1 SV=2	HUMAN		1
234	2	2	10.4	sp|P17900|SAP3_HUM	Ganglioside GM2 activator OS=Homo sapiens GN=GM2A PE=1 SV=4	HUMAN		1
235	2	2	14	sp|P05386|RLA1_HUM	60S acidic ribosomal protein P1 OS=Homo sapiens GN=RPLP1 PE=1 SV=1	HUMAN		1
236	2	2	8.6	sp|P02792|FRIL_HUM	Ferritin light chain OS=Homo sapiens GN=FTL PE=1 SV=2	HUMAN		1
237	2	2	1.4	sp|O60716|CTND1_HI	Catenin delta-1 OS=Homo sapiens GN=CTNND1 PE=1 SV=1	HUMAN		1
238	1.91	1.91	13	sp|Q5JNZ5|RS26L_HU	Putative 40S ribosomal protein S26-like 1 OS=Homo sapiens GN=RPS26P11 PE=5 SV=1	HUMAN		1
240	1.89	1.89	1.6	sp|P48960|CD97_HUM	CD97 antigen OS=Homo sapiens GN=CD97 PE=1 SV=4	HUMAN		1
241	1.86	1.86	12	sp|P05388|RLA0_HUM	60S acidic ribosomal protein P0 OS=Homo sapiens GN=RPLP0 PE=1 SV=1	HUMAN		1
242	1.86	1.86	7.2	sp|P00338|LDHA_HUI	L-lactate dehydrogenase A chain OS=Homo sapiens GN=LDHA PE=1 SV=2	HUMAN		1
243	1.85	1.85	3.5	sp|P11047|LAMC1_HI	Laminin subunit gamma-1 OS=Homo sapiens GN=LAMC1 PE=1 SV=3	HUMAN		1
244	1.84	1.84	3.5	sp|P22307|NLTP_HUM	Non-specific lipid-transfer protein OS=Homo sapiens GN=SCP2 PE=1 SV=2	HUMAN		2
245	1.82	1.82	18.5	sp|Q16762|THTR_HU	Thiosulfate sulfurtransferase OS=Homo sapiens GN=TST PE=1 SV=4	HUMAN		2
246	1.81	1.81	10.2	sp|Q9Y285|SYFA_HUM	Phenylalanine--tRNA ligase alpha subunit OS=Homo sapiens GN=FARSA PE=1 SV=3	HUMAN		2
247	1.8	1.8	23.3	sp|P47914|RL29_HUM	60S ribosomal protein L29 OS=Homo sapiens GN=RPL29 PE=1 SV=2	HUMAN		1
248	1.79	1.82	23.6	sp|O95563|MPC2_HU	Mitochondrial pyruvate carrier 2 OS=Homo sapiens GN=BRP44 PE=1 SV=1	HUMAN		1
249	1.79	1.79	6.9	sp|P16278|BGAL_HUI	Beta-galactosidase OS=Homo sapiens GN=GLB1 PE=1 SV=2	HUMAN		1
250	1.74	1.74	6.6	sp|P21397|AOFA_HUI	Amine oxidase [flavin-containing] A OS=Homo sapiens GN=MAOA PE=1 SV=1	HUMAN		2
251	1.74	1.74	9.2	sp|P30405|PPIF_HUM	Peptidyl-prolyl cis-trans isomerase F, mitochondrial OS=Homo sapiens GN=PPIF PE=1 SV=1	HUMAN		1
252	1.72	1.72	4.1	sp|P46821|MAP1B_H	Microtubule-associated protein 1B OS=Homo sapiens GN=MAP1B PE=1 SV=2	HUMAN		1
253	1.72	1.72	7.6	sp|P38606|VATA_HUM	V-type proton ATPase catalytic subunit A OS=Homo sapiens GN=ATP6V1A PE=1 SV=2	HUMAN		1
254	1.72	1.72	21.5	sp|P30044|PRDX5_HU	Peroxiredoxin-5, mitochondrial OS=Homo sapiens GN=PRDX5 PE=1 SV=4	HUMAN		2
255	1.71	1.71	8.8	sp|Q13423|NNTM_HI	NAD(P) transhydrogenase, mitochondrial OS=Homo sapiens GN=NNT PE=1 SV=3	HUMAN		1
256	1.7	1.7	14.6	sp|Q03135|CAV1_HUI	Caveolin-1 OS=Homo sapiens GN=CAV1 PE=1 SV=4	HUMAN		1
257	1.69	1.71	11	sp|P61247|RS3A_HUM	40S ribosomal protein S3a OS=Homo sapiens GN=RPS3A PE=1 SV=2	HUMAN		1
258	1.69	1.69	47.6	sp|P82909|RT36_HUM	28S ribosomal protein S36, mitochondrial OS=Homo sapiens GN=MRPS36 PE=1 SV=2	HUMAN		1
259	1.68	1.68	16.2	sp|Q96DB5|RMD1_HI	Regulator of microtubule dynamics protein 1 OS=Homo sapiens GN=FAM82B PE=1 SV=1	HUMAN		1
260	1.67	1.67	9.4	sp|O60568|PLOD3_HI	Procollagen-lysine,2-oxoglutarate 5-dioxygenase 3 OS=Homo sapiens GN=PLOD3 PE=1 SV=1	HUMAN		1
261	1.66	1.66	21.2	sp|O75348|VATG1_HU	V-type proton ATPase subunit G 1 OS=Homo sapiens GN=ATP6V1G1 PE=1 SV=3	HUMAN		1
262	1.66	1.66	18.6	sp|P63173|RL38_HUM	60S ribosomal protein L38 OS=Homo sapiens GN=RPL38 PE=1 SV=2	HUMAN		1
263	1.64	1.64	13.8	sp|Q9UHL4|DPP2_HU	Dipeptidyl peptidase 2 OS=Homo sapiens GN=DPP7 PE=1 SV=3	HUMAN		1
264	1.62	1.62	3.2	sp|Q10713|MPPA_HU	Mitochondrial-processing peptidase subunit alpha OS=Homo sapiens GN=PMPCA PE=1 SV=2	HUMAN		1
265	1.6	1.6	35.1	sp|P30049|ATPD_HUM	ATP synthase subunit delta, mitochondrial OS=Homo sapiens GN=ATP5D PE=1 SV=2	HUMAN		3
266	1.59	1.59	9.1	sp|Q08257|QOR_HUM	Quinone oxidoreductase OS=Homo sapiens GN=CRYZ PE=1 SV=1	HUMAN		1
267	1.58	1.62	17.2	sp|P40429|RL13A_HU	60S ribosomal protein L13a OS=Homo sapiens GN=RPL13A PE=1 SV=2	HUMAN		1
268	1.55	1.55	4	sp|P02751|FINC_HUM	Fibronectin OS=Homo sapiens GN=FN1 PE=1 SV=4	HUMAN		1
269	1.53	1.53	9	sp|P04746|AMYP_HU	Pancreatic alpha-amylase OS=Homo sapiens GN=AMY2A PE=1 SV=2	HUMAN		2
270	1.49	1.49	3	sp|Q9Y639|NPTN_HU	Neuroplastin OS=Homo sapiens GN=NPTN PE=1 SV=2	HUMAN		1
271	1.47	1.47	9.7	sp|P57105|SYJ2B_HUI	Synaptojanin-2-binding protein OS=Homo sapiens GN=SYNJ2BP PE=1 SV=2	HUMAN		1
272	1.44	1.44	23.3	sp|P62424|RL7A_HUM	60S ribosomal protein L7a OS=Homo sapiens GN=RPL7A PE=1 SV=2	HUMAN		1
273	1.44	1.44	13.3	sp|P30038|AL4A1_HU	Delta-1-pyrroline-5-carboxylate dehydrogenase, mitochondrial OS=Homo sapiens GN=ALDH4A1 PE=1 SV=3	HUMAN		1
274	1.44	1.44	5.8	sp|P28288|ABCD3_HU	ATP-binding cassette sub-family D member 3 OS=Homo sapiens GN=ABCD3 PE=1 SV=1	HUMAN		1
275	1.43	1.44	15	sp|P46781|RS9_HUM	40S ribosomal protein S9 OS=Homo sapiens GN=RPS9 PE=1 SV=3	HUMAN		1
276	1.41	1.41	9.5	sp|P02545|LMNA_HU	Prelamin-A/C OS=Homo sapiens GN=LMNA PE=1 SV=1	HUMAN		1
277	1.4	1.4	11.8	sp|P27348|1433T_HU	14-3-3 protein theta OS=Homo sapiens GN=YWHAQ PE=1 SV=1	HUMAN		1
278	1.39	1.39	14.1	sp|Q16795|NDUA9_H	NADH dehydrogenase [ubiquinone] 1 alpha subcomplex subunit 9, mitochondrial OS=Homo sapiens GN=NDUFA9 PE=1 SV=2	HUMAN		1
279	1.38	1.38	4.9	sp|Q9NZ01|TECR_HU	Trans-2,3-enoyl-CoA reductase OS=Homo sapiens GN=TECR PE=1 SV=1	HUMAN		1
280	1.37	1.37	12.1	sp|P49821|NDUV1_H	NADH dehydrogenase [ubiquinone] flavoprotein 1, mitochondrial OS=Homo sapiens GN=NDUFV1 PE=1 SV=4	HUMAN		1
281	1.34	1.34	14.6	sp|Q9UL46|PSME2_H	Proteasome activator complex subunit 2 OS=Homo sapiens GN=PSME2 PE=1 SV=4	HUMAN		1
282	1.33	1.33	11.3	sp|O60220|TIM8A_HU	Mitochondrial import inner membrane translocase subunit Tim8 A OS=Homo sapiens GN=TIMM8A PE=1 SV=1	HUMAN		1
283	1.32	1.32	4.1	sp|P31939|PUR9_HUM	Bifunctional purine biosynthesis protein PURH OS=Homo sapiens GN=ATIC PE=1 SV=3	HUMAN		1
284	1.31	1.31	5.3	sp|P19367|HXK1_HUM	Hexokinase-1 OS=Homo sapiens GN=HK1 PE=1 SV=3	HUMAN		1
285	1.31	1.31	19.6	sp|Q59GN2|R39L5_HU	Putative 60S ribosomal protein L39-like 5 OS=Homo sapiens GN=RPL39P5 PE=5 SV=2	HUMAN		1

Supplemental table S4: Proteins identified using Protein Pilot SDS-LC

N	Unused	Total	% Cov	Accession #	Name	Species	Peptides(95%)
1	88.06	88.06	38.2	sp|P35579|MYH9_HUMAN	Myosin-9 OS=Homo sapiens GN=MYH9 PE=1 SV=4	HUMAN	46
3	68.95	68.95	26.4	sp|P12111|CO6A3_HUMAN	Collagen alpha-3(VI) chain OS=Homo sapiens GN=COL6A3 PE=1 SV=5	HUMAN	40
7	56.93	56.93	81.1	sp|P07355|ANXA2_HUMAN	Annexin A2 OS=Homo sapiens GN=ANXA2 PE=1 SV=2	HUMAN	40
2	70	70	65.8	sp|P11021|GRP78_HUMAN	78 kDa glucose-regulated protein OS=Homo sapiens GN=HSPA5 PE=1 SV=2	HUMAN	37
10	53.01	53.47	60.9	sp|P04264|K2C1_HUMAN	Keratin, type II cytoskeletal 1 OS=Homo sapiens GN=KRT1 PE=1 SV=6	HUMAN	36
5	59.4	59.4	70.8	sp|P08670|VIME_HUMAN	Vimentin OS=Homo sapiens GN=VIM PE=1 SV=4	HUMAN	34
8	56.83	56.83	37.6	sp|P15144|AMPN_HUMAN	Aminopeptidase N OS=Homo sapiens GN=ANPEP PE=1 SV=4	HUMAN	33
4	60.69	60.69	19	sp|Q15149|PLEC_HUMAN	Plectin OS=Homo sapiens GN=PLEC PE=1 SV=3	HUMAN	30
9	56.21	56.21	45.2	sp|Q14697|GANAB_HUMAN	Neutral alpha-glucosidase AB OS=Homo sapiens GN=GANAB PE=1 SV=3	HUMAN	30
6	59.1	59.1	47.6	sp|P14625|ENPL_HUMAN	Endoplasmin OS=Homo sapiens GN=HSP90B1 PE=1 SV=1	HUMAN	29
23	35.68	35.68	72.7	sp|P23284|PPIB_HUMAN	Peptidyl-prolyl cis-trans isomerase B OS=Homo sapiens GN=PPIB PE=1 SV=2	HUMAN	28
13	45.59	45.59	60.4	sp|P25705|ATPA_HUMAN	ATP synthase subunit alpha, mitochondrial OS=Homo sapiens GN=ATP5A1 PE=1 SV=1	HUMAN	27
627	0.31	42.43	72.9	sp|A6NMY6|AXA2L_HUMAN	Putative annexin A2-like protein OS=Homo sapiens GN=ANXA2P2 PE=5 SV=2	HUMAN	27
12	45.69	45.69	58.9	sp|P07237|PDIA1_HUMAN	Protein disulfide-isomerase OS=Homo sapiens GN=P4HB PE=1 SV=3	HUMAN	26
15	45.04	45.04	60.2	sp|P30101|PDIA3_HUMAN	Protein disulfide-isomerase A3 OS=Homo sapiens GN=PDIA3 PE=1 SV=4	HUMAN	26
20	40.54	40.54	65.5	sp|P27797|CALR_HUMAN	Calreticulin OS=Homo sapiens GN=CALR PE=1 SV=1	HUMAN	26
17	42.21	42.21	51.7	sp|P38646|GRP75_HUMAN	Stress-70 protein, mitochondrial OS=Homo sapiens GN=HSPA9 PE=1 SV=2	HUMAN	25
11	50.11	50.11	31.6	sp|Q9NZM1|MYOF_HUMAN	Myoferlin OS=Homo sapiens GN=MYOF PE=1 SV=1	HUMAN	24
14	45.39	45.39	45.2	sp|P40939|ECHA_HUMAN	Trifunctional enzyme subunit alpha, mitochondrial OS=Homo sapiens GN=HADHA PE=1 SV=2	HUMAN	24
16	43.58	43.58	66	sp|P06576|ATPB_HUMAN	ATP synthase subunit beta, mitochondrial OS=Homo sapiens GN=ATP5B PE=1 SV=3	HUMAN	24
43	22.76	22.76	71.6	sp|P04179|SODM_HUMAN	Superoxide dismutase [Mn], mitochondrial OS=Homo sapiens GN=SOD2 PE=1 SV=2	HUMAN	24
26	34.04	34.04	60.3	sp|P60709|ACTB_HUMAN	Actin, cytoplasmic 1 OS=Homo sapiens GN=ACTB PE=1 SV=1	HUMAN	23
566	0.73	33.62	60.3	sp|P63261|ACTG_HUMAN	Actin, cytoplasmic 2 OS=Homo sapiens GN=ACTG1 PE=1 SV=1	HUMAN	23
21	39.08	39.4	53.3	sp|Q07065|CKAP4_HUMAN	Cytoskeleton-associated protein 4 OS=Homo sapiens GN=CKAP4 PE=1 SV=2	HUMAN	22
18	41.31	41.31	59.4	sp|P08133|ANXA6_HUMAN	Annexin A6 OS=Homo sapiens GN=ANXA6 PE=1 SV=3	HUMAN	21
29	32.27	32.27	49.1	sp|P00367|DHE3_HUMAN	Glutamate dehydrogenase 1, mitochondrial OS=Homo sapiens GN=GLUD1 PE=1 SV=2	HUMAN	21
19	40.69	40.69	37	sp|P12814|ACTN1_HUMAN	Alpha-actinin-1 OS=Homo sapiens GN=ACTN1 PE=1 SV=2	HUMAN	20
22	37.24	37.24	51.8	sp|P13667|PDIA4_HUMAN	Protein disulfide-isomerase A4 OS=Homo sapiens GN=PDIA4 PE=1 SV=2	HUMAN	20
32	30.24	30.24	71.6	sp|P04406|G3P_HUMAN	Glyceraldehyde-3-phosphate dehydrogenase OS=Homo sapiens GN=GAPDH PE=1 SV=3	HUMAN	20
24	35.23	35.23	73.9	sp|P21796|VDAC1_HUMAN	Voltage-dependent anion-selective channel protein 1 OS=Homo sapiens GN=VDAC1 PE=1 SV=2	HUMAN	19
27	34.41	34.41	47.9	sp|P55084|ECHB_HUMAN	Trifunctional enzyme subunit beta, mitochondrial OS=Homo sapiens GN=HADHB PE=1 SV=3	HUMAN	18
28	33.75	33.75	35.6	sp|P08473|NEP_HUMAN	Neprilysin OS=Homo sapiens GN=MME PE=1 SV=2	HUMAN	18
95	33.53	33.53	71.1	sp|P50454|SERPH_HUMAN	Serpin H1 OS=Homo sapiens GN=SERPINH1 PE=1 SV=2	HUMAN	18
34	12.9	32.42	37.2	sp|O43707|ACTN4_HUMAN	Alpha-actinin-4 OS=Homo sapiens GN=ACTN4 PE=1 SV=2	HUMAN	18
30	28.88	28.88	49.9	sp|P10809|CH60_HUMAN	60 kDa heat shock protein, mitochondrial OS=Homo sapiens GN=HSPD1 PE=1 SV=2	HUMAN	17
33	32.17	32.17	44.4	sp|P26038|MOES_HUMAN	Moesin OS=Homo sapiens GN=MSN PE=1 SV=3	HUMAN	16
31	29.19	29.19	57	sp|P35527|K1C9_HUMAN	Keratin, type I cytoskeletal 9 OS=Homo sapiens GN=KRT9 PE=1 SV=3	HUMAN	16
35	30.58	30.58	70.9	sp|Q99623|PHB2_HUMAN	Prohibitin-2 OS=Homo sapiens GN=PHB2 PE=1 SV=2	HUMAN	15
39	28.76	28.76	16.1	sp|Q13813|SPTN1_HUMAN	Spectrin alpha chain, non-erythrocytic 1 OS=Homo sapiens GN=SPTAN1 PE=1 SV=3	HUMAN	15
36	24.74	24.74	58.8	sp|P00387|NB5R3_HUMAN	NADH-cytochrome b5 reductase 3 OS=Homo sapiens GN=CYB5R3 PE=1 SV=3	HUMAN	15
37	28.05	28.27	74.1	sp|P08758|ANXA5_HUMAN	Annexin A5 OS=Homo sapiens GN=ANXA5 PE=1 SV=2	HUMAN	14
41	26.02	26.02	43.2	sp|P04843|RPN1_HUMAN	Dolichyl-diphosphooligosaccharide--protein glycosyltransferase subunit 1 OS=Homo sapiens GN=RPN1 PE=1 SV=1	HUMAN	14
42	23.42	23.42	57.5	sp|Q9BWM7|SFXN3_HUMAN	Sideroflexin-3 OS=Homo sapiens GN=SFXN3 PE=2 SV=2	HUMAN	14
51	22.92	22.92	30.2	sp|P27824|CALX_HUMAN	Calnexin OS=Homo sapiens GN=CANX PE=1 SV=2	HUMAN	14
52	20.44	20.44	40.2	sp|P24539|AT5F1_HUMAN	ATP synthase subunit b, mitochondrial OS=Homo sapiens GN=ATP5F1 PE=1 SV=2	HUMAN	14
38	20.17	22.23	36.3	sp|Q9H9B4|SFXN1_HUMAN	Sideroflexin-1 OS=Homo sapiens GN=SFXN1 PE=1 SV=4	HUMAN	14
58	25.31	25.31	30.6	sp|Q3SY69|AL1L2_HUMAN	Mitochondrial 10-formyltetrahydrofolate dehydrogenase OS=Homo sapiens GN=ALDH1L2 PE=1 SV=2	HUMAN	13
54	18.98	18.98	42.1	sp|P31930|QCR1_HUMAN	Cytochrome b-c1 complex subunit 1, mitochondrial OS=Homo sapiens GN=UQCRC1 PE=1 SV=3	HUMAN	13
45	23.67	23.67	29.5	sp|Q16822|PCKGM_HUMAN	Phosphoenolpyruvate carboxykinase [GTP], mitochondrial OS=Homo sapiens GN=PCK2 PE=1 SV=3	HUMAN	12
47	21.75	21.75	41.8	sp|P13645|K1C10_HUMAN	Keratin, type I cytoskeletal 10 OS=Homo sapiens GN=KRT10 PE=1 SV=6	HUMAN	12
47	20.98	20.98	30.3	sp|P07099|HYEP_HUMAN	Epoxide hydrolase 1 OS=Homo sapiens GN=EPHX1 PE=1 SV=1	HUMAN	12
48	20.93	20.93	40.5	sp|P34897|GLYM_HUMAN	Serine hydroxymethyltransferase, mitochondrial OS=Homo sapiens GN=SHMT2 PE=1 SV=3	HUMAN	12
69	17.54	17.54	35.2	sp|P17931|LEG3_HUMAN	Galectin-3 OS=Homo sapiens GN=LGALS3 PE=1 SV=5	HUMAN	12
46	21.36	21.36	18.7	sp|Q9P2E9|RRBP1_HUMAN	Ribosome-binding protein 1 OS=Homo sapiens GN=RRBP1 PE=1 SV=4	HUMAN	11
49	20.76	20.76	41.6	sp|Q9Y6N5|SQRD_HUMAN	Sulfide:quinone oxidoreductase, mitochondrial OS=Homo sapiens GN=SQRDL PE=1 SV=1	HUMAN	11
50	20.56	22.64	40.6	sp|P11142|HSP7C_HUMAN	Heat shock cognate 71 kDa protein OS=Homo sapiens GN=HSPA8 PE=1 SV=1	HUMAN	11
53	19.98	19.98	34.2	sp|Q7KZF4|SND1_HUMAN	Staphylococcal nuclease domain-containing protein 1 OS=Homo sapiens GN=SND1 PE=1 SV=1	HUMAN	11
54	19.83	19.83	38.2	sp|Q15084|PDIA6_HUMAN	Protein disulfide-isomerase A6 OS=Homo sapiens GN=PDIA6 PE=1 SV=1	HUMAN	11
71	17.39	17.39	34.7	sp|P00505|AATM_HUMAN	Aspartate aminotransferase, mitochondrial OS=Homo sapiens GN=GOT2 PE=1 SV=3	HUMAN	11
44	22.62	22.62	36.2	sp|P21397|AOFA_HUMAN	Amine oxidase [flavin-containing] A OS=Homo sapiens GN=MAOA PE=1 SV=1	HUMAN	10
55	19.7	19.7	20.7	sp|Q02218|ODO1_HUMAN	2-oxoglutarate dehydrogenase, mitochondrial OS=Homo sapiens GN=OGDH PE=1 SV=3	HUMAN	10
56	19.57	19.57	46	sp|P18124|RL7_HUMAN	60S ribosomal protein L7 OS=Homo sapiens GN=RPL7 PE=1 SV=1	HUMAN	10
57	19.46	19.46	24.4	sp|P05091|ALDH2_HUMAN	Aldehyde dehydrogenase, mitochondrial OS=Homo sapiens GN=ALDH2 PE=1 SV=2	HUMAN	10
62	18.09	18.09	15.9	sp|P21333|FLNA_HUMAN	Filamin-A OS=Homo sapiens GN=FLNA PE=1 SV=4	HUMAN	10
64	18.02	19.13	50.4	sp|P35232|PHB_HUMAN	Prohibitin OS=Homo sapiens GN=PHB PE=1 SV=1	HUMAN	10
66	17.87	17.87	43.5	sp|P07437|TBB5_HUMAN	Tubulin beta chain OS=Homo sapiens GN=TUBB PE=1 SV=2	HUMAN	10
110	10.88	18.36	40.4	sp|P35908|K22E_HUMAN	Keratin, type II cytoskeletal 2 epidermal OS=Homo sapiens GN=KRT2 PE=1 SV=2	HUMAN	10
59	18.76	18.76	17.5	sp|Q32P28|P3H1_HUMAN	Prolyl 3-hydroxylase 1 OS=Homo sapiens GN=LEPRE1 PE=1 SV=2	HUMAN	9
60	18.65	18.65	25.9	sp|P31040|DHSA_HUMAN	Succinate dehydrogenase [ubiquinone] flavoprotein subunit, mitochondrial OS=Homo sapiens GN=SDHA PE=1 SV=2	HUMAN	9
61	18.64	18.65	28.5	sp|O75390|CISY_HUMAN	Citrate synthase, mitochondrial OS=Homo sapiens GN=CS PE=1 SV=2	HUMAN	9
63	18.03	18.03	29.4	sp|P28331|NDUS1_HUMAN	NADH-ubiquinone oxidoreductase 75 kDa subunit, mitochondrial OS=Homo sapiens GN=NDUFS1 PE=1 SV=3	HUMAN	9
65	17.93	17.93	41	sp|P24752|THIL_HUMAN	Acetyl-CoA acetyltransferase, mitochondrial OS=Homo sapiens GN=ACAT1 PE=1 SV=1	HUMAN	9
67	17.7	17.7	25.4	sp|P39656|OST48_HUMAN	Dolichyl-diphosphooligosaccharide--protein glycosyltransferase 48 kDa subunit OS=Homo sapiens GN=DDOST PE=1 SV=4	HUMAN	9
68	17.64	17.64	62.5	sp|P62269|RS18_HUMAN	40S ribosomal protein S18 OS=Homo sapiens GN=RPS18 PE=1 SV=3	HUMAN	9
70	17.42	17.42	22.4	sp|P42704|LPPRC_HUMAN	Leucine-rich PPR motif-containing protein, mitochondrial OS=Homo sapiens GN=LRPPRC PE=1 SV=3	HUMAN	9
72	16.91	16.91	47	sp|P40926|MDHM_HUMAN	Malate dehydrogenase, mitochondrial OS=Homo sapiens GN=MDH2 PE=1 SV=3	HUMAN	9
74	16.14	16.14	28.9	sp|P22695|QCR2_HUMAN	Cytochrome b-c1 complex subunit 2, mitochondrial OS=Homo sapiens GN=UQCRC2 PE=1 SV=3	HUMAN	9
75	15.99	15.99	50.2	sp|P26373|RL13_HUMAN	60S ribosomal protein L13 OS=Homo sapiens GN=RPL13 PE=1 SV=4	HUMAN	9
78	15.42	15.42	29.2	sp|P07954|FUMH_HUMAN	Fumarate hydratase, mitochondrial OS=Homo sapiens GN=FH PE=1 SV=3	HUMAN	9
96	12.81	12.81	28.9	sp|P46781|RS9_HUMAN	40S ribosomal protein S9 OS=Homo sapiens GN=RPS9 PE=1 SV=3	HUMAN	9
98	12.64	12.64	27.1	sp|P07858|CATB_HUMAN	Cathepsin B OS=Homo sapiens GN=CTSB PE=1 SV=3	HUMAN	9
128	9.69	9.69	38	sp|Q8N8S9|TXND5_HUMAN	Thioredoxin domain-containing protein 5 OS=Homo sapiens GN=TXNDC5 PE=1 SV=2	HUMAN	9
296	3.97	16.11	12.9	sp|P35580|MYH10_HUMAN	Myosin-10 OS=Homo sapiens GN=MYH10 PE=1 SV=3	HUMAN	9
668	0.14	17.36	37.3	sp|P68371|TBB4B_HUMAN	Tubulin beta-4B chain OS=Homo sapiens GN=TUBB4B PE=1 SV=1	HUMAN	9
73	16.7	16.7	50.9	sp|P48735|IDHP_HUMAN	Isocitrate dehydrogenase [NADP], mitochondrial OS=Homo sapiens GN=IDH2 PE=1 SV=2	HUMAN	8
79	14.72	14.72	53.4	sp|P62249|RS16_HUMAN	40S ribosomal protein S16 OS=Homo sapiens GN=RPS16 PE=1 SV=2	HUMAN	8
89	13.16	13.16	44.6	sp|O00264|PGRC1_HUMAN	Membrane-associated progesterone receptor component 1 OS=Homo sapiens GN=PGRMC1 PE=1 SV=3	HUMAN	8
90	13.13	13.13	21.7	sp|Q96AY3|FKB10_HUMAN	Peptidyl-prolyl cis-trans isomerase FKBP10 OS=Homo sapiens GN=FKBP10 PE=1 SV=1	HUMAN	8
91	13.05	13.05	39.1	sp|P36578|RL4_HUMAN	60S ribosomal protein L4 OS=Homo sapiens GN=RPL4 PE=1 SV=5	HUMAN	8
76	15.52	15.52	10.8	sp|Q01082|SPTB2_HUMAN	Spectrin beta chain, non-erythrocytic 1 OS=Homo sapiens GN=SPTBN1 PE=1 SV=2	HUMAN	7
77	15.49	15.49	29.4	sp|P04181|OAT_HUMAN	Ornithine aminotransferase, mitochondrial OS=Homo sapiens GN=OAT PE=1 SV=1	HUMAN	7
80	14.44	14.44	30.5	sp|P49411|EFTU_HUMAN	Elongation factor Tu, mitochondrial OS=Homo sapiens GN=TUFM PE=1 SV=2	HUMAN	7
81	14.02	14.02	41.3	sp|Q02878|RL6_HUMAN	60S ribosomal protein L6 OS=Homo sapiens GN=RPL6 PE=1 SV=3	HUMAN	7
82	13.88	13.88	58.6	sp|P39019|RS19_HUMAN	40S ribosomal protein S19 OS=Homo sapiens GN=RPS19 PE=1 SV=2	HUMAN	7
83	13.86	13.86	26.8	sp|Q16181|SEPT7_HUMAN	Septin-7 OS=Homo sapiens GN=SEPT7 PE=1 SV=2	HUMAN	7
84	13.73	13.73	63.4	sp|O75947|ATP5H_HUMAN	ATP synthase subunit d, mitochondrial OS=Homo sapiens GN=ATP5H PE=1 SV=3	HUMAN	7
85	13.71	13.71	39.2	sp|P61313|RL15_HUMAN	60S ribosomal protein L15 OS=Homo sapiens GN=RPL15 PE=1 SV=2	HUMAN	7
87	13.26	13.26	31.9	sp|Q6NUK1|SCMC1_HUMAN	Calcium-binding mitochondrial carrier protein SCaMC-1 OS=Homo sapiens GN=SLC25A24 PE=1 SV=2	HUMAN	7
88	13.21	13.21	52.6	sp|P04083|ANXA1_HUMAN	Annexin A1 OS=Homo sapiens GN=ANXA1 PE=1 SV=2	HUMAN	7
94	12.97	12.97	44.8	sp|Q99714|HCD2_HUMAN	3-hydroxyacyl-CoA dehydrogenase type-2 OS=Homo sapiens GN=HSD17B10 PE=1 SV=3	HUMAN	7
97	12.67	12.67	47.5	sp|P13804|ETFA_HUMAN	Electron transfer flavoprotein subunit alpha, mitochondrial OS=Homo sapiens GN=ETFA PE=1 SV=1	HUMAN	7
101	11.93	11.93	54.2	sp|P27635|RL10_HUMAN	60S ribosomal protein L10 OS=Homo sapiens GN=RPL10 PE=1 SV=4	HUMAN	7
108	11.15	11.15	13.5	sp|P14314|GLU2B_HUMAN	Glucosidase 2 subunit beta OS=Homo sapiens GN=PRKCSH PE=1 SV=2	HUMAN	7
111	10.72	10.72	53.1	sp|P48047|ATPO_HUMAN	ATP synthase subunit O, mitochondrial OS=Homo sapiens GN=ATP5O PE=1 SV=1	HUMAN	7
86	13.52	13.52	62.7	sp|P13073|COX41_HUMAN	Cytochrome c oxidase subunit 4 isoform 1, mitochondrial OS=Homo sapiens GN=COX4I1 PE=1 SV=1	HUMAN	6
92	12.99	12.99	19.9	sp|O94832|MYO1D_HUMAN	Unconventional myosin-Id OS=Homo sapiens GN=MYO1D PE=1 SV=2	HUMAN	6
93	12.98	12.98	59.6	sp|P60660|MYL6_HUMAN	Myosin light polypeptide 6 OS=Homo sapiens GN=MYL6 PE=1 SV=2	HUMAN	6
99	12.17	12.17	32.6	sp|P05141|ADT2_HUMAN	ADP/ATP translocase 2 OS=Homo sapiens GN=SLC25A5 PE=1 SV=7	HUMAN	6
100	12.16	12.16	17.7	sp|P49748|ACADV_HUMAN	Very long-chain specific acyl-CoA dehydrogenase, mitochondrial OS=Homo sapiens GN=ACADVL PE=1 SV=1	HUMAN	6
102	11.89	11.89	27.9	sp|P11177|ODPB_HUMAN	Pyruvate dehydrogenase E1 component subunit beta, mitochondrial OS=Homo sapiens GN=PDHB PE=1 SV=3	HUMAN	6
104	11.57	11.57	30.5	sp|P30048|PRDX3_HUMAN	Thioredoxin-dependent peroxide reductase, mitochondrial OS=Homo sapiens GN=PRDX3 PE=1 SV=3	HUMAN	6
105	11.27	11.27	26.8	sp|P30040|ERP29_HUMAN	Endoplasmic reticulum resident protein 29 OS=Homo sapiens GN=ERP29 PE=1 SV=4	HUMAN	6
106	11.26	11.26	39.8	sp|O75489|NDUS3_HUMAN	NADH dehydrogenase [ubiquinone] iron-sulfur protein 3, mitochondrial OS=Homo sapiens GN=NDUFS3 PE=1 SV=1	HUMAN	6
107	11.23	11.23	30.2	sp|Q13011|ECH1_HUMAN	Delta(3,5)-Delta(2,4)-dienoyl-CoA isomerase, mitochondrial OS=Homo sapiens GN=ECH1 PE=1 SV=2	HUMAN	6
109	11.1	11.1	29.7	sp|P06733|ENOA_HUMAN	Alpha-enolase OS=Homo sapiens GN=ENO1 PE=1 SV=2	HUMAN	6
114	10.46	10.46	26.5	sp|O15173|PGRC2_HUMAN	Membrane-associated progesterone receptor component 2 OS=Homo sapiens GN=PGRMC2 PE=1 SV=1	HUMAN	6
115	10.4	10.4	15.5	sp|O14773|TPP1_HUMAN	Tripeptidyl-peptidase 1 OS=Homo sapiens GN=TPP1 PE=1 SV=2	HUMAN	6
119	10.1	10.1	35.6	sp|O43852|CALU_HUMAN	Calumenin OS=Homo sapiens GN=CALU PE=1 SV=2	HUMAN	6
121	10.03	10.03	43.9	sp|Q04837|SSBP_HUMAN	Single-stranded DNA-binding protein, mitochondrial OS=Homo sapiens GN=SSBP1 PE=1 SV=1	HUMAN	6
122	10.01	10.01	44.7	sp|P42766|RL35_HUMAN	60S ribosomal protein L35 OS=Homo sapiens GN=RPL35 PE=1 SV=2	HUMAN	6
124	9.84	9.84	23.9	sp|Q16795|NDUA9_HUMAN	NADH dehydrogenase [ubiquinone] 1 alpha subcomplex subunit 9, mitochondrial OS=Homo sapiens GN=NDUFA9 PE=1 SV=2	HUMAN	6
125	9.8	9.8	22.7	sp|Q9UHD8|SEPT9_HUMAN	Septin-9 OS=Homo sapiens GN=SEPT9 PE=1 SV=2	HUMAN	6

N	Unused	Total	% Cov	Accession #	Name	Species	Peptides(95%)
129	9.64	9.64	22.9	sp|P46777|RL5_HUMAN	60S ribosomal protein L5 OS=Homo sapiens GN=RPL5 PE=1 SV=3	HUMAN	6
130	9.56	9.56	44	sp|P09669|COX6C_HUMAN	Cytochrome c oxidase subunit 6C OS=Homo sapiens GN=COX6C PE=1 SV=2	HUMAN	6
136	9.19	9.19	35.3	sp|P63244|GBLP_HUMAN	Guanine nucleotide-binding protein subunit beta-2-like 1 OS=Homo sapiens GN=GNB2L1 PE=1 SV=3	HUMAN	6
143	8.66	8.66	50.9	sp|Q9UII2|ATIF1_HUMAN	ATPase inhibitor, mitochondrial OS=Homo sapiens GN=ATPIF1 PE=1 SV=1	HUMAN	6
165	7.76	7.76	19.6	sp|Q9BVK6|TMED9_HUMAN	Transmembrane emp24 domain-containing protein 9 OS=Homo sapiens GN=TMED9 PE=1 SV=2	HUMAN	6
191	6.66	6.66	55.7	sp|P62854|RS26_HUMAN	40S ribosomal protein S26 OS=Homo sapiens GN=RPS26 PE=1 SV=3	HUMAN	6
267	4.33	10.81	18.6	sp|P13647|K2C5_HUMAN	Keratin, type II cytoskeletal 5 OS=Homo sapiens GN=KRT5 PE=1 SV=3	HUMAN	6
373	2.3	2.3	20	sp|P02452|CO1A1_HUMAN	Collagen alpha-1(I) chain OS=Homo sapiens GN=COL1A1 PE=1 SV=5	HUMAN	6
103	11.76	11.76	33.3	sp|Q8ETX2|ACOT1_HUMAN	Acyl-coenzyme A thioesterase 1 OS=Homo sapiens GN=ACOT1 PE=1 SV=1	HUMAN	5
112	10.58	10.58	38	sp|P42765|THIM_HUMAN	3-ketoacyl-CoA thiolase, mitochondrial OS=Homo sapiens GN=ACAA2 PE=1 SV=2	HUMAN	5
113	10.58	10.58	32.6	sp|P36542|ATPG_HUMAN	ATP synthase subunit gamma, mitochondrial OS=Homo sapiens GN=ATP5C1 PE=1 SV=1	HUMAN	5
116	10.32	10.32	21.1	sp|Q14108|SCRB2_HUMAN	Lysosome membrane protein 2 OS=Homo sapiens GN=SCARB2 PE=1 SV=2	HUMAN	5
117	10.17	10.17	28.8	sp|Q15019|SEPT2_HUMAN	Septin-2 OS=Homo sapiens GN=SEPT2 PE=1 SV=1	HUMAN	5
118	10.13	10.13	26.8	sp|P50213|IDH3A_HUMAN	Isocitrate dehydrogenase [NAD] subunit alpha, mitochondrial OS=Homo sapiens GN=IDH3A PE=1 SV=1	HUMAN	5
120	10.05	10.05	32.3	sp|P30512|1A29_HUMAN	HLA class I histocompatibility antigen, A-29 alpha chain OS=Homo sapiens GN=HLA-A PE=2 SV=2	HUMAN	5
126	9.79	9.79	28	sp|P08559|ODPA_HUMAN	Pyruvate dehydrogenase E1 component subunit alpha, somatic form, mitochondrial OS=Homo sapiens GN=PDHA1 PE=1 SV=3	HUMAN	5
131	9.45	9.45	24.3	sp|P21912|DHSB_HUMAN	Succinate dehydrogenase [ubiquinone] iron-sulfur subunit, mitochondrial OS=Homo sapiens GN=SDHB PE=1 SV=3	HUMAN	5
132	9.37	9.37	34.6	sp|P22570|ADRO_HUMAN	NADPH:adrenodoxin oxidoreductase, mitochondrial OS=Homo sapiens GN=FDXR PE=1 SV=3	HUMAN	5
133	9.33	9.33	26.5	sp|P07339|CATD_HUMAN	Cathepsin D OS=Homo sapiens GN=CTSD PE=1 SV=1	HUMAN	5
135	9.27	9.27	24	sp|P02545|LMNA_HUMAN	Prelamin-A/C OS=Homo sapiens GN=LMNA PE=1 SV=1	HUMAN	5
137	9.06	9.06	50.7	sp|P61353|RL27_HUMAN	60S ribosomal protein L27 OS=Homo sapiens GN=RPL27 PE=1 SV=2	HUMAN	5
138	8.96	8.96	26.4	sp|Q9Y6C9|MTCH2_HUMAN	Mitochondrial carrier homolog 2 OS=Homo sapiens GN=MTCH2 PE=1 SV=1	HUMAN	5
139	8.92	8.92	13.8	sp|P13639|EF2_HUMAN	Elongation factor 2 OS=Homo sapiens GN=EEF2 PE=1 SV=4	HUMAN	5
140	8.9	8.9	24.1	sp|Q96I99|SUCB2_HUMAN	Succinyl-CoA ligase [GDP-forming] subunit beta, mitochondrial OS=Homo sapiens GN=SUCLG2 PE=1 SV=2	HUMAN	5
141	8.85	8.85	38.3	sp|P67936|TPM4_HUMAN	Tropomyosin alpha-4 chain OS=Homo sapiens GN=TPM4 PE=1 SV=3	HUMAN	5
146	8.35	8.35	25.4	sp|Q16698|DECR_HUMAN	2,4-dienoyl-CoA reductase, mitochondrial OS=Homo sapiens GN=DECR1 PE=1 SV=1	HUMAN	5
148	8.21	8.21	59.6	sp|P62241|RS8_HUMAN	40S ribosomal protein S8 OS=Homo sapiens GN=RPS8 PE=1 SV=2	HUMAN	5
149	8.2	8.2	36.1	sp|P45880|VDAC2_HUMAN	Voltage-dependent anion-selective channel protein 2 OS=Homo sapiens GN=VDAC2 PE=1 SV=2	HUMAN	5
150	8.18	8.18	41.4	sp|P62424|RL7A_HUMAN	60S ribosomal protein L7a OS=Homo sapiens GN=RPL7A PE=1 SV=2	HUMAN	5
159	8	8	30.8	sp|Q9BTV4|TMM43_HUMAN	Transmembrane protein 43 OS=Homo sapiens GN=TMEM43 PE=1 SV=1	HUMAN	5
168	7.61	7.61	17.7	sp|P36776|LONM_HUMAN	Lon protease homolog, mitochondrial OS=Homo sapiens GN=LONP1 PE=1 SV=2	HUMAN	5
181	7.05	7.05	17.2	sp|P15586|GNS_HUMAN	N-acetylglucosamine-6-sulfatase OS=Homo sapiens GN=GNS PE=1 SV=3	HUMAN	5
190	6.71	6.71	16	sp|Q00325|MPCP_HUMAN	Phosphate carrier protein, mitochondrial OS=Homo sapiens GN=SLC25A3 PE=1 SV=2	HUMAN	5
216	5.86	5.86	18.7	sp|Q13505|MTX1_HUMAN	Metaxin-1 OS=Homo sapiens GN=MTX1 PE=1 SV=2	HUMAN	5
222	5.65	5.65	20	sp|P08574|CY1_HUMAN	Cytochrome c1, heme protein, mitochondrial OS=Homo sapiens GN=CYC1 PE=1 SV=3	HUMAN	5
231	5.42	9.65	22.9	sp|P02533|K1C14_HUMAN	Keratin, type I cytoskeletal 14 OS=Homo sapiens GN=KRT14 PE=1 SV=4	HUMAN	5
127	9.73	9.73	24.7	sp|Q99798|ACON_HUMAN	Aconitate hydratase, mitochondrial OS=Homo sapiens GN=ACO2 PE=1 SV=2	HUMAN	4
134	9.3	10.37	32.3	sp|Q15293|RCN1_HUMAN	Reticulocalbin-1 OS=Homo sapiens GN=RCN1 PE=1 SV=1	HUMAN	4
142	8.72	8.72	12.7	sp|P11940|PABP1_HUMAN	Polyadenylate-binding protein 1 OS=Homo sapiens GN=PABPC1 PE=1 SV=2	HUMAN	4
144	8.51	8.51	23.8	sp|Q9BQE3|TBA1C_HUMAN	Tubulin alpha-1C chain OS=Homo sapiens GN=TUBA1C PE=1 SV=1	HUMAN	4
145	8.49	8.49	36.4	sp|P62277|RS13_HUMAN	40S ribosomal protein S13 OS=Homo sapiens GN=RPS13 PE=1 SV=2	HUMAN	4
147	8.24	8.24	15.4	sp|Q9NVA2|SEPT11_HUMAN	Septin-11 OS=Homo sapiens GN=SEPT11 PE=1 SV=3	HUMAN	4
151	8.16	8.16	72.3	sp|P80723|BASP1_HUMAN	Brain acid soluble protein 1 OS=Homo sapiens GN=BASP1 PE=1 SV=2	HUMAN	4
152	8.13	8.13	21.9	sp|P48449|ERG7_HUMAN	Lanosterol synthase OS=Homo sapiens GN=LSS PE=1 SV=1	HUMAN	4
153	8.11	8.11	20.1	sp|P07686|HEXB_HUMAN	Beta-hexosaminidase subunit beta OS=Homo sapiens GN=HEXB PE=1 SV=3	HUMAN	4
154	8.08	8.08	16.6	sp|Q02252|MMSA_HUMAN	Methylmalonate-semialdehyde dehydrogenase [acylating], mitochondrial OS=Homo sapiens GN=ALDH6A1 PE=1 SV=2	HUMAN	4
155	8.05	8.05	29.9	sp|P61247|RS3A_HUMAN	40S ribosomal protein S3a OS=Homo sapiens GN=RPS3A PE=1 SV=2	HUMAN	4
156	8.05	8.05	26.9	sp|Q3ZCQ8|TIM50_HUMAN	Mitochondrial import inner membrane translocase subunit TIM50 OS=Homo sapiens GN=TIMM50 PE=1 SV=2	HUMAN	4
157	8.03	8.03	40.1	sp|P62906|RL10A_HUMAN	60S ribosomal protein L10a OS=Homo sapiens GN=RPL10A PE=1 SV=2	HUMAN	4
158	8.02	8.02	23.5	sp|P30084|ECHM_HUMAN	Enoyl-CoA hydratase, mitochondrial OS=Homo sapiens GN=ECHS1 PE=1 SV=4	HUMAN	4
160	8	8	40.7	sp|P08865|RSSA_HUMAN	40S ribosomal protein SA OS=Homo sapiens GN=RPSA PE=1 SV=4	HUMAN	4
161	7.98	7.98	49.3	sp|P00167|CYB5_HUMAN	Cytochrome b5 OS=Homo sapiens GN=CYB5A PE=1 SV=2	HUMAN	4
162	7.92	7.92	22.6	sp|Q9UBS4|DJB11_HUMAN	DnaJ homolog subfamily B member 11 OS=Homo sapiens GN=DNAJB11 PE=1 SV=1	HUMAN	4
163	7.88	7.88	16.7	sp|Q969V3|NCLN_HUMAN	Nicalin OS=Homo sapiens GN=NCLN PE=1 SV=2	HUMAN	4
164	7.78	7.78	15.3	sp|P30038|AL4A1_HUMAN	Delta-1-pyrroline-5-carboxylate dehydrogenase, mitochondrial OS=Homo sapiens GN=ALDH4A1 PE=1 SV=3	HUMAN	4
166	7.74	7.74	17	sp|Q08257|QOR_HUMAN	Quinone oxidoreductase OS=Homo sapiens GN=CRYZ PE=1 SV=1	HUMAN	4
167	7.72	7.72	4.5	sp|Q07954|LRP1_HUMAN	Prolow-density lipoprotein receptor-related protein 1 OS=Homo sapiens GN=LRP1 PE=1 SV=2	HUMAN	4
169	7.54	7.54	54.3	sp|P10606|COX5B_HUMAN	Cytochrome c oxidase subunit 5B, mitochondrial OS=Homo sapiens GN=COX5B PE=1 SV=2	HUMAN	4
170	7.51	7.51	24.8	sp|P30837|AL1B1_HUMAN	Aldehyde dehydrogenase X, mitochondrial OS=Homo sapiens GN=ALDH1B1 PE=1 SV=3	HUMAN	4
171	7.48	7.48	53.5	sp|O96000|NDUBA_HUMAN	NADH dehydrogenase [ubiquinone] 1 beta subcomplex subunit 10 OS=Homo sapiens GN=NDUFB10 PE=1 SV=3	HUMAN	4
172	7.48	7.48	32.3	sp|P62917|RL8_HUMAN	60S ribosomal protein L8 OS=Homo sapiens GN=RPL8 PE=1 SV=2	HUMAN	4
173	7.45	7.45	15.8	sp|Q9UHG3|PCYOX_HUMAN	Prenylcysteine oxidase 1 OS=Homo sapiens GN=PCYOX1 PE=1 SV=3	HUMAN	4
174	7.31	7.31	26.9	sp|Q16762|THTR_HUMAN	Thiosulfate sulfurtransferase OS=Homo sapiens GN=TST PE=1 SV=4	HUMAN	4
175	7.29	7.29	45.8	sp|Q9P0J0|NDUAD_HUMAN	NADH dehydrogenase [ubiquinone] 1 alpha subcomplex subunit 13 OS=Homo sapiens GN=NDUFA13 PE=1 SV=3	HUMAN	4
176	7.24	7.24	29.8	sp|P62280|RS11_HUMAN	40S ribosomal protein S11 OS=Homo sapiens GN=RPS11 PE=1 SV=3	HUMAN	4
177	7.21	7.21	17.9	sp|P49821|NDUV1_HUMAN	NADH dehydrogenase [ubiquinone] flavoprotein 1, mitochondrial OS=Homo sapiens GN=NDUFV1 PE=1 SV=4	HUMAN	4
178	7.09	7.09	12	sp|P21589|5NTD_HUMAN	5'-nucleotidase OS=Homo sapiens GN=NT5E PE=1 SV=1	HUMAN	4
180	7.09	7.09	15.3	sp|P62873|GBB1_HUMAN	Guanine nucleotide-binding protein G(I)/G(S)/G(T) subunit beta-1 OS=Homo sapiens GN=GNB1 PE=1 SV=3	HUMAN	4
182	6.99	6.99	20.6	sp|P00558|PGK1_HUMAN	Phosphoglycerate kinase 1 OS=Homo sapiens GN=PGK1 PE=1 SV=3	HUMAN	4
183	6.97	6.97	60.8	sp|P61604|CH10_HUMAN	10 kDa heat shock protein, mitochondrial OS=Homo sapiens GN=HSPE1 PE=1 SV=2	HUMAN	4
184	6.95	6.95	28.6	sp|P38117|ETFB_HUMAN	Electron transfer flavoprotein subunit beta OS=Homo sapiens GN=ETFB PE=1 SV=3	HUMAN	4
185	6.91	6.91	19.3	sp|O94925|GLSK_HUMAN	Glutaminase kidney isoform, mitochondrial OS=Homo sapiens GN=GLS PE=1 SV=1	HUMAN	4
187	6.81	7.24	12.7	sp|P06865|HEXA_HUMAN	Beta-hexosaminidase subunit alpha OS=Homo sapiens GN=HEXA PE=1 SV=2	HUMAN	4
189	6.72	6.72	8.7	sp|O95782|AP2A1_HUMAN	AP-2 complex subunit alpha-1 OS=Homo sapiens GN=AP2A1 PE=1 SV=3	HUMAN	4
193	6.59	6.59	32.4	sp|P51149|RAB7A_HUMAN	Ras-related protein Rab-7a OS=Homo sapiens GN=RAB7A PE=1 SV=1	HUMAN	4
194	6.53	6.53	32.4	sp|P99999|CYC_HUMAN	Cytochrome c OS=Homo sapiens GN=CYCS PE=1 SV=2	HUMAN	4
195	6.51	6.51	49.1	sp|P30050|RL12_HUMAN	60S ribosomal protein L12 OS=Homo sapiens GN=RPL12 PE=1 SV=1	HUMAN	4
197	6.41	6.41	33	sp|P51571|SSRD_HUMAN	Translocon-associated protein subunit delta OS=Homo sapiens GN=SSR4 PE=1 SV=1	HUMAN	4
201	6.18	6.18	5.3	sp|P11047|LAMC1_HUMAN	Laminin subunit gamma-1 OS=Homo sapiens GN=LAMC1 PE=1 SV=3	HUMAN	4
210	6	6	11.8	sp|P15289|ARSA_HUMAN	Arylsulfatase A OS=Homo sapiens GN=ARSA PE=1 SV=3	HUMAN	4
215	5.86	5.86	58.4	sp|P62899|RL31_HUMAN	60S ribosomal protein L31 OS=Homo sapiens GN=RPL31 PE=1 SV=1	HUMAN	4
219	5.7	5.7	27	sp|P22090|RS4Y1_HUMAN	40S ribosomal protein S4, Y isoform 1 OS=Homo sapiens GN=RPS4Y1 PE=2 SV=2	HUMAN	4
225	5.55	5.55	9.8	sp|Q9Y4W6|AFG32_HUMAN	AFG3-like protein 2 OS=Homo sapiens GN=AFG3L2 PE=1 SV=2	HUMAN	4
227	5.45	5.45	22.1	sp|P46782|RS5_HUMAN	40S ribosomal protein S5 OS=Homo sapiens GN=RPS5 PE=1 SV=4	HUMAN	4
238	5.16	5.16	19.3	sp|Q8NBJ7|SUMF2_HUMAN	Sulfatase-modifying factor 2 OS=Homo sapiens GN=SUMF2 PE=1 SV=2	HUMAN	4
241	5.12	5.12	21.9	sp|P32322|PYCR1_HUMAN	Pyrroline-5-carboxylate reductase 1, mitochondrial OS=Homo sapiens GN=PYCR1 PE=1 SV=2	HUMAN	4
244	5.06	5.06	25.1	sp|P53597|SUCA_HUMAN	Succinyl-CoA ligase [ADP/GDP-forming] subunit alpha, mitochondrial OS=Homo sapiens GN=SUCLG1 PE=1 SV=4	HUMAN	4
253	4.71	4.71	8.2	sp|Q9NSE4|SYIM_HUMAN	Isoleucine--tRNA ligase, mitochondrial OS=Homo sapiens GN=IARS2 PE=1 SV=2	HUMAN	4
266	4.38	4.39	7.9	sp|O60568|PLOD3_HUMAN	Procollagen-lysine,2-oxoglutarate 5-dioxygenase 3 OS=Homo sapiens GN=PLOD3 PE=1 SV=1	HUMAN	4
310	3.63	3.63	11.5	sp|P00918|CAH2_HUMAN	Carbonic anhydrase 2 OS=Homo sapiens GN=CA2 PE=1 SV=2	HUMAN	4
513	1.4	6.12	17.9	sp|P08107|HSP71_HUMAN	Heat shock 70 kDa protein 1A/1B OS=Homo sapiens GN=HSPA1A PE=1 SV=5	HUMAN	4
624	0.32	9.45	23.8	sp|P12236|ADT3_HUMAN	ADP/ATP translocase 3 OS=Homo sapiens GN=SLC25A6 PE=1 SV=4	HUMAN	4
178	7.19	7.19	31.8	sp|P63104|1433Z_HUMAN	14-3-3 protein zeta/delta OS=Homo sapiens GN=YWHAZ PE=1 SV=1	HUMAN	3
186	6.87	6.87	75.9	sp|P61254|RL26_HUMAN	60S ribosomal protein L26 OS=Homo sapiens GN=RPL26 PE=1 SV=1	HUMAN	3
188	6.73	6.73	20.2	sp|P05388|RLA0_HUMAN	60S acidic ribosomal protein P0 OS=Homo sapiens GN=RPLP0 PE=1 SV=1	HUMAN	3
192	6.61	6.61	15.2	sp|P42126|ECI1_HUMAN	Enoyl-CoA delta isomerase 1, mitochondrial OS=Homo sapiens GN=ECI1 PE=1 SV=1	HUMAN	3
196	6.48	6.48	27.9	sp|P49755|TMEDA_HUMAN	Transmembrane emp24 domain-containing protein 10 OS=Homo sapiens GN=TMED10 PE=1 SV=2	HUMAN	3
198	6.27	6.27	18.1	sp|Q16891|IMMT_HUMAN	Mitochondrial inner membrane protein OS=Homo sapiens GN=IMMT PE=1 SV=1	HUMAN	3
199	6.23	6.23	7	sp|P07942|LAMB1_HUMAN	Laminin subunit beta-1 OS=Homo sapiens GN=LAMB1 PE=1 SV=2	HUMAN	3
200	6.23	6.23	28.4	sp|Q9UJZ1|STML2_HUMAN	Stomatin-like protein 2 OS=Homo sapiens GN=STOML2 PE=1 SV=1	HUMAN	3
202	6.15	6.15	24.4	sp|P60866|RS20_HUMAN	40S ribosomal protein S20 OS=Homo sapiens GN=RPS20 PE=1 SV=1	HUMAN	3
203	6.13	6.13	37.8	sp|P0CW22|RS17L_HUMAN	40S ribosomal protein S17-like OS=Homo sapiens GN=RPS17L PE=3 SV=1	HUMAN	3
204	6.1	6.73	13.9	sp|O95302|FKBP9_HUMAN	Peptidyl-prolyl cis-trans isomerase FKBP9 OS=Homo sapiens GN=FKBP9 PE=1 SV=2	HUMAN	3
205	6.1	6.1	72.3	sp|P62244|RS15A_HUMAN	40S ribosomal protein S15a OS=Homo sapiens GN=RPS15A PE=1 SV=2	HUMAN	3
206	6.03	6.03	28.4	sp|Q96D15|RCN3_HUMAN	Reticulocalbin-3 OS=Homo sapiens GN=RCN3 PE=1 SV=1	HUMAN	3
207	6.03	6.03	9.6	sp|P05023|AT1A1_HUMAN	Sodium/potassium-transporting ATPase subunit alpha-1 OS=Homo sapiens GN=ATP1A1 PE=1 SV=1	HUMAN	3
208	6.02	6.02	11.5	sp|Q13724|MOGS_HUMAN	Mannosyl-oligosaccharide glucosidase OS=Homo sapiens GN=MOGS PE=1 SV=5	HUMAN	3
209	6	6	37.1	sp|P60903|S10AA_HUMAN	Protein S100-A10 OS=Homo sapiens GN=S100A10 PE=1 SV=2	HUMAN	3
211	6	6	44.8	sp|Q96IX5|USMG5_HUMAN	Up-regulated during skeletal muscle growth protein 5 OS=Homo sapiens GN=USMG5 PE=1 SV=1	HUMAN	3
212	5.95	5.95	25.5	sp|Q16836|HCDH_HUMAN	Hydroxyacyl-coenzyme A dehydrogenase, mitochondrial OS=Homo sapiens GN=HADH PE=1 SV=3	HUMAN	3
213	5.92	5.92	10.2	sp|Q6DD88|ATL3_HUMAN	Atlastin-3 OS=Homo sapiens GN=ATL3 PE=1 SV=1	HUMAN	3
214	5.89	5.89	27.4	sp|P09382|LEG1_HUMAN	Galectin-1 OS=Homo sapiens GN=LGALS1 PE=1 SV=2	HUMAN	3
217	5.85	5.85	41.5	sp|P20671|H2A1D_HUMAN	Histone H2A type 1-D OS=Homo sapiens GN=HIST1H2AD PE=1 SV=2	HUMAN	3
218	5.74	5.74	40.5	sp|P50914|RL14_HUMAN	60S ribosomal protein L14 OS=Homo sapiens GN=RPL14 PE=1 SV=4	HUMAN	3
220	5.68	5.68	11.3	sp|Q9HDC9|APMAP_HUMAN	Adipocyte plasma membrane-associated protein OS=Homo sapiens GN=APMAP PE=1 SV=2	HUMAN	3
221	5.66	5.66	20.7	sp|Q9NVI7|ATD3A_HUMAN	ATPase family AAA domain-containing protein 3A OS=Homo sapiens GN=ATAD3A PE=1 SV=2	HUMAN	3
223	5.63	5.63	20	sp|Q969X5|ERGI1_HUMAN	Endoplasmic reticulum-Golgi intermediate compartment protein 1 OS=Homo sapiens GN=ERGIC1 PE=1 SV=1	HUMAN	3
224	5.6	5.6	12.7	sp|P43304|GPDM_HUMAN	Glycerol-3-phosphate dehydrogenase, mitochondrial OS=Homo sapiens GN=GPD2 PE=1 SV=3	HUMAN	3
226	5.51	5.51	10.8	sp|Q9Y4L1|HYOU1_HUMAN	Hypoxia up-regulated protein 1 OS=Homo sapiens GN=HYOU1 PE=1 SV=1	HUMAN	3
228	5.43	5.43	20.1	sp|P19404|NDUV2_HUMAN	NADH dehydrogenase [ubiquinone] flavoprotein 2, mitochondrial OS=Homo sapiens GN=NDUFV2 PE=1 SV=2	HUMAN	3
229	5.43	5.43	8.4	sp|P13674|P4HA1_HUMAN	Prolyl 4-hydroxylase subunit alpha-1 OS=Homo sapiens GN=P4HA1 PE=1 SV=2	HUMAN	3
230	5.43	5.43	22.4	sp|P09211|GSTP1_HUMAN	Glutathione S-transferase P OS=Homo sapiens GN=GSTP1 PE=1 SV=2	HUMAN	3

N	Unused	Total	% Cov	Accession #	Name	Species	Peptides(95%)	
232	5.36	5.36	40.4	sp|Q07020|RL18_HUMAN	60S ribosomal protein L18 OS=Homo sapiens GN=RPL18 PE=1 SV=2	HUMAN		3
233	5.34	5.34	8.1	sp|Q8NHP8|PLBL2_HUMAN	Putative phospholipase B-like 2 OS=Homo sapiens GN=PLBD2 PE=1 SV=2	HUMAN		3
234	5.31	5.31	24.8	sp|P47985|UCRI_HUMAN	Cytochrome b-c1 complex subunit Rieske, mitochondrial OS=Homo sapiens GN=UQCRFS1 PE=1 SV=2	HUMAN		3
236	5.24	5.24	24.3	sp|O14880|MGST3_HUMAN	Microsomal glutathione S-transferase 3 OS=Homo sapiens GN=MGST3 PE=1 SV=1	HUMAN		3
237	5.22	5.22	35.9	sp|P60763|RAC3_HUMAN	Ras-related C3 botulinum toxin substrate 3 OS=Homo sapiens GN=RAC3 PE=1 SV=1	HUMAN		3
239	5.12	5.12	17.4	sp|Q12907|LMAN2_HUMAN	Vesicular integral-membrane protein VIP36 OS=Homo sapiens GN=LMAN2 PE=1 SV=1	HUMAN		3
240	5.12	5.12	13.1	sp|P38606|VATA_HUMAN	V-type proton ATPase catalytic subunit A OS=Homo sapiens GN=ATP6V1A PE=1 SV=2	HUMAN		3
242	5.09	5.09	53.5	sp|O95168|NDUB4_HUMAN	NADH dehydrogenase [ubiquinone] 1 beta subcomplex subunit 4 OS=Homo sapiens GN=NDUFB4 PE=1 SV=3	HUMAN		3
245	5.03	5.03	26.7	sp|O95881|TXD12_HUMAN	Thioredoxin domain-containing protein 12 OS=Homo sapiens GN=TXNDC12 PE=1 SV=1	HUMAN		3
246	5	5	34.3	sp|P62491|RB11A_HUMAN	Ras-related protein Rab-11A OS=Homo sapiens GN=RAB11A PE=1 SV=3	HUMAN		3
247	4.98	4.98	18.3	sp|P53007|TXTP_HUMAN	Tricarboxylate transport protein, mitochondrial OS=Homo sapiens GN=SLC25A1 PE=1 SV=2	HUMAN		3
248	4.95	4.95	29.4	sp|P52565|GDIR1_HUMAN	Rho GDP-dissociation inhibitor 1 OS=Homo sapiens GN=ARHGDIA PE=1 SV=3	HUMAN		3
249	4.92	4.92	25.8	sp|P62081|RS7_HUMAN	40S ribosomal protein S7 OS=Homo sapiens GN=RPS7 PE=1 SV=1	HUMAN		3
251	4.74	4.74	46.1	sp|P22392|NDKB_HUMAN	Nucleoside diphosphate kinase B OS=Homo sapiens GN=NME2 PE=1 SV=1	HUMAN		3
252	4.74	4.74	43.7	sp|P62805|H4_HUMAN	Histone H4 OS=Homo sapiens GN=HIST1H4A PE=1 SV=2	HUMAN		3
256	4.64	4.64	15.3	sp|O02978|M2OM_HUMAN	Mitochondrial 2-oxoglutarate/malate carrier protein OS=Homo sapiens GN=SLC25A11 PE=1 SV=3	HUMAN		3
257	4.59	4.59	43.1	sp|P46779|RL28_HUMAN	60S ribosomal protein L28 OS=Homo sapiens GN=RPL28 PE=1 SV=3	HUMAN		3
258	4.54	4.54	19.6	sp|Q06830|PRDX1_HUMAN	Peroxiredoxin-1 OS=Homo sapiens GN=PRDX1 PE=1 SV=1	HUMAN		3
259	4.47	5.37	30.7	sp|Q29940|1B59_HUMAN	HLA class I histocompatibility antigen, B-59 alpha chain OS=Homo sapiens GN=HLA-B PE=2 SV=1	HUMAN		3
260	4.47	4.47	21.4	sp|P62841|RS15_HUMAN	40S ribosomal protein S15 OS=Homo sapiens GN=RPS15 PE=1 SV=2	HUMAN		3
261	4.45	4.45	26.4	sp|Q9UU7|KAD3_HUMAN	GTP:AMP phosphotransferase, mitochondrial OS=Homo sapiens GN=AK3 PE=1 SV=4	HUMAN		3
268	4.32	4.33	25.1	sp|P40429|RL13A_HUMAN	60S ribosomal protein L13a OS=Homo sapiens GN=RPL13A PE=1 SV=2	HUMAN		3
271	4.28	4.28	29.6	sp|P62910|RL32_HUMAN	60S ribosomal protein L32 OS=Homo sapiens GN=RPL32 PE=1 SV=2	HUMAN		3
272	4.26	4.26	18.9	sp|Q9UHL4|DPP2_HUMAN	Dipeptidyl peptidase 2 OS=Homo sapiens GN=DPP7 PE=1 SV=3	HUMAN		3
273	4.26	4.26	22.4	sp|Q96EY8|MMAB_HUMAN	Cob(I)yrinic acid a,c-diamide adenosyltransferase, mitochondrial OS=Homo sapiens GN=MMAB PE=1 SV=1	HUMAN		3
276	4.23	4.23	17	sp|P04075|ALDOA_HUMAN	Fructose-bisphosphate aldolase A OS=Homo sapiens GN=ALDOA PE=1 SV=2	HUMAN		3
280	4.12	4.12	34.3	sp|P51148|RAB5C_HUMAN	Ras-related protein Rab-5C OS=Homo sapiens GN=RAB5C PE=1 SV=2	HUMAN		3
281	4.1	4.1	14.7	sp|P08123|CO1A2_HUMAN	Collagen alpha-2(I) chain OS=Homo sapiens GN=COL1A2 PE=1 SV=7	HUMAN		3
282	4.09	4.1	16.5	sp|P55072|TERA_HUMAN	Transitional endoplasmic reticulum ATPase OS=Homo sapiens GN=VCP PE=1 SV=4	HUMAN		3
283	4.09	4.1	18	sp|Q53GQ0|DHB12_HUMAN	Estradiol 17-beta-dehydrogenase 12 OS=Homo sapiens GN=HSD17B12 PE=1 SV=2	HUMAN		3
287	4	4	9.5	sp|Q86Y23|HORN_HUMAN	Hornerin OS=Homo sapiens GN=HRNR PE=1 SV=2	HUMAN		3
300	3.78	3.78	7.1	sp|P62829|RL23_HUMAN	60S ribosomal protein L23 OS=Homo sapiens GN=RPL23 PE=1 SV=1	HUMAN		3
306	3.68	3.68	8.1	sp|P18206|VINC_HUMAN	Vinculin OS=Homo sapiens GN=VCL PE=1 SV=4	HUMAN		3
307	3.68	3.68	9.8	sp|O43819|SCO2_HUMAN	Protein SCO2 homolog, mitochondrial OS=Homo sapiens GN=SCO2 PE=1 SV=3	HUMAN		3
308	3.67	3.69	7.8	sp|P16278|BGAL_HUMAN	Beta-galactosidase OS=Homo sapiens GN=GLB1 PE=1 SV=2	HUMAN		3
309	3.67	3.68	7.5	sp|Q16134|ETFD_HUMAN	Electron transfer flavoprotein-ubiquinone oxidoreductase, mitochondrial OS=Homo sapiens GN=ETFDH PE=1 SV=2	HUMAN		3
311	3.61	3.61	42.6	sp|P56134|ATPK_HUMAN	ATP synthase subunit f, mitochondrial OS=Homo sapiens GN=ATPSJ2 PE=1 SV=3	HUMAN		3
312	3.6	3.6	16.6	sp|P83731|RL24_HUMAN	60S ribosomal protein L24 OS=Homo sapiens GN=RPL24 PE=1 SV=1	HUMAN		3
322	3.29	3.29	16.1	sp|P43235|CATK_HUMAN	Cathepsin K OS=Homo sapiens GN=CTSK PE=1 SV=1	HUMAN		3
323	3.29	3.29	12.3	sp|P54802|ANAG_HUMAN	Alpha-N-acetylglucosaminidase OS=Homo sapiens GN=NAGLU PE=1 SV=2	HUMAN		3
331	3.12	3.12	15.6	sp|O15382|BCAT2_HUMAN	Branched-chain-amino-acid aminotransferase, mitochondrial OS=Homo sapiens GN=BCAT2 PE=1 SV=2	HUMAN		3
332	3.11	3.12	4.7	sp|Q14956|GPNMB_HUMAN	Transmembrane glycoprotein NMB OS=Homo sapiens GN=GPNMB PE=1 SV=2	HUMAN		3
340	2.99	2.99	12.4	sp|P09622|DLDH_HUMAN	Dihydrolipoyl dehydrogenase, mitochondrial OS=Homo sapiens GN=DLD PE=1 SV=2	HUMAN		3
345	2.88	2.94	23.4	sp|Q12931|TRAP1_HUMAN	Heat shock protein 75 kDa, mitochondrial OS=Homo sapiens GN=TRAP1 PE=1 SV=3	HUMAN		3
349	2.8	2.8	25.8	sp|O95139|NDUB6_HUMAN	NADH dehydrogenase [ubiquinone] 1 beta subcomplex subunit 6 OS=Homo sapiens GN=NDUFB6 PE=1 SV=3	HUMAN		3
369	2.33	3.4	16.2	sp|O75439|MPPB_HUMAN	Mitochondrial-processing peptidase subunit beta OS=Homo sapiens GN=PMPCB PE=1 SV=2	HUMAN		3
388	2.13	4.18	26.2	sp|Q13162|PRDX4_HUMAN	Peroxiredoxin-4 OS=Homo sapiens GN=PRDX4 PE=1 SV=1	HUMAN		3
410	2	5.32	15	sp|P62879|GBB2_HUMAN	Guanine nucleotide-binding protein G(I)/G(S)/G(T) subunit beta-2 OS=Homo sapiens GN=GNB2 PE=1 SV=3	HUMAN		3
472	1.8	6.06	18.5	sp|P35241|RADI_HUMAN	Radixin OS=Homo sapiens GN=RDX PE=1 SV=1	HUMAN		3
495	1.59	3.84	31.4	sp|P62258|1433E_HUMAN	14-3-3 protein epsilon OS=Homo sapiens GN=YWHAE PE=1 SV=1	HUMAN		3
510	1.44	1.44	22.6	sp|Q969Q0|RL36L_HUMAN	60S ribosomal protein L36a-like OS=Homo sapiens GN=RPL36AL PE=1 SV=3	HUMAN		3
547	0.92	5.31	11.8	sp|P15311|EZRI_HUMAN	Ezrin OS=Homo sapiens GN=EZR PE=1 SV=4	HUMAN		3
657	0.19	0.19	19.3	sp|Q9BVC6|TM109_HUMAN	Transmembrane protein 109 OS=Homo sapiens GN=TMEM109 PE=1 SV=1	HUMAN		3
713	0.07	7.09	13.4	sp|P08238|HS90B_HUMAN	Heat shock protein HSP 90-beta OS=Homo sapiens GN=HSP90AB1 PE=1 SV=4	HUMAN		3
235	5.25	5.25	39.1	sp|P62263|RS14_HUMAN	40S ribosomal protein S14 OS=Homo sapiens GN=RPS14 PE=1 SV=3	HUMAN		2
243	5.07	5.07	13.8	sp|Q96EY7|PTCD3_HUMAN	Pentatricopeptide repeat-containing protein 3, mitochondrial OS=Homo sapiens GN=PTCD3 PE=1 SV=3	HUMAN		2
250	4.79	4.79	33.6	sp|O95182|NDUA7_HUMAN	NADH dehydrogenase [ubiquinone] 1 alpha subcomplex subunit 7 OS=Homo sapiens GN=NDUFA7 PE=1 SV=3	HUMAN		2
254	4.7	4.71	10.8	sp|Q5JRX3|PREP_HUMAN	Presequence protease, mitochondrial OS=Homo sapiens GN=PITRM1 PE=1 SV=2	HUMAN		2
255	4.65	4.65	11.6	sp|Q9BSJ8|ESYT1_HUMAN	Extended synaptotagmin-1 OS=Homo sapiens GN=ESYT1 PE=1 SV=1	HUMAN		2
262	4.44	4.44	12.7	sp|O95831|AIFM1_HUMAN	Apoptosis-inducing factor 1, mitochondrial OS=Homo sapiens GN=AIFM1 PE=1 SV=1	HUMAN		2
263	4.4	4.4	8.5	sp|P09110|THIK_HUMAN	3-ketoacyl-CoA thiolase, peroxisomal OS=Homo sapiens GN=ACAA1 PE=1 SV=2	HUMAN		2
264	4.39	4.39	16.1	sp|Q02809|PLOD1_HUMAN	Procollagen-lysine,2-oxoglutarate 5-dioxygenase 1 OS=Homo sapiens GN=PLOD1 PE=1 SV=2	HUMAN		2
265	4.39	4.39	12.6	sp|Q9UFN0|NP53A_HUMAN	Protein NipSnap homolog 3A OS=Homo sapiens GN=NIPSNAP3A PE=1 SV=2	HUMAN		2
269	4.3	4.3	36.6	sp|O14949|QCR8_HUMAN	Cytochrome b-c1 complex subunit 8 OS=Homo sapiens GN=UQCRQ PE=1 SV=4	HUMAN		2
270	4.28	4.97	12.4	sp|P07900|HS90A_HUMAN	Heat shock protein HSP 90-alpha OS=Homo sapiens GN=HSP90AA1 PE=1 SV=5	HUMAN		2
274	4.25	4.25	28	sp|P23396|RS3_HUMAN	40S ribosomal protein S3 OS=Homo sapiens GN=RPS3 PE=1 SV=2	HUMAN		2
275	4.25	4.25	23.5	sp|Q9Y2Q3|GSTK1_HUMAN	Glutathione S-transferase kappa 1 OS=Homo sapiens GN=GSTK1 PE=1 SV=3	HUMAN		2
277	4.19	4.19	13	sp|Q8NBJ5|GT251_HUMAN	Procollagen galactosyltransferase 1 OS=Homo sapiens GN=GLT25D1 PE=1 SV=1	HUMAN		2
278	4.17	4.17	12.6	sp|P51659|DHB4_HUMAN	Peroxisomal multifunctional enzyme type 2 OS=Homo sapiens GN=HSD17B4 PE=1 SV=3	HUMAN		2
279	4.14	4.14	29.7	sp|P46776|RL27A_HUMAN	60S ribosomal protein L27a OS=Homo sapiens GN=RPL27A PE=1 SV=2	HUMAN		2
284	4.09	4.09	13	sp|O94905|ERLN2_HUMAN	Erlin-2 OS=Homo sapiens GN=ERLIN2 PE=1 SV=1	HUMAN		2
285	4.05	4.05	26.8	sp|P51572|BAP31_HUMAN	B-cell receptor-associated protein 31 OS=Homo sapiens GN=BCAP31 PE=1 SV=3	HUMAN		2
286	4.02	4.02	30.2	sp|Q9Y6M9|NDUB9_HUMAN	NADH dehydrogenase [ubiquinone] 1 beta subcomplex subunit 9 OS=Homo sapiens GN=NDUFB9 PE=1 SV=3	HUMAN		2
288	4	4	30.2	sp|O14950|ML12B_HUMAN	Myosin regulatory light chain 12B OS=Homo sapiens GN=MYL12B PE=1 SV=2	HUMAN		2
289	4	4	8	sp|P60174|TPIS_HUMAN	Triosephosphate isomerase OS=Homo sapiens GN=TPI1 PE=1 SV=3	HUMAN		2
290	4	4	22.1	sp|P57105|SYJ2B_HUMAN	Synaptojanin-2-binding protein OS=Homo sapiens GN=SYNJ2BP PE=1 SV=2	HUMAN		2
291	4	4	20.2	sp|P10301|RRAS_HUMAN	Ras-related protein R-Ras OS=Homo sapiens GN=RRAS PE=1 SV=1	HUMAN		2
292	4	4	18.6	sp|P04216|THY1_HUMAN	Thy-1 membrane glycoprotein OS=Homo sapiens GN=THY1 PE=1 SV=2	HUMAN		2
293	4	4	20.2	sp|P02794|FRIH_HUMAN	Ferritin heavy chain OS=Homo sapiens GN=FTH1 PE=1 SV=2	HUMAN		2
294	4	4	8.5	sp|P09525|ANXA4_HUMAN	Annexin A4 OS=Homo sapiens GN=ANXA4 PE=1 SV=4	HUMAN		2
295	4	4	6.8	sp|O43837|IDH3B_HUMAN	Isocitrate dehydrogenase [NAD] subunit beta, mitochondrial OS=Homo sapiens GN=IDH3B PE=1 SV=2	HUMAN		2
297	3.9	3.9	11.1	sp|O00116|ADAS_HUMAN	Alkyldihydroxyacetonephosphate synthase, peroxisomal OS=Homo sapiens GN=AGPS PE=1 SV=1	HUMAN		2
298	3.88	3.88	5.2	sp|P04062|GLCM_HUMAN	Glucosylceramidase OS=Homo sapiens GN=GBA PE=1 SV=3	HUMAN		2
299	3.82	3.82	26	sp|Q969H8|CS010_HUMAN	UPF0556 protein C19orf10 OS=Homo sapiens GN=C19orf10 PE=1 SV=1	HUMAN		2
301	3.76	3.76	23.6	sp|P62913|RL11_HUMAN	60S ribosomal protein L11 OS=Homo sapiens GN=RPL11 PE=1 SV=2	HUMAN		2
302	3.74	3.74	10	sp|Q5JWF2|GNAS1_HUMAN	Guanine nucleotide-binding protein G(s) subunit alpha isoforms XLas OS=Homo sapiens GN=GNAS PE=1 SV=2	HUMAN		2
303	3.72	3.72	15	sp|Q16540|RM23_HUMAN	39S ribosomal protein L23, mitochondrial OS=Homo sapiens GN=MRPL23 PE=1 SV=1	HUMAN		2
304	3.7	3.7	21	sp|P62266|RS23_HUMAN	40S ribosomal protein S23 OS=Homo sapiens GN=RPS23 PE=1 SV=3	HUMAN		2
305	3.69	3.69	25.3	sp|P15880|RS2_HUMAN	40S ribosomal protein S2 OS=Homo sapiens GN=RPS2 PE=1 SV=2	HUMAN		2
313	3.55	3.55	12.4	sp|Q6YN16|HSDL2_HUMAN	Hydroxysteroid dehydrogenase-like protein 2 OS=Homo sapiens GN=HSDL2 PE=1 SV=1	HUMAN		2
314	3.54	3.54	22.5	sp|P84098|RL19_HUMAN	60S ribosomal protein L19 OS=Homo sapiens GN=RPL19 PE=1 SV=1	HUMAN		2
315	3.4	3.4	11.2	sp|P52907|CAZA1_HUMAN	F-actin-capping protein subunit alpha-1 OS=Homo sapiens GN=CAPZA1 PE=1 SV=3	HUMAN		2
317	3.37	3.37	8.6	sp|P11279|LAMP1_HUMAN	Lysosome-associated membrane glycoprotein 1 OS=Homo sapiens GN=LAMP1 PE=1 SV=3	HUMAN		2
318	3.36	3.36	11	sp|P19367|HXK1_HUMAN	Hexokinase-1 OS=Homo sapiens GN=HK1 PE=1 SV=3	HUMAN		2
319	3.36	3.36	22.2	sp|P30405|PPIF_HUMAN	Peptidyl-prolyl cis-trans isomerase F, mitochondrial OS=Homo sapiens GN=PPIF PE=1 SV=1	HUMAN		2
320	3.34	3.34	11.8	sp|P10515|ODP2_HUMAN	Dihydrolipoyllysine-residue acetyltransferase component of pyruvate dehydrogenase complex, mitochondrial OS=Homo sapiens GN=DLAT PE=1 SV=3	HUMAN		2
321	3.33	3.33	13.1	sp|P29992|GNA11_HUMAN	Guanine nucleotide-binding protein subunit alpha-11 OS=Homo sapiens GN=GNA11 PE=1 SV=2	HUMAN		2
325	3.28	3.28	13.7	sp|P41250|SYG_HUMAN	Glycine--tRNA ligase OS=Homo sapiens GN=GARS PE=1 SV=3	HUMAN		2
326	3.26	3.26	19.5	sp|P61803|DAD1_HUMAN	Dolichyl-diphosphooligosaccharide--protein glycosyltransferase subunit DAD1 OS=Homo sapiens GN=DAD1 PE=1 SV=3	HUMAN		2
327	3.25	3.25	4	sp|O75718|CRTAP_HUMAN	Cartilage-associated protein OS=Homo sapiens GN=CRTAP PE=1 SV=1	HUMAN		2
328	3.21	3.21	12.3	sp|Q9NX63|CHCH3_HUMAN	Coiled-coil-helix-coiled-coil-helix domain-containing protein 3, mitochondrial OS=Homo sapiens GN=CHCHD3 PE=1 SV=1	HUMAN		2
329	3.2	3.2	30.9	sp|Q07021|C1QBP_HUMAN	Complement component 1 Q subcomponent-binding protein, mitochondrial OS=Homo sapiens GN=C1QBP PE=1 SV=1	HUMAN		2
330	3.16	3.16	9.3	sp|P00338|LDHA_HUMAN	L-lactate dehydrogenase A chain OS=Homo sapiens GN=LDHA PE=1 SV=2	HUMAN		2
333	3.08	3.08	17.3	sp|P55809|SCOT1_HUMAN	Succinyl-CoA:3-ketoacid coenzyme A transferase 1, mitochondrial OS=Homo sapiens GN=OXCT1 PE=1 SV=1	HUMAN		2
334	3.08	3.08	13.9	sp|Q99653|CHP1_HUMAN	Calcineurin B homologous protein 1 OS=Homo sapiens GN=CHP1 PE=1 SV=3	HUMAN		2
335	3.06	3.06	7.7	sp|Q10471|GALT2_HUMAN	Polypeptide N-acetylgalactosaminyltransferase 2 OS=Homo sapiens GN=GALNT2 PE=1 SV=1	HUMAN		2
336	3.06	3.06	5.3	sp|Q9Y512|SAM50_HUMAN	Sorting and assembly machinery component 50 homolog OS=Homo sapiens GN=SAMM50 PE=1 SV=3	HUMAN		2
337	3.03	3.03	44.8	sp|Q9UI09|NDUAC_HUMAN	NADH dehydrogenase [ubiquinone] 1 alpha subcomplex subunit 12 OS=Homo sapiens GN=NDUFA12 PE=1 SV=1	HUMAN		2
341	2.98	2.98	13.6	sp|P11233|RALA_HUMAN	Ras-related protein Ral-A OS=Homo sapiens GN=RALA PE=1 SV=1	HUMAN		2
342	2.98	2.98	12.9	sp|O00217|NDUS8_HUMAN	NADH dehydrogenase [ubiquinone] iron-sulfur protein 8, mitochondrial OS=Homo sapiens GN=NDUFS8 PE=1 SV=1	HUMAN		2
343	2.93	2.93	9.4	sp|P54886|P5CS_HUMAN	Delta-1-pyrroline-5-carboxylate synthase OS=Homo sapiens GN=ALDH18A1 PE=1 SV=2	HUMAN		2
347	2.85	2.85	30.1	sp|P62750|RL23A_HUMAN	60S ribosomal protein L23a OS=Homo sapiens GN=RPL23A PE=1 SV=1	HUMAN		2
350	2.8	2.8	5.3	sp|Q14344|GNA13_HUMAN	Guanine nucleotide-binding protein subunit alpha-13 OS=Homo sapiens GN=GNA13 PE=1 SV=2	HUMAN		2
351	2.76	2.76	12.6	sp|P82933|RT09_HUMAN	28S ribosomal protein S9, mitochondrial OS=Homo sapiens GN=MRPS9 PE=1 SV=2	HUMAN		2
356	2.6	2.6	21.7	sp|O43181|NDUS4_HUMAN	NADH dehydrogenase [ubiquinone] iron-sulfur protein 4, mitochondrial OS=Homo sapiens GN=NDUFS4 PE=1 SV=1	HUMAN		2
357	2.58	2.58	38	sp|P20674|COX5A_HUMAN	Cytochrome c oxidase subunit 5A, mitochondrial OS=Homo sapiens GN=COX5A PE=1 SV=2	HUMAN		2
358	2.57	2.57	30.5	sp|Q9Y3U8|RL36_HUMAN	60S ribosomal protein L36 OS=Homo sapiens GN=RPL36 PE=1 SV=3	HUMAN		2
360	2.56	2.56	4.2	sp|Q9NUB1|ACS2L_HUMAN	Acetyl-coenzyme A synthetase 2-like, mitochondrial OS=Homo sapiens GN=ACSS1 PE=1 SV=2	HUMAN		2
366	2.39	2.39	10.1	sp|P59998|ARPC4_HUMAN	Actin-related protein 2/3 complex subunit 4 OS=Homo sapiens GN=ARPC4 PE=1 SV=3	HUMAN		2
374	2.3	2.3	30.3	sp|P02792|FRIL_HUMAN	Ferritin light chain OS=Homo sapiens GN=FTL PE=1 SV=2	HUMAN		2
380	2.23	2.23	25.8	sp|O95169|NDUB8_HUMAN	NADH dehydrogenase [ubiquinone] 1 beta subcomplex subunit 8, mitochondrial OS=Homo sapiens GN=NDUFB8 PE=1 SV=1	HUMAN		2
384	2.18	2.18	7.7	sp|Q96A33|CCD47_HUMAN	Coiled-coil domain-containing protein 47 OS=Homo sapiens GN=CCDC47 PE=1 SV=1	HUMAN		2

N	Unused	Total	% Cov	Accession #	Name	Species	Peptides(95%)	
392	2.12	2.12	7.1	sp|Q96HE7|ERO1A_HUMAN	ERO1-like protein alpha OS=Homo sapiens GN=ERO1L PE=1 SV=2	HUMAN		2
396	2.09	2.09	2.7	sp|O00410|IPO5_HUMAN	Importin-5 OS=Homo sapiens GN=IPO5 PE=1 SV=4	HUMAN		2
398	2.06	2.06	21	sp|P04792|HSPB1_HUMAN	Heat shock protein beta-1 OS=Homo sapiens GN=HSPB1 PE=1 SV=2	HUMAN		2
400	2.05	2.06	16.9	sp|O95292|VAPB_HUMAN	Vesicle-associated membrane protein-associated protein B/C OS=Homo sapiens GN=VAPB PE=1 SV=3	HUMAN		2
402	2.04	4.39	19.9	sp|P31946|1433B_HUMAN	14-3-3 protein beta/alpha OS=Homo sapiens GN=YWHAB PE=1 SV=3	HUMAN		2
411	2	3.53	21.6	sp|Q9Y277|VDAC3_HUMAN	Voltage-dependent anion-selective channel protein 3 OS=Homo sapiens GN=VDAC3 PE=1 SV=1	HUMAN		2
477	1.78	1.78	25.4	sp|Q9BYN8|RT26_HUMAN	28S ribosomal protein S26, mitochondrial OS=Homo sapiens GN=MRPS26 PE=1 SV=1	HUMAN		2
479	1.77	1.77	9.2	sp|P26885|FKBP2_HUMAN	Peptidyl-prolyl cis-trans isomerase FKBP2 OS=Homo sapiens GN=FKBP2 PE=1 SV=2	HUMAN		2
483	1.73	1.73	4.1	sp|P13473|LAMP2_HUMAN	Lysosome-associated membrane glycoprotein 2 OS=Homo sapiens GN=LAMP2 PE=1 SV=2	HUMAN		2
485	1.7	1.7	8.8	sp|P10253|LYAG_HUMAN	Lysosomal alpha-glucosidase OS=Homo sapiens GN=GAA PE=1 SV=4	HUMAN		2
488	1.69	1.69	7.9	sp|Q9NYU2|UGGG1_HUMAN	UDP-glucose:glycoprotein glucosyltransferase 1 OS=Homo sapiens GN=UGGT1 PE=1 SV=3	HUMAN		2
497	1.57	1.57	15.2	sp|O95299|NDUAA_HUMAN	NADH dehydrogenase [ubiquinone] 1 alpha subcomplex subunit 10, mitochondrial OS=Homo sapiens GN=NDUFA10 PE=1 SV=1	HUMAN		2
500	1.52	1.52	30.4	sp|P62851|RS25_HUMAN	40S ribosomal protein S25 OS=Homo sapiens GN=RPS25 PE=1 SV=1	HUMAN		2
501	1.51	1.51	13.7	sp|Q9HCD0|MCCB_HUMAN	Methylcrotonoyl-CoA carboxylase beta chain, mitochondrial OS=Homo sapiens GN=MCCC2 PE=1 SV=1	HUMAN		2
503	1.5	1.5	17.7	sp|Q16740|CLPP_HUMAN	Putative ATP-dependent Clp protease proteolytic subunit, mitochondrial OS=Homo sapiens GN=CLPP PE=1 SV=1	HUMAN		2
536	1.11	1.11	10.8	sp|P12109|CO6A1_HUMAN	Collagen alpha-1(VI) chain OS=Homo sapiens GN=COL6A1 PE=1 SV=3	HUMAN		2
550	0.9	3.14	18.2	sp|O75477|ERLN1_HUMAN	Erlin-1 OS=Homo sapiens GN=ERLIN1 PE=1 SV=1	HUMAN		2
557	0.79	5.88	65.5	sp|Q9UNX3|RL26L_HUMAN	60S ribosomal protein L26-like 1 OS=Homo sapiens GN=RPL26L1 PE=1 SV=1	HUMAN		2
581	0.59	3.47	12.6	sp|P61981|1433G_HUMAN	14-3-3 protein gamma OS=Homo sapiens GN=YWHAG PE=1 SV=2	HUMAN		2
675	0.12	5.1	35.5	sp|Q29960|1C16_HUMAN	HLA class I histocompatibility antigen, Cw-16 alpha chain OS=Homo sapiens GN=HLA-C PE=2 SV=1	HUMAN		2
316	3.37	3.37	27	sp|Q9BYD1|RM13_HUMAN	39S ribosomal protein L13, mitochondrial OS=Homo sapiens GN=MRPL13 PE=1 SV=1	HUMAN		1
324	3.28	3.29	13.4	sp|P49419|AL7A1_HUMAN	Alpha-aminoadipic semialdehyde dehydrogenase OS=Homo sapiens GN=ALDH7A1 PE=1 SV=5	HUMAN		1
338	3.01	3.01	7.9	sp|P02751|FINC_HUMAN	Fibronectin OS=Homo sapiens GN=FN1 PE=1 SV=4	HUMAN		1
339	3	3	26.3	sp|P62979|RS27A_HUMAN	Ubiquitin-40S ribosomal protein S27a OS=Homo sapiens GN=RPS27A PE=1 SV=2	HUMAN		1
344	2.91	2.91	13.4	sp|O00159|MYO1C_HUMAN	Unconventional myosin-Ic OS=Homo sapiens GN=MYO1C PE=1 SV=4	HUMAN		1
346	2.85	2.85	20.5	sp|O75306|NDUS2_HUMAN	NADH dehydrogenase [ubiquinone] iron-sulfur protein 2, mitochondrial OS=Homo sapiens GN=NDUFS2 PE=1 SV=2	HUMAN		1
348	2.82	2.82	23.6	sp|Q9Y2B0|CNPV2_HUMAN	Protein canopy homolog 2 OS=Homo sapiens GN=CNPY2 PE=1 SV=1	HUMAN		1
352	2.75	2.75	10.6	sp|Q9UBR2|CATZ_HUMAN	Cathepsin Z OS=Homo sapiens GN=CTSZ PE=1 SV=1	HUMAN		1
353	2.63	2.63	12.7	sp|Q6NVY1|HIBCH_HUMAN	3-hydroxyisobutyryl-CoA hydrolase, mitochondrial OS=Homo sapiens GN=HIBCH PE=1 SV=2	HUMAN		1
354	2.63	2.63	9.2	sp|P10619|PPGB_HUMAN	Lysosomal protective protein OS=Homo sapiens GN=CTSA PE=1 SV=2	HUMAN		1
355	2.63	2.63	6.8	sp|Q9Y639|NPTN_HUMAN	Neuroplastin OS=Homo sapiens GN=NPTN PE=1 SV=2	HUMAN		1
359	2.57	2.57	7.9	sp|Q13641|TPBG_HUMAN	Trophoblast glycoprotein OS=Homo sapiens GN=TPBG PE=1 SV=1	HUMAN		1
361	2.55	2.55	14.3	sp|P30533|AMRP_HUMAN	Alpha-2-macroglobulin receptor-associated protein OS=Homo sapiens GN=LRPAP1 PE=1 SV=1	HUMAN		1
362	2.51	2.51	18.2	sp|P31937|3HIDH_HUMAN	3-hydroxyisobutyrate dehydrogenase, mitochondrial OS=Homo sapiens GN=HIBADH PE=1 SV=2	HUMAN		1
363	2.43	2.43	20.1	sp|P67809|YBOX1_HUMAN	Nuclease-sensitive element-binding protein 1 OS=Homo sapiens GN=YBX1 PE=1 SV=3	HUMAN		1
364	2.41	2.41	14.1	sp|O75251|NDUS7_HUMAN	NADH dehydrogenase [ubiquinone] iron-sulfur protein 7, mitochondrial OS=Homo sapiens GN=NDUFS7 PE=1 SV=3	HUMAN		1
365	2.4	2.4	28.9	sp|P35268|RL22_HUMAN	60S ribosomal protein L22 OS=Homo sapiens GN=RPL22 PE=1 SV=2	HUMAN		1
367	2.38	2.38	7.5	sp|P23219|PGH1_HUMAN	Prostaglandin G/H synthase 1 OS=Homo sapiens GN=PTGS1 PE=1 SV=2	HUMAN		1
368	2.36	2.36	11.8	sp|P49257|LMAN1_HUMAN	Protein ERGIC-53 OS=Homo sapiens GN=LMAN1 PE=1 SV=2	HUMAN		1
370	2.32	2.32	20.2	sp|Q14257|RCN2_HUMAN	Reticulocalbin-2 OS=Homo sapiens GN=RCN2 PE=1 SV=1	HUMAN		1
371	2.32	2.32	26.2	sp|O00560|SDCB1_HUMAN	Syntenin-1 OS=Homo sapiens GN=SDCBP PE=1 SV=1	HUMAN		1
372	2.32	2.32	37.9	sp|O75964|ATP5L_HUMAN	ATP synthase subunit g, mitochondrial OS=Homo sapiens GN=ATP5L PE=1 SV=3	HUMAN		1
375	2.29	2.3	7	sp|P33121|ACSL1_HUMAN	Long-chain-fatty-acid--CoA ligase 1 OS=Homo sapiens GN=ACSL1 PE=1 SV=1	HUMAN		1
376	2.27	2.27	21.9	sp|O15145|ARPC3_HUMAN	Actin-related protein 2/3 complex subunit 3 OS=Homo sapiens GN=ARPC3 PE=1 SV=3	HUMAN		1
377	2.25	2.25	13.1	sp|P28838|AMPL_HUMAN	Cytosol aminopeptidase OS=Homo sapiens GN=LAP3 PE=1 SV=3	HUMAN		1
378	2.24	2.24	6.2	sp|O75746|CMC1_HUMAN	Calcium-binding mitochondrial carrier protein Aralar1 OS=Homo sapiens GN=SLC25A12 PE=1 SV=2	HUMAN		1
379	2.24	2.24	9.1	sp|P43307|SSRA_HUMAN	Translocon-associated protein subunit alpha OS=Homo sapiens GN=SSR1 PE=1 SV=3	HUMAN		1
381	2.2	2.2	23	sp|Q03135|CAV1_HUMAN	Caveolin-1 OS=Homo sapiens GN=CAV1 PE=1 SV=4	HUMAN		1
382	2.2	2.2	12.1	sp|P11310|ACADM_HUMAN	Medium-chain specific acyl-CoA dehydrogenase, mitochondrial OS=Homo sapiens GN=ACADM PE=1 SV=1	HUMAN		1
383	2.18	2.18	14.8	sp|Q9BYD3|RM04_HUMAN	39S ribosomal protein L4, mitochondrial OS=Homo sapiens GN=MRPL4 PE=1 SV=1	HUMAN		1
385	2.18	2.18	3.8	sp|O00754|MA2B1_HUMAN	Lysosomal alpha-mannosidase OS=Homo sapiens GN=MAN2B1 PE=1 SV=3	HUMAN		1
386	2.16	2.16	12.8	sp|Q9Y305|ACOT9_HUMAN	Acyl-coenzyme A thioesterase 9, mitochondrial OS=Homo sapiens GN=ACOT9 PE=1 SV=2	HUMAN		1
387	2.15	2.15	20.1	sp|P30044|PRDX5_HUMAN	Peroxiredoxin-5, mitochondrial OS=Homo sapiens GN=PRDX5 PE=1 SV=4	HUMAN		1
389	2.13	2.13	11.7	sp|P61978|HNRPK_HUMAN	Heterogeneous nuclear ribonucleoprotein K OS=Homo sapiens GN=HNRNPK PE=1 SV=1	HUMAN		1
390	2.13	2.13	9.4	sp|P21281|VATB2_HUMAN	V-type proton ATPase subunit B, brain isoform OS=Homo sapiens GN=ATP6V1B2 PE=1 SV=3	HUMAN		1
391	2.12	2.12	15.4	sp|P04040|CATA_HUMAN	Catalase OS=Homo sapiens GN=CAT PE=1 SV=3	HUMAN		1
393	2.1	2.1	21.7	sp|O43920|NDUS5_HUMAN	NADH dehydrogenase [ubiquinone] iron-sulfur protein 5 OS=Homo sapiens GN=NDUFS5 PE=1 SV=3	HUMAN		1
394	2.1	2.1	2.9	sp|Q969N2|PIGT_HUMAN	GPI transamidase component PIG-T OS=Homo sapiens GN=PIGT PE=1 SV=1	HUMAN		1
395	2.09	2.09	14.7	sp|P52209|6PGD_HUMAN	6-phosphogluconate dehydrogenase, decarboxylating OS=Homo sapiens GN=PGD PE=1 SV=3	HUMAN		1
397	2.08	2.08	35.8	sp|P62937|PPIA_HUMAN	Peptidyl-prolyl cis-trans isomerase A OS=Homo sapiens GN=PPIA PE=1 SV=2	HUMAN		1
399	2.06	2.06	19	sp|P30042|ES1_HUMAN	ES1 protein homolog, mitochondrial OS=Homo sapiens GN=C21orf33 PE=1 SV=3	HUMAN		1
401	2.05	2.05	16.3	sp|P18621|RL17_HUMAN	60S ribosomal protein L17 OS=Homo sapiens GN=RPL17 PE=1 SV=3	HUMAN		1
403	2.03	2.03	19.7	sp|Q9BPW8|NIPS1_HUMAN	Protein NipSnap homolog 1 OS=Homo sapiens GN=NIPSNAP1 PE=1 SV=1	HUMAN		1
404	2.03	2.03	15.2	sp|P36957|ODO2_HUMAN	Dihydrolipoyllysine-residue succinyltransferase component of 2-oxoglutarate dehydrogenase complex, mitochondrial OS=Homo sapiens GN=DLST PE=1 SV=4	HUMAN		1
405	2.01	2.01	21.9	sp|Q9Y2R9|RT07_HUMAN	28S ribosomal protein S7, mitochondrial OS=Homo sapiens GN=MRPS7 PE=1 SV=2	HUMAN		1
406	2.01	2.01	14.2	sp|P49189|AL9A1_HUMAN	4-trimethylaminobutyraldehyde dehydrogenase OS=Homo sapiens GN=ALDH9A1 PE=1 SV=3	HUMAN		1
407	2.01	2.01	7	sp|P36551|HEM6_HUMAN	Coproporphyrinogen-III oxidase, mitochondrial OS=Homo sapiens GN=CPOX PE=1 SV=3	HUMAN		1
408	2.01	2.01	16.2	sp|Q9NS69|TOM22_HUMAN	Mitochondrial import receptor subunit TOM22 homolog OS=Homo sapiens GN=TOMM22 PE=1 SV=3	HUMAN		1
409	2.01	2.01	11.7	sp|Q96AB3|ISOC2_HUMAN	Isochorismatase domain-containing protein 2, mitochondrial OS=Homo sapiens GN=ISOC2 PE=1 SV=1	HUMAN		1
412	2	2.44	11.8	sp|P04899|GNAI2_HUMAN	Guanine nucleotide-binding protein G(i) subunit alpha-2 OS=Homo sapiens GN=GNAI2 PE=1 SV=3	HUMAN		1
413	2	2	4.3	sp|Q9Y490|TLN1_HUMAN	Talin-1 OS=Homo sapiens GN=TLN1 PE=1 SV=3	HUMAN		1
414	2	2	11.4	sp|P23786|CPT2_HUMAN	Carnitine O-palmitoyltransferase 2, mitochondrial OS=Homo sapiens GN=CPT2 PE=1 SV=2	HUMAN		1
415	2	2	22.6	sp|P54819|KAD2_HUMAN	Adenylate kinase 2, mitochondrial OS=Homo sapiens GN=AK2 PE=1 SV=2	HUMAN		1
416	2	2	7.9	sp|P23246|SFPQ_HUMAN	Splicing factor, proline- and glutamine-rich OS=Homo sapiens GN=SFPQ PE=1 SV=2	HUMAN		1
417	2	2	25.8	sp|P10620|MGST1_HUMAN	Microsomal glutathione S-transferase 1 OS=Homo sapiens GN=MGST1 PE=1 SV=1	HUMAN		1
418	2	2	8.1	sp|P08195|4F2_HUMAN	4F2 cell-surface antigen heavy chain OS=Homo sapiens GN=SLC3A2 PE=1 SV=3	HUMAN		1
419	2	2	5.3	sp|O60313|OPA1_HUMAN	Dynamin-like 120 kDa protein, mitochondrial OS=Homo sapiens GN=OPA1 PE=1 SV=3	HUMAN		1
420	2	2	20.5	sp|Q9Y281|COF2_HUMAN	Cofilin-2 OS=Homo sapiens GN=CFL2 PE=1 SV=1	HUMAN		1
421	2	2	9.8	sp|Q9NP81|SYSM_HUMAN	Serine--tRNA ligase, mitochondrial OS=Homo sapiens GN=SARS2 PE=1 SV=1	HUMAN		1
422	2	2	25.1	sp|Q99470|SDF2_HUMAN	Stromal cell-derived factor 2 OS=Homo sapiens GN=SDF2 PE=1 SV=2	HUMAN		1
423	2	2	13.5	sp|Q8TC12|RDH11_HUMAN	Retinol dehydrogenase 11 OS=Homo sapiens GN=RDH11 PE=1 SV=2	HUMAN		1
424	2	2	27.8	sp|Q8N183|MIMIT_HUMAN	Mimitin, mitochondrial OS=Homo sapiens GN=NDUFAF2 PE=1 SV=1	HUMAN		1
425	2	2	12.7	sp|Q86WV6|TM173_HUMAN	Transmembrane protein 173 OS=Homo sapiens GN=TMEM173 PE=1 SV=1	HUMAN		1
426	2	2	4.3	sp|P16615|AT2A2_HUMAN	Sarcoplasmic/endoplasmic reticulum calcium ATPase 2 OS=Homo sapiens GN=ATP2A2 PE=1 SV=1	HUMAN		1
427	2	2	4.2	sp|Q9UBV2|SE1L1_HUMAN	Protein sel-1 homolog 1 OS=Homo sapiens GN=SEL1L PE=1 SV=3	HUMAN		1
428	2	2	6.4	sp|Q9NX20|RM16_HUMAN	39S ribosomal protein L16, mitochondrial OS=Homo sapiens GN=MRPL16 PE=1 SV=1	HUMAN		1
429	2	2	13	sp|Q9NR28|DBLOH_HUMAN	Diablo homolog, mitochondrial OS=Homo sapiens GN=DIABLO PE=1 SV=1	HUMAN		1
430	2	2	10.1	sp|Q12846|STX4_HUMAN	Syntaxin-4 OS=Homo sapiens GN=STX4 PE=1 SV=2	HUMAN		1
431	2	2	20.3	sp|P62847|RS24_HUMAN	40S ribosomal protein S24 OS=Homo sapiens GN=RPS24 PE=1 SV=1	HUMAN		1
432	2	2	21.4	sp|P56556|NDUA6_HUMAN	NADH dehydrogenase [ubiquinone] 1 alpha subcomplex subunit 6 OS=Homo sapiens GN=NDUFA6 PE=1 SV=3	HUMAN		1
433	2	2	10.8	sp|P50897|PPT1_HUMAN	Palmitoyl-protein thioesterase 1 OS=Homo sapiens GN=PPT1 PE=1 SV=1	HUMAN		1
434	2	2	11.6	sp|P24844|MYL9_HUMAN	Myosin regulatory light polypeptide 9 OS=Homo sapiens GN=MYL9 PE=1 SV=4	HUMAN		1
435	2	2	5.2	sp|P14384|CBPM_HUMAN	Carboxypeptidase M OS=Homo sapiens GN=CPM PE=1 SV=2	HUMAN		1
436	2	2	5	sp|P08962|CD63_HUMAN	CD63 antigen OS=Homo sapiens GN=CD63 PE=1 SV=2	HUMAN		1
437	2	2	2.8	sp|P06396|GELS_HUMAN	Gelsolin OS=Homo sapiens GN=GSN PE=1 SV=1	HUMAN		1
438	2	2	32.3	sp|O43678|NDUA2_HUMAN	NADH dehydrogenase [ubiquinone] 1 alpha subcomplex subunit 2 OS=Homo sapiens GN=NDUFA2 PE=1 SV=3	HUMAN		1
439	2	2	16.9	sp|Q9YSJ7|TIM9_HUMAN	Mitochondrial import inner membrane translocase subunit Tim9 OS=Homo sapiens GN=TIMM9 PE=1 SV=1	HUMAN		1
440	2	2	4.5	sp|Q9Y383|TMED7_HUMAN	Transmembrane emp24 domain-containing protein 7 OS=Homo sapiens GN=TMED7 PE=1 SV=2	HUMAN		1
441	2	2	4.3	sp|Q9Y2C4|EXOG_HUMAN	Nuclease EXOG, mitochondrial OS=Homo sapiens GN=EXOG PE=1 SV=2	HUMAN		1
442	2	2	7.6	sp|Q9UNL2|SSRG_HUMAN	Translocon-associated protein subunit gamma OS=Homo sapiens GN=SSR3 PE=1 SV=1	HUMAN		1
443	2	2	2.7	sp|Q9NP92|RT30_HUMAN	28S ribosomal protein S30, mitochondrial OS=Homo sapiens GN=MRPS30 PE=1 SV=2	HUMAN		1
444	2	2	3.2	sp|Q9HA77|SYCM_HUMAN	Probable cysteine--tRNA ligase, mitochondrial OS=Homo sapiens GN=CARS2 PE=1 SV=1	HUMAN		1
445	2	2	8.6	sp|Q9H3Z4|DNJC5_HUMAN	DnaJ homolog subfamily C member 5 OS=Homo sapiens GN=DNAJC5 PE=1 SV=1	HUMAN		1
446	2	2	7.8	sp|Q9GZV4|IF5A2_HUMAN	Eukaryotic translation initiation factor 5A-2 OS=Homo sapiens GN=EIF5A2 PE=1 SV=3	HUMAN		1
447	2	2	2.5	sp|Q96S52|PIGS_HUMAN	GPI transamidase component PIG-S OS=Homo sapiens GN=PIGS PE=1 SV=3	HUMAN		1
448	2	2	3.3	sp|Q13418|ILK_HUMAN	Integrin-linked protein kinase OS=Homo sapiens GN=ILK PE=1 SV=2	HUMAN		1
449	2	2	18.1	sp|P63220|RS21_HUMAN	40S ribosomal protein S21 OS=Homo sapiens GN=RPS21 PE=1 SV=1	HUMAN		1
450	2	2	5.9	sp|P62070|RRAS2_HUMAN	Ras-related protein R-Ras2 OS=Homo sapiens GN=RRAS2 PE=1 SV=1	HUMAN		1
451	2	2	3.6	sp|P55795|HNRH2_HUMAN	Heterogeneous nuclear ribonucleoprotein H2 OS=Homo sapiens GN=HNRNPH2 PE=1 SV=1	HUMAN		1
452	2	2	2.6	sp|P53634|CATC_HUMAN	Dipeptidyl peptidase 1 OS=Homo sapiens GN=CTSC PE=1 SV=2	HUMAN		1
453	2	2	2.2	sp|P39023|RL3_HUMAN	60S ribosomal protein L3 OS=Homo sapiens GN=RPL3 PE=1 SV=2	HUMAN		1
454	2	2	14	sp|P05386|RLA1_HUMAN	60S acidic ribosomal protein P1 OS=Homo sapiens GN=RPLP1 PE=1 SV=1	HUMAN		1
455	2	2	6.6	sp|Q75208|COQ9_HUMAN	Ubiquinone biosynthesis protein COQ9, mitochondrial OS=Homo sapiens GN=COQ9 PE=1 SV=1	HUMAN		1
456	2	2	7.8	sp|O60888|CUTA_HUMAN	Protein CutA OS=Homo sapiens GN=CUTA PE=1 SV=2	HUMAN		1
457	2	2	6.3	sp|O14521|DHSD_HUMAN	Succinate dehydrogenase [ubiquinone] cytochrome b small subunit, mitochondrial OS=Homo sapiens GN=SDHD PE=1 SV=1	HUMAN		1
458	1.96	2	28.4	sp|Q9GZT3|SLIRP_HUMAN	SRA stem-loop-interacting RNA-binding protein, mitochondrial OS=Homo sapiens GN=SLIRP PE=1 SV=1	HUMAN		1
459	1.96	2	7.6	sp|Q8IXI1|MIRO2_HUMAN	Mitochondrial Rho GTPase 2 OS=Homo sapiens GN=RHOT2 PE=1 SV=2	HUMAN		1
460	1.96	2	8.3	sp|P30049|ATPD_HUMAN	ATP synthase subunit delta, mitochondrial OS=Homo sapiens GN=ATP5D PE=1 SV=2	HUMAN		1
461	1.94	1.94	4.8	sp|P20930|FILA_HUMAN	Filaggrin OS=Homo sapiens GN=FLG PE=1 SV=3	HUMAN		1
462	1.93	2	46.9	sp|O00483|NDUA4_HUMAN	NADH dehydrogenase [ubiquinone] 1 alpha subcomplex subunit 4 OS=Homo sapiens GN=NDUFA4 PE=1 SV=1	HUMAN		1
463	1.9	1.9	6.9	sp|O75369|FLNB_HUMAN	Filamin-B OS=Homo sapiens GN=FLNB PE=1 SV=2	HUMAN		1
464	1.89	1.89	18.5	sp|Q9P0L0|VAPA_HUMAN	Vesicle-associated membrane protein-associated protein A OS=Homo sapiens GN=VAPA PE=1 SV=3	HUMAN		1

N	Unused	Total	% Cov	Accession #	Name	Species	Peptides(95%)	
465	1.89	1.89	8.7	sp|Q96QK1|VPS35_HUMAN	Vacuolar protein sorting-associated protein 35 OS=Homo sapiens GN=VPS35 PE=1 SV=2	HUMAN		1
466	1.89	1.89	16.7	sp|O75347|TBCA_HUMAN	Tubulin-specific chaperone A OS=Homo sapiens GN=TBCA PE=1 SV=3	HUMAN		1
467	1.86	1.86	3.3	sp|Q14974|IMB1_HUMAN	Importin subunit beta-1 OS=Homo sapiens GN=KPNB1 PE=1 SV=2	HUMAN		1
468	1.85	1.85	9.8	sp|P35237|SPB6_HUMAN	Serpin B6 OS=Homo sapiens GN=SERPINB6 PE=1 SV=3	HUMAN		1
469	1.82	1.82	16.2	sp|P15259|PGAM2_HUMAN	Phosphoglycerate mutase 2 OS=Homo sapiens GN=PGAM2 PE=1 SV=3	HUMAN		1
470	1.82	1.82	2.7	sp|P17050|NAGAB_HUMAN	Alpha-N-acetylgalactosaminidase OS=Homo sapiens GN=NAGA PE=1 SV=2	HUMAN		1
471	1.81	1.81	8.3	sp|Q9Y394|DHRS7_HUMAN	Dehydrogenase/reductase SDR family member 7 OS=Homo sapiens GN=DHRS7 PE=1 SV=1	HUMAN		1
473	1.8	1.8	12.9	sp|P43155|CACP_HUMAN	Carnitine O-acetyltransferase OS=Homo sapiens GN=CRAT PE=1 SV=5	HUMAN		1
474	1.8	1.8	7.1	sp|Q9Y257|PDIP2_HUMAN	Polymerase delta-interacting protein 2 OS=Homo sapiens GN=POLDIP2 PE=1 SV=1	HUMAN		1
475	1.8	1.8	27	sp|Q9UDW1|QCR9_HUMAN	Cytochrome b-c1 complex subunit 9 OS=Homo sapiens GN=UQCR10 PE=1 SV=3	HUMAN		1
476	1.8	1.8	8.5	sp|P60033|CD81_HUMAN	CD81 antigen OS=Homo sapiens GN=CD81 PE=1 SV=1	HUMAN		1
478	1.78	1.78	31.1	sp|Q8TCC3|RM30_HUMAN	39S ribosomal protein L30, mitochondrial OS=Homo sapiens GN=MRPL30 PE=1 SV=1	HUMAN		1
480	1.77	1.77	5.8	sp|P78417|GSTO1_HUMAN	Glutathione S-transferase omega-1 OS=Homo sapiens GN=GSTO1 PE=1 SV=2	HUMAN		1
481	1.74	1.74	2.4	sp|P51688|SPHM_HUMAN	N-sulphoglucosamine sulphohydrolase OS=Homo sapiens GN=SGSH PE=1 SV=1	HUMAN		1
482	1.73	1.73	17.6	sp|Q9P015|RM15_HUMAN	39S ribosomal protein L15, mitochondrial OS=Homo sapiens GN=MRPL15 PE=1 SV=1	HUMAN		1
484	1.72	1.72	11.3	sp|O75380|NDUS6_HUMAN	NADH dehydrogenase [ubiquinone] iron-sulfur protein 6, mitochondrial OS=Homo sapiens GN=NDUFS6 PE=1 SV=1	HUMAN		1
486	1.7	1.7	3.8	sp|Q92499|DDX1_HUMAN	ATP-dependent RNA helicase DDX1 OS=Homo sapiens GN=DDX1 PE=1 SV=2	HUMAN		1
487	1.7	1.7	15.5	sp|P42677|RS27_HUMAN	40S ribosomal protein S27 OS=Homo sapiens GN=RPS27 PE=1 SV=3	HUMAN		1
489	1.69	1.69	4.4	sp|P22314|UBA1_HUMAN	Ubiquitin-like modifier-activating enzyme 1 OS=Homo sapiens GN=UBA1 PE=1 SV=3	HUMAN		1
490	1.68	1.68	3.2	sp|P07602|SAP_HUMAN	Proactivator polypeptide OS=Homo sapiens GN=PSAP PE=1 SV=2	HUMAN		1
491	1.65	1.65	24	sp|Q96A26|F162A_HUMAN	Protein FAM162A OS=Homo sapiens GN=FAM162A PE=1 SV=2	HUMAN		1
492	1.64	1.64	4.7	sp|O75396|SC22B_HUMAN	Vesicle-trafficking protein SEC22b OS=Homo sapiens GN=SEC22B PE=1 SV=4	HUMAN		1
493	1.6	1.6	32.8	sp|O95298|NDUC2_HUMAN	NADH dehydrogenase [ubiquinone] 1 subunit C2 OS=Homo sapiens GN=NDUFC2 PE=1 SV=1	HUMAN		1
494	1.6	1.6	16.5	sp|P82912|RT11_HUMAN	28S ribosomal protein S11, mitochondrial OS=Homo sapiens GN=MRPS11 PE=1 SV=2	HUMAN		1
496	1.59	1.59	15.2	sp|P25398|RS12_HUMAN	40S ribosomal protein S12 OS=Homo sapiens GN=RPS12 PE=1 SV=3	HUMAN		1
498	1.57	1.57	3.6	sp|P40925|MDHC_HUMAN	Malate dehydrogenase, cytoplasmic OS=Homo sapiens GN=MDH1 PE=1 SV=4	HUMAN		1
499	1.53	1.53	7.7	sp|P42785|PCP_HUMAN	Lysosomal Pro-X carboxypeptidase OS=Homo sapiens GN=PRCP PE=1 SV=1	HUMAN		1
502	1.5	1.51	17.9	sp|Q15006|EMC2_HUMAN	ER membrane protein complex subunit 2 OS=Homo sapiens GN=EMC2 PE=1 SV=1	HUMAN		1
504	1.49	1.51	5.2	sp|Q86UE4|LYRIC_HUMAN	Protein LYRIC OS=Homo sapiens GN=MTDH PE=1 SV=2	HUMAN		1
505	1.49	1.51	4.4	sp|P04844|RPN2_HUMAN	Dolichyl-diphosphooligosaccharide--protein glycosyltransferase subunit 2 OS=Homo sapiens GN=RPN2 PE=1 SV=3	HUMAN		1
506	1.48	1.48	48.2	sp|P18077|RL35A_HUMAN	60S ribosomal protein L35a OS=Homo sapiens GN=RPL35A PE=1 SV=2	HUMAN		1
507	1.48	1.48	14.2	sp|Q9NUP9|LIN7C_HUMAN	Protein lin-7 homolog C OS=Homo sapiens GN=LIN7C PE=1 SV=1	HUMAN		1
508	1.46	1.46	23.7	sp|O00299|CLIC1_HUMAN	Chloride intracellular channel protein 1 OS=Homo sapiens GN=CLIC1 PE=1 SV=4	HUMAN		1
509	1.46	1.46	4.7	sp|P23142|FBLN1_HUMAN	Fibulin-1 OS=Homo sapiens GN=FBLN1 PE=1 SV=4	HUMAN		1
511	1.42	1.42	2.3	sp|P35613|BASI_HUMAN	Basigin OS=Homo sapiens GN=BSG PE=1 SV=2	HUMAN		1
512	1.41	1.41	4.9	sp|O00469|PLOD2_HUMAN	Procollagen-lysine,2-oxoglutarate 5-dioxygenase 2 OS=Homo sapiens GN=PLOD2 PE=1 SV=2	HUMAN		1
514	1.4	1.4	9.7	sp|Q9H061|T126A_HUMAN	Transmembrane protein 126A OS=Homo sapiens GN=TMEM126A PE=1 SV=1	HUMAN		1
515	1.4	1.4	3	sp|O96008|TOM40_HUMAN	Mitochondrial import receptor subunit TOM40 homolog OS=Homo sapiens GN=TOMM40 PE=1 SV=1	HUMAN		1
516	1.39	1.39	5.3	sp|P51398|RT29_HUMAN	28S ribosomal protein S29, mitochondrial OS=Homo sapiens GN=DAP3 PE=1 SV=1	HUMAN		1
517	1.38	1.38	3.1	sp|Q96TA1|NIBL1_HUMAN	Niban-like protein 1 OS=Homo sapiens GN=FAM129B PE=1 SV=3	HUMAN		1
518	1.38	1.38	4.1	sp|Q13510|ASAH1_HUMAN	Acid ceramidase OS=Homo sapiens GN=ASAH1 PE=1 SV=5	HUMAN		1
519	1.36	1.36	20.6	sp|Q8NRX2|RM17_HUMAN	39S ribosomal protein L17, mitochondrial OS=Homo sapiens GN=MRPL17 PE=1 SV=1	HUMAN		1
520	1.36	1.36	8.1	sp|O94760|DDAH1_HUMAN	N(G),N(G)-dimethylarginine dimethylaminohydrolase 1 OS=Homo sapiens GN=DDAH1 PE=1 SV=3	HUMAN		1
521	1.33	1.33	3	sp|O14656|TOR1A_HUMAN	Torsin-1A OS=Homo sapiens GN=TOR1A PE=1 SV=1	HUMAN		1
522	1.32	1.32	3.1	sp|Q14554|PDIA5_HUMAN	Protein disulfide-isomerase A5 OS=Homo sapiens GN=PDIA5 PE=1 SV=1	HUMAN		1
523	1.32	1.32	10.7	sp|P30536|TSPOA_HUMAN	Translocator protein OS=Homo sapiens GN=TSPO PE=1 SV=3	HUMAN		1

Supplemental table S5: PTM's detected using Mascot 2D-LC

prot_hit_num	prot_acc	prot_desc	prot_score	prot_mass	prot_matches	prot_cover	prot_pi	pep_query	pep_exp_mz	pep_exp_mr	pep_exp_z	pep_calc_mr	pep_delta	pep_start	pep_end	pep_miss	pep_score	pep_expect	pep_rank	pep_res_before	pep_seq	pep_res_after	pep_var_mod
26	PGRC1_HUMAN	Membrane-associated progesterone receptor com	185					5572	2375.94	2374.94	1	2374.93	0	173	192	1	83.56	1.60E-06	1	K	EGEEPTVYS	K	Phospho (ST)
5	GRP78_HUMAN	78 kDa glucose-regulated protein OS=Homo sapier	479					3883	1693.86	1692.86	1	1692.82	0.03	582	596	2	80.41	32	38	2.90E-06	1	K	Acetyl (K)
5	GRP78_HUMAN	78 kDa glucose-regulated protein OS=Homo sapier	480					3884	1693.87	1692.86	1	1692.82	0.04	582	596	2	36.82	27	38	0.067	1	K	Acetyl (K)
67	PPIA_HUMAN	Peptidyl-prolyl cis-trans isomerase A OS=Homo sap	119					5142	2118.96	2117.95	1	2118.05	-0.1	1	19	0	107.81	33	39	6.60E-09	1	-	Acetyl (N-term)
67	PPIA_HUMAN	Peptidyl-prolyl cis-trans isomerase A OS=Homo sap	120					5143	2119.04	2118.03	1	2118.05	-0.01	1	19	0	43.45	34	39	0.019	1	-	Acetyl (N-term)
68	2AAA_HUMAN	Serine/threonine-protein phosphatase 2A 65 kDa r	118					5209	2159.03	2158.02	1	2158.08	-0.05	2	21	0	77.79		39	7.30E-06	1	M	Acetyl (N-term)
68	2AAA_HUMAN	Serine/threonine-protein phosphatase 2A 65 kDa r	119					5210	2159.09	2158.08	1	2158.08	0	2	21	0	75.97	35	38	9.90E-06	1	M	Acetyl (N-term)
89	CKAP4_HUMAN	Cytoskeleton-associated protein 4 OS=Homo sapie	104					3432	1588.78	1587.78	1	1587.83	-0.05	541	554	1	37	30	38	0.075	1	K	Acetyl (K)
92	EXOC5_HUMAN	Exocyst complex component 5 OS=Homo sapiens (	103					5393	2272.04	2271.03	1	2271.06	-0.03	2	20	0	101.67	33	39	2.80E-08	1	M	Acetyl (N-term)
104	COX20_HUMAN	Cytochrome c oxidase protein 20 homolog OS=Hor	96	13283	2	10.2	9	2267	1320.6	1319.6	1	1319.6	0	2	13	0	93.52	34	37	1.20E-07	1	M	Acetyl (N-term)
104	COX20_HUMAN	Cytochrome c oxidase protein 20 homolog OS=Hor	97					2268	1320.61	1319.61	1	1319.6	0.01	2	13	0	33.51	29	37	0.13	1	M	Acetyl (N-term)
114	E41L3_HUMAN	Band 4.1-like protein 3 OS=Homo sapiens GN=EPB4	88					5962	2804.24	2803.24	1	2803.2	0.03	2	28	0	49.53		38	0.0041	1	M	Acetyl (N-term)
128	TIM8B_HUMAN	Mitochondrial import inner membrane translocase	81					2899	1472.68	1471.68	1	1471.68	0	2	14	0	79.99		38	3.40E-06	1	M	Acetyl (N-term)
133	EIF3M_HUMAN	Eukaryotic translation initiation factor 3 subunit M	79	42476	1	4.8	5.41	4941	2031.93	2030.93	1	2030.98	-0.05	2	19	0	79.17		39	5.00E-06	1	M	Acetyl (N-term)
172	IPO5_HUMAN	Importin-5 OS=Homo sapiens GN=IPO5 PE=1 SV=5	67					5915	2743.45	2742.44	1	2742.43	0.01	2	26	0	63.54		36	0.00011	1	M	Acetyl (N-term)
173	HMOX2_HUMAN	Heme oxygenase 2 OS=Homo sapiens GN=HMOX2	65	36010	2	12	5.31	4168	1765.78	1764.77	1	1764.79	-0.02	2	17	1	65.32	28	37	8.80E-05	1	M	Acetyl (N-term)

Supplemental table S6: PTM's detected using Mascot SDS-LC

prot_hit_num	prot_acc	prot_desc	prot_score	prot_mass	prot_match	prot_cover	prot_pi	pep_query	pep_exp_m	pep_exp_m	pep_exp_z	pep_calc_m	pep_delta	pep_start	pep_end	pep_miss	pep_score	pep_var_mod
2	ACTB_HUMAN	Actin, cytoplasmic 1 OS=Homo sapiens GN=ACTB PE=1 SV=2	2422					9323	1835.81	1834.8	1	1834.81	0	2	18	0	118.33	Acetyl (N-term); Propionamide (C)
101	RS18_HUMAN	40S ribosomal protein S18 OS=Homo sapiens GN=RPS18 PE=1 SV=3	281					7535	1621.94	1620.93	1	1620.94	0	2	14	1	64.45	Acetyl (N-term)
101	RS18_HUMAN	40S ribosomal protein S18 OS=Homo sapiens GN=RPS18 PE=1 SV=3	281					7536	1621.94	1620.93	1	1620.94	0	2	14	1	59.28	Acetyl (N-term)
119	SEP11_HUMAN	Septin-11 OS=Homo sapiens GN=SEPT11 PE=1 SV=3	253					5642	1439.75	1438.74	1	1438.75	-0.01	2	14	0	70.53	Acetyl (N-term)
119	SEP11_HUMAN	Septin-11 OS=Homo sapiens GN=SEPT11 PE=1 SV=3	253					5644	1439.76	1438.75	1	1438.75	0	2	14	0	62.39	Acetyl (N-term)
119	SEP11_HUMAN	Septin-11 OS=Homo sapiens GN=SEPT11 PE=1 SV=3	253					5645	1439.76	1438.75	1	1438.75	0	2	14	0	58.13	Acetyl (N-term)
164	ADT2_HUMAN	ADP/ATP translocase 2 OS=Homo sapiens GN=SLC25A5 PE=1 SV=7	193					10869	2152.14	2151.14	1	2151.12	0.01	2	23	1	61.24	Acetyl (N-term)
226	ETFB_HUMAN	Electron transfer flavoprotein subunit beta OS=Homo sapiens GN=ETFB PE=1 SV=5	143					4203	1291.74	1290.73	1	1290.7	0.03	192	202	1	36.79	Acetyl (K)
228	NDUB9_HUMAN	NADH dehydrogenase [ubiquinone] 1 beta subcomplex subunit 9 OS=Homo sapiens GN=NDUFB9 PE=1 SV=5	142					7350	1602.83	1601.82	1	1601.82	0	2	15	0	71.07	Acetyl (N-term)
242	EF2_HUMAN	Elongation factor 2 OS=Homo sapiens GN=EEF2 PE=1 SV=5	134					4435	1316.72	1315.71	1	1315.71	0	440	449	0	33.72	Acetyl (N-term)
249	RS11_HUMAN	40S ribosomal protein S11 OS=Homo sapiens GN=RPS11 PE=1 SV=4	129					653	874.43	873.43	1	873.42	0.01	2	8	0	43.85	Acetyl (N-term)
262	M2OM_HUMAN	Mitochondrial 2-oxoglutarate/malate carrier protein OS=Homo sapiens GN=SLC25A11 PE=1 SV=3	124					5674	1441.74	1440.73	1	1440.73	0	2	17	0	100.33	Acetyl (N-term)
264	NDUAC_HUMAN	NADH dehydrogenase [ubiquinone] 1 alpha subcomplex subunit 12 OS=Homo sapiens GN=NDUFA12 PE=1 SV=3	126					2890	1157.66	1156.66	1	1156.66	-0.01	1	9	1	70.96	Acetyl (N-term)
266	RL11_HUMAN	60S ribosomal protein L11 OS=Homo sapiens GN=RPL11 PE=1 SV=4	124					5694	1444.65	1443.64	1	1443.64	0	2	13	1	66.96	Acetyl (N-term)
266	RL11_HUMAN	60S ribosomal protein L11 OS=Homo sapiens GN=RPL11 PE=1 SV=6	124					9365	1842.88	1841.87	1	1841.87	0	2	16	2	30.87	Acetyl (N-term)
268	RB11A_HUMAN	Ras-related protein Rab-11A OS=Homo sapiens GN=RAB11A PE=1 SV=8	127					4429	1316.65	1315.64	1	1315.62	0.03	62	72	0	75.13	Acetyl (N-term)
268	RB11A_HUMAN	Ras-related protein Rab-11A OS=Homo sapiens GN=RAB11A PE=1 SV=9	127					4430	1316.67	1315.66	1	1315.62	0.04	62	72	0	31.1	Acetyl (N-term)
268	RB11B_HUMAN	Ras-related protein Rab-11B OS=Homo sapiens GN=RAB11B PE=1 SV=9	127					4429	1316.65	1315.64	1	1315.62	0.03	62	72	0	75.13	Acetyl (N-term)
268	RB11B_HUMAN	Ras-related protein Rab-11B OS=Homo sapiens GN=RAB11B PE=1 SV=10	127					4430	1316.67	1315.66	1	1315.62	0.04	62	72	0	31.1	Acetyl (N-term)
300	ATPK_HUMAN	ATP synthase subunit f, mitochondrial OS=Homo sapiens GN=ATP5J2 PE=1 SV=6	112					8555	1737.92	1736.91	1	1736.91	0	2	17	2	41.02	Acetyl (N-term); Propionamide (C)
301	CAH2_HUMAN	Carbonic anhydrase 2 OS=Homo sapiens GN=CA2 PE=1 SV=2	109	29228	6	11.5	6.87	1599	1013.47	1012.46	1	1012.45	0.01	2	9	0	49.5	Acetyl (N-term)
301	CAH2_HUMAN	Carbonic anhydrase 2 OS=Homo sapiens GN=CA2 PE=1 SV=3	109					1600	1013.47	1012.46	1	1012.45	0.01	2	9	0	31.72	Acetyl (N-term)
304	1C16_HUMAN	HLA class I histocompatibility antigen, Cw-16 alpha chain OS=Homo sapiens GN=HLA-C PE=2 SV=5	112					6821	1549.75	1548.74	1	1548.72	0.02	156	169	0	32.61	Acetyl (N-term); Propionamide (C)
309	RS5_HUMAN	40S ribosomal protein S5 OS=Homo sapiens GN=RPS5 PE=1 SV=9	109					9521	1870.9	1869.89	1	1869.9	-0.01	2	18	0	48.99	Acetyl (N-term)
310	GBB1_HUMAN	Guanine nucleotide-binding protein G(I)/G(S)/G(T) subunit beta-1 OS=Homo sapiens GN=GNB1 PE=1 SV=6	106					8470	1728.87	1727.87	1	1727.87	0	2	15	1	51.87	Acetyl (N-term)
310	GBB1_HUMAN	Guanine nucleotide-binding protein G(I)/G(S)/G(T) subunit beta-1 OS=Homo sapiens GN=GNB1 PE=1 SV=7	106					11234	2240.16	2239.15	1	2239.16	-0.01	2	19	2	54.14	Acetyl (N-term)
325	RL13A_HUMAN	60S ribosomal protein L13a OS=Homo sapiens GN=RPL13A PE=1 SV=2	100					3702	1240.68	1239.67	1	1239.68	-0.01	2	12	0	66.03	Acetyl (N-term)
329	RL28_HUMAN	60S ribosomal protein L28 OS=Homo sapiens GN=RPL28 PE=1 SV=3	98					3983	1268.65	1267.64	1	1267.65	-0.01	2	11	0	77.32	Acetyl (N-term)
329	RL28_HUMAN	60S ribosomal protein L28 OS=Homo sapiens GN=RPL28 PE=1 SV=3	98					3984	1268.66	1267.65	1	1267.65	0.01	2	11	0	41.04	Acetyl (N-term)
331	GBB2_HUMAN	Guanine nucleotide-binding protein G(I)/G(S)/G(T) subunit beta-2 OS=Homo sapiens GN=GNB2 PE=1 SV=3	97					8817	1770.9	1769.89	1	1769.89	0	2	15	1	71.19	Acetyl (N-term)
332	NDUB6_HUMAN	NADH dehydrogenase [ubiquinone] 1 beta subcomplex subunit 6 OS=Homo sapiens GN=NDUFB6 PE=1 SV=3	97	15479	4	25.8	9.63	3504	1221.62	1220.61	1	1220.6	0.01	2	11	1	43.87	Acetyl (N-term)
341	CAZA1_HUMAN	F-actin-capping protein subunit alpha-1 OS=Homo sapiens GN=CAPZA1 PE=1 SV=3	92					8416	1722.79	1721.78	1	1721.79	0	2	15	2	49.82	Acetyl (N-term)
369	SYFA_HUMAN	Phenylalanine--tRNA ligase alpha subunit OS=Homo sapiens GN=FARSA PE=1 SV=3	83	57528	1	2.2	7.31	3553	1226.67	1225.66	1	1225.67	-0.01	2	12	0	83.21	Acetyl (N-term)
371	COX20_HUMAN	Cytochrome c oxidase protein 20 homolog OS=Homo sapiens GN=COX20 PE=1 SV=2	83	13283	4	22.9	9	4472	1320.6	1319.59	1	1319.6	-0.01	2	13	0	77.16	Acetyl (N-term)
371	COX20_HUMAN	Cytochrome c oxidase protein 20 homolog OS=Homo sapiens GN=COX20 PE=1 SV=2	83					4473	1320.61	1319.6	1	1319.6	0	2	13	0	33.25	Acetyl (N-term)
377	1433F_HUMAN	14-3-3 protein eta OS=Homo sapiens GN=YWHAH PE=1 SV=4	82					2877	1156.61	1155.6	1	1155.6	0	2	10	1	36.37	Acetyl (N-term)
425	RS21_HUMAN	40S ribosomal protein S21 OS=Homo sapiens GN=RPS21 PE=1 SV=1	72					9055	1795.83	1794.83	1	1794.82	0	1	15	0	71.62	Acetyl (N-term)
430	DDAH1_HUMAN	N(G),N(G)-dimethylarginine dimethylaminohydrolase 1 OS=Homo sapiens GN=DDAH1 PE=1 SV=3	71					2308	1095.57	1094.57	1	1094.56	0	2	12	0	63.23	Acetyl (N-term)
436	SC61G_HUMAN	Protein transport protein Sec61 subunit gamma OS=Homo sapiens GN=SEC61G PE=2 SV=1	70					6391	1508.69	1507.68	1	1507.68	0	1	12	0	69.64	Acetyl (N-term)
480	K2C72_HUMAN	Keratin, type II cytoskeletal 72 OS=Homo sapiens GN=KRT72 PE=1 SV=2	60					1303	973.52	972.51	1	972.49	0.02	341	348	0	38.17	Acetyl (N-term)
480	K2C72_HUMAN	Keratin, type II cytoskeletal 72 OS=Homo sapiens GN=KRT72 PE=1 SV=2	60					1304	973.53	972.53	1	972.49	0.04	341	348	0	44.88	Acetyl (N-term)

Supplemental table S7: PTM's detected using Protein Pilot 2D-LC

Prec MW	Prec m/z	Prec z			Best Sequence	Modifications	Conf	Theor MW	z	
1692.897	1693.904	1	sp|P11021	78 kDa glucose-regulated protein OS=Homo sapiens GN=HSPA5 PE=1 SV=2	LGGKLSSEDKETMEK	Acetyl(K)@4	99	1692.824	1	
1562.612	1563.619	1	sp|P62158	Calmodulin OS=Homo sapiens GN=CALM1 PE=1 SV=2	ADQLTEEQIAEFK	Acetyl@N-term	99	1562.747	1	
1534.676	1535.683	1	sp|Q9BWN	Sideroflexin-3 OS=Homo sapiens GN=SFXN3 PE=2 SV=2	GELPLDINIQEPR	Acetyl@N-term	99	1534.799	1	
1239.585	1240.593	1	sp|P40429	60S ribosomal protein L13a OS=Homo sapiens GN=RPL13A PE=1 SV=2	AEVQVLVLDGR	Acetyl@N-term	99	1239.682	1	
1866.821	1867.828	1	sp|P63261	Actin, cytoplasmic 2 OS=Homo sapiens GN=ACTG1 PE=1 SV=1	EEEIAALVIDNGSGMCK	Acetyl@N-term, Deamidated(N)@11, Methylthio(C)@16	99	1866.805	1	
1866.834	1867.841	1	sp|P63261	Actin, cytoplasmic 2 OS=Homo sapiens GN=ACTG1 PE=1 SV=1	EEEIAALVIDNGSGMCK	Acetyl@N-term, Deamidated(N)@11, Methylthio(C)@16	99	1866.805	1	
1882.838	1883.846	1	sp|P63261	Actin, cytoplasmic 2 OS=Homo sapiens GN=ACTG1 PE=1 SV=1	EEEIAALVIDNGSGMCK	Acetyl@N-term, Deamidated(N)@11, Oxidation(M)@15, Methylthio(C)@16	99	1882.8	1	
1478.716	1479.723	1	sp|P02768	Serum albumin OS=Homo sapiens GN=ALB PE=1 SV=2	GEYKFQNALLVR	Acetyl(K)@4	99	1478.788	1	
1507.505	1508.512	1	sp|P60059	Protein transport protein Sec61 subunit gamma OS=Homo sapiens GN=SEC61G PE=2 SV=1	MDQVMQFVEPSR	Acetyl@N-term	99	1507.68	1	
1986.932	1987.939	1	sp|P62937	Peptidyl-prolyl cis-trans isomerase A OS=Homo sapiens GN=PPIA PE=1 SV=2	VNPTVFFDIAVDGEPLGR	Acetyl@N-term	99	1987.005	1	
2117.972	2118.979	1	sp|P62937	Peptidyl-prolyl cis-trans isomerase A OS=Homo sapiens GN=PPIA PE=1 SV=2	MVNPTVFFDIAVDGEPLGR	Acetyl@N-term	99	2118.046	1	
1866.615	1867.622	1	sp|P63261	Actin, cytoplasmic 2 OS=Homo sapiens GN=ACTG1 PE=1 SV=1	EEEIAALVIDNGSGMCK	Acetyl@N-term, Deamidated(N)@11, Methylthio(C)@16	99	1866.805	1	
1761.708	1762.716	1	sp|P04406	Glyceraldehyde-3-phosphate dehydrogenase OS=Homo sapiens GN=GAPDH PE=1 SV=3	ISWYDNEFGYSNR	Phospho(S)@2, Dioxidation(W)@3	99	1761.667	1	

Supplemental table S8: PTM's detected using Protein Pilot SDS-LC

Prec MW	Prec m/z	Prec z	Proteins	Best Sequence	Modifications	Conf	Theor MW	z
1890.61	1891.618	1	sp|P63261|AC Actin,cytoplasmic 2 OS=Homo sapiens GN=ACTG1 PE=1 SV=1	EEEIAALVIDNGSGMCK	Acetyl@N-term, Propionamide(C)@16	99.00	1890.87	1
1507.684	1508.692	1	sp|P60059|SC Protein transport protein Sec61 subunit gamma OS=Homo sapiens GN=SEC61G PE=2 SV=1	MDQVMQFVEPSR	Acetyl@N-term	99.00	1507.68	1
1094.57	1095.577	1	sp|O94760|DI N(G),N(G)-dimethylarginine dimethylaminohydrolase 1 OS=Homo sapiens GN=DDAH1 PE=1 SV=3	AGLGHPAAFGR	Acetyl@N-term	99.00	1094.562	1
1794.829	1795.836	1	sp|P63220|RS 40S ribosomal protein S21 OS=Homo sapiens GN=RPS21 PE=1 SV=1	MQNDAGEFVDLYVPR	Acetyl@N-term	99.00	1794.825	1
1769.89	1770.897	1	sp|P62879|GI Guanine nucleotide-binding protein G(I)/G(S)/G(T) subunit beta-2 OS=Homo sapiens GN=GNB2 PE=1 SV=3	SELEQLRQEAEQLR	Acetyl@N-term	99.00	1769.891	1
1721.784	1722.791	1	sp|P52907|CA F-actin-capping protein subunit alpha-1 OS=Homo sapiens GN=CAPZA1 PE=1 SV=3	ADFDDRVSDEEKVR	Acetyl@N-term	99.00	1721.786	1
1443.646	1444.653	1	sp|P62913|RL 60S ribosomal protein L11 OS=Homo sapiens GN=RPL11 PE=1 SV=2	AQDQGEKENPMR	Acetyl@N-term	99.00	1443.641	1
1601.821	1602.829	1	sp|Q9Y6M9|N NADH dehydrogenase [ubiquinone] 1 beta subcomplex subunit 9 OS=Homo sapiens GN=NDUFB9 PE=1 SV=3	AFLASGPYLTHQQK	Acetyl@N-term	99.00	1601.82	1
1239.678	1240.686	1	sp|P40429|RL 60S ribosomal protein L13a OS=Homo sapiens GN=RPL13A PE=1 SV=2	AEVQVLVLDGR	Acetyl@N-term	99.00	1239.682	1
1267.647	1268.655	1	sp|P46779|RL 60S ribosomal protein L28 OS=Homo sapiens GN=RPL28 PE=1 SV=3	SAHLQWMVVR	Acetyl@N-term	99.00	1267.65	1
1440.736	1441.743	1	sp|Q02978|M Mitochondrial 2-oxoglutarate/malate carrier protein OS=Homo sapiens GN=SLC25A11 PE=1 SV=3	AATASAGAGGIDGKPR	Acetyl@N-term	99.00	1440.732	1
1634.715	1635.722	1	sp|P32322|P5 Pyrroline-5-carboxylate reductase 1, mitochondrial OS=Homo sapiens GN=PYCR1 PE=1 SV=2	SVGFIGAGQLAFALAK	Acetyl@N-term, Oxidation(F)@12, Formyl(K)@16	99.00	1634.867	1
1869.896	1870.904	1	sp|P46782|RS 40S ribosomal protein S5 OS=Homo sapiens GN=RPS5 PE=1 SV=4	TEWETAAPAVAETPDIK	Acetyl@N-term	99.00	1869.9	1
1290.738	1291.745	1	sp|P38117|ET Electron transfer flavoprotein subunit beta OS=Homo sapiens GN=ETFB PE=1 SV=3	YATLPNIMKAK	Acetyl(K)@11	99.00	1290.701	1
1727.868	1728.875	1	sp|P62873|GI Guanine nucleotide-binding protein G(I)/G(S)/G(T) subunit beta-1 OS=Homo sapiens GN=GNB1 PE=1 SV=3	SELDQLRQEAEQLK	Acetyl@N-term	99.00	1727.869	1
2239.15	2240.157	1	sp|P62873|GI Guanine nucleotide-binding protein G(I)/G(S)/G(T) subunit beta-1 OS=Homo sapiens GN=GNB1 PE=1 SV=3	SELDQLRQEAEQLKNQIR	Acetyl@N-term	99.00	2239.156	1
1438.745	1439.752	1	sp|Q9NVA2|SI Septin-11 OS=Homo sapiens GN=SEPT11 PE=1 SV=3	AVAVGRPSNEELR	Acetyl@N-term	99.00	1438.753	1
1438.753	1439.76	1	sp|Q9NVA2|SI Septin-11 OS=Homo sapiens GN=SEPT11 PE=1 SV=3	AVAVGRPSNEELR	Acetyl@N-term	99.00	1438.753	1
1438.753	1439.76	1	sp|Q9NVA2|SI Septin-11 OS=Homo sapiens GN=SEPT11 PE=1 SV=3	AVAVGRPSNEELR	Acetyl@N-term	99.00	1438.753	1
1478.782	1479.789	1	sp|P02768|AL Serum albumin OS=Homo sapiens GN=ALB PE=1 SV=2	GEYKFQNALLVR	Acetyl(K)@4	99.00	1478.788	1
1478.789	1479.796	1	sp|P02768|AL Serum albumin OS=Homo sapiens GN=ALB PE=1 SV=2	GEYKFQNALLVR	Acetyl(K)@4	99.00	1478.788	1
1478.788	1479.795	1	sp|P02768|AL Serum albumin OS=Homo sapiens GN=ALB PE=1 SV=2	GEYKFQNALLVR	Acetyl(K)@4	99.00	1478.788	1
1478.789	1479.796	1	sp|P02768|AL Serum albumin OS=Homo sapiens GN=ALB PE=1 SV=2	GEYKFQNALLVR	Acetyl(K)@4	99.00	1478.788	1
2151.137	2152.144	1	sp|P05141|AL ADP/ATP translocase 2 OS=Homo sapiens GN=SLC25A5 PE=1 SV=7	TDAAVSFAKDFLAGGVAAAISK	Acetyl@N-term	99.00	2151.121	1
1620.934	1621.942	1	sp|P62269|RS 40S ribosomal protein S18 OS=Homo sapiens GN=RPS18 PE=1 SV=3	SLVIPEKFQHILR	Acetyl@N-term	99.00	1620.935	1
1620.933	1621.941	1	sp|P62269|RS 40S ribosomal protein S18 OS=Homo sapiens GN=RPS18 PE=1 SV=3	SLVIPEKFQHILR	Acetyl@N-term	99.00	1620.935	1
1604.85	1605.858	1	sp|Q9H9B4|SI Sideroflexin-1 OS=Homo sapiens GN=SFXN1 PE=1 SV=4	SGELPPNINIKEPR	Acetyl@N-term	99.00	1604.852	1
1834.806	1835.813	1	sp|P60709|AC Actin, cytoplasmic 1 OS=Homo sapiens GN=ACTB PE=1 SV=1	DDDIAALVVDNGSGMCK	Acetyl@N-term, Propionamide(C)@16	99.00	1834.808	1
1692.858	1693.865	1	sp|P11021|GF 78 kDa glucose-regulated protein OS=Homo sapiens GN=HSPA5 PE=1 SV=2	LGGKLSSEDKETMEK	Acetyl(K)@4	99.00	1692.824	1
2410.968	2411.976	1	sp|P04264|K2 Keratin, type II cytoskeletal 1 OS=Homo sapiens GN=KRT1 PE=1 SV=6	GGGGYGSGGSSYGSGGGSYGSGGGGGGGR	Phospho(S)@7, Dehydrated(S)@10, Phospho(S)@11	99.00	2410.824	1
2716.088	2717.095	1	sp|P04264|K2 Keratin, type II cytoskeletal 1 OS=Homo sapiens GN=KRT1 PE=1 SV=6	YGSGGGSYGSGGGGGGHGSYGSGSSSGGYR	Trioxidation(Y)@8, Phospho(S)@10, Oxidation(H)@17	99.00	2715.97	1

Study 4- Characterization of mitochondrial proteome in a severe case of ETF-QO deficiency.

Supplemental table S1: Total proteins identified in the MADD patient.

Protein Name	Accession Number	Protein MW	Protein PI	Peptide Count	Protein Score	Protein Score C.I. %	Functional cluster
14-3-3 protein beta/alpha OS=Homo sapiens GN=YWHAB PE=1 SV=3	1433B_HUMAN	28064.83008	4.76	9	208	100	Signal transduction
14-3-3 protein epsilon OS=Homo sapiens GN=YWHAE PE=1 SV=1	1433E_HUMAN	29155.41992	4.63	9	202	100	Signal transduction
14-3-3 protein eta OS=Homo sapiens GN=YWHAH PE=1 SV=4	1433F_HUMAN	28201.01953	4.76	10	94.5	100	Signal transduction
14-3-3 protein gamma OS=Homo sapiens GN=YWHAG PE=1 SV=2	1433G_HUMAN	28284.91016	4.8	8	92.4	100	Signal transduction
14-3-3 protein theta OS=Homo sapiens GN=YWHAQ PE=1 SV=1	1433T_HUMAN	27746.76953	4.68	9	137.0	100	Signal transduction
14-3-3 protein zeta/delta OS=Homo sapiens GN=YWHAZ PE=1 SV=1	1433Z_HUMAN	27727.73047	4.73	14	202.0	100	Signal transduction
2,4-dienoyl-CoA reductase, mitochondrial OS=Homo sapiens GN=DECR1 PE=1 SV=1	DECR_HUMAN	36044.80078	9.35	12	86.2	100	Metabolism
28S ribosomal protein S22, mitochondrial OS=Homo sapiens GN=MRPS22 PE=1 SV=1	RT22_HUMAN	41254.39063	7.7	19	290.0	100	Protein binding/folding
2-amino-3-ketobutyrate coenzyme A ligase, mitochondrial OS=Homo sapiens GN=GCAT PE=2 SV=1	KBL_HUMAN	45256.19922	8.3	11	62.4	99	Metabolism
3,2-trans-enoyl-CoA isomerase, mitochondrial OS=Homo sapiens GN=DCI PE=1 SV=1	D3D2_HUMAN	32795.23828	8.8	8	93.8	100	Metabolism
39S ribosomal protein L12, mitochondrial OS=Homo sapiens GN=MRPL12 PE=1 SV=2	RM12_HUMAN	21334.65039	9.04	6	58.5	97	DNA/RNA/protein biosynthesis
39S ribosomal protein L17, mitochondrial OS=Homo sapiens GN=MRPL17 PE=1 SV=1	RM17_HUMAN	20037.56055	10.12	10	57.9	97	DNA/RNA/protein biosynthesis
3-hydroxyacyl-CoA dehydrogenase type-2 OS=Homo sapiens GN=HSD17B10 PE=1 SV=3	HCD2_HUMAN	26906.10938	7.66	12	286.0	100	Metabolism
3-hydroxyisobutyrate dehydrogenase, mitochondrial OS=Homo sapiens GN=HIBADH PE=1 SV=2	3HIDH_HUMAN	35305.76172	8.38	7	451.0	100	Metabolism
3-ketoacyl-CoA thiolase, mitochondrial OS=Homo sapiens GN=ACAA2 PE=1 SV=2	THIM_HUMAN	41897.64063	8.32	14	143.0	100	Metabolism
3-mercaptopyruvate sulfurtransferase OS=Homo sapiens GN=MPST PE=1 SV=3	THTM_HUMAN	33157.64063	6.13	10	72.4	100	Metabolism
40S ribosomal protein S12 OS=Homo sapiens GN=RPS12 PE=1 SV=3	RS12_HUMAN	14505.48047	6.81	6	73.8	100	DNA/RNA/protein biosynthesis
40S ribosomal protein SA OS=Homo sapiens GN=RPSA PE=1 SV=4	RSSA_HUMAN	32833.42969	4.79	14	331.0	100	DNA/RNA/protein biosynthesis
60 kDa heat shock protein, mitochondrial OS=Homo sapiens GN=HSPD1 PE=1 SV=2	CH60_HUMAN	61016.37891	5.7	25	531.0	100	Protein binding/folding
60S acidic ribosomal protein P0 OS=Homo sapiens GN=RPLP0 PE=1 SV=1	RLA0_HUMAN	34251.80078	5.71	15	246.0	100	Protein binding/folding
60S acidic ribosomal protein P0-like OS=Homo sapiens PE=2 SV=1	RLA0L_HUMAN	34342.71875	5.41	10	153.0	100	Protein binding/folding
60S acidic ribosomal protein P2 OS=Homo sapiens GN=RPLP2 PE=1 SV=1	RLA2_HUMAN	11657.84961	4.42	7	194.0	100	Protein binding/folding
78 kDa glucose-regulated protein OS=Homo sapiens GN=HSPA5 PE=1 SV=2	GRP78_HUMAN	72288.42969	5.07	29	838.0	100	Protein binding/folding
Acetyl-CoA acetyltransferase, mitochondrial OS=Homo sapiens GN=ACAT1 PE=1 SV=1	THIL_HUMAN	45170.64063	8.98	17	235.0	100	Metabolism
Aconitate hydratase, mitochondrial OS=Homo sapiens GN=ACO2 PE=1 SV=2	ACON_HUMAN	85371.92188	7.36	7	72.7	100	Metabolism
Actin, alpha cardiac muscle 1 OS=Homo sapiens GN=ACTC1 PE=1 SV=1	ACTC_HUMAN	41991.87891	5.23	10	191.0	100	Structure
Actin, alpha skeletal muscle OS=Homo sapiens GN=ACTA1 PE=1 SV=1	ACTS_HUMAN	42023.85156	5.23	13	187.0	100	Structure
Actin, aortic smooth muscle OS=Homo sapiens GN=ACTA2 PE=1 SV=1	ACTA_HUMAN	41981.80078	5.23	9	145.0	100	Structure
Actin, cytoplasmic 1 OS=Homo sapiens GN=ACTB PE=1 SV=1	ACTB_HUMAN	41709.73047	5.29	11	164.0	100	Structure
Actin, cytoplasmic 2 OS=Homo sapiens GN=ACTG1 PE=1 SV=1	ACTG_HUMAN	41765.78906	5.31	18	381.0	100	Structure
Actin, gamma-enteric smooth muscle OS=Homo sapiens GN=ACTG2 PE=1 SV=1	ACTH_HUMAN	41849.78906	5.31	2	111.0	100	Structure
Actin-related protein 11 OS=Homo sapiens GN=ARP11 PE=2 SV=1	ARP11_HUMAN	23697.13086	5.36	2	66.6	100	Structure
Actin-related protein 3 OS=Homo sapiens GN=ACTR3 PE=1 SV=3	ARP3_HUMAN	47340.98047	5.61	15	244.0	100	Structure
Actin-related protein 3B OS=Homo sapiens GN=ACTR3B PE=1 SV=1	ARP3B_HUMAN	47577.16016	5.61	8	72.7	100	Structure
Acyl-coenzyme A thioesterase 1 OS=Homo sapiens GN=ACOT1 PE=1 SV=1	ACOT1_HUMAN	46248.05078	6.9	8	113.0	100	Metabolism
Acyl-coenzyme A thioesterase 2, mitochondrial OS=Homo sapiens GN=ACOT2 PE=1 SV=5	ACOT2_HUMAN	53203.76953	8.82	12	129.0	100	Metabolism
Adenosine deaminase OS=Homo sapiens GN=ADA PE=1 SV=3	ADA_HUMAN	40738.66016	5.63	9	161.0	100	Adhesion
Adenosine deaminase OS=Homo sapiens GN=ADA PE=1 SV=3	ADA_HUMAN	40738.66016	5.63	1	55.1	94	Adhesion
Adipocyte plasma membrane-associated protein OS=Homo sapiens GN=APMAP PE=1 SV=2	APMAP_HUMAN	46450.85156	5.82	12	124.0	100	Metabolism
Alcohol dehydrogenase [NADP+] OS=Homo sapiens GN=AKR1A1 PE=1 SV=3	AK1A1_HUMAN	36549.85156	6.32	8	64.3	99	Metabolism
Aldehyde dehydrogenase X, mitochondrial OS=Homo sapiens GN=ALDH1B1 PE=1 SV=2	AL1B1_HUMAN	57202.19922	6.36	18	310	100	Metabolism
Aldehyde dehydrogenase, mitochondrial OS=Homo sapiens GN=ALDH2 PE=1 SV=2	ALDH2_HUMAN	56345.62109	6.63	3	162	100	Metabolism
Alpha-aminoadipic semialdehyde dehydrogenase OS=Homo sapiens GN=ALDH7A1 PE=1 SV=4	AL7A1_HUMAN	55331.46094	6.44	14	185	100	Metabolism
Alpha-centractin OS=Homo sapiens GN=ACTR1A PE=1 SV=1	ACTZ_HUMAN	42586.89844	6.19	11	143	100	Transport
Alpha-enolase OS=Homo sapiens GN=ENO1 PE=1 SV=2	ENOA_HUMAN	47139.32031	7.01	20	340	100	Metabolism
Aminopeptidase N OS=Homo sapiens GN=ANPEP PE=1 SV=4	AMPN_HUMAN	109470.8828	5.31	4	57.6	96	Metabolism
Ankyrin repeat and LEM domain-containing protein 2 OS=Homo sapiens GN=ANKLE2 PE=1 SV=3	ANKL2_HUMAN	104056.6172	6.56	18	68.4	100	Structure
Annexin A2 OS=Homo sapiens GN=ANXA2 PE=1 SV=2	ANXA2_HUMAN	38579.80859	7.57	24	606	100	Signal transduction
Annexin A4 OS=Homo sapiens GN=ANXA4 PE=1 SV=4	ANXA4_HUMAN	35860.12109	5.84	16	185	100	Signal transduction
Annexin A5 OS=Homo sapiens GN=ANXA5 PE=1 SV=2	ANXA5_HUMAN	35914.39844	4.94	20	503	100	Signal transduction
Annexin A6 OS=Homo sapiens GN=ANXA6 PE=1 SV=3	ANXA6_HUMAN	75825.57031	5.42	23	148	100	Signal transduction
ATP synthase subunit alpha, mitochondrial OS=Homo sapiens GN=ATP5A1 PE=1 SV=1	ATPA_HUMAN	59713.58984	9.16	6	373	100	OXPHOS
ATP synthase subunit beta, mitochondrial OS=Homo sapiens GN=ATP5B PE=1 SV=3	ATPB_HUMAN	56524.60156	5.26	23	658	100	OXPHOS
ATP synthase subunit delta, mitochondrial OS=Homo sapiens GN=ATP5D PE=1 SV=2	ATPD_HUMAN	17479.18945	5.38	3	132	100	OXPHOS
Beta-actin-like protein 3 OS=Homo sapiens GN=ACTBL3 PE=1 SV=1	ACTBM_HUMAN	41988.83984	5.91	5	172	100	Structure
Beta-enolase OS=Homo sapiens GN=ENO3 PE=1 SV=4	ENOB_HUMAN	46902.28125	7.59	7	84.6	100	Metabolism
Beta-hexosaminidase subunit beta OS=Homo sapiens GN=HEXB PE=1 SV=3	HEXB_HUMAN	63071.17969	6.29	5	193	100	Metabolism
Calcium-binding mitochondrial carrier protein SCaMC-1 OS=Homo sapiens GN=SLC25A24 PE=1 SV=2	SCMC1_HUMAN	53320.33984	6	9	206	100	Signal transduction
Calcium-binding protein p22 OS=Homo sapiens GN=CHP PE=1 SV=3	CHP1_HUMAN	22442.33984	4.98	9	84.6	100	Signal transduction
Calmodulin OS=Homo sapiens GN=CALM1 PE=1 SV=2	CALM_HUMAN	16826.63008	4.09	3	224	100	Signal transduction
Calreticulin OS=Homo sapiens GN=CALR PE=1 SV=1	CALR_HUMAN	48111.82031	4.29	24	638	100	Signal transduction
Calumenin OS=Homo sapiens GN=CALU PE=1 SV=2	CALU_HUMAN	37083.53906	4.47	23	580	100	Protein binding/folding
Caspase-7 OS=Homo sapiens GN=CASP7 PE=1 SV=1	CASP7_HUMAN	34254.78906	5.72	7	57	96	Apoptosis
Cathepsin B OS=Homo sapiens GN=CTSB PE=1 SV=3	CATB_HUMAN	37796.82813	5.68	3	143	100	Proteolysis
Cathepsin D OS=Homo sapiens GN=CTSD PE=1 SV=1	CATD_HUMAN	44523.62109	6.1	7	231	100	Proteolysis
Cell division cycle protein 20 homolog OS=Homo sapiens GN=CDC20 PE=1 SV=2	CDC20_HUMAN	54588.62891	9.33	12	61	98	DNA/RNA/protein biosynthesis
Centlein OS=Homo sapiens GN=CNTLN PE=2 SV=4	CNTLN_HUMAN	161515.8906	8.28	24	56.1	95	DNA/RNA/protein biosynthesis
Centromere protein U OS=Homo sapiens GN=MLF1IP PE=1 SV=1	CENPU_HUMAN	47492.53906	9.18	13	59.3	98	DNA/RNA/protein biosynthesis
Centrosomal protein of 290 kDa OS=Homo sapiens GN=CEP290 PE=1 SV=2	CE290_HUMAN	290207.2813	5.75	28	56.1	95	DNA/RNA/protein biosynthesis
cGMP-dependent protein kinase 2 OS=Homo sapiens GN=PRKG2 PE=1 SV=1	KGP2_HUMAN	87377.20313	8.67	9	60.5	98	Signal transduction
Chloride intracellular channel protein 4 OS=Homo sapiens GN=CLIC4 PE=1 SV=4	CLIC4_HUMAN	28753.74023	5.45	12	142	100	Transport
Citrate synthase, mitochondrial OS=Homo sapiens GN=CS PE=1 SV=2	CISY_HUMAN	51679.51172	8.45	5	169	100	Metabolism
Cofilin-1 OS=Homo sapiens GN=CFL1 PE=1 SV=3	COF1_HUMAN	18490.66016	8.22	11	131	100	Signal transduction
Cofilin-2 OS=Homo sapiens GN=CFL2 PE=1 SV=1	COF2_HUMAN	18724.84961	7.66	6	73.3	100	Signal transduction
Coiled-coil domain-containing protein MTMR15 OS=Homo sapiens GN=MTMR15 PE=2 SV=4	MTMRF_HUMAN	114152	7.1	10	55.7	95	DNA/RNA/protein biosynthesis
Collagen alpha-1(I) chain OS=Homo sapiens GN=COL1A1 PE=1 SV=4	CO1A1_HUMAN	138826.5469	5.6	16	111	100	Structure
Collagen alpha-1(VI) chain OS=Homo sapiens GN=COL6A1 PE=1 SV=3	CO6A1_HUMAN	108462.0078	5.26	17	331	100	Structure
Complement component 1 Q subcomponent-binding protein, mitochondrial OS=Homo sapiens GN=C1QBP P	C1QBP_HUMAN	31342.60938	4.74	3	68.4	100	Signal transduction
CTTNBP2 N-terminal-like protein OS=Homo sapiens GN=CTTNBP2NL PE=1 SV=2	CT2NL_HUMAN	70114.78906	8.22	14	60.4	98	Structure
Cyclic AMP-dependent transcription factor ATF-3 OS=Homo sapiens GN=ATF3 PE=1 SV=2	ATF3_HUMAN	20562.68945	8.8	10	64.4	99	DNA/RNA/protein biosynthesis
Cystatin-B OS=Homo sapiens GN=CSTB PE=1 SV=2	CYTB_HUMAN	11132.58984	6.96	6	112	100	Proteolysis
Cytochrome b5 OS=Homo sapiens GN=CYB5A PE=1 SV=2	CYB5_HUMAN	15320.50977	4.88	6	147	100	OXPHOS
Cytochrome b-c1 complex subunit 1, mitochondrial OS=Homo sapiens GN=UQCRC1 PE=1 SV=3	QCR1_HUMAN	52612.42969	5.94	19	420	100	OXPHOS
Cytochrome b-c1 complex subunit 2, mitochondrial OS=Homo sapiens GN=UQCRC2 PE=1 SV=3	QCR2_HUMAN	48412.87891	8.74	11	134	100	OXPHOS
Cytochrome b-c1 complex subunit 7 OS=Homo sapiens GN=UQCRB PE=1 SV=2	QCR7_HUMAN	13521.98047	8.73	9	336	100	OXPHOS
Cytochrome b-c1 complex subunit Rieske, mitochondrial OS=Homo sapiens GN=UQCRFS1 PE=1 SV=2	UCRI_HUMAN	29649.35938	8.55	4	169	100	OXPHOS
Cytochrome c oxidase subunit 5A, mitochondrial OS=Homo sapiens GN=COX5A PE=1 SV=2	COX5A_HUMAN	16751.68945	6.3	5	188	100	OXPHOS
Cytosol aminopeptidase OS=Homo sapiens GN=LAP3 PE=1 SV=3	AMPL_HUMAN	56130.80859	8.03	7	81.3	100	Proteolysis
Death-associated protein kinase 2 OS=Homo sapiens GN=DAPK2 PE=1 SV=1	DAPK2_HUMAN	42871.32813	6.45	10	55.7	95	Apoptosis
Delta(3,5)-Delta(2,4)-dienoyl-CoA isomerase, mitochondrial OS=Homo sapiens GN=ECH1 PE=1 SV=2	ECH1_HUMAN	35793.37891	8.16	7	507	100	Metabolism
Delta-1-pyrroline-5-carboxylate dehydrogenase, mitochondrial OS=Homo sapiens GN=ALDH4A1 PE=1 SV=3	AL4A1_HUMAN	61680.58984	8.25	11	65	99	Metabolism/Redox
Desmin OS=Homo sapiens GN=DES PE=1 SV=3	DESM_HUMAN	53503.14844	5.21	8	136	100	Structure
Diablo homolog, mitochondrial OS=Homo sapiens GN=DIABLO PE=1 SV=1	DBLOH_HUMAN	27113.7207	5.68	12	300	100	Apoptosis
Dihydrolipoyllysine-residue succinyltransferase component of 2-oxoglutarate dehydrogenase complex,	ODO2_HUMAN	48698.44141	9.11	3	63	99	Metabolism
DNA polymerase zeta catalytic subunit OS=Homo sapiens GN=REV3L PE=1 SV=2	DPOLZ_HUMAN	352554.25	8.72	29	64.5	99	DNA/RNA/protein biosynthesis
DnaJ homolog subfamily B member 11 OS=Homo sapiens GN=DNAJB11 PE=1 SV=1	DJB11_HUMAN	40488.62109	5.81	6	93	100	Protein binding/folding
Dual specificity protein kinase TTK OS=Homo sapiens GN=TTK PE=1 SV=2	TTK_HUMAN	97011.09375	8.41	17	63.7	99	Structure
EH domain-binding protein 1 OS=Homo sapiens GN=EHBP1 PE=1 SV=3	EHBP1_HUMAN	139931.2656	5.24	17	56.1	95	OXPHOS
Electron transfer flavoprotein subunit alpha, mitochondrial OS=Homo sapiens GN=ETFA PE=1 SV=1	ETFA_HUMAN	35057.57813	8.62	7	188.0	100	OXPHOS
Electron transfer flavoprotein subunit beta OS=Homo sapiens GN=ETFB PE=1 SV=3	ETFB_HUMAN	27826.15039	8.24	9	195.0	100	OXPHOS
Elongation factor 1-alpha 1 OS=Homo sapiens GN=EEF1A1 PE=1 SV=1	EF1A1_HUMAN	50109.10938	9.1	6	104	100	DNA/RNA/protein biosynthesis
Elongation factor 2 OS=Homo sapiens GN=EEF2 PE=1 SV=4	EF2_HUMAN	95276.95313	6.41	15	209	100	DNA/RNA/protein biosynthesis

Protein Name	Accession Number	Protein MW	Protein PI	Peptide Count	Protein Score	Protein Score C.I. %	Functional cluster
Elongation factor Tu, mitochondrial OS=Homo sapiens GN=TUFM PE=1 SV=2	EFTU_HUMAN	49510.17969	7.26	17	327	100	DNA/RNA/protein biosynthesis
Endoplasmic reticulum protein ERp29 OS=Homo sapiens GN=ERP29 PE=1 SV=4	ERP29_HUMAN	28975.15039	6.77	13	214	100	Transport
Endoplasmin OS=Homo sapiens GN=HSP90B1 PE=1 SV=1	ENPL_HUMAN	92411.34375	4.76	27	532	100	Protein binding/folding/transport
Enoyl-CoA hydratase, mitochondrial OS=Homo sapiens GN=ECHS1 PE=1 SV=4	ECHM_HUMAN	31367.13086	8.34	12	222	100	Metabolism
Erlin-2 OS=Homo sapiens GN=ERLIN2 PE=1 SV=1	ERLN2_HUMAN	37815.44922	5.47	12	118	100	Structure
Eukaryotic initiation factor 4A-I OS=Homo sapiens GN=EIF4A1 PE=1 SV=1	IF4A1_HUMAN	46124.55078	5.32	14	140	100	DNA/RNA/protein biosynthesis
Eukaryotic initiation factor 4A-II OS=Homo sapiens GN=EIF4A2 PE=1 SV=2	IF4A2_HUMAN	46372.78125	5.33	12	122	100	DNA/RNA/protein biosynthesis
Eukaryotic translation initiation factor 5A-1 OS=Homo sapiens GN=EIF5A PE=1 SV=2	IF5A1_HUMAN	16821.40039	5.08	3	55.8	95	DNA/RNA/protein biosynthesis
Ezrin OS=Homo sapiens GN=EZR PE=1 SV=4	EZRI_HUMAN	69369.74219	5.94	10	68.1	100	Adhesion
F-actin-capping protein subunit alpha-1 OS=Homo sapiens GN=CAPZA1 PE=1 SV=3	CAZA1_HUMAN	32902.32813	5.45	6	83.5	100	Structure
F-box only protein 28 OS=Homo sapiens GN=FBXO28 PE=1 SV=1	FBX28_HUMAN	41123.39844	9.59	11	65.4	99	Proteolysis
FERM domain-containing protein 5 OS=Homo sapiens GN=FRMD5 PE=2 SV=1	FRMD5_HUMAN	65023.48828	8.62	14	63.4	99	Structure
Ferritin light chain OS=Homo sapiens GN=FTL PE=1 SV=2	FRIL_HUMAN	20007.09961	5.51	9	417.0	100	Transport/Redox
FK506-binding protein 10 OS=Homo sapiens GN=FKBP10 PE=1 SV=1	FKB10_HUMAN	64204.17969	5.36	22	441.0	100	Protein binding/folding
FK506-binding protein 9 OS=Homo sapiens GN=FKBP9 PE=1 SV=2	FKBP9_HUMAN	63043.51172	4.91	14	167.0	100	Protein binding/folding
Fructose-bisphosphate aldolase A OS=Homo sapiens GN=ALDOA PE=1 SV=2	ALDOA_HUMAN	39395.30078	8.3	11	179.0	100	Metabolism
Fumarate hydratase, mitochondrial OS=Homo sapiens GN=FH PE=1 SV=3	FUMH_HUMAN	54602.17188	8.85	21	334.0	100	Metabolism
Fumarylacetoacetate hydrolase domain-containing protein 1 OS=Homo sapiens GN=FAHD1 PE=1 SV=2	FAHD1_HUMAN	24826.73047	6.96	8	85.1	100	Metabolism
FUN14 domain-containing protein 2 OS=Homo sapiens GN=FUNDC2 PE=1 SV=2	FUND2_HUMAN	20662.71094	9.74	7	56.5	95	Unknown
Galectin-3 OS=Homo sapiens GN=LGALS3 PE=1 SV=5	LEG3_HUMAN	26136.05078	8.57	10	255.0	100	Apoptosis/Signal transduction
Gamma-enolase OS=Homo sapiens GN=ENO2 PE=1 SV=3	ENOG_HUMAN	47239	4.91	6	82.5	100	Metabolism
Girdin OS=Homo sapiens GN=CCDC88A PE=1 SV=2	GRDN_HUMAN	215909.1094	5.9	17	56.9	96	Signal transduction/Transport
Glucose-6-phosphate 1-dehydrogenase OS=Homo sapiens GN=G6PD PE=1 SV=4	G6PD_HUMAN	59218.98828	6.39	20	268.0	100	Metabolism
Glutamate dehydrogenase 1, mitochondrial OS=Homo sapiens GN=GLUD1 PE=1 SV=2	DHE3_HUMAN	61359.19141	7.66	20	403.0	100	Metabolism
Glutamate dehydrogenase 2, mitochondrial OS=Homo sapiens GN=GLUD2 PE=1 SV=2	DHE4_HUMAN	61395.42969	8.63	12	246.0	100	Metabolism
Glutaminase kidney isoform, mitochondrial OS=Homo sapiens GN=GLS PE=1 SV=1	GLSK_HUMAN	73413.89844	7.85	12	200.0	100	Metabolism
Glutathione S-transferase kappa 1 OS=Homo sapiens GN=GSTK1 PE=1 SV=3	GSTK1_HUMAN	25480.30078	8.5	8	90.0	100	Redox
Glutathione S-transferase P OS=Homo sapiens GN=GSTP1 PE=1 SV=2	GSTP1_HUMAN	23341.01953	5.43	5	94.4	100	Redox
Glyceraldehyde-3-phosphate dehydrogenase OS=Homo sapiens GN=GAPDH PE=1 SV=3	G3P_HUMAN	36030.39844	8.57	16	280	100	Metabolism
Glycerol-3-phosphate dehydrogenase, mitochondrial OS=Homo sapiens GN=GPD2 PE=1 SV=3	GPDM_HUMAN	80801.60938	7.57	18	166	100	Metabolism
GTP:AMP phosphotransferase mitochondrial OS=Homo sapiens GN=AK3 PE=1 SV=4	KAD3_HUMAN	25549.55078	9.15	12	228	100	Signal transduction
GTPase IMAP family member 8 OS=Homo sapiens GN=GIMAP8 PE=1 SV=2	GIMA8_HUMAN	74843.40625	8.62	15	56.8	96	Signal transduction
Guanine nucleotide-binding protein subunit beta-2-like 1 OS=Homo sapiens GN=GNB2L1 PE=1 SV=3	GBLP_HUMAN	35054.55859	7.6	19	395.0	100	Signal transduction
Heat shock cognate 71 kDa protein OS=Homo sapiens GN=HSPA8 PE=1 SV=1	HSP7C_HUMAN	70854.21875	5.37	13	147.0	100	Protein binding/folding
Heat shock protein beta-1 OS=Homo sapiens GN=HSPB1 PE=1 SV=2	HSPB1_HUMAN	22768.49023	5.98	9	253.0	100	Protein binding/folding
Heat shock protein HSP 90-beta OS=Homo sapiens GN=HSP90AB1 PE=1 SV=4	HS90B_HUMAN	83212.10156	4.97	14	209.0	100	Protein binding/folding
Histidine triad nucleotide-binding protein 2 OS=Homo sapiens GN=HINT2 PE=1 SV=1	HINT2_HUMAN	17151.24023	9.2	6	134.0	100	Apoptosis
Interleukin-25 OS=Homo sapiens GN=IL25 PE=1 SV=1	IL25_HUMAN	20316.96094	8.73	7	57.0	96	Signal transduction
Isochorismatase domain-containing protein 2, mitochondrial OS=Homo sapiens GN=ISOC2 PE=1 SV=1	ISOC2_HUMAN	22322.83984	7.67	4	57.4	96	Metabolism
Isocitrate dehydrogenase [NAD] subunit alpha, mitochondrial OS=Homo sapiens GN=IDH3A PE=1 SV=1	IDH3A_HUMAN	39566.07031	6.47	13	199.0	100	Metabolism
Isocitrate dehydrogenase [NADP] cytoplasmic OS=Homo sapiens GN=IDH1 PE=1 SV=2	IDHC_HUMAN	46629.51172	6.53	10	84.2	100	Metabolism
Keratin, type I cytoskeletal 9 OS=Homo sapiens GN=KRT9 PE=1 SV=3	K1C9_HUMAN	62026.80859	5.14	12	142.0	100	Structure
Keratin, type II cytoskeletal 1 OS=Homo sapiens GN=KRT1 PE=1 SV=6	K2C1_HUMAN	65999	8.15	12	84.5	100	Structure
Keratin, type II cytoskeletal 2 epidermal OS=Homo sapiens GN=KRT2 PE=1 SV=2	K22E_HUMAN	65393.21094	8.07	7	67.7	100	Structure
Keratin, type II cytoskeletal 6B OS=Homo sapiens GN=KRT6B PE=1 SV=5	K2C6B_HUMAN	60030.28906	8.09	8	57.9	97	Structure
Krueppel-like factor 2 OS=Homo sapiens GN=KLF2 PE=1 SV=2	KLF2_HUMAN	37395.78906	9.06	10	59.1	97	DNA/RNA/protein biosynthesis
Laminin subunit beta-1 OS=Homo sapiens GN=LAMB1 PE=1 SV=1	LAMB1_HUMAN	197936.6094	4.84	19	86.1	100	Structure
Laminin subunit gamma-1 OS=Homo sapiens GN=LAMC1 PE=1 SV=3	LAMC1_HUMAN	177488.5469	5.01	16	218.0	100	Structure
LIM and senescent cell antigen-like-containing domain protein 1 OS=Homo sapiens GN=LIMS1 PE=1 SV=4	LIMS1_HUMAN	37225.83984	8.43	13	61.1	98	Adhesion
Lipoamide acyltransferase component of branched-chain alpha-keto acid dehydrogenase complex, mitoch	ODB2_HUMAN	53452.92188	8.71	5	54.0	91.87383643	Metabolism
Liprin-alpha-3 OS=Homo sapiens GN=PPFIA3 PE=1 SV=3	LIPA3_HUMAN	133413.8438	5.53	19	62.3	99	Protein binding/folding
Lysozyme C OS=Homo sapiens GN=LYZ PE=1 SV=1	LYSC_HUMAN	16526.2793	9.38	2	101	100	Metabolism
Malate dehydrogenase, mitochondrial OS=Homo sapiens GN=MDH2 PE=1 SV=3	MDHM_HUMAN	35480.73047	8.92	17	394	100	Metabolism
Matrix-remodeling-associated protein 5 OS=Homo sapiens GN=MXRA5 PE=2 SV=2	MXRA5_HUMAN	312085.0313	8.57	27	55.7	95	Adhesion
Medium-chain specific acyl-CoA dehydrogenase, mitochondrial OS=Homo sapiens GN=ACADM PE=1 SV=1	ACADM_HUMAN	46558.57813	8.61	13	116.0	100	Metabolism
Methylcrotonoyl-CoA carboxylase beta chain, mitochondrial OS=Homo sapiens GN=MCCC2 PE=1 SV=1	MCCB_HUMAN	61294.41016	7.57	7	65.4	99	Metabolism
Microtubule-associated protein 1B OS=Homo sapiens GN=MAP1B PE=1 SV=1	MAP1B_HUMAN	270454	4.73	15	66.3	100	Structure
Mitochondrial import receptor subunit TOM40 homolog OS=Homo sapiens GN=TOMM40 PE=1 SV=1	TOM40_HUMAN	37869.14063	6.79	8	206	100	Transport
Mitochondrial inner membrane protein OS=Homo sapiens GN=IMMT PE=1 SV=1	IMMT_HUMAN	83626.35156	6.08	25	497	100	Protein binding/folding
Mitochondrial-processing peptidase subunit beta OS=Homo sapiens GN=PMPCB PE=1 SV=2	MPPB_HUMAN	54331.48828	6.38	15	191	100	Proteolysis
Mitogen-activated protein kinase kinase kinase 15 OS=Homo sapiens GN=MAP3K15 PE=2 SV=2	M3K15_HUMAN	147344.2656	5.42	19	66.5	100	Signal transduction
Mitogen-activated protein kinase scaffold protein 1 OS=Homo sapiens GN=MAPKSP1 PE=1 SV=1	MPKS1_HUMAN	13614.25977	6.73	8	153	100	Signal transduction
Moesin OS=Homo sapiens GN=MSN PE=1 SV=3	MOES_HUMAN	67777.78906	6.08	8	84.1	100	Adhesion
mTERF domain-containing protein 3, mitochondrial OS=Homo sapiens GN=MTERFD3 PE=1 SV=2	MTER3_HUMAN	44385.55859	9.15	8	54.3	92	DNA/RNA/protein biosynthesis
Myosin light polypeptide 6 OS=Homo sapiens GN=MYL6 PE=1 SV=2	MYL6_HUMAN	16919.13086	4.56	7	361	100	Structure
Myosin regulatory light chain 12B OS=Homo sapiens GN=MYL12B PE=1 SV=2	ML12B_HUMAN	19766.51953	4.71	5	218	100	Structure
Myosin regulatory light polypeptide 9 OS=Homo sapiens GN=MYL9 PE=1 SV=4	MYL9_HUMAN	19814.44922	4.8	5	85.3	100	Structure
NADH dehydrogenase [ubiquinone] 1 alpha subcomplex subunit 5 OS=Homo sapiens GN=NDUFA5 PE=1 SV	NDUA5_HUMAN	13450.16992	5.75	10	163.0	100	OXPHOS
NADH dehydrogenase [ubiquinone] flavoprotein 2, mitochondrial OS=Homo sapiens GN=NDUFV2 PE=1 SV	NDUV2_HUMAN	27374.00977	8.22	6	150.0	100	OXPHOS
NADH dehydrogenase [ubiquinone] iron-sulfur protein 3, mitochondrial OS=Homo sapiens GN=NDUFS3 PE	NDUS3_HUMAN	30222.71094	6.99	19	452.0	100	OXPHOS
NADH dehydrogenase [ubiquinone] iron-sulfur protein 6, mitochondrial OS=Homo sapiens GN=NDUFS6 PE	NDUS6_HUMAN	13702.82031	8.59	4	142.0	100	OXPHOS
NADH-ubiquinone oxidoreductase 75 kDa subunit, mitochondrial OS=Homo sapiens GN=NDUFS1 PE=1 SV	NDUS1_HUMAN	79416.53906	5.89	26	489.0	100	OXPHOS
Nebulin-related-anchoring protein OS=Homo sapiens GN=NRAP PE=2 SV=2	NRAP_HUMAN	196950.2969	9.24	25	56.3	95	Structure
Neutral alpha-glucosidase AB OS=Homo sapiens GN=GANAB PE=1 SV=3	GANAB_HUMAN	106806.6406	5.74	23	309.0	100	Metabolism
Nicotinamide N-methyltransferase OS=Homo sapiens GN=NNMT PE=1 SV=1	NNMT_HUMAN	29555.06055	5.56	6	87.7	100	Metabolism
Non-specific lipid-transfer protein OS=Homo sapiens GN=SCP2 PE=1 SV=2	NLTP_HUMAN	58955.60938	6.44	11	66.8	100	Transport
Nuclear apoptosis-inducing factor 1 OS=Homo sapiens GN=NAIF1 PE=1 SV=1	NAIF1_HUMAN	35142.30078	6.73	7	54.3	92	Apoptosis
Nucleoside diphosphate kinase A OS=Homo sapiens GN=NME1 PE=1 SV=1	NDKA_HUMAN	17137.66992	5.83	4	129.0	100	Metabolism/apoptosis
Nucleoside diphosphate kinase B OS=Homo sapiens GN=NME2 PE=1 SV=1	NDKB_HUMAN	17286.93945	8.52	8	255.0	100	Metabolism/apoptosis
Paraneoplastic antigen-like protein 6A OS=Homo sapiens GN=PNMA6A PE=2 SV=1	PNM6A_HUMAN	43847.37109	5.24	12	65.2	99	Unknown
Paraneoplastic antigen-like protein 6B OS=Homo sapiens GN=PNMA6B PE=2 SV=1	PNM6B_HUMAN	43978.48047	5.31	12	63.0	99	Unknown
Peptidyl-prolyl cis-trans isomerase A OS=Homo sapiens GN=PPIA PE=1 SV=2	PPIA_HUMAN	18000.88086	7.68	13	249.0	100	Metabolism
Peptidyl-prolyl cis-trans isomerase B OS=Homo sapiens GN=PPIB PE=1 SV=2	PPIB_HUMAN	23727.5293	9.42	14	352.0	100	Metabolism
Peroxidasin homolog OS=Homo sapiens GN=PXDN PE=1 SV=2	PXDN_HUMAN	165169.875	6.79	21	56.1	95	Redox
Peroxiredoxin-1 OS=Homo sapiens GN=PRDX1 PE=1 SV=1	PRDX1_HUMAN	22096.2793	8.27	10	130.0	100	Redox
Peroxiredoxin-2 OS=Homo sapiens GN=PRDX2 PE=1 SV=5	PRDX2_HUMAN	21878.24023	5.66	4	100.0	100	Redox
Peroxiredoxin-4 OS=Homo sapiens GN=PRDX4 PE=1 SV=1	PRDX4_HUMAN	30520.81055	5.86	12	207.0	100	Redox
Peroxiredoxin-5, mitochondrial OS=Homo sapiens GN=PRDX5 PE=1 SV=3	PRDX5_HUMAN	22012.49023	8.85	9	153.0	100	Redox
Peroxiredoxin-6 OS=Homo sapiens GN=PRDX6 PE=1 SV=3	PRDX6_HUMAN	25019.18945	6	14	307.0	100	Redox
Phosphatidylethanolamine-binding protein 1 OS=Homo sapiens GN=PEBP1 PE=1 SV=3	PEBP1_HUMAN	21043.66992	7.01	6	85.7	100	Signal transduction
Phosphoglycerate kinase 1 OS=Homo sapiens GN=PGK1 PE=1 SV=3	PGK1_HUMAN	44586.12891	8.3	9	105.0	100	Metabolism
Phosphoglycerate kinase 2 OS=Homo sapiens GN=PGK2 PE=1 SV=3	PGK2_HUMAN	44767.32813	8.74	3	64.0	99	Metabolism
Phosphoglycerate mutase 1 OS=Homo sapiens GN=PGAM1 PE=1 SV=2	PGAM1_HUMAN	28785.83008	6.67	10	116.0	100	Metabolism
Phosphoglycerate mutase 2 OS=Homo sapiens GN=PGAM2 PE=1 SV=3	PGAM2_HUMAN	28747.83984	8.99	4	75.0	100	Metabolism
Plasma kallikrein OS=Homo sapiens GN=KLKB1 PE=1 SV=1	KLKB1_HUMAN	71322.84375	8.6	14	56.1	95	Proteolysis
POTE ankyrin domain family member E OS=Homo sapiens GN=POTEE PE=1 SV=3	POTEE_HUMAN	121285.6563	5.83	9	189	100	Structure
POTE ankyrin domain family member F OS=Homo sapiens GN=POTEF PE=1 SV=2	POTEF_HUMAN	121366.6875	5.83	9	166	100	Structure
Procollagen-lysine,2-oxoglutarate 5-dioxygenase 3 OS=Homo sapiens GN=PLOD3 PE=1 SV=1	PLOD3_HUMAN	84731.46875	5.69	11	207	100	Redox
Profilin-1 OS=Homo sapiens GN=PFN1 PE=1 SV=2	PROF1_HUMAN	15044.55957	8.44	9	116	100	Structure
Prohibitin OS=Homo sapiens GN=PHB PE=1 SV=1	PHB_HUMAN	29785.90039	5.57	16	517	100	DNA/RNA/protein biosynthesis
Prohibitin-2 OS=Homo sapiens GN=PHB2 PE=1 SV=2	PHB2_HUMAN	33275.91016	9.83	14	354	100	DNA/RNA/protein biosynthesis
Proline-rich protein 4 OS=Homo sapiens GN=PRR4 PE=1 SV=2	PROL4_HUMAN	15115.63965	6.97	2	124	100	Signal transduction

Protein Name	Accession Number	Protein MW	Protein PI	Peptide Count	Protein Score	Protein Score C.I. %	Functional cluster
Prolyl 3-hydroxylase 1 OS=Homo sapiens GN=LEPRE1 PE=1 SV=2	P3H1_HUMAN	83341.07813	5.05	3	72	100	Signal transduction/Redox
Pro-MCH-like protein 1 OS=Homo sapiens GN=PMCHL1 PE=2 SV=2	MCHL1_HUMAN	9708.839844	5.71	5	61.9	99	Signal transduction
Proteasome subunit beta type-2 OS=Homo sapiens GN=PSMB2 PE=1 SV=1	PSB2_HUMAN	22821.67969	6.51	5	73.0	100	Proteolysis
Proteasome-associated protein ECM29 homolog OS=Homo sapiens GN=ECM29 PE=1 SV=2	ECM29_HUMAN	204160.375	6.74	19	61.8	99	Proteolysis
Protein Ag2 homolog OS=Homo sapiens GN=AG2 PE=1 SV=3	AG2_HUMAN	46085.35156	10.04	10	70.7	100	Unknown
Protein disulfide-isomerase A3 OS=Homo sapiens GN=PDIA3 PE=1 SV=4	PDIA3_HUMAN	56746.75	5.98	25	416.0	100	Signal transduction/Redox
Protein disulfide-isomerase A4 OS=Homo sapiens GN=PDIA4 PE=1 SV=2	PDIA4_HUMAN	72886.96875	4.96	10	64.1	99	Signal transduction/Redox
Protein disulfide-isomerase A6 OS=Homo sapiens GN=PDIA6 PE=1 SV=1	PDIA6_HUMAN	48091.26172	4.95	17	464.0	100	Redox
Protein disulfide-isomerase OS=Homo sapiens GN=P4HB PE=1 SV=3	PDIA1_HUMAN	57080.67188	4.76	24	475.0	100	Redox
Protein ECT2 OS=Homo sapiens GN=ECT2 PE=1 SV=3	ECT2_HUMAN	99987.27344	7.28	16	56.0	95	Apoptosis
Protein ETHE1, mitochondrial OS=Homo sapiens GN=ETHE1 PE=1 SV=2	ETHE1_HUMAN	27855.10938	6.35	8	149.0	100	Metabolism
Protein PAPPAS OS=Homo sapiens GN=PAPPAS PE=2 SV=1	PAPAS_HUMAN	12188.38965	9.78	7	57.2	96	Structure
Protein preY, mitochondrial OS=Homo sapiens GN=PREY PE=1 SV=1	PREY_HUMAN	12646.62012	9.45	5	58.1	97	Protein binding/folding
Protein Shroom3 OS=Homo sapiens GN=SHROOM3 PE=1 SV=1	SHRM3_HUMAN	216528.2344	7.75	23	62.6	99	Structure
Putative annexin A2-like protein OS=Homo sapiens GN=ANXA2P2 PE=5 SV=2	AXA2L_HUMAN	38634.82813	6.49	11	304.0	100	Signal transduction
Putative elongation factor 1-alpha-like 3 OS=Homo sapiens GN=EEF1AL3 PE=5 SV=1	EF1A3_HUMAN	50153.14844	9.15	7	110.0	100	DNA/RNA/protein biosynthesis
Putative endoplasmin-like protein OS=Homo sapiens GN=HSP90B2P PE=5 SV=1	ENPLL_HUMAN	45829.87891	5.14	7	74.0	100	Protein binding/folding
Putative heat shock protein HSP 90-alpha A2 OS=Homo sapiens GN=HSP90AA2 PE=1 SV=2	HS902_HUMAN	39340.42969	4.57	5	121.0	100	Protein binding/folding
Putative heat shock protein HSP 90-alpha A4 OS=Homo sapiens GN=HSP90AA4P PE=5 SV=1	HS904_HUMAN	47682.12109	5.07	1	73.3	100	Protein binding/folding
Putative heat shock protein HSP 90-beta-3 OS=Homo sapiens GN=HSP90AB3P PE=5 SV=1	H90B3_HUMAN	68281.96094	4.71	8	90.6	100	Protein binding/folding
Putative nucleoside diphosphate kinase OS=Homo sapiens GN=NME2P1 PE=5 SV=1	NDK8_HUMAN	15518.98047	8.76	5	163	100	Metabolism
Putative tropomyosin alpha-3 chain-like protein OS=Homo sapiens PE=5 SV=2	TPM3L_HUMAN	26252.91016	4.47	7	85.5	100	Structure
Putative uncharacterized protein FLJ45035 OS=Homo sapiens PE=5 SV=1	YD023_HUMAN	15487.54004	7.41	9	59.5	98	Unknown
Pyruvate dehydrogenase E1 component subunit beta, mitochondrial OS=Homo sapiens GN=PDHB PE=1 SV	ODPB_HUMAN	39208.03125	6.2	8	71.5	100	Metabolism
Radixin OS=Homo sapiens GN=RDX PE=1 SV=1	RADI_HUMAN	68521.39063	6.03	8	68.4	100	Structure
Reticulocalbin-1 OS=Homo sapiens GN=RCN1 PE=1 SV=1	RCN1_HUMAN	38866.16016	4.86	14	229.0	100	Signal transduction
Reticulocalbin-2 OS=Homo sapiens GN=RCN2 PE=1 SV=1	RCN2_HUMAN	36853.64063	4.26	11	159.0	100	Signal transduction
Reticulocalbin-3 OS=Homo sapiens GN=RCN3 PE=1 SV=1	RCN3_HUMAN	37470	4.74	11	339.0	100	Signal transduction
Reticulon-4-interacting protein 1, mitochondrial OS=Homo sapiens GN=RTN4IP1 PE=1 SV=2	RT4I1_HUMAN	43561.58984	9.22	12	63.4	99	Redox
Retinoblastoma-binding protein 6 OS=Homo sapiens GN=RBBP6 PE=1 SV=1	RBBP6_HUMAN	201441.7031	9.65	23	61.0	98	Protein binding/folding
Retinoic acid receptor responder protein 3 OS=Homo sapiens GN=RARRES3 PE=2 SV=1	TIG3_HUMAN	18167.26953	8.78	8	61.9	99	Signal transduction
Rho GDP-dissociation inhibitor 1 OS=Homo sapiens GN=ARHGDIA PE=1 SV=3	GDIR1_HUMAN	23192.69922	5.02	10	216.0	100	Signal transduction
Ribosome-binding protein 1 OS=Homo sapiens GN=RRBP1 PE=1 SV=4	RRBP1_HUMAN	152380.6719	8.69	12	71.1	100	Signal transduction/Transport
RNA-binding protein Raly OS=Homo sapiens GN=RALY PE=1 SV=1	RALY_HUMAN	32443.61914	9.2	8	73.5	100	DNA/RNA/protein biosynthesis
Septin-11 OS=Homo sapiens GN=SEPT11 PE=1 SV=3	SEP11_HUMAN	49367.19141	6.36	15	313.0	100	Structure
Septin-2 OS=Homo sapiens GN=SEPT2 PE=1 SV=1	SEPT2_HUMAN	41461.25	6.15	12	222.0	100	Structure
Serine hydroxymethyltransferase, mitochondrial OS=Homo sapiens GN=SHMT2 PE=1 SV=3	GLYM_HUMAN	55957.73047	8.76	10	64.0	99	Metabolism
Serine protease HTRA2, mitochondrial OS=Homo sapiens GN=HTRA2 PE=1 SV=2	HTRA2_HUMAN	48810.92969	10.07	10	78.9	100	Apoptosis/Proteolysis
Serpin H1 OS=Homo sapiens GN=SERPINH1 PE=1 SV=2	SERPH_HUMAN	46411.17969	8.75	17	268.0	100	Protein binding/folding
Serum albumin OS=Homo sapiens GN=ALB PE=1 SV=2	ALBU_HUMAN	69321.49219	5.92	5	112.0	100	Transport/Redox
Short-chain specific acyl-CoA dehydrogenase, mitochondrial OS=Homo sapiens GN=ACADS PE=1 SV=1	ACADS_HUMAN	44268.76172	8.13	7	70.6	100	Metabolism
Single-stranded DNA-binding protein, mitochondrial OS=Homo sapiens GN=SSBP1 PE=1 SV=1	SSBP_HUMAN	17249.0293	9.59	11	172.0	100	DNA/RNA/protein biosynthesis
Stress-70 protein, mitochondrial OS=Homo sapiens GN=HSPA9 PE=1 SV=2	GRP75_HUMAN	73634.77344	5.87	18	558.0	100	Protein binding/folding
Structural maintenance of chromosomes protein 4 OS=Homo sapiens GN=SMC4 PE=1 SV=2	SMC4_HUMAN	147090.5156	6.37	20	59.6	98	Structure
Succinate dehydrogenase [ubiquinone] flavoprotein subunit, mitochondrial OS=Homo sapiens GN=SDHA PE	DHSA_HUMAN	72645.28906	7.06	18	304	100	Metabolism
Succinyl-CoA:3-ketoacid-coenzyme A transferase 1, mitochondrial OS=Homo sapiens GN=OXCT1 PE=1 SV	SCOT1_HUMAN	56121.92969	7.14	11	106	100	Metabolism
Sulfatase-modifying factor 2 OS=Homo sapiens GN=SUMF2 PE=1 SV=1	SUMF2_HUMAN	33835.82031	7.79	8	110	100	Signal transduction
Superoxide dismutase [Mn], mitochondrial OS=Homo sapiens GN=SOD2 PE=1 SV=2	SODM_HUMAN	24706.55078	8.35	13	274	100	Redox
Synaptotagmin-like protein 3 OS=Homo sapiens GN=SYTL3 PE=2 SV=3	SYTL3_HUMAN	68516.32031	9.41	13	58.4	97	Signal transduction
Syntenin-1 OS=Homo sapiens GN=SDCBP PE=1 SV=1	SDCB1_HUMAN	32423.91992	7.05	5	72.5	100	Adhesion
T-complex protein 1 subunit alpha OS=Homo sapiens GN=CCT1 PE=1 SV=1	TCPA_HUMAN	60305.57813	5.8	12	209.0	100	Protein binding/folding
T-complex protein 1 subunit epsilon OS=Homo sapiens GN=CCT5 PE=1 SV=1	TCPE_HUMAN	59632.80859	5.45	17	167.0	100	Protein binding/folding
Tektin-3 OS=Homo sapiens GN=TEKT3 PE=1 SV=1	TEKT3_HUMAN	56600.53125	6.93	13	56.7	96	Structure
Thioredoxin domain-containing protein 5 OS=Homo sapiens GN=TXNDC5 PE=1 SV=2	TXND5_HUMAN	47598.66016	5.63	11	168	100	Redox
Thioredoxin-dependent peroxide reductase, mitochondrial OS=Homo sapiens GN=PRDX3 PE=1 SV=3	PRDX3_HUMAN	27675.16992	7.67	6	282	100	Redox
Transgelin OS=Homo sapiens GN=TAGLN PE=1 SV=4	TAGL_HUMAN	22596.42969	8.87	15	134	100	Signal transduction
Transgelin-2 OS=Homo sapiens GN=TAGLN2 PE=1 SV=3	TAGL2_HUMAN	22377.16992	8.41	13	107	100	Signal transduction
Translationally-controlled tumor protein OS=Homo sapiens GN=TPT1 PE=1 SV=1	TCTP_HUMAN	19582.58008	4.84	9	96.8	100	Apoptosis/Transport
Transmembrane protease, serine 11A OS=Homo sapiens GN=TMPRSS11A PE=1 SV=1	TM11A_HUMAN	47538.46094	9.32	11	61.7	99	Proteolysis
Triosephosphate isomerase OS=Homo sapiens GN=TPI1 PE=1 SV=2	TPIS_HUMAN	26652.74023	6.45	9	73.6	100	Metabolism
Tripeptidyl-peptidase 1 OS=Homo sapiens GN=TPP1 PE=1 SV=2	TPP1_HUMAN	61209.62891	6.01	4	85.9	100	Proteolysis/Protein binding/folding
Tropomyosin alpha-1 chain OS=Homo sapiens GN=TPM1 PE=1 SV=2	TPM1_HUMAN	32688.67969	4.69	11	107	100	Structure
Tropomyosin alpha-3 chain OS=Homo sapiens GN=TPM3 PE=1 SV=1	TPM3_HUMAN	32798.73828	4.68	16	307	100	Structure
Tropomyosin alpha-4 chain OS=Homo sapiens GN=TPM4 PE=1 SV=3	TPM4_HUMAN	28504.49023	4.67	8	250	100	Structure
Tropomyosin beta chain OS=Homo sapiens GN=TPM2 PE=1 SV=1	TPM2_HUMAN	32830.57031	4.66	5	141	100	Structure
Tubulin alpha-1A chain OS=Homo sapiens GN=TUBA1A PE=1 SV=1	TBA1A_HUMAN	50103.60938	4.94	15	406	100	Structure
Tubulin alpha-1B chain OS=Homo sapiens GN=TUBA1B PE=1 SV=1	TBA1B_HUMAN	50119.60156	4.94	16	481	100	Structure
Tubulin alpha-1C chain OS=Homo sapiens GN=TUBA1C PE=1 SV=1	TBA1C_HUMAN	49863.46094	4.96	14	460	100	Structure
Tubulin alpha-3E chain OS=Homo sapiens GN=TUBA3E PE=1 SV=2	TBA3E_HUMAN	49826.55859	5	2	114	100	Structure
Tubulin alpha-4A chain OS=Homo sapiens GN=TUBA4A PE=1 SV=1	TBA4A_HUMAN	49892.37109	4.95	14	345	100	Structure
Tubulin alpha-8 chain OS=Homo sapiens GN=TUBA8 PE=1 SV=1	TBA8_HUMAN	50061.55078	4.94	12	313	100	Structure
Tubulin beta chain OS=Homo sapiens GN=TUBB PE=1 SV=2	TBB5_HUMAN	49638.96875	4.78	14	198	100	Structure
Tubulin beta-2B chain OS=Homo sapiens GN=TUBB2B PE=1 SV=1	TBB2B_HUMAN	49920.94141	4.78	14	198	100	Structure
Tubulin beta-2C chain OS=Homo sapiens GN=TUBB2C PE=1 SV=1	TBB2C_HUMAN	49799	4.79	14	200	100	Structure
Tubulin beta-4 chain OS=Homo sapiens GN=TUBB4 PE=1 SV=2	TBB4_HUMAN	49553.89844	4.78	12	174	100	Structure
UPF0556 protein C19orf10 OS=Homo sapiens GN=C19orf10 PE=1 SV=1	CS010_HUMAN	18783.31055	6.2	5	107	100	Protein binding/folding
UPF0568 protein C14orf166 OS=Homo sapiens GN=C14orf166 PE=1 SV=1	CN166_HUMAN	28050.71094	6.19	2	91.6	100	Protein binding/folding
Vesicle-trafficking protein SEC22b OS=Homo sapiens GN=SEC22B PE=1 SV=3	SC22B_HUMAN	24724.75	8.67	10	196	100	Transport
Vimentin OS=Homo sapiens GN=VIM PE=1 SV=4	VIME_HUMAN	53619.07813	5.06	34	720	100	Structure
Voltage-dependent anion-selective channel protein 1 OS=Homo sapiens GN=VDAC1 PE=1 SV=2	VDAC1_HUMAN	30753.57031	8.62	19	442	100	Transport
Voltage-dependent anion-selective channel protein 2 OS=Homo sapiens GN=VDAC2 PE=1 SV=2	VDAC2_HUMAN	31546.55078	7.49	7	479	100	Transport
V-type proton ATPase catalytic subunit A OS=Homo sapiens GN=ATP6V1A PE=1 SV=2	VATA_HUMAN	68260.49219	5.35	18	249	100	Transport
Zinc finger protein 462 OS=Homo sapiens GN=ZNF462 PE=1 SV=3	ZN462_HUMAN	284505.875	7.53	27	57.2	96	DNA/RNA/protein biosynthesis

Supplemental figure S1 – Cluster analysis of identified proteins in functional clusters (according to Gene Ontology Annotation Database – GOA).

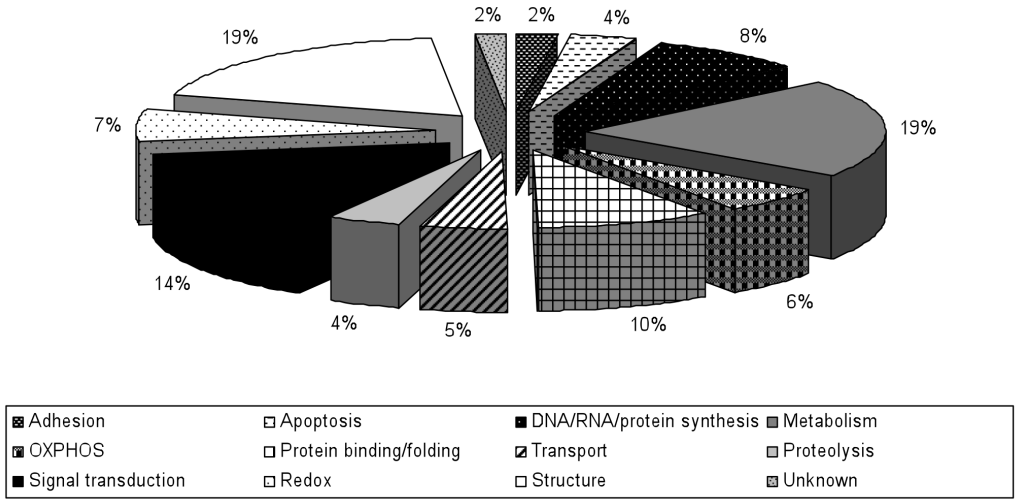

Supplemental figure S2: Differentially expressed proteins grouped according to Biological process (A) and Molecular function (B) (assigned by Panther).

A

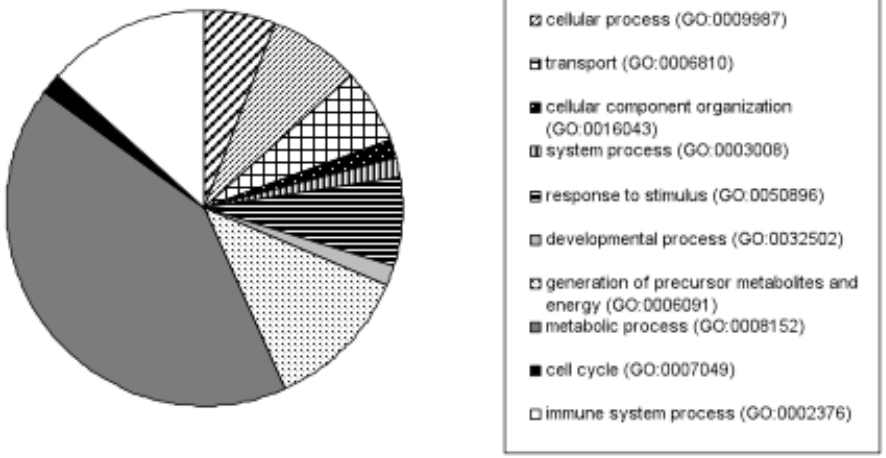

B

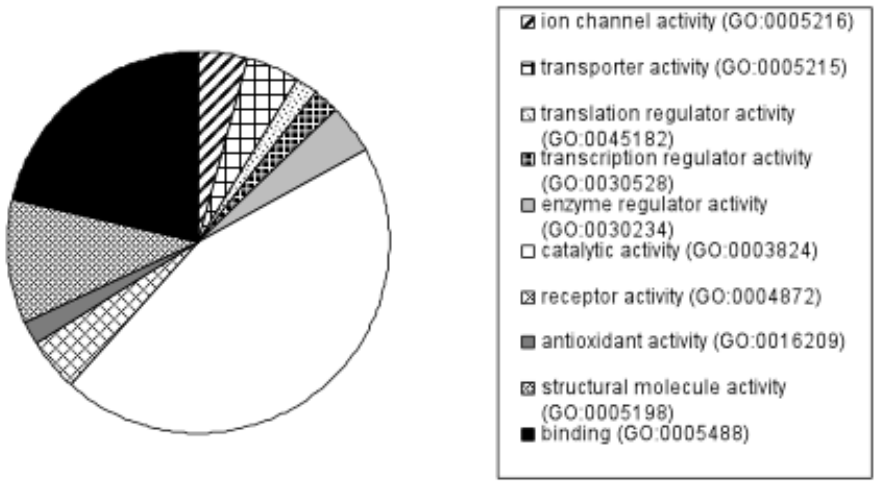

.

Study 5- Unravelling the impact of long-chain 3-hydroxyacyl-CoA dehydrogenase deficiency on mitochondrial proteome.

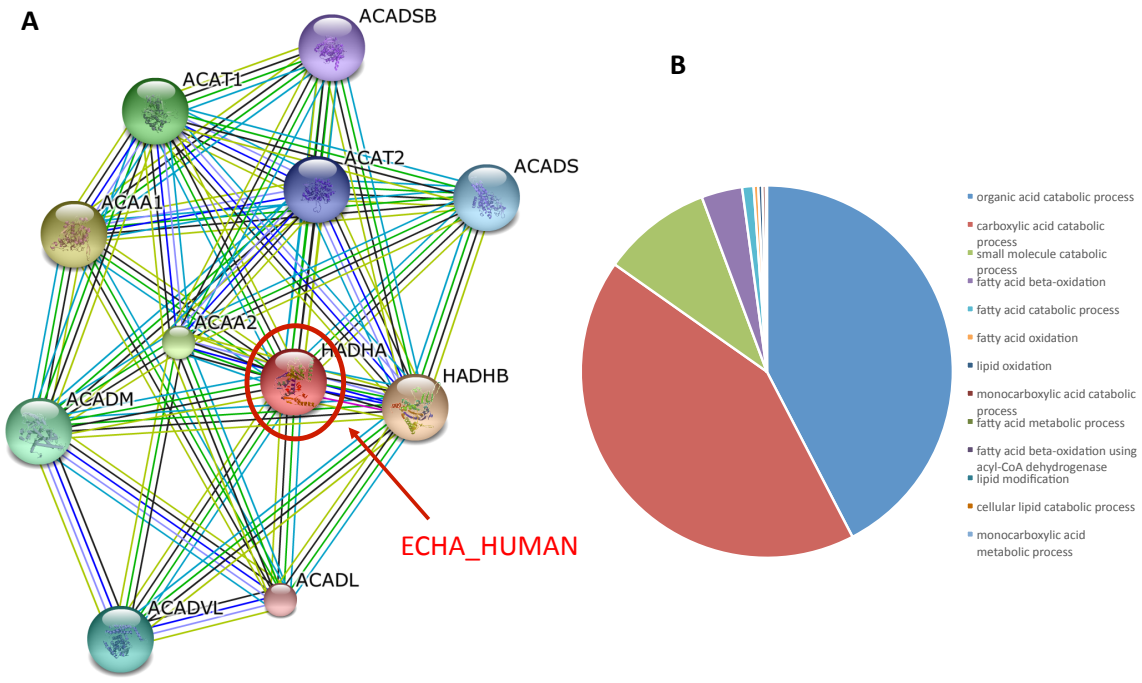

Supplemental figure S1 – (A) String analysis of the interaction of MTP α-subunit (ECHA_HUMAN), (B) Metabolic processes associated with MTP α-subunit according to G.O.

Supplemental table S1 – Primers sequences

Primer	Sequence
MT-ND1-F	CCCTAAAACCCGCCACATCT
MT-ND1-R	GAGCGATGGTGAGAGCTAAGGT
MT-ND4-F	CCATTCTCCTCCTATCCCTCAAC
MT-ND4-R	CACAATCTGATGTTTTGGTTAAACTATATTT
18S rRNA-F	GGCGTCCCCCAACTTCTTA
18S rRNA-R	GGGCATCACAGACCTGTTATTG

Supplemental table S2A – List of proteins identified by nanoLC-MS/MS.

Unused	Total	% Cov	Accession #	Name	Species	Peptides(95%)
344.53	344.53	78.3	sp|Q09666|AHNK_HUMAN	Neuroblast differentiation-associated protein AHNAK OS=Homo sapiens GN=AHNAK PE=1 SV=2	HUMAN	198
194.67	194.67	62.7	sp|P35579|MYH9_HUMAN	Myosin-9 OS=Homo sapiens GN=MYH9 PE=1 SV=4	HUMAN	121
74.46	74.46	94.7	sp|P07355|ANXA2_HUMAN	Annexin A2 OS=Homo sapiens GN=ANXA2 PE=1 SV=2	HUMAN	95
144.35	144.35	29.5	sp|Q15149|PLEC_HUMAN	Plectin OS=Homo sapiens GN=PLEC PE=1 SV=3	HUMAN	82
2	51.77	64.8	sp|P60709|ACTB_HUMAN	Actin, cytoplasmic 1 OS=Homo sapiens GN=ACTB PE=1 SV=1	HUMAN	82
51.77	51.77	64.8	sp|P63261|ACTG_HUMAN	Actin, cytoplasmic 2 OS=Homo sapiens GN=ACTG1 PE=1 SV=1	HUMAN	79
80.09	80.09	70.4	sp|P08670|VIME_HUMAN	Vimentin OS=Homo sapiens GN=VIM PE=1 SV=4	HUMAN	66
93.52	93.52	75.1	sp|P11021|GRP78_HUMAN	78 kDa glucose-regulated protein OS=Homo sapiens GN=HSPA5 PE=1 SV=2	HUMAN	65
89.77	89.77	81.5	sp|P07237|PDIA1_HUMAN	Protein disulfide-isomerase OS=Homo sapiens GN=P4HB PE=1 SV=3	HUMAN	64
65.64	65.64	52.9	sp|P02452|CO1A1_HUMAN	Collagen alpha-1(I) chain OS=Homo sapiens GN=COL1A1 PE=1 SV=5	HUMAN	57
66.38	67.38	72.9	sp|Q07065|CKAP4_HUMAN	Cytoskeleton-associated protein 4 OS=Homo sapiens GN=CKAP4 PE=1 SV=2	HUMAN	49
87.04	87.23	28.8	sp|P12111|CO6A3_HUMAN	Collagen alpha-3(VI) chain OS=Homo sapiens GN=COL6A3 PE=1 SV=5	HUMAN	46
76.18	76.18	54	sp|Q9P2E9|RRBP1_HUMAN	Ribosome-binding protein 1 OS=Homo sapiens GN=RRBP1 PE=1 SV=4	HUMAN	45
60.12	60.34	69.8	sp|P27797|CALR_HUMAN	Calreticulin OS=Homo sapiens GN=CALR PE=1 SV=1	HUMAN	45
67.27	67.49	63.9	sp|P38646|GRP75_HUMAN	Stress-70 protein, mitochondrial OS=Homo sapiens GN=HSPA9 PE=1 SV=2	HUMAN	44
79.93	79.93	30.3	sp|P21333|FLNA_HUMAN	Filamin-A OS=Homo sapiens GN=FLNA PE=1 SV=4	HUMAN	42
51.59	52.08	57	sp|P30101|PDIA3_HUMAN	Protein disulfide-isomerase A3 OS=Homo sapiens GN=PDIA3 PE=1 SV=4	HUMAN	41
4	31.97	50	sp|P63267|ACTH_HUMAN	Actin, gamma-enteric smooth muscle OS=Homo sapiens GN=ACTG2 PE=1 SV=1	HUMAN	39
62.88	63.05	54.9	sp|P14625|ENPL_HUMAN	Endoplasmin OS=Homo sapiens GN=HSP90B1 PE=1 SV=1	HUMAN	38
42.54	42.54	61.1	sp|P06576|ATPB_HUMAN	ATP synthase subunit beta, mitochondrial OS=Homo sapiens GN=ATP5B PE=1 SV=3	HUMAN	38
50.43	50.43	69	sp|P04406|G3P_HUMAN	Glyceraldehyde-3-phosphate dehydrogenase OS=Homo sapiens GN=GAPDH PE=1 SV=3	HUMAN	34
51.91	52.02	58.6	sp|P26038|MOES_HUMAN	Moesin OS=Homo sapiens GN=MSN PE=1 SV=3	HUMAN	30
49.26	49.26	33.1	sp|P15144|AMPN_HUMAN	Aminopeptidase N OS=Homo sapiens GN=ANPEP PE=1 SV=4	HUMAN	30
33.51	33.51	40.3	sp|P08123|CO1A2_HUMAN	Collagen alpha-2(I) chain OS=Homo sapiens GN=COL1A2 PE=1 SV=7	HUMAN	30
54.31	54.31	25.5	sp|P02751|FINC_HUMAN	Fibronectin OS=Homo sapiens GN=FN1 PE=1 SV=4	HUMAN	29
40.51	41	44.4	sp|Q05682|CALD1_HUMAN	Caldesmon OS=Homo sapiens GN=CALD1 PE=1 SV=3	HUMAN	28
42.79	43.13	47	sp|P27824|CALX_HUMAN	Calnexin OS=Homo sapiens GN=CANX PE=1 SV=2	HUMAN	26
40.93	40.93	64.2	sp|P10809|CH60_HUMAN	60 kDa heat shock protein, mitochondrial OS=Homo sapiens GN=HSPD1 PE=1 SV=2	HUMAN	26
34.12	34.12	51.1	sp|P07437|TBB5_HUMAN	Tubulin beta chain OS=Homo sapiens GN=TUBB PE=1 SV=2	HUMAN	26
30.99	30.99	64.9	sp|P04179|SODM_HUMAN	Superoxide dismutase [Mn], mitochondrial OS=Homo sapiens GN=SOD2 PE=1 SV=2	HUMAN	26
40.83	40.83	48.6	sp|P08133|ANXA6_HUMAN	Annexin A6 OS=Homo sapiens GN=ANXA6 PE=1 SV=3	HUMAN	24
36.05	36.05	62.2	sp|P50454|SERPH_HUMAN	Serpin H1 OS=Homo sapiens GN=SERPINH1 PE=1 SV=2	HUMAN	24
29.72	29.72	59.4	sp|O43852|CALU_HUMAN	Calumenin OS=Homo sapiens GN=CALU PE=1 SV=2	HUMAN	24
32.04	32.04	50.1	sp|P25705|ATPA_HUMAN	ATP synthase subunit alpha, mitochondrial OS=Homo sapiens GN=ATP5A1 PE=1 SV=1	HUMAN	23
31.18	31.18	45.4	sp|Q96AY3|FKB10_HUMAN	Peptidyl-prolyl cis-trans isomerase FKBP10 OS=Homo sapiens GN=FKBP10 PE=1 SV=1	HUMAN	22
28.89	43.98	28.2	sp|P35580|MYH10_HUMAN	Myosin-10 OS=Homo sapiens GN=MYH10 PE=1 SV=3	HUMAN	22
2.53	28.98	38.4	sp|P68371|TBB4B_HUMAN	Tubulin beta-4B chain OS=Homo sapiens GN=TUBB4B PE=1 SV=1	HUMAN	22
34.74	34.74	40.9	sp|O43707|ACTN4_HUMAN	Alpha-actinin-4 OS=Homo sapiens GN=ACTN4 PE=1 SV=2	HUMAN	21
28.73	28.85	39.4	sp|P00367|DHE3_HUMAN	Glutamate dehydrogenase 1, mitochondrial OS=Homo sapiens GN=GLUD1 PE=1 SV=2	HUMAN	21
18.16	18.16	47	sp|P02768|ALBU_HUMAN	Serum albumin OS=Homo sapiens GN=ALB PE=1 SV=2	HUMAN	21
38.3	38.3	39	sp|Q14697|GANAB_HUMAN	Neutral alpha-glucosidase AB OS=Homo sapiens GN=GANAB PE=1 SV=3	HUMAN	20
28.19	28.19	75	sp|P23284|PPIB_HUMAN	Peptidyl-prolyl cis-trans isomerase B OS=Homo sapiens GN=PPIB PE=1 SV=2	HUMAN	20
29.06	29.06	60.1	sp|P40926|MDHM_HUMAN	Malate dehydrogenase, mitochondrial OS=Homo sapiens GN=MDH2 PE=1 SV=3	HUMAN	18
12.48	30.06	28.1	sp|P12814|ACTN1_HUMAN	Alpha-actinin-1 OS=Homo sapiens GN=ACTN1 PE=1 SV=2	HUMAN	18
32.28	32.28	19.6	sp|Q9NZM1|MYOF_HUMAN	Myoferlin OS=Homo sapiens GN=MYOF PE=1 SV=1	HUMAN	17
29.55	33.45	41.5	sp|P11142|HSP7C_HUMAN	Heat shock cognate 71 kDa protein OS=Homo sapiens GN=HSPA8 PE=1 SV=1	HUMAN	17
25.89	25.89	37.3	sp|P68363|TBA1B_HUMAN	Tubulin alpha-1B chain OS=Homo sapiens GN=TUBA1B PE=1 SV=1	HUMAN	17
31.92	31.92	18.1	sp|Q13813|SPTA2_HUMAN	Spectrin alpha chain, brain OS=Homo sapiens GN=SPTAN1 PE=1 SV=3	HUMAN	16
30.02	30.02	61.3	sp|P06733|ENOA_HUMAN	Alpha-enolase OS=Homo sapiens GN=ENO1 PE=1 SV=2	HUMAN	16
26.44	26.71	66.1	sp|P67936|TPM4_HUMAN	Tropomyosin alpha-4 chain OS=Homo sapiens GN=TPM4 PE=1 SV=3	HUMAN	15
25.28	25.28	48.2	sp|Q15084|PDIA6_HUMAN	Protein disulfide-isomerase A6 OS=Homo sapiens GN=PDIA6 PE=1 SV=1	HUMAN	15
2	23.87	33.2	sp|Q9BQE3|TBA1C_HUMAN	Tubulin alpha-1C chain OS=Homo sapiens GN=TUBA1C PE=1 SV=1	HUMAN	15
23.07	23.07	41.5	sp|Q96D15|RCN3_HUMAN	Reticulocalbin-3 OS=Homo sapiens GN=RCN3 PE=1 SV=1	HUMAN	14
21.96	21.96	43.1	sp|P08758|ANXA5_HUMAN	Annexin A5 OS=Homo sapiens GN=ANXA5 PE=1 SV=2	HUMAN	14
20.58	20.58	41.5	sp|Q6NZI2|PTRF_HUMAN	Polymerase I and transcript release factor OS=Homo sapiens GN=PTRF PE=1 SV=1	HUMAN	14
18.41	18.41	42.4	sp|P17931|LEG3_HUMAN	Galectin-3 OS=Homo sapiens GN=LGALS3 PE=1 SV=5	HUMAN	14
17.58	17.58	30.8	sp|P04843|RPN1_HUMAN	Dolichyl-diphosphooligosaccharide--protein glycosyltransferase subunit 1 OS=Homo sapiens GN=RPN1 PE=1 SV=	HUMAN	14
2	24.49	47.9	sp|P07951|TPM2_HUMAN	Tropomyosin beta chain OS=Homo sapiens GN=TPM2 PE=1 SV=1	HUMAN	14
21.97	21.97	36.3	sp|P02545|LMNA_HUMAN	Prelamin-A/C OS=Homo sapiens GN=LMNA PE=1 SV=1	HUMAN	13
19.96	19.97	43.5	sp|Q15293|RCN1_HUMAN	Reticulocalbin-1 OS=Homo sapiens GN=RCN1 PE=1 SV=1	HUMAN	13
19.65	19.77	27.8	sp|P13667|PDIA4_HUMAN	Protein disulfide-isomerase A4 OS=Homo sapiens GN=PDIA4 PE=1 SV=2	HUMAN	13
17.09	17.09	92.2	sp|P61604|CH10_HUMAN	10 kDa heat shock protein, mitochondrial OS=Homo sapiens GN=HSPE1 PE=1 SV=2	HUMAN	13
0.86	16.25	28	sp|Q9BUF5|TBB6_HUMAN	Tubulin beta-6 chain OS=Homo sapiens GN=TUBB6 PE=1 SV=1	HUMAN	13
21.39	21.39	27.7	sp|P08473|NEP_HUMAN	Neprilysin OS=Homo sapiens GN=MME PE=1 SV=2	HUMAN	12
20.9	20.9	26.5	sp|P13639|EF2_HUMAN	Elongation factor 2 OS=Homo sapiens GN=EEF2 PE=1 SV=4	HUMAN	12
20.76	20.76	66.7	sp|Q02878|RL6_HUMAN	60S ribosomal protein L6 OS=Homo sapiens GN=RPL6 PE=1 SV=3	HUMAN	12
20.65	20.93	46.3	sp|Q5VTE0|EF1A3_HUMAN	Putative elongation factor 1-alpha-like 3 OS=Homo sapiens GN=EEF1A1P5 PE=5 SV=1	HUMAN	12
18.45	18.76	32.5	sp|P04264|K2C1_HUMAN	Keratin, type II cytoskeletal 1 OS=Homo sapiens GN=KRT1 PE=1 SV=6	HUMAN	12
18.31	18.31	30.1	sp|P40939|ECHA_HUMAN	Trifunctional enzyme subunit alpha, mitochondrial OS=Homo sapiens GN=HADHA PE=1 SV=2	HUMAN	12
16.66	16.66	24.9	sp|P55084|ECHB_HUMAN	Trifunctional enzyme subunit beta, mitochondrial OS=Homo sapiens GN=HADHB PE=1 SV=3	HUMAN	12
14.58	15.28	69.1	sp|P62937|PPIA_HUMAN	Peptidyl-prolyl cis-trans isomerase A OS=Homo sapiens GN=PPIA PE=1 SV=2	HUMAN	12
16.23	16.26	75.4	sp|Q99879|H2B1M_HUMAN	Histone H2B type 1-M OS=Homo sapiens GN=HIST1H2BM PE=1 SV=3	HUMAN	12
22.2	22.2	76.7	sp|P80723|BASP1_HUMAN	Brain acid soluble protein 1 OS=Homo sapiens GN=BASP1 PE=1 SV=2	HUMAN	11
21.4	21.48	22.5	sp|Q7KZF4|SND1_HUMAN	Staphylococcal nuclease domain-containing protein 1 OS=Homo sapiens GN=SND1 PE=1 SV=1	HUMAN	11
17.92	17.93	49.4	sp|P67809|YBOX1_HUMAN	Nuclease-sensitive element-binding protein 1 OS=Homo sapiens GN=YBX1 PE=1 SV=3	HUMAN	11
17.66	17.66	73.8	sp|P62158|CALM_HUMAN	Calmodulin OS=Homo sapiens GN=CALM1 PE=1 SV=2	HUMAN	11
16.6	16.6	29.8	sp|P04083|ANXA1_HUMAN	Annexin A1 OS=Homo sapiens GN=ANXA1 PE=1 SV=2	HUMAN	11
16.35	16.49	23.7	sp|P14314|GLU2B_HUMAN	Glucosidase 2 subunit beta OS=Homo sapiens GN=PRKCSH PE=1 SV=2	HUMAN	11
15.53	15.53	50.7	sp|P35232|PHB_HUMAN	Prohibitin OS=Homo sapiens GN=PHB PE=1 SV=1	HUMAN	11
15.03	15.03	68.9	sp|P60660|MYL6_HUMAN	Myosin light polypeptide 6 OS=Homo sapiens GN=MYL6 PE=1 SV=2	HUMAN	11
14.22	14.22	21.1	sp|P12109|CO6A1_HUMAN	Collagen alpha-1(VI) chain OS=Homo sapiens GN=COL6A1 PE=1 SV=3	HUMAN	11
13.25	13.25	30.7	sp|P24752|THIL_HUMAN	Acetyl-CoA acetyltransferase, mitochondrial OS=Homo sapiens GN=ACAT1 PE=1 SV=1	HUMAN	11
19.87	19.99	28.7	sp|P13674|P4HA1_HUMAN	Prolyl 4-hydroxylase subunit alpha-1 OS=Homo sapiens GN=P4HA1 PE=1 SV=2	HUMAN	10
19.51	19.51	44.4	sp|P14618|KPYM_HUMAN	Pyruvate kinase isozymes M1/M2 OS=Homo sapiens GN=PKM2 PE=1 SV=4	HUMAN	10
18.47	18.47	56.5	sp|P00387|NB5R3_HUMAN	NADH-cytochrome b5 reductase 3 OS=Homo sapiens GN=CYB5R3 PE=1 SV=3	HUMAN	10
17.93	17.93	41	sp|P36578|RL4_HUMAN	60S ribosomal protein L4 OS=Homo sapiens GN=RPL4 PE=1 SV=5	HUMAN	10
16.2	16.2	76.3	sp|P09382|LEG1_HUMAN	Galectin-1 OS=Homo sapiens GN=LGALS1 PE=1 SV=2	HUMAN	10

Unused	Total	% Cov	Accession #	Name	Species	Peptides(95%)
12	12	60.9	sp|P05387|RLA2_HUMAN	60S acidic ribosomal protein P2 OS=Homo sapiens GN=RPLP2 PE=1 SV=1	HUMAN	10
10.81	10.81	78.4	sp|P60903|S10AA_HUMAN	Protein S100-A10 OS=Homo sapiens GN=S100A10 PE=1 SV=2	HUMAN	10
10.7	10.7	24.3	sp|P36957|ODO2_HUMAN	Dihydrolipoyllysine-residue succinyltransferase component of 2-oxoglutarate dehydrogenase complex, mitochon	HUMAN	10
9.56	9.56	18.5	sp|P16070|CD44_HUMAN	CD44 antigen OS=Homo sapiens GN=CD44 PE=1 SV=3	HUMAN	10
9.54	16.79	35.9	sp|P09493|TPM1_HUMAN	Tropomyosin alpha-1 chain OS=Homo sapiens GN=TPM1 PE=1 SV=2	HUMAN	10
16.07	16.07	47.4	sp|P21796|VDAC1_HUMAN	Voltage-dependent anion-selective channel protein 1 OS=Homo sapiens GN=VDAC1 PE=1 SV=2	HUMAN	9
15.75	15.75	71.7	sp|P23528|COF1_HUMAN	Cofilin-1 OS=Homo sapiens GN=CFL1 PE=1 SV=3	HUMAN	9
15.06	15.06	21.1	sp|Q12797|ASPH_HUMAN	Aspartyl/asparaginyl beta-hydroxylase OS=Homo sapiens GN=ASPH PE=1 SV=3	HUMAN	9
14.32	14.32	55.2	sp|O14950|ML12B_HUMAN	Myosin regulatory light chain 12B OS=Homo sapiens GN=MYL12B PE=1 SV=2	HUMAN	9
14.28	14.28	60	sp|P39019|RS19_HUMAN	40S ribosomal protein S19 OS=Homo sapiens GN=RPS19 PE=1 SV=2	HUMAN	9
14.07	14.07	35.3	sp|P08865|RSSA_HUMAN	40S ribosomal protein SA OS=Homo sapiens GN=RPSA PE=1 SV=4	HUMAN	9
10.22	10.25	21.4	sp|P02461|CO3A1_HUMAN	Collagen alpha-1(III) chain OS=Homo sapiens GN=COL3A1 PE=1 SV=4	HUMAN	9
5.27	14.53	32.4	sp|P06753|TPM3_HUMAN	Tropomyosin alpha-3 chain OS=Homo sapiens GN=TPM3 PE=1 SV=1	HUMAN	9
17.37	17.37	53.1	sp|P26373|RL13_HUMAN	60S ribosomal protein L13 OS=Homo sapiens GN=RPL13 PE=1 SV=4	HUMAN	8
15.28	15.28	53.8	sp|Q06830|PRDX1_HUMAN	Peroxiredoxin-1 OS=Homo sapiens GN=PRDX1 PE=1 SV=1	HUMAN	8
15.24	15.24	25.8	sp|P39023|RL3_HUMAN	60S ribosomal protein L3 OS=Homo sapiens GN=RPL3 PE=1 SV=2	HUMAN	8
14.49	14.49	43.2	sp|P61247|RS3A_HUMAN	40S ribosomal protein S3a OS=Homo sapiens GN=RPS3A PE=1 SV=2	HUMAN	8
14.08	14.08	16.2	sp|P05023|AT1A1_HUMAN	Sodium/potassium-transporting ATPase subunit alpha-1 OS=Homo sapiens GN=ATP1A1 PE=1 SV=1	HUMAN	8
13.71	13.71	25.5	sp|P09622|DLDH_HUMAN	Dihydrolipoyl dehydrogenase, mitochondrial OS=Homo sapiens GN=DLD PE=1 SV=2	HUMAN	8
13.71	13.76	40.8	sp|P18621|RL17_HUMAN	60S ribosomal protein L17 OS=Homo sapiens GN=RPL17 PE=1 SV=3	HUMAN	8
13.71	13.71	42.8	sp|P30084|ECHM_HUMAN	Enoyl-CoA hydratase, mitochondrial OS=Homo sapiens GN=ECHS1 PE=1 SV=4	HUMAN	8
13.23	13.23	18	sp|P12110|CO6A2_HUMAN	Collagen alpha-2(VI) chain OS=Homo sapiens GN=COL6A2 PE=1 SV=4	HUMAN	8
13.2	13.2	22.6	sp|Q9NVI7|ATD3A_HUMAN	ATPase family AAA domain-containing protein 3A OS=Homo sapiens GN=ATAD3A PE=1 SV=2	HUMAN	8
11.52	11.52	26.2	sp|P07339|CATD_HUMAN	Cathepsin D OS=Homo sapiens GN=CTSD PE=1 SV=1	HUMAN	8
11.16	11.16	31.2	sp|P13804|ETFA_HUMAN	Electron transfer flavoprotein subunit alpha, mitochondrial OS=Homo sapiens GN=ETFA PE=1 SV=1	HUMAN	8
10.55	10.55	58.7	sp|P20674|COX5A_HUMAN	Cytochrome c oxidase subunit 5A, mitochondrial OS=Homo sapiens GN=COX5A PE=1 SV=2	HUMAN	8
10.19	10.29	61.4	sp|P07737|PROF1_HUMAN	Profilin-1 OS=Homo sapiens GN=PFN1 PE=1 SV=2	HUMAN	8
9.08	17.79	29.2	sp|P15311|EZRI_HUMAN	Ezrin OS=Homo sapiens GN=EZR PE=1 SV=4	HUMAN	8
6.81	6.81	26	sp|P35613|BASI_HUMAN	Basigin OS=Homo sapiens GN=BSG PE=1 SV=2	HUMAN	8
2.8	11.63	22.3	sp|P08107|HSP71_HUMAN	Heat shock 70 kDa protein 1A/1B OS=Homo sapiens GN=HSPA1A PE=1 SV=5	HUMAN	8
13.91	13.91	67.1	sp|P10412|H14_HUMAN	Histone H1.4 OS=Homo sapiens GN=HIST1H1E PE=1 SV=2	HUMAN	8
16.44	16.58	45.5	sp|P46777|RL5_HUMAN	60S ribosomal protein L5 OS=Homo sapiens GN=RPL5 PE=1 SV=3	HUMAN	7
15.52	15.57	46.9	sp|Q96AG4|LRC59_HUMAN	Leucine-rich repeat-containing protein 59 OS=Homo sapiens GN=LRRC59 PE=1 SV=1	HUMAN	7
14.38	14.38	12.4	sp|Q01082|SPTB2_HUMAN	Spectrin beta chain, brain 1 OS=Homo sapiens GN=SPTBN1 PE=1 SV=2	HUMAN	7
14.17	14.17	38.6	sp|P07858|CATB_HUMAN	Cathepsin B OS=Homo sapiens GN=CTSB PE=1 SV=3	HUMAN	7
14.16	14.21	14	sp|Q9NQC3|RTN4_HUMAN	Reticulon-4 OS=Homo sapiens GN=RTN4 PE=1 SV=2	HUMAN	7
13.56	13.56	30.4	sp|Q02818|NUCB1_HUMAN	Nucleobindin-1 OS=Homo sapiens GN=NUCB1 PE=1 SV=4	HUMAN	7
13.28	13.28	16.3	sp|Q9Y4L1|HYOU1_HUMAN	Hypoxia up-regulated protein 1 OS=Homo sapiens GN=HYOU1 PE=1 SV=1	HUMAN	7
12.91	12.91	63.1	sp|P14927|QCR7_HUMAN	Cytochrome b-c1 complex subunit 7 OS=Homo sapiens GN=UQCRB PE=1 SV=2	HUMAN	7
12.86	12.86	35.7	sp|P04075|ALDOA_HUMAN	Fructose-bisphosphate aldolase A OS=Homo sapiens GN=ALDOA PE=1 SV=2	HUMAN	7
12.75	12.75	24.3	sp|P07686|HEXB_HUMAN	Beta-hexosaminidase subunit beta OS=Homo sapiens GN=HEXB PE=1 SV=3	HUMAN	7
12.62	12.62	55.8	sp|P62750|RL23A_HUMAN	60S ribosomal protein L23a OS=Homo sapiens GN=RPL23A PE=1 SV=1	HUMAN	7
11.83	11.83	50.5	sp|P46782|RS5_HUMAN	40S ribosomal protein S5 OS=Homo sapiens GN=RPS5 PE=1 SV=4	HUMAN	7
11.79	11.9	25.9	sp|Q8NBS9|TXND5_HUMAN	Thioredoxin domain-containing protein 5 OS=Homo sapiens GN=TXNDC5 PE=1 SV=2	HUMAN	7
11.46	11.46	39.6	sp|P63000|RAC1_HUMAN	Ras-related C3 botulinum toxin substrate 1 OS=Homo sapiens GN=RAC1 PE=1 SV=1	HUMAN	7
11.36	11.36	57.6	sp|Q9UII2|ATIF1_HUMAN	ATPase inhibitor, mitochondrial OS=Homo sapiens GN=ATPIF1 PE=1 SV=1	HUMAN	7
10.49	10.58	24.4	sp|P34897|GLYM_HUMAN	Serine hydroxymethyltransferase, mitochondrial OS=Homo sapiens GN=SHMT2 PE=1 SV=3	HUMAN	7
9.41	13.51	9.6	sp|Q14315|FLNC_HUMAN	Filamin-C OS=Homo sapiens GN=FLNC PE=1 SV=3	HUMAN	7
8.58	8.58	41.3	sp|P12236|ADT3_HUMAN	ADP/ATP translocase 3 OS=Homo sapiens GN=SLC25A6 PE=1 SV=4	HUMAN	7
7.14	7.14	32.2	sp|P37802|TAGL2_HUMAN	Transgelin-2 OS=Homo sapiens GN=TAGLN2 PE=1 SV=3	HUMAN	7
6.16	6.16	23.9	sp|P07477|TRY1_HUMAN	Trypsin-1 OS=Homo sapiens GN=PRSS1 PE=1 SV=1	HUMAN	7
2.86	13.43	25	sp|P35241|RADI_HUMAN	Radixin OS=Homo sapiens GN=RDX PE=1 SV=1	HUMAN	7
2	12.72	20.2	sp|Q5T9A4|ATD3B_HUMAN	ATPase family AAA domain-containing protein 3B OS=Homo sapiens GN=ATAD3B PE=1 SV=1	HUMAN	7
12.91	12.91	14.1	sp|Q9Y490|TLN1_HUMAN	Talin-1 OS=Homo sapiens GN=TLN1 PE=1 SV=3	HUMAN	6
12.13	12.13	21.2	sp|P49411|EFTU_HUMAN	Elongation factor Tu, mitochondrial OS=Homo sapiens GN=TUFM PE=1 SV=2	HUMAN	6
12	12.62	13.2	sp|Q9Y2D5|AKAP2_HUMAN	A-kinase anchor protein 2 OS=Homo sapiens GN=AKAP2 PE=1 SV=3	HUMAN	6
11.96	12.02	14.2	sp|Q16822|PCKGM_HUMAN	Phosphoenolpyruvate carboxykinase [GTP], mitochondrial OS=Homo sapiens GN=PCK2 PE=1 SV=3	HUMAN	6
11.65	11.65	25.2	sp|Q16891|IMMT_HUMAN	Mitochondrial inner membrane protein OS=Homo sapiens GN=IMMT PE=1 SV=1	HUMAN	6
11.59	11.59	37.5	sp|Q99623|PHB2_HUMAN	Prohibitin-2 OS=Homo sapiens GN=PHB2 PE=1 SV=2	HUMAN	6
11.3	11.3	34.2	sp|P62424|RL7A_HUMAN	60S ribosomal protein L7a OS=Homo sapiens GN=RPL7A PE=1 SV=2	HUMAN	6
10.8	10.8	47.9	sp|P13073|COX41_HUMAN	Cytochrome c oxidase subunit 4 isoform 1, mitochondrial OS=Homo sapiens GN=COX4I1 PE=1 SV=1	HUMAN	6
10.72	10.72	15.5	sp|P27816|MAP4_HUMAN	Microtubule-associated protein 4 OS=Homo sapiens GN=MAP4 PE=1 SV=3	HUMAN	6
9.92	9.92	6.5	sp|Q07954|LRP1_HUMAN	Prolow-density lipoprotein receptor-related protein 1 OS=Homo sapiens GN=LRP1 PE=1 SV=2	HUMAN	6
9.69	9.69	26.3	sp|P01892|1A02_HUMAN	HLA class I histocompatibility antigen, A-2 alpha chain OS=Homo sapiens GN=HLA-A PE=1 SV=1	HUMAN	6
8.76	8.76	37.6	sp|P62899|RL31_HUMAN	60S ribosomal protein L31 OS=Homo sapiens GN=RPL31 PE=1 SV=1	HUMAN	6
8.57	8.58	45.2	sp|Q07020|RL18_HUMAN	60S ribosomal protein L18 OS=Homo sapiens GN=RPL18 PE=1 SV=2	HUMAN	6
8.5	8.5	14.4	sp|P05556|ITB1_HUMAN	Integrin beta-1 OS=Homo sapiens GN=ITGB1 PE=1 SV=2	HUMAN	6
8.44	8.44	7.9	sp|Q99715|COCA1_HUMAN	Collagen alpha-1(XII) chain OS=Homo sapiens GN=COL12A1 PE=1 SV=2	HUMAN	6
8.24	8.24	59.3	sp|P18859|ATP5J_HUMAN	ATP synthase-coupling factor 6, mitochondrial OS=Homo sapiens GN=ATP5J PE=1 SV=1	HUMAN	6
8.06	8.06	20	sp|Q9Y6N5|SQRD_HUMAN	Sulfide:quinone oxidoreductase, mitochondrial OS=Homo sapiens GN=SQRDL PE=1 SV=1	HUMAN	6
8	8	9.2	sp|O00469|PLOD2_HUMAN	Procollagen-lysine,2-oxoglutarate 5-dioxygenase 2 OS=Homo sapiens GN=PLOD2 PE=1 SV=2	HUMAN	6
8	8	42.5	sp|P00167|CYB5_HUMAN	Cytochrome b5 OS=Homo sapiens GN=CYB5A PE=1 SV=2	HUMAN	6
8	8	24.3	sp|P38117|ETFB_HUMAN	Electron transfer flavoprotein subunit beta OS=Homo sapiens GN=ETFB PE=1 SV=3	HUMAN	6
7.94	7.94	36.7	sp|P30048|PRDX3_HUMAN	Thioredoxin-dependent peroxide reductase, mitochondrial OS=Homo sapiens GN=PRDX3 PE=1 SV=3	HUMAN	6
7.6	7.6	17.4	sp|O95302|FKBP9_HUMAN	Peptidyl-prolyl cis-trans isomerase FKBP9 OS=Homo sapiens GN=FKBP9 PE=1 SV=2	HUMAN	6
7.55	7.56	22.8	sp|O75396|SC22B_HUMAN	Vesicle-trafficking protein SEC22b OS=Homo sapiens GN=SEC22B PE=1 SV=4	HUMAN	6
7.4	7.45	18.2	sp|P55072|TERA_HUMAN	Transitional endoplasmic reticulum ATPase OS=Homo sapiens GN=VCP PE=1 SV=4	HUMAN	6
7.16	7.16	31	sp|P61254|RL26_HUMAN	60S ribosomal protein L26 OS=Homo sapiens GN=RPL26 PE=1 SV=1	HUMAN	6
6.93	6.94	49.3	sp|Q04837|SSBP_HUMAN	Single-stranded DNA-binding protein, mitochondrial OS=Homo sapiens GN=SSBP1 PE=1 SV=1	HUMAN	6
6.9	6.9	18.5	sp|P22695|QCR2_HUMAN	Cytochrome b-c1 complex subunit 2, mitochondrial OS=Homo sapiens GN=UQCRC2 PE=1 SV=3	HUMAN	6
6.53	6.53	47.1	sp|P61313|RL15_HUMAN	60S ribosomal protein L15 OS=Homo sapiens GN=RPL15 PE=1 SV=2	HUMAN	6
4.39	4.39	48.4	sp|P47914|RL29_HUMAN	60S ribosomal protein L29 OS=Homo sapiens GN=RPL29 PE=1 SV=2	HUMAN	6
4.3	4.3	24.7	sp|Q03135|CAV1_HUMAN	Caveolin-1 OS=Homo sapiens GN=CAV1 PE=1 SV=4	HUMAN	6
2	8.15	40.3	sp|P05141|ADT2_HUMAN	ADP/ATP translocase 2 OS=Homo sapiens GN=SLC25A5 PE=1 SV=7	HUMAN	6
7.28	7.3	12.7	sp|Q13813|SPTN1_HUMAN	Spectrin alpha chain, non-erythrocytic 1 OS=Homo sapiens GN=SPTAN1 PE=1 SV=3	HUMAN	6
7.15	7.15	49.2	sp|Q7L7L0|H2A3_HUMAN	Histone H2A type 3 OS=Homo sapiens GN=HIST3H2A PE=1 SV=3	HUMAN	6
6.35	6.37	9.9	sp|Q14204|DYHC1_HUMAN	Cytoplasmic dynein 1 heavy chain 1 OS=Homo sapiens GN=DYNC1H1 PE=1 SV=5	HUMAN	6

Unused	Total	% Cov	Accession #	Name	Species	Peptides(95%)
0.75	9.22	63.4	sp|P16403|H12_HUMAN	Histone H1.2 OS=Homo sapiens GN=HIST1H1C PE=1 SV=2	HUMAN	6
11.2	11.2	32	sp|P07954|FUMH_HUMAN	Fumarate hydratase, mitochondrial OS=Homo sapiens GN=FH PE=1 SV=3	HUMAN	5
10.65	10.65	23	sp|O75390|CISY_HUMAN	Citrate synthase, mitochondrial OS=Homo sapiens GN=CS PE=1 SV=2	HUMAN	5
10.61	10.61	40.2	sp|P27635|RL10_HUMAN	60S ribosomal protein L10 OS=Homo sapiens GN=RPL10 PE=1 SV=4	HUMAN	5
10.12	10.12	55.9	sp|O75947|ATP5H_HUMAN	ATP synthase subunit d, mitochondrial OS=Homo sapiens GN=ATP5H PE=1 SV=3	HUMAN	5
10.07	10.26	13.6	sp|Q00341|VIGLN_HUMAN	Vigilin OS=Homo sapiens GN=HDLBP PE=1 SV=2	HUMAN	5
10.01	10.01	14.9	sp|P31040|DHSA_HUMAN	Succinate dehydrogenase [ubiquinone] flavoprotein subunit, mitochondrial OS=Homo sapiens GN=SDHA PE=1 S	HUMAN	5
10	10	32.5	sp|P29966|MARCS_HUMAN	Myristoylated alanine-rich C-kinase substrate OS=Homo sapiens GN=MARCKS PE=1 SV=4	HUMAN	5
10	10	25.5	sp|Q15019|SEPT2_HUMAN	Septin-2 OS=Homo sapiens GN=SEPT2 PE=1 SV=1	HUMAN	5
9.96	9.96	17.2	sp|O00159|MYO1C_HUMAN	Myosin-Ic OS=Homo sapiens GN=MYO1C PE=1 SV=4	HUMAN	5
9.82	9.82	37.7	sp|P00441|SODC_HUMAN	Superoxide dismutase [Cu-Zn] OS=Homo sapiens GN=SOD1 PE=1 SV=2	HUMAN	5
9.57	9.57	28.4	sp|Q9UJZ1|STML2_HUMAN	Stomatin-like protein 2 OS=Homo sapiens GN=STOML2 PE=1 SV=1	HUMAN	5
9.24	9.24	32.7	sp|P62906|RL10A_HUMAN	60S ribosomal protein L10a OS=Homo sapiens GN=RPL10A PE=1 SV=2	HUMAN	5
8.54	8.54	42.7	sp|P83731|RL24_HUMAN	60S ribosomal protein L24 OS=Homo sapiens GN=RPL24 PE=1 SV=1	HUMAN	5
8.09	8.09	12.6	sp|P18206|VINC_HUMAN	Vinculin OS=Homo sapiens GN=VCL PE=1 SV=4	HUMAN	5
7.88	7.88	39.9	sp|P30040|ERP29_HUMAN	Endoplasmic reticulum resident protein 29 OS=Homo sapiens GN=ERP29 PE=1 SV=4	HUMAN	5
7.56	7.56	38.3	sp|Q6IS14|IF5AL_HUMAN	Eukaryotic translation initiation factor 5A-1-like OS=Homo sapiens GN=EIF5AL1 PE=1 SV=2	HUMAN	5
7.46	7.46	34.8	sp|Q9UIJ7|KAD3_HUMAN	GTP:AMP phosphotransferase, mitochondrial OS=Homo sapiens GN=AK3 PE=1 SV=4	HUMAN	5
6.94	6.94	24	sp|P00505|AATM_HUMAN	Aspartate aminotransferase, mitochondrial OS=Homo sapiens GN=GOT2 PE=1 SV=3	HUMAN	5
6.54	6.54	19.6	sp|Q9NVA2|SEP11_HUMAN	Septin-11 OS=Homo sapiens GN=SEPT11 PE=1 SV=3	HUMAN	5
6.38	6.38	61.9	sp|Q99880|H2B1L_HUMAN	Histone H2B type 1-L OS=Homo sapiens GN=HIST1H2BL PE=1 SV=3	HUMAN	5
6.35	6.35	42.5	sp|P62249|RS16_HUMAN	40S ribosomal protein S16 OS=Homo sapiens GN=RPS16 PE=1 SV=2	HUMAN	5
6	6	14.4	sp|O14773|TPP1_HUMAN	Tripeptidyl-peptidase 1 OS=Homo sapiens GN=TPP1 PE=1 SV=2	HUMAN	5
5.88	5.88	15.8	sp|Q00325|MPCP_HUMAN	Phosphate carrier protein, mitochondrial OS=Homo sapiens GN=SLC25A3 PE=1 SV=2	HUMAN	5
5.21	5.21	33.3	sp|P30050|RL12_HUMAN	60S ribosomal protein L12 OS=Homo sapiens GN=RPL12 PE=1 SV=1	HUMAN	5
4.05	4.05	46.4	sp|P62857|RS28_HUMAN	40S ribosomal protein S28 OS=Homo sapiens GN=RPS28 PE=1 SV=1	HUMAN	5
3.02	9.54	44.8	sp|P24844|MYL9_HUMAN	Myosin regulatory light polypeptide 9 OS=Homo sapiens GN=MYL9 PE=1 SV=4	HUMAN	5
2.01	8.02	31	sp|P30443|1A01_HUMAN	HLA class I histocompatibility antigen, A-1 alpha chain OS=Homo sapiens GN=HLA-A PE=1 SV=1	HUMAN	5
1.56	6.25	6.1	sp|O75369|FLNB_HUMAN	Filamin-B OS=Homo sapiens GN=FLNB PE=1 SV=2	HUMAN	5
1.32	10.83	19.2	sp|P08238|HS90B_HUMAN	Heat shock protein HSP 90-beta OS=Homo sapiens GN=HSP90AB1 PE=1 SV=4	HUMAN	5
4.08	4.11	73.5	sp|Q71DI3|H32_HUMAN	Histone H3.2 OS=Homo sapiens GN=HIST2H3A PE=1 SV=3	HUMAN	5
3.39	3.39	32.6	sp|Q15365|PCBP1_HUMAN	Poly(rC)-binding protein 1 OS=Homo sapiens GN=PCBP1 PE=1 SV=2	HUMAN	5
2.07	2.07	35.2	sp|P26641|EF1G_HUMAN	Elongation factor 1-gamma OS=Homo sapiens GN=EEF1G PE=1 SV=3	HUMAN	5
9.34	9.41	25.4	sp|P07900|HS90A_HUMAN	Heat shock protein HSP 90-alpha OS=Homo sapiens GN=HSP90AA1 PE=1 SV=5	HUMAN	4
9.03	9.03	52.9	sp|P62241|RS8_HUMAN	40S ribosomal protein S8 OS=Homo sapiens GN=RPS8 PE=1 SV=2	HUMAN	4
8.96	8.96	11.9	sp|P07996|TSP1_HUMAN	Thrombospondin-1 OS=Homo sapiens GN=THBS1 PE=1 SV=2	HUMAN	4
8.88	8.93	10.6	sp|Q3SY69|AL1L2_HUMAN	Mitochondrial 10-formyltetrahydrofolate dehydrogenase OS=Homo sapiens GN=ALDH1L2 PE=1 SV=2	HUMAN	4
8.68	8.68	46.3	sp|P04792|HSPB1_HUMAN	Heat shock protein beta-1 OS=Homo sapiens GN=HSPB1 PE=1 SV=2	HUMAN	4
8.62	8.62	24.3	sp|Q9UBS4|DJB11_HUMAN	DnaJ homolog subfamily B member 11 OS=Homo sapiens GN=DNAJB11 PE=1 SV=1	HUMAN	4
8.47	8.47	65.1	sp|P14854|CX6B1_HUMAN	Cytochrome c oxidase subunit 6B1 OS=Homo sapiens GN=COX6B1 PE=1 SV=2	HUMAN	4
8.37	8.37	39.5	sp|P62701|RS4X_HUMAN	40S ribosomal protein S4, X isoform OS=Homo sapiens GN=RPS4X PE=1 SV=2	HUMAN	4
8.27	8.27	14.2	sp|P49748|ACADV_HUMAN	Very long-chain specific acyl-CoA dehydrogenase, mitochondrial OS=Homo sapiens GN=ACADVL PE=1 SV=1	HUMAN	4
8.21	8.21	18.7	sp|P13645|K1C10_HUMAN	Keratin, type I cytoskeletal 10 OS=Homo sapiens GN=KRT10 PE=1 SV=6	HUMAN	4
8.09	8.8	23.5	sp|Q8IVF2|AHNK2_HUMAN	Protein AHNAK2 OS=Homo sapiens GN=AHNAK2 PE=1 SV=2	HUMAN	4
8.04	8.04	14.3	sp|Q16643|DREB_HUMAN	Drebrin OS=Homo sapiens GN=DBN1 PE=1 SV=4	HUMAN	4
8.01	8.01	13.1	sp|O95202|LETM1_HUMAN	LETM1 and EF-hand domain-containing protein 1, mitochondrial OS=Homo sapiens GN=LETM1 PE=1 SV=1	HUMAN	4
8	8	16.4	sp|O00461|GOLI4_HUMAN	Golgi integral membrane protein 4 OS=Homo sapiens GN=GOLIM4 PE=1 SV=1	HUMAN	4
8	8	22.6	sp|P11177|ODPB_HUMAN	Pyruvate dehydrogenase E1 component subunit beta, mitochondrial OS=Homo sapiens GN=PDHB PE=1 SV=3	HUMAN	4
8	8.12	9.1	sp|P51659|DHB4_HUMAN	Peroxisomal multifunctional enzyme type 2 OS=Homo sapiens GN=HSD17B4 PE=1 SV=3	HUMAN	4
8	8	32.8	sp|P84157|MXRA7_HUMAN	Matrix-remodeling-associated protein 7 OS=Homo sapiens GN=MXRA7 PE=1 SV=1	HUMAN	4
8	8	23.9	sp|Q16795|NDUA9_HUMAN	NADH dehydrogenase [ubiquinone] 1 alpha subcomplex subunit 9, mitochondrial OS=Homo sapiens GN=NDUFA	HUMAN	4
8	8	23	sp|Q9NR28|DBLOH_HUMAN	Diablo homolog, mitochondrial OS=Homo sapiens GN=DIABLO PE=1 SV=1	HUMAN	4
7.95	7.95	36.6	sp|P62917|RL8_HUMAN	60S ribosomal protein L8 OS=Homo sapiens GN=RPL8 PE=1 SV=2	HUMAN	4
7.9	7.9	5.2	sp|Q5JWF2|GNAS1_HUMAN	Guanine nucleotide-binding protein G(s) subunit alpha isoforms XLas OS=Homo sapiens GN=GNAS PE=1 SV=2	HUMAN	4
7.85	7.85	12.9	sp|P04040|CATA_HUMAN	Catalase OS=Homo sapiens GN=CAT PE=1 SV=3	HUMAN	4
7.81	7.81	31.8	sp|Q14847|LASP1_HUMAN	LIM and SH3 domain protein 1 OS=Homo sapiens GN=LASP1 PE=1 SV=2	HUMAN	4
7.73	7.73	13.5	sp|P22307|NLTP_HUMAN	Non-specific lipid-transfer protein OS=Homo sapiens GN=SCP2 PE=1 SV=2	HUMAN	4
7.67	7.67	20.7	sp|P49821|NDUV1_HUMAN	NADH dehydrogenase [ubiquinone] flavoprotein 1, mitochondrial OS=Homo sapiens GN=NDUFV1 PE=1 SV=4	HUMAN	4
7.59	7.59	32.2	sp|P30533|AMRP_HUMAN	Alpha-2-macroglobulin receptor-associated protein OS=Homo sapiens GN=LRPAP1 PE=1 SV=1	HUMAN	4
7.58	7.58	45.9	sp|P46781|RS9_HUMAN	40S ribosomal protein S9 OS=Homo sapiens GN=RPS9 PE=1 SV=3	HUMAN	4
7.56	7.56	35.3	sp|P61224|RAP1B_HUMAN	Ras-related protein Rap-1b OS=Homo sapiens GN=RAP1B PE=1 SV=1	HUMAN	4
7.52	7.52	18.6	sp|P42765|THIM_HUMAN	3-ketoacyl-CoA thiolase, mitochondrial OS=Homo sapiens GN=ACAA2 PE=1 SV=2	HUMAN	4
7.37	7.37	37.9	sp|P18124|RL7_HUMAN	60S ribosomal protein L7 OS=Homo sapiens GN=RPL7 PE=1 SV=1	HUMAN	4
7.3	7.3	28.4	sp|Q01995|TAGL_HUMAN	Transgelin OS=Homo sapiens GN=TAGLN PE=1 SV=4	HUMAN	4
7.28	7.28	21.2	sp|P61586|RHOA_HUMAN	Transforming protein RhoA OS=Homo sapiens GN=RHOA PE=1 SV=1	HUMAN	4
7.26	7.26	23.3	sp|Q16836|HCDH_HUMAN	Hydroxyacyl-coenzyme A dehydrogenase, mitochondrial OS=Homo sapiens GN=HADH PE=1 SV=3	HUMAN	4
7.25	7.26	56.7	sp|P06703|S10A6_HUMAN	Protein S100-A6 OS=Homo sapiens GN=S100A6 PE=1 SV=1	HUMAN	4
7.14	7.21	9.4	sp|P46940|IQGA1_HUMAN	Ras GTPase-activating-like protein IQGAP1 OS=Homo sapiens GN=IQGAP1 PE=1 SV=1	HUMAN	4
7.05	7.05	20	sp|O15460|P4HA2_HUMAN	Prolyl 4-hydroxylase subunit alpha-2 OS=Homo sapiens GN=P4HA2 PE=1 SV=1	HUMAN	4
6.87	6.92	7.1	sp|Q9NYU2|UGGG1_HUMAN	UDP-glucose:glycoprotein glucosyltransferase 1 OS=Homo sapiens GN=UGGT1 PE=1 SV=3	HUMAN	4
6.78	6.78	27.1	sp|O75915|PRAF3_HUMAN	PRA1 family protein 3 OS=Homo sapiens GN=ARL6IP5 PE=1 SV=1	HUMAN	4
6.64	6.95	6.9	sp|P07942|LAMB1_HUMAN	Laminin subunit beta-1 OS=Homo sapiens GN=LAMB1 PE=1 SV=2	HUMAN	4
6.64	6.64	34.3	sp|P31949|S10AB_HUMAN	Protein S100-A11 OS=Homo sapiens GN=S100A11 PE=1 SV=2	HUMAN	4
6.61	6.61	26.9	sp|P45880|VDAC2_HUMAN	Voltage-dependent anion-selective channel protein 2 OS=Homo sapiens GN=VDAC2 PE=1 SV=2	HUMAN	4
6.59	6.59	50.7	sp|P09669|COX6C_HUMAN	Cytochrome c oxidase subunit 6C OS=Homo sapiens GN=COX6C PE=1 SV=2	HUMAN	4
6.52	6.52	26.6	sp|Q07021|C1QBP_HUMAN	Complement component 1 Q subcomponent-binding protein, mitochondrial OS=Homo sapiens GN=C1QBP PE=1	HUMAN	4
6.47	6.47	66.3	sp|P63220|RS21_HUMAN	40S ribosomal protein S21 OS=Homo sapiens GN=RPS21 PE=1 SV=1	HUMAN	4
6.44	6.44	20.6	sp|O15173|PGRC2_HUMAN	Membrane-associated progesterone receptor component 2 OS=Homo sapiens GN=PGRMC2 PE=1 SV=1	HUMAN	4
6.26	6.26	23.5	sp|P23396|RS3_HUMAN	40S ribosomal protein S3 OS=Homo sapiens GN=RPS3 PE=1 SV=2	HUMAN	4
6.08	6.08	22.9	sp|P31937|3HIDH_HUMAN	3-hydroxyisobutyrate dehydrogenase, mitochondrial OS=Homo sapiens GN=HIBADH PE=1 SV=2	HUMAN	4
6	6.09	43.7	sp|P0CW22|RS17L_HUMAN	40S ribosomal protein S17-like OS=Homo sapiens GN=RPS17L PE=3 SV=1	HUMAN	4
5.79	5.81	17.9	sp|P48735|IDHP_HUMAN	Isocitrate dehydrogenase [NADP], mitochondrial OS=Homo sapiens GN=IDH2 PE=1 SV=2	HUMAN	4
5.77	5.77	39.4	sp|O75489|NDUS3_HUMAN	NADH dehydrogenase [ubiquinone] iron-sulfur protein 3, mitochondrial OS=Homo sapiens GN=NDUFS3 PE=1 SV	HUMAN	4
5.74	5.77	42.9	sp|P30049|ATPD_HUMAN	ATP synthase subunit delta, mitochondrial OS=Homo sapiens GN=ATP5D PE=1 SV=2	HUMAN	4
5.72	5.72	28	sp|P51149|RAB7A_HUMAN	Ras-related protein Rab-7a OS=Homo sapiens GN=RAB7A PE=1 SV=1	HUMAN	4
5.7	5.7	12.7	sp|O94925|GLSK_HUMAN	Glutaminase kidney isoform, mitochondrial OS=Homo sapiens GN=GLS PE=1 SV=1	HUMAN	4
5.67	5.67	37.6	sp|P26447|S10A4_HUMAN	Protein S100-A4 OS=Homo sapiens GN=S100A4 PE=1 SV=1	HUMAN	4

Unused	Total	% Cov	Accession #	Name	Species	Peptides(95%)
5.54	5.54	37.2	sp|P50914|RL14_HUMAN	60S ribosomal protein L14 OS=Homo sapiens GN=RPL14 PE=1 SV=4	HUMAN	4
5.19	5.19	8.9	sp|P15586|GNS_HUMAN	N-acetylglucosamine-6-sulfatase OS=Homo sapiens GN=GNS PE=1 SV=3	HUMAN	4
4.98	4.98	39.2	sp|P46776|RL27A_HUMAN	60S ribosomal protein L27a OS=Homo sapiens GN=RPL27A PE=1 SV=2	HUMAN	4
4.97	4.97	57.6	sp|P62861|RS30_HUMAN	40S ribosomal protein S30 OS=Homo sapiens GN=FAU PE=1 SV=1	HUMAN	4
4.9	4.9	62.3	sp|P56385|ATP5I_HUMAN	ATP synthase subunit e, mitochondrial OS=Homo sapiens GN=ATP5I PE=1 SV=2	HUMAN	4
4.65	4.65	76.8	sp|P62273|RS29_HUMAN	40S ribosomal protein S29 OS=Homo sapiens GN=RPS29 PE=1 SV=2	HUMAN	4
4.16	4.16	32.3	sp|P62280|RS11_HUMAN	40S ribosomal protein S11 OS=Homo sapiens GN=RPS11 PE=1 SV=3	HUMAN	4
4.14	4.14	14.9	sp|P39656|OST48_HUMAN	Dolichyl-diphosphooligosaccharide--protein glycosyltransferase 48 kDa subunit OS=Homo sapiens GN=DDOST PE	HUMAN	4
4.04	4.04	8.7	sp|Q5JRX3|PREP_HUMAN	Presequence protease, mitochondrial OS=Homo sapiens GN=PITRM1 PE=1 SV=2	HUMAN	4
4	4	6.3	sp|P06756|ITAV_HUMAN	Integrin alpha-V OS=Homo sapiens GN=ITGAV PE=1 SV=2	HUMAN	4
4	4.86	17.7	sp|Q13162|PRDX4_HUMAN	Peroxiredoxin-4 OS=Homo sapiens GN=PRDX4 PE=1 SV=1	HUMAN	4
4	6	20.7	sp|Q29940|1B59_HUMAN	HLA class I histocompatibility antigen, B-59 alpha chain OS=Homo sapiens GN=HLA-B PE=2 SV=1	HUMAN	4
3.68	6.61	27.5	sp|P61981|1433G_HUMAN	14-3-3 protein gamma OS=Homo sapiens GN=YWHAG PE=1 SV=2	HUMAN	4
3.53	3.53	13.9	sp|P21397|AOFA_HUMAN	Amine oxidase [flavin-containing] A OS=Homo sapiens GN=MAOA PE=1 SV=1	HUMAN	4
3.43	4.71	81.8	sp|A8MW06|TMSL3_HUMAN	Thymosin beta-4-like protein 3 OS=Homo sapiens GN=TMSL3 PE=2 SV=1	HUMAN	4
3.35	3.39	12.3	sp|Q96I99|SUCB2_HUMAN	Succinyl-CoA ligase [GDP-forming] subunit beta, mitochondrial OS=Homo sapiens GN=SUCLG2 PE=1 SV=2	HUMAN	4
4.14	4.14	18.9	sp|P26022|PTX3_HUMAN	Pentraxin-related protein PTX3 OS=Homo sapiens GN=PTX3 PE=1 SV=3	HUMAN	4
3.93	3.93	24.3	sp|O00571|DDX3X_HUMAN	ATP-dependent RNA helicase DDX3X OS=Homo sapiens GN=DDX3X PE=1 SV=3	HUMAN	4
3.77	3.77	13.3	sp|Q15907|RB11B_HUMAN	Ras-related protein Rab-11B OS=Homo sapiens GN=RAB11B PE=1 SV=4	HUMAN	4
3.47	3.47	9.6	sp|Q8WWI1|LMO7_HUMAN	LIM domain only protein 7 OS=Homo sapiens GN=LMO7 PE=1 SV=3	HUMAN	4
3.16	3.16	32.8	sp|Q29960|1C16_HUMAN	HLA class I histocompatibility antigen, Cw-16 alpha chain OS=Homo sapiens GN=HLA-C PE=2 SV=1	HUMAN	4
2.83	2.83	14.7	sp|P24534|EF1B_HUMAN	Elongation factor 1-beta OS=Homo sapiens GN=EEF1B2 PE=1 SV=3	HUMAN	4
2.81	2.81	21.7	sp|P11940|PABP1_HUMAN	Polyadenylate-binding protein 1 OS=Homo sapiens GN=PABPC1 PE=1 SV=2	HUMAN	4
2.09	2.09	9.8	sp|Q53TN4|CYBR1_HUMAN	Cytochrome b reductase 1 OS=Homo sapiens GN=CYBRD1 PE=1 SV=1	HUMAN	4
2.03	2.03	19.5	sp|P16949|STMN1_HUMAN	Stathmin OS=Homo sapiens GN=STMN1 PE=1 SV=3	HUMAN	4
2.03	2.03	11.4	sp|Q07157|ZO1_HUMAN	Tight junction protein ZO-1 OS=Homo sapiens GN=TJP1 PE=1 SV=3	HUMAN	4
1.29	1.29	6.8	sp|Q9NR12|PDLI7_HUMAN	PDZ and LIM domain protein 7 OS=Homo sapiens GN=PDLIM7 PE=1 SV=1	HUMAN	4
0.74	2.4	34.3	sp|P16104|H2AX_HUMAN	Histone H2A.x OS=Homo sapiens GN=H2AFX PE=1 SV=2	HUMAN	4
7.89	7.89	30.3	sp|P62841|RS15_HUMAN	40S ribosomal protein S15 OS=Homo sapiens GN=RPS15 PE=1 SV=2	HUMAN	3
6.84	6.84	38.6	sp|P62753|RS6_HUMAN	40S ribosomal protein S6 OS=Homo sapiens GN=RPS6 PE=1 SV=1	HUMAN	3
6.77	6.77	7.7	sp|P11047|LAMC1_HUMAN	Laminin subunit gamma-1 OS=Homo sapiens GN=LAMC1 PE=1 SV=3	HUMAN	3
6.74	6.74	19.7	sp|P00558|PGK1_HUMAN	Phosphoglycerate kinase 1 OS=Homo sapiens GN=PGK1 PE=1 SV=3	HUMAN	3
6.74	6.74	33.9	sp|P63104|1433Z_HUMAN	14-3-3 protein zeta/delta OS=Homo sapiens GN=YWHAZ PE=1 SV=1	HUMAN	3
6.67	6.72	24.6	sp|P43235|CATK_HUMAN	Cathepsin K OS=Homo sapiens GN=CTSK PE=1 SV=1	HUMAN	3
6.53	6.53	28.9	sp|Q9BVK6|TMED9_HUMAN	Transmembrane emp24 domain-containing protein 9 OS=Homo sapiens GN=TMED9 PE=1 SV=2	HUMAN	3
6.33	6.33	12.6	sp|P05091|ALDH2_HUMAN	Aldehyde dehydrogenase, mitochondrial OS=Homo sapiens GN=ALDH2 PE=1 SV=2	HUMAN	3
6.32	6.32	47.7	sp|Q99878|H2A1J_HUMAN	Histone H2A type 1-J OS=Homo sapiens GN=HIST1H2AJ PE=1 SV=3	HUMAN	3
6.04	6.04	14.7	sp|P53597|SUCA_HUMAN	Succinyl-CoA ligase [ADP/GDP-forming] subunit alpha, mitochondrial OS=Homo sapiens GN=SUCLG1 PE=1 SV=4	HUMAN	3
6.04	6.08	14.7	sp|Q9Y6M1|IF2B2_HUMAN	Insulin-like growth factor 2 mRNA-binding protein 2 OS=Homo sapiens GN=IGF2BP2 PE=1 SV=2	HUMAN	3
6.03	6.03	39.1	sp|P04216|THY1_HUMAN	Thy-1 membrane glycoprotein OS=Homo sapiens GN=THY1 PE=1 SV=2	HUMAN	3
6.03	6.03	43.4	sp|P62269|RS18_HUMAN	40S ribosomal protein S18 OS=Homo sapiens GN=RPS18 PE=1 SV=3	HUMAN	3
6	6	6.6	sp|O00754|MA2B1_HUMAN	Lysosomal alpha-mannosidase OS=Homo sapiens GN=MAN2B1 PE=1 SV=3	HUMAN	3
6	6	10.2	sp|O60568|PLOD3_HUMAN	Procollagen-lysine,2-oxoglutarate 5-dioxygenase 3 OS=Homo sapiens GN=PLOD3 PE=1 SV=1	HUMAN	3
6	6.06	8.4	sp|P28331|NDUS1_HUMAN	NADH-ubiquinone oxidoreductase 75 kDa subunit, mitochondrial OS=Homo sapiens GN=NDUFS1 PE=1 SV=3	HUMAN	3
6	6	9.7	sp|P36776|LONM_HUMAN	Lon protease homolog, mitochondrial OS=Homo sapiens GN=LONP1 PE=1 SV=2	HUMAN	3
6	6	18.5	sp|P52907|CAZA1_HUMAN	F-actin-capping protein subunit alpha-1 OS=Homo sapiens GN=CAPZA1 PE=1 SV=3	HUMAN	3
6	6.04	20.5	sp|P61978|HNRPK_HUMAN	Heterogeneous nuclear ribonucleoprotein K OS=Homo sapiens GN=HNRNPK PE=1 SV=1	HUMAN	3
6	6.03	26.5	sp|Q14257|RCN2_HUMAN	Reticulocalbin-2 OS=Homo sapiens GN=RCN2 PE=1 SV=1	HUMAN	3
6	6.05	15.1	sp|Q86UE4|LYRIC_HUMAN	Protein LYRIC OS=Homo sapiens GN=MTDH PE=1 SV=2	HUMAN	3
6	6	24.9	sp|Q9HAV7|GRPE1_HUMAN	GrpE protein homolog 1, mitochondrial OS=Homo sapiens GN=GRPEL1 PE=1 SV=2	HUMAN	3
5.9	5.9	18.6	sp|P80303|NUCB2_HUMAN	Nucleobindin-2 OS=Homo sapiens GN=NUCB2 PE=1 SV=2	HUMAN	3
5.88	5.88	34.3	sp|P48047|ATPO_HUMAN	ATP synthase subunit O, mitochondrial OS=Homo sapiens GN=ATP5O PE=1 SV=1	HUMAN	3
5.81	5.83	27.6	sp|P99999|CYC_HUMAN	Cytochrome c OS=Homo sapiens GN=CYCS PE=1 SV=2	HUMAN	3
5.76	5.76	29.1	sp|Q9NX63|CHCH3_HUMAN	Coiled-coil-helix-coiled-coil-helix domain-containing protein 3, mitochondrial OS=Homo sapiens GN=CHCHD3 PE	HUMAN	3
5.72	5.78	16.1	sp|P60174|TPIS_HUMAN	Triosephosphate isomerase OS=Homo sapiens GN=TPI1 PE=1 SV=3	HUMAN	3
5.72	5.76	9.8	sp|Q13557|KCC2D_HUMAN	Calcium/calmodulin-dependent protein kinase type II subunit delta OS=Homo sapiens GN=CAMK2D PE=1 SV=3	HUMAN	3
5.6	5.71	16.6	sp|Q9UHD8|SEPT9_HUMAN	Septin-9 OS=Homo sapiens GN=SEPT9 PE=1 SV=2	HUMAN	3
5.55	5.55	28.6	sp|Q9Y2B0|CNPY2_HUMAN	Protein canopy homolog 2 OS=Homo sapiens GN=CNPY2 PE=1 SV=1	HUMAN	3
5.46	5.46	20.9	sp|P55145|MANF_HUMAN	Mesencephalic astrocyte-derived neurotrophic factor OS=Homo sapiens GN=MANF PE=1 SV=3	HUMAN	3
5.4	5.4	6.3	sp|Q9BSJ8|ESYT1_HUMAN	Extended synaptotagmin-1 OS=Homo sapiens GN=ESYT1 PE=1 SV=1	HUMAN	3
5.36	5.36	34.8	sp|Q9H0U4|RAB1B_HUMAN	Ras-related protein Rab-1B OS=Homo sapiens GN=RAB1B PE=1 SV=1	HUMAN	3
5.34	5.34	8.6	sp|Q13283|G3BP1_HUMAN	Ras GTPase-activating protein-binding protein 1 OS=Homo sapiens GN=G3BP1 PE=1 SV=1	HUMAN	3
5.21	5.21	20.2	sp|P05388|RLA0_HUMAN	60S acidic ribosomal protein P0 OS=Homo sapiens GN=RPLP0 PE=1 SV=1	HUMAN	3
5.15	5.15	10.9	sp|P07602|SAP_HUMAN	Proactivator polypeptide OS=Homo sapiens GN=PSAP PE=1 SV=2	HUMAN	3
5.15	5.15	23.8	sp|P62266|RS23_HUMAN	40S ribosomal protein S23 OS=Homo sapiens GN=RPS23 PE=1 SV=3	HUMAN	3
5.09	5.09	24.3	sp|P30044|PRDX5_HUMAN	Peroxiredoxin-5, mitochondrial OS=Homo sapiens GN=PRDX5 PE=1 SV=4	HUMAN	3
5.08	5.09	8.1	sp|O60716|CTND1_HUMAN	Catenin delta-1 OS=Homo sapiens GN=CTNND1 PE=1 SV=1	HUMAN	3
5.06	5.06	17.7	sp|Q70UQ0|IKIP_HUMAN	Inhibitor of nuclear factor kappa-B kinase-interacting protein OS=Homo sapiens GN=IKBIP PE=1 SV=1	HUMAN	3
5.05	5.05	11.2	sp|Q13724|MOGS_HUMAN	Mannosyl-oligosaccharide glucosidase OS=Homo sapiens GN=MOGS PE=1 SV=5	HUMAN	3
4.99	4.99	12.2	sp|O43491|E41L2_HUMAN	Band 4.1-like protein 2 OS=Homo sapiens GN=EPB41L2 PE=1 SV=1	HUMAN	3
4.89	4.89	11	sp|P06396|GELS_HUMAN	Gelsolin OS=Homo sapiens GN=GSN PE=1 SV=1	HUMAN	3
4.85	4.85	33.8	sp|P69905|HBA_HUMAN	Hemoglobin subunit alpha OS=Homo sapiens GN=HBA1 PE=1 SV=2	HUMAN	3
4.8	4.8	41.4	sp|P35268|RL22_HUMAN	60S ribosomal protein L22 OS=Homo sapiens GN=RPL22 PE=1 SV=2	HUMAN	3
4.73	4.73	19.3	sp|P00338|LDHA_HUMAN	L-lactate dehydrogenase A chain OS=Homo sapiens GN=LDHA PE=1 SV=2	HUMAN	3
4.6	4.6	17.6	sp|Q99714|HCD2_HUMAN	3-hydroxyacyl-CoA dehydrogenase type-2 OS=Homo sapiens GN=HSD17B10 PE=1 SV=3	HUMAN	3
4.42	4.42	6.6	sp|Q5JPE7|NOMO2_HUMAN	Nodal modulator 2 OS=Homo sapiens GN=NOMO2 PE=1 SV=1	HUMAN	3
4.41	4.41	12.1	sp|Q99798|ACON_HUMAN	Aconitate hydratase, mitochondrial OS=Homo sapiens GN=ACO2 PE=1 SV=2	HUMAN	3
4.36	4.42	35.7	sp|P84098|RL19_HUMAN	60S ribosomal protein L19 OS=Homo sapiens GN=RPL19 PE=1 SV=1	HUMAN	3
4.26	4.31	12.1	sp|Q14956|GPNMB_HUMAN	Transmembrane glycoprotein NMB OS=Homo sapiens GN=GPNMB PE=1 SV=2	HUMAN	3
4.22	4.22	6.9	sp|Q02218|ODO1_HUMAN	2-oxoglutarate dehydrogenase, mitochondrial OS=Homo sapiens GN=OGDH PE=1 SV=3	HUMAN	3
4.17	4.17	10.3	sp|P54886|P5CS_HUMAN	Delta-1-pyrroline-5-carboxylate synthase OS=Homo sapiens GN=ALDH18A1 PE=1 SV=2	HUMAN	3
4.12	4.12	64.4	sp|P05204|HMGN2_HUMAN	Non-histone chromosomal protein HMG-17 OS=Homo sapiens GN=HMGN2 PE=1 SV=3	HUMAN	3
4.08	4.08	26.5	sp|P49755|TMEDA_HUMAN	Transmembrane emp24 domain-containing protein 10 OS=Homo sapiens GN=TMED10 PE=1 SV=2	HUMAN	3
4.07	4.07	23.2	sp|P14209|CD99_HUMAN	CD99 antigen OS=Homo sapiens GN=CD99 PE=1 SV=1	HUMAN	3
4	4	20.9	sp|P14174|MIF_HUMAN	Macrophage migration inhibitory factor OS=Homo sapiens GN=MIF PE=1 SV=4	HUMAN	3
4	6	11.5	sp|P47755|CAZA2_HUMAN	F-actin-capping protein subunit alpha-2 OS=Homo sapiens GN=CAPZA2 PE=1 SV=3	HUMAN	3
4	4	19.6	sp|P52565|GDIR1_HUMAN	Rho GDP-dissociation inhibitor 1 OS=Homo sapiens GN=ARHGDIA PE=1 SV=3	HUMAN	3

Unused	Total	% Cov	Accession #	Name	Species	Peptides(95%)
4	4	9.9	sp|Q02809|PLOD1_HUMAN	Procollagen-lysine,2-oxoglutarate 5-dioxygenase 1 OS=Homo sapiens GN=PLOD1 PE=1 SV=2	HUMAN	3
3.89	3.9	50.4	sp|P10606|COX5B_HUMAN	Cytochrome c oxidase subunit 5B, mitochondrial OS=Homo sapiens GN=COX5B PE=1 SV=2	HUMAN	3
3.33	6.09	17.3	sp|P62258|1433E_HUMAN	14-3-3 protein epsilon OS=Homo sapiens GN=YWHAE PE=1 SV=1	HUMAN	3
3.2	4.21	17.2	sp|P04899|GNAI2_HUMAN	Guanine nucleotide-binding protein G(i) subunit alpha-2 OS=Homo sapiens GN=GNAI2 PE=1 SV=3	HUMAN	3
3.19	3.19	12	sp|P47985|UCRI_HUMAN	Cytochrome b-c1 complex subunit Rieske, mitochondrial OS=Homo sapiens GN=UQCRFS1 PE=1 SV=2	HUMAN	3
3.16	4.74	12.8	sp|Q16181|SEPT7_HUMAN	Septin-7 OS=Homo sapiens GN=SEPT7 PE=1 SV=2	HUMAN	3
3.12	3.12	19.8	sp|Q9BVC6|TM109_HUMAN	Transmembrane protein 109 OS=Homo sapiens GN=TMEM109 PE=1 SV=1	HUMAN	3
2.08	2.14	16.7	sp|P54819|KAD2_HUMAN	Adenylate kinase 2, mitochondrial OS=Homo sapiens GN=AK2 PE=1 SV=2	HUMAN	3
2.05	2.08	13	sp|Q9UNL2|SSRG_HUMAN	Translocon-associated protein subunit gamma OS=Homo sapiens GN=SSR3 PE=1 SV=1	HUMAN	3
2	4.35	12.6	sp|P16989|DBPA_HUMAN	DNA-binding protein A OS=Homo sapiens GN=CSDA PE=1 SV=4	HUMAN	3
2	5.71	25.6	sp|P31946|1433B_HUMAN	14-3-3 protein beta/alpha OS=Homo sapiens GN=YWHAB PE=1 SV=3	HUMAN	3
1.41	2.39	20.5	sp|P61106|RAB14_HUMAN	Ras-related protein Rab-14 OS=Homo sapiens GN=RAB14 PE=1 SV=4	HUMAN	3
0.11	4.12	37.1	sp|P62820|RAB1A_HUMAN	Ras-related protein Rab-1A OS=Homo sapiens GN=RAB1A PE=1 SV=3	HUMAN	3
2.75	2.75	19.8	sp|P23246|SFPQ_HUMAN	Splicing factor, proline- and glutamine-rich OS=Homo sapiens GN=SFPQ PE=1 SV=2	HUMAN	3
2.61	3.08	16.2	sp|P07195|LDHB_HUMAN	L-lactate dehydrogenase B chain OS=Homo sapiens GN=LDHB PE=1 SV=2	HUMAN	3
2.35	2.35	14	sp|P02786|TFR1_HUMAN	Transferrin receptor protein 1 OS=Homo sapiens GN=TFRC PE=1 SV=2	HUMAN	3
2.27	2.27	17.4	sp|Q15233|NONO_HUMAN	Non-POU domain-containing octamer-binding protein OS=Homo sapiens GN=NONO PE=1 SV=4	HUMAN	3
2.15	2.15	20.1	sp|P18669|PGAM1_HUMAN	Phosphoglycerate mutase 1 OS=Homo sapiens GN=PGAM1 PE=1 SV=2	HUMAN	3
2.11	2.11	11.2	sp|P09486|SPRC_HUMAN	SPARC OS=Homo sapiens GN=SPARC PE=1 SV=1	HUMAN	3
2.06	2.06	11.8	sp|P22314|UBA1_HUMAN	Ubiquitin-like modifier-activating enzyme 1 OS=Homo sapiens GN=UBA1 PE=1 SV=3	HUMAN	3
2.03	2.03	16.5	sp|Q9UBR2|CATZ_HUMAN	Cathepsin Z OS=Homo sapiens GN=CTSZ PE=1 SV=1	HUMAN	3
2.02	2.02	9.8	sp|P11586|C1TC_HUMAN	C-1-tetrahydrofolate synthase, cytoplasmic OS=Homo sapiens GN=MTHFD1 PE=1 SV=3	HUMAN	3
2.02	2.02	4.2	sp|P61619|S61A1_HUMAN	Protein transport protein Sec61 subunit alpha isoform 1 OS=Homo sapiens GN=SEC61A1 PE=1 SV=2	HUMAN	3
2	2	11.2	sp|O14684|PTGES_HUMAN	Prostaglandin E synthase OS=Homo sapiens GN=PTGES PE=1 SV=2	HUMAN	3
2	2	7.9	sp|O43175|SERA_HUMAN	D-3-phosphoglycerate dehydrogenase OS=Homo sapiens GN=PHGDH PE=1 SV=4	HUMAN	3
2	2	14.9	sp|P01037|CYTN_HUMAN	Cystatin-SN OS=Homo sapiens GN=CST1 PE=1 SV=3	HUMAN	3
2	2	8.1	sp|P13796|PLSL_HUMAN	Plastin-2 OS=Homo sapiens GN=LCP1 PE=1 SV=6	HUMAN	3
2	2	10.2	sp|P55769|NH2L1_HUMAN	NHP2-like protein 1 OS=Homo sapiens GN=NHP2L1 PE=1 SV=3	HUMAN	3
2	2	12.9	sp|P78417|GSTO1_HUMAN	Glutathione S-transferase omega-1 OS=Homo sapiens GN=GSTO1 PE=1 SV=2	HUMAN	3
2	2.01	6.9	sp|Q13045|FLII_HUMAN	Protein flightless-1 homolog OS=Homo sapiens GN=FLII PE=1 SV=2	HUMAN	3
2	2	8.6	sp|Q15717|ELAV1_HUMAN	ELAV-like protein 1 OS=Homo sapiens GN=ELAVL1 PE=1 SV=2	HUMAN	3
2	2	23.5	sp|Q5JXB2|UE2NL_HUMAN	Putative ubiquitin-conjugating enzyme E2 N-like OS=Homo sapiens GN=UBE2NL PE=1 SV=1	HUMAN	3
2	2	15.9	sp|Q92841|DDX17_HUMAN	Probable ATP-dependent RNA helicase DDX17 OS=Homo sapiens GN=DDX17 PE=1 SV=2	HUMAN	3
2	2	4.7	sp|Q969M3|YIPF5_HUMAN	Protein YIPF5 OS=Homo sapiens GN=YIPF5 PE=1 SV=1	HUMAN	3
2	2	3.7	sp|Q96EP5|DAZP1_HUMAN	DAZ-associated protein 1 OS=Homo sapiens GN=DAZAP1 PE=1 SV=1	HUMAN	3
2	2.27	7.7	sp|Q9Y3I0|RTCB_HUMAN	tRNA-splicing ligase RtcB homolog OS=Homo sapiens GN=C22orf28 PE=1 SV=1	HUMAN	3
1.94	1.94	8.9	sp|P11166|GTR1_HUMAN	Solute carrier family 2, facilitated glucose transporter member 1 OS=Homo sapiens GN=SLC2A1 PE=1 SV=2	HUMAN	3
1.92	1.92	23.6	sp|Q9UBI6|GBG12_HUMAN	Guanine nucleotide-binding protein G(I)/G(S)/G(O) subunit gamma-12 OS=Homo sapiens GN=GNG12 PE=1 SV=3	HUMAN	3
1.89	1.89	7.4	sp|P00533|EGFR_HUMAN	Epidermal growth factor receptor OS=Homo sapiens GN=EGFR PE=1 SV=2	HUMAN	3
1.82	1.82	4.2	sp|O96008|TOM40_HUMAN	Mitochondrial import receptor subunit TOM40 homolog OS=Homo sapiens GN=TOMM40 PE=1 SV=1	HUMAN	3
1.82	1.82	5.8	sp|P34932|HSP74_HUMAN	Heat shock 70 kDa protein 4 OS=Homo sapiens GN=HSPA4 PE=1 SV=4	HUMAN	3
1.82	1.82	8.9	sp|Q16563|SYPL1_HUMAN	Synaptophysin-like protein 1 OS=Homo sapiens GN=SYPL1 PE=1 SV=1	HUMAN	3
1.77	1.77	16.9	sp|A6NIZ1|RP1BL_HUMAN	Ras-related protein Rap-1b-like protein OS=Homo sapiens PE=2 SV=1	HUMAN	3
1.77	1.77	6	sp|P27487|DPP4_HUMAN	Dipeptidyl peptidase 4 OS=Homo sapiens GN=DPP4 PE=1 SV=2	HUMAN	3
1.77	1.77	11.7	sp|Q13561|DCTN2_HUMAN	Dynactin subunit 2 OS=Homo sapiens GN=DCTN2 PE=1 SV=4	HUMAN	3
1.76	1.77	35	sp|O60361|NDK8_HUMAN	Putative nucleoside diphosphate kinase OS=Homo sapiens GN=NME2P1 PE=5 SV=1	HUMAN	3
1.72	1.73	9.8	sp|Q16543|CDC37_HUMAN	Hsp90 co-chaperone Cdc37 OS=Homo sapiens GN=CDC37 PE=1 SV=1	HUMAN	3
1.59	1.59	9.4	sp|P27695|APEX1_HUMAN	DNA-(apurinic or apyrimidinic site) lyase OS=Homo sapiens GN=APEX1 PE=1 SV=2	HUMAN	3
1.51	1.51	7.8	sp|O95168|NDUB4_HUMAN	NADH dehydrogenase [ubiquinone] 1 beta subcomplex subunit 4 OS=Homo sapiens GN=NDUFB4 PE=1 SV=3	HUMAN	3
1.51	1.51	19.2	sp|P19623|SPEE_HUMAN	Spermidine synthase OS=Homo sapiens GN=SRM PE=1 SV=1	HUMAN	3
1.51	1.51	11.7	sp|P61009|SPCS3_HUMAN	Signal peptidase complex subunit 3 OS=Homo sapiens GN=SPCS3 PE=1 SV=1	HUMAN	3
1.49	1.49	28.2	sp|P62979|RS27A_HUMAN	Ubiquitin-40S ribosomal protein S27a OS=Homo sapiens GN=RPS27A PE=1 SV=2	HUMAN	3
1.48	1.54	12.2	sp|Q9ULC3|RAB23_HUMAN	Ras-related protein Rab-23 OS=Homo sapiens GN=RAB23 PE=1 SV=1	HUMAN	3
1.46	1.46	9.3	sp|Q7L576|CYFP1_HUMAN	Cytoplasmic FMR1-interacting protein 1 OS=Homo sapiens GN=CYFIP1 PE=1 SV=1	HUMAN	3
1.44	2.07	6.8	sp|P20020|AT2B1_HUMAN	Plasma membrane calcium-transporting ATPase 1 OS=Homo sapiens GN=ATP2B1 PE=1 SV=3	HUMAN	3
1.42	1.43	38.1	sp|Q86V81|THOC4_HUMAN	THO complex subunit 4 OS=Homo sapiens GN=ALYREF PE=1 SV=3	HUMAN	3
1.41	1.41	10.9	sp|P26599|PTBP1_HUMAN	Polypyrimidine tract-binding protein 1 OS=Homo sapiens GN=PTBP1 PE=1 SV=1	HUMAN	3
1.41	1.41	7.4	sp|Q969E2|SCAM4_HUMAN	Secretory carrier-associated membrane protein 4 OS=Homo sapiens GN=SCAMP4 PE=2 SV=1	HUMAN	3
1.4	1.41	3.5	sp|P11717|MPRI_HUMAN	Cation-independent mannose-6-phosphate receptor OS=Homo sapiens GN=IGF2R PE=1 SV=3	HUMAN	3
1.38	1.39	7.2	sp|P50281|MMP14_HUMAN	Matrix metalloproteinase-14 OS=Homo sapiens GN=MMP14 PE=1 SV=3	HUMAN	3
1.38	1.38	5.7	sp|P50416|CPT1A_HUMAN	Carnitine O-palmitoyltransferase 1, liver isoform OS=Homo sapiens GN=CPT1A PE=1 SV=2	HUMAN	3
1.33	1.33	13.2	sp|Q9Y678|COPG1_HUMAN	Coatomer subunit gamma-1 OS=Homo sapiens GN=COPG1 PE=1 SV=1	HUMAN	3
1.27	1.27	46.8	sp|Q07955|SRSF1_HUMAN	Serine/arginine-rich splicing factor 1 OS=Homo sapiens GN=SRSF1 PE=1 SV=2	HUMAN	3
1.23	1.23	16.6	sp|O43390|HNRPR_HUMAN	Heterogeneous nuclear ribonucleoprotein R OS=Homo sapiens GN=HNRNPR PE=1 SV=1	HUMAN	3
1.21	1.21	5.2	sp|Q9GZV4|IF5A2_HUMAN	Eukaryotic translation initiation factor 5A-2 OS=Homo sapiens GN=EIF5A2 PE=1 SV=3	HUMAN	3
1.2	1.21	12.5	sp|Q05193|DYN1_HUMAN	Dynamin-1 OS=Homo sapiens GN=DNM1 PE=1 SV=2	HUMAN	3
1.14	1.14	7.8	sp|Q99729|ROAA_HUMAN	Heterogeneous nuclear ribonucleoprotein A/B OS=Homo sapiens GN=HNRNPAB PE=1 SV=2	HUMAN	3
1.1	1.1	24.3	sp|P27105|STOM_HUMAN	Erythrocyte band 7 integral membrane protein OS=Homo sapiens GN=STOM PE=1 SV=3	HUMAN	3
1.1	1.1	18.6	sp|Q9Y230|RUVB2_HUMAN	RuvB-like 2 OS=Homo sapiens GN=RUVBL2 PE=1 SV=3	HUMAN	3
1.05	1.05	20.4	sp|Q13404|UB2V1_HUMAN	Ubiquitin-conjugating enzyme E2 variant 1 OS=Homo sapiens GN=UBE2V1 PE=1 SV=2	HUMAN	3
1.04	1.04	16.9	sp|O60831|PRAF2_HUMAN	PRA1 family protein 2 OS=Homo sapiens GN=PRAF2 PE=1 SV=1	HUMAN	3
1.01	1.01	16.7	sp|Q8TF09|DLRB2_HUMAN	Dynein light chain roadblock-type 2 OS=Homo sapiens GN=DYNLRB2 PE=1 SV=1	HUMAN	3
0.98	0.98	8	sp|P43243|MATR3_HUMAN	Matrin-3 OS=Homo sapiens GN=MATR3 PE=1 SV=2	HUMAN	3
0.96	0.96	14	sp|Q9NZU5|LMCD1_HUMAN	LIM and cysteine-rich domains protein 1 OS=Homo sapiens GN=LMCD1 PE=1 SV=1	HUMAN	3
0.95	1.78	9.5	sp|Q7Z794|K2C1B_HUMAN	Keratin, type II cytoskeletal 1b OS=Homo sapiens GN=KRT77 PE=1 SV=3	HUMAN	3
0.95	0.96	7.8	sp|Q8WWI5|CTL1_HUMAN	Choline transporter-like protein 1 OS=Homo sapiens GN=SLC44A1 PE=1 SV=1	HUMAN	3
0.94	0.95	7.1	sp|Q8TDI7|TMC2_HUMAN	Transmembrane channel-like protein 2 OS=Homo sapiens GN=TMC2 PE=2 SV=3	HUMAN	3
0.92	0.92	12.5	sp|Q07812|BAX_HUMAN	Apoptosis regulator BAX OS=Homo sapiens GN=BAX PE=1 SV=1	HUMAN	3
0.89	0.89	9	sp|O15427|MOT4_HUMAN	Monocarboxylate transporter 4 OS=Homo sapiens GN=SLC16A3 PE=1 SV=1	HUMAN	3
0.87	0.87	12	sp|Q9BWM7|SFXN3_HUMAN	Sideroflexin-3 OS=Homo sapiens GN=SFXN3 PE=2 SV=2	HUMAN	3
0.84	0.84	18.8	sp|P49207|RL34_HUMAN	60S ribosomal protein L34 OS=Homo sapiens GN=RPL34 PE=1 SV=3	HUMAN	3
0.82	0.82	1.9	sp|P16435|NCPR_HUMAN	NADPH--cytochrome P450 reductase OS=Homo sapiens GN=POR PE=1 SV=2	HUMAN	3
0.77	0.78	10.2	sp|P20908|CO5A1_HUMAN	Collagen alpha-1(V) chain OS=Homo sapiens GN=COL5A1 PE=1 SV=3	HUMAN	3
0.76	0.77	9.7	sp|P28482|MK01_HUMAN	Mitogen-activated protein kinase 1 OS=Homo sapiens GN=MAPK1 PE=1 SV=3	HUMAN	3
0.76	0.77	28.2	sp|Q15056|IF4H_HUMAN	Eukaryotic translation initiation factor 4H OS=Homo sapiens GN=EIF4H PE=1 SV=5	HUMAN	3
0.74	0.74	45.1	sp|P62891|RL39_HUMAN	60S ribosomal protein L39 OS=Homo sapiens GN=RPL39 PE=2 SV=2	HUMAN	3
0.7	0.91	3.8	sp|Q16850|CP51A_HUMAN	Lanosterol 14-alpha demethylase OS=Homo sapiens GN=CYP51A1 PE=1 SV=3	HUMAN	3

Unused	Total	% Cov	Accession #	Name	Species	Peptides(95%)
0.51	0.51	7.8	sp|Q01518|CAP1_HUMAN	Adenylyl cyclase-associated protein 1 OS=Homo sapiens GN=CAP1 PE=1 SV=5	HUMAN	3
0.45	2.95	34.6	sp|Q8IUE6|H2A2B_HUMAN	Histone H2A type 2-B OS=Homo sapiens GN=HIST2H2AB PE=1 SV=3	HUMAN	3
0.33	0.33	18.5	sp|P11234|RALB_HUMAN	Ras-related protein Ral-B OS=Homo sapiens GN=RALB PE=1 SV=1	HUMAN	3
0.22	0.22	17.2	sp|Q9BZ23|PANK2_HUMAN	Pantothenate kinase 2, mitochondrial OS=Homo sapiens GN=PANK2 PE=1 SV=3	HUMAN	3
0.16	0.31	6.3	sp|Q7Z4H8|KDEL2_HUMAN	KDEL motif-containing protein 2 OS=Homo sapiens GN=KDELC2 PE=1 SV=2	HUMAN	3
5.51	5.51	9.1	sp|P16615|AT2A2_HUMAN	Sarcoplasmic/endoplasmic reticulum calcium ATPase 2 OS=Homo sapiens GN=ATP2A2 PE=1 SV=1	HUMAN	2
5.15	5.15	75	sp|P63313|TYB10_HUMAN	Thymosin beta-10 OS=Homo sapiens GN=TMSB10 PE=1 SV=2	HUMAN	2
4.93	4.93	15.3	sp|Q9NZN4|EHD2_HUMAN	EH domain-containing protein 2 OS=Homo sapiens GN=EHD2 PE=1 SV=2	HUMAN	2
4.62	4.67	5.6	sp|O95782|AP2A1_HUMAN	AP-2 complex subunit alpha-1 OS=Homo sapiens GN=AP2A1 PE=1 SV=3	HUMAN	2
4.43	4.48	22.5	sp|P06748|NPM_HUMAN	Nucleophosmin OS=Homo sapiens GN=NPM1 PE=1 SV=2	HUMAN	2
4.37	4.37	29.6	sp|Q99497|PARK7_HUMAN	Protein DJ-1 OS=Homo sapiens GN=PARK7 PE=1 SV=2	HUMAN	2
4.36	4.36	15.4	sp|Q8NC51|PAIRB_HUMAN	Plasminogen activator inhibitor 1 RNA-binding protein OS=Homo sapiens GN=SERBP1 PE=1 SV=2	HUMAN	2
4.34	4.34	37.9	sp|P25398|RS12_HUMAN	40S ribosomal protein S12 OS=Homo sapiens GN=RPS12 PE=1 SV=3	HUMAN	2
4.32	4.32	15.2	sp|Q16698|DECR_HUMAN	2,4-dienoyl-CoA reductase, mitochondrial OS=Homo sapiens GN=DECR1 PE=1 SV=1	HUMAN	2
4.31	4.31	22.4	sp|P22626|ROA2_HUMAN	Heterogeneous nuclear ribonucleoproteins A2/B1 OS=Homo sapiens GN=HNRNPA2B1 PE=1 SV=2	HUMAN	2
4.27	4.27	15.1	sp|Q9Y639|NPTN_HUMAN	Neuroplastin OS=Homo sapiens GN=NPTN PE=1 SV=2	HUMAN	2
4.24	4.24	6.8	sp|Q13423|NNTM_HUMAN	NAD(P) transhydrogenase, mitochondrial OS=Homo sapiens GN=NNT PE=1 SV=3	HUMAN	2
4.24	4.24	17.5	sp|Q9BS26|ERP44_HUMAN	Endoplasmic reticulum resident protein 44 OS=Homo sapiens GN=ERP44 PE=1 SV=1	HUMAN	2
4.09	4.09	23.9	sp|P10620|MGST1_HUMAN	Microsomal glutathione S-transferase 1 OS=Homo sapiens GN=MGST1 PE=1 SV=1	HUMAN	2
4.08	4.08	25.9	sp|P15880|RS2_HUMAN	40S ribosomal protein S2 OS=Homo sapiens GN=RPS2 PE=1 SV=2	HUMAN	2
4.07	4.07	10.3	sp|P11279|LAMP1_HUMAN	Lysosome-associated membrane glycoprotein 1 OS=Homo sapiens GN=LAMP1 PE=1 SV=3	HUMAN	2
4.07	4.07	43.9	sp|P62244|RS15A_HUMAN	40S ribosomal protein S15a OS=Homo sapiens GN=RPS15A PE=1 SV=2	HUMAN	2
4.05	4.05	31.3	sp|O95816|BAG2_HUMAN	BAG family molecular chaperone regulator 2 OS=Homo sapiens GN=BAG2 PE=1 SV=1	HUMAN	2
4.04	4.04	31.9	sp|P51148|RAB5C_HUMAN	Ras-related protein Rab-5C OS=Homo sapiens GN=RAB5C PE=1 SV=2	HUMAN	2
4.04	4.04	21.1	sp|P62070|RRAS2_HUMAN	Ras-related protein R-Ras2 OS=Homo sapiens GN=RRAS2 PE=1 SV=1	HUMAN	2
4.03	4.03	13.8	sp|O43493|TGON2_HUMAN	Trans-Golgi network integral membrane protein 2 OS=Homo sapiens GN=TGOLN2 PE=1 SV=2	HUMAN	2
4.03	4.04	9.3	sp|P83111|LACTB_HUMAN	Serine beta-lactamase-like protein LACTB, mitochondrial OS=Homo sapiens GN=LACTB PE=1 SV=2	HUMAN	2
4.03	4.05	14.3	sp|Q9Y680|FKBP7_HUMAN	Peptidyl-prolyl cis-trans isomerase FKBP7 OS=Homo sapiens GN=FKBP7 PE=1 SV=1	HUMAN	2
4.02	4.02	29.4	sp|P62081|RS7_HUMAN	40S ribosomal protein S7 OS=Homo sapiens GN=RPS7 PE=1 SV=1	HUMAN	2
4.02	4.08	24.8	sp|Q9Y2Q3|GSTK1_HUMAN	Glutathione S-transferase kappa 1 OS=Homo sapiens GN=GSTK1 PE=1 SV=3	HUMAN	2
4	4	24.8	sp|O00560|SDCB1_HUMAN	Syntenin-1 OS=Homo sapiens GN=SDCBP PE=1 SV=1	HUMAN	2
4	4	7.3	sp|O75306|NDUS2_HUMAN	NADH dehydrogenase [ubiquinone] iron-sulfur protein 2, mitochondrial OS=Homo sapiens GN=NDUFS2 PE=1 SV	HUMAN	2
4	4	8.8	sp|P11310|ACADM_HUMAN	Medium-chain specific acyl-CoA dehydrogenase, mitochondrial OS=Homo sapiens GN=ACADM PE=1 SV=1	HUMAN	2
4	4	14.5	sp|P19338|NUCL_HUMAN	Nucleolin OS=Homo sapiens GN=NCL PE=1 SV=3	HUMAN	2
4	4	14.4	sp|P30086|PEBP1_HUMAN	Phosphatidylethanolamine-binding protein 1 OS=Homo sapiens GN=PEBP1 PE=1 SV=3	HUMAN	2
4	4.01	8.7	sp|P42785|PCP_HUMAN	Lysosomal Pro-X carboxypeptidase OS=Homo sapiens GN=PRCP PE=1 SV=1	HUMAN	2
4	4	7.7	sp|P50990|TCPQ_HUMAN	T-complex protein 1 subunit theta OS=Homo sapiens GN=CCT8 PE=1 SV=4	HUMAN	2
4	4	10.3	sp|P52272|HNRPM_HUMAN	Heterogeneous nuclear ribonucleoprotein M OS=Homo sapiens GN=HNRNPM PE=1 SV=3	HUMAN	2
4	4	35	sp|P82909|RT36_HUMAN	28S ribosomal protein S36, mitochondrial OS=Homo sapiens GN=MRPS36 PE=1 SV=2	HUMAN	2
4	4	7.4	sp|Q14699|RFTN1_HUMAN	Raftlin OS=Homo sapiens GN=RFTN1 PE=1 SV=4	HUMAN	2
4	4	20.7	sp|Q15819|UB2V2_HUMAN	Ubiquitin-conjugating enzyme E2 variant 2 OS=Homo sapiens GN=UBE2V2 PE=1 SV=4	HUMAN	2
4	4	26	sp|Q15836|VAMP3_HUMAN	Vesicle-associated membrane protein 3 OS=Homo sapiens GN=VAMP3 PE=1 SV=3	HUMAN	2
4	4.01	8.5	sp|Q96HE7|ERO1A_HUMAN	ERO1-like protein alpha OS=Homo sapiens GN=ERO1L PE=1 SV=2	HUMAN	2
4	4	11.8	sp|Q99442|SEC62_HUMAN	Translocation protein SEC62 OS=Homo sapiens GN=SEC62 PE=1 SV=1	HUMAN	2
4	4	25.4	sp|Q9NS69|TOM22_HUMAN	Mitochondrial import receptor subunit TOM22 homolog OS=Homo sapiens GN=TOMM22 PE=1 SV=3	HUMAN	2
4	4	14	sp|Q9Y5M8|SRPRB_HUMAN	Signal recognition particle receptor subunit beta OS=Homo sapiens GN=SRPRB PE=1 SV=3	HUMAN	2
3.96	3.96	35.2	sp|P46783|RS10_HUMAN	40S ribosomal protein S10 OS=Homo sapiens GN=RPS10 PE=1 SV=1	HUMAN	2
3.94	4.05	9.6	sp|P06865|HEXA_HUMAN	Beta-hexosaminidase subunit alpha OS=Homo sapiens GN=HEXA PE=1 SV=2	HUMAN	2
3.92	3.92	5.7	sp|Q9UGT4|SUSD2_HUMAN	Sushi domain-containing protein 2 OS=Homo sapiens GN=SUSD2 PE=1 SV=1	HUMAN	2
3.9	4.4	36.4	sp|O00264|PGRC1_HUMAN	Membrane-associated progesterone receptor component 1 OS=Homo sapiens GN=PGRMC1 PE=1 SV=3	HUMAN	2
3.86	3.86	17	sp|Q6NUK1|SCMC1_HUMAN	Calcium-binding mitochondrial carrier protein SCaMC-1 OS=Homo sapiens GN=SLC25A24 PE=1 SV=2	HUMAN	2
3.84	3.84	16.1	sp|P09496|CLCA_HUMAN	Clathrin light chain A OS=Homo sapiens GN=CLTA PE=1 SV=1	HUMAN	2
3.82	3.82	10.3	sp|P29401|TKT_HUMAN	Transketolase OS=Homo sapiens GN=TKT PE=1 SV=3	HUMAN	2
3.74	3.74	7.6	sp|P49257|LMAN1_HUMAN	Protein ERGIC-53 OS=Homo sapiens GN=LMAN1 PE=1 SV=2	HUMAN	2
3.68	3.68	19.8	sp|P15259|PGAM2_HUMAN	Phosphoglycerate mutase 2 OS=Homo sapiens GN=PGAM2 PE=1 SV=3	HUMAN	2
3.67	3.68	16.4	sp|O15260|SURF4_HUMAN	Surfeit locus protein 4 OS=Homo sapiens GN=SURF4 PE=1 SV=3	HUMAN	2
3.64	3.64	7.8	sp|P49419|AL7A1_HUMAN	Alpha-aminoadipic semialdehyde dehydrogenase OS=Homo sapiens GN=ALDH7A1 PE=1 SV=5	HUMAN	2
3.64	3.64	8.7	sp|Q32P28|P3H1_HUMAN	Prolyl 3-hydroxylase 1 OS=Homo sapiens GN=LEPRE1 PE=1 SV=2	HUMAN	2
3.62	3.62	40.6	sp|P62987|RL40_HUMAN	Ubiquitin-60S ribosomal protein L40 OS=Homo sapiens GN=UBA52 PE=1 SV=2	HUMAN	2
3.6	3.6	9.4	sp|Q9HCC0|MCCB_HUMAN	Methylcrotonoyl-CoA carboxylase beta chain, mitochondrial OS=Homo sapiens GN=MCCC2 PE=1 SV=1	HUMAN	2
3.58	3.58	8.5	sp|P01023|A2MG_HUMAN	Alpha-2-macroglobulin OS=Homo sapiens GN=A2M PE=1 SV=3	HUMAN	2
3.51	3.56	31.1	sp|P60866|RS20_HUMAN	40S ribosomal protein S20 OS=Homo sapiens GN=RPS20 PE=1 SV=1	HUMAN	2
3.49	3.49	22	sp|O00299|CLIC1_HUMAN	Chloride intracellular channel protein 1 OS=Homo sapiens GN=CLIC1 PE=1 SV=4	HUMAN	2
3.4	3.4	15	sp|P00403|COX2_HUMAN	Cytochrome c oxidase subunit 2 OS=Homo sapiens GN=MT-CO2 PE=1 SV=1	HUMAN	2
3.36	3.36	8.1	sp|P35221|CTNA1_HUMAN	Catenin alpha-1 OS=Homo sapiens GN=CTNNA1 PE=1 SV=1	HUMAN	2
3.36	3.36	7.5	sp|P36551|HEM6_HUMAN	Coproporphyrinogen-III oxidase, mitochondrial OS=Homo sapiens GN=CPOX PE=1 SV=3	HUMAN	2
3.36	3.36	15.6	sp|Q00688|FKBP3_HUMAN	Peptidyl-prolyl cis-trans isomerase FKBP3 OS=Homo sapiens GN=FKBP3 PE=1 SV=1	HUMAN	2
3.32	3.34	12.8	sp|Q13011|ECH1_HUMAN	Delta(3,5)-Delta(2,4)-dienoyl-CoA isomerase, mitochondrial OS=Homo sapiens GN=ECH1 PE=1 SV=2	HUMAN	2
3.29	3.29	12.5	sp|P24539|AT5F1_HUMAN	ATP synthase subunit b, mitochondrial OS=Homo sapiens GN=ATP5F1 PE=1 SV=2	HUMAN	2
3.28	3.28	21.1	sp|P51572|BAP31_HUMAN	B-cell receptor-associated protein 31 OS=Homo sapiens GN=BCAP31 PE=1 SV=3	HUMAN	2
3.19	3.21	39.4	sp|P16401|H15_HUMAN	Histone H1.5 OS=Homo sapiens GN=HIST1H1B PE=1 SV=3	HUMAN	2
3.19	3.19	9.5	sp|P55209|NP1L1_HUMAN	Nucleosome assembly protein 1-like 1 OS=Homo sapiens GN=NAP1L1 PE=1 SV=1	HUMAN	2
3.16	3.16	34.5	sp|P26885|FKBP2_HUMAN	Peptidyl-prolyl cis-trans isomerase FKBP2 OS=Homo sapiens GN=FKBP2 PE=1 SV=2	HUMAN	2
3.15	3.15	9.1	sp|P53634|CATC_HUMAN	Dipeptidyl peptidase 1 OS=Homo sapiens GN=CTSC PE=1 SV=2	HUMAN	2
3.14	3.19	6.9	sp|Q9Y2J2|E41L3_HUMAN	Band 4.1-like protein 3 OS=Homo sapiens GN=EPB41L3 PE=1 SV=2	HUMAN	2
3.1	3.1	17.9	sp|Q969H8|CS010_HUMAN	UPF0556 protein C19orf10 OS=Homo sapiens GN=C19orf10 PE=1 SV=1	HUMAN	2
3.03	3.03	11.9	sp|P43307|SSRA_HUMAN	Translocon-associated protein subunit alpha OS=Homo sapiens GN=SSR1 PE=1 SV=3	HUMAN	2
3.01	3.01	7.8	sp|P30038|AL4A1_HUMAN	Delta-1-pyrroline-5-carboxylate dehydrogenase, mitochondrial OS=Homo sapiens GN=ALDH4A1 PE=1 SV=3	HUMAN	2
3.01	3.01	14	sp|Q96CG8|CTHR1_HUMAN	Collagen triple helix repeat-containing protein 1 OS=Homo sapiens GN=CTHRC1 PE=1 SV=1	HUMAN	2
3	3.17	25.6	sp|P30405|PPIF_HUMAN	Peptidyl-prolyl cis-trans isomerase F, mitochondrial OS=Homo sapiens GN=PPIF PE=1 SV=1	HUMAN	2
2.98	2.98	10	sp|P19404|NDUV2_HUMAN	NADH dehydrogenase [ubiquinone] flavoprotein 2, mitochondrial OS=Homo sapiens GN=NDUFV2 PE=1 SV=2	HUMAN	2
2.96	2.96	14.6	sp|Q9H361|PABP3_HUMAN	Polyadenylate-binding protein 3 OS=Homo sapiens GN=PABPC3 PE=1 SV=2	HUMAN	2
2.93	2.93	12.7	sp|Q9HDC9|APMAP_HUMAN	Adipocyte plasma membrane-associated protein OS=Homo sapiens GN=APMAP PE=1 SV=2	HUMAN	2
2.92	2.92	15.9	sp|P47756|CAPZB_HUMAN	F-actin-capping protein subunit beta OS=Homo sapiens GN=CAPZB PE=1 SV=4	HUMAN	2
2.91	2.94	23.7	sp|Q9Y696|CLIC4_HUMAN	Chloride intracellular channel protein 4 OS=Homo sapiens GN=CLIC4 PE=1 SV=4	HUMAN	2
2.84	2.84	9.2	sp|P26572|MGAT1_HUMAN	Alpha-1,3-mannosyl-glycoprotein 2-beta-N-acetylglucosaminyltransferase OS=Homo sapiens GN=MGAT1 PE=2 S	HUMAN	2
2.81	2.81	13.6	sp|P84095|RHOG_HUMAN	Rho-related GTP-binding protein RhoG OS=Homo sapiens GN=RHOG PE=1 SV=1	HUMAN	2

Unused	Total	% Cov	Accession #	Name	Species	Peptides(95%)
2.8	2.82	12.3	sp|P07099|HYEP_HUMAN	Epoxide hydrolase 1 OS=Homo sapiens GN=EPHX1 PE=1 SV=1	HUMAN	2
2.77	2.77	43.1	sp|P46778|RL21_HUMAN	60S ribosomal protein L21 OS=Homo sapiens GN=RPL21 PE=1 SV=2	HUMAN	2
2.75	2.75	12.6	sp|Q96CW1|AP2M1_HUMAN	AP-2 complex subunit mu OS=Homo sapiens GN=AP2M1 PE=1 SV=2	HUMAN	2
2.66	2.66	13	sp|Q5JNZ5|RS26L_HUMAN	Putative 40S ribosomal protein S26-like 1 OS=Homo sapiens GN=RPS26P11 PE=5 SV=1	HUMAN	2
2.66	2.66	7.9	sp|Q92504|S39A7_HUMAN	Zinc transporter SLC39A7 OS=Homo sapiens GN=SLC39A7 PE=1 SV=2	HUMAN	2
2.65	2.65	15	sp|P21589|5NTD_HUMAN	5'-nucleotidase OS=Homo sapiens GN=NT5E PE=1 SV=1	HUMAN	2
2.53	2.53	11.2	sp|Q9ULV4|COR1C_HUMAN	Coronin-1C OS=Homo sapiens GN=CORO1C PE=1 SV=1	HUMAN	2
2.52	2.52	29.7	sp|P02511|CRYAB_HUMAN	Alpha-crystallin B chain OS=Homo sapiens GN=CRYAB PE=1 SV=2	HUMAN	2
2.52	2.55	25.2	sp|P42766|RL35_HUMAN	60S ribosomal protein L35 OS=Homo sapiens GN=RPL35 PE=1 SV=2	HUMAN	2
2.48	2.48	4.4	sp|P08648|ITA5_HUMAN	Integrin alpha-5 OS=Homo sapiens GN=ITGA5 PE=1 SV=2	HUMAN	2
2.29	2.29	24.8	sp|P46779|RL28_HUMAN	60S ribosomal protein L28 OS=Homo sapiens GN=RPL28 PE=1 SV=3	HUMAN	2
2.27	2.27	12.1	sp|O75477|ERLN1_HUMAN	Erlin-1 OS=Homo sapiens GN=ERLIN1 PE=1 SV=1	HUMAN	2
2.25	2.25	13.4	sp|P04062|GLCM_HUMAN	Glucosylceramidase OS=Homo sapiens GN=GBA PE=1 SV=3	HUMAN	2
2.23	2.23	33.1	sp|P62277|RS13_HUMAN	40S ribosomal protein S13 OS=Homo sapiens GN=RPS13 PE=1 SV=2	HUMAN	2
2.2	2.2	28	sp|Q9H299|SH3L3_HUMAN	SH3 domain-binding glutamic acid-rich-like protein 3 OS=Homo sapiens GN=SH3BGRL3 PE=1 SV=1	HUMAN	2
2.04	2.04	22.7	sp|P61769|B2MG_HUMAN	Beta-2-microglobulin OS=Homo sapiens GN=B2M PE=1 SV=1	HUMAN	2
2.02	2.02	14.9	sp|P02792|FRIL_HUMAN	Ferritin light chain OS=Homo sapiens GN=FTL PE=1 SV=2	HUMAN	2
2.02	2.02	19.1	sp|P20645|MPRD_HUMAN	Cation-dependent mannose-6-phosphate receptor OS=Homo sapiens GN=M6PR PE=1 SV=1	HUMAN	2
2	2	16.4	sp|O60783|RT14_HUMAN	28S ribosomal protein S14, mitochondrial OS=Homo sapiens GN=MRPS14 PE=1 SV=1	HUMAN	2
2	2	7.1	sp|O95571|ETHE1_HUMAN	Protein ETHE1, mitochondrial OS=Homo sapiens GN=ETHE1 PE=1 SV=2	HUMAN	2
2	2	6.4	sp|P04181|OAT_HUMAN	Ornithine aminotransferase, mitochondrial OS=Homo sapiens GN=OAT PE=1 SV=1	HUMAN	2
2	4.05	36.8	sp|P05386|RLA1_HUMAN	60S acidic ribosomal protein P1 OS=Homo sapiens GN=RPLP1 PE=1 SV=1	HUMAN	2
2	4	22.9	sp|P10301|RRAS_HUMAN	Ras-related protein R-Ras OS=Homo sapiens GN=RRAS PE=1 SV=1	HUMAN	2
2	4.62	16.7	sp|P27348|1433T_HUMAN	14-3-3 protein theta OS=Homo sapiens GN=YWHAQ PE=1 SV=1	HUMAN	2
2	4.01	13.5	sp|P50995|ANX11_HUMAN	Annexin A11 OS=Homo sapiens GN=ANXA11 PE=1 SV=1	HUMAN	2
2	2.94	26.7	sp|P60981|DEST_HUMAN	Destrin OS=Homo sapiens GN=DSTN PE=1 SV=3	HUMAN	2
2	2.87	19.5	sp|P61026|RAB10_HUMAN	Ras-related protein Rab-10 OS=Homo sapiens GN=RAB10 PE=1 SV=1	HUMAN	2
2	2.85	9.5	sp|Q14344|GNA13_HUMAN	Guanine nucleotide-binding protein subunit alpha-13 OS=Homo sapiens GN=GNA13 PE=1 SV=2	HUMAN	2
2	2.87	17.4	sp|Q15286|RAB35_HUMAN	Ras-related protein Rab-35 OS=Homo sapiens GN=RAB35 PE=1 SV=1	HUMAN	2
1.68	1.68	30.9	sp|P18077|RL35A_HUMAN	60S ribosomal protein L35a OS=Homo sapiens GN=RPL35A PE=1 SV=2	HUMAN	2
1.66	2.54	6.5	sp|P54136|SYRC_HUMAN	Arginine--tRNA ligase, cytoplasmic OS=Homo sapiens GN=RARS PE=1 SV=2	HUMAN	2
1.61	1.61	9	sp|P10515|ODP2_HUMAN	Dihydrolipoyllysine-residue acetyltransferase component of pyruvate dehydrogenase complex, mitochondrial OS	HUMAN	2
1.5	3.69	16.6	sp|P09525|ANXA4_HUMAN	Annexin A4 OS=Homo sapiens GN=ANXA4 PE=1 SV=4	HUMAN	2
1.43	1.43	19.2	sp|P30041|PRDX6_HUMAN	Peroxiredoxin-6 OS=Homo sapiens GN=PRDX6 PE=1 SV=3	HUMAN	2
1.82	1.82	37.6	sp|P38159|RBMX_HUMAN	RNA-binding motif protein, X chromosome OS=Homo sapiens GN=RBMX PE=1 SV=3	HUMAN	2
1.2	1.2	32.7	sp|P20340|RAB6A_HUMAN	Ras-related protein Rab-6A OS=Homo sapiens GN=RAB6A PE=1 SV=3	HUMAN	2
0.99	0.99	11	sp|Q99439|CNN2_HUMAN	Calponin-2 OS=Homo sapiens GN=CNN2 PE=1 SV=4	HUMAN	2
0.74	0.74	22.9	sp|P49368|TCPG_HUMAN	T-complex protein 1 subunit gamma OS=Homo sapiens GN=CCT3 PE=1 SV=4	HUMAN	2
0.63	0.63	13.6	sp|O14737|PDCD5_HUMAN	Programmed cell death protein 5 OS=Homo sapiens GN=PDCD5 PE=1 SV=3	HUMAN	2
0.62	0.62	25.2	sp|Q7L8A9|VASH1_HUMAN	Vasohibin-1 OS=Homo sapiens GN=VASH1 PE=1 SV=1	HUMAN	2
0.6	0.61	15.6	sp|Q16658|FSCN1_HUMAN	Fascin OS=Homo sapiens GN=FSCN1 PE=1 SV=3	HUMAN	2
0.58	0.58	5.6	sp|Q8N4U5|T11L2_HUMAN	T-complex protein 11-like protein 2 OS=Homo sapiens GN=TCP11L2 PE=2 SV=1	HUMAN	2
0.56	0.56	11.1	sp|Q16186|ADRM1_HUMAN	Proteasomal ubiquitin receptor ADRM1 OS=Homo sapiens GN=ADRM1 PE=1 SV=2	HUMAN	2
0.55	0.55	5.1	sp|P20810|ICAL_HUMAN	Calpastatin OS=Homo sapiens GN=CAST PE=1 SV=4	HUMAN	2
0.51	0.51	17.9	sp|Q15654|TRIP6_HUMAN	Thyroid receptor-interacting protein 6 OS=Homo sapiens GN=TRIP6 PE=1 SV=3	HUMAN	2
0.48	0.48	9.8	sp|Q9UBK2|PRGC1_HUMAN	Peroxisome proliferator-activated receptor gamma coactivator 1-alpha OS=Homo sapiens GN=PPARGC1A PE=1 S	HUMAN	2
0.45	0.46	7.1	sp|Q15751|HERC1_HUMAN	Probable E3 ubiquitin-protein ligase HERC1 OS=Homo sapiens GN=HERC1 PE=1 SV=2	HUMAN	2
0.45	0.46	12.5	sp|Q6JBY9|CPZIP_HUMAN	CapZ-interacting protein OS=Homo sapiens GN=RCSD1 PE=1 SV=1	HUMAN	2
0.44	0.45	3.2	sp|O43374|RASL2_HUMAN	Ras GTPase-activating protein 4 OS=Homo sapiens GN=RASA4 PE=2 SV=2	HUMAN	2
0.44	0.44	18.9	sp|O75781|PALM_HUMAN	Paralemmin-1 OS=Homo sapiens GN=PALM PE=1 SV=2	HUMAN	2
0.41	0.41	19.5	sp|O14979|HNRDL_HUMAN	Heterogeneous nuclear ribonucleoprotein D-like OS=Homo sapiens GN=HNRPDL PE=1 SV=3	HUMAN	2
0.41	0.41	8.6	sp|Q96JN8|NEUL4_HUMAN	Neuralized-like protein 4 OS=Homo sapiens GN=NEURL4 PE=1 SV=2	HUMAN	2
0.4	0.4	8.5	sp|Q09028|RBBP4_HUMAN	Histone-binding protein RBBP4 OS=Homo sapiens GN=RBBP4 PE=1 SV=3	HUMAN	2
0.39	0.39	7.8	sp|P51397|DAP1_HUMAN	Death-associated protein 1 OS=Homo sapiens GN=DAP PE=1 SV=3	HUMAN	2
0.39	0.39	13.6	sp|Q16555|DPYL2_HUMAN	Dihydropyrimidinase-related protein 2 OS=Homo sapiens GN=DPYSL2 PE=1 SV=1	HUMAN	2
0.39	0.39	9.5	sp|Q96TA1|NIBL1_HUMAN	Niban-like protein 1 OS=Homo sapiens GN=FAM129B PE=1 SV=3	HUMAN	2
0.38	0.38	4.3	sp|Q9H3N1|TMX1_HUMAN	Thioredoxin-related transmembrane protein 1 OS=Homo sapiens GN=TMX1 PE=1 SV=1	HUMAN	2
0.37	0.37	14.3	sp|Q71UM5|RS27L_HUMAN	40S ribosomal protein S27-like OS=Homo sapiens GN=RPS27L PE=1 SV=3	HUMAN	2
0.36	0.36	37.8	sp|P84103|SRSF3_HUMAN	Serine/arginine-rich splicing factor 3 OS=Homo sapiens GN=SRSF3 PE=1 SV=1	HUMAN	2
0.35	0.53	4.9	sp|P40261|NNMT_HUMAN	Nicotinamide N-methyltransferase OS=Homo sapiens GN=NNMT PE=1 SV=1	HUMAN	2
0.34	0.34	4.4	sp|P48742|LHX1_HUMAN	LIM/homeobox protein Lhx1 OS=Homo sapiens GN=LHX1 PE=1 SV=2	HUMAN	2
0.33	0.33	12.6	sp|O75064|DEN4B_HUMAN	DENN domain-containing protein 4B OS=Homo sapiens GN=DENND4B PE=1 SV=4	HUMAN	2
0.32	0.32	10	sp|P14866|HNRPL_HUMAN	Heterogeneous nuclear ribonucleoprotein L OS=Homo sapiens GN=HNRNPL PE=1 SV=2	HUMAN	2
0.32	0.33	11.6	sp|Q9H444|CHM4B_HUMAN	Charged multivesicular body protein 4b OS=Homo sapiens GN=CHMP4B PE=1 SV=1	HUMAN	2
0.31	0.32	2.6	sp|O14617|AP3D1_HUMAN	AP-3 complex subunit delta-1 OS=Homo sapiens GN=AP3D1 PE=1 SV=1	HUMAN	2
0.3	0.3	4.7	sp|P43490|NAMPT_HUMAN	Nicotinamide phosphoribosyltransferase OS=Homo sapiens GN=NAMPT PE=1 SV=1	HUMAN	2
0.29	0.29	14.9	sp|P09429|HMGB1_HUMAN	High mobility group protein B1 OS=Homo sapiens GN=HMGB1 PE=1 SV=3	HUMAN	2
0.28	0.28	5.5	sp|P15559|NQO1_HUMAN	NAD(P)H dehydrogenase [quinone] 1 OS=Homo sapiens GN=NQO1 PE=1 SV=1	HUMAN	2
0.26	0.26	11.7	sp|A6NC98|CC88B_HUMAN	Coiled-coil domain-containing protein 88B OS=Homo sapiens GN=CCDC88B PE=1 SV=1	HUMAN	2
0.26	0.26	4.1	sp|O75534|CSDE1_HUMAN	Cold shock domain-containing protein E1 OS=Homo sapiens GN=CSDE1 PE=1 SV=2	HUMAN	2
0.26	0.26	8.4	sp|Q6DT37|MRCKG_HUMAN	Serine/threonine-protein kinase MRCK gamma OS=Homo sapiens GN=CDC42BPG PE=1 SV=2	HUMAN	2
0.26	0.26	15.5	sp|Q96FQ6|S10AG_HUMAN	Protein S100-A16 OS=Homo sapiens GN=S100A16 PE=1 SV=1	HUMAN	2
0.25	0.25	19.1	sp|Q7Z7L8|CK096_HUMAN	Uncharacterized protein C11orf96 OS=Homo sapiens GN=C11orf96 PE=1 SV=3	HUMAN	2
0.25	0.25	8.8	sp|Q8NEB9|PK3C3_HUMAN	Phosphatidylinositol 3-kinase catalytic subunit type 3 OS=Homo sapiens GN=PIK3C3 PE=1 SV=1	HUMAN	2
0.24	0.24	8.6	sp|P40121|CAPG_HUMAN	Macrophage-capping protein OS=Homo sapiens GN=CAPG PE=1 SV=2	HUMAN	2
0.24	0.24	7.2	sp|Q68EM7|RHG17_HUMAN	Rho GTPase-activating protein 17 OS=Homo sapiens GN=ARHGAP17 PE=1 SV=1	HUMAN	2
0.24	0.49	13	sp|Q92930|RAB8B_HUMAN	Ras-related protein Rab-8B OS=Homo sapiens GN=RAB8B PE=1 SV=2	HUMAN	2
0.24	0.24	10.6	sp|Q96N66|MBOA7_HUMAN	Lysophospholipid acyltransferase 7 OS=Homo sapiens GN=MBOAT7 PE=1 SV=2	HUMAN	2
0.23	0.23	4.1	sp|P04844|RPN2_HUMAN	Dolichyl-diphosphooligosaccharide--protein glycosyltransferase subunit 2 OS=Homo sapiens GN=RPN2 PE=1 SV=	HUMAN	2
0.23	0.24	5.2	sp|Q1MSJ5|CSPP1_HUMAN	Centrosome and spindle pole-associated protein 1 OS=Homo sapiens GN=CSPP1 PE=1 SV=4	HUMAN	2
0.23	0.23	29.8	sp|Q9Y3Y2|CHTOP_HUMAN	Chromatin target of PRMT1 protein OS=Homo sapiens GN=CHTOP PE=1 SV=2	HUMAN	2
0.22	0.23	6.8	sp|O95466|FMNL_HUMAN	Formin-like protein 1 OS=Homo sapiens GN=FMNL1 PE=1 SV=3	HUMAN	2
0.21	0.21	5.4	sp|Q14974|IMB1_HUMAN	Importin subunit beta-1 OS=Homo sapiens GN=KPNB1 PE=1 SV=2	HUMAN	2
0.21	0.22	15.8	sp|Q9Y5X1|SNX9_HUMAN	Sorting nexin-9 OS=Homo sapiens GN=SNX9 PE=1 SV=1	HUMAN	2
0.2	0.2	5.6	sp|P54289|CA2D1_HUMAN	Voltage-dependent calcium channel subunit alpha-2/delta-1 OS=Homo sapiens GN=CACNA2D1 PE=1 SV=3	HUMAN	2
0.19	0.19	11.3	sp|Q9H5N1|RABE2_HUMAN	Rab GTPase-binding effector protein 2 OS=Homo sapiens GN=RABEP2 PE=1 SV=2	HUMAN	2
0.18	0.62	7.6	sp|P08195|4F2_HUMAN	4F2 cell-surface antigen heavy chain OS=Homo sapiens GN=SLC3A2 PE=1 SV=3	HUMAN	2

Unused	Total	% Cov	Accession #	Name	Species	Peptides(95%)
0.18	0.18	10.1	sp|Q92974|ARHG2_HUMAN	Rho guanine nucleotide exchange factor 2 OS=Homo sapiens GN=ARHGEF2 PE=1 SV=4	HUMAN	2
0.18	0.18	8.6	sp|Q9ULI4|KI26A_HUMAN	Kinesin-like protein KIF26A OS=Homo sapiens GN=KIF26A PE=1 SV=3	HUMAN	2
0.17	0.18	12.4	sp|Q08379|GOGA2_HUMAN	Golgin subfamily A member 2 OS=Homo sapiens GN=GOLGA2 PE=1 SV=3	HUMAN	2
0.17	0.19	15.4	sp|Q9BR39|JPH2_HUMAN	Junctophilin-2 OS=Homo sapiens GN=JPH2 PE=1 SV=2	HUMAN	2
0.17	0.17	5.6	sp|Q9BX10|GTPB2_HUMAN	GTP-binding protein 2 OS=Homo sapiens GN=GTPBP2 PE=2 SV=1	HUMAN	2
0.17	0.18	2.3	sp|Q9Y4B4|ARIP4_HUMAN	Helicase ARIP4 OS=Homo sapiens GN=RAD54L2 PE=1 SV=4	HUMAN	2
0.16	0.16	2.8	sp|P30926|ACHB4_HUMAN	Neuronal acetylcholine receptor subunit beta-4 OS=Homo sapiens GN=CHRNB4 PE=1 SV=2	HUMAN	2
0.16	0.18	5.2	sp|Q8WXH0|SYNE2_HUMAN	Nesprin-2 OS=Homo sapiens GN=SYNE2 PE=1 SV=3	HUMAN	2
0.15	0.16	14.6	sp|O60762|DPM1_HUMAN	Dolichol-phosphate mannosyltransferase OS=Homo sapiens GN=DPM1 PE=1 SV=1	HUMAN	2
0.15	0.15	5.1	sp|Q53H54|TYW2_HUMAN	tRNA wybutosine-synthesizing protein 2 homolog OS=Homo sapiens GN=TRMT12 PE=1 SV=1	HUMAN	2
0.14	0.29	7.1	sp|Q32MK0|MYLK3_HUMAN	Myosin light chain kinase 3 OS=Homo sapiens GN=MYLK3 PE=2 SV=3	HUMAN	2
0.14	0.14	7.4	sp|Q8IY95|TM192_HUMAN	Transmembrane protein 192 OS=Homo sapiens GN=TMEM192 PE=1 SV=1	HUMAN	2
0.14	0.15	8.1	sp|Q9H0U3|MAGT1_HUMAN	Magnesium transporter protein 1 OS=Homo sapiens GN=MAGT1 PE=1 SV=1	HUMAN	2
0.11	0.11	7.3	sp|P00491|PNPH_HUMAN	Purine nucleoside phosphorylase OS=Homo sapiens GN=PNP PE=1 SV=2	HUMAN	2
0.11	0.11	2.6	sp|Q96JM2|ZN462_HUMAN	Zinc finger protein 462 OS=Homo sapiens GN=ZNF462 PE=1 SV=3	HUMAN	2
0.11	0.11	5.8	sp|Q96PE1|GP124_HUMAN	G-protein coupled receptor 124 OS=Homo sapiens GN=GPR124 PE=1 SV=2	HUMAN	2
0.1	0.1	3	sp|P25787|PSA2_HUMAN	Proteasome subunit alpha type-2 OS=Homo sapiens GN=PSMA2 PE=1 SV=2	HUMAN	2
0.1	0.1	8.7	sp|Q8IV13|CCNJL_HUMAN	Cyclin-J-like protein OS=Homo sapiens GN=CCNJL PE=2 SV=3	HUMAN	2
0.09	0.09	4.5	sp|A2VDF0|FUCM_HUMAN	Fucose mutarotase OS=Homo sapiens GN=FUOM PE=1 SV=2	HUMAN	2
2.92	2.92	31.1	sp|P62910|RL32_HUMAN	60S ribosomal protein L32 OS=Homo sapiens GN=RPL32 PE=1 SV=2	HUMAN	1
2.92	2.92	21.6	sp|Q02543|RL18A_HUMAN	60S ribosomal protein L18a OS=Homo sapiens GN=RPL18A PE=1 SV=2	HUMAN	1
2.74	2.74	32	sp|P62913|RL11_HUMAN	60S ribosomal protein L11 OS=Homo sapiens GN=RPL11 PE=1 SV=2	HUMAN	1
2.71	2.71	17	sp|P11233|RALA_HUMAN	Ras-related protein Ral-A OS=Homo sapiens GN=RALA PE=1 SV=1	HUMAN	1
2.61	2.61	8.8	sp|Q9BTV4|TMM43_HUMAN	Transmembrane protein 43 OS=Homo sapiens GN=TMEM43 PE=1 SV=1	HUMAN	1
2.59	2.59	14.7	sp|P60953|CDC42_HUMAN	Cell division control protein 42 homolog OS=Homo sapiens GN=CDC42 PE=1 SV=2	HUMAN	1
2.58	2.58	5.2	sp|P31930|QCR1_HUMAN	Cytochrome b-c1 complex subunit 1, mitochondrial OS=Homo sapiens GN=UQCRC1 PE=1 SV=3	HUMAN	1
2.55	2.55	9.4	sp|Q14108|SCRB2_HUMAN	Lysosome membrane protein 2 OS=Homo sapiens GN=SCARB2 PE=1 SV=2	HUMAN	1
2.53	2.53	16.6	sp|Q8N183|MIMIT_HUMAN	Mimitin, mitochondrial OS=Homo sapiens GN=NDUFAF2 PE=1 SV=1	HUMAN	1
2.49	2.49	7.6	sp|P13473|LAMP2_HUMAN	Lysosome-associated membrane glycoprotein 2 OS=Homo sapiens GN=LAMP2 PE=1 SV=2	HUMAN	1
2.45	2.45	15.7	sp|P21912|DHSB_HUMAN	Succinate dehydrogenase [ubiquinone] iron-sulfur subunit, mitochondrial OS=Homo sapiens GN=SDHB PE=1 SV=	HUMAN	1
2.42	2.42	15.2	sp|P62263|RS14_HUMAN	40S ribosomal protein S14 OS=Homo sapiens GN=RPS14 PE=1 SV=3	HUMAN	1
2.41	2.41	12.3	sp|P61019|RAB2A_HUMAN	Ras-related protein Rab-2A OS=Homo sapiens GN=RAB2A PE=1 SV=1	HUMAN	1
2.4	2.4	23.7	sp|Q9P0L0|VAPA_HUMAN	Vesicle-associated membrane protein-associated protein A OS=Homo sapiens GN=VAPA PE=1 SV=3	HUMAN	1
2.39	2.39	4.4	sp|P35222|CTNB1_HUMAN	Catenin beta-1 OS=Homo sapiens GN=CTNNB1 PE=1 SV=1	HUMAN	1
2.39	2.39	18.4	sp|P61353|RL27_HUMAN	60S ribosomal protein L27 OS=Homo sapiens GN=RPL27 PE=1 SV=2	HUMAN	1
2.35	2.35	19.7	sp|P49753|ACOT2_HUMAN	Acyl-coenzyme A thioesterase 2, mitochondrial OS=Homo sapiens GN=ACOT2 PE=1 SV=6	HUMAN	1
2.34	2.34	7.7	sp|P10619|PPGB_HUMAN	Lysosomal protective protein OS=Homo sapiens GN=CTSA PE=1 SV=2	HUMAN	1
2.26	2.26	5.8	sp|Q13488|VPP3_HUMAN	V-type proton ATPase 116 kDa subunit a isoform 3 OS=Homo sapiens GN=TCIRG1 PE=1 SV=3	HUMAN	1
2.25	2.25	10.6	sp|Q96A33|CCD47_HUMAN	Coiled-coil domain-containing protein 47 OS=Homo sapiens GN=CCDC47 PE=1 SV=1	HUMAN	1
2.24	2.26	15.3	sp|Q96HY6|DDRGK_HUMAN	DDRGK domain-containing protein 1 OS=Homo sapiens GN=DDRGK1 PE=1 SV=2	HUMAN	1
2.23	2.23	3	sp|Q04721|NOTC2_HUMAN	Neurogenic locus notch homolog protein 2 OS=Homo sapiens GN=NOTCH2 PE=1 SV=3	HUMAN	1
2.19	2.19	22.3	sp|Q4V9L6|TM119_HUMAN	Transmembrane protein 119 OS=Homo sapiens GN=TMEM119 PE=2 SV=1	HUMAN	1
2.15	2.15	12.2	sp|P30837|AL1B1_HUMAN	Aldehyde dehydrogenase X, mitochondrial OS=Homo sapiens GN=ALDH1B1 PE=1 SV=3	HUMAN	1
2.14	2.14	15.4	sp|O14561|ACPM_HUMAN	Acyl carrier protein, mitochondrial OS=Homo sapiens GN=NDUFAB1 PE=1 SV=3	HUMAN	1
2.14	2.14	19.1	sp|P49773|HINT1_HUMAN	Histidine triad nucleotide-binding protein 1 OS=Homo sapiens GN=HINT1 PE=1 SV=2	HUMAN	1
2.14	2.19	6	sp|Q00610|CLH1_HUMAN	Clathrin heavy chain 1 OS=Homo sapiens GN=CLTC PE=1 SV=5	HUMAN	1
2.13	2.18	6.5	sp|P46939|UTRO_HUMAN	Utrophin OS=Homo sapiens GN=UTRN PE=1 SV=2	HUMAN	1
2.12	2.12	61.5	sp|P07919|QCR6_HUMAN	Cytochrome b-c1 complex subunit 6, mitochondrial OS=Homo sapiens GN=UQCRH PE=1 SV=2	HUMAN	1
2.1	2.16	7.1	sp|P61160|ARP2_HUMAN	Actin-related protein 2 OS=Homo sapiens GN=ACTR2 PE=1 SV=1	HUMAN	1
2.09	2.09	29.2	sp|O75531|BAF_HUMAN	Barrier-to-autointegration factor OS=Homo sapiens GN=BANF1 PE=1 SV=1	HUMAN	1
2.09	2.13	6.7	sp|P46821|MAP1B_HUMAN	Microtubule-associated protein 1B OS=Homo sapiens GN=MAP1B PE=1 SV=2	HUMAN	1
2.07	2.07	18.7	sp|P33316|DUT_HUMAN	Deoxyuridine 5'-triphosphate nucleotidohydrolase, mitochondrial OS=Homo sapiens GN=DUT PE=1 SV=4	HUMAN	1
2.07	2.07	21.7	sp|P62888|RL30_HUMAN	60S ribosomal protein L30 OS=Homo sapiens GN=RPL30 PE=1 SV=2	HUMAN	1
2.07	2.09	6.3	sp|Q96QK1|VPS35_HUMAN	Vacuolar protein sorting-associated protein 35 OS=Homo sapiens GN=VPS35 PE=1 SV=2	HUMAN	1
2.07	2.07	30.6	sp|Q99584|S10AD_HUMAN	Protein S100-A13 OS=Homo sapiens GN=S100A13 PE=1 SV=1	HUMAN	1
2.06	2.06	19.7	sp|P02100|HBE_HUMAN	Hemoglobin subunit epsilon OS=Homo sapiens GN=HBE1 PE=1 SV=2	HUMAN	1
2.06	2.06	17.6	sp|P21291|CSRP1_HUMAN	Cysteine and glycine-rich protein 1 OS=Homo sapiens GN=CSRP1 PE=1 SV=3	HUMAN	1
2.06	2.08	11.4	sp|Q0ZGT2|NEXN_HUMAN	Nexilin OS=Homo sapiens GN=NEXN PE=1 SV=1	HUMAN	1
2.06	2.08	6.8	sp|Q14764|MVP_HUMAN	Major vault protein OS=Homo sapiens GN=MVP PE=1 SV=4	HUMAN	1
2.05	2.05	7	sp|O75718|CRTAP_HUMAN	Cartilage-associated protein OS=Homo sapiens GN=CRTAP PE=1 SV=1	HUMAN	1
2.05	2.05	20.4	sp|O95169|NDUB8_HUMAN	NADH dehydrogenase [ubiquinone] 1 beta subcomplex subunit 8, mitochondrial OS=Homo sapiens GN=NDUFB8	HUMAN	1
2.05	2.05	9.5	sp|Q02952|AKA12_HUMAN	A-kinase anchor protein 12 OS=Homo sapiens GN=AKAP12 PE=1 SV=4	HUMAN	1
2.05	2.05	16.9	sp|Q96FZ7|CHMP6_HUMAN	Charged multivesicular body protein 6 OS=Homo sapiens GN=CHMP6 PE=1 SV=3	HUMAN	1
2.05	2.05	17.4	sp|Q9P0J0|NDUAD_HUMAN	NADH dehydrogenase [ubiquinone] 1 alpha subcomplex subunit 13 OS=Homo sapiens GN=NDUFA13 PE=1 SV=3	HUMAN	1
2.04	2.04	4.8	sp|P53396|ACLY_HUMAN	ATP-citrate synthase OS=Homo sapiens GN=ACLY PE=1 SV=3	HUMAN	1
2.04	2.06	5.6	sp|P62873|GBB1_HUMAN	Guanine nucleotide-binding protein G(I)/G(S)/G(T) subunit beta-1 OS=Homo sapiens GN=GNB1 PE=1 SV=3	HUMAN	1
2.04	2.04	7.7	sp|Q10471|GALT2_HUMAN	Polypeptide N-acetylgalactosaminyltransferase 2 OS=Homo sapiens GN=GALNT2 PE=1 SV=1	HUMAN	1
2.04	2.04	9.2	sp|Q8WUM4|PDC6I_HUMAN	Programmed cell death 6-interacting protein OS=Homo sapiens GN=PDCD6IP PE=1 SV=1	HUMAN	1
2.04	2.04	11.6	sp|Q9UHB6|LIMA1_HUMAN	LIM domain and actin-binding protein 1 OS=Homo sapiens GN=LIMA1 PE=1 SV=1	HUMAN	1
2.03	2.03	13.9	sp|P08574|CY1_HUMAN	Cytochrome c1, heme protein, mitochondrial OS=Homo sapiens GN=CYC1 PE=1 SV=3	HUMAN	1
2.03	2.03	6.7	sp|P23634|AT2B4_HUMAN	Plasma membrane calcium-transporting ATPase 4 OS=Homo sapiens GN=ATP2B4 PE=1 SV=2	HUMAN	1
2.03	2.03	8	sp|Q53GQ0|DHB12_HUMAN	Estradiol 17-beta-dehydrogenase 12 OS=Homo sapiens GN=HSD17B12 PE=1 SV=2	HUMAN	1
2.03	2.03	9.2	sp|Q96DB5|RMD1_HUMAN	Regulator of microtubule dynamics protein 1 OS=Homo sapiens GN=FAM82B PE=1 SV=1	HUMAN	1
2.02	2.02	7.5	sp|O95831|AIFM1_HUMAN	Apoptosis-inducing factor 1, mitochondrial OS=Homo sapiens GN=AIFM1 PE=1 SV=1	HUMAN	1
2.02	2.02	9.1	sp|P25325|THTM_HUMAN	3-mercaptopyruvate sulfurtransferase OS=Homo sapiens GN=MPST PE=1 SV=3	HUMAN	1
2.02	2.02	8.8	sp|P43304|GPDM_HUMAN	Glycerol-3-phosphate dehydrogenase, mitochondrial OS=Homo sapiens GN=GPD2 PE=1 SV=3	HUMAN	1
2.02	2.76	20.8	sp|P45877|PPIC_HUMAN	Peptidyl-prolyl cis-trans isomerase C OS=Homo sapiens GN=PPIC PE=1 SV=1	HUMAN	1
2.02	2.02	8.9	sp|Q14165|MLEC_HUMAN	Malectin OS=Homo sapiens GN=MLEC PE=1 SV=1	HUMAN	1
2.02	2.05	9.4	sp|Q9HAV0|GBB4_HUMAN	Guanine nucleotide-binding protein subunit beta-4 OS=Homo sapiens GN=GNB4 PE=1 SV=3	HUMAN	1
2.02	2.02	7.6	sp|Q9NSE4|SYIM_HUMAN	Isoleucine--tRNA ligase, mitochondrial OS=Homo sapiens GN=IARS2 PE=1 SV=2	HUMAN	1
2.01	2.04	7.1	sp|O60313|OPA1_HUMAN	Dynamin-like 120 kDa protein, mitochondrial OS=Homo sapiens GN=OPA1 PE=1 SV=3	HUMAN	1
2.01	2.02	12.3	sp|P20073|ANXA7_HUMAN	Annexin A7 OS=Homo sapiens GN=ANXA7 PE=1 SV=3	HUMAN	1
2.01	2.55	12	sp|Q9H4M9|EHD1_HUMAN	EH domain-containing protein 1 OS=Homo sapiens GN=EHD1 PE=1 SV=2	HUMAN	1
2	2	4.3	sp|O00217|NDUS8_HUMAN	NADH dehydrogenase [ubiquinone] iron-sulfur protein 8, mitochondrial OS=Homo sapiens GN=NDUFS8 PE=1 SV	HUMAN	1
2	2.02	5.1	sp|O00410|IPO5_HUMAN	Importin-5 OS=Homo sapiens GN=IPO5 PE=1 SV=4	HUMAN	1
2	2	10.9	sp|O14494|LPP1_HUMAN	Lipid phosphate phosphohydrolase 1 OS=Homo sapiens GN=PPAP2A PE=1 SV=1	HUMAN	1
2	2	6.1	sp|O14495|LPP3_HUMAN	Lipid phosphate phosphohydrolase 3 OS=Homo sapiens GN=PPAP2B PE=1 SV=1	HUMAN	1

Unused	Total	% Cov	Accession #	Name	Species	Peptides(95%)
2	2	7.8	sp|O14745|NHRF1_HUMAN	Na(+)/H(+) exchange regulatory cofactor NHE-RF1 OS=Homo sapiens GN=SLC9A3R1 PE=1 SV=4	HUMAN	1
2	2	8.6	sp|O14880|MGST3_HUMAN	Microsomal glutathione S-transferase 3 OS=Homo sapiens GN=MGST3 PE=1 SV=1	HUMAN	1
2	2	9.6	sp|O14908|GIPC1_HUMAN	PDZ domain-containing protein GIPC1 OS=Homo sapiens GN=GIPC1 PE=1 SV=2	HUMAN	1
2	2	3.6	sp|O15127|SCAM2_HUMAN	Secretory carrier-associated membrane protein 2 OS=Homo sapiens GN=SCAMP2 PE=1 SV=2	HUMAN	1
2	2	8.4	sp|O15145|ARPC3_HUMAN	Actin-related protein 2/3 complex subunit 3 OS=Homo sapiens GN=ARPC3 PE=1 SV=3	HUMAN	1
2	2	8	sp|O15269|SPTC1_HUMAN	Serine palmitoyltransferase 1 OS=Homo sapiens GN=SPTLC1 PE=1 SV=1	HUMAN	1
2	2.1	14.6	sp|O15400|STX7_HUMAN	Syntaxin-7 OS=Homo sapiens GN=STX7 PE=1 SV=4	HUMAN	1
2	2	11.7	sp|O43399|TPD54_HUMAN	Tumor protein D54 OS=Homo sapiens GN=TPD52L2 PE=1 SV=2	HUMAN	1
2	2	15.4	sp|O43504|HBXIP_HUMAN	Hepatitis B virus X-interacting protein OS=Homo sapiens GN=HBXIP PE=1 SV=1	HUMAN	1
2	2.01	5.8	sp|O43776|SYNC_HUMAN	Asparagine--tRNA ligase, cytoplasmic OS=Homo sapiens GN=NARS PE=1 SV=1	HUMAN	1
2	2	17.3	sp|O60493|SNX3_HUMAN	Sorting nexin-3 OS=Homo sapiens GN=SNX3 PE=1 SV=3	HUMAN	1
2	2	4.2	sp|O60506|HNRPQ_HUMAN	Heterogeneous nuclear ribonucleoprotein Q OS=Homo sapiens GN=SYNCRIP PE=1 SV=2	HUMAN	1
2	2	8.1	sp|O60664|PLIN3_HUMAN	Perilipin-3 OS=Homo sapiens GN=PLIN3 PE=1 SV=3	HUMAN	1
2	2	24.6	sp|O75348|VATG1_HUMAN	V-type proton ATPase subunit G 1 OS=Homo sapiens GN=ATP6V1G1 PE=1 SV=3	HUMAN	1
2	2	14.1	sp|O75381|PEX14_HUMAN	Peroxisomal membrane protein PEX14 OS=Homo sapiens GN=PEX14 PE=1 SV=1	HUMAN	1
2	2	19	sp|O75438|NDUB1_HUMAN	NADH dehydrogenase [ubiquinone] 1 beta subcomplex subunit 1 OS=Homo sapiens GN=NDUFB1 PE=1 SV=1	HUMAN	1
2	2.02	8.2	sp|O76031|CLPX_HUMAN	ATP-dependent Clp protease ATP-binding subunit clpX-like, mitochondrial OS=Homo sapiens GN=CLPX PE=1 SV=:	HUMAN	1
2	2	6	sp|O94919|ENDD1_HUMAN	Endonuclease domain-containing 1 protein OS=Homo sapiens GN=ENDOD1 PE=1 SV=2	HUMAN	1
2	2	7.5	sp|P04004|VTNC_HUMAN	Vitronectin OS=Homo sapiens GN=VTN PE=1 SV=1	HUMAN	1
2	2	20.3	sp|P04921|GLPC_HUMAN	Glycophorin-C OS=Homo sapiens GN=GYPC PE=1 SV=1	HUMAN	1
2	2	7	sp|P05198|IF2A_HUMAN	Eukaryotic translation initiation factor 2 subunit 1 OS=Homo sapiens GN=EIF2S1 PE=1 SV=3	HUMAN	1
2	2.03	7	sp|P07585|PGS2_HUMAN	Decorin OS=Homo sapiens GN=DCN PE=1 SV=1	HUMAN	1
2	2	16.3	sp|P07910|HNRPC_HUMAN	Heterogeneous nuclear ribonucleoproteins C1/C2 OS=Homo sapiens GN=HNRNPC PE=1 SV=4	HUMAN	1
2	2	5.5	sp|P08240|SRPR_HUMAN	Signal recognition particle receptor subunit alpha OS=Homo sapiens GN=SRPR PE=1 SV=2	HUMAN	1
2	2.32	22.9	sp|P09651|ROA1_HUMAN	Heterogeneous nuclear ribonucleoprotein A1 OS=Homo sapiens GN=HNRNPA1 PE=1 SV=5	HUMAN	1
2	2	3.3	sp|P10253|LYAG_HUMAN	Lysosomal alpha-glucosidase OS=Homo sapiens GN=GAA PE=1 SV=4	HUMAN	1
2	2	8.7	sp|P11498|PYC_HUMAN	Pyruvate carboxylase, mitochondrial OS=Homo sapiens GN=PC PE=1 SV=2	HUMAN	1
2	2	8.5	sp|P15289|ARSA_HUMAN	Arylsulfatase A OS=Homo sapiens GN=ARSA PE=1 SV=3	HUMAN	1
2	2	8.6	sp|P19367|HXK1_HUMAN	Hexokinase-1 OS=Homo sapiens GN=HK1 PE=1 SV=3	HUMAN	1
2	2.02	7.6	sp|P19525|E2AK2_HUMAN	Interferon-induced, double-stranded RNA-activated protein kinase OS=Homo sapiens GN=EIF2AK2 PE=1 SV=2	HUMAN	1
2	2	12.6	sp|P20042|IF2B_HUMAN	Eukaryotic translation initiation factor 2 subunit 2 OS=Homo sapiens GN=EIF2S2 PE=1 SV=2	HUMAN	1
2	2.06	7.2	sp|P22033|MUTA_HUMAN	Methylmalonyl-CoA mutase, mitochondrial OS=Homo sapiens GN=MUT PE=1 SV=4	HUMAN	1
2	2	7	sp|P23368|MAOM_HUMAN	NAD-dependent malic enzyme, mitochondrial OS=Homo sapiens GN=ME2 PE=1 SV=1	HUMAN	1
2	2	7.8	sp|P29992|GNA11_HUMAN	Guanine nucleotide-binding protein subunit alpha-11 OS=Homo sapiens GN=GNA11 PE=1 SV=2	HUMAN	1
2	2	9	sp|P30042|ES1_HUMAN	ES1 protein homolog, mitochondrial OS=Homo sapiens GN=C21orf33 PE=1 SV=3	HUMAN	1
2	2.02	4.4	sp|P31939|PUR9_HUMAN	Bifunctional purine biosynthesis protein PURH OS=Homo sapiens GN=ATIC PE=1 SV=3	HUMAN	1
2	2.01	4.9	sp|P31943|HNRH1_HUMAN	Heterogeneous nuclear ribonucleoprotein H OS=Homo sapiens GN=HNRNPH1 PE=1 SV=4	HUMAN	1
2	2	4.3	sp|P36269|GGT5_HUMAN	Gamma-glutamyltransferase 5 OS=Homo sapiens GN=GGT5 PE=1 SV=2	HUMAN	1
2	2	6.7	sp|P36542|ATPG_HUMAN	ATP synthase subunit gamma, mitochondrial OS=Homo sapiens GN=ATP5C1 PE=1 SV=1	HUMAN	1
2	2	4.8	sp|P43155|CACP_HUMAN	Carnitine O-acetyltransferase OS=Homo sapiens GN=CRAT PE=1 SV=5	HUMAN	1
2	2	11.9	sp|P43487|RANG_HUMAN	Ran-specific GTPase-activating protein OS=Homo sapiens GN=RANBP1 PE=1 SV=1	HUMAN	1
2	2	6.1	sp|P46199|IF2M_HUMAN	Translation initiation factor IF-2, mitochondrial OS=Homo sapiens GN=MTIF2 PE=1 SV=2	HUMAN	1
2	2.03	7.2	sp|P48643|TCPE_HUMAN	T-complex protein 1 subunit epsilon OS=Homo sapiens GN=CCT5 PE=1 SV=1	HUMAN	1
2	2	5.5	sp|P49721|PSB2_HUMAN	Proteasome subunit beta type-2 OS=Homo sapiens GN=PSMB2 PE=1 SV=1	HUMAN	1
2	2.05	7.7	sp|P49768|PSN1_HUMAN	Presenilin-1 OS=Homo sapiens GN=PSEN1 PE=1 SV=1	HUMAN	1
2	2	12.2	sp|P50402|EMD_HUMAN	Emerin OS=Homo sapiens GN=EMD PE=1 SV=1	HUMAN	1
2	2	5.3	sp|P50552|VASP_HUMAN	Vasodilator-stimulated phosphoprotein OS=Homo sapiens GN=VASP PE=1 SV=3	HUMAN	1
2	2	6.6	sp|P54802|ANAG_HUMAN	Alpha-N-acetylglucosaminidase OS=Homo sapiens GN=NAGLU PE=1 SV=2	HUMAN	1
2	2	7.1	sp|P54920|SNAA_HUMAN	Alpha-soluble NSF attachment protein OS=Homo sapiens GN=NAPA PE=1 SV=3	HUMAN	1
2	2	6.8	sp|P55060|XPO2_HUMAN	Exportin-2 OS=Homo sapiens GN=CSE1L PE=1 SV=3	HUMAN	1
2	2	4.1	sp|P55884|EIF3B_HUMAN	Eukaryotic translation initiation factor 3 subunit B OS=Homo sapiens GN=EIF3B PE=1 SV=3	HUMAN	1
2	2	16	sp|P56134|ATPK_HUMAN	ATP synthase subunit f, mitochondrial OS=Homo sapiens GN=ATP5J2 PE=1 SV=3	HUMAN	1
2	2	15.2	sp|P57105|SYJ2B_HUMAN	Synaptojanin-2-binding protein OS=Homo sapiens GN=SYNJ2BP PE=1 SV=2	HUMAN	1
2	2.02	12.3	sp|P60033|CD81_HUMAN	CD81 antigen OS=Homo sapiens GN=CD81 PE=1 SV=1	HUMAN	1
2	2	17.7	sp|P60059|SC61G_HUMAN	Protein transport protein Sec61 subunit gamma OS=Homo sapiens GN=SEC61G PE=2 SV=1	HUMAN	1
2	2	13.6	sp|P60842|IF4A1_HUMAN	Eukaryotic initiation factor 4A-I OS=Homo sapiens GN=EIF4A1 PE=1 SV=1	HUMAN	1
2	2	10.1	sp|P61966|AP1S1_HUMAN	AP-1 complex subunit sigma-1A OS=Homo sapiens GN=AP1S1 PE=1 SV=1	HUMAN	1
2	2.03	25.2	sp|P62805|H4_HUMAN	Histone H4 OS=Homo sapiens GN=HIST1H4A PE=1 SV=2	HUMAN	1
2	2	26.9	sp|P62942|FKB1A_HUMAN	Peptidyl-prolyl cis-trans isomerase FKBP1A OS=Homo sapiens GN=FKBP1A PE=1 SV=2	HUMAN	1
2	2	12.9	sp|P63208|SKP1_HUMAN	S-phase kinase-associated protein 1 OS=Homo sapiens GN=SKP1 PE=1 SV=2	HUMAN	1
2	2	6.1	sp|P68402|PA1B2_HUMAN	Platelet-activating factor acetylhydrolase IB subunit beta OS=Homo sapiens GN=PAFAH1B2 PE=1 SV=1	HUMAN	1
2	2.12	15.6	sp|P82663|RT25_HUMAN	28S ribosomal protein S25, mitochondrial OS=Homo sapiens GN=MRPS25 PE=1 SV=1	HUMAN	1
2	2.06	14.5	sp|Q04941|PLP2_HUMAN	Proteolipid protein 2 OS=Homo sapiens GN=PLP2 PE=1 SV=1	HUMAN	1
2	2	8	sp|Q08431|MFGM_HUMAN	Lactadherin OS=Homo sapiens GN=MFGE8 PE=1 SV=2	HUMAN	1
2	2	7.8	sp|Q13405|RM49_HUMAN	39S ribosomal protein L49, mitochondrial OS=Homo sapiens GN=MRPL49 PE=1 SV=1	HUMAN	1
2	2	8	sp|Q13418|ILK_HUMAN	Integrin-linked protein kinase OS=Homo sapiens GN=ILK PE=1 SV=2	HUMAN	1
2	2	8.8	sp|Q13641|TPBG_HUMAN	Trophoblast glycoprotein OS=Homo sapiens GN=TPBG PE=1 SV=1	HUMAN	1
2	2	6.9	sp|Q14157|UBP2L_HUMAN	Ubiquitin-associated protein 2-like OS=Homo sapiens GN=UBAP2L PE=1 SV=2	HUMAN	1
2	2	14.1	sp|Q14249|NUCG_HUMAN	Endonuclease G, mitochondrial OS=Homo sapiens GN=ENDOG PE=1 SV=4	HUMAN	1
2	2	16.4	sp|Q15005|SPCS2_HUMAN	Signal peptidase complex subunit 2 OS=Homo sapiens GN=SPCS2 PE=1 SV=3	HUMAN	1
2	2	8.4	sp|Q15006|TTC35_HUMAN	Tetratricopeptide repeat protein 35 OS=Homo sapiens GN=TTC35 PE=1 SV=1	HUMAN	1
2	2	4.6	sp|Q15758|AAAT_HUMAN	Neutral amino acid transporter B(0) OS=Homo sapiens GN=SLC1A5 PE=1 SV=2	HUMAN	1
2	2	22.2	sp|Q15843|NEDD8_HUMAN	NEDD8 OS=Homo sapiens GN=NEDD8 PE=1 SV=1	HUMAN	1
2	2	11.3	sp|Q86UU1|PHLB1_HUMAN	Pleckstrin homology-like domain family B member 1 OS=Homo sapiens GN=PHLDB1 PE=1 SV=1	HUMAN	1
2	2	9.6	sp|Q86WA6|BPHL_HUMAN	Valacyclovir hydrolase OS=Homo sapiens GN=BPHL PE=1 SV=1	HUMAN	1
2	2	12.3	sp|Q86Y82|STX12_HUMAN	Syntaxin-12 OS=Homo sapiens GN=STX12 PE=1 SV=1	HUMAN	1
2	2	6	sp|Q8N129|CNPY4_HUMAN	Protein canopy homolog 4 OS=Homo sapiens GN=CNPY4 PE=2 SV=1	HUMAN	1
2	2	5.3	sp|Q8N1G4|LRC47_HUMAN	Leucine-rich repeat-containing protein 47 OS=Homo sapiens GN=LRRC47 PE=1 SV=1	HUMAN	1
2	2	5.4	sp|Q8N357|CB018_HUMAN	Transmembrane protein C2orf18 OS=Homo sapiens GN=C2orf18 PE=1 SV=1	HUMAN	1
2	2.15	10.1	sp|Q8N490|PNKD_HUMAN	Probable hydrolase PNKD OS=Homo sapiens GN=PNKD PE=1 SV=2	HUMAN	1
2	2	5.6	sp|Q8N766|K0090_HUMAN	Uncharacterized protein KIAA0090 OS=Homo sapiens GN=KIAA0090 PE=1 SV=1	HUMAN	1
2	2	5.3	sp|Q8NBJ5|GT251_HUMAN	Procollagen galactosyltransferase 1 OS=Homo sapiens GN=GLT25D1 PE=1 SV=1	HUMAN	1
2	2	4.3	sp|Q8NBJ7|SUMF2_HUMAN	Sulfatase-modifying factor 2 OS=Homo sapiens GN=SUMF2 PE=1 SV=2	HUMAN	1
2	2	20.6	sp|Q8TAD7|OCC1_HUMAN	Overexpressed in colon carcinoma 1 protein OS=Homo sapiens GN=OCC1 PE=1 SV=2	HUMAN	1
2	2	4.7	sp|Q8WVM8|SCFD1_HUMAN	Sec1 family domain-containing protein 1 OS=Homo sapiens GN=SCFD1 PE=1 SV=4	HUMAN	1
2	2.01	5.5	sp|Q92508|PIEZ1_HUMAN	Piezo-type mechanosensitive ion channel component 1 OS=Homo sapiens GN=PIEZO1 PE=1 SV=4	HUMAN	1
2	2.05	8.5	sp|Q92805|GOGA1_HUMAN	Golgin subfamily A member 1 OS=Homo sapiens GN=GOLGA1 PE=1 SV=3	HUMAN	1

Unused	Total	% Cov	Accession #	Name	Species	Peptides(95%)
2	2	10.2	sp|Q96CX2|KCD12_HUMAN	BTB/POZ domain-containing protein KCTD12 OS=Homo sapiens GN=KCTD12 PE=1 SV=1	HUMAN	1
2	2	6.7	sp|Q96EY7|PTCD3_HUMAN	Pentatricopeptide repeat-containing protein 3, mitochondrial OS=Homo sapiens GN=PTCD3 PE=1 SV=3	HUMAN	1
2	2	10.5	sp|Q96I23|PREY_HUMAN	Protein preY, mitochondrial OS=Homo sapiens GN=PREY PE=1 SV=1	HUMAN	1
2	2.01	7.4	sp|Q96P63|SPB12_HUMAN	Serpin B12 OS=Homo sapiens GN=SERPINB12 PE=1 SV=1	HUMAN	1
2	2	8.8	sp|Q96RQ3|MCCA_HUMAN	Methylcrotonoyl-CoA carboxylase subunit alpha, mitochondrial OS=Homo sapiens GN=MCCC1 PE=1 SV=3	HUMAN	1
2	2	5.1	sp|Q99536|VAT1_HUMAN	Synaptic vesicle membrane protein VAT-1 homolog OS=Homo sapiens GN=VAT1 PE=1 SV=2	HUMAN	1
2	2	8.4	sp|Q99757|THIOM_HUMAN	Thioredoxin, mitochondrial OS=Homo sapiens GN=TXN2 PE=1 SV=2	HUMAN	1
2	2	6.4	sp|Q99832|TCPH_HUMAN	T-complex protein 1 subunit eta OS=Homo sapiens GN=CCT7 PE=1 SV=2	HUMAN	1
2	2	8.1	sp|Q9BRA2|TXD17_HUMAN	Thioredoxin domain-containing protein 17 OS=Homo sapiens GN=TXNDC17 PE=1 SV=1	HUMAN	1
2	2	6.6	sp|Q9BRK5|CAB45_HUMAN	45 kDa calcium-binding protein OS=Homo sapiens GN=SDF4 PE=1 SV=1	HUMAN	1
2	2	7.4	sp|Q9BXK5|B2L13_HUMAN	Bcl-2-like protein 13 OS=Homo sapiens GN=BCL2L13 PE=1 SV=1	HUMAN	1
2	2	8.4	sp|Q9BYD1|RM13_HUMAN	39S ribosomal protein L13, mitochondrial OS=Homo sapiens GN=MRPL13 PE=1 SV=1	HUMAN	1
2	2.06	16.5	sp|Q9BYD2|RM09_HUMAN	39S ribosomal protein L9, mitochondrial OS=Homo sapiens GN=MRPL9 PE=1 SV=2	HUMAN	1
2	2	10.3	sp|Q9BYD3|RM04_HUMAN	39S ribosomal protein L4, mitochondrial OS=Homo sapiens GN=MRPL4 PE=1 SV=1	HUMAN	1
2	2.01	6.7	sp|Q9BZF1|OSBL8_HUMAN	Oxysterol-binding protein-related protein 8 OS=Homo sapiens GN=OSBPL8 PE=1 SV=3	HUMAN	1
2	2	6.7	sp|Q9C0C2|TB182_HUMAN	182 kDa tankyrase-1-binding protein OS=Homo sapiens GN=TNKS1BP1 PE=1 SV=4	HUMAN	1
2	2	3.4	sp|Q9H2V7|SPNS1_HUMAN	Protein spinster homolog 1 OS=Homo sapiens GN=SPNS1 PE=1 SV=1	HUMAN	1
2	2	7.4	sp|Q9H4A6|GOLP3_HUMAN	Golgi phosphoprotein 3 OS=Homo sapiens GN=GOLPH3 PE=1 SV=1	HUMAN	1
2	2	7.4	sp|Q9H4I3|TRABD_HUMAN	TraB domain-containing protein OS=Homo sapiens GN=TRABD PE=2 SV=1	HUMAN	1
2	2	9	sp|Q9HA77|SYCM_HUMAN	Probable cysteine--tRNA ligase, mitochondrial OS=Homo sapiens GN=CARS2 PE=1 SV=1	HUMAN	1
2	2	11.6	sp|Q9NRV9|HEBP1_HUMAN	Heme-binding protein 1 OS=Homo sapiens GN=HEBP1 PE=1 SV=1	HUMAN	1
2	2	5.7	sp|Q9NRX2|RM17_HUMAN	39S ribosomal protein L17, mitochondrial OS=Homo sapiens GN=MRPL17 PE=1 SV=1	HUMAN	1
2	2	9	sp|Q9NSD9|SYFB_HUMAN	Phenylalanine--tRNA ligase beta chain OS=Homo sapiens GN=FARSB PE=1 SV=3	HUMAN	1
2	2	12.7	sp|Q9NZU7|CABP1_HUMAN	Calcium-binding protein 1 OS=Homo sapiens GN=CABP1 PE=1 SV=5	HUMAN	1
2	2.06	9.6	sp|Q9P0K7|RAI14_HUMAN	Ankycorbin OS=Homo sapiens GN=RAI14 PE=1 SV=2	HUMAN	1
2	2	8.5	sp|Q9UBQ7|GRHPR_HUMAN	Glyoxylate reductase/hydroxypyruvate reductase OS=Homo sapiens GN=GRHPR PE=1 SV=1	HUMAN	1
2	2	7.9	sp|Q9UG63|ABCF2_HUMAN	ATP-binding cassette sub-family F member 2 OS=Homo sapiens GN=ABCF2 PE=1 SV=2	HUMAN	1
2	2	7.9	sp|Q9UH62|ARMX3_HUMAN	Armadillo repeat-containing X-linked protein 3 OS=Homo sapiens GN=ARMCX3 PE=1 SV=1	HUMAN	1
2	2	9.8	sp|Q9UJU6|DBNL_HUMAN	Drebrin-like protein OS=Homo sapiens GN=DBNL PE=1 SV=1	HUMAN	1
2	2.02	22.9	sp|Q9UKY7|CDV3_HUMAN	Protein CDV3 homolog OS=Homo sapiens GN=CDV3 PE=1 SV=1	HUMAN	1
2	2	7.1	sp|Q9UL46|PSME2_HUMAN	Proteasome activator complex subunit 2 OS=Homo sapiens GN=PSME2 PE=1 SV=4	HUMAN	1
2	2	14	sp|Q9UMX5|NENF_HUMAN	Neudesin OS=Homo sapiens GN=NENF PE=1 SV=1	HUMAN	1
2	2	19.2	sp|Q9UMY4|SNX12_HUMAN	Sorting nexin-12 OS=Homo sapiens GN=SNX12 PE=1 SV=3	HUMAN	1
2	2.02	10.2	sp|Q9UQ80|PA2G4_HUMAN	Proliferation-associated protein 2G4 OS=Homo sapiens GN=PA2G4 PE=1 SV=3	HUMAN	1
2	2	4.5	sp|Q9Y285|SYFA_HUMAN	Phenylalanine--tRNA ligase alpha chain OS=Homo sapiens GN=FARSA PE=1 SV=3	HUMAN	1
2	2	9.2	sp|Q9Y3A5|SBDS_HUMAN	Ribosome maturation protein SBDS OS=Homo sapiens GN=SBDS PE=1 SV=4	HUMAN	1
2	2	20.1	sp|Q9Y3E5|PTH2_HUMAN	Peptidyl-tRNA hydrolase 2, mitochondrial OS=Homo sapiens GN=PTRH2 PE=1 SV=1	HUMAN	1
2	2.38	7.4	sp|Q9Y4G6|TLN2_HUMAN	Talin-2 OS=Homo sapiens GN=TLN2 PE=1 SV=4	HUMAN	1
2	2	25.3	sp|Q9Y5L4|TIM13_HUMAN	Mitochondrial import inner membrane translocase subunit Tim13 OS=Homo sapiens GN=TIMM13 PE=1 SV=1	HUMAN	1
1.92	2	7.4	sp|P50213|IDH3A_HUMAN	Isocitrate dehydrogenase [NAD] subunit alpha, mitochondrial OS=Homo sapiens GN=IDH3A PE=1 SV=1	HUMAN	1
1.9	2.02	6.3	sp|P63244|GBLP_HUMAN	Guanine nucleotide-binding protein subunit beta-2-like 1 OS=Homo sapiens GN=GNB2L1 PE=1 SV=3	HUMAN	1
1.9	1.9	6.3	sp|Q9NVH1|DJC11_HUMAN	DnaJ homolog subfamily C member 11 OS=Homo sapiens GN=DNAJC11 PE=1 SV=2	HUMAN	1
1.89	1.89	7.3	sp|P48960|CD97_HUMAN	CD97 antigen OS=Homo sapiens GN=CD97 PE=1 SV=4	HUMAN	1
1.89	1.89	7.1	sp|Q12841|FSTL1_HUMAN	Follistatin-related protein 1 OS=Homo sapiens GN=FSTL1 PE=1 SV=1	HUMAN	1
1.89	1.89	21.9	sp|Q9Y3B8|ORN_HUMAN	Oligoribonuclease, mitochondrial OS=Homo sapiens GN=REXO2 PE=1 SV=3	HUMAN	1
1.88	2	9.1	sp|P26006|ITA3_HUMAN	Integrin alpha-3 OS=Homo sapiens GN=ITGA3 PE=1 SV=5	HUMAN	1
1.82	1.82	7.6	sp|P08962|CD63_HUMAN	CD63 antigen OS=Homo sapiens GN=CD63 PE=1 SV=2	HUMAN	1
1.81	1.81	23.8	sp|P15954|COX7C_HUMAN	Cytochrome c oxidase subunit 7C, mitochondrial OS=Homo sapiens GN=COX7C PE=1 SV=1	HUMAN	1
1.81	1.81	38.1	sp|Q9Y3U8|RL36_HUMAN	60S ribosomal protein L36 OS=Homo sapiens GN=RPL36 PE=1 SV=3	HUMAN	1
1.77	1.88	6.2	sp|P28838|AMPL_HUMAN	Cytosol aminopeptidase OS=Homo sapiens GN=LAP3 PE=1 SV=3	HUMAN	1
1.77	1.83	9	sp|Q13084|RM28_HUMAN	39S ribosomal protein L28, mitochondrial OS=Homo sapiens GN=MRPL28 PE=1 SV=4	HUMAN	1
1.74	1.74	16.8	sp|Q16864|VATF_HUMAN	V-type proton ATPase subunit F OS=Homo sapiens GN=ATP6V1F PE=1 SV=2	HUMAN	1
1.72	1.72	9.4	sp|O43920|NDUS5_HUMAN	NADH dehydrogenase [ubiquinone] iron-sulfur protein 5 OS=Homo sapiens GN=NDUFS5 PE=1 SV=3	HUMAN	1
1.72	1.72	15.5	sp|Q16718|NDUA5_HUMAN	NADH dehydrogenase [ubiquinone] 1 alpha subcomplex subunit 5 OS=Homo sapiens GN=NDUFA5 PE=1 SV=3	HUMAN	1
1.72	1.72	11	sp|Q92520|FAM3C_HUMAN	Protein FAM3C OS=Homo sapiens GN=FAM3C PE=1 SV=1	HUMAN	1
1.7	1.7	9.4	sp|P13987|CD59_HUMAN	CD59 glycoprotein OS=Homo sapiens GN=CD59 PE=1 SV=1	HUMAN	1
1.7	1.7	25	sp|P22392|NDKB_HUMAN	Nucleoside diphosphate kinase B OS=Homo sapiens GN=NME2 PE=1 SV=1	HUMAN	1
1.68	1.68	5.6	sp|O95817|BAG3_HUMAN	BAG family molecular chaperone regulator 3 OS=Homo sapiens GN=BAG3 PE=1 SV=3	HUMAN	1
1.66	1.66	7	sp|P42704|LPPRC_HUMAN	Leucine-rich PPR motif-containing protein, mitochondrial OS=Homo sapiens GN=LRPPRC PE=1 SV=3	HUMAN	1
1.64	1.64	10.5	sp|O75367|H2AY_HUMAN	Core histone macro-H2A.1 OS=Homo sapiens GN=H2AFY PE=1 SV=4	HUMAN	1
1.64	2.08	12.7	sp|P51991|ROA3_HUMAN	Heterogeneous nuclear ribonucleoprotein A3 OS=Homo sapiens GN=HNRNPA3 PE=1 SV=2	HUMAN	1
1.64	1.65	20.7	sp|Q00059|TFAM_HUMAN	Transcription factor A, mitochondrial OS=Homo sapiens GN=TFAM PE=1 SV=1	HUMAN	1
1.64	1.64	7.8	sp|Q9NTJ5|SAC1_HUMAN	Phosphatidylinositide phosphatase SAC1 OS=Homo sapiens GN=SACM1L PE=1 SV=2	HUMAN	1
1.62	1.62	8.7	sp|Q9Y295|DRG1_HUMAN	Developmentally-regulated GTP-binding protein 1 OS=Homo sapiens GN=DRG1 PE=1 SV=1	HUMAN	1
1.6	1.6	5.3	sp|Q99613|EIF3C_HUMAN	Eukaryotic translation initiation factor 3 subunit C OS=Homo sapiens GN=EIF3C PE=1 SV=1	HUMAN	1
1.59	1.59	10.4	sp|P14384|CBPM_HUMAN	Carboxypeptidase M OS=Homo sapiens GN=CPM PE=1 SV=2	HUMAN	1
1.59	1.59	48.9	sp|P62072|TIM10_HUMAN	Mitochondrial import inner membrane translocase subunit Tim10 OS=Homo sapiens GN=TIMM10 PE=1 SV=1	HUMAN	1
1.55	1.55	17.3	sp|O95292|VAPB_HUMAN	Vesicle-associated membrane protein-associated protein B/C OS=Homo sapiens GN=VAPB PE=1 SV=3	HUMAN	1
1.55	1.55	10.1	sp|P33908|MA1A1_HUMAN	Mannosyl-oligosaccharide 1,2-alpha-mannosidase IA OS=Homo sapiens GN=MAN1A1 PE=1 SV=3	HUMAN	1
1.54	1.54	5.9	sp|P13489|RINI_HUMAN	Ribonuclease inhibitor OS=Homo sapiens GN=RNH1 PE=1 SV=2	HUMAN	1
1.52	1.52	3.4	sp|Q9HBR0|S38AA_HUMAN	Putative sodium-coupled neutral amino acid transporter 10 OS=Homo sapiens GN=SLC38A10 PE=1 SV=2	HUMAN	1
1.51	1.51	4.5	sp|O75083|WDR1_HUMAN	WD repeat-containing protein 1 OS=Homo sapiens GN=WDR1 PE=1 SV=4	HUMAN	1
1.5	1.5	16.2	sp|Q9Y6M9|NDUB9_HUMAN	NADH dehydrogenase [ubiquinone] 1 beta subcomplex subunit 9 OS=Homo sapiens GN=NDUFB9 PE=1 SV=3	HUMAN	1
1.49	1.49	6.2	sp|P49406|RM19_HUMAN	39S ribosomal protein L19, mitochondrial OS=Homo sapiens GN=MRPL19 PE=1 SV=2	HUMAN	1
1.49	1.49	6.8	sp|Q14103|HNRPD_HUMAN	Heterogeneous nuclear ribonucleoprotein D0 OS=Homo sapiens GN=HNRNPD PE=1 SV=1	HUMAN	1
1.48	1.49	10.3	sp|Q969G5|PRDBP_HUMAN	Protein kinase C delta-binding protein OS=Homo sapiens GN=PRKCDBP PE=1 SV=3	HUMAN	1
1.46	1.46	7	sp|P80404|GABT_HUMAN	4-aminobutyrate aminotransferase, mitochondrial OS=Homo sapiens GN=ABAT PE=1 SV=3	HUMAN	1
1.44	1.44	12.5	sp|Q99538|LGMN_HUMAN	Legumain OS=Homo sapiens GN=LGMN PE=1 SV=1	HUMAN	1
1.43	1.43	8.5	sp|O75251|NDUS7_HUMAN	NADH dehydrogenase [ubiquinone] iron-sulfur protein 7, mitochondrial OS=Homo sapiens GN=NDUFS7 PE=1 SV	HUMAN	1
1.43	1.43	5.5	sp|Q92896|GSLG1_HUMAN	Golgi apparatus protein 1 OS=Homo sapiens GN=GLG1 PE=1 SV=2	HUMAN	1
1.41	1.41	9.9	sp|O94766|B3GA3_HUMAN	Galactosylgalactosylxylosylprotein 3-beta-glucuronosyltransferase 3 OS=Homo sapiens GN=B3GAT3 PE=1 SV=2	HUMAN	1
1.39	1.39	38.1	sp|P61927|RL37_HUMAN	60S ribosomal protein L37 OS=Homo sapiens GN=RPL37 PE=1 SV=2	HUMAN	1
1.37	1.37	7.7	sp|P61158|ARP3_HUMAN	Actin-related protein 3 OS=Homo sapiens GN=ACTR3 PE=1 SV=3	HUMAN	1
1.36	1.41	5.8	sp|Q5JRA6|MIA3_HUMAN	Melanoma inhibitory activity protein 3 OS=Homo sapiens GN=MIA3 PE=1 SV=1	HUMAN	1
1.36	1.41	13.5	sp|Q9Y6C9|MTCH2_HUMAN	Mitochondrial carrier homolog 2 OS=Homo sapiens GN=MTCH2 PE=1 SV=1	HUMAN	1
1.35	1.35	7.6	sp|P21980|TGM2_HUMAN	Protein-glutamine gamma-glutamyltransferase 2 OS=Homo sapiens GN=TGM2 PE=1 SV=2	HUMAN	1
1.35	1.35	5.9	sp|Q8WX93|PALLD_HUMAN	Palladin OS=Homo sapiens GN=PALLD PE=1 SV=3	HUMAN	1

Unused	Total	% Cov	Accession #	Name	Species	Peptides(95%)
1.35	1.35	12.2	sp|Q9UNE7|CHIP_HUMAN	E3 ubiquitin-protein ligase CHIP OS=Homo sapiens GN=STUB1 PE=1 SV=2	HUMAN	1
1.34	1.34	20	sp|P63173|RL38_HUMAN	60S ribosomal protein L38 OS=Homo sapiens GN=RPL38 PE=1 SV=2	HUMAN	1
1.32	1.36	5.2	sp|Q14789|GOGB1_HUMAN	Golgin subfamily B member 1 OS=Homo sapiens GN=GOLGB1 PE=1 SV=2	HUMAN	1
1.28	1.28	6	sp|Q9H2D6|TARA_HUMAN	TRIO and F-actin-binding protein OS=Homo sapiens GN=TRIOBP PE=1 SV=3	HUMAN	1
1.27	1.27	5.9	sp|Q9UHQ9|NB5R1_HUMAN	NADH-cytochrome b5 reductase 1 OS=Homo sapiens GN=CYB5R1 PE=1 SV=1	HUMAN	1
1.24	1.24	6.8	sp|O43837|IDH3B_HUMAN	Isocitrate dehydrogenase [NAD] subunit beta, mitochondrial OS=Homo sapiens GN=IDH3B PE=1 SV=2	HUMAN	1
1.24	1.24	3	sp|P23142|FBLN1_HUMAN	Fibulin-1 OS=Homo sapiens GN=FBLN1 PE=1 SV=4	HUMAN	1
1.24	1.24	33.3	sp|Q5VTU8|AT5EL_HUMAN	ATP synthase subunit epsilon-like protein, mitochondrial OS=Homo sapiens GN=ATP5EP2 PE=1 SV=1	HUMAN	1
1.23	1.23	45	sp|P62829|RL23_HUMAN	60S ribosomal protein L23 OS=Homo sapiens GN=RPL23 PE=1 SV=1	HUMAN	1
1.23	1.25	6.6	sp|P78344|IF4G2_HUMAN	Eukaryotic translation initiation factor 4 gamma 2 OS=Homo sapiens GN=EIF4G2 PE=1 SV=1	HUMAN	1
1.2	1.2	13.4	sp|O95563|BR44_HUMAN	Brain protein 44 OS=Homo sapiens GN=BRP44 PE=1 SV=1	HUMAN	1
1.17	1.17	11	sp|Q6UWF9|F180A_HUMAN	Protein FAM180A OS=Homo sapiens GN=FAM180A PE=2 SV=1	HUMAN	1
1.13	1.13	4.6	sp|Q9HCU0|CD248_HUMAN	Endosialin OS=Homo sapiens GN=CD248 PE=1 SV=1	HUMAN	1
1.12	1.12	24.3	sp|O75964|ATP5L_HUMAN	ATP synthase subunit g, mitochondrial OS=Homo sapiens GN=ATP5L PE=1 SV=3	HUMAN	1
1.11	1.11	16.6	sp|Q9BX68|HINT2_HUMAN	Histidine triad nucleotide-binding protein 2, mitochondrial OS=Homo sapiens GN=HINT2 PE=1 SV=1	HUMAN	1
1.07	1.07	28.8	sp|P62851|RS25_HUMAN	40S ribosomal protein S25 OS=Homo sapiens GN=RPS25 PE=1 SV=1	HUMAN	1
1.06	1.06	4.8	sp|O94832|MYO1D_HUMAN	Myosin-Id OS=Homo sapiens GN=MYO1D PE=1 SV=2	HUMAN	1
1.05	1.05	8.4	sp|Q14247|SRC8_HUMAN	Src substrate cortactin OS=Homo sapiens GN=CTTN PE=1 SV=2	HUMAN	1
1.04	1.04	13.2	sp|P03928|ATP8_HUMAN	ATP synthase protein 8 OS=Homo sapiens GN=MT-ATP8 PE=1 SV=1	HUMAN	1
1.01	1.01	9	sp|P09543|CN37_HUMAN	2',3'-cyclic-nucleotide 3'-phosphodiesterase OS=Homo sapiens GN=CNP PE=1 SV=2	HUMAN	1
1	1	13.7	sp|Q14696|MESD_HUMAN	LDLR chaperone MESD OS=Homo sapiens GN=MESDC2 PE=1 SV=2	HUMAN	1
0.98	0.98	6.9	sp|Q9UHG3|PCYOX_HUMAN	Prenylcysteine oxidase 1 OS=Homo sapiens GN=PCYOX1 PE=1 SV=3	HUMAN	1
0.95	0.95	8.7	sp|P40925|MDHC_HUMAN	Malate dehydrogenase, cytoplasmic OS=Homo sapiens GN=MDH1 PE=1 SV=4	HUMAN	1
0.95	0.95	2.8	sp|P49189|AL9A1_HUMAN	4-trimethylaminobutyraldehyde dehydrogenase OS=Homo sapiens GN=ALDH9A1 PE=1 SV=3	HUMAN	1
0.95	0.95	15.5	sp|P59998|ARPC4_HUMAN	Actin-related protein 2/3 complex subunit 4 OS=Homo sapiens GN=ARPC4 PE=1 SV=3	HUMAN	1
0.94	0.96	16.7	sp|P32969|RL9_HUMAN	60S ribosomal protein L9 OS=Homo sapiens GN=RPL9 PE=1 SV=1	HUMAN	1
0.94	0.94	7.3	sp|Q96AB3|ISOC2_HUMAN	Isochorismatase domain-containing protein 2, mitochondrial OS=Homo sapiens GN=ISOC2 PE=1 SV=1	HUMAN	1
0.94	0.94	6.8	sp|Q9HC07|TM165_HUMAN	Transmembrane protein 165 OS=Homo sapiens GN=TMEM165 PE=1 SV=1	HUMAN	1
0.92	0.92	10.3	sp|Q13740|CD166_HUMAN	CD166 antigen OS=Homo sapiens GN=ALCAM PE=1 SV=2	HUMAN	1
0.87	0.87	2.8	sp|P08236|BGLR_HUMAN	Beta-glucuronidase OS=Homo sapiens GN=GUSB PE=1 SV=2	HUMAN	1
0.82	0.82	2.8	sp|O60637|TSN3_HUMAN	Tetraspanin-3 OS=Homo sapiens GN=TSPAN3 PE=2 SV=1	HUMAN	1
0.79	0.79	14.7	sp|O94760|DDAH1_HUMAN	N(G),N(G)-dimethylarginine dimethylaminohydrolase 1 OS=Homo sapiens GN=DDAH1 PE=1 SV=3	HUMAN	1
0.76	0.76	5.3	sp|P33121|ACSL1_HUMAN	Long-chain-fatty-acid--CoA ligase 1 OS=Homo sapiens GN=ACSL1 PE=1 SV=1	HUMAN	1
0.76	0.76	9.4	sp|Q9H553|ALG2_HUMAN	Alpha-1,3/1,6-mannosyltransferase ALG2 OS=Homo sapiens GN=ALG2 PE=2 SV=1	HUMAN	1
0.74	0.74	24.3	sp|P51571|SSRD_HUMAN	Translocon-associated protein subunit delta OS=Homo sapiens GN=SSR4 PE=1 SV=1	HUMAN	1
0.73	0.73	11.6	sp|O60784|TOM1_HUMAN	Target of Myb protein 1 OS=Homo sapiens GN=TOM1 PE=1 SV=2	HUMAN	1
0.72	0.72	15.3	sp|P17568|NDUB7_HUMAN	NADH dehydrogenase [ubiquinone] 1 beta subcomplex subunit 7 OS=Homo sapiens GN=NDUFB7 PE=1 SV=4	HUMAN	1
0.7	0.7	2.9	sp|Q16832|DDR2_HUMAN	Discoidin domain-containing receptor 2 OS=Homo sapiens GN=DDR2 PE=1 SV=2	HUMAN	1
0.69	0.69	9.5	sp|Q14152|EIF3A_HUMAN	Eukaryotic translation initiation factor 3 subunit A OS=Homo sapiens GN=EIF3A PE=1 SV=1	HUMAN	1
0.67	0.67	5.9	sp|Q9UP95|S12A4_HUMAN	Solute carrier family 12 member 4 OS=Homo sapiens GN=SLC12A4 PE=1 SV=2	HUMAN	1
0.66	0.67	8.2	sp|Q9BXL7|CAR11_HUMAN	Caspase recruitment domain-containing protein 11 OS=Homo sapiens GN=CARD11 PE=1 SV=3	HUMAN	1
0.64	0.68	11.7	sp|P29692|EF1D_HUMAN	Elongation factor 1-delta OS=Homo sapiens GN=EEF1D PE=1 SV=5	HUMAN	1
0.64	0.64	6.8	sp|P54727|RD23B_HUMAN	UV excision repair protein RAD23 homolog B OS=Homo sapiens GN=RAD23B PE=1 SV=1	HUMAN	1
0.63	0.63	5.6	sp|O95479|G6PE_HUMAN	GDH/6PGL endoplasmic bifunctional protein OS=Homo sapiens GN=H6PD PE=1 SV=2	HUMAN	1
0.62	0.62	6.3	sp|Q15942|ZYX_HUMAN	Zyxin OS=Homo sapiens GN=ZYX PE=1 SV=1	HUMAN	1
0.61	0.61	10.7	sp|P30536|TSPOA_HUMAN	Translocator protein OS=Homo sapiens GN=TSPO PE=1 SV=3	HUMAN	1
0.59	0.62	7.5	sp|Q9UH65|SWP70_HUMAN	Switch-associated protein 70 OS=Homo sapiens GN=SWAP70 PE=1 SV=1	HUMAN	1
0.58	0.58	8.3	sp|P16278|BGAL_HUMAN	Beta-galactosidase OS=Homo sapiens GN=GLB1 PE=1 SV=2	HUMAN	1
0.58	0.59	7.9	sp|P46013|KI67_HUMAN	Antigen KI-67 OS=Homo sapiens GN=MKI67 PE=1 SV=2	HUMAN	1
0.57	0.57	11.3	sp|P62847|RS24_HUMAN	40S ribosomal protein S24 OS=Homo sapiens GN=RPS24 PE=1 SV=1	HUMAN	1
0.57	0.57	5.6	sp|Q14019|COTL1_HUMAN	Coactosin-like protein OS=Homo sapiens GN=COTL1 PE=1 SV=3	HUMAN	1
0.56	0.56	4.1	sp|P06241|FYN_HUMAN	Tyrosine-protein kinase Fyn OS=Homo sapiens GN=FYN PE=1 SV=3	HUMAN	1
0.56	0.56	9.9	sp|P09110|THIK_HUMAN	3-ketoacyl-CoA thiolase, peroxisomal OS=Homo sapiens GN=ACAA1 PE=1 SV=2	HUMAN	1
0.55	0.56	4.2	sp|Q6PI48|SYDM_HUMAN	Aspartate--tRNA ligase, mitochondrial OS=Homo sapiens GN=DARS2 PE=1 SV=1	HUMAN	1
0.53	0.53	9	sp|P02749|APOH_HUMAN	Beta-2-glycoprotein 1 OS=Homo sapiens GN=APOH PE=1 SV=3	HUMAN	1
0.46	0.46	3	sp|O94874|UFL1_HUMAN	E3 UFM1-protein ligase 1 OS=Homo sapiens GN=UFL1 PE=1 SV=2	HUMAN	1
0.46	0.47	25.1	sp|P40429|RL13A_HUMAN	60S ribosomal protein L13a OS=Homo sapiens GN=RPL13A PE=1 SV=2	HUMAN	1
0.45	0.45	7.9	sp|P05090|APOD_HUMAN	Apolipoprotein D OS=Homo sapiens GN=APOD PE=1 SV=1	HUMAN	1
0.39	0.39	5.1	sp|Q15436|SC23A_HUMAN	Protein transport protein Sec23A OS=Homo sapiens GN=SEC23A PE=1 SV=2	HUMAN	1
0.39	0.4	9.6	sp|Q6YN16|HSDL2_HUMAN	Hydroxysteroid dehydrogenase-like protein 2 OS=Homo sapiens GN=HSDL2 PE=1 SV=1	HUMAN	1
0.35	0.35	4.1	sp|P06744|G6PI_HUMAN	Glucose-6-phosphate isomerase OS=Homo sapiens GN=GPI PE=1 SV=4	HUMAN	1
0.32	0.32	6.7	sp|P17987|TCPA_HUMAN	T-complex protein 1 subunit alpha OS=Homo sapiens GN=TCP1 PE=1 SV=1	HUMAN	1
0.2	0.2	16.5	sp|Q86Y30|BAGE2_HUMAN	B melanoma antigen 2 OS=Homo sapiens GN=BAGE2 PE=2 SV=1	HUMAN	1
0.13	0.13	43.4	sp|Q969Q0|RL36L_HUMAN	60S ribosomal protein L36a-like OS=Homo sapiens GN=RPL36AL PE=1 SV=3	HUMAN	1
0.1	0.16	8.2	sp|Q9UNQ0|ABCG2_HUMAN	ATP-binding cassette sub-family G member 2 OS=Homo sapiens GN=ABCG2 PE=1 SV=3	HUMAN	1
0.09	0.09	7.6	sp|P48382|RFX5_HUMAN	DNA-binding protein RFX5 OS=Homo sapiens GN=RFX5 PE=1 SV=1	HUMAN	1
0.09	0.09	6.4	sp|P51970|NDUA8_HUMAN	NADH dehydrogenase [ubiquinone] 1 alpha subcomplex subunit 8 OS=Homo sapiens GN=NDUFA8 PE=1 SV=3	HUMAN	1
0.09	0.09	6.6	sp|Q9H6S3|ES8L2_HUMAN	Epidermal growth factor receptor kinase substrate 8-like protein 2 OS=Homo sapiens GN=EPS8L2 PE=1 SV=2	HUMAN	1
0.08	0.11	5.8	sp|P12270|TPR_HUMAN	Nucleoprotein TPR OS=Homo sapiens GN=TPR PE=1 SV=3	HUMAN	1
0.08	0.08	2	sp|P23942|PRPH2_HUMAN	Peripherin-2 OS=Homo sapiens GN=PRPH2 PE=1 SV=1	HUMAN	1
0.08	0.08	7.9	sp|Q14444|CAPR1_HUMAN	Caprin-1 OS=Homo sapiens GN=CAPRIN1 PE=1 SV=2	HUMAN	1
0.08	0.08	5.2	sp|Q96S59|RANB9_HUMAN	Ran-binding protein 9 OS=Homo sapiens GN=RANBP9 PE=1 SV=1	HUMAN	1

Supplemental table S2B - Differentially expressed proteins identified by comparative analysis of mitochondrial fraction of each of the patients studied with control subjects by nanoLC-MS/MS with iTRAQ labeling.

Protein	Acess Number	Pt1	Pt2
14-3-3 protein beta/alpha OS=Homo sapiens GN=YWHAB PE=1 SV=3	1433B_HUMAN	1.48	1.51
14-3-3 protein epsilon OS=Homo sapiens GN=YWHAE PE=1 SV=1	1433E_HUMAN	1.41	1.11
14-3-3 protein gamma OS=Homo sapiens GN=YWHAG PE=1 SV=2	1433G_HUMAN	1.47	1.58
14-3-3 protein theta OS=Homo sapiens GN=YWHAQ PE=1 SV=1	1433T_HUMAN	1.60	1.49
14-3-3 protein zeta/delta OS=Homo sapiens GN=YWHAZ PE=1 SV=1	1433Z_HUMAN	1.83	1.67
2-oxoglutarate dehydrogenase. mitochondrial	ODO1_HUMAN	NS	0.59
40S ribosomal protein S28 OS=Homo sapiens GN=RPS28 PE=1 SV=1	RS28_HUMAN	1.12	0.55
40S ribosomal protein S8 OS=Homo sapiens GN=RPS8 PE=1 SV=2	RS8_HUMAN	1.18	1.49
60S ribosomal protein L21 OS=Homo sapiens GN=RPL21 PE=1 SV=2	RL21_HUMAN	1.39	1.05
60S ribosomal protein L29 OS=Homo sapiens GN=RPL29 PE=1 SV=2	RL29_HUMAN	1.61	1.48
60S ribosomal protein L8 OS=Homo sapiens GN=RPL8 PE=1 SV=2	RL8_HUMAN	1.25	1.40
7-dehydrocholesterol reductase OS=Homo sapiens GN=DHCR7 PE=1 SV=1	DHCR7_HUMAN	1.32	0.99
A-kinase anchor protein 2 OS=Homo sapiens GN=AKAP2 PE=1 SV=3	AKAP2_HUMAN	1.44	1.57
Actin. cytoplasmic 1 OS=Homo sapiens GN=ACTB PE=1 SV=1	ACTB_HUMAN	1.45	1.31
Adenylyl cyclase-associated protein 1 OS=Homo sapiens GN=CAP1 PE=1 SV=5	CAP1_HUMAN	1.33	1.56
Alpha-actinin-4 OS=Homo sapiens GN=ACTN4 PE=1 SV=2	ACTN4_HUMAN	1.41	1.41
Alpha-enolase OS=Homo sapiens GN=ENO1 PE=1 SV=2	ENOA_HUMAN	1.39	1.69
Aminopeptidase N OS=Homo sapiens GN=ANPEP PE=1 SV=4	AMPN_HUMAN	1.53	1.24
Annexin A1 OS=Homo sapiens GN=ANXA1 PE=1 SV=2	ANXA1_HUMAN	1.52	0.80
Annexin A2 OS=Homo sapiens GN=ANXA2 PE=1 SV=2	ANXA2_HUMAN	2.03	1.66
Annexin A6 OS=Homo sapiens GN=ANXA6 PE=1 SV=3	ANXA6_HUMAN	1.75	1.50
Aspartyl/asparaginyl beta-hydroxylase OS=Homo sapiens GN=ASPH PE=1 SV=3	ASPH_HUMAN	0.86	0.60
Basigin OS=Homo sapiens GN=BSG PE=1 SV=2	BASI_HUMAN	1.44	1.10
Beta-hexosaminidase subunit beta OS=Homo sapiens GN=HEXB PE=1 SV=3	HEXB_HUMAN	0.79	0.61
Brain acid soluble protein 1	BASP1_HUMAN	1.06	1.61
Calmodulin OS=Homo sapiens GN=CALM1 PE=1 SV=2	CALM_HUMAN	1.80	1.59
Calumenin OS=Homo sapiens GN=CALU PE=1 SV=2	CALU_HUMAN	0.54	0.99
Catenin alpha-1 OS=Homo sapiens GN=CTNNA1 PE=1 SV=1	CTNA1_HUMAN	1.31	1.01
Cathepsin B OS=Homo sapiens GN=CTSB PE=1 SV=3	CATB_HUMAN	2.15	1.21
CD166 antigen	CD166_HUMAN	NS	1.68
Cofilin-1 OS=Homo sapiens GN=CFL1 PE=1 SV=3	COF1_HUMAN	1.67	1.65
Collagen alpha-1(I) chain OS=Homo sapiens GN=COL1A1 PE=1 SV=5	CO1A1_HUMAN	0.70	1.42
Collagen alpha-2(I) chain OS=Homo sapiens GN=COL1A2 PE=1 SV=7	CO1A2_HUMAN	1.04	1.34
Core histone macro-H2A.1 OS=Homo sapiens GN=H2AFY PE=1 SV=4	H2AY_HUMAN	0.68	0.83
Coronin-1C OS=Homo sapiens GN=CORO1C PE=1 SV=1	COR1C_HUMAN	1.53	1.44
Cysteine and glycine-rich protein 1 OS=Homo sapiens GN=CSRP1 PE=1 SV=3	CSRP1_HUMAN	1.79	1.23
Cytochrome b-c1 complex subunit 1. mitochondrial	QCR1_HUMAN	NS	0.63
Cytoskeleton-associated protein 4 OS=Homo sapiens GN=CKAP4 PE=1 SV=2	CKAP4_HUMAN	0.66	0.83
Dihydropyrimidinase-related protein 2 OS=Homo sapiens GN=DPYSL2 PE=1 SV=1	DPYL2_HUMAN	1.66	1.36
Dolichyl-diphosphooligosaccharide--protein glycosyltransferase subunit 1 OS=Homo sapiens GN=RPN1 PE=1 SV=1	RPN1_HUMAN	0.69	0.76
Drebrin OS=Homo sapiens GN=DBN1 PE=1 SV=4	DREB_HUMAN	1.76	1.29
Dynactin subunit 2 OS=Homo sapiens GN=DCTN2 PE=1 SV=4	DCTN2_HUMAN	1.53	1.36
Elongation factor 1-delta OS=Homo sapiens GN=EEF1D PE=1 SV=5	EF1D_HUMAN	1.37	1.56
Elongation factor 1-gamma OS=Homo sapiens GN=EEF1G PE=1 SV=3	EF1G_HUMAN	1.27	1.52
Emerin OS=Homo sapiens GN=EMD PE=1 SV=1	EMD_HUMAN	0.64	0.70
Endoplasmin OS=Homo sapiens GN=HSP90B1 PE=1 SV=1	ENPL_HUMAN	0.72	0.63
Epidermal growth factor receptor OS=Homo sapiens GN=EGFR PE=1 SV=2	EGFR_HUMAN	1.72	1.26
Erlin-1 OS=Homo sapiens GN=ERLIN1 PE=1 SV=1	ERLN1_HUMAN	0.88	0.70
Eukaryotic initiation factor 4A-II OS=Homo sapiens GN=EIF4A2 PE=1 SV=2	IF4A2_HUMAN	1.49	1.42
Ezrin OS=Homo sapiens GN=EZR PE=1 SV=4	EZRI_HUMAN	1.62	1.58
F-actin-capping protein subunit alpha-1 OS=Homo sapiens GN=CAPZA1 PE=1 SV=3	CAZA1_HUMAN	1.56	1.38
F-actin-capping protein subunit alpha-2 OS=Homo sapiens GN=CAPZA2 PE=1 SV=3	CAZA2_HUMAN	1.36	1.23
Fatty acid synthase OS=Homo sapiens GN=FASN PE=1 SV=3	FAS_HUMAN	0.76	0.68
Galectin-1 OS=Homo sapiens GN=LGALS1 PE=1 SV=2	LEG1_HUMAN	1.64	1.53
Galectin-3 OS=Homo sapiens GN=LGALS3 PE=1 SV=5	LEG3_HUMAN	2.34	1.60
Glyceraldehyde-3-phosphate dehydrogenase OS=Homo sapiens GN=GAPDH PE=1 SV=3	G3P_HUMAN	1.21	1.54
Guanine nucleotide-binding protein G(i) subunit alpha-2 OS=Homo sapiens GN=GNAI2 PE=1 SV=3	GNAI2_HUMAN	2.24	1.49
Guanine nucleotide-binding protein G(s) subunit alpha isoforms XLas OS=Homo sapiens GN=GNAS PE=1 SV=2	GNAS1_HUMAN	1.36	1.12
Heat shock protein beta-1 OS=Homo sapiens GN=HSPB1 PE=1 SV=2	HSPB1_HUMAN	1.48	1.41
Heat shock protein HSP 90-alpha OS=Homo sapiens GN=HSP90AA1 PE=1 SV=5	HS90A_HUMAN	1.36	1.07
Heterogeneous nuclear ribonucleoprotein A1 OS=Homo sapiens GN=HNRNPA1 PE=1 SV=5	ROA1_HUMAN	0.70	1.17
Heterogeneous nuclear ribonucleoprotein M OS=Homo sapiens GN=HNRNPM PE=1 SV=3	HNRPM_HUMAN	0.69	0.84
Heterogeneous nuclear ribonucleoprotein U OS=Homo sapiens GN=HNRNPU PE=1 SV=6	HNRPU_HUMAN	0.63	0.94
Heterogeneous nuclear ribonucleoproteins A2/B1 OS=Homo sapiens GN=HNRNPA2B1 PE=1 SV=2	ROA2_HUMAN	0.59	0.81
Histone H1.4 OS=Homo sapiens GN=HIST1H1E PE=1 SV=2	H14_HUMAN	0.55	0.94
Histone H1.5 OS=Homo sapiens GN=HIST1H1B PE=1 SV=3	H15_HUMAN	0.52	0.86
Histone H2A type 1-C OS=Homo sapiens GN=HIST1H2AC PE=1 SV=3	H2A1C_HUMAN	0.68	0.85
Histone H2A type 1-J	H2A1J_HUMAN	0.35	NS
Histone H2B type 1-L OS=Homo sapiens GN=HIST1H2BL PE=1 SV=3	H2B1L_HUMAN	0.56	0.96
Histone H3.1 OS=Homo sapiens GN=HIST1H3A PE=1 SV=2	H31_HUMAN	0.67	0.88
Histone H4 OS=Homo sapiens GN=HIST1H4A PE=1 SV=2	H4_HUMAN	0.54	0.90
HLA class I histocompatibility antigen. A-3 alpha chain OS=Homo sapiens GN=HLA-A PE=1 SV=2	1A03_HUMAN	1.53	0.80
Hydroxyacyl-coenzyme A dehydrogenase. mitochondrial	HCDH_HUMAN	NS	0.65
Hypoxia up-regulated protein 1 OS=Homo sapiens GN=HYOU1 PE=1 SV=1	HYOU1_HUMAN	0.73	0.66
Inhibitor of nuclear factor kappa-B kinase-interacting protein OS=Homo sapiens GN=IKBIP PE=1 SV=1	IKIP_HUMAN	0.59	0.80
LIM and SH3 domain protein 1 OS=Homo sapiens GN=LASP1 PE=1 SV=2	LASP1_HUMAN	1.47	1.65
LIM domain only protein 7 OS=Homo sapiens GN=LMO7 PE=1 SV=3	LMO7_HUMAN	1.07	1.39
Magnesium transporter protein 1 OS=Homo sapiens GN=MAGT1 PE=1 SV=1	MAGT1_HUMAN	0.83	0.69

Protein	Acess Number	Pt1	Pt2
Microtubule-associated protein 4 OS=Homo sapiens GN=MAP4 PE=1 SV=3	MAP4_HUMAN	1.28	1.30
Moesin OS=Homo sapiens GN=MSN PE=1 SV=3	MOES_HUMAN	1.87	1.73
Myosin regulatory light polypeptide 9 OS=Homo sapiens GN=MYL9 PE=1 SV=4	MYL9_HUMAN	0.48	0.37
Myosin-10 OS=Homo sapiens GN=MYH10 PE=1 SV=3	MYH10_HUMAN	0.76	0.62
Myristoylated alanine-rich C-kinase substrate	MARCS_HUMAN	1.62	2.17
N-acetylglucosamine-6-sulfatase OS=Homo sapiens GN=GNS PE=1 SV=3	GNS_HUMAN	1.10	0.67
Neprilysin OS=Homo sapiens GN=MME PE=1 SV=2	NEP_HUMAN	1.51	1.30
Neuroblast differentiation-associated protein AHNAK OS=Homo sapiens GN=AHNAK PE=1 SV=2	AHNK_HUMAN	1.73	1.54
Neuroplastin OS=Homo sapiens GN=NPTN PE=1 SV=2	NPTN_HUMAN	1.32	1.49
Neutral alpha-glucosidase AB OS=Homo sapiens GN=GANAB PE=1 SV=3	GANAB_HUMAN	0.79	0.70
Neutral amino acid transporter B(0) OS=Homo sapiens GN=SLC1A5 PE=1 SV=2	AAAT_HUMAN	1.15	0.67
Non-POU domain-containing octamer-binding protein OS=Homo sapiens GN=NONO PE=1 SV=4	NONO_HUMAN	0.67	0.99
Peptidyl-prolyl cis-trans isomerase A OS=Homo sapiens GN=PPIA PE=1 SV=2	PPIA_HUMAN	1.78	1.15
Peptidyl-prolyl cis-trans isomerase B OS=Homo sapiens GN=PPIB PE=1 SV=2	PPIB_HUMAN	0.61	0.66
Peptidyl-prolyl cis-trans isomerase FKBP10 OS=Homo sapiens GN=FKBP10 PE=1 SV=1	FKB10_HUMAN	0.88	0.64
Peptidyl-prolyl cis-trans isomerase FKBP9 OS=Homo sapiens GN=FKBP9 PE=1 SV=2	FKBP9_HUMAN	0.65	0.54
Peroxiredoxin-1 OS=Homo sapiens GN=PRDX1 PE=1 SV=1	PRDX1_HUMAN	1.18	1.55
Peroxisomal multifunctional enzyme type 2	DHB4_HUMAN	0.64	0.61
Phosphoenolpyruvate carboxykinase [GTP]. mitochondrial OS=Homo sapiens GN=PCK2 PE=1 SV=3	PCKGM_HUMAN	0.75	0.63
Phosphoglycerate kinase 1 OS=Homo sapiens GN=PGK1 PE=1 SV=3	PGK1_HUMAN	0.66	0.69
Phosphoglycerate mutase 1 OS=Homo sapiens GN=PGAM1 PE=1 SV=2	PGAM1_HUMAN	1.41	1.08
Plasma membrane calcium-transporting ATPase 1 OS=Homo sapiens GN=ATP2B1 PE=1 SV=3	AT2B1_HUMAN	1.42	1.02
Plasma membrane calcium-transporting ATPase 4 OS=Homo sapiens GN=ATP2B4 PE=1 SV=2	AT2B4_HUMAN	1.96	1.09
Prelamin-A/C OS=Homo sapiens GN=LMNA PE=1 SV=1	LMNA_HUMAN	0.56	0.96
Procollagen-lysine.2-oxoglutarate 5-dioxygenase 2 OS=Homo sapiens GN=PLOD2 PE=1 SV=2	PLOD2_HUMAN	0.58	1.15
Proliferation-associated protein 2G4 OS=Homo sapiens GN=PA2G4 PE=1 SV=3	PA2G4_HUMAN	1.35	1.10
Prolyl 4-hydroxylase subunit alpha-1 OS=Homo sapiens GN=P4HA1 PE=1 SV=2	P4HA1_HUMAN	0.64	0.69
Prostaglandin E synthase OS=Homo sapiens GN=PTGES PE=1 SV=2	PTGES_HUMAN	0.61	0.85
Protein AHNAK2 OS=Homo sapiens GN=AHNAK2 PE=1 SV=2	AHNK2_HUMAN	1.84	0.91
Protein disulfide-isomerase A3 OS=Homo sapiens GN=PDIA3 PE=1 SV=4	PDIA3_HUMAN	0.70	0.58
Protein disulfide-isomerase A4 OS=Homo sapiens GN=PDIA4 PE=1 SV=2	PDIA4_HUMAN	0.73	0.56
Protein disulfide-isomerase A6 OS=Homo sapiens GN=PDIA6 PE=1 SV=1	PDIA6_HUMAN	0.77	0.64
Protein disulfide-isomerase OS=Homo sapiens GN=P4HB PE=1 SV=3	PDIA1_HUMAN	0.66	0.77
Protein S100-A10	S10AA_HUMAN	2.71	1.90
Protein S100-A11	S10AB_HUMAN	2.41	1.96
Protein S100-A4	S10A4_HUMAN	1.69	1.38
Protein S100-A6	S10A6_HUMAN	NS	1.50
Putative elongation factor 1-alpha-like 3	EF1A3_HUMAN	1.58	2.21
Putative RNA-binding protein 3 OS=Homo sapiens GN=RBM3 PE=1 SV=1	RBM3_HUMAN	0.70	0.98
Pyruvate kinase isozymes M1/M2 OS=Homo sapiens GN=PKM PE=1 SV=4	KPYM_HUMAN	1.35	1.46
Radixin OS=Homo sapiens GN=RDX PE=1 SV=1	RADI_HUMAN	1.71	1.51
Ras-related C3 botulinum toxin substrate 1	RAC1_HUMAN	1.70	NS
Ras-related protein Rab-11B OS=Homo sapiens GN=RAB11B PE=1 SV=4	RB11B_HUMAN	1.44	1.07
Ras-related protein Rab-7a OS=Homo sapiens GN=RAB7A PE=1 SV=1	RAB7A_HUMAN	1.41	0.81
Ras-related protein Rab-8B OS=Homo sapiens GN=RAB8B PE=1 SV=2	RAB8B_HUMAN	1.30	1.01
Reticulocalbin-3 OS=Homo sapiens GN=RCN3 PE=1 SV=1	RCN3_HUMAN	0.55	0.50
Ribosome-binding protein 1 OS=Homo sapiens GN=RRBP1 PE=1 SV=4	RRBP1_HUMAN	0.78	1.43
Septin-2 OS=Homo sapiens GN=SEPT2 PE=1 SV=1	SEPT2_HUMAN	0.97	1.30
Serine hydroxymethyltransferase. mitochondrial OS=Homo sapiens GN=SHMT2 PE=1 SV=3	GLYM_HUMAN	0.90	0.69
Serine/arginine-rich splicing factor 1 OS=Homo sapiens GN=SRSF1 PE=1 SV=2	SRSF1_HUMAN	0.67	0.90
Serpin H1 OS=Homo sapiens GN=SERPINH1 PE=1 SV=2	SERPH_HUMAN	0.45	0.53
Sodium/potassium-transporting ATPase subunit alpha-1 OS=Homo sapiens GN=ATP1A1 PE=1 SV=1	AT1A1_HUMAN	1.63	1.22
Solute carrier family 2. facilitated glucose transporter member 1 OS=Homo sapiens GN=SLC2A1 PE=1 SV=2	GTR1_HUMAN	0.89	0.58
Spectrin beta chain. non-erythrocytic 1 OS=Homo sapiens GN=SPTBN1 PE=1 SV=2	SPTB2_HUMAN	1.30	1.20
Splicing factor. proline- and glutamine-rich OS=Homo sapiens GN=SFPQ PE=1 SV=2	SFPQ_HUMAN	0.62	0.80
Stathmin OS=Homo sapiens GN=STMN1 PE=1 SV=3	STMN1_HUMAN	1.89	1.59
Superoxide dismutase [Mn]. mitochondrial	SODM_HUMAN	0.41	1.54
Thioredoxin domain-containing protein 5 OS=Homo sapiens GN=TXNDC5 PE=1 SV=2	TXND5_HUMAN	0.61	0.53
Thrombospondin-1 OS=Homo sapiens GN=THBS1 PE=1 SV=2	TSP1_HUMAN	0.67	0.63
Thymosin beta-10 OS=Homo sapiens GN=TMSB10 PE=1 SV=2	TYB10_HUMAN	2.01	2.60
Transforming protein RhoA OS=Homo sapiens GN=RHOA PE=1 SV=1	RHOA_HUMAN	1.50	1.16
Transgelin OS=Homo sapiens GN=TAGLN PE=1 SV=4	TAGL_HUMAN	1.01	1.45
Transgelin-2 OS=Homo sapiens GN=TAGLN2 PE=1 SV=3	TAGL2_HUMAN	1.41	1.39
Transketolase OS=Homo sapiens GN=TKT PE=1 SV=3	TKT_HUMAN	1.37	0.99
Translocon-associated protein subunit gamma OS=Homo sapiens GN=SSR3 PE=1 SV=1	SSRG_HUMAN	0.77	0.62
Tropomyosin alpha-4 chain	TPM4_HUMAN	1.63	1.51
Tubulin alpha-1A chain OS=Homo sapiens GN=TUBA1A PE=1 SV=1	TBA1A_HUMAN	1.66	1.73
Tubulin beta chain OS=Homo sapiens GN=TUBB PE=1 SV=2	TBB5_HUMAN	1.57	1.62
Tubulin beta-4B chain OS=Homo sapiens GN=TUBB4B PE=1 SV=1	TBB4B_HUMAN	1.56	1.47
Tubulin beta-6 chain OS=Homo sapiens GN=TUBB6 PE=1 SV=1	TBB6_HUMAN	1.52	1.78
Unconventional myosin-Id OS=Homo sapiens GN=MYO1D PE=1 SV=2	MYO1D_HUMAN	0.69	1.13
Vigilin OS=Homo sapiens GN=HDLBP PE=1 SV=2	VIGLN_HUMAN	0.74	0.64
Vinculin OS=Homo sapiens GN=VCL PE=1 SV=4	VINC_HUMAN	1.43	1.13
WD repeat-containing protein 1 OS=Homo sapiens GN=WDR1 PE=1 SV=4	WDR1_HUMAN	1.46	1.01
WD repeat-containing protein 7 OS=Homo sapiens GN=WDR7 PE=2 SV=2	WDR7_HUMAN	0.89	0.60

NS - not significative

Study 6- Disclosing the differences in mitochondrial pathway modulation between severe and mild multiple acyl-CoA dehydrogenation deficiencies.

Supplemental table S1 – List of proteins identified by nanoLC-MS/MS.

N	Unused	Total	% Cov	Accession #	Name	Species	Peptides(95%)
1	155.85	155.85	65.7	sp|P35579|MYH9_HUMAN	Myosin-9 OS=Homo sapiens GN=MYH9 PE=1 SV=4	HUMAN	124
2	117.36	117.36	59.2	sp|Q09666|AHNK_HUMAN	Neuroblast differentiation-associated protein AHNAK OS=Homo sapiens GN=AHNAK PE=1 SV=2	HUMAN	72
269	2	42.65	77.1	sp|P60709|ACTB_HUMAN	Actin, cytoplasmic 1 OS=Homo sapiens GN=ACTB PE=1 SV=1	HUMAN	63
3	65.84	65.84	77.7	sp|P08670|VIME_HUMAN	Vimentin OS=Homo sapiens GN=VIM PE=1 SV=4	HUMAN	63
10	42.65	42.65	77.1	sp|P63261|ACTG_HUMAN	Actin, cytoplasmic 2 OS=Homo sapiens GN=ACTG1 PE=1 SV=1	HUMAN	59
6	56.85	56.85	59.5	sp|P02452|CO1A1_HUMAN	Collagen alpha-1(I) chain OS=Homo sapiens GN=COL1A1 PE=1 SV=5	HUMAN	59
4	62.29	62.29	69.1	sp|P11021|GRP78_HUMAN	78 kDa glucose-regulated protein OS=Homo sapiens GN=HSPA5 PE=1 SV=2	HUMAN	57
8	46.87	46.87	78	sp|P07237|PDIA1_HUMAN	Protein disulfide-isomerase OS=Homo sapiens GN=P4HB PE=1 SV=3	HUMAN	44
7	49.81	49.81	82	sp|P07355|ANXA2_HUMAN	Annexin A2 OS=Homo sapiens GN=ANXA2 PE=1 SV=2	HUMAN	43
5	57.7	57.7	35.4	sp|P21333|FLNA_HUMAN	Filamin-A OS=Homo sapiens GN=FLNA PE=1 SV=4	HUMAN	40
13	37.93	37.93	70.9	sp|Q07065|CKAP4_HUMAN	Cytoskeleton-associated protein 4 OS=Homo sapiens GN=CKAP4 PE=1 SV=2	HUMAN	34
14	37.85	37.85	27.5	sp|Q15149|PLEC_HUMAN	Plectin OS=Homo sapiens GN=PLEC PE=1 SV=3	HUMAN	33
26	24.58	24.58	59.4	sp|P06576|ATPB_HUMAN	ATP synthase subunit beta, mitochondrial OS=Homo sapiens GN=ATP5B PE=1 SV=3	HUMAN	31
20	27.7	27.7	56	sp|P50454|SERPH_HUMAN	Serpin H1 OS=Homo sapiens GN=SERPINH1 PE=1 SV=2	HUMAN	30
11	41.55	41.58	59.2	sp|P27797|CALR_HUMAN	Calreticulin OS=Homo sapiens GN=CALR PE=1 SV=1	HUMAN	28
9	43.2	43.35	49.7	sp|P14625|ENPL_HUMAN	Endoplasmin OS=Homo sapiens GN=HSP90B1 PE=1 SV=1	HUMAN	28
12	38.95	38.95	52	sp|Q9P2E9|RRBP1_HUMAN	Ribosome-binding protein 1 OS=Homo sapiens GN=RRBP1 PE=1 SV=4	HUMAN	28
15	32.85	32.85	66	sp|P04406|G3P_HUMAN	Glyceraldehyde-3-phosphate dehydrogenase OS=Homo sapiens GN=GAPDH PE=1 SV=3	HUMAN	27
31	19.34	19.34	55.3	sp|P02768|ALBU_HUMAN	Serum albumin OS=Homo sapiens GN=ALB PE=1 SV=2	HUMAN	26
16	31.89	31.96	50.1	sp|P38646|GRP75_HUMAN	Stress-70 protein, mitochondrial OS=Homo sapiens GN=HSPA9 PE=1 SV=2	HUMAN	26
22	26.86	26.86	52.9	sp|P10809|CH60_HUMAN	60 kDa heat shock protein, mitochondrial OS=Homo sapiens GN=HSPD1 PE=1 SV=2	HUMAN	25
18	28.19	28.44	50.7	sp|P30101|PDIA3_HUMAN	Protein disulfide-isomerase A3 OS=Homo sapiens GN=PDIA3 PE=1 SV=4	HUMAN	25
21	26.86	26.86	48.1	sp|P08123|CO1A2_HUMAN	Collagen alpha-2(I) chain OS=Homo sapiens GN=COL1A2 PE=1 SV=7	HUMAN	24
270	2	21.72	58.2	sp|P63267|ACTH_HUMAN	Actin, gamma-enteric smooth muscle OS=Homo sapiens GN=ACTG2 PE=1 SV=1	HUMAN	23
19	28.06	28.41	42.1	sp|Q05682|CALD1_HUMAN	Caldesmon OS=Homo sapiens GN=CALD1 PE=1 SV=3	HUMAN	22
27	23.61	23.61	25.7	sp|P15144|AMPN_HUMAN	Aminopeptidase N OS=Homo sapiens GN=ANPEP PE=1 SV=4	HUMAN	21
36	16.72	16.72	50.3	sp|P25705|ATPA_HUMAN	ATP synthase subunit alpha, mitochondrial OS=Homo sapiens GN=ATP5A1 PE=1 SV=1	HUMAN	21
17	29.63	29.63	26.1	sp|P12111|CO6A3_HUMAN	Collagen alpha-3(VI) chain OS=Homo sapiens GN=COL6A3 PE=1 SV=5	HUMAN	20
30	19.45	19.45	32.6	sp|Q14697|GANAB_HUMAN	Neutral alpha-glucosidase AB OS=Homo sapiens GN=GANAB PE=1 SV=3	HUMAN	20
34	17.99	17.99	25.9	sp|O43707|ACTN4_HUMAN	Alpha-actinin-4 OS=Homo sapiens GN=ACTN4 PE=1 SV=2	HUMAN	17
23	26.71	26.95	54.6	sp|P26038|MOES_HUMAN	Moesin OS=Homo sapiens GN=MSN PE=1 SV=3	HUMAN	17
40	14.9	14.9	86.8	sp|P60660|MYL6_HUMAN	Myosin light polypeptide 6 OS=Homo sapiens GN=MYL6 PE=1 SV=2	HUMAN	17
196	2.85	14.77	21.8	sp|P12814|ACTN1_HUMAN	Alpha-actinin-1 OS=Homo sapiens GN=ACTN1 PE=1 SV=2	HUMAN	16
28	21.13	21.13	46.8	sp|Q15084|PDIA6_HUMAN	Protein disulfide-isomerase A6 OS=Homo sapiens GN=PDIA6 PE=1 SV=1	HUMAN	16
33	18.56	18.56	66.5	sp|Q96D15|RCN3_HUMAN	Reticulocalbin-3 OS=Homo sapiens GN=RCN3 PE=1 SV=1	HUMAN	16
56	10.12	10.12	70.5	sp|P62158|CALM_HUMAN	Calmodulin OS=Homo sapiens GN=CALM1 PE=1 SV=2	HUMAN	15
37	15.8	15.8	33.3	sp|Q96AY3|FKB10_HUMAN	Peptidyl-prolyl cis-trans isomerase FKBP10 OS=Homo sapiens GN=FKBP10 PE=1 SV=1	HUMAN	15
25	26.12	26.12	23.3	sp|Q99715|COCA1_HUMAN	Collagen alpha-1(XII) chain OS=Homo sapiens GN=COL12A1 PE=1 SV=2	HUMAN	14
49	12.08	12.08	58.5	sp|P19105|ML12A_HUMAN	Myosin regulatory light chain 12A OS=Homo sapiens GN=MYL12A PE=1 SV=2	HUMAN	14
65	8.68	8.68	47.9	sp|P62937|PPIA_HUMAN	Peptidyl-prolyl cis-trans isomerase A OS=Homo sapiens GN=PPIA PE=1 SV=2	HUMAN	14
39	15.03	15.03	49.1	sp|P07437|TBB5_HUMAN	Tubulin beta chain OS=Homo sapiens GN=TUBB PE=1 SV=2	HUMAN	14
24	26.24	26.24	18.2	sp|P02751|FINC_HUMAN	Fibronectin OS=Homo sapiens GN=FN1 PE=1 SV=4	HUMAN	13
32	18.68	18.68	67.6	sp|P23284|PPIB_HUMAN	Peptidyl-prolyl cis-trans isomerase B OS=Homo sapiens GN=PPIB PE=1 SV=2	HUMAN	13
54	10.57	10.57	47.2	sp|P67936|TPM4_HUMAN	Tropomyosin alpha-4 chain OS=Homo sapiens GN=TPM4 PE=1 SV=3	HUMAN	13
74	7.47	17.41	30.2	sp|P35580|MYH10_HUMAN	Myosin-10 OS=Homo sapiens GN=MYH10 PE=1 SV=3	HUMAN	12
29	19.77	19.77	21.7	sp|Q9Y490|TLN1_HUMAN	Talin-1 OS=Homo sapiens GN=TLN1 PE=1 SV=3	HUMAN	12
35	16.81	16.81	43.4	sp|Q9BQE3|TBA1C_HUMAN	Tubulin alpha-1C chain OS=Homo sapiens GN=TUBA1C PE=1 SV=1	HUMAN	12
375	1.54	10.97	40.5	sp|Q13885|TBB2A_HUMAN	Tubulin beta-2A chain OS=Homo sapiens GN=TUBB2A PE=1 SV=1	HUMAN	12
48	12.29	12.29	49.5	sp|O43852|CALU_HUMAN	Calumenin OS=Homo sapiens GN=CALU PE=1 SV=2	HUMAN	11
43	13.64	13.64	21.9	sp|P04843|RPN1_HUMAN	Dolichyl-diphosphooligosaccharide--protein glycosyltransferase subunit 1 OS=Homo sapiens GN	HUMAN	11
38	15.24	15.24	13.6	sp|P01023|A2MG_HUMAN	Alpha-2-macroglobulin OS=Homo sapiens GN=A2M PE=1 SV=3	HUMAN	10
41	13.95	13.95	30	sp|P06733|ENOA_HUMAN	Alpha-enolase OS=Homo sapiens GN=ENO1 PE=1 SV=2	HUMAN	10
46	12.66	12.66	30.7	sp|P07858|CATB_HUMAN	Cathepsin B OS=Homo sapiens GN=CTSB PE=1 SV=3	HUMAN	10
44	12.92	12.96	46.4	sp|P04179|SODM_HUMAN	Superoxide dismutase [Mn], mitochondrial OS=Homo sapiens GN=SOD2 PE=1 SV=2	HUMAN	10
228	2.2	15.16	43.7	sp|Q71U36|TBA1A_HUMAN	Tubulin alpha-1A chain OS=Homo sapiens GN=TUBA1A PE=1 SV=1	HUMAN	10
50	11.8	11.8	63.7	sp|P09382|LEG1_HUMAN	Galectin-1 OS=Homo sapiens GN=LGALS1 PE=1 SV=2	HUMAN	8
60	9.91	9.91	23.6	sp|P13667|PDIA4_HUMAN	Protein disulfide-isomerase A4 OS=Homo sapiens GN=PDIA4 PE=1 SV=2	HUMAN	8
79	6.9	6.9	30.5	sp|Q15293|RCN1_HUMAN	Reticulocalbin-1 OS=Homo sapiens GN=RCN1 PE=1 SV=1	HUMAN	8
51	11.24	11.24	21.3	sp|Q01082|SPTB2_HUMAN	Spectrin beta chain, non-erythrocytic 1 OS=Homo sapiens GN=SPTBN1 PE=1 SV=2	HUMAN	8
127	4.19	7.94	41.6	sp|P09493|TPM1_HUMAN	Tropomyosin alpha-1 chain OS=Homo sapiens GN=TPM1 PE=1 SV=2	HUMAN	8
426	0.72	6.78	29.2	sp|P06753|TPM3_HUMAN	Tropomyosin alpha-3 chain OS=Homo sapiens GN=TPM3 PE=1 SV=1	HUMAN	8
250	2.05	11.07	34.7	sp|P04350|TBB4A_HUMAN	Tubulin beta-4A chain OS=Homo sapiens GN=TUBB4A PE=1 SV=2	HUMAN	8
53	10.63	10.63	20	sp|Q00341|VIGLN_HUMAN	Vigilin OS=Homo sapiens GN=HDLBP PE=1 SV=2	HUMAN	8
45	12.81	12.92	25.7	sp|P27824|CALX_HUMAN	Calnexin OS=Homo sapiens GN=CANX PE=1 SV=2	HUMAN	7
200	2.82	2.93	21.3	sp|P00367|DHE3_HUMAN	Glutamate dehydrogenase 1, mitochondrial OS=Homo sapiens GN=GLUD1 PE=1 SV=2	HUMAN	7
47	12.46	12.46	49.8	sp|P00387|NB5R3_HUMAN	NADH-cytochrome b5 reductase 3 OS=Homo sapiens GN=CYB5R3 PE=1 SV=3	HUMAN	7
80	6.9	6.9	44.1	sp|P35232|PHB_HUMAN	Prohibitin OS=Homo sapiens GN=PHB PE=1 SV=1	HUMAN	7
113	4.87	4.87	15.7	sp|O15460|P4HA2_HUMAN	Prolyl 4-hydroxylase subunit alpha-2 OS=Homo sapiens GN=P4HA2 PE=1 SV=1	HUMAN	7
58	10	10	39.9	sp|Q15019|SEPT2_HUMAN	Septin-2 OS=Homo sapiens GN=SEPT2 PE=1 SV=1	HUMAN	7
64	9.14	9.14	25.8	sp|Q7KZF4|SND1_HUMAN	Staphylococcal nuclease domain-containing protein 1 OS=Homo sapiens GN=SND1 PE=1 SV=1	HUMAN	7
42	13.78	13.78	19	sp|P07996|TSP1_HUMAN	Thrombospondin-1 OS=Homo sapiens GN=THBS1 PE=1 SV=2	HUMAN	7
104	5.82	5.82	28.8	sp|O75396|SC22B_HUMAN	Vesicle-trafficking protein SEC22b OS=Homo sapiens GN=SEC22B PE=1 SV=4	HUMAN	7
78	7.01	7.01	40.5	sp|P61247|RS3A_HUMAN	40S ribosomal protein S3a OS=Homo sapiens GN=RPS3A PE=1 SV=2	HUMAN	6
69	8.03	8.03	20.1	sp|P24752|THIL_HUMAN	Acetyl-CoA acetyltransferase, mitochondrial OS=Homo sapiens GN=ACAT1 PE=1 SV=1	HUMAN	6
61	9.79	9.79	28.6	sp|P07339|CATD_HUMAN	Cathepsin D OS=Homo sapiens GN=CTSD PE=1 SV=1	HUMAN	6
271	2	7.11	22.6	sp|P17661|DESM_HUMAN	Desmin OS=Homo sapiens GN=DES PE=1 SV=3	HUMAN	6
70	8	8	29.9	sp|P49411|EFTU_HUMAN	Elongation factor Tu, mitochondrial OS=Homo sapiens GN=TUFM PE=1 SV=2	HUMAN	6
59	10	10	33	sp|P04075|ALDOA_HUMAN	Fructose-bisphosphate aldolase A OS=Homo sapiens GN=ALDOA PE=1 SV=2	HUMAN	6
55	10.16	12.99	24.2	sp|P11142|HSP7C_HUMAN	Heat shock cognate 71 kDa protein OS=Homo sapiens GN=HSPA8 PE=1 SV=1	HUMAN	6
141	4	8.11	61.6	sp|P24844|MYL9_HUMAN	Myosin regulatory light polypeptide 9 OS=Homo sapiens GN=MYL9 PE=1 SV=4	HUMAN	6
87	6.57	6.57	34.4	sp|Q6NZI2|PTRF_HUMAN	Polymerase I and transcript release factor OS=Homo sapiens GN=PTRF PE=1 SV=1	HUMAN	6
99	6	6.03	12.3	sp|P46940|IQGA1_HUMAN	Ras GTPase-activating-like protein IQGAP1 OS=Homo sapiens GN=IQGAP1 PE=1 SV=1	HUMAN	6
62	9.76	9.76	25.9	sp|Q8NBS9|TXND5_HUMAN	Thioredoxin domain-containing protein 5 OS=Homo sapiens GN=TXNDC5 PE=1 SV=2	HUMAN	6
76	7.33	7.33	19.7	sp|P40939|ECHA_HUMAN	Trifunctional enzyme subunit alpha, mitochondrial OS=Homo sapiens GN=HADHA PE=1 SV=2	HUMAN	6
52	10.69	10.69	38.9	sp|P26373|RL13_HUMAN	60S ribosomal protein L13 OS=Homo sapiens GN=RPL13 PE=1 SV=4	HUMAN	5
85	6.65	6.65	51.3	sp|P08758|ANXA5_HUMAN	Annexin A5 OS=Homo sapiens GN=ANXA5 PE=1 SV=2	HUMAN	5
130	4.12	4.12	22.4	sp|P08133|ANXA6_HUMAN	Annexin A6 OS=Homo sapiens GN=ANXA6 PE=1 SV=3	HUMAN	5
86	6.61	6.61	9.8	sp|P16070|CD44_HUMAN	CD44 antigen OS=Homo sapiens GN=CD44 PE=1 SV=3	HUMAN	5
115	4.8	4.8	24.1	sp|Q9NZN4|EHD2_HUMAN	EH domain-containing protein 2 OS=Homo sapiens GN=EHD2 PE=1 SV=2	HUMAN	5
72	7.81	7.81	34.9	sp|P68104|EF1A1_HUMAN	Elongation factor 1-alpha 1 OS=Homo sapiens GN=EEF1A1 PE=1 SV=1	HUMAN	5
92	6.33	6.33	20.2	sp|P13639|EF2_HUMAN	Elongation factor 2 OS=Homo sapiens GN=EEF2 PE=1 SV=4	HUMAN	5
105	5.55	5.55	13	sp|Q9BSJ8|ESYT1_HUMAN	Extended synaptotagmin-1 OS=Homo sapiens GN=ESYT1 PE=1 SV=1	HUMAN	5
101	5.91	6.93	12.7	sp|Q14315|FLNC_HUMAN	Filamin-C OS=Homo sapiens GN=FLNC PE=1 SV=3	HUMAN	5

N	Unused	Total	% Cov	Accession #	Name	Species	Peptides(95%)	
75	7.41	7.41	20.1	sp|P14314|GLU2B_HUMAN	Glucosidase 2 subunit beta OS=Homo sapiens GN=PRKCSH PE=1 SV=2	HUMAN	5	
96	6.06	6.06	21.4	sp|P01892|1A02_HUMAN	HLA class I histocompatibility antigen, A-2 alpha chain OS=Homo sapiens GN=HLA-A PE=1 SV=1	HUMAN	5	
419	0.78	5.21	29.3	sp|P10314|1A32_HUMAN	HLA class I histocompatibility antigen, A-32 alpha chain OS=Homo sapiens GN=HLA-A PE=2 SV=2	HUMAN	5	
84	6.65	6.65	45.9	sp|Q96AG4|LRC59_HUMAN	Leucine-rich repeat-containing protein 59 OS=Homo sapiens GN=LRRC59 PE=1 SV=1	HUMAN	5	
66	8.47	8.47	42.3	sp|P40926|MDHM_HUMAN	Malate dehydrogenase, mitochondrial OS=Homo sapiens GN=MDH2 PE=1 SV=3	HUMAN	5	
63	9.2	9.2	14.8	sp|Q9NZM1|MYOF_HUMAN	Myoferlin OS=Homo sapiens GN=MYOF PE=1 SV=1	HUMAN	5	
93	6.32	6.32	24.5	sp|Q02818|NUCB1_HUMAN	Nucleobindin-1 OS=Homo sapiens GN=NUCB1 PE=1 SV=4	HUMAN	5	
179	3.35	3.35	10.3	sp|Q16822|PCKGM_HUMAN	Phosphoenolpyruvate carboxykinase [GTP], mitochondrial OS=Homo sapiens GN=PCK2 PE=1 SV	HUMAN	5	
94	6.18	6.18	59.8	sp|P60903|S10AA_HUMAN	Protein S100-A10 OS=Homo sapiens GN=S100A10 PE=1 SV=2	HUMAN	5	
57	10	10	17.9	sp|Q9NQC3|RTN4_HUMAN	Reticulon-4 OS=Homo sapiens GN=RTN4 PE=1 SV=2	HUMAN	5	
218	2.39	2.39	11.6	sp|Q9Y6N5|SQRD_HUMAN	Sulfide:quinone oxidoreductase, mitochondrial OS=Homo sapiens GN=SQRDL PE=1 SV=1	HUMAN	5	
109	5.25	5.25	29.7	sp|P46783|RS10_HUMAN	40S ribosomal protein S10 OS=Homo sapiens GN=RPS10 PE=1 SV=1	HUMAN	4	
180	3.32	3.32	61.4	sp|P39019|RS19_HUMAN	40S ribosomal protein S19 OS=Homo sapiens GN=RPS19 PE=1 SV=2	HUMAN	4	
160	3.85	3.85	46.4	sp|P62857|RS28_HUMAN	40S ribosomal protein S28 OS=Homo sapiens GN=RPS28 PE=1 SV=1	HUMAN	4	
81	6.74	6.74	44.6	sp|P46782|RS5_HUMAN	40S ribosomal protein S5 OS=Homo sapiens GN=RPS5 PE=1 SV=4	HUMAN	4	
73	7.48	7.48	34	sp|P62081|RS7_HUMAN	40S ribosomal protein S7 OS=Homo sapiens GN=RPS7 PE=1 SV=1	HUMAN	4	
97	6.04	6.04	27.1	sp|P08865|RSSA_HUMAN	40S ribosomal protein SA OS=Homo sapiens GN=RPSA PE=1 SV=4	HUMAN	4	
103	5.88	5.88	44.7	sp|P50914|RL14_HUMAN	60S ribosomal protein L14 OS=Homo sapiens GN=RPL14 PE=1 SV=4	HUMAN	4	
148	4	4	27.2	sp|P04083|ANXA1_HUMAN	Annexin A1 OS=Homo sapiens GN=ANXA1 PE=1 SV=2	HUMAN	4	
108	5.35	5.35	15.3	sp|P35613|BASI_HUMAN	Basigin OS=Homo sapiens GN=BSG PE=1 SV=2	HUMAN	4	
71	8	8	37.4	sp|P80723|BASP1_HUMAN	Brain acid soluble protein 1 OS=Homo sapiens GN=BASP1 PE=1 SV=2	HUMAN	4	
68	8.29	8.29	52.4	sp|P23528|COF1_HUMAN	Cofilin-1 OS=Homo sapiens GN=CFL1 PE=1 SV=3	HUMAN	4	
98	6.01	6.01	19.2	sp|P12109|CO6A1_HUMAN	Collagen alpha-1(VI) chain OS=Homo sapiens GN=COL6A1 PE=1 SV=3	HUMAN	4	
95	6.13	6.13	48.2	sp|Q07021|C1QBP_HUMAN	Complement component 1 Q subcomponent-binding protein, mitochondrial OS=Homo sapiens	HUMAN	4	
125	4.23	4.23	35.1	sp|P00167|CYB5_HUMAN	Cytochrome b5 OS=Homo sapiens GN=CYB5A PE=1 SV=2	HUMAN	4	
162	3.8	3.8	12	sp|P54886|P5CS_HUMAN	Delta-1-pyrroline-5-carboxylate synthase OS=Homo sapiens GN=ALDH18A1 PE=1 SV=2	HUMAN	4	
67	8.46	8.46	22.2	sp|P09622|DLDH_HUMAN	Dihydrolipoyl dehydrogenase, mitochondrial OS=Homo sapiens GN=DLD PE=1 SV=2	HUMAN	4	
417	0.82	5.13	25.8	sp|P15311|EZRI_HUMAN	Ezrin OS=Homo sapiens GN=EZR PE=1 SV=4	HUMAN	4	
132	4.12	4.12	33.3	sp|O00264|PGRC1_HUMAN	Membrane-associated progesterone receptor component 1 OS=Homo sapiens GN=PGRMC1 PE	HUMAN	4	
272	2	3.72	11.1	sp|P20742|PZP_HUMAN	Pregnancy zone protein OS=Homo sapiens GN=PZP PE=1 SV=4	HUMAN	4	
135	4.09	4.09	23.7	sp|P11177|ODPB_HUMAN	Pyruvate dehydrogenase E1 component subunit beta, mitochondrial OS=Homo sapiens GN=PDH	HUMAN	4	
116	4.76	4.76	11.6	sp|O14773|TPP1_HUMAN	Tripeptidyl-peptidase 1 OS=Homo sapiens GN=TPP1 PE=1 SV=2	HUMAN	4	
124	4.28	4.28	59.8	sp|P61604|CH10_HUMAN	10 kDa heat shock protein, mitochondrial OS=Homo sapiens GN=HSPE1 PE=1 SV=2	HUMAN	3	
181	3.31	3.32	57.8	sp|P0CW22|RS17L_HUMAN	40S ribosomal protein S17-like OS=Homo sapiens GN=RPS17L PE=3 SV=1	HUMAN	3	
107	5.41	5.41	44.5	sp|P62701|RS4X_HUMAN	40S ribosomal protein S4, X isoform OS=Homo sapiens GN=RPS4X PE=1 SV=2	HUMAN	3	
198	2.84	2.84	28.1	sp|P62753|RS6_HUMAN	40S ribosomal protein S6 OS=Homo sapiens GN=RPS6 PE=1 SV=1	HUMAN	3	
167	3.58	3.58	38	sp|P62241|RS8_HUMAN	40S ribosomal protein S8 OS=Homo sapiens GN=RPS8 PE=1 SV=2	HUMAN	3	
152	4	4	47.8	sp|P05387|RLA2_HUMAN	60S acidic ribosomal protein P2 OS=Homo sapiens GN=RPLP2 PE=1 SV=1	HUMAN	3	
216	2.41	2.41	30.3	sp|P30050|RL12_HUMAN	60S ribosomal protein L12 OS=Homo sapiens GN=RPL12 PE=1 SV=1	HUMAN	3	
235	2.15	2.15	38.1	sp|P46778|RL21_HUMAN	60S ribosomal protein L21 OS=Homo sapiens GN=RPL21 PE=1 SV=2	HUMAN	3	
102	5.91	5.91	43	sp|P62750|RL23A_HUMAN	60S ribosomal protein L23a OS=Homo sapiens GN=RPL23A PE=1 SV=1	HUMAN	3	
128	4.16	4.16	52.2	sp|P47914|RL29_HUMAN	60S ribosomal protein L29 OS=Homo sapiens GN=RPL29 PE=1 SV=2	HUMAN	3	
112	4.98	4.98	29	sp|P39023|RL3_HUMAN	60S ribosomal protein L3 OS=Homo sapiens GN=RPL3 PE=1 SV=2	HUMAN	3	
164	3.78	3.78	35.2	sp|P62899|RL31_HUMAN	60S ribosomal protein L31 OS=Homo sapiens GN=RPL31 PE=1 SV=1	HUMAN	3	
83	6.68	6.68	33.7	sp|P46777|RL5_HUMAN	60S ribosomal protein L5 OS=Homo sapiens GN=RPL5 PE=1 SV=3	HUMAN	3	
82	6.73	6.73	23.9	sp|Q12797|ASPH_HUMAN	Aspartyl/asparaginyl beta-hydroxylase OS=Homo sapiens GN=ASPH PE=1 SV=3	HUMAN	3	
156	4	4	31.6	sp|P30049|ATPD_HUMAN	ATP synthase subunit delta, mitochondrial OS=Homo sapiens GN=ATP5D PE=1 SV=2	HUMAN	3	
303	2	2	41.7	sp|P18859|ATP5J_HUMAN	ATP synthase-coupling factor 6, mitochondrial OS=Homo sapiens GN=ATP5J PE=1 SV=1	HUMAN	3	
188	3.15	3.15	20.2	sp|Q03135|CAV1_HUMAN	Caveolin-1 OS=Homo sapiens GN=CAV1 PE=1 SV=4	HUMAN	3	
199	2.84	2.84	15.8	sp|Q9ULV4|COR1C_HUMAN	Coronin-1C OS=Homo sapiens GN=CORO1C PE=1 SV=1	HUMAN	3	
100	6	6	22.7	sp|P31930|QCR1_HUMAN	Cytochrome b-c1 complex subunit 1, mitochondrial OS=Homo sapiens GN=UQCRC1 PE=1 SV=3	HUMAN	3	
154	4	4	15.5	sp|P22695|QCR2_HUMAN	Cytochrome b-c1 complex subunit 2, mitochondrial OS=Homo sapiens GN=UQCRC2 PE=1 SV=3	HUMAN	3	
157	4	4	42.9	sp|P07919|QCR6_HUMAN	Cytochrome b-c1 complex subunit 6, mitochondrial OS=Homo sapiens GN=UQCRH PE=1 SV=2	HUMAN	3	
88	6.53	6.53	56.8	sp|P14927|QCR7_HUMAN	Cytochrome b-c1 complex subunit 7 OS=Homo sapiens GN=UQCRB PE=1 SV=2	HUMAN	3	
114	4.82	4.82	43.8	sp|P99999|CYC_HUMAN	Cytochrome c OS=Homo sapiens GN=CYCS PE=1 SV=2	HUMAN	3	
123	4.34	4.34	50	sp|P20674|COX5A_HUMAN	Cytochrome c oxidase subunit 5A, mitochondrial OS=Homo sapiens GN=COX5A PE=1 SV=2	HUMAN	3	
151	4	4	16.8	sp|P13804|ETFA_HUMAN	Electron transfer flavoprotein subunit alpha, mitochondrial OS=Homo sapiens GN=ETFA PE=1 SV	HUMAN	3	
182	3.31	3.31	25.7	sp|P30040|ERP29_HUMAN	Endoplasmic reticulum resident protein 29 OS=Homo sapiens GN=ERP29 PE=1 SV=4	HUMAN	3	
120	4.43	4.43	47.4	sp|P63241|IF5A1_HUMAN	Eukaryotic translation initiation factor 5A-1 OS=Homo sapiens GN=EIF5A PE=1 SV=2	HUMAN	3	
91	6.37	6.37	23.2	sp|P17931|LEG3_HUMAN	Galectin-3 OS=Homo sapiens GN=LGALS3 PE=1 SV=5	HUMAN	3	
242	2.09	4.13	20.1	sp|P17066|HSP76_HUMAN	Heat shock 70 kDa protein 6 OS=Homo sapiens GN=HSPA6 PE=1 SV=2	HUMAN	3	
90	6.38	6.38	53.1	sp|Q99878|H2AJ_HUMAN	Histone H2A type 1-J OS=Homo sapiens GN=HIST1H2AJ PE=1 SV=3	HUMAN	3	
402	1.07	3.37	25.4	sp|P30685|1B35_HUMAN	HLA class I histocompatibility antigen, B-35 alpha chain OS=Homo sapiens GN=HLA-B PE=1 SV=1	HUMAN	3	
111	5.02	5.02	24.6	sp|O75489|NDUS3_HUMAN	NADH dehydrogenase [ubiquinone] iron-sulfur protein 3, mitochondrial OS=Homo sapiens GN=I	HUMAN	3	
214	2.49	2.49	15.3	sp|P08473|NEP_HUMAN	Neprilysin OS=Homo sapiens GN=MME PE=1 SV=2	HUMAN	3	
106	5.51	5.51	35.4	sp|Q15365|PCBP1_HUMAN	Poly(rC)-binding protein 1 OS=Homo sapiens GN=PCBP1 PE=1 SV=2	HUMAN	3	
172	3.54	3.54	21.3	sp|O75915|PRAF3_HUMAN	PRA1 family protein 3 OS=Homo sapiens GN=ARL6IP5 PE=1 SV=1	HUMAN	3	
89	6.49	6.49	20.6	sp|O60568|PLOD3_HUMAN	Procollagen-lysine,2-oxoglutarate 5-dioxygenase 3 OS=Homo sapiens GN=PLOD3 PE=1 SV=1	HUMAN	3	
110	5.21	5.21	30.4	sp|Q99623|PHB2_HUMAN	Prohibitin-2 OS=Homo sapiens GN=PHB2 PE=1 SV=2	HUMAN	3	
138	4.03	4.03	10.7	sp|Q07954|LRP1_HUMAN	Prolow-density lipoprotein receptor-related protein 1 OS=Homo sapiens GN=LRP1 PE=1 SV=2	HUMAN	3	
173	3.5	3.5	29.4	sp|P13674|P4HA1_HUMAN	Prolyl 4-hydroxylase subunit alpha-1 OS=Homo sapiens GN=P4HA1 PE=1 SV=2	HUMAN	3	
185	3.21	3.21	38.2	sp|O95571|ETHE1_HUMAN	Protein ETHE1, mitochondrial OS=Homo sapiens GN=ETHE1 PE=1 SV=2	HUMAN	3	
146	4	4	20.5	sp|P14618|KPYM_HUMAN	Pyruvate kinase isozymes M1/M2 OS=Homo sapiens GN=PKM PE=1 SV=4	HUMAN	3	
203	2.79	2.79	30	sp|P51149|RAB7A_HUMAN	Ras-related protein Rab-7a OS=Homo sapiens GN=RAB7A PE=1 SV=1	HUMAN	3	
262	2.02	2.02	14.1	sp|P62834|RAP1A_HUMAN	Ras-related protein Rap-1A OS=Homo sapiens GN=RAP1A PE=1 SV=1	HUMAN	3	
143	4	4.1	23.3	sp|Q14257|RCN2_HUMAN	Reticulocalbin-2 OS=Homo sapiens GN=RCN2 PE=1 SV=1	HUMAN	3	
77	7.2	7.2	42.3	sp|Q01995|TAGL_HUMAN	Transgelin OS=Homo sapiens GN=TAGLN PE=1 SV=4	HUMAN	3	
261	2.02	2.02	15.7	sp|Q9UNL2|SSRG_HUMAN	Translocon-associated protein subunit gamma OS=Homo sapiens GN=SSR3 PE=1 SV=1	HUMAN	3	
215	2.42	2.42	46.6	sp|P82909|RT36_HUMAN	28S ribosomal protein S36, mitochondrial OS=Homo sapiens GN=MRPS36 PE=1 SV=2	HUMAN	2	
267	2.01	2.01	14.6	sp|P42765|THIM_HUMAN	3-ketoacyl-CoA thiolase, mitochondrial OS=Homo sapiens GN=ACAA2 PE=1 SV=2	HUMAN	2	
187	3.16	3.16	31.1	sp|P25398|RS12_HUMAN	40S ribosomal protein S12 OS=Homo sapiens GN=RPS12 PE=1 SV=3	HUMAN	2	
122	4.36	4.36	37.9	sp|P62841|RS15_HUMAN	40S ribosomal protein S15 OS=Homo sapiens GN=RPS15 PE=1 SV=2	HUMAN	2	
390	1.24	1.24	23.3	sp|P62249|RS16_HUMAN	40S ribosomal protein S16 OS=Homo sapiens GN=RPS16 PE=1 SV=2	HUMAN	2	
163	3.78	3.78	44.7	sp|P62269|RS18_HUMAN	40S ribosomal protein S18 OS=Homo sapiens GN=RPS18 PE=1 SV=3	HUMAN	2	
298	2	2	55.4	sp|P63220|RS21_HUMAN	40S ribosomal protein S21 OS=Homo sapiens GN=RPS21 PE=1 SV=1	HUMAN	2	
209	2.61	2.61	42.1	sp|P62847|RS24_HUMAN	40S ribosomal protein S24 OS=Homo sapiens GN=RPS24 PE=1 SV=1	HUMAN	2	
247	2.07	2.07	53.6	sp|P62273|RS29_HUMAN	40S ribosomal protein S29 OS=Homo sapiens GN=RPS29 PE=1 SV=2	HUMAN	2	
134	4.09	4.1	67.8	sp|P62861|RS30_HUMAN	40S ribosomal protein S30 OS=Homo sapiens GN=FAU PE=1 SV=1	HUMAN	2	
165	3.72	3.72	35.1	sp|P46781|RS9_HUMAN	40S ribosomal protein S9 OS=Homo sapiens GN=RPS9 PE=1 SV=3	HUMAN	2	
161	3.82	3.9	23.4	sp|P18621|RL17_HUMAN	60S ribosomal protein L17 OS=Homo sapiens GN=RPL17 PE=1 SV=3	HUMAN	2	
192	2.97	2.97	37.2	sp|P84098|RL19_HUMAN	60S ribosomal protein L19 OS=Homo sapiens GN=RPL19 PE=1 SV=1	HUMAN	2	
204	2.75	2.75	37.2	sp|P36578|RL4_HUMAN	60S ribosomal protein L4 OS=Homo sapiens GN=RPL4 PE=1 SV=5	HUMAN	2	
189	3.08	3.11	56.3	sp|Q02878|RL6_HUMAN	60S ribosomal protein L6 OS=Homo sapiens GN=RPL6 PE=1 SV=3	HUMAN	2	

N	Unused	Total	% Cov	Accession #	Name	Species	Peptides(95%)	
150	4	4	29	sp|P18124|RL7_HUMAN	60S ribosomal protein L7 OS=Homo sapiens GN=RPL7 PE=1 SV=1	HUMAN	2	
177	3.4	3.4	13.6	sp|Q99798|ACON_HUMAN	Aconitate hydratase, mitochondrial OS=Homo sapiens GN=ACO2 PE=1 SV=2	HUMAN	2	
324	2	2	24.2	sp|O15145|ARPC3_HUMAN	Actin-related protein 2/3 complex subunit 3 OS=Homo sapiens GN=ARPC3 PE=1 SV=3	HUMAN	2	
153	4	4	22.2	sp|P54819|KAD2_HUMAN	Adenylate kinase 2, mitochondrial OS=Homo sapiens GN=AK2 PE=1 SV=2	HUMAN	2	
254	2.04	2.04	15.7	sp|P27144|KAD4_HUMAN	Adenylate kinase isoenzyme 4, mitochondrial OS=Homo sapiens GN=AK4 PE=1 SV=1	HUMAN	2	
166	3.7	3.7	19.1	sp|P12236|ADT3_HUMAN	ADP/ATP translocase 3 OS=Homo sapiens GN=SLC25A6 PE=1 SV=4	HUMAN	2	
195	2.91	2.91	6.9	sp|P54802|ANAG_HUMAN	Alpha-N-acetylglucosaminidase OS=Homo sapiens GN=NAGLU PE=1 SV=2	HUMAN	2	
274	2	2.1	8.6	sp|Q9NVD7|PARVA_HUMAN	Alpha-parvin OS=Homo sapiens GN=PARVA PE=1 SV=1	HUMAN	2	
168	3.57	3.57	18.1	sp|Q9NVI7|ATD3A_HUMAN	ATPase family AAA domain-containing protein 3A OS=Homo sapiens GN=ATAD3A PE=1 SV=2	HUMAN	2	
176	3.41	3.41	16.9	sp|P07686|HEXB_HUMAN	Beta-hexosaminidase subunit beta OS=Homo sapiens GN=HEXB PE=1 SV=3	HUMAN	2	
190	3.03	3.03	13.8	sp|Q13557|KCC2D_HUMAN	Calcium/calmodulin-dependent protein kinase type II subunit delta OS=Homo sapiens GN=CAM	HUMAN	2	
366	1.69	1.69	30.5	sp|P13987|CD59_HUMAN	CD59 glycoprotein OS=Homo sapiens GN=CD59 PE=1 SV=1	HUMAN	2	
183	3.28	3.28	13	sp|P14209|CD99_HUMAN	CD99 antigen OS=Homo sapiens GN=CD99 PE=1 SV=1	HUMAN	2	
205	2.75	2.75	19.2	sp|P12110|CO6A2_HUMAN	Collagen alpha-2(VI) chain OS=Homo sapiens GN=COL6A2 PE=1 SV=4	HUMAN	2	
312	2	2	10.6	sp|P36551|HEM6_HUMAN	Coproporphyrinogen-III oxidase, mitochondrial OS=Homo sapiens GN=CPOX PE=1 SV=3	HUMAN	2	
208	2.63	2.63	37.9	sp|Q96HY6|DDRGK_HUMAN	DDRGK domain-containing protein 1 OS=Homo sapiens GN=DDRGK1 PE=1 SV=2	HUMAN	2	
292	2	2	12.7	sp|P10515|ODP2_HUMAN	Dihydrolipoyllysine-residue acetyltransferase component of pyruvate dehydrogenase complex,	HUMAN	2	
227	2.21	2.22	16.8	sp|P36957|ODO2_HUMAN	Dihydrolipoyllysine-residue succinyltransferase component of 2-oxoglutarate dehydrogenase co	HUMAN	2	
158	3.92	3.92	11.5	sp|P53634|CATC_HUMAN	Dipeptidyl peptidase 1 OS=Homo sapiens GN=CTSC PE=1 SV=2	HUMAN	2	
273	2	3.43	33.9	sp|P16989|DBPA_HUMAN	DNA-binding protein A OS=Homo sapiens GN=CSDA PE=1 SV=4	HUMAN	2	
147	4	4	14.4	sp|Q9H4M9|EHD1_HUMAN	EH domain-containing protein 1 OS=Homo sapiens GN=EHD1 PE=1 SV=2	HUMAN	2	
131	4.12	4.12	25.2	sp|P30084|ECHM_HUMAN	Enoyl-CoA hydratase, mitochondrial OS=Homo sapiens GN=ECHS1 PE=1 SV=4	HUMAN	2	
121	4.38	4.38	16.2	sp|Q14240|IF4A2_HUMAN	Eukaryotic initiation factor 4A-II OS=Homo sapiens GN=EIF4A2 PE=1 SV=2	HUMAN	2	
302	2	2	17.7	sp|P20042|IF2B_HUMAN	Eukaryotic translation initiation factor 2 subunit 2 OS=Homo sapiens GN=EIF2S2 PE=1 SV=2	HUMAN	2	
268	2.01	2.01	22.3	sp|P02792|FRIL_HUMAN	Ferritin light chain OS=Homo sapiens GN=FTL PE=1 SV=2	HUMAN	2	
411	0.87	1.57	7.8	sp|O75369|FLNB_HUMAN	Filamin-B OS=Homo sapiens GN=FLNB PE=1 SV=2	HUMAN	2	
380	1.43	1.43	11.2	sp|O00461|GOLI4_HUMAN	Golgi integral membrane protein 4 OS=Homo sapiens GN=GOLIM4 PE=1 SV=1	HUMAN	2	
315	2	2	10.7	sp|P04899|GNAI2_HUMAN	Guanine nucleotide-binding protein G(i) subunit alpha-2 OS=Homo sapiens GN=GNAI2 PE=1 SV=	HUMAN	2	
358	1.78	4.02	10.8	sp|P08238|HS90B_HUMAN	Heat shock protein HSP 90-beta OS=Homo sapiens GN=HSP90AB1 PE=1 SV=4	HUMAN	2	
307	2	2	26.2	sp|Q5QNW6|H2B2F_HUMAN	Histone H2B type 2-F OS=Homo sapiens GN=HIST2H2BF PE=1 SV=3	HUMAN	2	
169	3.55	3.55	13.3	sp|Q9Y4L1|HYOU1_HUMAN	Hypoxia up-regulated protein 1 OS=Homo sapiens GN=HYOU1 PE=1 SV=1	HUMAN	2	
439	0.57	2.79	19.9	sp|Q9Y6M1|IF2B2_HUMAN	Insulin-like growth factor 2 mRNA-binding protein 2 OS=Homo sapiens GN=IGF2BP2 PE=1 SV=2	HUMAN	2	
145	4	4	14.7	sp|O00425|IF2B3_HUMAN	Insulin-like growth factor 2 mRNA-binding protein 3 OS=Homo sapiens GN=IGF2BP3 PE=1 SV=2	HUMAN	2	
174	3.5	3.5	22.1	sp|P48735|IDHP_HUMAN	Isocitrate dehydrogenase [NADP], mitochondrial OS=Homo sapiens GN=IDH2 PE=1 SV=2	HUMAN	2	
144	4	4	21.6	sp|P04264|K2C1_HUMAN	Keratin, type II cytoskeletal 1 OS=Homo sapiens GN=KRT1 PE=1 SV=6	HUMAN	2	
251	2.05	2.05	13.7	sp|P11279|LAMP1_HUMAN	Lysosome-associated membrane glycoprotein 1 OS=Homo sapiens GN=LAMP1 PE=1 SV=3	HUMAN	2	
355	1.85	1.85	20.9	sp|P14174|MIF_HUMAN	Macrophage migration inhibitory factor OS=Homo sapiens GN=MIF PE=1 SV=4	HUMAN	2	
331	2	2	13.4	sp|Q9NS69|TOM22_HUMAN	Mitochondrial import receptor subunit TOM22 homolog OS=Homo sapiens GN=TOMM22 PE=1	HUMAN	2	
117	4.7	4.7	13.6	sp|Q16891|IMMT_HUMAN	Mitochondrial inner membrane protein OS=Homo sapiens GN=IMMT PE=1 SV=1	HUMAN	2	
308	2	2	8	sp|Q10713|MPPA_HUMAN	Mitochondrial-processing peptidase subunit alpha OS=Homo sapiens GN=PMPCA PE=1 SV=2	HUMAN	2	
119	4.49	4.49	23.8	sp|P29966|MARCS_HUMAN	Myristoylated alanine-rich C-kinase substrate OS=Homo sapiens GN=MARCKS PE=1 SV=4	HUMAN	2	
136	4.05	4.05	7.6	sp|P15586|GNS_HUMAN	N-acetylglucosamine-6-sulfatase OS=Homo sapiens GN=GNS PE=1 SV=3	HUMAN	2	
450	0.42	0.42	22.9	sp|Q9Y6M9|NDUB9_HUMAN	NADH dehydrogenase [ubiquinone] 1 beta subcomplex subunit 9 OS=Homo sapiens GN=NDUFB	HUMAN	2	
186	3.17	3.17	11.8	sp|Q9Y639|NPTN_HUMAN	Neuroplastin OS=Homo sapiens GN=NPTN PE=1 SV=2	HUMAN	2	
118	4.55	4.55	59.6	sp|P67809|YBOX1_HUMAN	Nuclease-sensitive element-binding protein 1 OS=Homo sapiens GN=YBX1 PE=1 SV=3	HUMAN	2	
266	2.01	2.01	11.9	sp|P80303|NUCB2_HUMAN	Nucleobindin-2 OS=Homo sapiens GN=NUCB2 PE=1 SV=2	HUMAN	2	
191	2.99	2.99	19.4	sp|P06748|NPM_HUMAN	Nucleophosmin OS=Homo sapiens GN=NPM1 PE=1 SV=2	HUMAN	2	
219	2.35	2.35	11.8	sp|O95302|FKBP9_HUMAN	Peptidyl-prolyl cis-trans isomerase FKBP9 OS=Homo sapiens GN=FKBP9 PE=1 SV=2	HUMAN	2	
159	3.9	3.9	26.1	sp|Q06830|PRDX1_HUMAN	Peroxiredoxin-1 OS=Homo sapiens GN=PRDX1 PE=1 SV=1	HUMAN	2	
263	2.01	2.02	21.9	sp|P30041|PRDX6_HUMAN	Peroxiredoxin-6 OS=Homo sapiens GN=PRDX6 PE=1 SV=3	HUMAN	2	
139	4.02	4.02	11.1	sp|O00469|PLOD2_HUMAN	Procollagen-lysine,2-oxoglutarate 5-dioxygenase 2 OS=Homo sapiens GN=PLOD2 PE=1 SV=2	HUMAN	2	
126	4.21	4.21	25.7	sp|P07737|PROF1_HUMAN	Profilin-1 OS=Homo sapiens GN=PFN1 PE=1 SV=2	HUMAN	2	
155	4	4	25.8	sp|Q9Y2B0|CNPY2_HUMAN	Protein canopy homolog 2 OS=Homo sapiens GN=CNPY2 PE=1 SV=1	HUMAN	2	
317	2	2	16.4	sp|Q99497|PARK7_HUMAN	Protein DJ-1 OS=Homo sapiens GN=PARK7 PE=1 SV=2	HUMAN	2	
311	2	2	10.4	sp|P49257|LMAN1_HUMAN	Protein ERGIC-53 OS=Homo sapiens GN=LMAN1 PE=1 SV=2	HUMAN	2	
352	2	2	15.2	sp|P31949|S10AB_HUMAN	Protein S100-A11 OS=Homo sapiens GN=S100A11 PE=1 SV=2	HUMAN	2	
171	3.54	3.54	7.2	sp|Q9UBV2|SE1L1_HUMAN	Protein sel-1 homolog 1 OS=Homo sapiens GN=SEL1L PE=1 SV=3	HUMAN	2	
342	2	2	4.2	sp|Q9C0H2|TTYH3_HUMAN	Protein tweety homolog 3 OS=Homo sapiens GN=TTYH3 PE=1 SV=3	HUMAN	2	
175	3.48	3.48	15.7	sp|Q13283|G3BP1_HUMAN	Ras GTPase-activating protein-binding protein 1 OS=Homo sapiens GN=G3BP1 PE=1 SV=1	HUMAN	2	
133	4.12	4.12	19	sp|P61026|RAB10_HUMAN	Ras-related protein Rab-10 OS=Homo sapiens GN=RAB10 PE=1 SV=1	HUMAN	2	
363	1.72	4	11	sp|Q15286|RAB35_HUMAN	Ras-related protein Rab-35 OS=Homo sapiens GN=RAB35 PE=1 SV=1	HUMAN	2	
137	4.04	4.04	19.8	sp|Q9NVA2|SEP11_HUMAN	Septin-11 OS=Homo sapiens GN=SEPT11 PE=1 SV=3	HUMAN	2	
142	4	4.13	24.6	sp|P34897|GLYM_HUMAN	Serine hydroxymethyltransferase, mitochondrial OS=Homo sapiens GN=SHMT2 PE=1 SV=3	HUMAN	2	
345	2	2	12.8	sp|Q04837|SSBP_HUMAN	Single-stranded DNA-binding protein, mitochondrial OS=Homo sapiens GN=SSBP1 PE=1 SV=1	HUMAN	2	
213	2.52	2.52	14.3	sp|P13637|AT1A3_HUMAN	Sodium/potassium-transporting ATPase subunit alpha-3 OS=Homo sapiens GN=ATP1A3 PE=1 SV	HUMAN	2	
149	4	4	21.4	sp|Q9UJZ1|STML2_HUMAN	Stomatin-like protein 2 OS=Homo sapiens GN=STOML2 PE=1 SV=1	HUMAN	2	
129	4.14	4.14	13.7	sp|P31040|DHSA_HUMAN	Succinate dehydrogenase [ubiquinone] flavoprotein subunit, mitochondrial OS=Homo sapiens G	HUMAN	2	
194	2.96	2.96	70.5	sp|P62328|TYB4_HUMAN	Thymosin beta-4 OS=Homo sapiens GN=TMSB4X PE=1 SV=2	HUMAN	2	
289	2	2	36.9	sp|P20290|BTF3_HUMAN	Transcription factor BTF3 OS=Homo sapiens GN=BTF3 PE=1 SV=1	HUMAN	2	
243	2.09	2.09	22.6	sp|P37802|TAGL2_HUMAN	Transgelin-2 OS=Homo sapiens GN=TAGLN2 PE=1 SV=3	HUMAN	2	
257	2.03	2.03	19.6	sp|P43307|SSRA_HUMAN	Translocon-associated protein subunit alpha OS=Homo sapiens GN=SSR1 PE=1 SV=3	HUMAN	2	
212	2.54	2.54	17.7	sp|P55084|ECHB_HUMAN	Trifunctional enzyme subunit beta, mitochondrial OS=Homo sapiens GN=HADHB PE=1 SV=3	HUMAN	2	
140	4.02	4.02	16.2	sp|Q13641|TPBG_HUMAN	Trophoblast glycoprotein OS=Homo sapiens GN=TPBG PE=1 SV=1	HUMAN	2	
184	3.26	3.26	8.9	sp|P07477|TRY1_HUMAN	Trypsin-1 OS=Homo sapiens GN=PRSS1 PE=1 SV=1	HUMAN	2	
440	0.55	2.76	7.3	sp|P07478|TRY2_HUMAN	Trypsin-2 OS=Homo sapiens GN=PRSS2 PE=1 SV=1	HUMAN	2	
325	2	2	12.3	sp|Q9Y224|CN166_HUMAN	UPF0568 protein C14orf166 OS=Homo sapiens GN=C14orf166 PE=1 SV=1	HUMAN	2	
178	3.38	3.38	11.2	sp|P18206|VINC_HUMAN	Vinculin OS=Homo sapiens GN=VCL PE=1 SV=4	HUMAN	2	
170	3.55	3.55	14.8	sp|P21796|VDAC1_HUMAN	Voltage-dependent anion-selective channel protein 1 OS=Homo sapiens GN=VDAC1 PE=1 SV=2	HUMAN	2	
197	2.85	2.85	63.7	sp|P83731|RL24_HUMAN	60S ribosomal protein L24 OS=Homo sapiens GN=RPL24 PE=1 SV=1	HUMAN	2	
441	0.55	0.55	17.7	sp|Q9Y295|DRG1_HUMAN	Developmentally-regulated GTP-binding protein 1 OS=Homo sapiens GN=DRG1 PE=1 SV=1	HUMAN	2	
252	2.04	2.04	11.6	sp|P04062|GLCM_HUMAN	Glucosylceramidase OS=Homo sapiens GN=GBA PE=1 SV=3	HUMAN	2	
225	2.22	2.22	45.4	sp|P04792|HSPB1_HUMAN	Heat shock protein beta-1 OS=Homo sapiens GN=HSPB1 PE=1 SV=2	HUMAN	2	
258	2.02	2.05	14.1	sp|P13797|PLST_HUMAN	Plastin-3 OS=Homo sapiens GN=PLS3 PE=1 SV=4	HUMAN	2	
206	2.73	2.73	13.5	sp|Q13813|SPTN1_HUMAN	Spectrin alpha chain, non-erythrocytic 1 OS=Homo sapiens GN=SPTAN1 PE=1 SV=3	HUMAN	2	
193	2.97	2.97	40.6	sp|P62987|RL40_HUMAN	Ubiquitin-60S ribosomal protein L40 OS=Homo sapiens GN=UBA52 PE=1 SV=2	HUMAN	2	
517	0.09	0.09	27.4	sp|P62424|RL7A_HUMAN	60S ribosomal protein L7a OS=Homo sapiens GN=RPL7A PE=1 SV=2	HUMAN	2	
369	1.62	1.62	6.5	sp|Q02218|ODO1_HUMAN	2-oxoglutarate dehydrogenase, mitochondrial OS=Homo sapiens GN=OGDH PE=1 SV=3	HUMAN	1	
412	0.87	0.87	13.7	sp|Q16698|DECR_HUMAN	2,4-dienoyl-CoA reductase, mitochondrial OS=Homo sapiens GN=DECR1 PE=1 SV=1	HUMAN	1	
295	2	2	31	sp|Q99714|HCD2_HUMAN	3-hydroxyacyl-CoA dehydrogenase type-2 OS=Homo sapiens GN=HSD17B10 PE=1 SV=3	HUMAN	1	
322	2	2	10.1	sp|P31937|3HIDH_HUMAN	3-hydroxyisobutyrate dehydrogenase, mitochondrial OS=Homo sapiens GN=HIBADH PE=1 SV=2	HUMAN	1	
290	2	2	18.9	sp|P09110|THIK_HUMAN	3-ketoacyl-CoA thiolase, peroxisomal OS=Homo sapiens GN=ACAA1 PE=1 SV=2	HUMAN	1	
444	0.51	0.51	18.4	sp|P62280|RS11_HUMAN	40S ribosomal protein S11 OS=Homo sapiens GN=RPS11 PE=1 SV=3	HUMAN	1	
403	1.06	1.06	21.2	sp|P62263|RS14_HUMAN	40S ribosomal protein S14 OS=Homo sapiens GN=RPS14 PE=1 SV=3	HUMAN	1	

N	Unused	Total	% Cov	Accession #	Name	Species	Peptides(95%)	
249	2.06	2.06	33.9	sp|P62244|RS15A_HUMAN	40S ribosomal protein S15a OS=Homo sapiens GN=RPS15A PE=1 SV=2	HUMAN	1	
236	2.15	2.15	26.3	sp|P15880|RS2_HUMAN	40S ribosomal protein S2 OS=Homo sapiens GN=RPS2 PE=1 SV=2	HUMAN	1	
359	1.77	1.77	24.5	sp|P62266|RS23_HUMAN	40S ribosomal protein S23 OS=Homo sapiens GN=RPS23 PE=1 SV=3	HUMAN	1	
229	2.2	2.21	19.3	sp|P23396|RS3_HUMAN	40S ribosomal protein S3 OS=Homo sapiens GN=RPS3 PE=1 SV=2	HUMAN	1	
275	2	2.06	18.4	sp|P05386|RLA1_HUMAN	60S acidic ribosomal protein P1 OS=Homo sapiens GN=RPLP1 PE=1 SV=1	HUMAN	1	
392	1.22	1.22	36.5	sp|P27635|RL10_HUMAN	60S ribosomal protein L10 OS=Homo sapiens GN=RPL10 PE=1 SV=4	HUMAN	1	
234	2.16	2.16	35.5	sp|P62906|RL10A_HUMAN	60S ribosomal protein L10a OS=Homo sapiens GN=RPL10A PE=1 SV=2	HUMAN	1	
393	1.2	1.2	14	sp|P62913|RL11_HUMAN	60S ribosomal protein L11 OS=Homo sapiens GN=RPL11 PE=1 SV=2	HUMAN	1	
381	1.42	1.42	44.1	sp|P61313|RL15_HUMAN	60S ribosomal protein L15 OS=Homo sapiens GN=RPL15 PE=1 SV=2	HUMAN	1	
379	1.46	1.46	19.9	sp|Q02543|RL18A_HUMAN	60S ribosomal protein L18a OS=Homo sapiens GN=RPL18A PE=1 SV=2	HUMAN	1	
389	1.24	1.24	26.9	sp|Q9UNX3|RL26L_HUMAN	60S ribosomal protein L26-like 1 OS=Homo sapiens GN=RPL26L1 PE=1 SV=1	HUMAN	1	
394	1.18	1.18	30.2	sp|P61353|RL27_HUMAN	60S ribosomal protein L27 OS=Homo sapiens GN=RPL27 PE=1 SV=2	HUMAN	1	
336	2	2	16.5	sp|P62888|RL30_HUMAN	60S ribosomal protein L30 OS=Homo sapiens GN=RPL30 PE=1 SV=2	HUMAN	1	
386	1.32	1.32	29.9	sp|P49207|RL34_HUMAN	60S ribosomal protein L34 OS=Homo sapiens GN=RPL34 PE=1 SV=3	HUMAN	1	
434	0.65	0.65	35.3	sp|P62891|RL39_HUMAN	60S ribosomal protein L39 OS=Homo sapiens GN=RPL39 PE=2 SV=2	HUMAN	1	
278	2	2	5.6	sp|Q02952|AKA12_HUMAN	A-kinase anchor protein 12 OS=Homo sapiens GN=AKAP12 PE=1 SV=4	HUMAN	1	
543	0.06	0.07	9.3	sp|Q9Y2D5|AKAP2_HUMAN	A-kinase anchor protein 2 OS=Homo sapiens GN=AKAP2 PE=1 SV=3	HUMAN	1	
418	0.81	0.81	17.2	sp|Q96CM8|ACSF2_HUMAN	Acyl-CoA synthetase family member 2, mitochondrial OS=Homo sapiens GN=ACSF2 PE=1 SV=2	HUMAN	1	
431	0.66	0.66	10.6	sp|P49753|ACOT2_HUMAN	Acyl-coenzyme A thioesterase 2, mitochondrial OS=Homo sapiens GN=ACOT2 PE=1 SV=6	HUMAN	1	
230	2.2	2.2	20.4	sp|Q9HDC9|APMAP_HUMAN	Adipocyte plasma membrane-associated protein OS=Homo sapiens GN=APMAP PE=1 SV=2	HUMAN	1	
420	0.78	0.78	16.4	sp|Q10588|BST1_HUMAN	ADP-ribosyl cyclase 2 OS=Homo sapiens GN=BST1 PE=1 SV=2	HUMAN	1	
300	2	2	11.2	sp|P30837|AL1B1_HUMAN	Aldehyde dehydrogenase X, mitochondrial OS=Homo sapiens GN=ALDH1B1 PE=1 SV=3	HUMAN	1	
314	2	2	12.4	sp|P05091|ALDH2_HUMAN	Aldehyde dehydrogenase, mitochondrial OS=Homo sapiens GN=ALDH2 PE=1 SV=2	HUMAN	1	
244	2.09	2.09	12.2	sp|P54920|SNAA_HUMAN	Alpha-soluble NSF attachment protein OS=Homo sapiens GN=NAPA PE=1 SV=3	HUMAN	1	
527	0.08	0.08	11.9	sp|O95831|AIFM1_HUMAN	Apoptosis-inducing factor 1, mitochondrial OS=Homo sapiens GN=AIFM1 PE=1 SV=1	HUMAN	1	
313	2	2	10.5	sp|P15289|ARSA_HUMAN	Arylsulfatase A OS=Homo sapiens GN=ARSA PE=1 SV=3	HUMAN	1	
201	2.8	2.8	24.4	sp|P00505|AATM_HUMAN	Aspartate aminotransferase, mitochondrial OS=Homo sapiens GN=GOT2 PE=1 SV=3	HUMAN	1	
231	2.2	2.2	26.7	sp|O75947|ATP5H_HUMAN	ATP synthase subunit d, mitochondrial OS=Homo sapiens GN=ATP5H PE=1 SV=3	HUMAN	1	
248	2.06	2.06	36.2	sp|P48047|ATPO_HUMAN	ATP synthase subunit O, mitochondrial OS=Homo sapiens GN=ATP5O PE=1 SV=1	HUMAN	1	
286	2	2	7.7	sp|Q9UG63|ABCF2_HUMAN	ATP-binding cassette sub-family F member 2 OS=Homo sapiens GN=ABCF2 PE=1 SV=2	HUMAN	1	
297	2	2	7.8	sp|Q92499|DDX1_HUMAN	ATP-dependent RNA helicase DDX1 OS=Homo sapiens GN=DDX1 PE=1 SV=2	HUMAN	1	
283	2	2	11.5	sp|O43491|E41L2_HUMAN	Band 4.1-like protein 2 OS=Homo sapiens GN=EPB41L2 PE=1 SV=1	HUMAN	1	
350	2	2	8.4	sp|P61769|B2MG_HUMAN	Beta-2-microglobulin OS=Homo sapiens GN=B2M PE=1 SV=1	HUMAN	1	
409	0.91	0.91	6.4	sp|P06865|HEXA_HUMAN	Beta-hexosaminidase subunit alpha OS=Homo sapiens GN=HEXA PE=1 SV=2	HUMAN	1	
370	1.62	1.62	6.1	sp|O75844|FACE1_HUMAN	CAAX prenyl protease 1 homolog OS=Homo sapiens GN=ZMPSTE24 PE=1 SV=2	HUMAN	1	
238	2.13	2.13	16.8	sp|P13861|KAP2_HUMAN	cAMP-dependent protein kinase type II-alpha regulatory subunit OS=Homo sapiens GN=PRKAR2	HUMAN	1	
376	1.51	1.51	8.7	sp|Q9BXL7|CAR11_HUMAN	Caspase recruitment domain-containing protein 11 OS=Homo sapiens GN=CARD11 PE=1 SV=3	HUMAN	1	
323	2	2	9.3	sp|P04040|CATA_HUMAN	Catalase OS=Homo sapiens GN=CAT PE=1 SV=3	HUMAN	1	
328	2	2	14.4	sp|P21964|COMT_HUMAN	Catechol O-methyltransferase OS=Homo sapiens GN=COMT PE=1 SV=2	HUMAN	1	
232	2.18	2.18	12.2	sp|P35222|CTNB1_HUMAN	Catenin beta-1 OS=Homo sapiens GN=CTNNB1 PE=1 SV=1	HUMAN	1	
221	2.3	2.3	9.2	sp|P08962|CD63_HUMAN	CD63 antigen OS=Homo sapiens GN=CD63 PE=1 SV=2	HUMAN	1	
351	2	2	8.5	sp|P60033|CD81_HUMAN	CD81 antigen OS=Homo sapiens GN=CD81 PE=1 SV=1	HUMAN	1	
360	1.77	1.77	4.1	sp|P48960|CD97_HUMAN	CD97 antigen OS=Homo sapiens GN=CD97 PE=1 SV=4	HUMAN	1	
384	1.33	1.33	11	sp|P60953|CDC42_HUMAN	Cell division control protein 42 homolog OS=Homo sapiens GN=CDC42 PE=1 SV=2	HUMAN	1	
464	0.3	0.3	14.1	sp|Q96GE4|CEP95_HUMAN	Centrosomal protein of 95 kDa OS=Homo sapiens GN=CEP95 PE=1 SV=1	HUMAN	1	
371	1.6	1.6	7.5	sp|Q6UVK1|CSPG4_HUMAN	Chondroitin sulfate proteoglycan 4 OS=Homo sapiens GN=CSPG4 PE=1 SV=2	HUMAN	1	
217	2.41	2.41	12.2	sp|O75390|CISY_HUMAN	Citrate synthase, mitochondrial OS=Homo sapiens GN=CS PE=1 SV=2	HUMAN	1	
365	1.7	1.77	7.5	sp|Q00610|CLH1_HUMAN	Clathrin heavy chain 1 OS=Homo sapiens GN=CLTC PE=1 SV=5	HUMAN	1	
368	1.66	1.66	23.7	sp|P47985|UCRI_HUMAN	Cytochrome b-c1 complex subunit Rieske, mitochondrial OS=Homo sapiens GN=UQCRFS1 PE=1	HUMAN	1	
210	2.58	2.58	14.2	sp|P13073|COX41_HUMAN	Cytochrome c oxidase subunit 4 isoform 1, mitochondrial OS=Homo sapiens GN=COX4I1 PE=1 S	HUMAN	1	
220	2.32	2.32	51.2	sp|P14854|CX6B1_HUMAN	Cytochrome c oxidase subunit 6B1 OS=Homo sapiens GN=COX6B1 PE=1 SV=2	HUMAN	1	
353	2	2	14.3	sp|P15954|COX7C_HUMAN	Cytochrome c oxidase subunit 7C, mitochondrial OS=Homo sapiens GN=COX7C PE=1 SV=1	HUMAN	1	
329	2	2	12.6	sp|P08574|CY1_HUMAN	Cytochrome c1, heme protein, mitochondrial OS=Homo sapiens GN=CYC1 PE=1 SV=3	HUMAN	1	
373	1.59	1.59	9.8	sp|P28838|AMPL_HUMAN	Cytosol aminopeptidase OS=Homo sapiens GN=LAP3 PE=1 SV=3	HUMAN	1	
321	2	2	23	sp|P33316|DUT_HUMAN	Deoxyuridine 5'-triphosphate nucleotidohydrolase, mitochondrial OS=Homo sapiens GN=DUT P	HUMAN	1	
341	2	2	5	sp|Q9NR28|DBLOH_HUMAN	Diablo homolog, mitochondrial OS=Homo sapiens GN=DIABLO PE=1 SV=1	HUMAN	1	
423	0.74	0.74	14	sp|Q9UBS4|DJB11_HUMAN	DnaJ homolog subfamily B member 11 OS=Homo sapiens GN=DNAJB11 PE=1 SV=1	HUMAN	1	
404	1.05	1.05	20.4	sp|P39656|OST48_HUMAN	Dolichyl-diphosphooligosaccharide--protein glycosyltransferase 48 kDa subunit OS=Homo sapie	HUMAN	1	
256	2.03	2.03	8.9	sp|P04844|RPN2_HUMAN	Dolichyl-diphosphooligosaccharide--protein glycosyltransferase subunit 2 OS=Homo sapiens GN	HUMAN	1	
255	2.03	2.03	13.7	sp|Q16643|DREB_HUMAN	Drebrin OS=Homo sapiens GN=DBN1 PE=1 SV=4	HUMAN	1	
432	0.65	0.66	7.8	sp|Q96JB1|DYH8_HUMAN	Dynein heavy chain 8, axonemal OS=Homo sapiens GN=DNAH8 PE=1 SV=2	HUMAN	1	
245	2.08	2.08	20.7	sp|Q969X5|ERGI1_HUMAN	Endoplasmic reticulum-Golgi intermediate compartment protein 1 OS=Homo sapiens GN=ERGIC	HUMAN	1	
294	2	2	11.9	sp|O75477|ERLN1_HUMAN	Erlin-1 OS=Homo sapiens GN=ERLIN1 PE=1 SV=1	HUMAN	1	
296	2	2	8.3	sp|Q96HE7|ERO1A_HUMAN	ERO1-like protein alpha OS=Homo sapiens GN=ERO1L PE=1 SV=2	HUMAN	1	
566	0.05	0.05	7.5	sp|Q9Y2L1|RRP44_HUMAN	Exosome complex exonuclease RRP44 OS=Homo sapiens GN=DIS3 PE=1 SV=2	HUMAN	1	
459	0.34	0.34	7.5	sp|Q9Y4F1|FARP1_HUMAN	FERM, RhoGEF and pleckstrin domain-containing protein 1 OS=Homo sapiens GN=FARP1 PE=1 S	HUMAN	1	
335	2	2	12	sp|Q12841|FSTL1_HUMAN	Follistatin-related protein 1 OS=Homo sapiens GN=FSTL1 PE=1 SV=1	HUMAN	1	
348	2	2	12.4	sp|P17900|SAP3_HUMAN	Ganglioside GM2 activator OS=Homo sapiens GN=GM2A PE=1 SV=4	HUMAN	1	
415	0.84	0.84	7.3	sp|P17302|CXA1_HUMAN	Gap junction alpha-1 protein OS=Homo sapiens GN=GJA1 PE=1 SV=2	HUMAN	1	
421	0.77	0.77	7.9	sp|Q92896|GSLG1_HUMAN	Golgi apparatus protein 1 OS=Homo sapiens GN=GLG1 PE=1 SV=2	HUMAN	1	
253	2.04	2.04	18.9	sp|Q9UIJ7|KAD3_HUMAN	GTP:AMP phosphotransferase, mitochondrial OS=Homo sapiens GN=AK3 PE=1 SV=4	HUMAN	1	
416	0.83	0.83	13	sp|Q14344|GNA13_HUMAN	Guanine nucleotide-binding protein subunit alpha-13 OS=Homo sapiens GN=GNA13 PE=1 SV=2	HUMAN	1	
442	0.55	0.55	14.9	sp|P09601|HMOX1_HUMAN	Heme oxygenase 1 OS=Homo sapiens GN=HMOX1 PE=1 SV=1	HUMAN	1	
301	2	2	15.5	sp|P30519|HMOX2_HUMAN	Heme oxygenase 2 OS=Homo sapiens GN=HMOX2 PE=1 SV=2	HUMAN	1	
378	1.47	1.47	25.9	sp|P69892|HBG2_HUMAN	Hemoglobin subunit gamma-2 OS=Homo sapiens GN=HBG2 PE=1 SV=2	HUMAN	1	
299	2	2	16.6	sp|P52597|HNRPF_HUMAN	Heterogeneous nuclear ribonucleoprotein F OS=Homo sapiens GN=HNRNPF PE=1 SV=3	HUMAN	1	
281	2	2	8.6	sp|P19367|HXK1_HUMAN	Hexokinase-1 OS=Homo sapiens GN=HK1 PE=1 SV=3	HUMAN	1	
429	0.69	0.7	17.2	sp|P09429|HMGB1_HUMAN	High mobility group protein B1 OS=Homo sapiens GN=HMGB1 PE=1 SV=3	HUMAN	1	
260	2.02	2.02	38.7	sp|Q9BX68|HINT2_HUMAN	Histidine triad nucleotide-binding protein 2, mitochondrial OS=Homo sapiens GN=HINT2 PE=1 S	HUMAN	1	
480	0.22	0.22	13.1	sp|Q16836|HCDH_HUMAN	Hydroxyacyl-coenzyme A dehydrogenase, mitochondrial OS=Homo sapiens GN=HADH PE=1 SV=	HUMAN	1	
276	2	2.03	8.6	sp|O00410|IPO5_HUMAN	Importin-5 OS=Homo sapiens GN=IPO5 PE=1 SV=4	HUMAN	1	
382	1.41	1.41	17.4	sp|Q70UQ0|IKIP_HUMAN	Inhibitor of nuclear factor kappa-B kinase-interacting protein OS=Homo sapiens GN=IKBIP PE=1	HUMAN	1	
304	2	2	6.4	sp|P08648|ITA5_HUMAN	Integrin alpha-5 OS=Homo sapiens GN=ITGA5 PE=1 SV=2	HUMAN	1	
202	2.79	2.83	12.8	sp|P05556|ITB1_HUMAN	Integrin beta-1 OS=Homo sapiens GN=ITGB1 PE=1 SV=2	HUMAN	1	
433	0.65	0.66	9.7	sp|Q13418|ILK_HUMAN	Integrin-linked protein kinase OS=Homo sapiens GN=ILK PE=1 SV=2	HUMAN	1	
265	2.01	2.01	9.3	sp|P19525|E2AK2_HUMAN	Interferon-induced, double-stranded RNA-activated protein kinase OS=Homo sapiens GN=EIF2A	HUMAN	1	
287	2	2	5.1	sp|Q9NSE4|SYIM_HUMAN	Isoleucine--tRNA ligase, mitochondrial OS=Homo sapiens GN=IARS2 PE=1 SV=2	HUMAN	1	
410	0.88	0.88	14.1	sp|P35527|K1C9_HUMAN	Keratin, type I cytoskeletal 9 OS=Homo sapiens GN=KRT9 PE=1 SV=3	HUMAN	1	
372	1.59	1.71	11.8	sp|Q9NSB2|KRT84_HUMAN	Keratin, type II cuticular Hb4 OS=Homo sapiens GN=KRT84 PE=1 SV=2	HUMAN	1	
319	2	2	7	sp|Q08431|MFGM_HUMAN	Lactadherin OS=Homo sapiens GN=MFGE8 PE=1 SV=2	HUMAN	1	
428	0.7	0.7	9.2	sp|P48449|ERG7_HUMAN	Lanosterol synthase OS=Homo sapiens GN=LSS PE=1 SV=1	HUMAN	1	
356	1.8	1.8	24.9	sp|Q14847|LASP1_HUMAN	LIM and SH3 domain protein 1 OS=Homo sapiens GN=LASP1 PE=1 SV=2	HUMAN	1	
291	2	2	7.3	sp|O00754|MA2B1_HUMAN	Lysosomal alpha-mannosidase OS=Homo sapiens GN=MAN2B1 PE=1 SV=3	HUMAN	1	

N	Unused	Total	% Cov	Accession #	Name	Species	Peptides(95%)	
211	2.55	2.55	14.2	sp|Q14108|SCRB2_HUMAN	Lysosome membrane protein 2 OS=Homo sapiens GN=SCARB2 PE=1 SV=2	HUMAN	1	
223	2.25	2.25	4.9	sp|P13473|LAMP2_HUMAN	Lysosome-associated membrane glycoprotein 2 OS=Homo sapiens GN=LAMP2 PE=1 SV=2	HUMAN	1	
518	0.09	0.09	9.1	sp|Q14764|MVP_HUMAN	Major vault protein OS=Homo sapiens GN=MVP PE=1 SV=4	HUMAN	1	
285	2	2	15.1	sp|Q13724|MOGS_HUMAN	Mannosyl-oligosaccharide glucosidase OS=Homo sapiens GN=MOGS PE=1 SV=5	HUMAN	1	
407	0.92	0.92	8.2	sp|O75448|MED24_HUMAN	Mediator of RNA polymerase II transcription subunit 24 OS=Homo sapiens GN=MED24 PE=1 SV=	HUMAN	1	
282	2	2	17.1	sp|P11310|ACADM_HUMAN	Medium-chain specific acyl-CoA dehydrogenase, mitochondrial OS=Homo sapiens GN=ACADM I	HUMAN	1	
364	1.72	1.72	15.7	sp|O15173|PGRC2_HUMAN	Membrane-associated progesterone receptor component 2 OS=Homo sapiens GN=PGRMC2 PE=	HUMAN	1	
408	0.92	0.92	4.8	sp|Q9HCC0|MCCB_HUMAN	Methylcrotonoyl-CoA carboxylase beta chain, mitochondrial OS=Homo sapiens GN=MCCC2 PE=	HUMAN	1	
333	2	2	15.4	sp|Q8N183|MIMIT_HUMAN	Mimitin, mitochondrial OS=Homo sapiens GN=NDUFAF2 PE=1 SV=1	HUMAN	1	
279	2	2	8.9	sp|Q3SY69|AL1L2_HUMAN	Mitochondrial 10-formyltetrahydrofolate dehydrogenase OS=Homo sapiens GN=ALDH1L2 PE=1	HUMAN	1	
357	1.8	1.8	21.1	sp|P62072|TIM10_HUMAN	Mitochondrial import inner membrane translocase subunit Tim10 OS=Homo sapiens GN=TIMM	HUMAN	1	
391	1.23	1.23	37.9	sp|Q9Y5L4|TIM13_HUMAN	Mitochondrial import inner membrane translocase subunit Tim13 OS=Homo sapiens GN=TIMM	HUMAN	1	
332	2	2	81.1	sp|Q96B49|TOM6_HUMAN	Mitochondrial import receptor subunit TOM6 homolog OS=Homo sapiens GN=TOMM6 PE=1 SV	HUMAN	1	
361	1.77	1.77	25.3	sp|O43678|NDUA2_HUMAN	NADH dehydrogenase [ubiquinone] 1 alpha subcomplex subunit 2 OS=Homo sapiens GN=NDUF	HUMAN	1	
427	0.72	0.72	19.7	sp|P19404|NDUV2_HUMAN	NADH dehydrogenase [ubiquinone] flavoprotein 2, mitochondrial OS=Homo sapiens GN=NDUF\	HUMAN	1	
338	2	2	4.8	sp|O75306|NDUS2_HUMAN	NADH dehydrogenase [ubiquinone] iron-sulfur protein 2, mitochondrial OS=Homo sapiens GN=I	HUMAN	1	
277	2	2.03	6.9	sp|P16435|NCPR_HUMAN	NADPH--cytochrome P450 reductase OS=Homo sapiens GN=POR PE=1 SV=2	HUMAN	1	
320	2	2	9.2	sp|P50897|PPT1_HUMAN	Palmitoyl-protein thioesterase 1 OS=Homo sapiens GN=PPT1 PE=1 SV=1	HUMAN	1	
437	0.58	0.58	28.4	sp|P20962|PTMS_HUMAN	Parathymosin OS=Homo sapiens GN=PTMS PE=1 SV=2	HUMAN	1	
339	2	2	6.9	sp|O14908|GIPC1_HUMAN	PDZ domain-containing protein GIPC1 OS=Homo sapiens GN=GIPC1 PE=1 SV=2	HUMAN	1	
458	0.35	0.35	8.9	sp|P26022|PTX3_HUMAN	Pentraxin-related protein PTX3 OS=Homo sapiens GN=PTX3 PE=1 SV=3	HUMAN	1	
438	0.58	0.58	10.5	sp|Q9NYL4|FKB11_HUMAN	Peptidyl-prolyl cis-trans isomerase FKBP11 OS=Homo sapiens GN=FKBP11 PE=1 SV=1	HUMAN	1	
305	2	2	13.9	sp|Q9Y680|FKBP7_HUMAN	Peptidyl-prolyl cis-trans isomerase FKBP7 OS=Homo sapiens GN=FKBP7 PE=1 SV=1	HUMAN	1	
226	2.22	2.22	17	sp|Q13162|PRDX4_HUMAN	Peroxiredoxin-4 OS=Homo sapiens GN=PRDX4 PE=1 SV=1	HUMAN	1	
284	2	2	11	sp|P51659|DHB4_HUMAN	Peroxisomal multifunctional enzyme type 2 OS=Homo sapiens GN=HSD17B4 PE=1 SV=3	HUMAN	1	
306	2	2	8.1	sp|Q9Y285|SYFA_HUMAN	Phenylalanine--tRNA ligase alpha subunit OS=Homo sapiens GN=FARSA PE=1 SV=3	HUMAN	1	
347	2	2	9.1	sp|P30086|PEBP1_HUMAN	Phosphatidylethanolamine-binding protein 1 OS=Homo sapiens GN=PEBP1 PE=1 SV=3	HUMAN	1	
400	1.1	1.1	11.8	sp|P18669|PGAM1_HUMAN	Phosphoglycerate mutase 1 OS=Homo sapiens GN=PGAM1 PE=1 SV=2	HUMAN	1	
224	2.24	2.24	18.1	sp|Q8NC51|PAIRB_HUMAN	Plasminogen activator inhibitor 1 RNA-binding protein OS=Homo sapiens GN=SERBP1 PE=1 SV=	HUMAN	1	
293	2	2	4.9	sp|P09619|PGFRB_HUMAN	Platelet-derived growth factor receptor beta OS=Homo sapiens GN=PDGFRB PE=1 SV=1	HUMAN	1	
425	0.73	0.73	8.2	sp|O15031|PLXB2_HUMAN	Plexin-B2 OS=Homo sapiens GN=PLXNB2 PE=1 SV=3	HUMAN	1	
233	2.16	2.17	15.3	sp|P11940|PABP1_HUMAN	Polyadenylate-binding protein 1 OS=Homo sapiens GN=PABPC1 PE=1 SV=2	HUMAN	1	
413	0.86	0.86	13.5	sp|Q10471|GALT2_HUMAN	Polypeptide N-acetylgalactosaminyltransferase 2 OS=Homo sapiens GN=GALNT2 PE=1 SV=1	HUMAN	1	
240	2.11	2.11	8.2	sp|P07602|SAP_HUMAN	Proactivator polypeptide OS=Homo sapiens GN=PSAP PE=1 SV=2	HUMAN	1	
334	2	2	8.1	sp|Q8N129|CNPY4_HUMAN	Protein canopy homolog 4 OS=Homo sapiens GN=CNPY4 PE=2 SV=1	HUMAN	1	
354	2	2	9.5	sp|O75629|CREG1_HUMAN	Protein CREG1 OS=Homo sapiens GN=CREG1 PE=1 SV=1	HUMAN	1	
280	2	2	18.2	sp|Q86UE4|LYRIC_HUMAN	Protein LYRIC OS=Homo sapiens GN=MTDH PE=1 SV=2	HUMAN	1	
237	2.14	2.14	41.1	sp|P06703|S10A6_HUMAN	Protein S100-A6 OS=Homo sapiens GN=S100A6 PE=1 SV=1	HUMAN	1	
385	1.33	1.33	4.7	sp|Q9H2V7|SPNS1_HUMAN	Protein spinster homolog 1 OS=Homo sapiens GN=SPNS1 PE=1 SV=1	HUMAN	1	
326	2	2	30.4	sp|Q5JNZ5|RS26L_HUMAN	Putative 40S ribosomal protein S26-like 1 OS=Homo sapiens GN=RPS26P11 PE=5 SV=1	HUMAN	1	
309	2	2	17.7	sp|P62070|RRAS2_HUMAN	Ras-related protein R-Ras2 OS=Homo sapiens GN=RRAS2 PE=1 SV=1	HUMAN	1	
388	1.3	1.3	20.9	sp|P61020|RAB5B_HUMAN	Ras-related protein Rab-5B OS=Homo sapiens GN=RAB5B PE=1 SV=1	HUMAN	1	
396	1.14	1.14	22.8	sp|P11234|RALB_HUMAN	Ras-related protein Ral-B OS=Homo sapiens GN=RALB PE=1 SV=1	HUMAN	1	
327	2	2	17.4	sp|P62745|RHOB_HUMAN	Rho-related GTP-binding protein RhoB OS=Homo sapiens GN=RHOB PE=1 SV=1	HUMAN	1	
405	0.99	0.99	6.9	sp|P16615|AT2A2_HUMAN	Sarcoplasmic/endoplasmic reticulum calcium ATPase 2 OS=Homo sapiens GN=ATP2A2 PE=1 SV=	HUMAN	1	
377	1.51	1.51	12.9	sp|Q8WVM8|SCFD1_HUMAN	Sec1 family domain-containing protein 1 OS=Homo sapiens GN=SCFD1 PE=1 SV=4	HUMAN	1	
401	1.08	1.09	26.5	sp|Q16181|SEPT7_HUMAN	Septin-7 OS=Homo sapiens GN=SEPT7 PE=1 SV=2	HUMAN	1	
443	0.51	0.51	9.7	sp|Q9UHD8|SEPT9_HUMAN	Septin-9 OS=Homo sapiens GN=SEPT9 PE=1 SV=2	HUMAN	1	
456	0.39	0.39	6.3	sp|O00506|STK25_HUMAN	Serine/threonine-protein kinase 25 OS=Homo sapiens GN=STK25 PE=1 SV=1	HUMAN	1	
465	0.29	0.29	26.2	sp|P11309|PIM1_HUMAN	Serine/threonine-protein kinase pim-1 OS=Homo sapiens GN=PIM1 PE=1 SV=3	HUMAN	1	
318	2	2	7.9	sp|Q96P63|SPB12_HUMAN	Serpin B12 OS=Homo sapiens GN=SERPINB12 PE=1 SV=1	HUMAN	1	
414	0.86	0.86	13.9	sp|P53597|SUCA_HUMAN	Succinyl-CoA ligase [ADP/GDP-forming] subunit alpha, mitochondrial OS=Homo sapiens GN=SUC	HUMAN	1	
399	1.1	1.1	26.6	sp|Q8NBJ7|SUMF2_HUMAN	Sulfatase-modifying factor 2 OS=Homo sapiens GN=SUMF2 PE=1 SV=2	HUMAN	1	
222	2.26	2.26	11.9	sp|O15260|SURF4_HUMAN	Surfeit locus protein 4 OS=Homo sapiens GN=SURF4 PE=1 SV=3	HUMAN	1	
288	2	2	20.4	sp|Q99536|VAT1_HUMAN	Synaptic vesicle membrane protein VAT-1 homolog OS=Homo sapiens GN=VAT1 PE=1 SV=2	HUMAN	1	
346	2	2	13.1	sp|P57105|SYJ2B_HUMAN	Synaptojanin-2-binding protein OS=Homo sapiens GN=SYNJ2BP PE=1 SV=2	HUMAN	1	
264	2.01	2.01	24.6	sp|Q86Y82|STX12_HUMAN	Syntaxin-12 OS=Homo sapiens GN=STX12 PE=1 SV=1	HUMAN	1	
387	1.32	1.32	10	sp|O15400|STX7_HUMAN	Syntaxin-7 OS=Homo sapiens GN=STX7 PE=1 SV=4	HUMAN	1	
340	2	2	11.1	sp|O00560|SDCB1_HUMAN	Syntenin-1 OS=Homo sapiens GN=SDCBP PE=1 SV=1	HUMAN	1	
310	2	2	12.1	sp|P50991|TCPD_HUMAN	T-complex protein 1 subunit delta OS=Homo sapiens GN=CCT4 PE=1 SV=4	HUMAN	1	
374	1.55	1.55	18.8	sp|P30048|PRDX3_HUMAN	Thioredoxin-dependent peroxide reductase, mitochondrial OS=Homo sapiens GN=PRDX3 PE=1 S	HUMAN	1	
241	2.1	2.1	14.9	sp|P04216|THY1_HUMAN	Thy-1 membrane glycoprotein OS=Homo sapiens GN=THY1 PE=1 SV=2	HUMAN	1	
259	2.02	2.02	11.5	sp|Q92616|GCN1L_HUMAN	Translational activator GCN1 OS=Homo sapiens GN=GCN1L1 PE=1 SV=6	HUMAN	1	
435	0.63	0.63	12	sp|Q9UGP8|SEC63_HUMAN	Translocation protein SEC63 homolog OS=Homo sapiens GN=SEC63 PE=1 SV=2	HUMAN	1	
362	1.74	1.74	33.5	sp|P51571|SSRD_HUMAN	Translocon-associated protein subunit delta OS=Homo sapiens GN=SSR4 PE=1 SV=1	HUMAN	1	
207	2.69	2.69	20	sp|Q9BVK6|TMED9_HUMAN	Transmembrane emp24 domain-containing protein 9 OS=Homo sapiens GN=TMED9 PE=1 SV=2	HUMAN	1	
430	0.66	0.68	7.5	sp|Q9BTV4|TMM43_HUMAN	Transmembrane protein 43 OS=Homo sapiens GN=TMEM43 PE=1 SV=1	HUMAN	1	
367	1.66	1.76	4.6	sp|Q8N357|CB018_HUMAN	Transmembrane protein C2orf18 OS=Homo sapiens GN=C2orf18 PE=1 SV=1	HUMAN	1	
383	1.33	1.33	16.4	sp|P53007|TXTP_HUMAN	Tricarboxylate transport protein, mitochondrial OS=Homo sapiens GN=SLC25A1 PE=1 SV=2	HUMAN	1	
424	0.73	0.74	7.9	sp|O75386|TULP3_HUMAN	Tubby-related protein 3 OS=Homo sapiens GN=TULP3 PE=1 SV=2	HUMAN	1	
406	0.97	0.97	5.2	sp|Q14157|UBP2L_HUMAN	Ubiquitin-associated protein 2-like OS=Homo sapiens GN=UBAP2L PE=1 SV=2	HUMAN	1	
395	1.15	1.15	14	sp|Q92575|UBXN4_HUMAN	UBX domain-containing protein 4 OS=Homo sapiens GN=UBXN4 PE=1 SV=2	HUMAN	1	
398	1.12	1.12	6.4	sp|Q9NYU2|UGGG1_HUMAN	UDP-glucose:glycoprotein glucosyltransferase 1 OS=Homo sapiens GN=UGGT1 PE=1 SV=3	HUMAN	1	
239	2.11	2.11	8.7	sp|O00159|MYO1C_HUMAN	Unconventional myosin-Ic OS=Homo sapiens GN=MYO1C PE=1 SV=4	HUMAN	1	
344	2	2	3	sp|Q13488|VPP3_HUMAN	V-type proton ATPase 116 kDa subunit a isoform 3 OS=Homo sapiens GN=TCIRG1 PE=1 SV=3	HUMAN	1	
316	2	2	36.4	sp|O75348|VATG1_HUMAN	V-type proton ATPase subunit G 1 OS=Homo sapiens GN=ATP6V1G1 PE=1 SV=3	HUMAN	1	
246	2.07	2.07	10	sp|P50552|VASP_HUMAN	Vasodilator-stimulated phosphoprotein OS=Homo sapiens GN=VASP PE=1 SV=3	HUMAN	1	
349	2	2	16	sp|Q15836|VAMP3_HUMAN	Vesicle-associated membrane protein 3 OS=Homo sapiens GN=VAMP3 PE=1 SV=3	HUMAN	1	
330	2	2	10.8	sp|Q9P0L0|VAPA_HUMAN	Vesicle-associated membrane protein-associated protein A OS=Homo sapiens GN=VAPA PE=1 SV	HUMAN	1	
337	2	2	9.9	sp|P45880|VDAC2_HUMAN	Voltage-dependent anion-selective channel protein 2 OS=Homo sapiens GN=VDAC2 PE=1 SV=2	HUMAN	1	
343	2	2	4.9	sp|Q15043|S39AE_HUMAN	Zinc transporter ZIP14 OS=Homo sapiens GN=SLC39A14 PE=1 SV=3	HUMAN	1	
462	0.31	0.31	9.7	sp|Q8IYH5|ZZZ3_HUMAN	ZZ-type zinc finger-containing protein 3 OS=Homo sapiens GN=ZZZ3 PE=1 SV=1	HUMAN	1	